INTERPRETING FOSSILS OF FLY-SPECK FUNGI USING COMPARATIVE ANATOMY AND PHYLOGENETICS

by

Ludovic Le Renard

B.Sc., Université Montpellier 2, 2009

M.Sc., Université Paris Descartes, 2011

A THESIS SUBMITTED IN PARTIAL FULFILLMENT OF

THE REQUIREMENTS FOR THE DEGREE OF

Doctor of Philosophy

in

THE FACULTY OF GRADUATE AND POSTDOCTORAL STUDIES

(Botany)

THE UNIVERSITY OF BRITISH COLUMBIA

(Vancouver)

December 2019

The following individuals certify that they have read, and recommend to the Faculty of Graduate and Postdoctoral Studies for acceptance, the dissertation entitled:

Interpreting fossils of fly-speck fungi using comparative anatomy and phylogenetics

submitted by Ludovic Le Renard in partial fulfillment of the requirements for

the degree of Doctor of Philosophy

in Botany

Examining Committee:

Mary Berbee, Botany
Co-supervisor

Ruth Stockey, Oregon State University, Botany
Co-supervisor

Sean Graham, Botany
Supervisory Committee Member

Wayne Maddison, Zoology
Supervisory Committee Member

Jim Kronstad, Microbiology & Immunology
University Examiner

Quentin Cronk, Botany
University Examiner

Abstract

Critical interpretations of fossil fungi combined with phylogenies of living species have the potential to reveal patterns of character evolution and to inform estimates of the geological timing of fungal radiations. Some of the best fungal fossils are of thyriothecia, formed by fly-speck fungi. A thyriothecium is a minute fungal sporulating structure, with a flat scutellum and a shield-like upper surface. Scutella have distinctive cell patterns that are formed by a sequence of hyphal branching and septation. However, for thyriothecial species, phylogenies from DNA sequence data and illustrations of scutella remain have been limited. In Chapter 2, I present a comprehensive phylogeny of thyriothecial Dothideomycetes based on 4251 nucelotides for 320 taxa, contributing new nuclear rDNA sequence data for 14 thyriothecial fungi. I code character states for taxa including 60 thyriothecial species and then estimate ancestral character states using the Bayesian posterior distribution of topologies from my dataset to account for phylogenetic uncertainty. Radiate thyriothecia are only found in Class Dothideomycetes, where they seem to have evolved independently at least three times. In Chapters 3, 4 and 5, I describe new species of Cretaceous scutellum fossils. Scutella can be abundant on fossilized leaf cuticles and are well documented in deposits of Eocene age and younger (<45 Ma). To better sample earlier fossils, I studied thyriothecia from clays from Early Cretaceous Dutch Gap Canal beds (dated 125–113 Ma). I dissolved the inorganic matrix and selected organic, fossilized fragments of plant cuticle showing signs of fungal colonization. Of hundreds of fungal reproductive structures on 281 cuticle fragments, I describe thyriothecia that were preserved well enough to be coded for their characters. Chapter 3 describes *Protographum luttrellii*, a fossil that shares characters with extant Aulographaceae. Chapters 4 and 5 describe thyriothecial taxa with character combinations not seen in extant species. The most common Cretaceous thyriothecia differ substantially from their extant relatives. My work demonstrates that it is possible to extend fossil evidence of lineages of Dothideomycetes further back in time, by surveying fungi on fossilized plant cuticles and integrating comparative anatomy and phylogeny in their interpretation.

Lay Summary

My thesis focuses on the evolution of fly-speck fungi, microfungi that appear as minute black reproductive structures called 'thyriothecia' on the surfaces of plant leaves and stems, resembling fly droppings. Thyriothecia produce spores below a scutellum, a small, shield-like plate of fungal filaments. Scutella are common as fossils. I collected fossilized scutella from Lower Cretaceous, 113–121 million-year-old clays from Virginia by digesting away the inorganic matrix and saving the organic fossils. For comparison with the fossils, I used living species, creating a database of their shapes, habitats, and development, and analyzed their evolutionary relationships using DNA sequences. The comparisons helped me to discover three new species of fossil fly-speck fungi. One fossil, *Protographum luttrellii* is the most ancient fly-speck fungus that belongs to a fungal family that is still alive today. My work extends knowledge of the evolutionary diversity of forms of fungi and improves interpretation of fungal fossils.

Preface

I developed my research topic, initially using a database that I helped to produce and to publish (Berbee, M., **Le Renard, L.**, Carmean, D., 2014. Online access to the Kalgutkar and Jansonius database of fossil fungi. Palynology 39:103–109).

Chapter 2 is prepared for submission as **Le Renard, L.,** Firmino, André L., Pereira, Olinto L., Stockey, Ruth A., Berbee, Mary L., Character evolution of modern fly-speck fungi (Ascomycota) and implications for interpreting thyriothecial fossils. I was responsible for finding new taxa and determining DNA sequences. Under Berbee's supervision, I performed all the analyses, made all the illustrations, and prepared initial drafts of the manuscript. Firmino and Pereira contributed important sequence data and specimens that were instrumental to my interpretations. Berbee participated in writing and structuring of the manuscript. Stockey helped integrate the fossil data in a coherent way.

Chapter 3 was submitted to the journal *Mycologia* and reviewed favorably on October 15th 2019 as "**Le Renard, L.,** Stockey, R. A., Upchurch, G., Berbee M. L. A new epiphyllous fly-speck fungus from the Early Cretaceous Potomac group of Virginia (125–112 Ma): *Protographum luttrellii gen. et sp. nov.* I performed all the analyses and generated new sequences of Aulographaceae."

Chapter 4 is prepared for submission as: "**Le Renard, L.,** Stockey, R. A., Upchurch, G., Berbee M.L. *Bleximothyrites ostiolatus gen*. *et sp. nov*. a unique fly-speck fungus (Dothideomycetes) from the Lower Cretaceous."

Chapter 5 is prepared for submission as "**Le Renard, L.,** Stockey, R. A., Upchurch, G., Berbee M.L. Cretaceous fungal scutella from the Lower Potomac Group Zone 1: *Stomatothyrites placocentrus gen. et sp. nov.*, a dothideomycete colonizer of conifer stomata."

In Chapter 3, 4 and 5, I prepared living and fossil fungi for microscopic analysis, illustrated them, and performed all analyses. Upchurch provided the Cretaceous fossiliferous clay and helped with fossil plant cuticle identification. I prepared the manuscripts under Stockey's supervision and Berbee participated in the writing.

Table of Contents

List of Tables

List of Figures

Acknowledgements

I would like to thank my two supervisors, Mary Berbee and Ruth Stockey for enduring and supporting me in my difficult choice to work with fossils of fungi, the opportunity of a lifetime. I wish to thank my committee members Sean Graham and Wayne Maddison for their feedback and support, and precious advice throughout my degree.

I thank Dr. Randal A. Mindell (Qualicum Beach Museum) for his suggestions and assistance in modifying fossil cuticle extraction protocol. He gave me the confidence to work with fossil debris in search for fungi *my own way*. I want to thank Gar Rothwell, for his help assembling illustrative plates as well as for his comments, advice, stories and the endless knowledge about fossil plants he is willing to share. I thank Dr. Rolf W. Mathewes (Simon Fraser University) for processing fossil samples with hydrofluoric acid and for his suggestion for handling dispersed phytodebris.

I thank the Organisation for Tropical Studies and the Comisión Nacional para la Gestión de la Biodeiversidad, especially Francisco Campos Rivera and Bernal Mattarita Carranza for allowing me to collect tropical fungi in the research station of La Selva in Costa Rica. Additionally, I want to thank Marybel Soto Gomez for her invaluable help editing application documents in Spanish.

I also wish to thank Sueli Valéria Ribeiro at the herbarium of the Universidade Federal de Viçosa, Ann Bogaerts at the Botanical Garden of Meise, Kyle Gervers and Joey Spatafora at the herbarium of Oregon State University, Arien van Iperen and Pedro Crous at the Westerdijk Fungal Biodiversity Institute and Olivia Lee at the herbarium of the University of British

Columbia for their help processing herbarium loans. I thank Robert Lücking from the Botanischer Garten und Botanisches Museum Berlin for gifts of lichen specimens.

The opportunity I was given to be a Teaching Assistant through the Biology program contributed to my salary and trained me to be a more effective teacher. To those inspiring teachers I assisted: Mary Berbee, Julia Costa, Luis Gonzalez Torres, Jill Jankowski, Wayne Maddison and Jeanette Whitton: *merci beaucoup*!

Thanks to the Biodiversity BRITE travel award (2015), I had the opportunity to go collect epiphyllous fungi in Costa Rica and to sample important fungi for my project. MSA Mentor student travel awards allowed to me to attend the conference of the Mycological Society of America in 2016 and share my research with the community.

Thanks to the former members of the Berbee lab who helped and whose interest for fungal evolution reinforces my desire to work with fossils: Ben Auxier, Anna Bazzicalupo and Jaclyn Dee. I also want to thank other like-minded students, who became friends and were supportive, Sean McCotter, Ana Radojičić, Marybel Soto Gomez, Vicent Billy, Pierre Rogy and Florent Mazel.

A special thank you to the people who lived with me A. Muqeet, M. Haque, and H. Lee, M. Radtke, and those who hosted me in Oregon, Alija Mujic, Charlotte Johston and her husband Dan. Finally, I cannot thank all my family enough, for being supportive while I was away from for so long, so that I could study fossil fungi.

Chapter 1: Introduction

1.1 Summary

In this chapter, I aim at refining our vision of fungal evolution on land through time, with an emphasis on the members of the most diverse phylum: Ascomycota. I chose to study fungal fossils with the goal of extending the repertoire of calibration points available to infer fungal divergence times, and ultimately provide a better picture of ascomycete diversity through time. I show that a single fossil suggests that Ascomycota evolved during the Paleozoic, while subsequent fossil evidence is more than 200 Ma younger. While living fungi are increasingly characterized through barcode DNA sequencing, fossil fungi can only be described using morphological characters. This results in a dual classification, where species concepts of fungal fossils intersect with those of living fungi only infrequently. To remedy this, it is necessary to use the insights gained from molecular phylogenetics and assess the phylogenetic significance of morphological characters found in fossils. As suggested by the available fossil record of Ascomycota, fly-speck fungi represent a major group of fungi available in the fossil record that are found across the globe by the Lower Cretaceous. The study of additional fossils from the same age will undoubtedly contribute additional evidence of their evolution, and is likely to yield new calibration points to infer the ages of ascomycete divergences.

1.2 Biology and systematics of Ascomycota

The phylum Ascomycota Caval.-Sm. is the most thoroughly sampled group of fungi in terrestrial ecosystems (McLaughlin and Spatafora, 2015). During sexual reproduction, most fungi in this lineage form ascomata, structures to develop and liberate their meiotic spores (Fig. 1.1). Variation in the morphology of the ascomata remains important in assigning taxa to clades (Eriksson and Winka, 1997). Asexual dispersal in ascomycetes is widespread and involves hyphal tip differentiation into spores by various means (Hughes, 1953b). The systematic significance of asexual characters requires more caution in interpretation than sexual structures (Seifert and

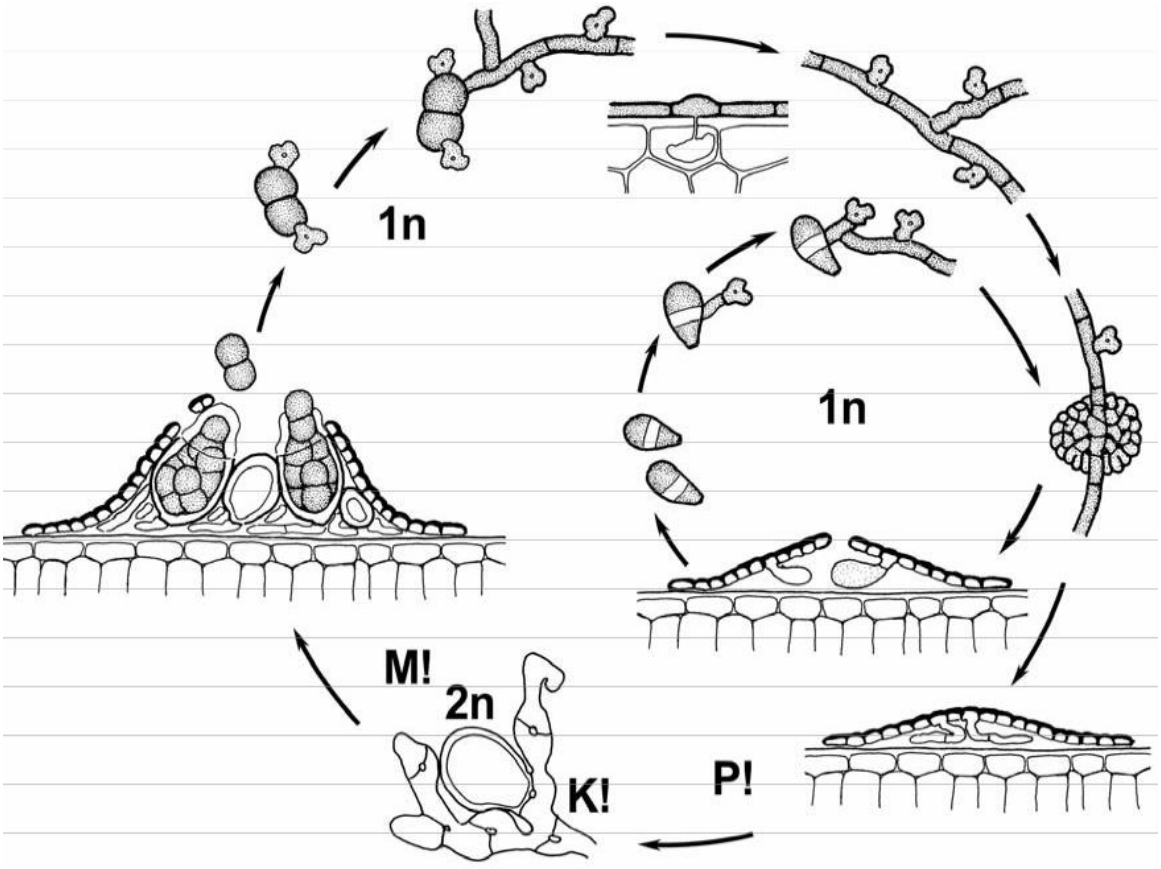

Figure 1.1 Holomorphic life cycle of *Asterina* and its asexual *Asterostomella* state. Abbreviations: 1n = haploid, 2n = diploid, K! = karyogamy, M! = meiosis, P! = plasmogamy. From T.A. Hofmann (2009) with permission from the author.

Gams, 2001; Seifert et al., 2011). Organismal concepts of fungi often involve both modes of reproduction and may be termed holomorphs (Fig.1.1).

Ascomycota, together with Basidiomycota Doweld, form Subkingdom Dikarya Hibbett, T.Y. James & Vilgalys (Fig 1.2), which encompasses most terrestrial lineages of fungi (Hibbett et al., 2018). Their success on land, together with recent molecular inference, all point toward a terrestrial ancestor for Dikarya that scavenged plant carbohydrates for its nutrition (Chang et al., 2015; Spatafora et al., 2017). Timing of the evolutionary radiations that led to the present diversity of Dikarya, however, is poorly known, and may have been tied to the radiation of particular lineages of vascular plants, or plant products (Arnold et al., 2009; Schoch et al., 2009b).

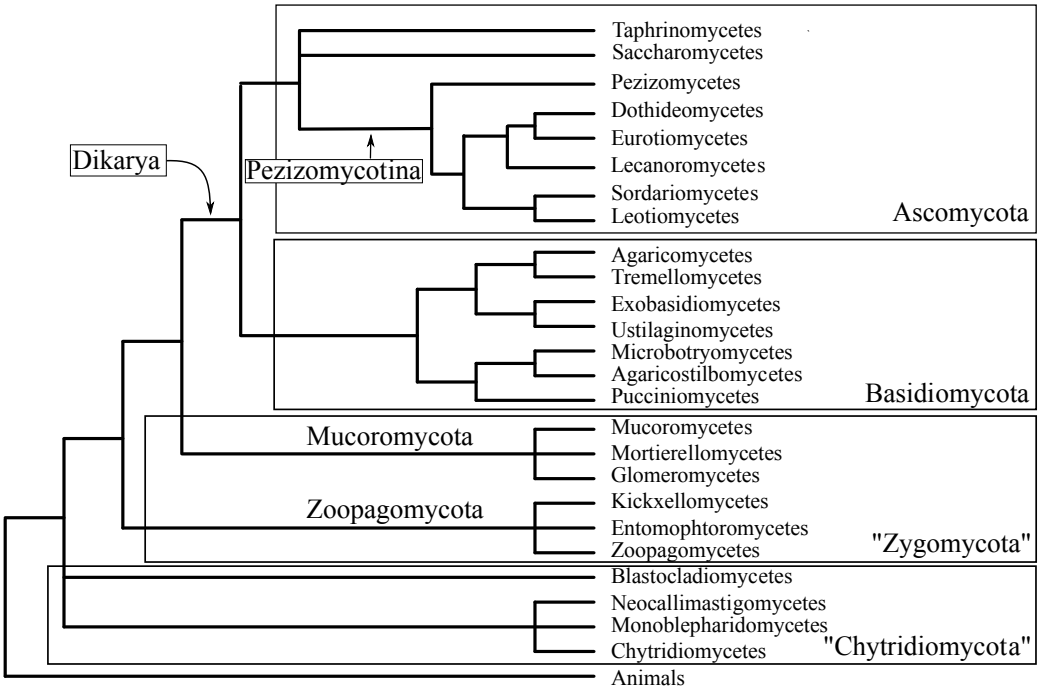

Figure 1.2 Phylogenetic relationships between major classes of Fungi. Topology based on Spatafora et al. (2017). Note, Spatafora et al. (2017) clarifies that "Zygomycota" and "Chytridiomycota" each consist of two paraphyletic phyla.

INTERNATIONAL CHRONOSTRATIGRAPHIC CHART

IUGS

www.stratigraphy.org

International Commission on Stratigraphy

v 2019/05

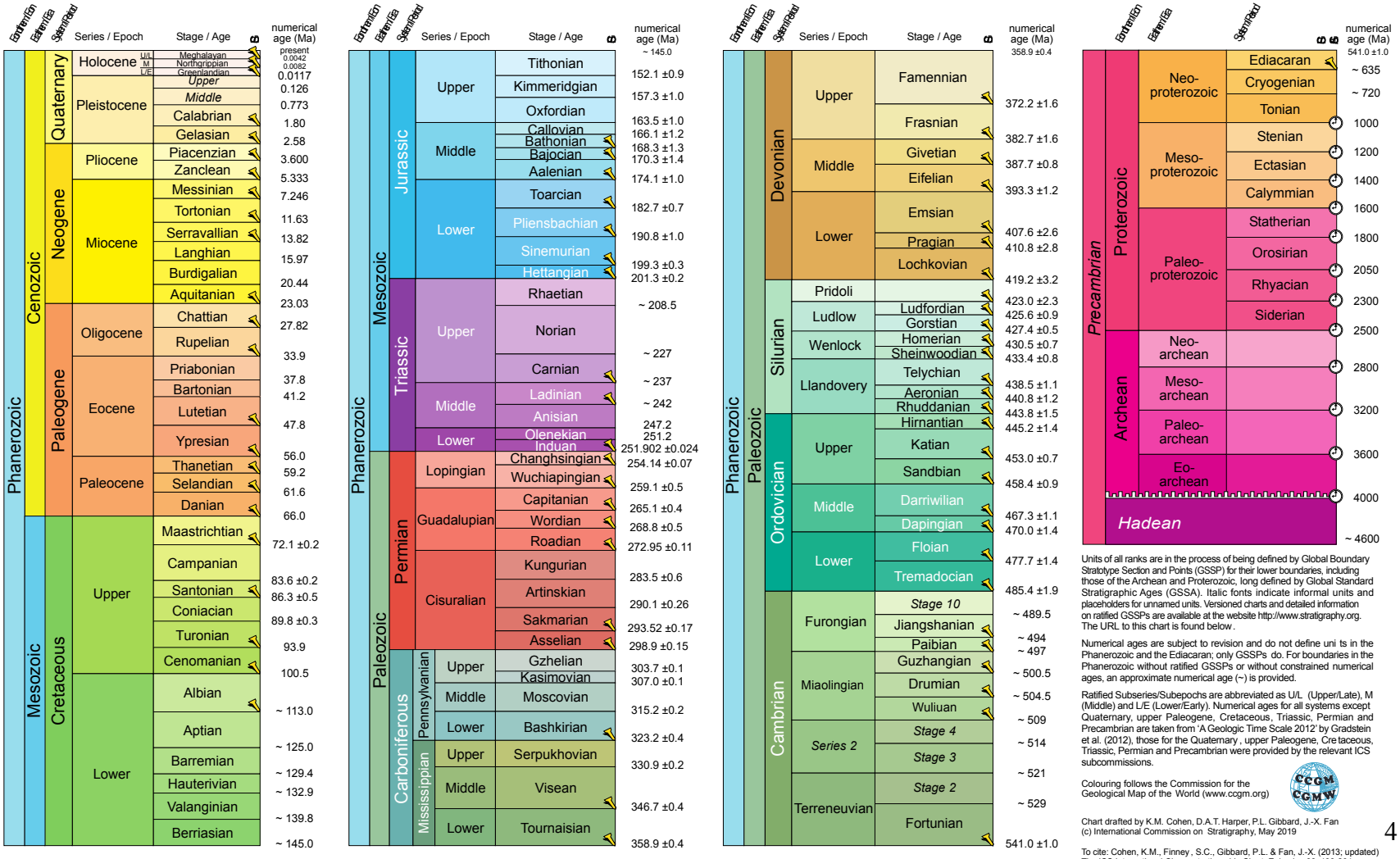

Units of all ranks are in the process of being defined by Global Boundary Stratotype Section and Points (GSSP) for their lower boundaries, including those of the Archean and Proterozoic, long defined by Global Standard Stratigraphic Ages (GSSA). Italic fonts indicate informal units and placeholders for unnamed units. Versioned charts and detailed information on ratified GSSPs are available at the website http://www.stratigraphy.org. The URL to this chart is found below.

Numerical ages are subject to revision and do not define uni ts in the Phanerozoic and the Ediacaran; only GSSPs do. For boundaries in the Phanerozoic without ratified GSSPs or without constrained numerical ages, an approximate numerical age (~) is provided.

Ratified Subseries/Subepochs are abbreviated as U/L (Upper/Late), M (Middle) and L/E (Lower/Early). Numerical ages for all systems except Quaternary, upper Paleogene, Cretaceous, Triassic, Permian and Precambrian are taken from 'A Geologic Time Scale 2012' by Gradstein et al. (2012), those for the Quaternary, upper Paleogene, Cretaceous, Triassic, Permian and Precambrian were provided by the relevant ICS subcommissions.

Colouring follows the Commission for the Geological Map of the World (www.cgm.org)

Chart drafted by K.M. Cohen, D.A.T. Harper, P.L. Gibbard, J.-X. Fan

To cite: Cohen, K.M., Finney, S.C., Gibbard, P.L. & Fan, J.-X. (2013; updated) The ICS International Chronostratigraphic Chart. Episodes 36: 199-204.

URL: http://www.stratigraphy.org/ICSchart/ChronostratChart2019-05.pdf

Figure 1.3 International Chronostratigraphic Chart, v 2019/05.
See legend below chart. Global Boundary Stratotype Section and Points are displayed in the chart by small golden-spike icons at the base of the divisions that they define. Global Standard Stratigraphic Ages are indicated similarly by clock icons (Cohen et al., 2019). Reprinted with permission from The International Commission on Stratigraphy.

1.3 Fossil Ascomycota

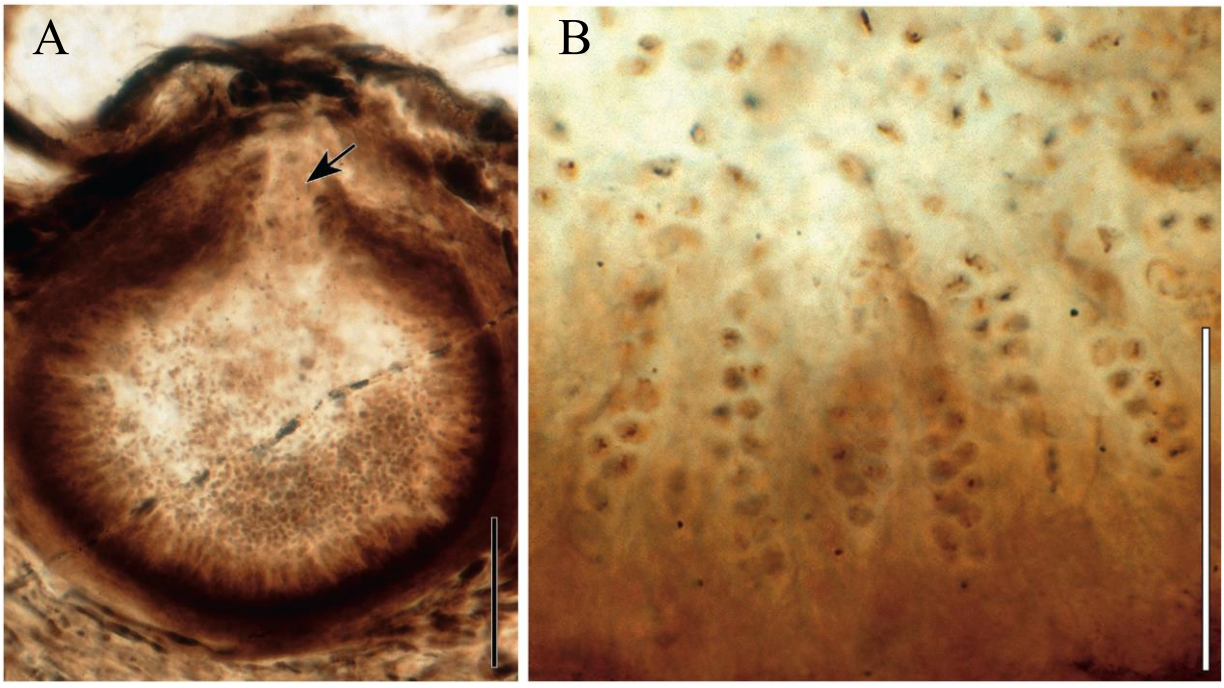

Figure 1.4 Morphology of *Paleopyrenomycites devonicus*.
A. Cross section through individual sporocarp, showing opening through an ostiole (arrow). B. Content of sporocarp magnified, showing sporangia usually interpreted to be asci. Reproduced from Taylor et al. (2015) with permission from authors and Elsevier.

The oldest widely accepted fossil of Dikarya, *Paleopyrenomycites devonicus* Taylor, Hass, Kerp, M. Krings & Hanlin, was found in the Early Devonian (Fig. 1.3) Rhynie chert (≈ 420 Ma, Fig. 1.4), associated with axes of *Asteroxylon mackiei* Kidston & Lang, an early lycopod. *Paleopyrenomycites devonicus* is considered to be a representative of phylum Ascomycota due to the presence of an ascoma containing asci (Fig. 1.4), the synapomorphy for

the phylum. However, the morphological characters of the fossil are challenging to interpret and it does not fit into any modern clade of Ascomycota (Taylor et al., 2005). Although the preservation is amazing, some of its characters are not so clearly visible that they can be referred to homologous structures (*e.g.* the fossil is described as having "operculate asci", but an operculum is not clearly visible in the micrographs). Some of the characters of *P. devonicus* are prone to convergence, and for example, the ostiole, a distinct apical pore in the ascoma (Fig. 1.4A) has evolved in at least four separate clades of Ascomycota. The characters of the fossil, as interpreted by the authors, do not appear in combination in any extant taxa. For example, in extant taxa, operculate asci only occur in apothecial ascomata (lacking an ostiole), not in perithecia as in the fossil (Hansen and Pfister, 2006). Ascomata with an ostiole are supposedly associated with forcible ascospore discharge (Roper et al., 2008), but the ascospore shape and orientation in *P. devonicus* are not consistent with forcible discharge.

The multiple Paleozoic traces of Basidiomycota (Dennis, 1970; Krings et al., 2011b) come from the vegetative characters of the group: the presence of a clamp connection at the septum of a hypha. Clamp connections, although a synapomorphy in members of Basidiomycota, provide no information about the kinds of basidiomycetes that may have evolved by this time. They do, however, confirm the presence of Dikarya-specific traits in the middle Paleozoic, and thus, at least, the presence of the stem lineage of Ascomycota.

After the Devonian appearance of *P. devonicus*, subsequent evidence of sexual reproduction in fossil taxa of Ascomycota does not appear until the late Mesozoic, during the Cretaceous period (Fig. 1.3) (Alvin and Muir, 1970; Kalgutkar and Sigler, 1995; Smith et al., 2004; Van der Ham and Dortangs, 2005; Bronson et al., 2013). The phylogenetic interpretations of the Cretaceous fossils are open to debate; they, however, all resemble taxa in Pezizomycotina.

Further, the groups represented by the Cretaceous fossils may have arisen much earlier, so the fossils do not necessarily provide useful minimal ages for taxa. On the other hand, many fossil Dikarya from Tertiary deposits can be assigned to known monophyletic groups of fungi, although again, the age of the fossils are often thought to be younger than the age of the groups they represent (Berbee and Taylor, 2010; Prieto and Wedin, 2013; Beimforde et al., 2014; Schmidt et al., 2014).

The publication of (Kalgutkar and Jansonius, 2000) is a cornerstone summary of species of fossil fungi published up to 2000. It comprises descriptions of 1004 valid fossil form taxa among which 703 are spore taxa, almost all illustrated. Berbee and Carmean translated the text into a Web accessible database, and I prepared illustrations with scale bars from the assembled plates of the synopsis (Fig. 1.5A).

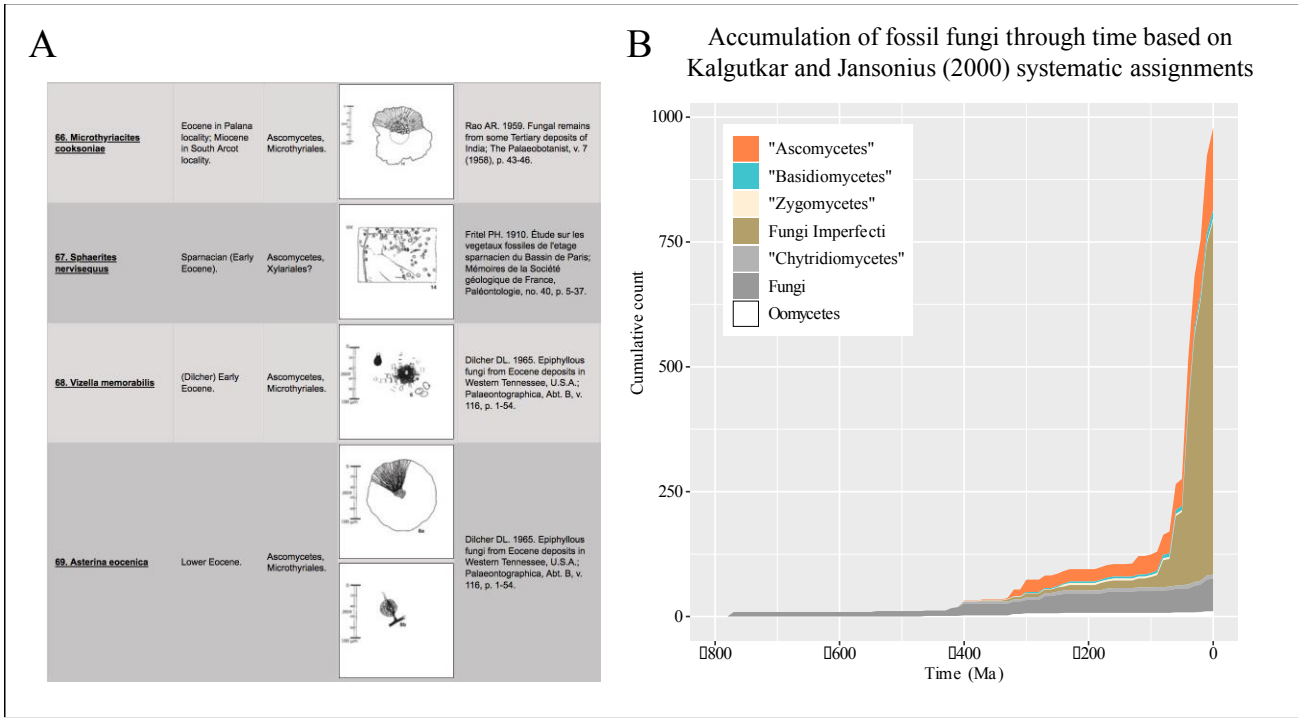

Figure 1.5 The online version of the Kalgutkar and Jansonius database of fossil fungi. Being able to search through the fossil record of fungi greatly improves communication in paleomycology (<https://advance.science.sfu.ca/fungi/fossils/Kalgutkar_and_Jansonius/>). A. Screenshot of the database, showing ascomycetes taxa sorted by geological age. B. Accumulation of fossil fungi through time based on Kalgutkar and Jansonius (2000) systematic assignments into classes of fungi.

Form species, used in Kalgutkar and Jansonius (2000), are not to be considered as real taxa. They are morphospecies that might include individuals belonging to very different modern groups of organisms because those form genera are defined on characters prone to convergence. For example, the form genus *Brachysporisporites* Lange & Smith resembles taxa in the living genus *Sporidesmium* Link, which was recently shown to be polyphyletic (Shenoy et al., 2006). The taxonomic diversity presented in the synopsis nonetheless indicates a majority of spores (Fig. 1.5B, classified in "Fungi Imperfecti") followed by a large number of ascomycetes fungi (more than 150 taxa).

1.4 Estimates of age of lineages is limited by available fossil calibrations

The molecular clock analyses of fungi inferred to this point have revealed two major problems: (i) Estimates are based heavily on the interpretation of the single fossil, *P. devonicus*; and depending on the interpretation of this fossil, estimates for the divergence between Basidiomycota and Ascomycota can vary between 452 and 1485 Ma (Berbee and Taylor, 2010), (ii) Estimates suggest a Paleozoic to early Mesozoic radiation of Pezizomycotina, giving rise to Ascomycota classes Dothideomycetes O.E. Erikss. & Winka, Sordariomycetes O.E. Erikss. & Winka, Lecanoromycetes O.E. Erikss. & Winka, and Eurotiomycetes O.E. Erikss. & Winka (Eriksson and Winka, 1997; Beimforde et al., 2014). These classes share the same mechanism of

forcible ascospore discharge, which presumably evolved from a common ancestor (Trail, 2007). However, spores associated with forcible discharge generally have a distinctive shape with acute ends and regular outline (Roper et al., 2008; Fritz et al., 2013). Spores with this shape do not appear in the fossil record until the Cretaceous (Kalgutkar and Jansonius 2000), for example with the form genus *Dicellaesporites antarcticus* Kalgutkar. Further, many pre-Cretaceous fossils classified in "Ascomycetes" by Kalgutkar and Jansonius (2000) instead represent lineages diverging prior to the evolution of Dikarya (Krings et al., 2011a; Krings and Taylor, 2012; Krings et al., 2014).

The conflict between the first evidence of forcibly dispersed ascospores in the Cretaceous with the Devonian ascoma is puzzling, and resolving the conflict requires a deeper understanding of the fossil lineages and their closest extant relatives. Besides dispersed spores, the next most frequently described fossils are those of thyriothecia (Elsik, 1978; Kalgutkar and Jansonius, 2000; Berbee et al., 2014). Understanding the evolution of the thyriothecium and of its associated morphological characters is paramount to the appropriate interpretation of their extensive fossil record.

1.5 Analysis of molecular phylogeny, morphological character states, and fossil record of fly-speck fungi (Dothideomycetes, Ascomycota)

Fly-speck fungi are the epiphyllous fungi that are the focus of my dissertation. All of them form black reproductive thyriothecia that are easily mistaken for fly droppings. Thyriothecia are minute (50 µm to 2 mm in diameter), circular to elongated structures covered by a scutellum, a plate appressed to the surface of living and dead leaves or stems of vascular plants (Fig. 1.6A–E), and covering spore producing tissue (Arnaud, 1918; Stevens and Manter,

1925; Doidge, 1942). How these fungi interact with their host plants is unclear, but some appear to be asymptomatic biotrophic parasites on living hosts (Fig. 1.6 F, G), while others are found in leaf litter (Guerrero et al., 2011; Wu et al., 2011b; Hongsanan et al., 2014b). At maturity, spores of thyriothecial fungi are shed through an ostiole (Fig. 1.6 H–O) or through slits.

These fungi are unusually easy to recognize in the fossil record because of their distinctive thyriothecia (Fig. 1.6). Because it is usually possible to remove a thyriothecium from the surface of a leaf without affecting the plant tissue (note the left side of the sectioned thyriothecium detaching from the leaf in Fig. 1.6O), these fungi are epiphyllous, in contrast to otherwise similar fungi that are embedded in their host and consume the tissue that surrounds them. The morphology and anatomy of the thyriothecia, together with tools of molecular biology (for extant taxa), are used to describe and assign thyriothecial fungi to a known group, or clade. My dissertation extends the molecular data available for modern fly-speck fungi, contributes to their Cretaceous fossil record, clarifies their associated morphologicalcharacters and critically considers the use of these fossils as calibration points in a molecular clock analysis.

1.6 Interpretation of evolutionary patterns of thyriothecial development and anatomy based on extant species.

All the thyriothecial fungi sampled to date are members of the class Dothideomycetes (Schoch et al., 2009a; Wu et al., 2011b; Wu et al., 2012; Wu et al., 2014b). Due to several technical problems, they are, however, poorly represented in GenBank and are almost absent from phylogenetic studies of modern taxa. One problem is geographical; most species are tropical, while most mycologists work primarily in temperate lands. Then, their small fruiting bodies are scattered across leaves, and different species often cohabit the same leaf. Great care is needed to avoid mixed DNA populations when sampling thyriothecia from a leaf surface.

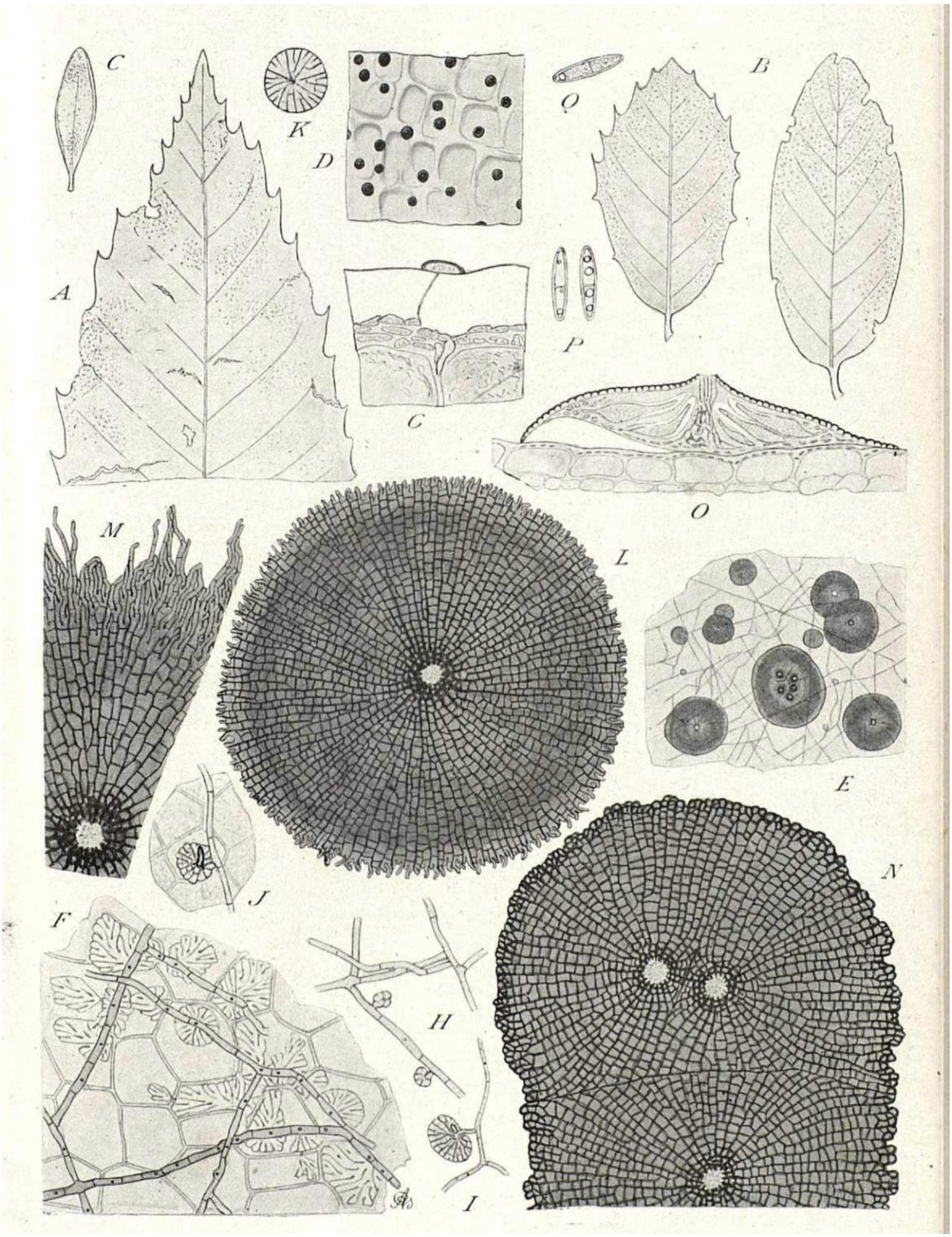
C
K
D
Q
B
A
P
C
O
M
L
E
J
N
F
H
I

Figure 1.6 Line drawings of *Microthyrium microscopicum* Desm. from Arnaud (1918). A-C. On leaves of: A. *Castanea sativa* Mill., adaxial. B. *Quercus ilex* L., adaxial. C. *Buxus sempervirens* L., abaxial. D. Thyriothecia on leaf fragment, enlarged. F. Epidermis with external mycelium and internal *mycélium en palmettes*. G. Section of epidermis with appressorium connecting subcuticular mycelium to a superficial appressorium. H-K. External mycelium and young thyriothecia. L–N. Mature thyriothecia. O. Cross section of a thyriothecium. P–Q. Immature ascospores. A, D, I–L, O on *C. sativa*; B, E, G, H, N, P on *Q. ilex* and C, F, M on *B. sempervirens*. Magnification (originally printed size 15 x 23 cm): A–C, original size; D = x10; E = x50; F, H-O = x375; G, Q = x1000.

Fly-speck fungi were originally classified in order Microthyriales D. Arnaud., in class Dothideomycetes. Recent molecular studies have shown that the Microthyriales, and the families within the order, are not monophyletic. The majority of the sequences recovered seem to belong to a poorly defined group of Dothideomycetes (Wu *et al.*, 2011, Fig. 2). Divergent sequences from thyriothecia seem related to other epiphyllous Dothideomycetes clades. Some of these sequences may represent contamination from non-target species occurring together on the same leaf. Alternatively, thyriothecia may have arisen by evolutionary convergences in distantly related lineages.

Characters that may be important in identifying thyriothecial fungi to clade include the patterns of cells of the scutellum (Fig.1.6 K–N) the type of dehiscence of the scutellum, and the shapes of hyphae in the superficial mycelium (Fig. 1.6F-H). These characters are available not only in extant specimens, but also in fossil thyriothecia on cuticles, making this group of fungi an excellent candidate to link fossil and present diversity.

1.7 Thyriothecial fungi as interpretable fossils

Epiphyllous fungal fossils are unusual among fossil fungi in that they are relatively consistent in their association with hosts. Based on my experience with these fungi, they seem consistently

present when their hosts are present and whenever accumulation moisture allows their development. Thus, ages of the first fossil thyriothecia may indicate the age of origin of the group.

Thyriothecial fungi display morphological characters that are unique among fossil fungi; they represent more than 80 form-genera, ranging from Early Cretaceous (Alvin and Muir, 1970) to Tertiary deposits (Dilcher, 1965). Many of the same characters are used to classify fossil and extant taxa. The oldest convincing fossil thyriothecia are found in Lower and Upper Cretaceous deposits (Alvin and Muir, 1970; Pons and Boureau, 1977), while the majority of the form-taxa published are from Paleocene, Eocene and Miocene ages (Kalgutkar and Jansonius, 2000). The first appearance of a type of thyriothecial anatomy in the fossil record can act as a valuable indicator of the minimum age of a clade. However, complicating interpretation, spores are missing for most thyriothecial fossils and the only characters available, scutellum anatomy and development, had not been critically assessed or interpreted phylogenetically, prior to my dissertation research.

1.8 Fossil material used in my work

Dutch Gap Canal fossil clays are part of the Potomac Group beds that consistently yield plant cuticles, with fungi on them (Upchurch and Doyle, 1981; Upchurch, G., Texas State University, personal communication). The Potomac Group fossil record of preserved leaves and of dispersed spores and pollen grains has been important in reconstructing patterns of early angiosperm evolution (Fig. 1.7) (Upchurch, 1981, 1984b, a). Because the pollen is produced and dispersed in abundance, its continuity may be reliable enough to provide a maximum age for the Eudicots

clade (Doyle, 2012). I have analyzed some of the epiphyllous fungi from the Dutch Gap Canal fossil clays. Even though fungal thyriothecia are not as abundant as pollen in the fossil.

My major goal in this dissertation is to compare the anatomy of fossil and extant fungi and ultimately relate character distribution in the fossil record to phylogenetic distribution in extant material. I analyzed scutellum anatomy and development in modern taxa. To be consistent in character definitions, I produced detailed illustrations of the characters. Using the Dutch Gap Canal fossil clays borrowed from Texas State University, I documented and described three taxa forming thyriothecia in the Aptian, Cretaceous (Chapters 3, 4 and 5). Although the phylogenetic distribution of taxa forming thyriothecia is still incompletely characterized, two out of three new fossil taxa contributed have characters that were never found in living taxa. Re-defining loosely defined morphological characters was important to fine-tune interpretation of fossil material, and to capture changes in the morphogenetic ability of the different lineages of fungi forming thyriothecia. The systematic interpretation resulting from my analysis represents a conservative method of integrating new fossils of fungi in the available systematics of fungi.
record, they are more abundant and diverse than any other types of known fossilized fungi (Kalgutkar and Jansonius, 2000).

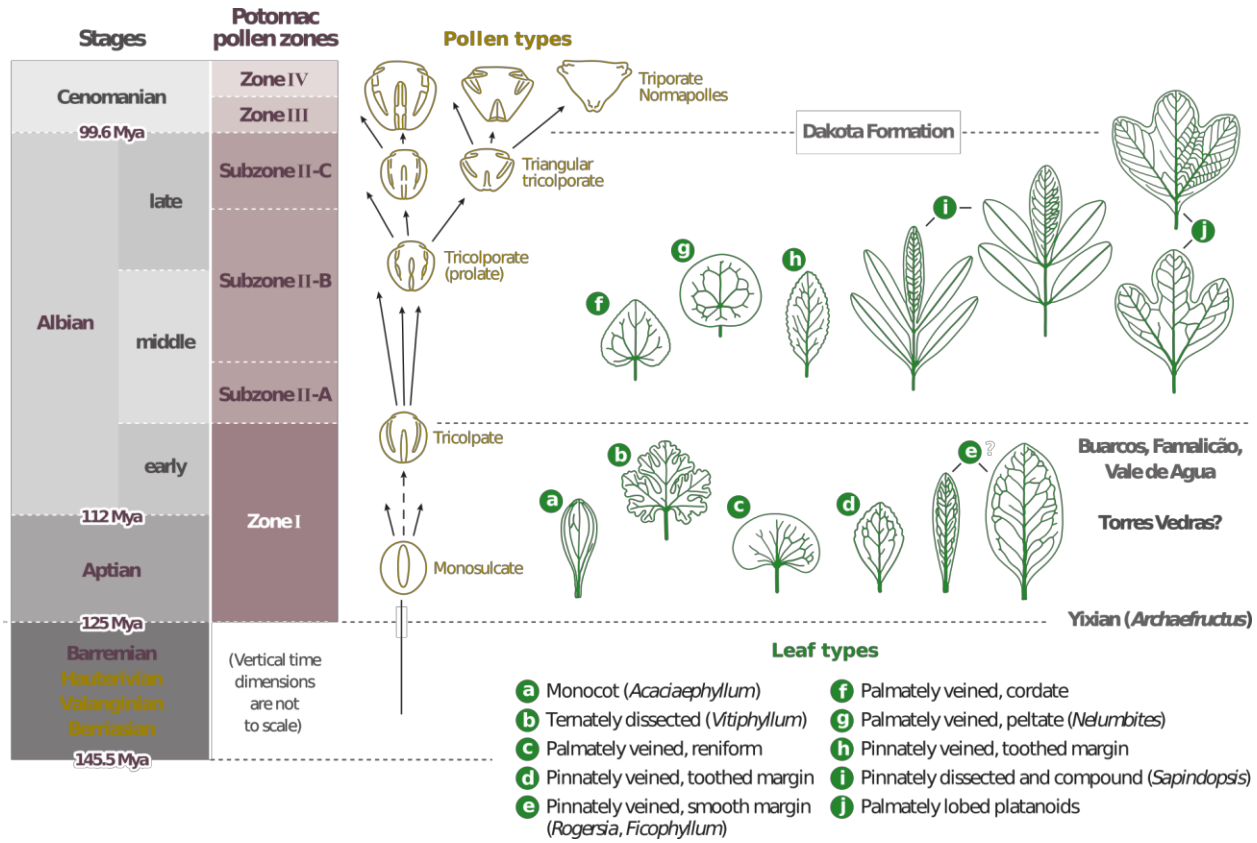

Figure 1.7 Paleobotanical significance of the stratigraphic sequence of the Potomac Group beds (from Doyle, 2012).

Stratigraphic sequence of major angiosperm pollen and leaf types in the Potomac Group of eastern North America, with correlations of plant-bearing localities in other geographic areas. Abbreviation: Ma, million years ago. Permission to reproduce obtained from J. Doyle and Annual Reviews inc.

Chapter 2: Character evolution of modern fly-speck fungi and implications for interpreting thyriothecial fossils

2.1 Summary

Fossils show that fly-speck fungi have been reproducing with small, black thyriothecia on leaf surfaces for ~250 million years. Here, I analyze characters of extant thyriothecial fungi to develop a phylogenetic framework for interpreting the fossil taxa. I placed 59 extant fly-speck fungi in a phylogeny of 320 ascomycetes using nuclear ribosomal large and small subunit sequences, including newly determined sequences from 9 specimens. I coded states of 11 morphological characters using original observations and literature. I reconstructed ancestral character states using BayesTraits and maximum likelihood. Using parsimony, the morphological character matrix, and the molecular phylogeny, I analyzed the relationships of three Mesozoic fossils. Thyriothecia evolved convergently from multiple lineages of superficial, leaf-inhabiting ascomycetes. Radiate and ostiolate scutellum organization is restricted to Dothideomycetes; scutellum initiation by intercalary septation of a single hypha characterizes Asterinales and Asterotexiales. Scutella in Microthyriales are initiated apically on a lateral hyphal branch and in Aulographaceae (Order *incertae sedis*), by coordinated growth of two or more adjacent hyphae. Patterns of hyphal branching in scutella facilitate distinguishing among orders. Parsimony analysis resolves the three fossils as Dothideomycetes, and one is further resolved as a member of of a clade comprising Microthyriales and Zeloasperisporiales within Dothideomycetes. This is the most comprehensive study of thyriothecial fungi and their relatives to date. My phylogeny and matrix of character states of modern taxa provide a new, objective

basis for interpreting thyriothecial fossils, and contribute to improving understanding of morphological evolution and geological ages of Dothideomycetes.

2.2 Introduction

Fly-speck fungi are ascomycetes that appear as minute (50 μm to 2 mm in diameter) black reproductive structures called thyriothecia. Thyriothecia differ from other reproductive structures of Ascomycota in having scutella, small, thin, darkly pigmented, shield-like plates that cover spore-producing tissue. The margins of scutella are appressed to the surfaces of living or dead leaves or stems of vascular plants (Arnaud, 1917b, 1918, 1925; Stevens and Ryan, 1939; Wu et al., 2011b; Wu et al., 2014a). Fly-speck fungi are common throughout the world (Arnaud, 1918; Doidge, 1942; Batista, 1959; Batista et al., 1969; Holm and Holm, 1991), especially abundant in tropical rainforests, where they grow in species mixtures on leaf surfaces (Batista, 1959; Hughes, 1976; Hofmann and Piepenbring, 2011; Firmino, 2016). Scutella of fly-speck fungi are also common as fossils (Elsik, 1978; Kalgutkar and Jansonius, 2000). My interest in these fungi is rooted in a desire to interpret the phylogenetic significance of the hundreds of fossil forms found in palynological preparations and on preserved cuticles of plant fossils (Kalgutkar and Jansonius, 2000; Taylor et al., 2015). Fossil fly-speck scutella have long been classified into form genera and form species that carry minimal phylogenetic information, and are based on a few characters that have not been used in the taxonomy of extant thyriothecia. Analyzing the systematic distribution of scutellum characters in extant fly-speck fungal lineages is a necessary first step for interpreting their numerous fossils.

Scutella of thyriothecia are recognizable in part because they develop above the plant cuticle, in contrast to many other kinds of minute ascomycete fruiting bodies that begin within

host tissue and break through to the leaf surface only when spores are ready for dispersal. How fly-speck fungi interact with their host plants is unclear, but some appear to be asymptomatic biotrophic parasites (on living hosts) while others are found in leaf litter (Hofmann, 2009; Wu et al., 2011b). Like other leaf-inhabiting fungi, many fly-speck fungi form appressoria, specialized hyphal cells from which a penetration peg allows the fungus to invade host tissues (Parbery and Emmett, 1977) or enter the host directly through a stoma (Hofmann, 2009; Firmino, 2016). By accumulating turgor pressure and directing growth toward the host through a small melanized ring, appressoria connect superficial portions of the fungal thallus to internal structures referred to as hypostromata when made of dense hyphal to stromatic structures (Hofmann, 2009; Firmino, 2016), or as "palmettes" of flattened, intercellular, dichotomous hyphae (Ducomet, 1907; Arnaud, 1918).

Several aspects of fly-speck fungus biology make it challenging to relate their morphology to phylogeny. First, thyriothecia are small, and so it can be difficult to find enough individuals of the same species for morphological or molecular systematic analysis. Second, in fossilized material, fly-speck fungi appear in mixtures with other epiphyllous fungi, which can complicate distinguishing among species (Dilcher, 1965; Phipps and Rember, 2004). For extant species, Hofmann (2009) and Firmino (2016) noted mixed species of *Asterina* growing together, and Ellis (1976) described closely related, co-occurring species in the type collection of the genus *Microthyrium*. For sequence analysis, species should ideally be isolated and grown in pure culture. While some fly-speck fungi grow (slowly) in pure culture (Firmino, 2016), other species do not (Hofmann, 2009); overall, they are poorly represented in culture collections.

Of the thyriothecial fungi analyzed so far with molecular phylogenetics, most can be classified to orders within Dothideomycetes, although the relationships among orders is poorly

resolved. A series of recent sequence-based papers has challenged the long-held view (Arnaud, 1918; Doidge, 1919; Clements and Shear, 1931; Gäumann, 1952; Kirk et al., 2008) that thyriothecial fungi are monophyletic. Hofmann's (2009) sequencing of nuclear DNA sequences showed that thyriothecial *Asterina* species group with plant pathogenic fungi in the order Venturiales. Wu et al. (2011b) included a broader sampling of thyriothecial fungi and found them to be scattered across four orders of Dothideomycetes, although with low support from bootstrap values or posterior probabilities. A phylogenetic analysis by Guatimosim et al. (2015) showed that similar-looking thyriothecial fungi fall into two orders, Asterinales and Asterotexiales, but again, support for relationships among orders was poor. Mapook et al (2016) and Hernández-Restrepo et al. (2019) showed that species of thyriothecial and thyriothecium-like fungi in Muyocopronales form a strongly supported sister group to Dyfrolomycetales, distant from any other thyriothecial fungi. Even more distant is a monophyletic group of two thyriothecial *Micropeltis* species that is nested among non-lichenized fungi in Ostropomycetidae, Lecanoromycetes, far removed from other thyriothecial clades (Hongsanan and Hyde, 2017).

In spite of this recent progress, the challenges involved in collecting sufficient tissue from fly-speck fungi remain, and their sequences are still poorly represented in GenBank and in phylogenetic studies. About 150 sequences were available, representing 18 genera, as of January 2019, contrasting with the more than 50 genera documented in recent publications (Hofmann, 2009; Wu et al., 2011a; Wu et al., 2011b; Hongsanan et al., 2014b; Wu et al., 2014a; Mapook et al., 2016a), and close to ~150 generic names available in families of thyriothecial fungi (Wijayawardene et al., 2014).

To interpret the fossil record of fly-speck fungi, my goals include increasing the molecular phylogenetic sampling of extant representatives and related taxa in the Ascomycota

class Dothideomycetes. Although availability of specimens continues to limit study of these fungi, my project brings new cultures, herbarium specimens, and sequences into the public domain. Using new and previously published data, my first aim is to infer a molecular phylogeny that samples as widely as possible from the lineages of fly-speck fungi and their possible close relatives. Second, I characterize species in each lineage morphologically, and reconstruct morphological ancestral character states throughout the phylogeny. Third, I use the molecular tree, comparative morphology, and inferred ancestral character states to discuss the phylogenetic affinities of three fly-speck fossils.

2.3 Materials and methods

2.3.1 Taxon sampling

I assembled a dataset of 320 ascomycete taxa including 59 fly-speck fungi. I obtained sequence data from new collections, from pure cultures where possible, found in Canada, Costa Rica (Permit nºR002-2014-OT-CONAGEBIO) and France. Pure cultures were established by crushing individual thyriothecia under an inverted compound microscope using insect pin (size 0, Austerlitz insect pins, Slavkov u Brna, Czech Republic) and then transferring individual spores or groups of spores onto water agar + ampicillin + kanamycin (1 mM) for germination. Germinating spores were transferred to antibiotic-free nutritive media under a dissecting microscope. The resulting cultures have been deposited in the Westerdijk Institute, Netherlands (Appendix S1, strains labelled with an asterisk).

Sequence data for nuclear ribosomal large subunit (LSU) and small subunit (SSU) DNA from thyriothecial taxa and their closest relatives were recovered from GenBank using a series of BLAST searches (Appendix A.1). The use of these two loci was pragmatic; for most of the

relatives of thyriothecial fungi including other leaf-inhabiting fungi and lichenized fungi, only ribosomal DNA (rDNA) data were available (Lumbsch et al., 2005). I also included published sequences from lichenized fungi or lichen associated fungi that shared the epiphyllous habitat with thyriothecial fungi. I selected outgroups to represent classes related to Dothideomycetes. In addition, near full-length to full-length LSU and SSU data were retrieved from 13 whole genome projects with the help of BLAST searches and by using the JGI MycoCosm Portal (Grigoriev et al., 2013) (Appendix A.2).

2.3.2 DNA extraction, amplification, sequencing

I successfully isolated four strains in pure culture, including *Lembosina* sp. CBS 144007, *L. aulographoides* CBS 143809, *Microthyrium macrosporum* CBS 143810, and cf. *Stomiopeltis* sp. CBS 143811. I harvested mycelium from culture media for genomic DNA extraction using the Qiagen DNeasy Plant Minikit (QIAGEN Inc., Mississauga, Ontario). I isolated a strain corresponding to the voucher of cf. *Stomiopeltis* sp. UBC-F33041 in pure culture and extracted its DNA, but the isolate stopped growing after a few culture transfers. I performed the PCR reactions using PureTaq™ Ready-To-Go™ PCR beads (Amersham Biosciences, Piscataway, New Jersey), following manufacturer instructions. I performed amplifications using fungal specific rDNA primers reported in James et al. (2006): BMB-BR, NS1, NS3, NS6, NS8, NS20, NS23, NS51, ITS2, LIC1460R, LIC2197, LR0R, LR3R, LR5, LR5R, LR7R, LR8, LR10, LR11, LR10R, LR12, LR13. I used uncultured dried specimens of *Micropeltis* F. Stevens & Manter, *Scolecopeltidium* F. Stevens & Manter and Asterotexiaceae Firmino, O.L. Pereira & Crous (*Micropeltis* sp. UBC-F33034, *Scolecopeltidium* spp. UBC-F33033 and UBC-F33035, Asterotexiaceae sp. UBC-F33036) as templates for direct DNA amplification (Lee and Taylor,

1990) of the 5' 1 kb of LSU (LR0R-LR8), a region known to be informative for thyriothecial fungi (Hofmann et al., 2010; Wu et al., 2011b; Guatimosim et al., 2015). I pipetted a cocktail of 12.5 µL of water and primers at a concentration of 1.0 µM each into a PCR reaction tube containing a PureTaq™ Ready-To-Go™ PCR bead, and I kept the tubes on ice. For each taxon: (i) I mounted a thyriothecium in a drop of sterile water, observed it under the compound microscope to ascertain identity, presence of ascospores, and absence of contaminant material; (ii) I crushed the thyriothecium firmly in between slide and coverslip, and (iii) I pipetted ~10-13 µL of the crushed ascospore material in water from the coverslip and the slide into a waiting PCR reaction tube, which was then vortexed briefly. The final volume of liquid in each tube was ~25 µL, and the final concentration of each primer was 0.5 µM. I ran the PCR reactions for 40 cycles with an annealing temperature of 50ºC and an elongation temperature of 72ºC. I performed direct amplifications on the first 700-1000 bp of LSU using primers LR0R-LR8, with an annealing temperature of 55ºC initially yielded weak PCR product. I then diluted weak PCR products 100 to 1000 times and re-amplified LSU with internal primers to increase product concentration for sequencing (see Mitchel, 2015, for similar methods).

2.3.3 Phylogenetic inference

I first aligned the LSU and SSU rDNA sequences using the iterative refinement method G-INS-I in MAAFT v7 (Katoh and Standley, 2013). I trimmed out introns manually in Mesquite (Maddison and Maddison, 2015) and I realigned the resulting sequences with MAAFT. I then manually excluded ambiguously aligned positions in Mesquite (Baldauf, 2003; Harrison and Langdale, 2006). The resulting concatenated dataset spanned 4552 aligned nucleotide positions. I ran JModeltest 2 (Darriba et al., 2012) on the CIPRES portal (Miller et al., 2010) and selected

the GTR+G model for individual genes. I ran RAxML v.8 (Stamatakis, 2014) on two partitions (one for each gene) and 1000 independent maximum likelihood searches, again running on CIPRES. I assessed branch support using 1000 bootstrap replicates (BS) (Felsenstein, 1985). I performed Bayesian analysis using MrBayes 3.2 Metropolis Coupled Monte Carlo algorithm (Ronquist et al., 2012). For the Bayesian analysis, I ran four independent searches with each eight MCMC chains for 160 million generations sampling every 5000 trees, using 128 processors of 2 Gb each on a Compute Canada cluster (cedar.computecanada.ca). Following test runs, I adjusted the heating parameter to 0.03, optimizing the search space so that swap frequencies were between 0.3 and 0.7, as the MrBayes 3.2 manual advises. I discarded 50% of the samples as burn-in. I used Tracer 1.5 to determine effective sample size (≥200), and the R package "rwty" (Warren et al., 2017) to assess the convergence of independent runs. I considered clades with >70% ML bootstrap support and >0.95 Bayesian posterior probability to be moderately well supported.

Preliminary results suggested that some taxa at various ranks were not monophyletic. To explore the fit of the data to alternative hypotheses concerning monophyly, I set monophyly constraints as single individual branches and found the most likely tree given each constraint using 100 independent "thorough" searches in RAxML. I then generated per-site log likelihoods of each ML tree given the constraint, and performed an approximately unbiased (AU) test (Shimodaira, 2002) using CONSEL (Shimodaira and Hasegawa, 2001). I rejected hypotheses receiving a probability below 0.05 in the AU test (Appendix A.4). I specifically tested in turn the monophyly of (i) Asterinales and Asterotexiales, (ii) Microthyriales and Zeloasperisporiales, (iii) Radiate thyriothecia, (iv) *Asterina* and (v) *Lembosia*.

2.3.4 Observation and scoring of morphological characters

Table 2.1 Specimens consulted for scoring characters. Taxa in grey are species scored based on a surrogate specimen, not sequenced.

IH code	Herbarium accession	Country	Collector	Order	Taxon
VIC	42822	Brazil	A.L. Firmino	Asterinales	*Asterina melastomatis*
VIC	42823	Brazil	A.L. Firmino	Asterinales	*Asterina chrysophylli*
VIC	42814	Brazil	O.L. Pereira & A.L. Firmino	Asterotexiales	*Asterotexis cucurbitacearum*
VIC	42818	Brazil	A.L. Firmino	Asterinales	*Prillieuxina baccharidincola*
VIC	42514	Brazil	A.L. Firmino, D.B. Pinho & O.L. Pereira	Asterinales	*Batistinula gallesiae*
VIC	42450	Brazil	M. Silva & O.L. Pereira	Asterinales	*Parmularia styracis*
VIC	39748	Brazil	R.W. Barreto	Asterotexiales	*Inocyclus angularis*
VIC	31939	Brazil	E. Guatimosim	Asterotexiales	*Rhagadolobiopsis thelypteridis*
BR	5030012458426	Spain	Ertz D.	Asterotexiales	*Hemigrapha atlantica*
BR	5030020189138; 5030020188124	Belgium	Ertz D.	Asterotexiales	*Buelliella poetschii*
UBC	F33036	Canada	L. Le Renard	Asterotexiales	Asterotexiaceae sp.
UBC	F33036	Costa Rica	L. Le Renard	Asterotexiales	Asterotexiaceae sp.
UBC	F33038	Canada	L. Le Renard	Incertae sedis	*Aulographum* sp.
UBC	F33037	Canada	L. Le Renard	Incertae sedis	*Lembosina aulographoides*
UBC	F33044	Canada	L. Le Renard	Incertae sedis	*Lembosina* sp.
UBC	F33045	Canada	L. Le Renard	Incertae sedis	*Lembosina* sp.

UBC	F33031	France	L. Le Renard	Microthyriales	*Microthyrium ilicinum*
UBC	F33039	Canada	L. Le Renard	Microthyriales	*Microthyrium macrosporum*
UBC	F33040	Canada	L. Le Renard	Venturiales	cf. *Stomiopeltis* sp.
UBC	F33041	Canada	L. Le Renard	Venturiales	cf. *Stomiopeltis* sp.
UBC	F33032	Canada	L. Le Renard	Microthyriales	*Lichenopeltella pinophylla*
UBC	F33033	Costa Rica	L. Le Renard	Ostropales	*Scolecopeltidium* sp.
UBC	F33034	Costa Rica	L. Le Renard	Ostropales	*Micropeltis* sp.
UBC	F33035	Costa Rica	L. Le Renard	Ostropales	*Scolecopeltidium* sp.
UBC	L47305	Canada	Curtis R. Bjork, Danielle Bourassa	Monoblastiales	*Acrocordia cavata* for *A. subglobosa*
UBC	F3143	Canada	M.E. Barr	Capnodiales	*Schizothyrium gaultheriae* for *S. pomi*
UBC	F23788	Canada	Tanay Bose	Capnodiales	*Fumiglobus pieridicola*
UBC	F33043	Canada	L. Le Renard	Lichenostigmatales	*Seuratia millardetii*

Table 2.1 lists the 28 specimens examined directly for morphological analysis; scoring for the remaining 292 taxa was based on interpretations of published illustrations and the literature (Appendix S3). To study the hyphal structure of the dorsal surface of scutella, and to look for appressoria, I peeled thyriothecia together with their surface hyphae off leaf surfaces using nail polish, as in Hosagoudar and Kapoor (1985). I examined thyriothecial features using a Leica DMRB (Leitz) DIC microscope, and photographed at 400x or 1000x with a Leica DFC420 digital color camera. Many scutella were more cone-shaped than strictly flat, and investigating their hyphae required views from multiple focal planes. I attempted to use confocal microscopy

to visualize hyphal organization, staining a specimen of *Microthyrium* with 0.1 mg/mL Calcofluor white (Sigma, St. Louis, Missouri). The calcofluor revealed internal asci and some septa, but hyphae of the scutellum were obscured by autofluorescence and pigmentation, and I pursued this approach no further. Subsequently, I assembled stacks of bright field or differential interference contrast (DIC) images at different focal planes to capture details of scutella and mycelia, following Harper (2015, p. 64, §4.3.1) and suggestions from Bercovici et al. (2009).

Table 2.2 Definitions of characters and their states, with reference to examples from illustrations in plates

Character	Definition	Examples
I. Habitat - Substrate		
0–On rock or soil	On rock or other inorganic substrates.	Rock inhabiting (*Saxomyces* sp.), ground dwelling lichen (*Simonyella variegata*)
1–Superficial on plants	On leaves, stems, fruit; superficial, closely associated with cuticle.	On living leaves, *Asterina melastomatis,* **Fig.3 J**, or on dead leaves, *Microthyrium macrosporum* Fig.4 **B**
2–On lichens	On lichen thallus.	Obligately lichenicolous, *Hemigrapha atlantica*
3–Immersed in plants	In bark or in woody parts of plants, in or under a plant's epidermis.	Taxa bursting through woody parts (*Dothidea sambuci*), on decorticated material (*Natipusilla bellaspora*), or as part of corticolous lichens thalli (*Trypethelium elutheriae*)
4–Other	Various habitats that are not the focus of this study and that are poorly sampled here. Includes taxa that inhabit dung, are endoparasites, or are mycorrhizal.	*Coenococcum geophillum, Phaeotrichum atkisonii*

Table 2.2 cont.

II- Lichenized		
0–Non-lichenized		*Asterina melastomatis* Fig. 3**P, Q**
1–Lichenized		*Graphis scripta*
III- Sporocarp type		
0–Apothecioid	Hymenium exposed at maturity.	*Abrothallus usneae*
1–Perithecioid	Ostiolated.	*Acrospermum graminearum*
2–Thyriothecioid	Flat, appressed, ascomata, sporogenous tissue covered by a pigmented scutellum (comprise catathecia, which unlike most thyriothecia have a pigmented ventral wall).	*Microthyrium macrosporum*
3–Cleistothecioid	No preformed opening (include chasmothecia).	*Lepidopterella palustris*
IV- Lower wall		
0–Unpigmented	Lower wall of sporocarp either absent or made up of one or a few layers of unpigmented cells, contrasting with the darker upper sporocarp wall.	*Microthyrium* spp.
1–Pigmented	Lower wall of sporocarp present and concolorous to the rest of the ascoma. It does not include host tissue and is thus not a hypostroma.	*Lichenopeltella pinophylla* **Fig. 4 G**

Table 2.2 cont.

V- Dehiscence		
0–Ostiole	Any dorsal pore by which spores are freed from an ascigerous or pycnidial sporocarp.	Opening of most Pleosporalean fungi
1-Irregular slit	Elongated opening formed by cracking or splitting of the scutellum. The splitting is irregular in that upon opening, it usually propagates radially between lateral walls of neighboring hyphae but it can also propagate transversely across hyphae. The split does not appear to follow pre-formed lines of dehiscence.	*Prilleuxinia baccharidincola* **Fig. 3 K**
2–Regular slit	Elongated opening formed in a regular fashion that does not propagate irregularly.	Opening found in hysterothecia and lirella, *Hysteropatella elliptica*, *Graphis scripta*
3–No dehiscence	Sporocarp closed when mature, no mechanism of dehiscence as part of sporocarp growth.	*Piedraia hortae*
4–Exposed at maturity	Sporocarp mostly open, sporogenous tissue is exposed throughout its development	*Abrothallus* spp., *Seuratia millardetii*

Table 2.2 cont.

VI- Locule circumference		
0–circular	Sporocarp enlarges from a center in all direction at about the same pace so that it appears round in dorsal view.	Asterinaceae **Fig. 3 H–J**, Microthyriaceae **Fig. 4 A–D, G–J**
1–elongate	Sporocarp elongates as it enlarges from a central area into one or more 'arms.'	*Lembosina aulographoides* **Fig. 5 B**
VII- Radiate ascomatal wall		
0–Non-radiate	No signs of a common central origin; distal hyphae cannot be traced back to central area of a sporocarp.	*Micropeltis spp., Schizothyrium pomi*
1–Radiating hyphae	Most or all of the distal hyphae of the scutellum can be traced back to their parental hyphae at or near the center of the sporocarp.	*Asterina spp., Microthyriumspp. Fig. 3–5*

Table 2.2 cont.

VIII- Branching pattern (in hyphae of sporocarp wall)		
0–Pseudoparenchyma unspecified **Fig. 2 A**	Any wall of hyphal origin where linear hyphal filaments can no longer be discerned. Instead, walls are composed of polyhedral cells, and the original planes of transverse cell divisions cannot be recognized.	Most pseudothecia **Fig. 2A a, b**
1–Isotomous overlapping **Fig. 2 C**	Scutellum hyphae radiate, isotomous dichotomies predominate where in each pair of dichotomous branches, one hyphal branch is wider than its sister. Hyphal segments occasionally show evidence of overlapping their neighbors.	*Asterina* spp. **Fig.2C e**
2–Isotomous, non-overlapping **Fig. 2 D**	Scutellum hyphae radiate, isotomous dichotomies and anisotomous dichotomies coexist but hyphal segments do not show evidence of overlapping their neighbors.	*Microthyrium macrosporum* **Fig. 2h**
3–Isotomous pseudomonopodial **Fig.2 E**	Scutellum hyphae radiate with few isotomous dichotomies; abundant evidence of overlap; pseudomonopodial dichotomies predominate and are most evident at the periphery of the scutellum	*Lembosia* spp., *Aulographum* spp. **Fig. 2 i**
4–Untraceable **Fig. 2 F**	Scutellum hyphae not radiate or if radiate, they cannot be traced from the sporocarp center to its margin. Isotomous dichotomies are few and neighboring hyphae frequently overlap.	*Schizothyrium* sp., *Micropeltis* spp., *Stomiopeltis* sp. **Fig. 2j-k, Pl. 3 A, C**

Table 2.2 cont.

IX- Appressed margin		
0–No appressed margin	Ascoma without defined, appressed margin. Instead, the ascoma wall usually curves upwards, forming a flask or disc shape.	*Pleospora herbarum*, appressed margin not applicable; ascoma is flask-shaped
1–Crenulate	Margin of ascoma made of well-defined hyphal tips, each tip bulging out beyond the longitudinal wall shared by adjacent cells.	*Asterina melastomatis*
2–Entire	Hyphal tips appear trucate, blunt, at least in young specimens. In mature specimens, the blunt tips may give rise to a fringe of tapering hyphae that are 2-5 times narrower than their mother cells.	*Microthyrium macrosporum*
3–Anastomosing	Marginal hyphae of ascomata continue outwards, connecting or merging with surrounding superficial mycelium; hyphal tips not discernable.	*Schizothyrium pomi*, *Prilleuxina baccharidincola* **Fig. 3 K**
X- Lateral Appressoria		
0–Absent	Appressoria absent or intercalary if present	*Aulographum* sp. **Pl. 3 E-G**
1–Present	Appressoria lateral, branching directly from superficial hyphae.	*Asterina melastomatis* **Fig. 3 P-S**

Table 2.2 cont.

XI- Initiation of sporocarp		
0–Tip of generator hypha	Generator hypha is a short lateral branch of a superficial hypha on a plant surface. The scutellum is derived from a single cell of the generator hypha, and it overgrows generator hyphae at maturity.	*Microthyrium* spp. **Fig. 2D g, h**
1–Intercalary; below generator hypha	Generator hypha is an intercalary (more rarely terminal) portion of a hypha that is superficial on a plant surface. The generator hypha remains above the scutellum at maturity.	Asterinales, Asterotexiales **Fig. 2C c, d, e**
2–From spores	Generator hypha absent; a scutellum grows directly from each part-spore and becomes confluent with surrounding scutella as it enlarges.	*Asterotexis cucurbitacearum* **Fig. 3 E-F**
3–From host stomata	Generator hypha indiscernable. Scutellum arises directly from hyphae growing up through the stoma (likely from a hypostroma) and covers guard cells and stomatal complex at maturity.	*Rhagadolobiopsis thelypteridis* **Fig. 3 G**
4–Coordinated generator hyphae	More than one intercalary generator hypha participates in forming a single thyriothecium. A generator hypha gives rise to the first dichotomous scutellum cells and this differentiation propagates to adjacent portions of the same hypha as well as to nearby hyphae, all of which become generator hyphae and contribute to the same scutellum.	*Aulographum* sp. **Fig. 2E i1**

Table 2.2 shows my working definitions for scoring 11 morphological or habitat characters, considering sporocarp features of both asexual, conidium producing structures and sexual ascomata. When possible, I used morphological and sequence information from the same specimen (Appendix A.3). My original observations of specimens, shown in the results, were particularly important for coding thyriothecial characters that also appear in fossils. Published written descriptions are rarely detailed enough to allow coding of subtle characters such as ascoma development or hyphal branching patterns, but I did extract character state information from published illustrations (Appendix A.3). Some characters are rarely reported or illustrated, and had to be coded as missing data for many taxa. Appressoria are one such character, visible in surface mycelium of extant and fossil thyriothecial taxa, but rarely noted in publications on other fungi. Similarly, thyriothecial development can be coded in extant and fossil taxa because different stages are exposed on the surfaces of leaves. Development in most other Dothideomycetes is more difficult to observe, leading to much missing data (Appendix A.3).

2.3.5 Analysis of morphological characters

I performed maximum likelihood ancestral character state reconstruction on the most likely tree in Mesquite version 3.31 (Maddison and Maddison, 2015) for the scored characters. Maximum likelihood reconstructions were computed using the Markov k-state 1-parameter (MK1) model (Lewis, 2001). Likelihood ratio tests showed that the MK1 model, which assumes equal rates of forward and reverse transitions between all states for each character was more likely than an asymmetrical, 2-parameter model for the five binary characters in my dataset. I reconstructed character states on the single, most likely tree.

To take phylogenetic uncertainty into account for state reconstructions, I also performed reconstruction using BayesTraits V3 (Pagel and Meade, 2007). In BayesTraits, I used the Multistate ML search algorithm, which estimates different rates for every state transition, with the option MLtries set to 100, a setting which led to consistent results in preliminary runs. Each character was reconstructed for 208 nodes out of the 319 nodes of my tree (labelled in Appendix S7). The proportion of each state for each node was calculated from its mean value over the 5000 trees chosen randomly from the among the 32,000 trees in the posterior distribution of trees in chain 1 of my MrBayes analysis. I considered any character state reconstructions with > 0.7 of both posterior probability (from BayesTraits) and proportional likelihood (ML) to be supported.

2.3.6 Analysis of fossils

I selected three fossils reported as thyriothecial from the literature that were well enough illustrated to be coded for morphology (Fig. 6). These include the oldest dispersed thyriothecium-like structure (Mishra et al., 2018), a dispersed *Lichenopeltella*-like form (Monga et al., 2015) for which cell patterns could be analyzed, and *Asterina eocenica* Dilcher found on leaf associated with mycelium (Dilcher, 1965). I coded their character states from the illustrations and compared them with extant taxa sharing similar combinations of characters (Appendix A.3).

To infer the phylogenetic relationships of each of the three fossils, I used the most likely, 320-taxon tree from the rDNA analysis as a topological constraint. I analyzed the relationships of one fossil at a time, using the 11 characters morphological data set, scored for the 320 extant and one of the fossil taxa (Appendix A.3). With branch-and-bound searches in PAUP 4.0a166 (Swofford 2003), I found the most parsimonious positions of each fossil, given the rooted

constraint tree. Alignments, phylograms, and cladograms are available from TreeBASE (Submission ID: 25212).

2.4 Results

2.4.1 Distribution of thyriothecium forming fungi

Thyriothecium forming fungi appear polyphyletic, as expected (Fig. 2.1). All but Micropeltidaceae are included in class Dothideomycetes (Fig. 2.1). Within Dothideomycetes, thyriothecial fungi appear widely distributed, stemming from a poorly resolved backbone **(**Fig. 2.1, Appendix S7).

Character reconstructions show that the ancestors of most clades of thyriothecial fungi produced superficial ascomata on leaves (Fig. 2.1, Appendix S8). However, beyond that generalization, the closest relatives of thyriothecial taxa vary in habitat, nutritional modes, and ascoma type (Appendices A.8–A.10). Asterotexiales form a well-supported clade rich in thyriothecial forms, including the type species *Asterotexis cucurbitacearum*. Of the 35 Asterotexiales taxa sampled, 20 are thyriothecial and 19 are epiphyllous (Appendices A.3). Clade A, one of three clades diverging near the base of the Asterotexiales includes 19 thyriothecial taxa and 18 of the epiphyllous species (Appendix A.7) in Asterotexiales. However, Clade A also includes *Buelliella poetschii*, an apothecioid lichen parasite and *Mycosphaerella pneumatophorae*, which produced an perithecioid ascomata in (rather than superficially on) plant tissue.

Clade B species were recently classified in Asterinales (see (Ertz and Diederich, 2015)) but here, they group instead with Asterotexiales (Appendix A.7). Clade B includes 14 species, most of which are apothecioid parasites of lichens, although two are corticolous, and one species,

Morenoina calamicola is thyriothecial and epiphyllous (Appendices A.7, A.8, A.10). The third clade is represented by *Geastrumia polystigmatis*, an epiphyllous species known only by its asexual state, that has yet to be formally classified to order. Aulographaceae, represented by six thyriothecial taxa, is recovered as the sister group of Asterotexiales, but the relationship receives low branch support.

A clade of five orders including Microthyriales and Venturiales receives 88% bootstrap support and 100% posterior probability (Appendix A.7). Of these, Microthyriales and Zeloasperisporiales are thyriothecial and epiphyllous, but their close relatives in Natipusillales are freshwater cleistothecioid fungi that fruit on decorticated wood (Fig. 2.1, Appendices A.3, A.8, A.10). Although Venturiales includes a few thyriothecial species, most of its members are perithecioid leaf and stem parasites causing, for example, apple scab and black knot of plum (Fig. 2.1, Appendices A.3, A.8, A.10).

Most Capnodiales are generally perithecioid, but the order also includes thyriothecial species (Fig. 2.1, Appendix A.10). The order Asterinales is nested in Capnodiales with 99% Bayesian posterior probability but with negligible likelihood bootstrap support (Appendix A.7). Asterinales is represented here by the type species *Asterina melastomatis*, and by sequences from three collections of *Parmularia styracis*, the type species of Parmulariaceae (Appendix A.7). Asterinales also includes anamorphic folicolous fungi and *Aulographina eucalypti*, a plant pathogen that causes leaf spots around its thyriothecia. Three thyriothecial taxa in Capnodiales are not closely related to one another or to Asterinales: *Peltaster fructicola, Schizothyrium pomi* and *Stomiopeltis versicolor* (Appendix A.10). The genus *Stomiopeltis* is polyphyletic, as the other species in this genus were recovered in other clades: *Stomiopeltis betulae* appears in

Microthyriales and two species tentatively identified as *Stomiopeltis* form a clade with *Tothia fuscella* in Venturiales (Appendix A.7).

Muyocopronales represents a strongly supported example of convergent origin of thyriothecia (Fig. 1, Appendices A.7, A.10). Muyocopronales thyriothecia have several cell layers of lightly pigmented, pseudoparenchymatous cells below their outer, darkly pigmented scutellum (see illustrations of Mapook et al., 2016b). The scutellum thickness makes detailed analysis of their hyphal branching pattern challenging. Like Asterinales and Asterotexiales, the scutella of Muyocopronales have crenulate margins and scutellum hyphae appear radial. As with Microthyriales, Muyocopronales thyriothecia are ostiolate.

Micropeltidaceae provides another strongly supported example of convergent thyriothecial morphology. The family is nested among Ostropomycetidae in Lecanoromycetes rather than Dothideomycetes (Fig. 2.1, Appendix A.7). The scutellum of Micropeltidaceae is distinctive in that it is ostiolate and formed as a flat, compact reticulum-like network of overlapping hyphae. As illustrated by Hofmann and Piepenbring (2006), the hyphae do not appear to radiate from the centre to the margins of the scutellum.

2.4.2 Lower sporocarp walls in thyriothecia are missing

Unlike most ascomata, thyriothecia usually lack a differentiated lower wall, a layer of pigmented fungal tissue that would separate sporogenous tissue from the substrate (Fig. 2.1, Appendices A.5, S11). Out of 59 thyriothecial species included here, only four have a pigmented, differentiated lower wall (Appendices A.5, A.11). Lower walls are hypothesized to be present in the ancestor of Dothideomycetes based on 100% proportional likelihood and 58% support from BayesTraits (Node 1 in Fig. 2.1, Appendices A.3, A.11). The most recent common ancestor of

Asterotexiales and Aulographaceae is hypothesized to lack a differentiated lower wall, but the loss of the wall could have occurred along several alternative ancestral branches (Appendix A.5). The common ancestor of Microthyriales and Zeloasperisporiales is hypothesized to lack a lower wall, with 84% proportional likelihood and 61% posterior probability, but again, the point where the lower wall was lost is not resolved (Appendices A.5 and A.11). Similarly, likelihood reconstructions suggest that lower walls were lost within Asterinales after *Parmularia styracis* diverged from the clade with *Asterina melastomatis* (Fig. 2.1, Appendix A.11) and that Muyocopronales lost a lower wall after divergence from a shared ancestor with Dyfrolomycetales (Fig. 2.1).

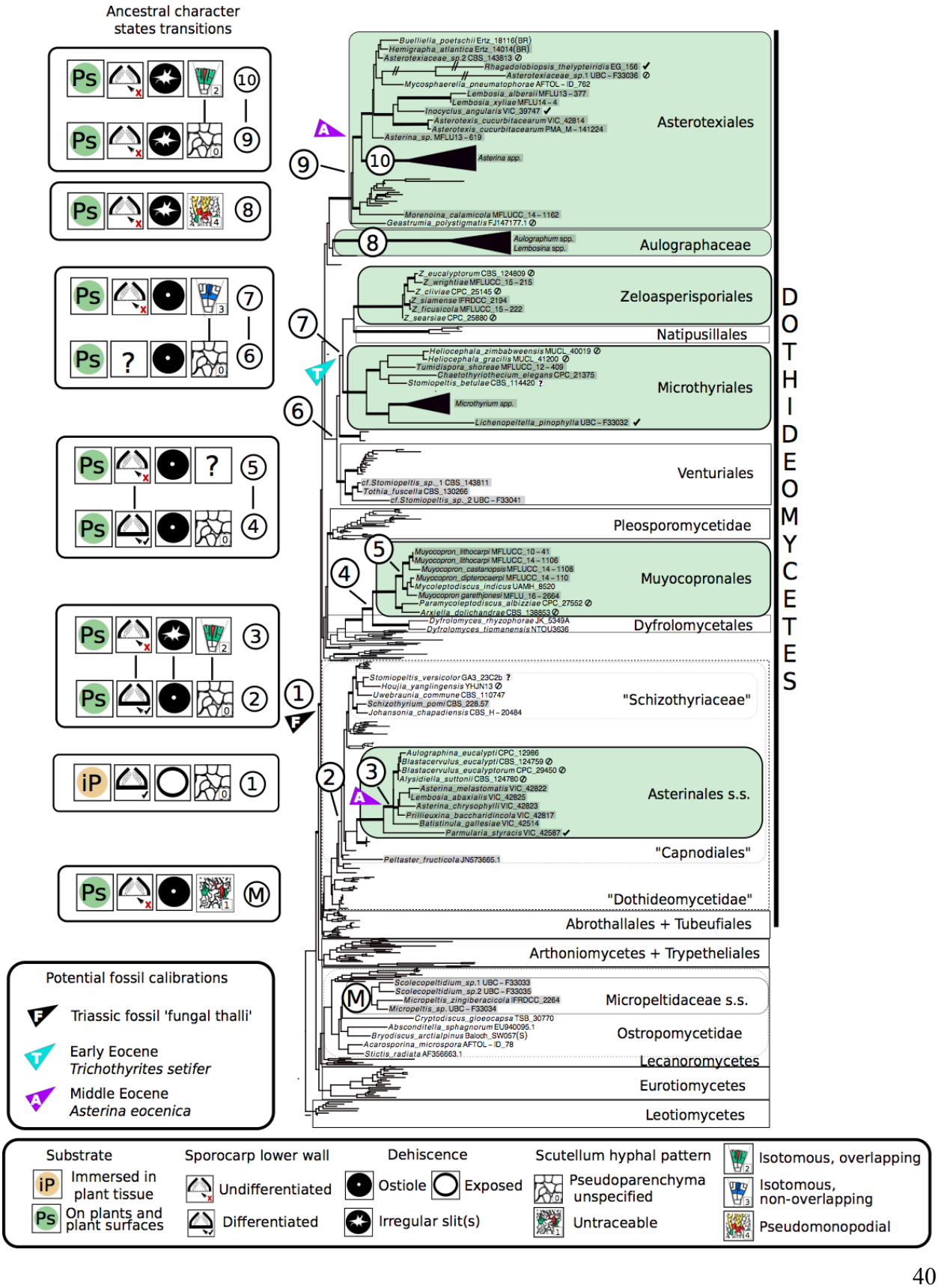
Ancestral character states transitions
Ps
iP
?
Buelliella_poetschii Ertz_18116(BR)
Hemigrapha_atlantica Ertz_14014(BR)
Asterotexiaceae_sp.2 CBS_143813
Rhagadolobiopsis_thelypteiridis EG_156
Asterotexiaceae_sp.1 UBC – F33036
Mycosphaerella_pneumatophorae AFTOL – ID_762
Lembosia_albersii MFLU13 – 377
Lembosia_xyliae MFLU14 – 4
Inocyclus_angularis VIC_39747
Asterotexis_cucurbitacearum VIC_42814
Asterotexis_cucurbitacearum PMA_M – 141224
Asterina_sp. MFLU13 – 619
Asterina spp.
Asterotexiales
Morenoina_calamicola MFLUCC_14 – 1162
Geastrumia_polystigmatis FJ147177.1
Aulographum spp.
Lembosina spp.
Aulographaceae
Z_eucalyptorum CBS_124809
Z_wrightiae MFLUCC_15 – 215
Z_cliviae CPC_25145
Z_siamense IFRDCC_2194
Z_ficusicola MFLUCC_15 – 222
Z_searsiae CPC_25880
Zeloasperisporiales
Natipusillales
Heliocephala_zimbabweensis MUCL_40019
Heliocephala_gracilis MUCL_41200
Tumidispora_shoreae MFLUCC_12 – 409
Chaetothyriothecium_elegans CPC_21375
Stomiopeltis_betulae CBS_114420
Microthyrium spp.
Lichenopeltella_pinophylla UBC – F33032
Microthyriales
cf.Stomiopeltis_sp._1 CBS_143811
Tothia_fuscella CBS_130266
cf.Stomiopeltis_sp._2 UBC – F33041
Venturiales
Pleosporomycetidae
Muyocopron_lithocarpi MFLUCC_10 – 41
Muyocopron_lithocarpi MFLUCC_14 – 1106
Muyocopron_castanopsis MFLUCC_14 – 1108
Muyocopron_dipterocaerpi MFLUCC_14 – 110
Mycoleptodiscus_indicus UAMH_8520
Muyocopron garethjonesi MFLU_16 – 2664
Paramycoleptodiscus_albizziae CPC_27552
Arxiella_dolichandrae CBS_138853
Muyocopronales
Dyfrolomyces_rhyzophorae JK_5349A
Dyfrolomyces_tiomanensis NTOU3636
Dyfrolomycetales
Stomiopeltis_versicolor GA3_23C2b
Houjia_yanglingensis YHJN13
Uwebraunia_commune CBS_110747
Schizothyrium_pomi CBS_226.57
Johansonia_chapadiensis CBS_H – 20484
"Schizothyriaceae"
Aulographina_eucalypti CPC_12986
Blastacervulus_eucalypti CBS_124759
Blastacervulus_eucalyptorum CPC_29450
Alysidiella_suttonii CBS_124780
Asterina_melastomatis VIC_42822
Lembosia_abaxialis VIC_42825
Asterina_chrysophylli VIC_42823
Prillieuxina_baccharidincola VIC_42817
Batistinula_gallesiae VIC_42514
Parmularia_styracis VIC_42587
Asterinales s.s.
"Capnodiales"
Peltaster_fructicola JN573665.1
"Dothideomycetidae"
Abrothallales + Tubeufiales
Arthoniomycetes + Trypetheliales
Scolecopeltidium_sp.1 UBC – F33033
Scolecopeltidium_sp.2 UBC – F33035
Micropeltis_zingiberacicola IFRDCC_2264
Micropeltis_sp. UBC – F33034
Micropeltidaceae s.s.
Cryptodiscus_gloeocapsa TSB_30770
Absconditella_sphagnorum EU940095.1
Bryodiscus_arctialpinus Baloch_SW057(S)
Acarosporina_microspora AFTOL – ID_78
Stictis_radiata AF356663.1
Ostropomycetidae
Lecanoromycetes
Eurotiomycetes
Leotiomycetes
DOTHIDEOMYCETES
Potential fossil calibrations
Triassic fossil 'fungal thalli'
Early Eocene
Trichothyrites setifer
Middle Eocene
Asterina eocenica
Substrate
Immersed in plant tissue
On plants and plant surfaces
Sporocarp lower wall
Undifferentiated
Differentiated
Dehiscence
Ostiole
Exposed
Irregular slit(s)
Scutellum hyphal pattern
Pseudoparenchyma unspecified
Untraceable
Isotomous, overlapping
Isotomous, non-overlapping
Pseudomonopodial

Figure 2.1 Phylogeny and character state transitions supporting convergent evolution of fly-speck fungal morphology.
Numbers on boxes left of tree match labelled nodes in tree and represent transitions between reconstructed ancestral states that received >0.7 proportional likelihood for characters for substrate, sporocarp lower wall, dehiscence and scutellum hyphal pattern following bottom legend. Shaded boxes indicate taxa forming thyriothecia. Clades with radiate scutella are in green boxes. When thyriothecia have a differentiated lower wall they are labelled with a tick mark. Taxa labelled with question mark represent suspected thyriothecia and taxa with a slashed circle are only known from asexual stages. Nodes labelled with arrowheads and letters represent fossils combining characters that are reconstructed for these nodes or their descendent nodes, following the legend on the left. Maximum likelihood phylogeny resulting from concatenated LSU and SSU rDNA data for 320 taxa; black thickened branches had bootstrap support > 70% and posterior probability > 0.95.

2.4.3 Transition in dehiscence mechanisms of thyriothecia

The mechanism of spore release from ascomata varies among the closest relatives of Dothideomycetes, and among thyriothecial taxa (Appendix A.12). Likelihood reconstructions suggest that ancestral Dothideomycetes opened with an ostiole (Fig. 2.1); BayesTraits reconstructions favor opening by a regular slit and show ancestral forms with slits subsequently giving rise to ostiolate clades that diversified further (Appendices A.5 and A.12). A transition to irregular slits is reconstructed somewhere before the most recent common ancestor of Asterotexiales and Aulographaceae (Figs. 2.1,2. 3, Appendix A12). A convergent transition from ostioles to irregular slits appeared along the branch nested in Capnodiales that leads to Asterinales. Developmentally, the irregular slits result from cracking between the adjacent hyphae that make up the scutellum (Fig. 2.3 L, M). The precise location of the opening remains unclear until dehiscence. Slit-forming genera sometimes produce ostioles in their asexual or spermatial states (Fig. 2.3). In *Aulographaceae*, and possibly also in species of *Lembosia*, the slit appears early in development as a line of lightly pigmented cells, but the crack follows

longitudinal walls and propagates beyond the less pigmented area (Fig. 2.5). Less common among Dothideomycetes as a whole, and thyriothecial taxa in particular, are regular slits that follow a pre-determined pattern without further propagation. Regular slits appear to have originated twice among thyriothecial taxa, being present in *Parmularia* in Asterinales, and in *Inocyclus angularis* in Asterotexiales, but not in their inferred common ancestor (Appendix A.12). Regular slits are also found in taxa producing hysterothecia and lirella (such as *Farlowiella charmichaeliana, Hysterographium fraxinii*, *Melasipileopsis* cf. *diplasiospora, Stictographa lentiginosa*), which at maturity may look more like apothecia than thyriothecia (Appendix A.12).

Ancestral ostioles appear to have been retained in Microthyriales and Muyocopronales (Figs. 2.1, 2.4, Appendix A.12), but the mode of dehiscence and ancestral states are unknown in Zeloasperisporiales. The common ancestor of Micropeltidaceae probably released spores through an ostiolate thyriothecium which is hypothesized to be derived from the apothecium that is shared by other members of Ostropomycetidae in Lecanoromycetes (Appendix A.12).

2.4.4 Radiate scutellum development and systematics

Scutella of thyriothecia are either made up of radiating hyphae that can be traced from their distal tips to their central point of origin (Figs. 2.1–2.5), or of hyphae that are not radiate and cannot be traced back to their origin (Figs 2.1, 2.2, 2.5). Non-radiating thyriothecial patterns appear in six widely scattered lineages, five in Dothideomycetes and one in Micropeltidaceae, Lecanoromycetes (Fig. 2.1). This indicates convergent origins of this fruiting body, as the non-radiate thyriothecia form supported clades with taxa with other sporocarp types (Fig. 2.1, Appendix A.7). Radiating patterns of thyriothecia are restricted to class Dothideomycetes (Fig. 1,

Appendices A.5, A.14) and are reconstructed to have originated convergently from ancestors with non-radiating patterns. Independent transitions to radiating patterns appear to have taken place in the evolution of Asterinales and Muyocopronales, supported in both RAxML and Mr Bayes analyses of ancestral states (Appendix A.14). In Asterotexiales, Aulographaceae, and somewhere among Microthyriales and Zeloasperisporiales, results between methods conflicted, and one or multiple transitions to radiate thyriothecia may have occurred in each clade (Appendix A.14). Non-radiating patterns are widely distributed throughout the phylogeny (Fig. 2.1). For example, thyriothecia of Micropeltidaceae in class Lecanoromycetes consistently lack radiate scutella (Fig. 2.1, node M; Appendices A.5, A.14).

2.4.5 Phylogenetic distribution of hyphal branching patterns of thyriothecial scutella

Likelihood consistently reconstructs pseudoparenchymatous ascomatal walls of polyhedral cells as the ancestral state at the base of Dothideomycetes and Lecanoromycetes, (Fig. 2.1, 2.2, Appendix A.15). However, corresponding BayesTraits reconstructions are equivocal (Appendices A.5, A.14). Among thyriothecial fungi, branching patterns of hyphae forming scutella are usually distinctive compared with more the widespread, and possibly ancestral, pseudoparenchymatous type.

Scutella with isotomous overlapping branching are reconstructed as possibly ancestral at the base of Clade A in Asterotexiales (proportional likelihood 68%, BayesTraits 52%) and for Asterinales after the divergence of *Parmularia styracis* (proportional likelihood 100%, BayesTraits 56%), with increasing support for reconstructions with this state among more recently diverging nodes (Appendices A.5, A.15). Isotomous branching patterns in thyriothecia expand the scutellum circumference mainly by duplicating files of cells through apical, nearly

equal isotomous dichotomies, resulting first in a “Y” shaped cell with a basal septum, and then in three cells, after additional septa delimit the two arms of the “Y” as separate cells (Figs. 2.2B, 2.3A, 2.3B, 2.3H**)**. In some cases, one of the two branches overlaps the other, growing downward and disappearing below its neighbors (Figs. 2.2C, 2.3D, 2.3I). Septa are sometimes aligned around part of the circumference of the scutellum, resulting in partial concentric rings of septa, (cf. Fig. 3.8 "d" in Hofmann 2009). Pigmentation in older parts of the scutellum contrasts with more translucent tips at the margin of scutellum hyphae (Fig. 2.3H, 2.3J, 2.3K).

In Microthyriales, scutellum hyphae usually branch dichotomously without overlap. While their branching is usually isotomous, anisotomous branching also occurs, producing hyphal tips of unequal width (Fig. 2.4H inset). A septum sometimes forms at the base of only one of the two new hyphal tips, resulting in a roughly 'L' shaped proximal cell (Figs. 2.2D, 2.4B; cf. Fig 15E Wu et al. 2011). The anisotomous expansion is reconstructed in the common ancestor of Zeloasperisporiales with 81% proportional likelihood (Fig. 2.1) but only 21% posterior probability from BayesTraits (Appendix A.5). Septa are angular (Figs. 2.2C, 2.4B, 2.4G, 2.4H) and constrictions at septa are infrequent, resulting in trapezoidal to nearly rectangular cells with sharp angles. Partially aligned septations in adjacent hyphae sometimes result in a pattern of incomplete concentric rings. Early stages of thyriothecium development may be isotomous in Microthyriaceae (Figs. 2.2D, 2.4C, 2.4I, 2.4J) making the distinction between anisotomy and isotomy most visible in fully grown structures (Fig. 2.2D).

Scutella with pseudomonopodial branching are restricted to Aulographaceae. The common ancestor of Aulographaceae is reconstructed with pseudomonopodial branching with 99% proportional likelihood and 28% posterior probability. In this growth form, the tip of dominant hyphae grows at the circumference of the expanding scutellum, each producing a series

of short lateral branches (Fig. 2.2E, 2.5B inset, 2.5D) that overlap with neighboring hyphae. Hyphae curve as they grow, and septa only form in the oldest hyphal segments. This results in a scutellum of irregular, multi-lobed cells (Fig. 2.2E). Distal tips at the appressed margin are rounded, and uniform in diameter (Fig. 2.5B, 2.5D, 2.5H). Within Aulographaceae, the construction of scutella is similar in *Lembosina* (Fig. 2.5B) and *Aulographum* (Figs. 2.5D, 2.5G, 2.5H; Appendix A.7).

Scutellum hyphae in some thyriothecial species in Venturiales and Capnodiales in Dothideomycetes, and in all Micropeltidaceae in Lecanoromycetes are "untraceable" (Fig. 2.1). This can be due to dark pigmentation, or to curved or meandering scutellum hyphae that overlap and obscure one another, resulting in a "*textura intricata*" or "*textura epidermoidea*" (Kirk et al., 2008; Figs. 2.2F, 2.5A, 2.5C, 2.5F).

2.4.6 Locule circumference shape

In most Dothideomycetes, the circumference of the locule within the ascoma is approximately round. Elongate locules are less common and are scattered across the phylogeny.

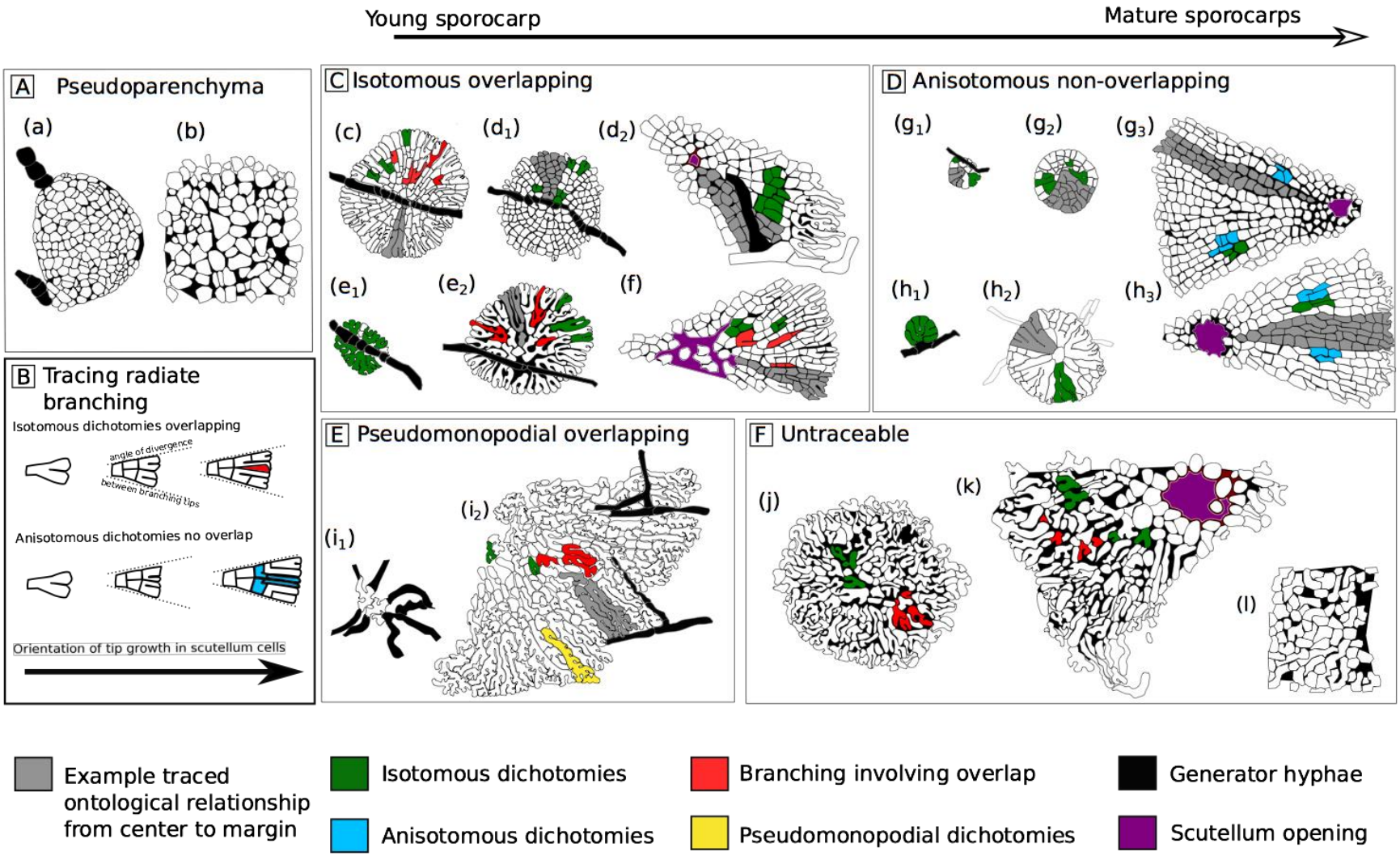
Young sporocarp
Mature sporocarps
A Pseudoparenchyma
(a)
(b)
B Tracing radiate branching
Isotomous dichotomies overlapping
angle of divergence between branching tips
Anisotomous dichotomies no overlap
Orientation of tip growth in scutellum cells
C Isotomous overlapping
(c)
(d1)
(d2)
(e1)
(e2)
(f)
D Anisotomous non-overlapping
(g1)
(g2)
(g3)
(h1)
(h2)
(h3)
E Pseudomonopodial overlapping
(i1)
(i2)
F Untraceable
(j)
(k)
(l)
Example traced ontological relationship from center to margin
Isotomous dichotomies
Anisotomous dichotomies
Branching involving overlap
Pseudomonopodial dichotomies
Generator hyphae
Scutellum opening

Figure 2.2 Scutellum initiation and interpretation of branching.
A, Ancestors of thyriothecial fungi with pseudoparenchymatous walls (a–b). B, Radiate scutella grow by successive dichotomies followed by cross-wall formation; isotomous dichotomies, hyphae of similar width often overlap (top); anisotomous dichotomies, hyphae of different width rarely overlap (bottom). C, Scutella with isotomous dichotomies and overlap (c, e) may not show evidence of overlap in certain specimens ($d_{1\text{-}2}$) as well as young specimens (e_1), often borne from single intercalary generator hypha persisting above scutella at maturity (c, $d_{1\text{-}2}$, $e_{1\text{-}2}$). D, Scutella with anisotomous dichotomies and no overlap when mature (g_3–h_3) start with only isotomous dichotomies ($g_{1\text{-}2}$, $h_{1\text{-}2}$), also often borne from a lateral generator hypha (g_1, h_1), overgrown (g_2, h) and untraceable at maturity. E, Scutella with monopodial branching (i_2) often borne from multiple adjacent generator hyphae (i_1). F, Untraceable scutellum branching pattern (j–l) cannot be traced to generator hypha. Grey areas in drawings show traceable sequences of branching. Representative scutellum cells colored to show isotomous, anisotomous and monopodial branching, evidence of overlap, generator hyphae and opening of scutellum. Sources of drawings: a *Fumiglobus pieridicola* UBC-F33205; b *Pleospora herbarum* UBC-F4461; c *Batistinula gallesiae* VIC 42514 ; d Asterotexiaceae sp. UBC F33036; e *Asterina chrysophylli* VIC 42823; f Asterotexiaceae sp. CBS 143813; g *Microthyrium ilicinum* CBS 143808; h from *M. macrosporum* CBS 143810, i *Aulographum* sp. CBS 143545, j *Stomiopeltis* sp. UBC F33041, k *Stomiopeltis* sp. CBS 143811 and l *Peltaster cerophilus* redrawn from Fig. 2M in (Medjedović et al., 2014).

Thyriothecial species with elongate locules are inferred to be closely related to species with round locules (Appendix A.13), contrary to predictions from the current classification (Wu et al., 2011b). For example, ascoma shape, which was used to separate the elongate *Lembosia* from circular *Asterina*, fails to predict relationships. Instead, species of both genera appear in both Asterotexiales and in Asterinales (Fig. 2.1, Appendix A.7). In tree topology tests, constraining

either *Asterina* or *Lembosia* to be monophyletic is rejected with strong support (Appendix 4).

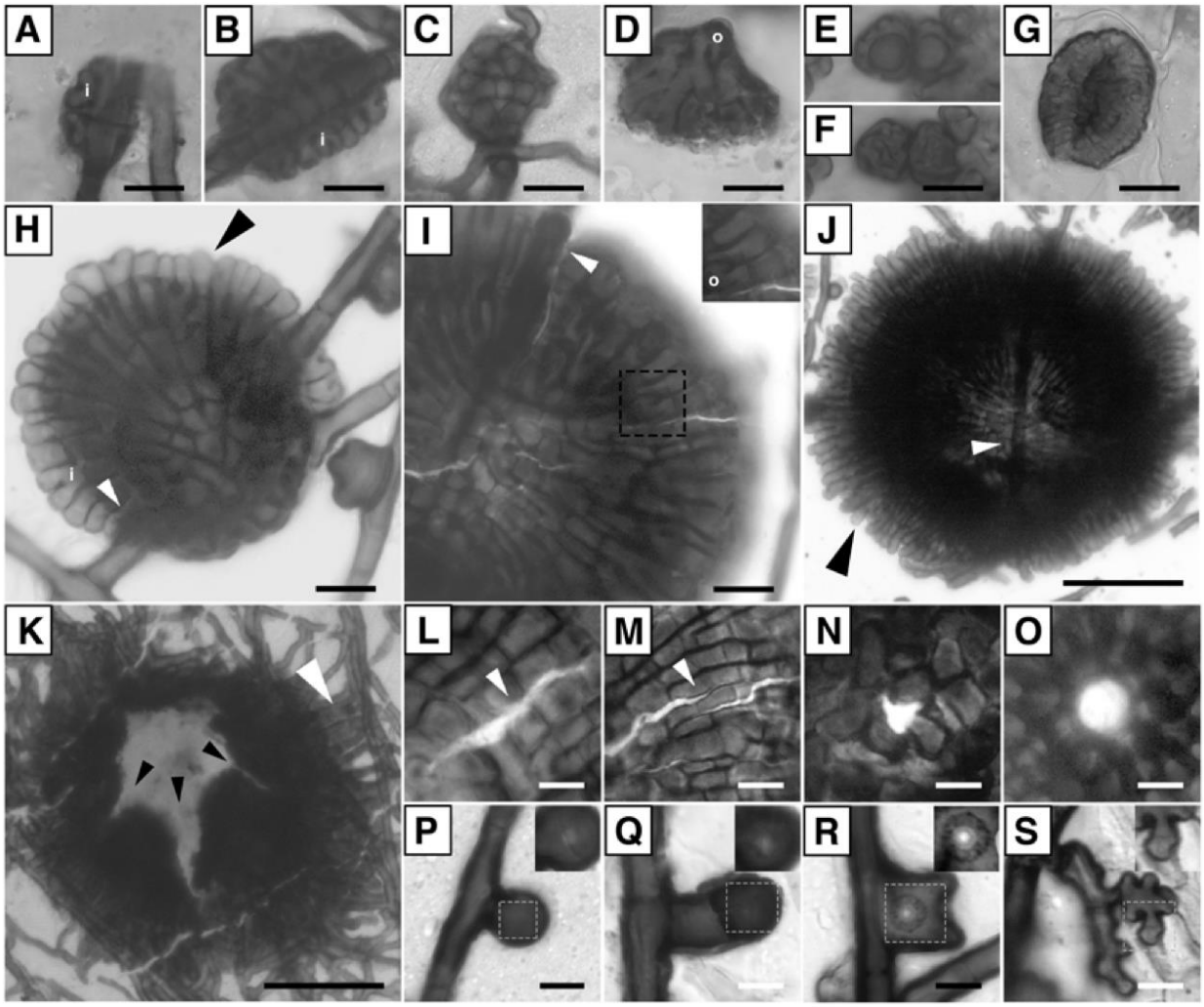

Figure 2.3 Morphological characters of Asterinales and Asterotexiales in dorsal view. A–C, Meristogenous intercalary initiation of ascoma in *Asterina*-like fungi involves septation of generator hypha and successive rounds of isotomous dichotomies (i). D–G, Alternative modes of initiation of scutellum in Asterotexiaceae, unknown (D), from spores (E, F) or from stomata (G), showing evidence of overlap (o). H–J, Majority of scutella of *Asterina*-like fungi have a generator hypha persisting above the scutellum at maturity (white arrow); scutellum margin shows lightly pigmented isotomous dichotomies (i); tips crenulate at maturity (black arrow). K, Margin of *Prillieuxina baccharidincola* differs in having margin anastomosing with surrounding mycelium (white arrow) although it shares other characters like dehiscence through radially arranged irregular slit (black arrows). L-M, Irregular slit follows longitudinal walls of scutellum cells (arrow). N-O, Ostiolate

opening associated with early ascomatal stage (N), anamorphic or spermatial stage (O) with evenly pigmented cells lining ostiole. P–S, Variation in lateral appressoria morphology in Asterinales and Asterotexiales showing characteristic melanized ring at lower focal plane (inset, representing area in dashed grey box).
Cells labelled with i represent example of mother cell of isotomous dichotomies, those labelled o represent cells leading to overlap between neighboring cells. Scales A–D, H–I, 10 µm; E–G, 20 µm; J–K, 50 µm; L–S, 5 µm. A, I, J, P, Q *Asterina melastomatis* VIC 52822, 1, 4, 6, 2 and 2 f.p. respectively; B, *Asterina chrysophylli* VIC 42823, 4 f.p.; C, O, Asterotexiaceae sp. CBS 143813, 2 f.p. each; D, *Hemigrapha atlantica* BR 14014, 1 f.p.; E, F, *Asterotexis cucurbitacearum* VIC 42814, 1 f.p. each; G, L, *Rhagadolobiopsis thelypteridis* EG156; H, R, *Batistinula gallesiae* VIC 42514, 10 and 2 focal planes (f.p.) respectively; K, N, *Prillieuxina baccharidincola* VIC 42817; M, Asterotexiaceae sp. UBC F33036, 11 f.p.; S, *Asterina* sp. (VUL. 341b), 2 f.p.;

2.4.7 Scutellum margins

Thyriothecia are unusual in that the margins of the scutellum are pressed to the surface of a host--a leaf or a lichen--and the characters of the hyphae at the scutellum margin differ across clades. Other kinds of ascomata lack a direct homolog to the scutellum margin, because their outer walls curve up from the substrate. In Aulographaceae, Asterotexiales, Asterinales and Muyocopronales, the scutellum margins often look crenulate or finely scalloped, because the dome-shaped hyphal tips bulge out around the circumference (Figs. 2.3H, 2.3J, 2.5A, 2.5C, 2.5D; Appendix A.16). In some species, for example in *Prillieuxina baccharidincola* (Fig. 2.3K) and in some *Stomiopeltis*-like species (Fig. 2.5A), the scutellum cells continue to grow at the margin, anastomosing with other superficial hyphae on the leaf surface, so that the margin of the scutellum is poorly defined and continuous with the surface mycelium. In Microthyriales and Zeloasperisporiales, scutellum margins are often entire, the scutellum hyphae ending as truncate tips aligned around the circumference (Figs. 2.4D, 2.4F, 2.4L). In *Microthyrium*, the hyphal tips of scutella that have finished radial expansion will narrow and continue to grow, forming a short

fringe at the scutellum periphery (Figs. 2.4B, 2.4L). Fringe hyphae look more tightly appressed to the host surface than central portions of scutella in these cases.

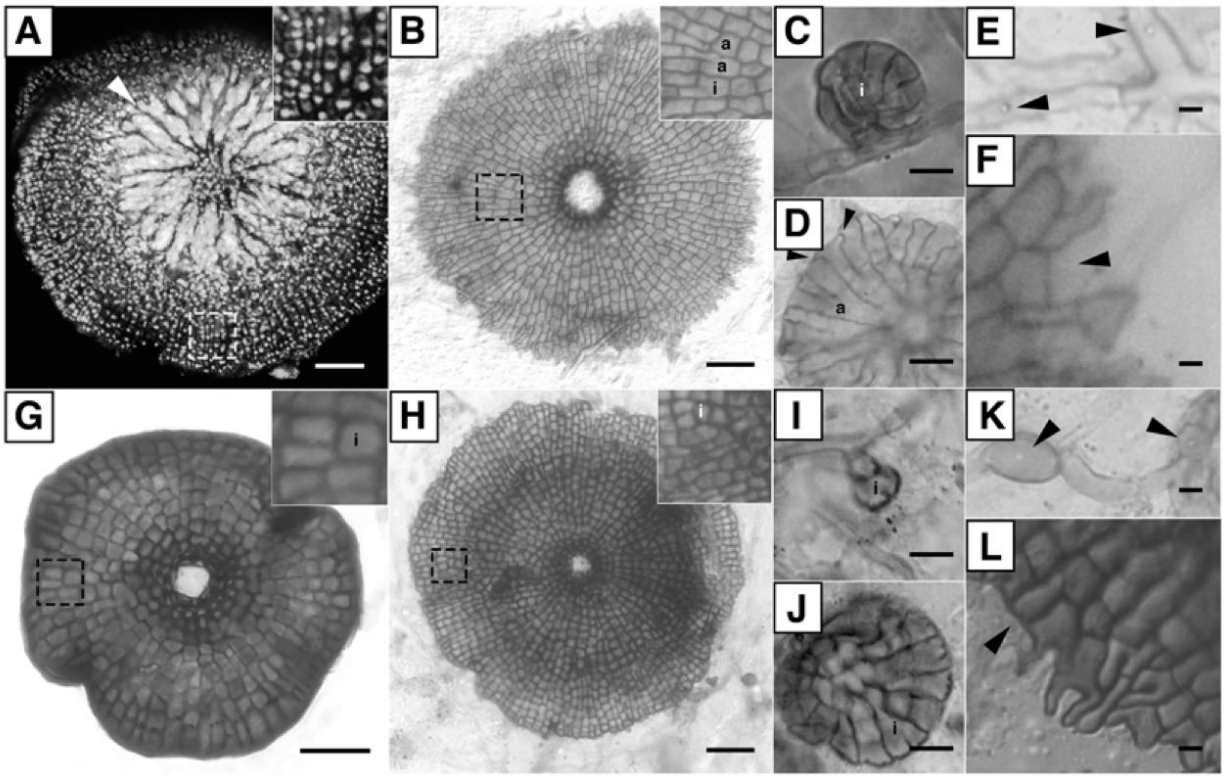

Figure 2.4 Morphological characters of Microthyriales in dorsal view.
A, Calcofluor staining of *Microthyrium* sp. revealing uneven staining of cells of scutellum, showing radially arranged hymenium below scutellum more strongly stained than scutellum cells. Inset shows uneven staining of scutellum due to dark pigments. B, G, H, Scutella with ostiole, lined by small and darkly pigmented cells, insets show examples of interpretable dichotomies. All scutella show isotomous dichotomies (i) and only members of Microthyriales and allies show anisotomous dichotomies (a). C, D, I, J, Early stage of growth showing initiation from lateral branches and appressed distal margin with blunt tips. E, K, Variation of intercalary appressoria morphology formed in a regular (E) or swollen (K) hypha segment, showing melanized rings (arrows). F, L, Margin of mature scutella showing blunt tips (arrows) or branching further into irregular meandering fringes with tapering, round or bulging tips (L). Scales, A–C, 20 µm; D, 10 µm; E–I, 5 µm. A, *Microthyrium* sp., 44 f.p.; B–F, *Microthyrium macrosporum* CBS 143810, with 4, 3, 1, 1 and 1 focal planes (f.p.), respectively; G, *Lichenopeltella pinophylla*, CBS 143816, 14 f.p.; H–L, *M. ilicinum* CBS 143808, with 4, 1, 3 and 2 f.p. respectively.

2.4.8 Lateral appressoria

Appressoria are widely distributed across thyriothecium-forming Dothideomycetes and are varied in their morphology and position. Conspicuous, pigmented, lateral appressoria are only produced by Asterinales and Asterotexiales (Figs. 2.3P–2.3S; Appendices A.5, A.17). The appressoria are usually unicellular (Figs. 2.3P, 2.3R) but in some species may be two-celled (Figs. 2.3Q, 2.4S) (Hofmann, 2009, Figs. 3.8; 3.14; 3.21; 3.24; 3.31; 3.56). The lateral appressoria may be swollen, lobed or minimally differentiated, and they branch from surface hyphae. I coded thyriothecial taxa of Asterinales and Asterotexiales that lack appressoria or produce them below the scutellum rather than on surface hyphae as absent for this character.

Other kinds of appressoria appear in other thyriothecial clades. Inconspicuous, hyaline, intercalary appressoria are produced by some Microthyriales (Figs. 2.5E, 2.5K). All Aulographaceae examined have intercalary appressoria on swollen cells with a conspicuous melanized ring (Fig. 2.5E), and strains isolated in pure culture form an appressorium regularly in each segment of somatic hyphae. Species of *Stomiopeltis* form infrequent, intercalary appressoria with a hyaline ring that contrasts with the pigmentation of the hyphae (Fig. 2.5G). The hyphae bearing the appressoria may be swollen (Figs. 2.5F, 2.5G). BayesTraits reconstructs lateral appressoria as present in the most recent shared ancestor of Asterotexiales, and as present in the most recent shared ancestor of Asterinales, while likelihood reconstructs them as ancestral only for lineages that have diverged more recently from one another (Appendix A.17).

2.4.9 Initiation of thyriothecia

Development of thyriothecia begins with distinctive, lineage-specific patterns of coordinated hyphal growth and septation in the species where observation was possible. I could directly

observe different developmental stages of 18 taxa (Table 2.1) and analyze development for 14 additional taxa from published illustrations (Appendix A.3). Otherwise, data on development is scarce and ancestral state reconstructions are equivocal where data are missing (Appendices A.5, S18).

A single "generator hypha" (Hofmann, 2009) initiates the thyriothecia by first developing multiple, closely spaced intercalary septa only in Asterinales and Asterotexiales, of taxa analyzed here (Figs. 2.2C, 2.3A–2.3C, 2.3H–2.3J). Each of the delimited cells then gives rise to transverse, adjacent, dichotomizing hyphal tips that together form the scutellum. The generator hypha remains above the dorsal surface of the mature scutella and is visible even in mature thyriothecia (Figs. 2.2C, 2.3I–2.3J). Ascomata in one Asterotexiales species, *Rhagadolobiopsis thelypteridis*, are initiated directly over host stomata, as shown by Guatimosim et al. (2014b) and in Fig. 2.3G here; in *Asterotexis cucurbitacearum,* they are initiated directly from ascospores (Figs. 2.3E, 2.3F).

In contrast to the widespread intercalary origin among Asterinales and Asterotexiales, all Microthyriales examined initiate their ascomata at the tip of a generator hypha located on a short lateral branch of a surface hypha (Figs. 2.2D, 2.3C, 2.3I). The generator hypha does not become highly septate, but instead its tip gives rise to a succession of dichotomously branched, closely appressed hyphal tips that develop into a scutellum. The scutellum in Microthyriales overgrows to cover the generator hypha, and so that the generator hypha can no longer be seen in older scutella (Figs. 2.3A, 2.3B, 2.3G, 2.3H).

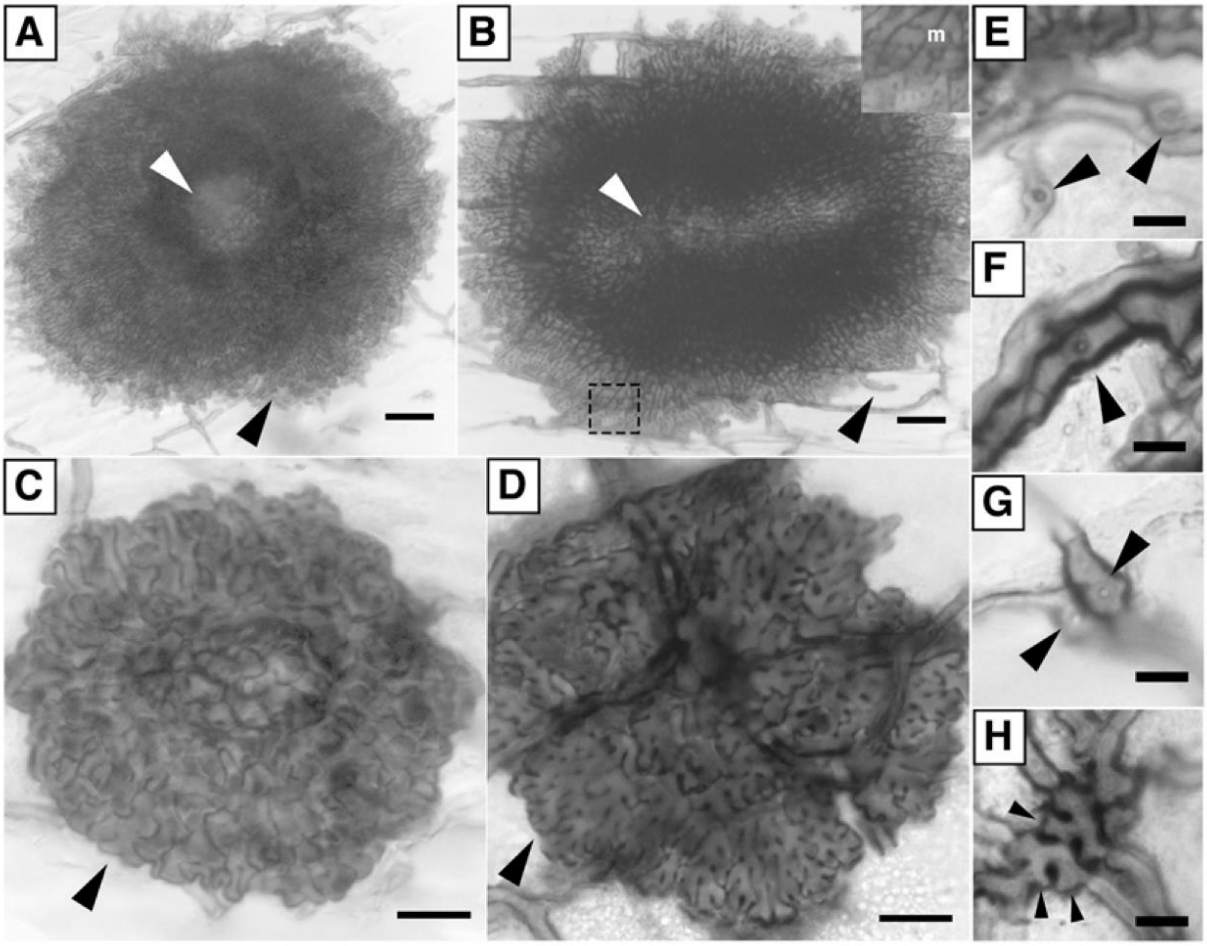

Figure 2.5 Morphological characters of Aulographaceae and some *Stomiopeltis* spp. s.l. in dorsal view.

A, *Stomiopeltis*-like scutellum morphology with wide ostiole (white arrow) and free hyphal tips at distal appressed margin (black arrow). B, Aulographaceae scutellum morphology with lighter area where irregular slit dehiscence will take place (white arrow), and appressed distal margin with free hyphae. C, *Stomiopeltis*-like scutellum at early stage of development with appressed distal tips adhering to their neighbors (arrow). D, Aulographaceae scutellum at early stage of development with appressed distal tips adhering to their neighbors (arrow). E–G, Intercalary appressoria with melanized ring (arrow). H, Scutellum initiation symphiogenous, with multiple hyphal tips originating from distinct surface hyphae (arrow). Scales, A, B, 20 µm; C, D, 10 µm; E–H, 5 µm. A, C, F, *Stomiopeltis* sp. UBC F33041, 5, 6 and 1 stacked focal planes (f.p.) respectively; B, *Lembosina aulographoides* CBS 143809, 4 f.p., D, G, H, *Aulographum* sp. CBS 143545, 1 f.p.; E, *Stomiopeltis* sp. UBC F33040, 1 f.p.

Of all the Aulographaceae observed, three species of *Lembosina* and one species of *Aulographum* initiated their ascomata with coordinated development from multiple generator hyphae. Adjacent intercalary portions of the multiple generator hyphae developed abutting, transverse branches that contributed to forming a single scutellum (Figs. 2.2E, 2.5H). At a later stage, radially arranged hyphae form monopodial branching units that cover the upper surface of the hyphal aggregate (Fig. 2.5D), each hypha resembling monopodial branching stems in plants.

2.4.10 Case studies using thyriothecial fossils

Morphological characters of thyriothecial scutella and mycelia offer a range of variation, allowing phylogenetically informed interpretations of published fossils. I looked for the oldest geological occurrence of thyriothecia and two younger and more interpretable fossils on the basis of their morphology (Fig. 2.6; Appendix A.3). Each phylogenetic analysis of a fossil yielded more than one equally parsimonious tree, given the morphological dataset and the rDNA likelihood constraint tree. All of the optimal trees were 232 steps and were the same length as the constraint tree without any fossils.

Triassic dispersed scutellum

The oldest evidence of a radiate fungal scutellum is a fossil from the Early Triassic of India (Induan, ~251 Ma) referred to as a "fungal thallus" but not identified to species or genus. The fossil is from a palynological sample that was rich in land plant cuticle and spores (Mishra et al. 2018, Fig. 8j). It shares five characters with extant thyriothecial taxa. Like extant radial thyriothecia, it is made up of hypha-like filaments that are closely appressed along their sides. The filaments are regularly septate into trapezoidal cells that form partial, concentric rings. Some

of the filaments dichotomize. A central circular opening appears to be an ostiole surrounded by a ring of very dark cells. Where the scutellum margin is in focus, it appears to be crenulate (Fig. 2.6A) (Appendix A.3).

I found 28 equally parsimonious positions for this fossil relative to the constraint tree. Based on its five coded characters, the fossil could cluster with thyriothecial taxa in Asterinales, Asterotexiales and Microthyriales. Missing character state data from some extant taxa increased the number of possible, equally parsimonious positions for the fossil to anamorphs of Zeloasperiasporiales. A strict consensus of the 28 trees resulted in a polytomy of 45 lineages, all stemming from the most recent ancestor of all Dothideomycetes (Fig. 2.1; Appendix A.19).

Microthyriaceous fossil

Trichothyrites setifer (Cookson) Saxena & Mishra, a fossil from the early Eocene (Ypresian, 56–47.8 Ma) sediments of India is illustrated by Monga et al. (2015) (Fig. 2.6B). While this specimen is from dispersed material, rather than in situ on a leaf surface, it shares seven characters with extant *Lichenopeltella pinophylla* and six characters with other thyriothecial Microthyriales. It has a circular multicellular thallus. The radiate scutellum has an entire margin and shows the presence of a lower wall (Fig. 2.6B, arrowhead). The scutellum branching pattern is mostly isotomous, but also shows anisotomous dichotomies. Its central ostiole is surrounded by papillate cells. Papillate ostioles, although uncommon, occur in *Chaetothyriothecium elegans* and *Lichenopeltella pinophylla*. However, *C. elegans* lacks a differentiated lower wall. My ancestral state reconstructions for the ancestor of Microthyriales and Zeloasperisporiales suggests it grew a circular, radiate and ostiolate thyriothecium without a differentiated lower

wall, and produced isotomous and anisotomous dichotomies without overlap and an entire margin (Appendix A.5).

I found 16 equally parsimonious trees resolving *T. setifer* in my phylogeny of living fungi. The strict consensus position of this fossil suggests it shares affinities with the clade containing Microthyriales and Zeloasperisporiales (Fig. 2.1, Appendix A.20). Among the 16 reconstructions, *T. setifer* is alternatively placed in Microthyriales; as sister to Microthyriales (10/16); as sister to asexual taxa in Zeloasperisporiales (that are missing data for characters of the ascoma) (3/16); as the sister to the perithecioid Natipusillales (2/16); or as the sister to all these lineages (Fig. 2.1, Appendix A.20).

Asterina fossil

The early Eocene (56-48 Ma) *Asterina eocenica* Dilcher (1965) is found on leaves of *Chrysobalanus* and consists of circular, multicellular thalli and mycelia that are preserved in different states of development, allowing comparison with extant Asterinales and Asterotexiales. The lower wall of the fossil scutellum is absent, and dehiscence is by means of an irregular slit. The pattern of branching of the scutellum is isotomous with overlapping hyphae, and the margin is crenulate, as in living *Asterina.* The sporocarp is initiated with an intercalary generator hypha (Fig. 2.6C). The mycelium bears appressoria. My ancestral state reconstructions for the ancestors of clades containing *Asterina* species suggest that they evolved from ancestors that were superficial on leaves, producing radiate thyriothecia that initiated from an intercalary generator hypha, with a crenulate margin, and branching through isotomous dichotomies leading to overlap of scutellum hyphae, with opening through irregular slits (Appendix A.5).

A strict consensus of the 23 equally parsimonious trees places *A. eocenica* in a polytomy at the base of Dothideomycetes (Appendix A.21). *Asterina eocenica* shares all 11 morphological characters with three extant taxa in Asterinales and with nine in Asterotexiales (Fig. 2.6C, Appendix A.3). Consistent with the shared characters, 18 of the individual phylogenies show *A. eocenica* within or as sister to Asterotexiales (Appendix A.22), and five show it in, or as sister to Asterinales (Appendix A.23).

2.5 Discussion

Results from my molecular phylogeny of 306 species including 59 species of thyriothecial taxa combined with critical analysis of 11 morphological characters of extant Dothideomycetes offer grounds for cautious optimism for incorporating thyriothecial fossil data into the broader picture of fungal evolution. Ancestral state reconstructions show that convergent evolution of thyriothecia in Dothideomycetes likely began among fungi that produced pseudoparenchymatous-walled sporocarps on surfaces of plant cuticles. My reconstructions suggest that radiate scutella arose at least three times within epiphyllous Dothideomycetes. With the evolution of radiate thyriothecial forms came distinctive patterns of development in the hyphal branching and septation patterns of scutella. Future surveys of fungi on fossilized plant cuticle will make possible further tests or refinement of these predictions about the early stages of thyriothecial fungal evolution. Their association with leaf cuticles makes thyriothecial fossils easier to collect and to interpret than many other kinds of fungal fossils. Analysis of thyriothecial fossils has the potential to reveal interpretable patterns of origin and diversification of important lineages of filamentous ascomycetes.

2.5.1 A dispersed scutellum as evidence of Triassic Dothideomycetes

Among my sampling of extant taxa, radiate scutella are restricted to Dothideomycetes. Further, ancestral state reconstructions show radiate thyriothecia as a derived character state that arose convergently, but only among epiphyllous Dothideomycetes. As the parsimony analysis shows, given available data, the scutellum-like "fungal thallus" of Mishra et al. (2018, Fig. 8j) provides evidence of Dothideomycetes from the Early Triassic (~251 Ma). Consistent with results from the parsimony analysis, the combination of an ostiole and a scutellum with dichotomous branching that is found in the fossil was also reconstructed to be ancestral for Asterinales, Asterotexiales, and Microthyriales. The fossil could represent a member of any of these groups. However, this fossil likely represents the oldest fossil evidence of thyriothecia.

2.5.2 Fossil evidence of Microthyriales

Monga (2015, Pl.2 Fig.18) illustrates the fossil *Trichothyrites setifer* (Cookson) Saxena & Misra. Like the "fungal thallus" discussed above, *T. setifer* is from a sample rich in land plant material, but its substrate is unknown. *Trichothyrites* specimens (synonym of *Notothyrites*, see Kalgutkar and Jansonius, 2000), interpreted as members of Trichothyriaceae have frequently been reported in the fossil record throughout the Tertiary (Kalgutkar and Jansonius, 2000). Although classified in Microthyriaceae, extant *Lichenopeltella* shares multiple characters with Trichothyriaceae (Appendix S3), including an entire margin, a papillate ostiole, a scutellum with isotomous and anisotomous dichotomies, and a differentiated lower wall that can be seen in the overlapping septation patters of the transparent upper and lower walls continuous with the scutellum, and an entire margin (Spooner and Kirk, 1990). This distinctive type of microthyriaceous thyriothecium with a lower wall is also known as a 'catathecium' and is characteristic of Trichothyriaceae. The

only extant taxon I sampled with this morphology, *Lichenopeltella*, did not show evidence of anisotomous dichotomies, but they do occur in the genus: available illustrations of *L. arctomiae* show anisotomous dichotomies in the scutellum of this species (Fig. 1 in Pérez-Ortega and Spribille, 2009).

Although *T. setifer* is more similar to *Lichenopeltella* than any other taxa in my dataset, some of its shared characters including ostiolate thyriothecia are reconstructed as ancestral in the larger clade encompassing Zeloasperisporiales, Natipusillales and Microthyriales. Three of six taxa in Zeloasperisporiales are only known from hyphomycetous anamorphs and are missing data for the sporocarp. A differentiated lower wall also occurs in non-thyriothecial ascomata of Natipusillales. As a result of missing data and plesiomorphic characters, *T. setifer* appears equally parsimoniously within Microthyriales; as the sister lineage to Microthyriales, Natipusillales, or Zeloasperisporiales, and as a sister to the clade including all of these taxa.

At present, early Eocene (56–47.8 Ma) *T. setifer* (Monga et al., 2015) represents the most convincing early evidence for catathecia, and thus of the clade including Microthyriales. Investigating Paleocene deposits may very well yield further and older evidence of the divergence of taxa with catathecia from those with thyriothecia in the order Microthyriales. For more formal testing, the molecular phylogenetic positions of extant taxa of *Actinopeltis*, *Lichenopeltella*, *Trichothyrium* and *Trichothyrina* should be established, and their morphology analyzed for comparison with the fossils.

2.5.3 *Asterina*-like fossils could represent either Asterinales or Asterotexiales

Contrary to my expectations, combining close morphological observations and the molecular phylogeny revealed no clade-specific morphological differences between Asterinales and

Asterotexiales. Guatimosim et al. (2015) showed that Asterinales and Asterotexiales both include taxa with scutellum dehiscence by irregular cracks, and superficial hyphae bearing lateral appressoria. *Lembosia* species (characterized by with elongate thyriothecial outlines) occur nested among both Asterinales and Asterotexiales species with round thyriothecial outlines.

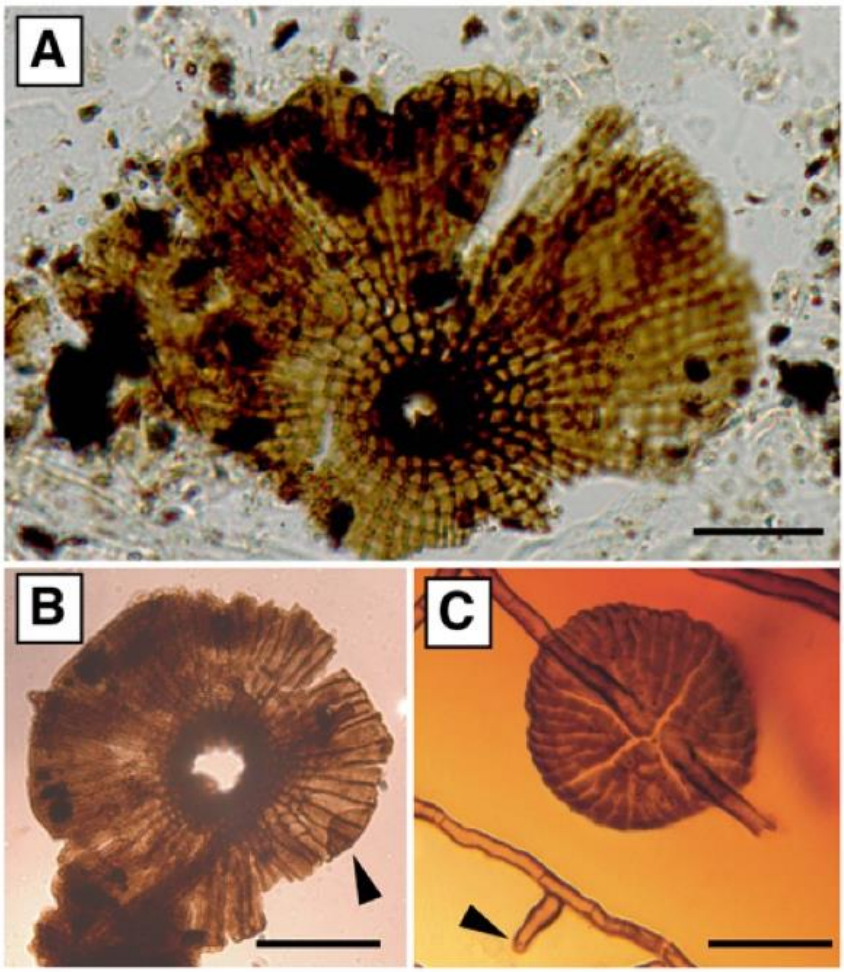

Figure 2.6 Reproduction of fossil illustrations used in case studies.
A. Triassic dispersed 'fungal thalli', courtesy Mishra et al. (2018), reproduced with the permission of Springer Nature; B.S.I.P. 15524, J36-4. B. Early Eocene dispersed *Trichothyrites setifer* with lower wall seen by transparence (arrowhead), reproduced with permission from Monga et al. (2015); B.S.I.P. 15297, U41/3. C. Middle Eocene *Asterina eocenica* on cuticle of *Chrysobalanus* sp. described in Dilcher (1965), illustration courtesy Steven Manchester, reproduced from Taylor et al. (2015), with permission from Elsevier; Florida Museum of Natural history, l.f. 87. Scales, 20µm.

Hofmann's (2009) thesis contains elegant drawings from diverse species, documenting the common intercalary origin of thyriothecia, starting with septation in a generator hypha. At the time of her thesis, the distinction between Asterinales and Asterotexiales had yet to be discovered and Hofmann lacked sequence data to link her observations to clades. My analysis of species of Asterinales and Asterotexiales shows that development and scutellum branching as Hofmann described are common to both orders. The orders share additional characters illustrated here, including intercalary initiation of scutellum formation, and crenulate scutellum margins, characters that were sometimes illustrated in great detail in early works, without receiving further attention (Arnaud, 1918; Doidge, 1919; Viégas, 1944).

Liu et al. (2017) interpreted Asterotexiales as "Asterinales sensu stricto" and suggested that the Asterinales, represented by a clade of six species and their LSU rDNA sequences, all from Brazil, should be considered "Asterinales sensu lato". However, the six Brazilian Asterinales species that were sequenced include *Asterina melastomatis* (from the epitype specimen of the Asterinales), which means that the ordinal name applies to their clade. If a single sequence had been involved, or if the disputed Brazilian Asterinales were from a clade of fungi commonly amplified from leaf surfaces in other studies, contamination by non-target DNAs might seem a possible explanation for the presence of morphologically similar species in phylogenetically divergent groups. However, the several Brazilian sequences are from species in five genera of thyriothecium forming taxa: *Batistinula*, *Prillieuxina*, *Parmularia*, *Asterina*, and *Lembosia*. Together, the sequences representing Asterinales form a novel clade. In the absence of any contradictory evidence, the sequences must be assumed to come from their target fungi (Guatimosim et al., 2015).

Asterinales also include a clade consisting of *Alysidiella suttonii* and *Blastacervulus* spp., both known only from their asexual states (Cheewangkoon et al., 2012; Giraldo et al., 2017); and *Aulographina eucalypti*, a parasite on leaves of various eucalyptus species that forms elongate thyriothecia (Wall and Keane, 1984). The sequence from the culture *A. eucalypti* (CPC 12986) was published without illustration of the source material (Cheewangkoon et al., 2012). Like most Asterinales, *Alysidiella suttonii* and *Blastacervulus* spp. share a folicolous habitat, and their growth is almost exclusively superficial. I speculate that the radiating pattern of growth of hyphae in the subcuticular stroma of *Blastacervulus eucalypti* may be related to radial growth of thyriothecial hyphae. However, whether *Alysidiella suttonii* and *Blastacervulus* spp. form thyriothecia is unclear.

It is possible that more molecular data may resolve Asterinales and Asterotexiales as sister groups of one another, consistent with their morphological similarities. Tree topology tests did not rule out a sister relationship between the two orders (Appendix S4). Although the orders consistently appear unrelated in published phylogenies, their separation never receives strong bootstrap support or high posterior probabilities (Guatimosim et al., 2015; Firmino, 2016; Liu et al., 2017 and Fig. 1). With cultures now available representing Asterotexiales (Asterotexiaceae sp. 2 CBS 143813) and Asterinales (*Alysidiella suttonii* CBS 12478) it should soon be possible to expand available sequences beyond the ~1 kb of 28S ribosomal DNA per taxon that currently limits phylogenetic resolution. If Asterinales and Asterotexiales are sister groups, a phylogenetic analysis of their morphological characters, including dehiscence type, scutellum branching and pattern of initiation of sporocarp, should likely allow unambiguous assignment of fossils to their clade.

Asterina eocenica from the Middle Eocene (48.6-37.2) of western Tennessee (Dilcher,

1965; Elsik and Dilcher, 1974) is the oldest fossil that combines a convincing Asterinales/Asterotexiales suite of characters. The exquisitely preserved scutella of *A. eocenica* show clear isotomous dichotomies with overlap (Figs. 64 and 65 in Dilcher, 1965). This places the fossil with clades of thyriothecia in which hyphae branch dichotomously at their apices to produce radial scutella (Farr, 1969; Reynolds and Gilbert, 2005; Hofmann and Piepenbring, 2011; Guatimosim et al., 2015). Dichotomous branching is infrequent among fungi, where branching is usually initiated some micrometers behind the hyphal apex. *Asterina eocenica* has nine out of 11 characters shared by Asterinales and Asterotexiales. The development of thyriothecia of *A. eocenica* is typical of Asterinales and Asterotexiales, with initiation by closely spaced septa forming in a generator hypha. The generator hypha persists on the dorsal side of the scutellum (Figs. 59, 60, 63, 64 and 65 in Dilcher, 1965). Like Asterinales and Asterotexiales, *A. eocenica* has slit-like dehiscence (Figs. 63 and 65 in Dilcher 1965), an undifferentiated lower wall (Figs. 61, 63, 65 and 66 in Dilcher, 1965), and some elongate, 1-celled tapering lateral hyphal projections described as appressoria (Figs. 57 and 59 in Dilcher, 1965). In their otherwise detailed and useful review of fossils, Samarakoon et al. (2019) assign *A. eocenica* to crown group Asterinales (=Asterotexiales) and give its minimum age as Paleocene 54 Ma. The Paleocene age appears to be an error, because it is inconsistent with Elsik and Dilcher (1974)'s analysis of pollen and spores that assigned a more recent Middle Eocene age to the fossil's source material from the Lawrence Clay Pit. None of the characters of *A. eocenica* justify positioning it in the crown group of either order as opposed to a stem relationship of either order, and as the parsimony analysis shows, it could equally well represent Asterinales and Asterotexiales. A strong implication of the close similarity of Asterinales and Asterotexiales is that even a beautiful, complete fossil like *A. eocenica* cannot be assigned to one order versus the

other.

2.6 Conclusion

Much cryptic diversity in Dothideomycetes consists of minute leaf dwelling fungi (Arx and Müller, 1954; Müller and von Arx, 1962; von Arx and Müller, 1975). As my analysis shows, epiphyllous fungi together with lichenized, lichenicolous and aquatic fungi are all relevant to the evolution of thyriothecia, but they have been studied by different mycologists who sequenced different loci for phylogenetic analysis (Dhanasekaran et al., 2006; Miadlikowska et al., 2006; Etayo, 2010). The sequencing of the 5' end of the LSU was common across most studies, but choices of other loci varied. I anticipate that sequencing of more Dothideomycetes genomes, including some from the new isolates from this study from cultures available through the Westerdijk Institute, will contribute to improved resolution of relationships.

My molecular phylogeny of a broad sampling of thyriothecial taxa and their closest relatives leads to testable predictions about the sequence of early events in their evolutionary history. Thorough morphological analysis here revealed differences in scutellum morphology, development and hyphal branching patterns that distinguish Asterinales/Asterotexiales, Microthyriales, Aulographaceae, Muyocopronales and Micropeltidaceae. Analyzing and coding morphological characters offers an objective pathway toward comparing fossils to extant taxa and ultimately to incorporating fossils into phylogenies. The fidelity of association of characters with extant lineages should be tested across a broader range of taxa using morphological and molecular phylogenetic analysis. Undoubtedly, further study will help reveal convergence and variation, and perhaps additional distinctive synapomorphies. My analyses suggest scutellum characters can link fossils on leaf cuticle to phylogenetic lineages, offering rewarding insights into fungal evolution through geological time. However limited fossilized characters may be,

documenting equivalent anatomical features in extant taxa helps communicate the significance of fossil morphologies, increasing their value for paleomycology.

Chapter 3: A new epiphyllous fly-speck fungus from the Early Cretaceous Potomac Group of Virginia (125–112 Ma): *Protographum luttrellii gen. et sp. nov.*

3.1 Summary

Fly-speck fungi reproduce via thyriothecia that consist of sporogenous tissue appressed to cuticle surfaces of plant leaves and covered by a shield-like scutellum. Thyriothecial scutella likely evolved repeatedly in Dothideomycetes (Ascomycota), and their morphology varies by lineage. Fly-speck fungi have an exceptionally good fossil record that begins in the Mesozoic. The interpretation of scutellum characters in fossils may provide insights into the origins of Dothideomycetes and help calibrate the timing of ascomycete evolution. From sediments of the Lower Cretaceous (125–112 Ma) Potomac Group of Virginia, from Dutch Gap Canal, lower Zone 1, I found scutella similar to those of extant Aulographaceae (Dothideomycetes), attached to a single piece of dispersed coniferous cuticle. I analyzed hyphae and scutellum development among four extant Aulographaceae species for comparison with the fossil. The excellent preservation of fungi on the leaf cuticle surface allows me to infer a developmental sequence for the fossil. Scutellum development begins with coordinated growth of multiple neighboring generator hyphae, and continues with hyphae producing two-dimensional pseudomonopodial, dichotomous, radial growth. Asci and ascospores were not found. I coded states for seven morphological characters using direct observations of the fossil and eight extant taxa, and using the literature for 28 others. I inferred a phylogeny using nuclear 18S and 28S rDNA of 36 extant taxa, 34 Dothideomycetes and two Arthoniomycetes. The phylogeny includes newly determined sequences from five species, two from Aulographaceae. With a branch-and-bound search, I

inferred the most parsimonious placements of the fossil given the molecular tree topology. Optimal fossil placements included several stem lineages near Aulographaceae and Asterotexiales, and placement within crown Aulographaceae. I describe the fossil morphotype as *Protographum luttrellii gen. et sp. nov.* The fossil provides the oldest evidence of morphological characters restricted among extant fungi to Aulographaceae.

3.2 Introduction

Fungi have traditionally been classified on the basis of their structure and life cycle (Gäumann, 1952; Webster and Weber, 2007). More recently fungal DNA has revolutionized our understanding of their evolutionary relationships and patterns (Schmitt et al., 2005; Hibbett, 2007; Larsson, 2007; Schoch et al., 2009b; Lumbsch and Leavitt, 2011), and many formerly accepted phylogenetic hypotheses based on structural synapomorphies have been replaced by phylogenies inferred using DNA sequence analysis. However, morphological and anatomical characters are virtually all that is available from the fossil record, and so analysis of structural characters is key to incorporating fossils in reconstructions of the evolutionary history of fungi. Paleomycological research combining high-quality anatomical illustrations and up-to-date phylogenetic hypotheses provides an increasingly useful framework for pursuing such goals (Taylor et al., 2015).

The fossil record includes Mesozoic evidence of fly-speck fungi (Stevens and Manter, 1925) in the form of distinctive sporocarps referred to as thyriothecia (Vijaya and Murthy, 2012; Sun et al., 2015; Taylor et al., 2015; Mishra et al., 2018). In extant fungi, thyriothecia are sexual structures, ascoma that produce asci and ascospores; similar-looking asexual structures are known as pycnothyria (Kirk et al., 2008; Hofmann et al., 2010; Hongsanan et al., 2016) (Chapter

2). Extant thyriothecia and pycnothyria form flattened, circular to elongate sporocarps lacking a lower wall (Kirk et al., 2008) that grow appressed to plant surfaces (Arnaud, 1918; Stevens and Manter, 1925).

The scutellum, or shield-like dorsal surface of thyriothecia of extant taxa varies in morphology, and its hyphal patterning can be diagnostic for species, genera, or even higher taxa (Hofmann, 2009; Wu et al., 2011b; Guatimosim et al., 2015; Hongsanan and Hyde, 2017) (Chapter 2). Scutella are typically formed by radial growth of dark-walled hyphae that dichotomize at their tips (Arnaud, 1918; Doidge, 1919; Stevens and Manter, 1925). Dichotomies are typically but not always "isotomous" or similar in size (Chapter 2). This growth pattern distinguishes thyriothecia and pycnothyria from other kinds of sporocarps in Dothideomycetes, which have pseudoparenchymatous walls and do not develop by dichotomous branching (Chapter 2).

Most fossil fly-speck fungi consist only of scutella and superficial hyphae. Kalgutkar and Jansonius (2000) published a synopsis of the available reports of fossil fungal form-genera, translated into a searchable public database (Berbee et al., 2014) that includes 131 taxonomic records for fly-speck species (originally classified as Microthyriales). These fungi are among the most abundantly documented Mesozoic and Cenozoic fungi, with records spanning the Triassic to the Holocene (Bajpai and Maheshwari, 1987; Kalgutkar and Jansonius, 2000; Sun et al., 2015; Mishra et al., 2018). When found on plant cuticles and associated with hyphae, fossils of thyriothecioid scutella may provide convincing evidence of fungal affinities. Even in the absence of ascospores and asci, the patterns of branching of the dichotomizing hyphae of the scutellum may be systematically diagnostic.

During a survey of angiospermous plant remains from the Lower Cretaceous Potomac Group, Upchurch recognized abundant evidence for fungal colonization on the cuticles of leaf surfaces (Upchurch and Doyle, 1981; Upchurch, 1984a, b). The processing of additional Potomac Group (lower Zone 1) sediments has revealed an abundance of fungal remains on gymnosperm leaf cuticles. Here I characterized and named a fossil fungal morphotype that has scutella at different developmental stages. Its morphology resembles living Aulographaceae (Dothideomycetes). For comparison with the fossil, I also described stages of development of extant Aulographaceae represented by *Lembosina* and *Aulographum*, with particular emphasis on the generator hyphae, the first hyphae to differentiate to begin forming the scutellum. I scored characters of extant and fossil fungi, yielding a morphological data matrix of seven characters for parsimony-based inference of fossil placement, using a phylogeny of extant Dothideomycetes as a topological constraint.

3.3 Material and methods

3.3.1 Fossil fungi

The leaf fossils and associated fungi come from a clay bed exposed on the south side of Dutch Gap Canal, James River, Virginia (Hickey and Doyle, 1977; Upchurch and Doyle, 1981; Upchurch, 1984b). The Dutch Gap Canal (37.376°, -77.3593°; locality DMNH 128) is dated as lower Zone I of Brenner (1963), or Aptian (125–112 Ma) based its palynoflora (Doyle and Hickey, 1976; Upchurch and Doyle, 1981; Doyle and Upchurch, 2014, and references therein). The described materials come from the base of the sequence in a claybed exposed at low tide. This bed yielded shoots of the extinct conifer *Pseudofrenelopsis parceramosa*, leaf macrofossils

of the extinct bennettitalean gymnosperm *Dioonites buchianus*, and shoots of early herbaceous angiosperms (Upchurch and Doyle, 1981; Doyle and Upchurch, 2014; Jud, 2015).

I modified a cuticle extraction protocol from Upchurch (1989) as follows. I immersed 200 g of clay in saturated household trisodium phosphate solution (TSP; Rescochem, Québec) and added 10% hydrogen peroxide (H_2O_2) to release cuticles from the matrix. The solution was left to react slowly for up to 36 h. I collected accumulated foam containing organic debris at regular intervals (3–6 h). Upon collection, organic debris was rinsed in 70% ethanol, extracted in two fractions using 200 µm and 90 µm sieves, and stored in 50% ethanol. Silicate-rich samples were processed (by Rolf Mathewes) in concentrated 20% HF for two days. These fractions were washed with water and stored in 50% ethanol. I inspected the stored cuticles in solution under a dissecting microscope, and I sampled individual cuticles with signs of fungal, with the aid of an insect pin (size 0, Austerlitz insect pins, Slavkov u Brna, Czech Republic). I further processed dark cuticles in 10% KOH and heated to 60 C for up to two days, removing cleared cuticles from the liquid before any fungal structure disappeared. Up to 10 cuticle fragments were spread onto each glass slide with the aid of insect pins using the dissecting microscope. Cuticles were then mounted in Eukitt, a xylene-based mounting medium (O. Kindler GmbH, Freiburg, Germany).

3.3.2 Microscopy and image processing

I observed extant and fossil fungi using a Leica DMRB (Leitz, Germany) DIC microscope and photographed at 200X, 400X, or under immersion oil at 1000X with a Leica DFC420 digital color camera. I assembled more than one focal plane into brightfield stacks in Photoshop CC 2015.1.2 (1990 – 2019, Adobe Systems, Ottawa, Canada), following Harper (2015) and using suggestions from Bercovici et al. (2009). Many of the dark fungal structures contrast with the

cleared cuticles and benefitted from post processing using the gamma correction setting in Photoshop to reveal the outline of scutellum hyphae in greater detail.

3.3.3 Morphology of modern Aulographaceae

For comparison with the fossil, I analyzed hyphae and development of thyriothecia in Aulographaceae using herbarium specimens of *Aulographum* sp. (UBC F33038), three species of *Lembosina* (UBC F33037, UBC F33044 and UBC F33045), and their corresponding pure cultures: CBS 143545, CBS 144007, CBS 143809 and CBS 143815, Westerdijk Fungal Biodiversity Institute, Utrecht, Netherlands. Additionally, I incubated slide cultures of *Aulographum* sp. (CBS 143545) in petri dishes on cornmeal agar kept moist for 12 weeks, to observe growth.

3.3.4 Molecular and morphological phylogenetic analysis

I sampled 36 taxa that include thyriothecial lineages, their closest relatives in Dothideomycetes, and two species in Arthoniomycetes as outgroups (Appendix B.1). The Dothideomycetes included three Asterinales and seven related taxa in Dothideomycetidae; four Microthyriales plus six related taxa in Phaeotrichales, Natipusillales, and Venturiales; six Asterotexiales; and two Aulographaceae used in the developmental studies described above. Additional samples included four Pleosporomycetidae, one Tubeufiales and one Patellariales (Appendix B.1). The taxa I chose from Asterotexiales and Asterinales represent a small subset of the full morphological diversity of these orders (Hongsanan et al., 2014b; Ertz and Diederich, 2015; Guatimosim et al., 2015). I retrieved sequences for target taxa using BLAST searches from GenBank or from the Joint Genome Institute (JGI) using 28S or 18S nuclear rDNA as a query (permissions for using

Aulographum hederae CBS 113979, *Patellaria atrata* CBS 101060 and *Trichodelitschia bisporula* CBS 262.69 JGI genome data were granted by J. Spatafora, Oregon State University). I selected sequences that were linked to publications with photographs and descriptions of the specimen for inclusion in alignments.

Sequences and morphological characters from the same specimen were not initially available for all of my target taxa. I determined new sequences from pure cultures, where possible, that corresponded to herbarium collections available for morphological study. I established cultures by crushing individual thyriothecia under an inverted compound microscope and using an insect pin (size 0, Austerlitz insect pins, Slavkov u Brna, Czech Republic) to transfer individual spores or groups of spores onto water agar with 1 mM ampicillin and 1 mM kanamycin, for germination. I transferred germinating spores to antibiotic-free nutritive media under a dissecting microscope. I harvested mycelia in pure culture from culture media, and I extracted DNA using the QIAGEN DNeasy Plant Minikit (QIAGEN Inc., Toronto, Ontario). Amplifications were performed with PureTaq Ready-To-Go PCR (polymerase chain reaction) beads (Amersham Biosciences, Piscataway, New Jersey), following manufacturer instructions, using the standard PCR primers for 28S and 18S rDNA genes listed in James et al. (2006).

I collected Asterotexiaceae sp. UBC-F33036 in Costa Rica (Permit nºR002-2014-OT-CONAGEBIO) but I could not be isolate it in pure culture. I instead directly amplified the first (5'-end) 1 kb of 28S rDNA (using primers LR0R-LR8) from dried tissue (Lee and Taylor, 1990). I prepared PCR reaction tubes containing a PureTaq Ready-To-Go PCR bead, 12.5 µL of water and primers at a concentration of 1.0 µM and kept the tubes on ice. I mounted thyriothecia in a drop of sterile water, checked under the compound microscope, crushed firmly between slide and coverslip, and pipetted into the waiting PCR reaction tube for a final reaction volume of ~25 µL,

and final primer concentration 0.5 μM each. I ran the PCR reactions for 40 cycles with an annealing temperature of 50 C. For Sanger sequencing, I used ABI PRISM BigDye Terminator Cycle Sequencing Kit V3.1 following the manufacturer instructions (Life Technologies-Applied Biosystems, Burlington, Canada). I assembled sequences using Sequencher ver. 4.10.1 (Gene Codes, Ann Arbor, Michigan).

I aligned sequences using the iterative refinement method G-INS-I in MAAFT v7 (Katoh and Standley, 2013). Using Mesquite version 3.31, I manually optimized the alignment or excluded ambiguously aligned position (Maddison and Maddison, 2015). The resulting concatenated dataset spans 4248 nucleotide positions. I ran JModeltest 2 (Darriba et al., 2012) and recovered the GTR+G model for individual genes. I used RAxML v.8 (Stamatakis, 2014) with 100 independent searches to find the tree with the maximum likelihood (ML). Topological support was assessed with 1000 bootstrap replicates (BS). Bayesian analysis was performed using MrBayes 3.2.6 (Ronquist et al., 2012), using two independent searches with four Metropolis coupled Monte Carlo (MCMC) chains each, for 20 million generations, sampling every 1000th tree. I used Tracer 1.5 to determine the effective sample size (≥200) and assess convergence. Jmodeltest 2, RaxML v.8 and MrBayes 3.2.6 analyses were run on the CIPRES portal (Miller et al., 2010).

Morphological character coding and parsimony analysis.— I scored morphological characters for taxa included in my phylogenetic analysis based on published descriptions, illustrations or direct observations (Appendix B.2). The eight taxa scored from direct observation are *Asterina melastomatis* VIC 42822*, Asterotexiaceae* sp. UBC F33036, CBS 143813*, Batistinula gallesiae* VIC 42514*, Lembosia abaxialis* VIC 42825*, Lichenopeltella pinophylla* UBC F33032*, Microthyrium ilicinum* UBC F33031; and two of the four Aulographaceae species used in

analyses of development described above: *Aulographum* sp. UBC F33038, CBS 143545 and *Lembosina* sp. UBC F33044, CBS 144007 (Appendix B.2). The scored characters include substrate type (on rock or soil, superficial on plants, lichenicolous or immersed in plants); sporocarp type (apothecioid, perithecioid; thyriothecioid or cleistothecioid); dehiscence mode (ostiole, irregular slit, regular slit, no dehiscence or exposed at maturity); locule circumference (circular or elongate); scutellum hyphal branching type (pseudoparenchyma, isotomous dichotomies or pseudomonopodial dichotomies); state of scutellum margin (not appressed, crenulate or entire) and lateral appressoria (present or absent). I used the maximum likelihood tree obtained using nucleotide data to constrain the topology of all of the taxa except the fossil in a branch-and-bound parsimony search. The most parsimonious positions of the fossil, given the backbone constraint topology and the morphological matrix were inferred using PAUP 4.0a165 (Swofford, 2003). Alignments, phylograms, and cladograms are available from TreeBASE (Submission ID: 24642).

3.4 Results

3.4.1 Description

The fossil sporocarps occur on a single piece of conifer cuticle, 1 x 2 mm, which shows three rows of stomata (Fig. 3.1A). At least two distinct fungal morphotypes are found along with bisaccate pollen on the same cuticle (Fig. 3.1A). Fourteen stomata are colonized by dark, circular structures 110–130 μm in diameter (Fig. 3.1A–C). These large structures are common on other cuticles from the Dutch Gap Canal site and are described in detail in Chapter 5. Some of these were apparently old sporocarps that were broken (Fig. 3.1A–C). Growing alongside these large stomatal colonizers or in their broken sporocarps are 17 small, circular to elongate sporocarps

preserved in different stages of scutellum development. These are connected to surface (superficial) mycelium (Fig. 3.1B–G). One of the 17 sporocarps is larger than the others, and its identification as the same fungus is uncertain (Fig. 3.1C); this sporocarp is discussed separately below.

The new taxon described below as "*Protographum luttrellii*" refers to the 16 small sporocarps associated with mycelia that are not colonizing stomata. They are scattered on the plant cuticle and range in size from 20–60 µm diameter (Fig. 3.1D–F). Each young scutellum is attached to its surrounding, superficial, septate mycelium at three or more points by multiple generator hyphae (Fig. 3.1D–F). One young scutellum is surrounded by the broken remains from a larger, old or infected sporocarp of one of the stomatal colonizers (Fig. 3.1B). All of these small structures represent the upper walls of thyriothecioid sporocarps or scutella, as they sit directly on the plant cuticle instead of being embedded below it, and they show radiate hyphal branching rather than a pseudoparenchymatous stroma.

Most of these scutella are round (Fig. 3.1D, F), measuring up to 30–50 µm in diameter, but they appear to elongate as they grow larger as in the specimen in Fig. 3.1E, which is 68 x 38 µm. The hyphae that make up the scutellum are 1–3 µm wide and branch dichotomously. Branching is "pseudomonopodial", with one branch from a dichotomous pair elongating beyond the other, resulting in candelabra-like segments that radiate out from a central area (Fig. 3.1B–F, H–J). Cross septa occur infrequently in the older, central parts of the scutellum and may be absent from the distal portions of individual hyphae (Fig. 3.1H–J). Hyphae often dichotomize near the periphery of scutella, and the rounded distal tips of hyphae give the scutellum a crenulate margin (Fig. 3.1D–F). The overlap of some hyphae obscures the radial organization in certain scutella (Fig. 3.1D). Observing the stages of growth of the scutella, development appears

to originate from several generator hyphae, and multiple hyphae coordinate their growth to form a continuous, flattened scutellum.

3.4.2 Large associated sporocarp

The largest scutellum has a more markedly elliptical shape than most of the scutella described above and measures 208 x 96 μm (Fig. 3.1C). It is much more elongate, and is three times larger than the somewhat elliptical structure in 3.1E. The large scutellum shows a subtle line of pigmentation suggestive of a longitudinal dehiscence slit (Fig. 3.1C). This scutellum is attached to at least three generator hyphae (Fig. 1C), and sits next to a row of three sporocarps of the stomatal colonizer, growing over two of them. The large scutellum shows little evidence of apical dichotomous branching, and the candelabra-like segments seen in younger forms of *P. luttrellii* are absent (Fig. 3.1G, K). Instead, septate hyphae in the central zone appear to be formed of rectangular to lobate cells, 4–6 x 2–3 μm (Fig. 3.1K). These central cells are obscured by elongate hyphal segments 5–20 x 1–2 μm that overlap, and their course is hard to follow from the centre to the margin of the scutellum. Near the edge of the scutellum, however, hyphae are unbranched and tend to run parallel to one another (Fig. 3.1G, 1K). I was unable to evaluate whether the large associated scutellum described here represented *P. luttrellii*, due to the absence of intermediate stages in the developmental sequence of the scutellum. Further comparisons of this large scutellum will have to await the discovery of more fossil material of the same type.

Close examination of the mycelium associated with *P. luttrellii* and the larger scutellum reveals two appressorium-like swellings, each with a pigmented ring resembling a penetration peg (Fig. 3.1L–M), similar to the appressoria of other Dothideomycetes (Parbery and Emmett, 1977). One swelling, with a ~0.3 μm wide ring is found on a hypha attached near the edge of the larger unidentified scutellum (Fig. 3.1L). The other 0.6 μm wide ring is on superficial mycelium

attached to a young scutellum of *P. luttrellii* (Fig. 3.1M). I could not follow hyphae from these swellings below the cuticle, however, and no subcuticular mycelium was found in the most heavily colonized area of the cuticle.

3.4.3 Molecular identity and morphology of newly contributed Aulographaceae

In BLAST searches, the 28S sequence of *Aulographum* sp. UBC F33038 (CBS 143545) shares 96.8% nucleotide identity with each of two 28S GenBank fragments (KM386980, KM386981) from *Aulographum hederae* and is 98.7% identical to a 28S region from the *A. hederae* CBS 113979 genome, sequenced by JGI. *Lembosina* sp. (CBS 144007) shares 99.8% identity with *Lembosina aulographoides* (CPC:33049) GenBank fragments, 83% identity with the *A. hederae* GenBank fragments and 93% with the CBS 113979 isolate sequence, consistent with its classification as a member of Aulographaceae. All other top hits were from distantly related Dothideomycetes, which is consistent with the phylogenetic results noted below.

Morphologically, species of *Aulographum* and *Lembosina* share several features with each other (Fig. 3.2A–F). The four taxa examined were associated with angiosperm plant cuticles. Their abundant, grey, olive brown to dark brown hyphae penetrate host plants through appressoria (Fig. 3.2G–I), stomata (Fig. 3.2J) and possibly trichomes (Fig. 3.2K). Below the cuticle, inconspicuous to abundant subcuticular hyphae show evidence of dichotomies and form a dense prosenchyma (Fig. 3.2N).

Central/initial branching of the scutellum usually begins with multiple neighboring surface generator hyphae (sometimes only one, as in Fig. 3.2F) that initiate repeated dichotomous branching in close proximity, within a few micrometers of one another (Fig. 3.2D–E). Later in development, the hyphal tips branch dichotomously, one branch continuing to

elongate radially and the other remaining short. The lateral walls of hyphae remain in contact with one another. This gives rise to the pseudomonopodial, radiate scutellum pattern (Fig. 3.2D–F). Each hyphal segment from a generator hypha may remain non-septate for much of its length (Fig. 3.2E). These hyphae eventually become septate and pigmented in older scutella (Fig. 3.2F).

Pseudomonopodial dichotomies occur throughout scutellum growth and can be seen in the most distal portions of dehiscent scutella. The lower wall of the sporocarp (ascoma) is hyaline and undifferentiated (Fig. 2P). Dehiscence occurs through one or more irregular slits running along the scutellum lengthwise (Fig. 3.2A, B). Asci are ovoid to oblong, and evanescent at maturity (Fig. 3.2P, Q). Ascospores are once-septate, hyaline, smooth or light brown, and finely verrucose at maturity (Fig. 3.2R–T).

Characters that distinguish the four species include habitat, the frequency of formation of appressoria, the dimensions of the scutellum, and the patterns of hyphal growth in their host plants. Characters from herbarium specimens, all collected from Vancouver BC, Canada, and their associated cultures are reported below for each species.

Aulographum sp. specimen UBC F33038 (Fig. 3.2A, D, G–J, L–N, R) was found on bleached, white leaves from leaf litter of *Ilex aquifolium,* forming superficial ascomata, mostly abaxial along the central vein (Fig. 3.2A). On the same leaf with *Aulographum* sp. UBC F33038, a species of *Microthyrium* produced scattered ascomata on both leaf surfaces (Fig. 3.2A). Thyriothecia of *Aulographum* sp. UBC F33038 are connected to superficial hyphae that are (1–)2–4(–5) µm wide with frequent appressoria in locally swollen (4–5 µm wide) segments, each with a more or less pronounced melanized ring reaching 0.6–1 µm in diameter (Fig. 3.2G–I). Superficial mycelium is abundant, contrasting with the light grey to hyaline mycelium of *Microthyrium* (Fig. 3.2L). The close proximity of *Aulographum* sp. UBC F33038 to

Microthyrium sp. (Fig 2A) made surveying its mycelium within the host plant somewhat challenging, but I could confirm the whole fungus connection by following superficial mycelium from thyriothecia of *Aulographum* sp. UBC F33038 across multiple focal planes, through the host cuticle and into host intercellular spaces. Appressoria (Fig. 3.2L–M) connect to hyphae within the host that branch and form a dense prosenchymatous layer (Fig. 3.2M). In areas where both taxa co-occur, their hyphae often follow one another (Fig. 3.2G–H, L). Figure 2N shows a suspected instance of opportunistic fungivory by *Aulographum* sp. UBC F33038 on *Microthyrium*, where the browner hypha of *Aulographum* formed an appressorium where it crossed hyaline hyphae of *Microthyrium* (Fig. 3.2N). Ascomata of *Aulographum* sp. UBC F33038 are 140–750 µm x 75–150 µm in smaller ellipsoid to larger strap-shaped scutella (> 300 µm), and are simple or less frequently branched to form X- or Y-shaped patterns. Infrequently, young, circular thyriothecia of *Aulographum* sp. UBC F33038 exhibit a distinct ostiole, possibly representing a spermatial or conidial stage. Mature asci discharge hyaline ascospores, 14–18 x 2.5–3 µm (Fig. 3.2R). Non-discharged ascospores become lightly pigmented after a month of exposure to light.

A slide culture of CBS 143545 ex *Aulographum* sp. UBC F33038 produces abundant pigmented mycelium with typical swollen appressoria (Fig. 3.2I). It also produces ostiolate, circular spermatial or conidial pycnothyria up to 50 µm diam. Like the original specimen on its host, *Aulographum* sp. in culture produces large, elongate ascomata that open by a dehiscence slit when pressed by the hard surface of a Petri dish or a slide.

The second species, *Lembosina aulographoides*, represented by specimen UBC F33037 (Fig. 3.2B–C, E–F, J–K, Q), was found on white stems (where cuticle remains the longest before periderm production) of ornamental *Rhododendron* cf. *ponticum*, forming superficial ascomata in

clusters on aging branches. Ascomata are frequently intermixed with *Leptopeltis* sp. and less frequently with aeroterrestrial algae (phylum Chlorophyta) accumulating at the edge of their scutellum. The grey to brown, superficial hyphae attached to scutella of *L. aulographoides* follow host cell outlines in most places, making them difficult to see. Appressoria in this species, although infrequent and hard to find, occur as swollen cells with a lightly pigmented, melanized ring. Most mature ascomata are circular, ellipsoid or slightly lunate (Fig. 3.2B–C, F), reaching 160–530 x 100–330 µm, or less frequently are strap-shaped like those of *Aulographum*. Mature ascospores are 18–24 x 8–10 µm; and pseudoparaphyses are present but evanescent (Fig. 3.2Q). Culture CBS 143809 from the collection UBC F33037 of *L. aulographoides* grows slowly and did not produce ascomata.

The third species of *Lembosina*, represented by specimen UBC F33044 (Fig. 3.2O, P), was found on the previous year's dead and upright stems of ornamental *Euphorbia* cf. *characias.* The colonized stems are white where cuticle remains, or grey or brown where decorticated. Superficial ascomata are intermixed with *Leptopeltis* sp., *Diplodia* sp. and with aeroterrestrial algae that accumulated at the edge of the scutella (Fig. 3.2O–P). Superficial hyphae produced frequent appressoria or entered the stems via stomata. No direct interaction with *Leptopeltis* sp. was observed. Mature ascomata are circular or ellipsoid, 160–500 x 120–280 µm. Mature ascospores are 20–25 x 8–10 µm, and pseudoparaphyses are present. Culture CBS 144007 from collection UBC F33044 grows slowly without producing ascomata.

The fourth species, *Lembosina* sp. specimen UBC F33045 (Fig. 3.2T), consisted of five ascomata on the stem of dried *Laurus nobilis*. One ascoma was used to isolate the strain, two were vouchered and the remaining two were used for imaging. A cuticular peel could not be obtained for this taxon. The only mature ascoma that could be measured was 600 x 350 µm and

contained four mature ascospores, 20–23 x 8–11 µm (Fig. 3.2T), and two appressoria were attached to a scutellum in one preparation. The culture CBS 143815 from UBC F33045 grows slowly without producing ascomata.

Phylogenetic analyses.—Maximum likelihood and Bayesian phylogenetic searches yield similar topologies for my 36-taxon dataset that includes 12 thyriothecial species. Of the four thyriothecium-forming lineages, Asterinales appears nested in Dothideomycetidae (BS = 93, PP = 1), Asterotexiales and Aulographaceae appear as sister taxa although with poor support (BS = 32, PP = 0.64), and Microthyriales are supported as sister to Venturiales and Natipusillales (BS = 90, PP = 1) (Fig. 3.3).

A branch-and-bound search using the morphological data that included *P. luttrellii* yielded four equally parsimonious trees of 49 steps. These equally parsimonious solutions are consistent with alternative possible schemes for the evolution of scutellum branching. The scutellum in the common ancestor of Asterotexiales and Aulographaceae could either have had isotomous dichotomies (state "1") or pseudomonopodial dichotomies (state "2"). In trees where isotomous dichotomies (state "1") are reconstructed as ancestral to Asterotexiales and Aulographaceae, *P. luttrellii* appears as sister to, or nested in Aulographaceae (Fig. 3.3, alternative "a"). In the trees where pseudomonopodial dichotomies are assumed to be ancestral in Asterotexiales and Aulographaceae, *P. luttrellii* can be reconstructed on the stem leading to the common ancestor, or as a sister group to Asterotexiales that diverged prior to the gain of isotomous dichotomies (FIG.3, alternative "b").

3.5 Taxonomy

Class: Dothideomycetes O.E. Erikss. & Winka

Family: Aulographaceae Luttr. ex P.M. Kirk, P.F. Cannon & J.C. David

Genus: ***Protographum*** Le Renard, Upchurch, Stockey & Berbee *gen. nov.*

MycoBank no: MB831507

Typification: *Protographum luttrellii* Le Renard, Upchurch, Stockey & Berbee

Etymology: The generic epithet Proto- refers to the first of its kind, -graph refers to the genus *Aulographum* that it resembles.

Diagnosis: Mycelium superficial on leaves with intercalary appressoria, hyphae septate. Sporocarp shield-like, covered by scutellum (upper wall), appressed to host surface, circular or elongate. Scutella made of pseudomonopodial, dichotomously branching and radiating hyphae; scutellum connected to surrounding mycelium by multiple generator hyphae.

Protographum luttrellii Le Renard, Upchurch, Stockey & Berbee *sp. nov.* Fig. 3.1

MycoBank no: MB831508

Typification: USA: Virginia, Potomac Group, lower Zone 1, *Pseudofrenelopsis parceramosa* bed; Aptian (Lower Cretaceous, 125–113 Ma). **Holotype** specimen occurring in slide DG 083 fragment B (England Finder coordinates M43-O43, label on specimen slide to the right), deposited in the Denver Museum of Nature and Science under slide EPI.53110.

Etymology: The species is named in honor of the late Everett S. Luttrell, University of Georgia, for his contributions to the study of Aulographaceae and other thyriothecial Dothideomycetes.

Diagnosis: Superficial mycelium composed of septate hyphae, 1–3 µm wide; appressoria infrequent. Thyriothecia represented by shield-like scutella appressed to host leaf surface, circular to elongate in largest specimens. Young scutella 20–60 µm diam, connected to

surrounding mycelium by multiple generator hyphae; made of pseudomonopodial dichotomously branching hyphae, 1–3 μm wide, radiating from generator hyphae and overlapping with one another, mostly non-septate; few cross-septa laid in older, proximal portion of hyphae.

Notes: *Protographum luttrellii* is distinguished from other fossil taxa by pseudomonopodial dichotomous branching in a scutellum initiated by multiple generator hyphae. Due to its lack of asci and ascospores and of a known mode of dehiscence (ostiole vs. slit) the fossil cannot be placed in a living genus.

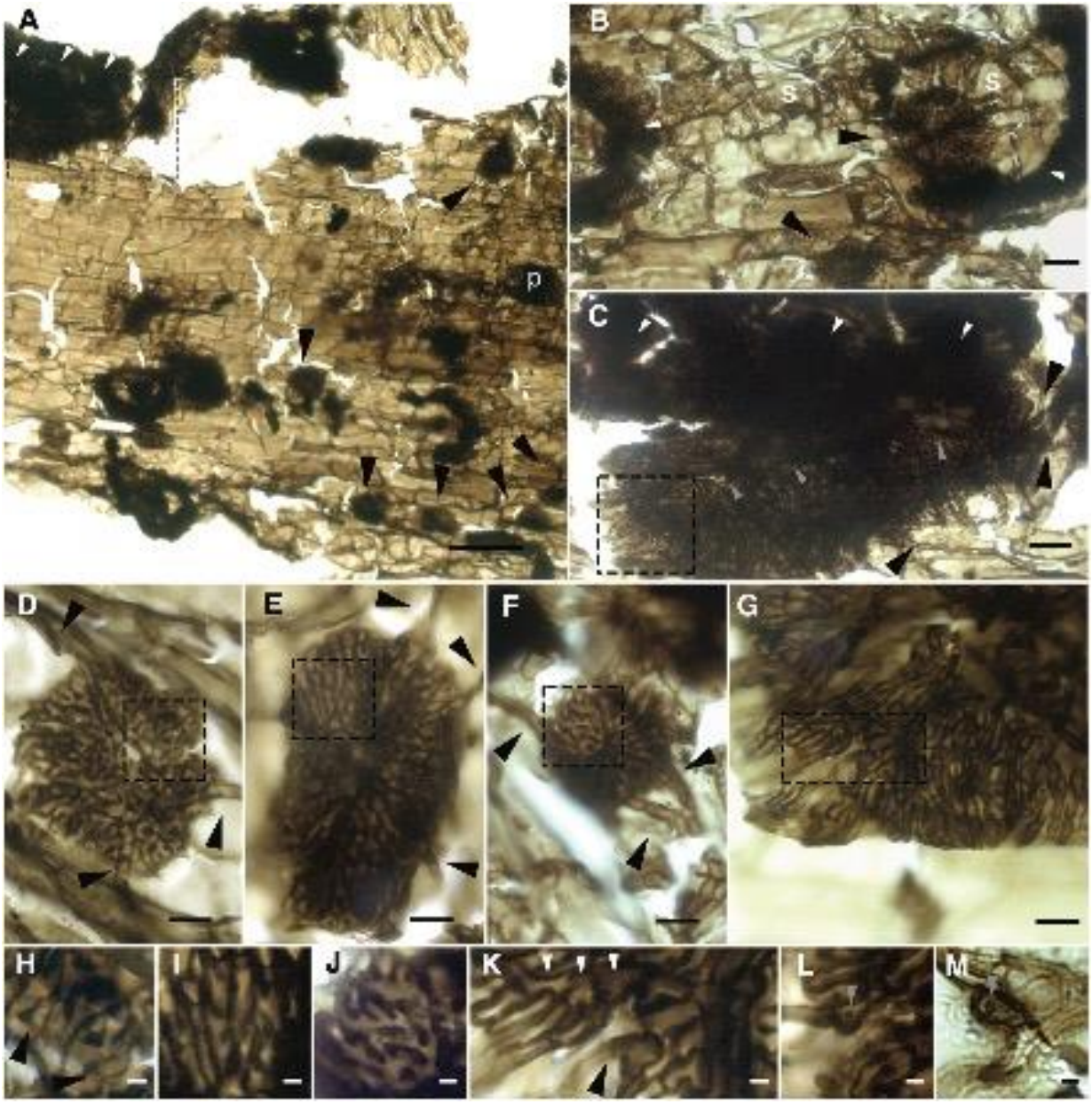

Figure 3.1 Fossils of *Protographum luttrellii gen. et sp. nov.* on Lower Cretaceous (125–112 Ma) cuticle of unknown conifer.

Holotype, DMNS EPI.53110. A. Overview of cuticle with *P. luttrellii* (black arrowheads), which does not emerge from stomata, in contrast to *Stomatothyrites placocentrus*, described in Chapter 5, arising from stomata aligned in rows (white arrowheads); pollen grain (P). B. Closer view of two *P. luttrellii* scutella (black arrowheads), one on old sporocarp (white arrowheads) of the colonizer of stomata (S). C. Large thyriothecium associated with *P. luttrellii*, growing next to row of colonized stomata (white arrowheads); connected to surrounding mycelium in at least three points (black arrowheads). Possible, faint line of

dehiscence (grey arrowheads). D-F. Young thyriothecia of *P. luttrellii* initiated from at least three surface hyphae (black arrowheads). G. Close up of dashed box of Fig. 1C. Note pseudomonopodial dichotomous branching less obvious than in smaller scutella; septation and overlap between neighboring hyphae obscures evidence of early hyphal branching. H-J. Higher magnification of boxes of Fig.1D-F respectively, showing pseudomonopodial dichotomous branching; septa restricted to proximal segments of hyphae (black arrowheads). K. Area in dashed box of Fig.1G magnified, showing hyphal segments that may have originated through septation of pseudomonopodial dichotomies (white arrowheads). Elongate hyphal segments distal to septa (black arrowhead) are unbranched. L, M. Intercalary appressoria with penetration pegs (grey arrowheads). L. Appressorium connected to large sporocarp in C. M. Appressorium connected to hypha of smaller sporocarp. Illustration of manually assembled stacks of three and two focal planes in Figs. D and E, respectively. All other illustrations are of a single focal plane.
Bars: A = 50 µm; B, C = 20 µm; D, E, F, G = 10 µm; H, I, J, K, L, M = 2 µm.

3.6 Discussion

3.6.1 Affinities of *Protographum*, comparisons with living taxa

The fungus *P. luttrellii,* which is borne appressed superficially on leaf surfaces of conifer cuticle, produces radiate sporocarps (scutella) that are initiated from generator hyphae and surrounded by superficial hyphae, as is characteristic of thyriothecial Dothideomycetes (Hofmann, 2009; Wu et al., 2011b; Hyde et al., 2013; Guatimosim et al., 2015). Here, I show that scutellum development in *P. luttrellii* is initiated from multiple generator hyphae and expands with pseudomonopodial, dichotomously branching hyphae also found in extant fungi in Aulographaceae.

3.6.2 Phylogeny and morphology of extant Aulographaceae

Analyses of *Lembosina* and *Aulographum* nuclear rDNA sequences revealed that they form a strongly supported clade of Dothideomycetes. *Aulographum hederae* represented the family Aulographaceae in a molecular phylogenetic study by Hongsanan et al. (2014b) and JGI

sequenced the genome of the same species, *A. hederae* CBS 113979. BLAST searches confirmed that my isolate of *Aulographum* sp. is closely related to *A. hederae.* As in previous analyses that also included sequences of *Aulographum hederae* (Wu et al., 2011b; Hongsanan et al., 2014b; Guatimosim et al., 2015; Liu et al., 2017; Dai et al., 2018), my phylogeny shows Aulographaceae and Asterotexiales as sister to Dothideomycetes. Sister group relationships of Aulographaceae are poorly supported and appear variable in different studies (Hongsanan et al., 2014b; Guatimosim et al., 2015). Despite the consistent lack of backbone resolution, my analysis and all previous analyses agree in showing the family to be nested within Dothideomycetes.

Comparison of the scutellum pattern of *P. luttrellii* with other radiate thyriothecioid fungi requires additional, careful analysis of living members of Aulographaceae. Scutella in Microthyriales, Asterinales and Asterotexiales are initiated by dichotomously branching hyphae, which progressively cover a circular surface through repeated isotomous dichotomies, producing branches of equal size that adhere laterally and grow radially to form the scutellum (Wu et al., 2011b; Hongsanan et al., 2014b; Guatimosim et al., 2015). However, in illustrations from previous studies of Aulographaceae, the dark pigmentation of the scutellum obscured phylogenetically informative details of its hyphal branching (Muthappa, 1969; von Arx and Müller, 1975; Hyde et al., 2013). Eriksson noted that scutella of Aulographaceae consist of "irregularly arranged, meandering cells and not radiating square cells" (1981), as in Microthyriaceae or Asterinaceae. I show that these meandering cells in Aulographaceae can be characterized as pseudomonopodial dichotomously branching hyphae in which septation is often delayed. This type of branching and septation distinguishes scutella of Aulographaceae from other thyriothecioid genera described as meandering (="maeandrisch plectenchymatische"),

including Plochmopeltinae (Theissen, 1914) or species sometimes referred to as *Stomiopeltis* (Luttrell, 1946).

A scutellum with pseudomonopodial branching is not restricted to Aulographaceae but the combination of scutella developing from multiple, superficial generator hyphae is as yet known only from Aulographaceae (Chapter 2). Pseudomonopodial branching occurs in at least the distal part of the scutellum in other species e.g. *Asterina ekmanii* (Hofmann, 2009, Fig. 3.16), *Maublancia myrtacearum* (Arnaud, 1918, Pl. XXVIII), *Maurodothella dothideoides* (Arnaud, 1918, Pl. XIV) and *Hariotula loranthi* (Arnaud, 1918, Pl. XLIV) (Arnaud, 1918; Doidge, 1919; Hofmann, 2009), but because the phylogenetic relationships of these other species are untested, the extent of convergence of pseudomonopodial branching is currently unknown. All these taxa produce scutella from a single superficial generator hypha except *H. loranthi* (Arnaud, 1918, p. 201), in which the scutella arise directly from under the host cuticle rather than from superficial generator hyphae.

The superficial mycelium and the subcuticular structures of Aulographaceae provide additional characters that may become more relevant to fossil interpretation when more extant taxa are examined. While appressoria are reported as being absent in *Aulographum* (Hyde et al., 2013; Hongsanan et al., 2014b), they are produced regularly by *Aulographum* sp. UBC F33038 both in situ and in culture. *Lembosina* spp. produce only occasional appressoria that penetrate dead tissue of living hosts (Chapter 2). Thus, like other fungi in Aulographaceae, *Protographum luttrellii* has appressoria.

Although the presence of appressoria has sometimes been used to differentiate biotrophic and hemibiotrophic fungi from necrotrophs (Perfect and Green, 2001; Moore et al., 2011; De Silva et al., 2016), biotrophy can only be confirmed with the discovery of haustoria in living host

cells (Diéguez-Uribeondo et al., 2005; Gachomo et al., 2006). The biotrophic relationship of Asterinales to their hosts is well documented (Arnaud, 1918; Hofmann, 2009; Guatimosim et al., 2015), but the same is not true of other thyriothecial fungi. Appressoria are formed by a wide range of fungi (Emmett and Parbery, 1975; Parbery and Emmett, 1977), and endophytic growth of hyphae in a dead host can happen long after appressorium formation (Brown, 1975). As shown here, and as implied by Hongsanan et al. (2014b) culture collection number MFLUCC 13-0001, Aulographaceae can grow in culture, and so are at least facultatively saprobic. Although the mycelia of Aulographaceae are found in dead tissue of living or dead plants, the developmental stages of colonization have yet to be studied. Thus, it remains possible that they can have a biotrophic phase. Against this background of uncertainty about extant taxa, is also unclear whether the fossilized fungus was biotrophic.

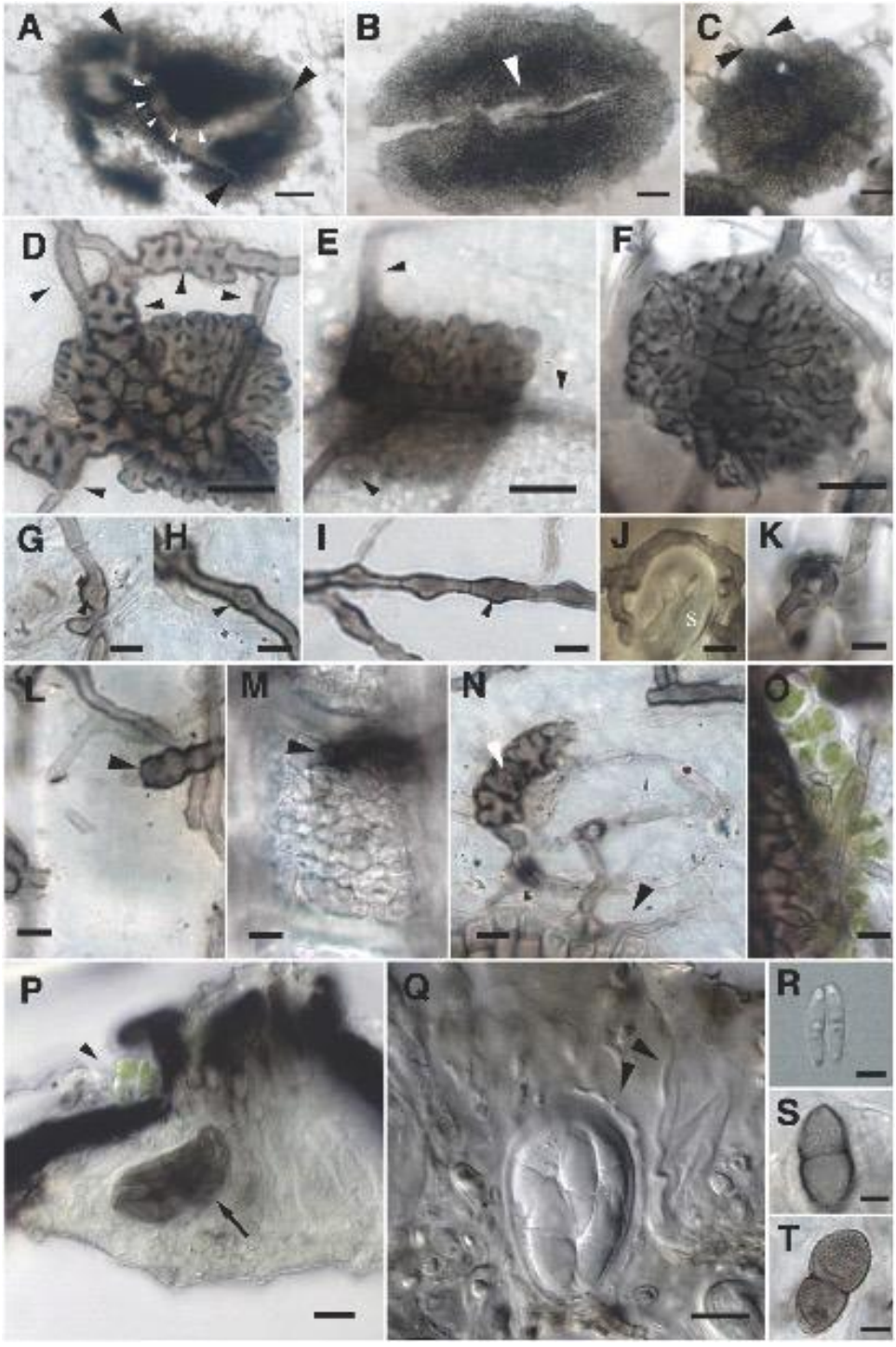
A
B
C
D
E
F
G
H
I
J
K
L
M
N
O
P
Q
R
S
T

Figure 3.2 Morphological characters of extant Aulographaceae.
A. Mature thyriothecium of *Aulographum* sp. UBC F33038 splits along irregular slits (black arrowheads) to reveal thyriothecium of *Microthyrium sp*. (white arrowheads) that it had overgrown. B, C. *Lembosina aulographoides* UBC F33037. B. Mature thyriothecium with elongate outline; irregular longitudinal slit (white arrowhead). C. Opaque thyriothecium grows around hyaline host trichome (black arrowheads). D. Early development in *Aulographum* sp. where multiple generator hyphae cooperate in scutellum formation (black arrowheads). E, F. Early development in *L. aulographoides*. E. Thyriothecium initiated from multiple generator hyphae (black arrowheads). F. Thyriothecium from single generator hypha. G, H. Intercalary appressoria and penetration pegs (black arrowheads) from *Aulographum* sp. on leaf cuticle. I. Appressoria in every hyphal segment of *Aulographum* sp. (CBS 143545 ex UBC F33038) grown on microscope slide. J. Hyphae of *L. aulographoides* surrounding stoma (S) of *Rhododendron*. K. Hyphae of *L. aulographoides* penetrating host at base of trichome. L, M. *Aulographum* sp. connection between hyphae on leaf surface and subcuticular internal hyphae at different focal planes. L. Surface hypha with appressorium (black arrowhead). M. Within host epidermal cells, appressorium out of focus (black arrowhead), but intricate pattern of intercellular growth revealed. N. *Aulographum* sp. pigmented hypha with penetration peg (white arrowhead) growing over and possibly parasitizing light-colored hypha attached to near-by thyriothecium of *Microthyrium* sp. (black arrowhead). O, P. *Lembosina* sp. (UBC F33044). O. Algae aggregated around scutellum. P. Cross section showing mature ascus (black arrow) and algae sticking to scutellum (black arrowhead). Q. Young asci and pseudoparaphyses (black arrowheads) of *Lembosina aulographoides.* R, S, T. Ascospores of three species of *Aulographaceae*. R. *Aulographum* sp. S. *L. aulographoides.* T. *Lembosina sp.* UBC F-33045. Illustration of manually assembled stacks of two focal planes in Figs. A, J; three focal planes in Figs. D, S; 5, 9 and 6 focal planes in Figs. B, C and F, respectively. All other illustrations are of a single focal plane.
Bars: A = 50 µm; B, C = 20 µm; D, E, F, P, Q = 10 µm; G, H, I, J, K L, M, N, O, R, S, T = 5 µm.

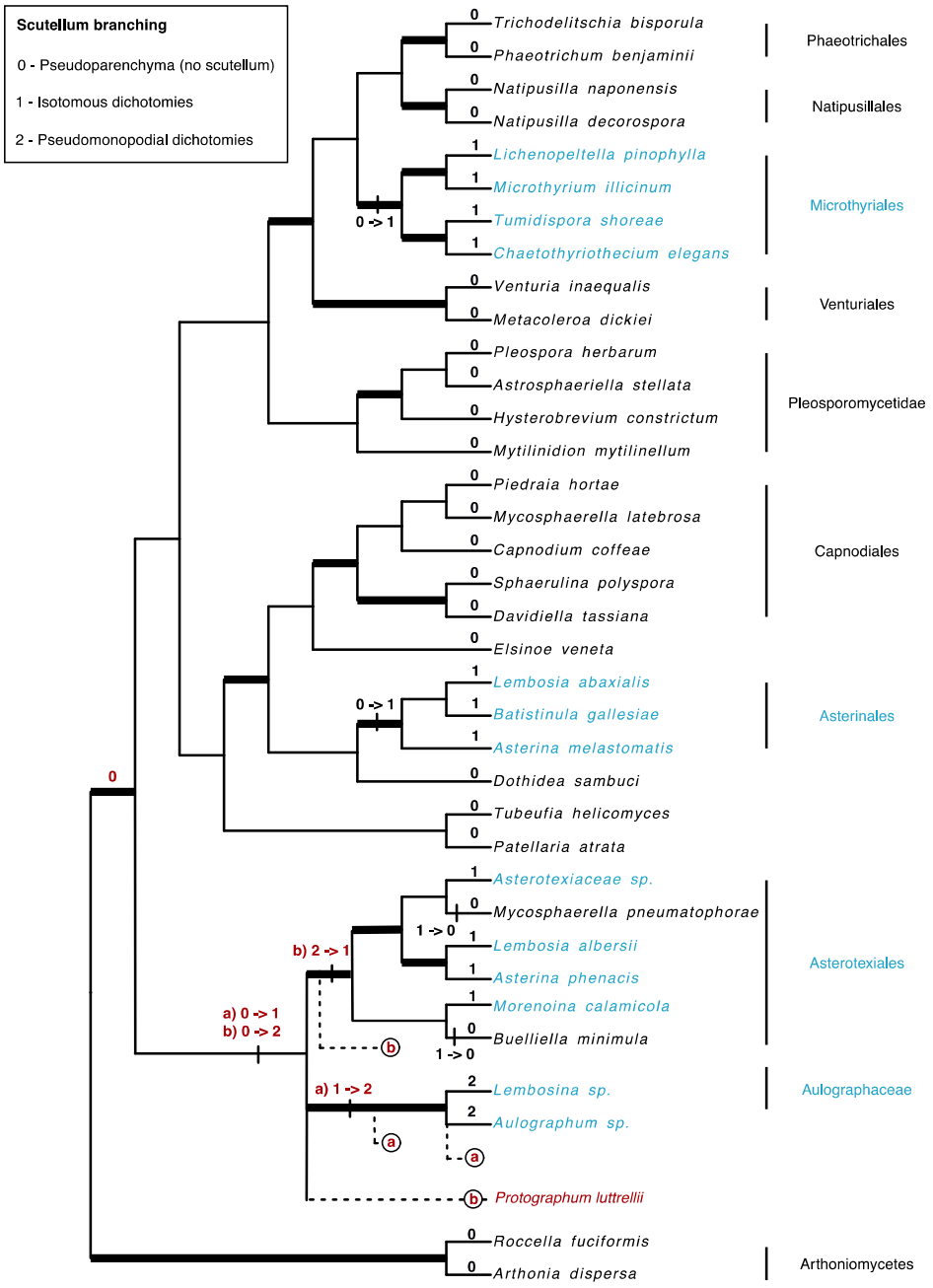

Figure 3.3 Most parsimonious placement of the fossil *P. luttrellii* in a constrained phylogeny of 36 Dothideomycetes.

Dashed branches represent alternative character transitions 'a' or 'b.' The branch labelled *P. luttrellii* represent one of the four equally parsimonious solutions and is equivalent to the strict consensus tree of all four possible scenarios. Thickened branches indicate maximum likelihood bootstrap probabilities > 80% and MrBayes posterior probabilities = 1 from the molecular phylogeny. Blue indicates thyriothecial scutella; red indicates fossil taxon.

3.6.3 Comparison of *Protographum luttrellii* to other fossils of thyriothecioid sporocarps

The oldest of the fossils that might represent Dothideomycetes-like thyriothecioid fungi comes from the Lower Triassic of India (Induan, ~251 Ma, Mishra et al., 2018, Fig. 8j). This fossil, identified only as a "fungal thallus" was found in a core sample from a palynological survey (Mishra et al., 2018, Fig. 8j). It is a roughly circular structure of radiating, hypha-like filaments that appear to dichotomize. Its filaments have regular cross septa giving rise to cells that appear square in dorsal view, forming partial concentric rings. Thick-walled cells with small lumina surround an ostiole-like central opening in the centre. The outer tips of filaments bow outwards, giving the structure a scalloped margin. This Indian specimen lacks pseudomonopodial dichotomous hyphae as seen in *Protographum,* and the structure was found dispersed (not associated with a host), so the development of a scutellum or the host plant cannot be assessed. While the Indian specimen probably represents a fungus in Dothideomycetes, it is probably not a member of Aulographaceae, and it is therefore distant from *Protographum*.

Dilcher (1965) described *Plochmopeltidella* antiqua from the early Eocene of western Tennessee from the surfaces of cuticle of *Sapindus*. These fungi are represented by scutella that are 50–75 μm in diameter, round but not radiate, and lacking a well-defined margin. They are composed of tightly interwoven hyphae of equal width with no evidence of dichotomies. Scutella appear to originate from multiple generator hyphae as in *Protographum*, but are pseudoparenchymatous rather than radiate in construction. *Plochmopeltidella antiqua* resembles extant *Plochmopeltidella* (Micropeltidaceae), with which it shares a number of characters (Dilcher, 1965).

Bannister et al. (2016) illustrated a late Eocene radiate scutellum from the Pikopiko Fossil Forest site of New Zealand. This specimen has not been named, but the scutellum was

described as circular to elongate, 27–50 μm in diameter, with interwoven convoluted hyphae, and radiate marginal hyphae that give the margin a slightly fringed appearance (Bannister et al., 2016, Fig. 3I). No ostiole, superficial hyphae or spores were reported. The illustration of this structure (Bannister et al., 2016, Fig. 3I) shows that its hyphae produced pseudomonopodial dichotomies, most of which can be traced to the centre of the scutellum, as in *Protographum*. It is possible that this fossil scutellum represents an Eocene occurrence of Aulographaceae; however, the multiple generator hyphae that would further support identification are not evident in the photograph.

Fossils of *Euthythyrites oleinitis* on cuticles of *Oleinites willsii* from the middle Miocene Yallourn Brown Coal (Australia) are described from two illustrated specimens (Pl.12, Figs.12–13 of Cookson, 1947). Cookson (1947) and Kalgutkar and Jansonius (2000) proposed affinities of *E. oleinitis* with *Aulographum hederae* var. *oleae* and *Lembosiopsis oleae*, both reported from extant oleaceous leaves. As with some specimens of *Aulographum* and *Lembosina*, fossils of *E. oleinitis* show branching sporocarps, one of which is Y-shaped. The sporocarps open by an irregular slit, and are connected to superficial mycelium at multiple points. Unlike *P. luttrellii* and Aulographaceae, scutella of *E. oleinitis* show dichotomous branching without overlap and they produce aligned, regularly septate hyphae distinct in growth form from pseudomonopodial dichotomies. The development and the appressed margin of scutella in *E. oleinitis* cannot be seen in the illustrations provided.

Fossils of various stages of development of *Euthythyrites morenoinitis* were found on cuticle of suspected Myrtaceae (Selkirk, 1969, Figs. 40–47; 1975) from the early Miocene of Kiandra (Australia). Selkirk (1975) compared *E. morenoinitis* to extant *Lembosina*, *Echidnodella* and *Morenoina*. Like these three extant genera and others in Asterinales and Asterotexiales

(*Aulographina, Cirsosina, Dothidasteromella, Echidnodes, Lembosia*), *Euthythyrites morenoinitis* shows branched (Y-shaped) and unbranched, elongated scutella opening by a longitudinally oriented, irregular slit. Unlike *P. luttrellii* and Aulographaceae (e.g., *Lembosina*), scutella of *E. morenoinitis* are initiated from an intercalary generator hypha, and the scutellum grows with aligned, regularly septate hyphae that form isotomous dichotomies that do not overlap one another.

3.6.4 Significance

Protographum luttrellii is the oldest described fossil fungus with morphological characters known only in extant Aulographaceae. In comparing *P. luttrellii* to the known fossil record of Dothideomycetes, it becomes obvious that more studies of the morphology of extant taxa are necessary to put thyriothecial fungi into a proper phylogenetic context. In the absence of data on the development of sporocarps from one or multiple hyphae in most taxa used in my analysis, I cannot yet use these distinctive characters of Aulographaceae in formal parsimony analysis. However, I hypothesize that the initiation of scutella from multiple generator hyphae seen in *P. luttrellii* supports an affinity with Aulographaceae.

However much *P. luttrellii* looks like modern Aulographaceae, my phylogenetic analysis cannot yet resolve when the distinguishing characters found in this fossil evolved relative to the phylogeny of Dothideomycetes. For now, the ability of *P. luttrellii* to calibrate age of divergence in Dothideomycetes is uncertain, and depends on the timing of scutellum character evolution. We cannot rule out an early origin among crown Dothideomycetes for the characters in *P. luttrellii* (see Fig. 3.3). The Triassic "fungal thallus" (Mishra et al., 2018, Fig. 8j) is tangible evidence of Dothideomycetes of twice the age of *P. luttrellii*, and the age of crown

Dothideomycetes estimated by molecular clock analyses is even older, ~384 Ma (Lutzoni et al., 2018) or 267-430 Ma (Beimforde et al., 2014).

The power of *P. luttrellii* to constrain geological ages will increase if additional sampling of extant taxa suggests that characters such as initiation from multiple generator hyphae evolved within the Aulographaceae crown group (Chapter 2). *Protographum luttrellii* might then be old enough to constrain the geological age estimates for the Aulographaceae crown group. Whatever its phylogenetic position, the value of *P. luttrellii* goes beyond constraining the age of a lineage because it documents the minimum age for its combination of characters, information that may never be available from a phylogeny of modern taxa.

A molecular phylogeny combined with analysis of a matrix of morphological characters offers an objective basis for interpretation of fossil fungi that was previously lacking. Phylogenetic studies of change through time among fossil angiosperm leaves and pollen from Potomac Group fossils contributed robust information on geological age and character evolution in plants (Hickey and Doyle; Doyle and Upchurch). As with fossil pollen and leaves, close analysis of fly-speck fungi diversification through time has the potential increase the reliability of inferences about timing and patterns of evolution among Dothideomycetes and more broadly, among Ascomycota. Tracking Aulographaceae through the fossil record could prove fruitful as it seems their divergence from other living taxa lies among the deepest nodes of Dothideomycetes.

3.7 Conclusion

An appropriate focus on characters of fly-speck fungi using fossils opens the door for a better appreciation of their evolution through the combined study of extant and fossil characters. my phylogeny combined with a matrix of morphological characters offers an objective basis for

interpreting fossil fungi that has previously been lacking. The great diversity of extant scutella described by mycologists is matched by a diverse range of fossil forms that may or may not resemble extant lineages. I look forward to an increased appreciation of the diversity of thyriothecium-forming fungi because their fossil record is more promising than is currently recognized. They are found throughout the late Mesozoic and all the Cenozoic (Berbee et al., 2014). These fungi can be sampled reliably, and many thyriothecioid taxa exhibit unique character combinations that have escaped the notice of taxonomists until now. Tracking Aulographaceae through the fossil record could prove fruitful as it seems their divergence from other living taxa lies among the deepest nodes of Dothideomycetes. Comparative anatomy of fossil fungi will undoubtedly reveal new patterns of morphological evolution in Dothideomycetes and improve my understanding of those distinct evolutionary attempts that led to the variety of thyriothecia seen today.

Chapter 4: *Bleximothyrites ostiolatus gen. et sp. nov.* a unique fly-speck fungus (Dothideomycetes) from the Lower Cretaceous

4.1 Summary

I found well preserved thyriothecia (flat fungal sporocarps) growing on gymnosperm cuticle, in a survey of dispersed plant cuticles from the Lower Cretaceous of Virginia. Detailed analysis of their anatomy allows comparison of the fossil to extant taxa that form thyriothecia. Maceration of clays from the Potomac Group, lower Zone 1 (Aptian, 125–113 Ma) yielded a gymnospermous leaf cuticle with both abaxial and adaxial surfaces colonized by a single fungus producing multiple thyriothecia. I used a combined molecular and morphological dataset comprising 15 extant thyriothecia and 28 of their known relatives in Dothideomycetes to search for the most parsimonious placement of the fossil fungus. *Bleximothyrites ostiolatus gen. et sp. nov.* is the first fossil collected *in situ* on cuticle that produced thyriothecia sharing an ostiole and a radiate, dichotomizing hyphal construction common among living species. It is the second thyriothecial species described from the lower Potomac Group. Fly-speck fungi with radiate scutella appear to have evolved convergently in Dothideomycetes and my phylogenetic inferences place *B. ostiolatus* in several optimal positions, in each clade that contains ostiolate scutella. Like some modern taxa, thyriothecia of *B. ostiolatus* are connected to superficial mycelium, to intercalary and lateral appressoria, and to an extensive subcuticular *mycélium en palmettes*. *Bleximothyrites ostiolatus* provides early evidence of character state combinations and *in situ* growth habit of a thyriothecial dothideomycete. The scutellum of *B. ostiolatus* in dorsal view differs from available known lineages, and this fossil likely represents an extinct, or as yet unsampled, group of fly-speck fungi.

4.2 Introduction

Fungal taxonomic diversity appears to increase through the Cretaceous and Paleogene (reviewed in Tiffney and Barghoorn (1974). A variety of leaf-dwelling ascomycetous fungi enter the fossil record at the same time (Tiffney and Barghoorn, 1974; Elsik, 1978, 1993; Kalgutkar and Jansonius, 2000; Taylor et al., 2015) that flowering plants were diversifying (Friis et al., 2011; Doyle, 2012). The fossil record of ascomycetous fly-speck fungi on Lower Cretaceous plant cuticles reflects this pattern (Krassilov, 1967; Martínez, 1968; Alvin and Muir, 1970; Bajpai and Maheshwari, 1987; Estévez-Gallardo et al., 2015), as this type of sporocarp became increasingly diverse during the Paleogene (Dilcher, 1965; Selkirk, 1975; Elsik, 1978, 1993; Kalgutkar and Jansonius, 2000; Berbee et al., 2014; Taylor et al., 2015).

Fly-speck fungi form thyriothecia, which are flat and circular sporocarps that are superficial on plant surfaces, in which a scutellum, a shield of pigmented hyphae, overlies the spore-producing tissue (Arnaud, 1918; Stevens and Manter, 1925; Wu et al., 2011b; Guatimosim et al., 2015). Some thyriothecial species release spores through an ostiole, a circular opening in the scutellum (Eriksson, 1981; Hyde et al., 2013) (Chapter 2). The scutellum may be radiate, formed by hyphae that can be traced out from the centre of the scutellum to the margin, or nonradiate, formed by hyphae that are intertwined and cannot be traced (Luttrell, 1946) (Chapter 2). The tips of the scutellum hyphae of some genera branch isodichotomously into two, roughly equal branches (Chapter 2), while others produce anisotomous branches that appear pseudomonopodial (Chapter 2, 3). Until DNA sequence data became available, taxa with radiate scutella were classified in Microthyriales G. Arnaud, and taxa with non-radiate scutella were placed in Hemisphaeriales Theiss. (Arnaud, 1918; Stevens and Manter, 1925; Müller and von Arx, 1962). Additional characters relating to the mycelium, spores and scutellum dehiscence

helped to further distinguish families and genera (Stevens and Manter, 1925; Stevens and Ryan, 1939; Luttrell, 1946; Müller and von Arx, 1962; Eriksson, 1981). Phylogenetic studies using nuclear rDNA sequences showed that the non-radiate Hemisphaeriales evolved convergently in different classes of Ascomycota (Hongsanan and Hyde, 2017), while the radiate forms that were originally placed in Microthyriales are distributed in different clades within a single class, Dothideomycetes O.E. Erikss. & Winka. Clades of radiate thyriothecia include Asterinales M.E. Barr ex D. Hawksw. & O.E. Erikss, Asterotexiales Firmino, O.L. Pereira & Crous, Aulographaceae Luttr. ex P.M. Kirk, P.F. Cannon & J.C. David (Order *Incertae sedis*), Microthyriales, Muyocopronales Mapook, Boonmee & K.D. Hyde and Zeloasperisporiales Hongsanan & K.D. Hyde (Hofmann et al., 2010; Hofmann and Piepenbring, 2011; Wu et al., 2011b; Hyde et al., 2013; Hongsanan et al., 2014b; Ertz and Diederich, 2015; Guatimosim et al., 2015; Hongsanan et al., 2016). Combinations of characters relating to mycelium, thyriothecium dehiscence mechanism (Wu et al., 2011b; Hongsanan et al., 2015) and ascus and ascospore morphology (Mapook et al., 2016a; Mapook et al., 2016b) help characterize some of these lineages. Scutellum morphology can also be phylogenetically informative (Hongsanan and Hyde, 2017) (Chapter 2). Additionally, appressoria, hyphal structures that the fly-speck fungi usually uses to enter the host plant, are anatomically diverse and may be systematically informative (Arnaud, 1918; Hofmann, 2009; Guatimosim et al., 2015).

Because fossil fly-speck fungi are usually found preserved as scutella with mycelium, without the underlying spore producing tissue, their classification has relied on anatomical characterization of scutellum and mycelium (Kalgutkar and Jansonius, 2000). The best characterized fossils of thyriothecia are from the Eocene and include *Asterina eocenica* Dilcher (Dilcher, 1965) and *Trichothyrites setifer* (Cookson) Saxena & Misra (Smith, 1980), as shown in

Chapter 2. These fossils serve to record the origin of crown lineages of Dothideomycetes. *Asterina eocenica* was found on angiosperm cuticle, preserved with its mycelium and spores, and is so complete that Dilcher (Dilcher, 1965) placed this fossil in *Asterina* Lév., a living genus. Dispersed fossils of *T. setifer* resemble the living genus *Lichenopeltella* Höhn., provisionally placed in Microthyriales (Chapter 2). Geologically older Cretaceous thyriothecia tend not to resemble any particular lineage of living fly-speck fungi that have yet been included in molecular analyses (Krassilov, 1967; Martínez, 1968; Alvin and Muir, 1970; Bajpai and Maheshwari, 1987; Estévez-Gallardo et al., 2015), with the exception of *Protographum luttrellii* Le Renard, Upchurch, Stockey & Berbee in Aulographaceae (Chapter 3). A detailed characterization of scutella and associated mycelia allows new fossils to be interpreted using phylogenetic approaches (Chapter 2).

In a survey of angiosperms from the Lower Cretaceous Potomac Group, Upchurch recognized abundant fungal colonization on the cuticles of leaf surfaces (Upchurch and Doyle, 1981; Upchurch, 1984a, b). Chapter 3 and the current study of additional Potomac Group (lower Zone 1) sediments reveal abundant fungal remains on gymnosperm leaf cuticles. Here, I describe a fossil fungal morphotype with scutella at different developmental stages, collected from a leaf of an extinct gymnosperm. I infer the phylogenetic relationships of ostiolate and radiate thyriothecial lineages and their sister clades using available nuclear rDNA sequences, and score the morphology of the fossil and the extant taxon. By using the resulting rDNA topology as a constraint, I infer most parsimonious placements of the fossil fungus using a matrix of morphological characters.

4.3 Materials and methods

Fossils were collected on the south side of Dutch Gap Canal, near James River, Virginia (Hickey and Doyle, 1977; Upchurch and Doyle, 1981; Upchurch, 1984b). Dutch Gap Canal sediments (37.3760000°, -77.3593000°, locality DMNH 128) consist of clay beds exposed at low tide, dated as lower Zone I of Brenner (1963), or Aptian (125–113 Ma) based on the palynoflora (Doyle and Hickey, 1976; Upchurch and Doyle, 1981; Doyle and Upchurch, 2014, and references therein). Sampled clays are from the so-called *Pseudofrenelopsis* bed, the lowest exposed sediments, which also yielded shoots of *Pseudofrenelopsis parceramosa* (Fontaine) Watson, leaves of the extinct bennettitalean gymnosperm *Dioonites buchianus* Fontaine, and shoots of early herbaceous angiosperms (Upchurch and Doyle, 1981; Doyle and Upchurch, 2014; Jud, 2015).

4.3.1 Cuticle preparation

I modified a cuticle extraction protocol from Upchurch (1989) by immersing 200 g of clay in saturated household trisodium phosphate solution (TSP; Rescochem, Québec**)** and adding 10% hydrogen peroxide (H_2O_2) to release cuticles from the matrix. The solution was left to react slowly for up to 36 h, and I collected the accumulated foam containing organic debris at regular intervals (3–6 h). This organic debris was rinsed in 70% EtOH, extracted in two fractions using 200 µm and 90 µm sieves, and stored in 50% ethanol. Cuticles were examined in solution under the dissecting microscope, and those with fungal colonization were removed with an insect pin (size 0, Austerlitz insect pins, Slavkov u Brna, Czech Republic). Cuticle fragments were spread onto a glass slide using insect pins under a dissecting microscope. Specimens were then mounted in Eukitt, xylene soluble mounting medium (O. Kindler GmbH, Freiburg, Germany). The

holotype is deposited in the Department of Earth Sciences, Denver Museum of Nature and Science, Denver, CO, under Accession 2019-55, slide #EPI 53111. The fungal holotype specimen is on the surface of a single gymnosperm cuticle, broken in two pieces mounted on the same slide. A second cuticle of the same host plant species, also illustrated here, was found among other cuticles and was deposited at DMNS, slide #EPI 53112 (cuticle fragment DG-106.A, England Finder coordinates J47–N42; label on specimen slide to the right).

4.3.2 Microscopy and image processing

Plant cuticles and fungi were observed using different setups: a Leica DMRB (Leitz, Germany) DIC microscope with a Leica DFC420 digital color camera, or a Powerphase (Phase One, Copenhagen) digital scanning camera mounted on a Leitz Aristophot bellows camera, or a Zeiss WL compound microscope. I assembled more than one focal plane into brightfield stacks in Photoshop CC 2015.1.2 (1990 – 2019, Adobe Systems, California) following Harper (2015), and using suggestions from Bercovici et al. (2009). Many of the dark fungal structures contrast with the cleared cuticles and benefit from post processing, using image adjustments settings in Photoshop to reveal the outline of scutellum hyphae in greater detail.

4.3.3 Phylogenetic analyses

Using available nuclear rDNA large subunit (LSU) and small subunit (SSU) sequence data from 41 taxa of Dothideomycetes and two outgroups, I inferred a phylogeny of the five main lineages of fungi that form radiate thyriothecia. For each lineage containing thyriothecial sporocarps, I included non-thyriothecial sister taxa when known. The dataset includes four taxa in Microthyriales and six taxa in sister clades Phaeotrichales Ariyaw., Jian K. Liu & K.D. Hyde,

Natipusillales Raja, Shearer, A.N. Mill. & K.D. Hyde, and Venturiales Yin. Zhang, C.L. Schoch & K.D. Hyde, three thyriothecium-forming Asterotexiales and two of their non-thyriothecial relatives, and three taxa in Muyocopronales and two of their perithecioid relatives in the Dyfrolomycetales K.L. Pang, K.D. Hyde & E.B.G. Jones. The remaining two lineages, Asterinales (three taxa) and Aulographaceae (two taxa), are poorly sampled to date, and their closest relatives are still unknown within Dothideomycetes. I included taxa in distant diverse lineages of Dothideomycetes from the following well characterized orders (Hyde et al., 2013): Abrothallales Pérez-Ort. & Suija, Capnodiales Woron., Dothideales Lindau, Hysteriales Lindau, Mytilinidiales E. Boehm, C.L. Schoch & Spatafora, Patellariales D. Hawksw. & O.E. Erikss., Pleosporales Luttr. ex M.E. Barr and Tubeufiales Boonmee & K.D. Hyde; and two outgroup taxa in Class Arthoniomycetes O.E. Erikss. & Winka (Appendix S1).

Sequences of the LSU and SSU regions of rDNA genes were each aligned using the iterative refinement method G-INS-I in MAAFT v7 (Katoh and Standley, 2013), manually excluding positions that were ambiguously aligned in Mesquite version 3.31 (Maddison and Maddison, 2015), resulting in a concatenated dataset of two partitions spanning 2578 nucleotide positions. I used JModeltest 2 (Darriba et al., 2012) to recover the GTR+G model for each partitions (LSU and SSU), and used RaxML v.8 (Stamatakis, 2014) to search of the best tree, with 500 independent searches (Appendix S2). Branch support was assessed with 1000 bootstrap replicates (BS) (Felsenstein, 1985). For Bayesian analysis, I used MrBayes 3.2.6 and two independent searches with four MCMC chains each, for 20 million generations, sampling every 1000 trees (Appendix S3). The convergence of independent runs was assessed using Tracer 1.6 (Rambaut and Drummond, 2013), and posterior probabilities (PP) summarized on the most likely topology after I discarded 25% of burn-in. I used the online CIPRES portal to run JModeltest,

RaxML and MrBayes analyses (Miller et al., 2010). I then used the most likely topology from RAxML as a topological constraint to find the most parsimonious placement of the fossil as described below.

4.3.4 Matrix of morphological characters and parsimony analysis

I assembled a matrix of nine characters found in the fossil fungus that could also be scored for extant, vouchered taxa with available rDNA sequences based on published illustrations and descriptions, Appendix S4. The characters used in the analysis include the *sporulation substrate* (on mineral substrates; superficial on plants; on lichens; immersed in plants), *sporocarp type* (apothecioid; perithecioid; thyriothecioid; cleistothecioid), state of the *sporocarp lower wall* (undifferentiated; differentiated), state of the *ostiole* (absent in all life stages; present at least in one sporulating stage), *sporocarp outline* (circular; elongate), *sporocarp* type (non-radiate; radiate), *hyphal branching pattern of sporocarp wall* (pseudoparenchymatous; isodichotomous; pseudomonopodial dichotomies), state of the *hyphal tips at appressed margin of scutellum* (absent/pseudoparenchymatous; aligned rounded tips; aligned blunt tips; divergent, rounded tips), *appressoria with pigmented penetration peg* (absent; present) and type of *sporocarp lower wall* (unpigmented; pigmented). The resulting character matrix for extant and new fossil taxa is presented in Appendix S4, including the literature or vouchered specimens consulted for scoring characters. The most parsimonious position(s) of the fossil taxon were inferred for the morphological matrix, with a molecular constraint topology, using branch-and-bound search in PAUP 4.0a166 (Swofford 2003). Alignments, phylograms, and cladograms are available from TreeBASE (Submission ID: 25164).

4.4 Results

4.4.1 Host cuticle colonized by fungus

The fossil thyriothecia occur on both adaxial and abaxial surfaces of the cuticle of a gymnospermous leaf (Fig. 4.1A–1B, arrows). Dispersed pollen found on the cuticle surface is gymnospermous and of the *Classopollis* Pflug and *Eucommiidites* Erdtman types. The cuticles of the upper and lower leaf surfaces on the holotype were split apart during preparation and remain together on the same slide (Fig. 4.1A–1B, labelled). A similar cuticle without the fungal infection is illustrated in Fig. 4.3. The leaf is amphistomatic (Fig. 4.1A). Epidermal cells on the leaf adaxial surface are rectangular, with horizontal or oblique end walls, and are 82.5 μm (40–125 μm) long by 22.5 μm (15–30 μm) wide (Fig. 4.1A). They are organized into distinct rows and are more elongate and regular in shape than those on the abaxial surface (Fig. 4.1A). All pavement (epidermal) cells have similar cuticular thickness; thick- and thin-walled cells are absent. The anticlinal wall contour is predominantly straight to curved, never undulate. Stomata are sparse on the adaxial epidermis and are similar in structure to those of the abaxial epidermis.

Cells of the abaxial epidermis are 50 μm (35–65 μm) long by 25 μm (18–32 μm) wide. Abaxial epidermal cells are quadrangular to polygonal near the stomata, and more rectangular in stomatal free zones (Fig. 4.1A–1C). Thick-and thin-walled cells are absent. The anticlinal wall contour ranges from straight to curved and is never undulate. Stomata are dense on the abaxial epidermis and form a zone in which the stomata are scattered and not in regular rows (Fig. 4.1A–1B). Stomatal complexes average 60 μm (48–72 μm) long by 54 μm wide (42–66 μm). Guard cells are sunken and of the gymnospermous type, with raised poles, polar extensions, and a lack of stomatal ledges. Guard cells average 16.5 μm long (12–21 μm) by 7.5 μm wide (6–9 μm) and are oriented parallel to oblique to the long axis of the leaf (Figs. 1D, 2A–2C). Transversely

oriented stomata have not been observed. Stomatal openings are up to 6 μm wide. Papillae are absent.

Stomatal complexes are monocyclic, with subsidiary cells that are darker in color and have thicker cuticle than the surrounding epidermal (pavement) cells (Fig. 4.1A–1C). Four to six subsidiary cells occur per stomatal complex, with five and six being the most common numbers (Figs. 4.1D, 4.2A–4.2C). Occasionally subsidiary cells from adjacent stomata contact one another (Figs. 4.1C, 4.2A), but no stomatal complexes share subsidiary cells. Polar subsidiary cells can be absent (e.g., Fig. 4.1D, lower right), and the poles of the guard cells often coincide with a lateral subsidiary cell wall. Polar extensions are more easily visible when they do not overlap a subsidiary cell wall flange (Fig. 4.2B, upper left). Encircling cells are weakly developed (Fig. 4.1A–1D).

4.4.2 Description of fungi

Leaf surfaces show abundant fungal remains (Fig. 4.1A–1B), and subcuticular hyphae (Fig.4. 2D–2E) are common throughout. Sixteen fungal fruiting bodies of the same type have been identified on the adaxial surface of the leaf and five on the abaxial surface (Fig. 4.1A–1B). These sporocarps are circular, shield-like, and are each covered by a scutellum (upper wall) that is appressed to the host surface at its margins (Fig. 4.3A–4.3D). Most scutella are broken, and only the appressed margins remain, although four are completely preserved (three illustrated in Fig. 4.1A–4.1B). Scutella are 85–240 μm in diameter, composed of intermingling hyphae (1–4 μm wide) radiating out from the centre, and are preserved in different stages of development (Fig. 4.3A, 4.3C–4.3D). Branching of the hyphae is isodichotomous, and septation is present throughout (Fig. 4.3A, 4.3D). In the most complete sporocarps, an ostiole is seen at the centre of

the scutellum (Figs. 4.1A–4.1B, 4.3A–4.3D). Hyphal branching is dense near the ostiole, and hyphae appear pseudoparenchymatous (Fig. 4.3A–4.3B). Hyphae at the edge of older (larger) scutella branch less frequently, overlap, and diverge from the radial alignment (Fig. 4.3C–4.3E). In smaller scutella, this character is less prominent (Fig. 4.3A), and the hyphae do not taper at the growing tip (Fig. 4.3A); tapering is seen only in larger and broken scutella (Fig. 4.3D–4.3E). Tapering hyphae are 2 μm wide or less at the margins of older scutella, and less densely septate than in the centre of the scutellum (Fig. 4.3E).

Although fungal spores were found on both cuticle surfaces, they were not attached or found inside scutella (Fig. 4.3F–4.3G), so the connection is unclear. Spores are smooth, ellipsoidal, laterally flattened, 12 μm long by 8 μm wide, with a blunt base and an apical pore (Fig. 4.3F–4.3G).

Subcuticular mycelium is found below all scutella (Fig. 4.2E). The mycelium indiscriminately colonizes stomatal complexes, subsidiary cells, and epidermal cells (Figs. 4.2D–4.2E, 4.4A–4D). Subcuticular hyphae show dense, dendritic branching patterns (Fig. 4.4A–4.4E), forming extensive *mycélium en palmettes* (Ducomet, 1907). This subcuticular mycelium forms anisodichotomies at first, where some hyphae become wider than their adjacent branches (Fig. 4.4A). As it enlarges and covers individual host cells, this mycelium appears particularly dense and conspicuous on the cuticle at cell wall flanges, appressed in the lower face of the cuticle (Figs. 4.2D–4.2E, 4.4A–4.4C). Hyphae of the subcuticular mycelium show small, dark, punctate structures, < 1 μm in diameter, that I interpret as penetration pegs (Figs. 4.2E, 4.4D–4.4E). On close examination of the cuticle surface, superficial hyphae are found to be connected to the subcuticular mycelium via appressoria (Fig. 4.4B, 4.4F–4.4G). Appressoria are often associated with swollen hyphal segments, up to 5μm wide, which display pigmented penetration

pegs (Fig. 4.4B, 4.4F–4.4G). Seen from the top, *mycélium en palmettes* growing at a right angle appears on both sides of the host cell walls (Fig. 4.4B–4.4C). The *mycélium en palmettes* also proliferates from one cell to another, within the cuticle (Fig. 4.4A)., branching profusely and coating individual epidermal cells (Fig.4. 4B, 4.4D).

4.4.3 Phylogenetic analysis

The maximum likelihood search resulted in a completely resolved tree, while the consensus tree from the posterior distribution of the MrBayes analysis included a polytomy around the deepest divergences in Dothideomycetes (Appendices C.2, C.3). Both maximum likelihood and Bayesian analyses resulted in topologies with five distinct and supported lineages of radiate thyriothecium forming fungi (Fig. 4. 5, Appendices C.2, C.3). In both analyses, lineages forming thyriothecia were polyphyletic. Taxa in Aulographaceae, represented by *Aulographum* Lib. and *Lembosina* Theiss. formed a monophyletic group (BS=100, PP=1). The sister clade of Aulographaceae in the best tree has negligible bootstrap and Bayesian support (BS=26, PP=0.22). Asterinales and Asterotexiales were both found to be monophyletic (BS=100, PP=1, and BS=87, PP=99, respectively). Although the trees indicated a sister relationship between Asterinales and Asterotexiales, this result received low branch support (BS=23, PP=0.23). Taxa in Muyocopronales form a clade (BS=1, PP=100) that is supported as the sister group of Dyfrolomycetales (BS=100, PP=1), an order that is also well supported (BS=100, PP=1). Microthyriales formed a clade (BS=86, PP=1) that is the sister group of Phaeotrichales and Natipusillales; and all three orders consistently grouped together with the order Venturiales in both analyses with moderate to strong support (BS=72, PP=1).

Possible relationships of the fossils were inferred using a parsimony analysis with the nine morphological characters that could be coded for *B. ostiolatus* and for 11 extant taxa in my dataset (Appendix C.4). The remaining 33 taxa could not be scored for the presence of appressoria. A branch-and-bound search revealed 14 equally parsimonious trees (= 14 possible fossil placements) of 62 steps that were compatible with the topological constraint from the likelihood phylogeny (Fig. 4.5).

The consensus position of *B. ostiolatus* is among unresolved, early branches in the phylogeny of Dothideomycetes (Fig. 4.5). *Bleximothyrites ostiolatus* shares eight morphological characters with *Microthyrium ilicinum.* Three of the fourteen equally parsimonious placements of *B. ostiolatus* occur near the divergence of *M. ilicinum* (Fig.4.5, labelled in red) from its sister clade *Lichenopeltella pinophylla.* The eleven remaining most parsimonious placements suggest possible affinities of *B. ostiolatus* with taxa that are missing data (Fig. 4.5, labelled in turquoise). Radiate and ostiolate thyriothecial taxa missing data for appressoria include *Chaetothyriothecium elegans* Hongsanan & K.D. Hyde and *Tumidispora shoreae* (both in Microthyriales), *Muyocopron dipterocarpi* and *M. lithocarpi* (in Muyocopronales) and *Discopycnothyrium palmae* (in Asterotexiales). Because these five taxa also shared seven characters with *B. ostiolatus*, they allowed for equally parsimonious placements of the fossil with two additional taxa in Microthyriales, one taxon in Asterotexiales and two taxa in Muyocopronales. The unique mode of branching and organization in distal margins of *B. ostiolatus* scutella (Fig. 4.3) can for now be considered unique and an autapomorphy of the fossil taxon.

4.5 Taxonomy

Phylum: Ascomycota Caval.-Sm.

Class: Dothideomycetes O.E. Erikss. & Winka

Family: Incertae sedis

Genus: *Bleximothyrites* Le Renard, Upchurch, Stockey & Berbee *gen. nov.*—MycoBank number: MB832577

Generic diagnosis: Mycelium superficial on leaves, hyphae septate with intercalary and lateral appressoria (Fig. 4.4B, 4.4F, 4.4G). Sporocarp circular, covered by a shield-like dorsal scutellum, appressed to host surface. Scutella radiate, composed of intermingling hyphae radiating out from centre through isodichotomous branching diagnostic of Dothideomycetes thyriothecia (Fig. 4.3A). Hyphal branching at centre of scutellum dense (Fig. 4.4A–4.4B, 4.4D). Hyphae at scutellum edge branch less frequently, overlap, diverging from radial alignment (Fig. 4.4B–4.4E). Hyphal tips narrow near margin of scutellum (Fig. 4.4E).

Comments: *Bleximothyrites ostiolatus* is distinguished from other fossil taxa by the ostiolate scutella with isodichotomous branching hyphae that diverge from radial alignment distally. Due to its lack of asci and ascospores, the fossil cannot be placed in a living genus

Etymology—The generic name bléximo- comes from the Greek for "a confused mass of something twisted together", and refers to the entangling of hyphae at the edge of the scutellum. Thyr refers to the thyriothecia it produces (thureos = shield in Greek); and the suffix -ites indicates its fossil nature.

Type species: *Bleximothyrites ostiolatus* Le Renard, Upchurch, Stockey & Berbee *sp. nov.*—MycoBank number: MB832578.

Figs. 4.1A, 4.1B, 4.2D, 4.2E, 4.3A–4.3E, 4.4

Specific Diagnosis: Thyriothecium ostiolate, radiate, with isodichotomous branching, lower wall undifferentiated (Fig. 4.4A–4.4D), a plesiomorphic combination in Dothideomycetes

thyriothecia. Area near ostiole with pseudoparenchymatous hyphae. Surface hyphae connected to subcuticular mycelium via appressoria with pigmented, penetration pegs. Sub-cuticular hyphae dendritic, forming extensive *mycélium en palmettes* (palm-frond-like lobes of densely branching subcuticular hyphae) of uncertain systematic importance.

Etymology: The specific epithet refers to the presence of an ostiole.

Holotype *hic designatus*: Slide DG-090 deposited in the Department of Earth Sciences, Denver Museum of Nature and Science, Denver, CO, under Accession 2019-55, slide #EPI 53111. Specimen is on surface of gymnospermous cuticle.

Locality: The Dutch Gap Canal locality (37° 22’ 33.8” N, 77° 21’ 33.6” W; UTM 291098.50 Easting, 4139202.60 Northing, locality DMNH 128), James River, Virginia.

Stratigraphic position and age: Potomac Group, lower Zone 1, *Pseudofrenelopsis parceramosa* bed; Aptian (Lower Cretaceous, 125–113 Ma).

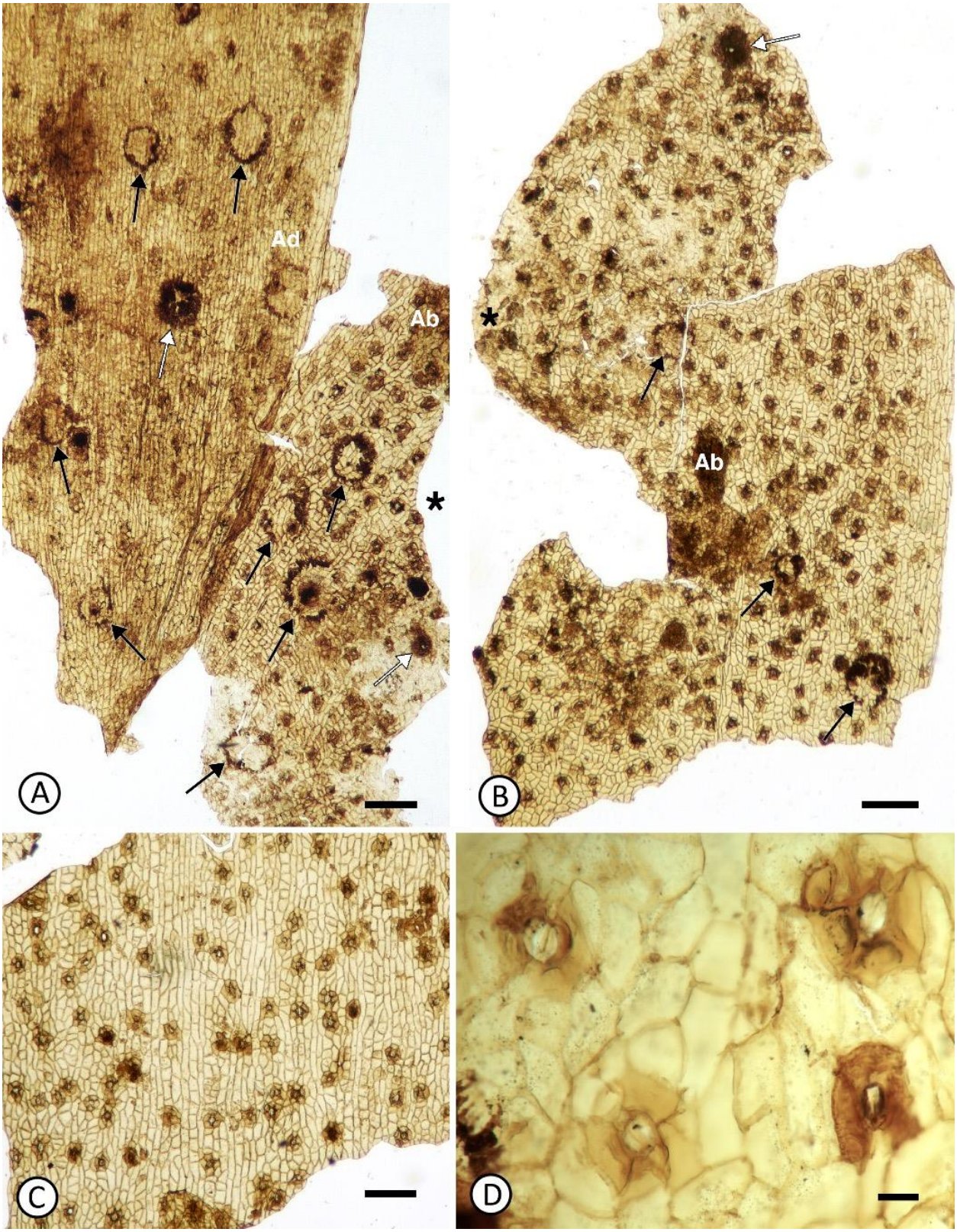
Ad
Ab
*
A
Ab
*
B
C
D

Figure 4.1 Fossils of *Bleximothyrites ostiolatus gen. et sp. nov.* on Lower Cretaceous (125–112 Ma) cuticle.

A, B. Overview of cuticle of single leaf colonized by *B. ostiolatus*. Two cuticle fragments were attached at edges labelled with stars (*), fungal thyriothecia, black arrows; Holotype, DMNS EPI.53111. A. Cuticle colonized by thyriothecia of *B. ostiolatus;* abaxial (Ab), adaxial (Ad) surface of same cuticle. Note: stomata on abaxial side more numerous than adaxial surface. B. Smaller fragment showing only abaxial surface (Ab) in second piece of cuticle in Fig. 5.1A. Complete fungal scutella indicated with white arrows; broken sporocarps with black arrows. C, D. Gymnosperm cuticle similar to host of *Bleximothyrites*, not colonized by fungus, DMNS EPI.53112. C. Overview of cuticle. D. stomatal complexes. Bars: 200 µm (A–C), 20 µm (D).

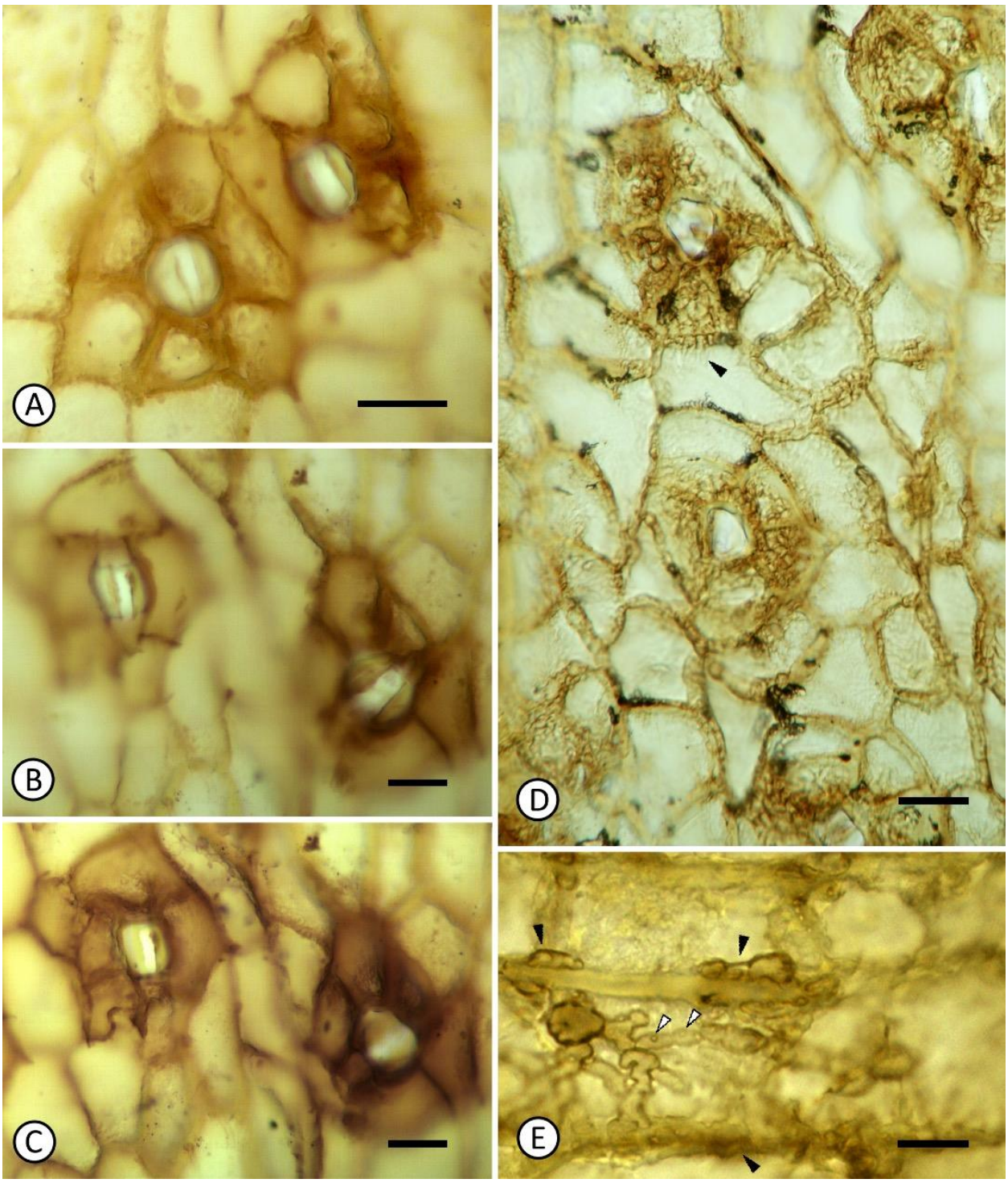
A
B
C
D
E

Figure 4.2 Morphology of host plant cuticle and fungal colonization by *Bleximothyrites ostiolatus gen. et sp. nov.*
A. Two adjacent stomatal complexes from uncolonized cuticle showing brown pigmentation of thick cuticle on subsidiary cells in absence of fungus. Three focal planes (f.p.) stacked; DMNS EPI.53112. B, C, Uncolonized stomatal complexes at two different focal planes; DMNS EPI.53112. B. Stomata at level of sunken guard cell cuticle showing polar extension. C. Stomatal complexes showing four and five subsidiary cells. D. Epidermis and stomatal complexes colonized by mycelium of *B. ostiolatus* at boundary between host cells. Note mycelium changes orientation toward the upper surface of host cell, and branches dichotomously before going out of focus, lining lower face of cuticle; black arrowhead; Holotype DMNS EPI.53111. E. Subcuticular mycelium showing irregular, lobed cells connected to surface mycelium by dark penetration pegs (white arrowheads), and hyphae at cell flanges in cross section, following lower cuticle surface labelled (black arrowheads). Holotype DMNS EPI.53111. Bars: 20 µm (A–D), 10 µm (E).

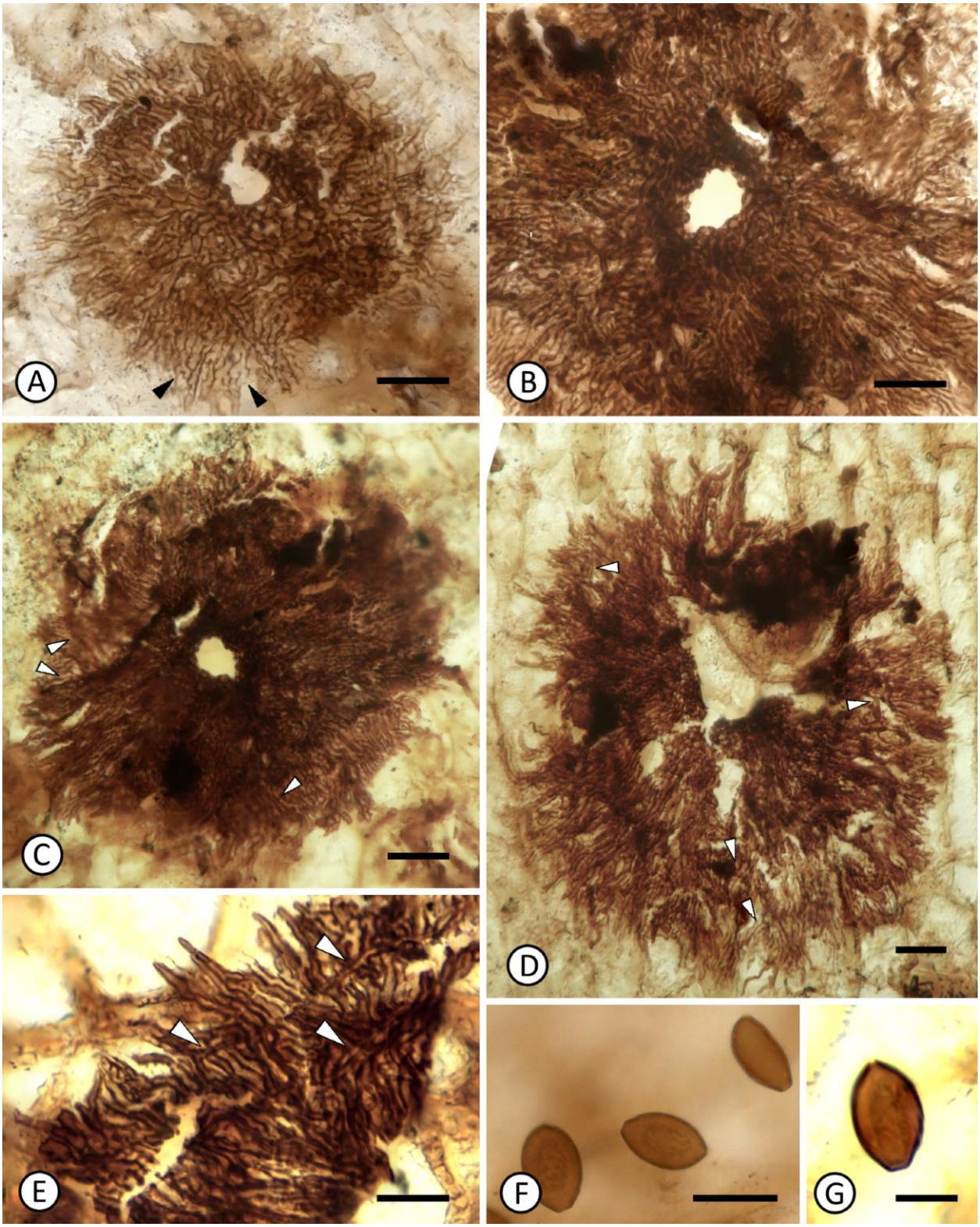
A
B
C
D
E
F
G

Figure 4.3 Morphology of scutella in *Bleximothyrites ostiolatus gen. et sp. nov.*
A. Small sporocarp, showing radiate, ostiolate scutellum produced by successive isodichotomies (black arrowheads). Note pseudoparenchyma around ostiole; eight focal planes (f.p.) stacked. B. Central area of ostiole in large sporocarp showing transition from pseudoparenchyma near ostiole to more radiating hyphae of distal zone; eight f.p. stacked. C, D. Mature thyriothecium with distal hyphae deviating from radial alignment of scutellum (white arrowheads); C and D each from three f.p. stacked. E. Distal margin of mature scutellum showing hyphae deviating from radial alignment of scutellum (white arrowheads) and tapering hyphal tips. F, G. Conidia of associated unknown fossil taxon showing blunt scar on one end and apical germ pore. F and G each from three f.p. stacked. Holotype DMNS EPI.53111. Bars: 10 µm (A–B, E–F); 20 µm (C–D); 5 µm (G).

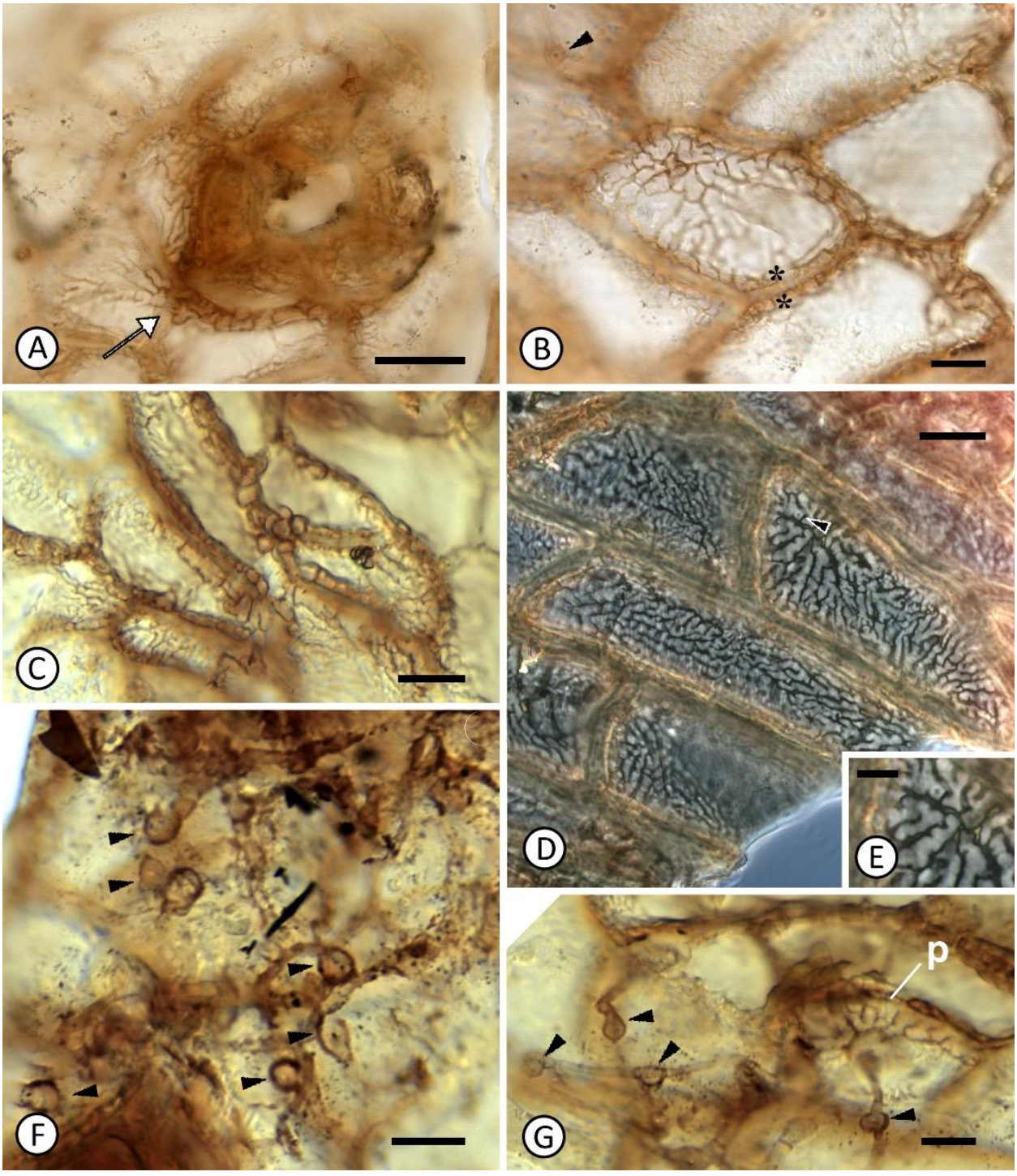
A
B
C
D
E
F
G
p

Figure 4.4 Pattern of host colonization in *Bleximothyrites ostiolatus gen. et sp. nov.*, superficial mycelium and subcuticular *mycélium en palmettes.*
A. Subcuticular mycelium producing flat, densely branching *mycélium en palmettes* in stomatal complex, intercellular area of epidermal cells and proliferating to adjacent cells within cuticle (white arrow). B. Subcuticular mycelium forming radiating *mycélium en palmettes* in epidermal cells; appressed on either side of host cell flanges, (*). Appressorium on cuticle surface (black arrowhead). C. Intercellular mycelium (between walls of epidermal cells) is continuous with flattened palmettes coating underside of cuticle. D. *Mycélium en palmettes* in phase-contrast of cuticle, showing extensive network of palmettes coating host cells and bearing penetration peg (black arrowhead). E. Inset from D showing palmettes at higher magnification with pigmented penetration peg (upper, centre). F, G. Superficial mycelium with appressoria in swollen hyphal segments (black arrowheads), showing penetration peg as black or hyaline dot in centre. Note that appressoria and their penetration pegs can be followed below cuticle to *mycélium en palmettes* (p). Holotype DMNS EPI.53111. Bars = 20 µm (A, C), 10 µm (B, D, F, G), 5 µm (E)

4.6 Discussion

4.6.1 The host plant

Cuticles have been studied from relatively few gymnosperm macrofossils from the Potomac Group, and so the affinities of the host plant must be determined by comparison to gymnosperm macrofossils from other Cretaceous sites. The host here most likely represents a non-papillate ginkgophyte or a cycad, but the generalized suite of characters preserved in the cuticle means that probable affinities must be determined through the process of exclusion, rather than by the presence of one or more specialized features diagnostic of major lineages. The absence of paracytic stomatal complexes eliminates Bennettitales and Gnetales of the *Welwitschia* + *Gnetum* clade (Florin, 1933; Martens, 1971), while the absence of stomata in distinct rows eliminates Czekanowskiales and extant conifers (Florin, 1933; Ash, 1994) and the absence of papillate subsidiary cells eliminates many species of *Nilssonia* (Watson and Cusack, 2005). The absence of thick- and thin-walled cells eliminates the zamioid clade of crown group cycads;

while the absence of a distinctly oblique fabric to the pavement cells eliminates crown group cycads (Pant and Nautiyal, 1963; Greguss, 1968). Among extinct cycads, the absence of striations eliminates the genus *Ctenis* (Watson and Cusack, 2005). Among ginkgophytes, the absence of papillae eliminates the genus *Ginkgo* (Quan et al., 2010) and other species with papillate stomatal complexes; while the presence of typical gymnospermous stomata eliminates Caytoniales, which have such angiospermous features as stomatal poles level with the stomatal pore, and well-developed stomatal ledges (Harris, 1932; Barbacka and Boka, 2000).

Among Cretaceous gymnosperms, the suite of characters found in my cuticle is similar to several non-papillate ginkgophytes, in particular with the qualitative features of the abaxial epidermis are very similar to those of *Eretmophyllum/Nehvizdyella* (Kvacek et al., 2005). The suite of characters found in my fossil cuticle is also similar to that found in some species of the extinct cycad genus *Pseudoctenis*, with the caveat that many *Pseudoctenis* species have more subsidiary cells per stomatal complex than the fossils derscribed here (7–10 or more) (Watson and Cusack, 2005). By this process of elimination, the host most likely represents a non-papillate ginkgophyte or a cycad among the known lineages of seed plants.

4.6.2 *Mycélium en palmettes* and their potential taxonomic significance

Ducomet (1907) first described *mycélium en palmettes* similar to that of *B. ostiolatus* in other folicolous ascomycetes. The presence of extensive *mycélium en palmettes* has been only documented in a few living fungi, both in thyriothecial and non-thyriothecial taxa (Ducomet, 1907; Arnaud, 1917a; Hughes, 1953a). Arnaud (1918) illustrated only two species of fly-speck fungi as having subcuticular *mycélium en palmettes*: *Microthyrium microscopicum* Desm. (Microthyriales) and *Lembosina psychotriae* (G. Arnaud) Arx (Aulographaceae). All the rest of

the many fly-speck fungi illustrated by Arnaud (1918) grew haustoria shortly after host penetration, without apparent *mycélium en palmettes*. Most taxa in Dothideomycetes ever reported to produce *mycélium en palmettes* are in the order Venturiales (Ducomet, 1907; Hughes, 1953a). This raises the possibility, which could be addressed with a comparative study of host penetration in folicolous taxa, that *mycélium en palmettes* had a single origin in Dothideomycetes, in the ancestor of the clade encompassing Microthyriales and Venturiales. If they prove to be taxonomically restricted in Dothideomycetes, the combination of *mycélium en palmettes* with thyriothecia will be useful in classification of both extant and fossil species.

4.6.3 Comparison to other fossils of thyriothecia

The synopsis of published reports for fossil fungal form-genera of Kalgutkar and Jansonius (2000), which was translated into a searchable public database (Berbee et al., 2014), includes 131 taxonomic records for fly-speck fungi. These are among the most abundantly documented Mesozoic and Cenozoic fungi, with fossil records from the Triassic to the Holocene (Bajpai and Maheshwari, 1987; Kalgutkar and Jansonius, 2000; Sun et al., 2015; Mishra et al., 2018). Thyriothecioid scutella that are associated with hyphae and on plant cuticles provide convincing evidence of fungal affinities. The patterns of branching of the dichotomizing hyphae of the scutellum may aid in finer-scale identification, even in the absence of ascospores and asci.

Stomiopeltites cretaceus Alvin & Muir (1970) from the Lower Cretaceous Wealden Formation is the oldest described taxon with flattened, ostiolate scutella that also shows overlapping hyphae. Their scutella are borne on shoots of a conifer resembling *Frenelopsis* Schenk. Although described as non-radiate, the authors report radiating hyphae at the margins of young scutella (Alvin & Muir, 1970). Comparisons of *Bleximothyrites ostiolatus* to *S. cretaceus*

are difficult, as specimens were illustrated almost exclusively using SEM, and the characters of branching and surface mycelium looked for using light microscopy were obscured. In contrast to *B. ostiolatus*, hyphae that form the scutella of *S. cretaceus* overlap throughout the entire radius of the scutellum, not just at the margins. A second specimen described as *S. cretaceus*, from a leaf of *Frenelopsis* from the Upper Cretaceous (middle Cenomanian) of Anjou, France, is also ostiolate with a non-radiate scutellum (Pons and Boureau, 1977). Both specimens of *S. cretaceus* are attached to surface mycelium that lacks the appressoria and subcuticular mycelium seen in *B. ostiolatus*.

The fungal taxon *Mariusia andegavensis* Pons & Boureau (1977), also from cuticle of *Frenelopsis*, from the Upper Cretaceous (middle Cenomanian) locality in Anjou, France (Pons and Boureau, 1977), is represented by several scutella at different stages of development. Young scutella of *M. andegavensis* show radiate hyphae with dichotomies. Older scutella may or may not appear radiate, and hyphae at the margin of the scutellum are densely septate and do not protrude beyond the margins, in contrast to those of *B. ostiolatus*. Similar to the mycelium of *B. ostiolatus*, *M. andegavensis* produces abundant intercalary appressoria associated with penetration pegs and with *mycélium en palmettes* (Pons and Boureau, 1977). In contrast to *B. ostiolatus*, the young *mycélium en palmettes* of *M. andegavensis* appear as hemispheric lobes of dichotomies, rather than elongate, anisodichotomous branches (Fig. 4.4A). The ostiole of *M. andegavensis* is about four times wider than that seen in *B. ostiolatus* at maturity.

Other specimens of *Mariusia andegavensis* on *Frenelopsis* have been described from the Lower Cretaceous (middle to upper Albian) Escucha Formation of Spain (Estévez-Gallardo et al., 2015). All the specimens are large, apparently mature, and the scutella look radiate, like *B. ostiolatus* and unlike the holotype of *M. andegavensis* (Pons and Boureau, 1977). However,

scutellum hyphae do not show septation as in *B. ostiolatus*. These *M. andegavensis* specimens do not appear to have surface mycelium as in *B. ostiolatus*. The ostioles in the Spanish specimens are also very large, up to twice the size of those of *B. ostiolatus*, and the area around the ostiole does not show the pseudoparenchymatous hyphae seen in the fossils described here.

Stomiopeltites plectilis (Dilcher) Kalgutkar & Jansonius (2000) was originally described by Dilcher (1965) from the Middle Eocene of Tennessee on the surface of *Sapindus* L. leaves. Only the margins of the scutellum appear radiate from among the several fruiting bodies at different stages of development, and the mycelium does not bear appressoria (Dilcher, 1965) as in *B. ostiolatus*. Mature scutella of *S. plectilis* are ostiolate, and pseudoparenchyma extends beyond the rim of the ostiole to the margin of the scutellum (Dilcher, 1965), unlike the localized pseudoparenchyma in *B. ostiolatus*. The marginal hyphae in *S. plectilis* overlap one another, as in *B. ostiolatus*, but the hyphae do not extend beyond the margin of the scutellum.

Several *Plochmopeltinites* species have been described in the past but Cookson (1947) and Selkirk (1969, 1975) restrict *Plochmopeltinites masonii* to specimens that are radiate, ostiolate, and found in situ. Cookson's (1947, Fig. 14) specimen comes from Traralgon, east of Yallourn, Victoria, Australia, from an Oligocene/Miocene ligneous clay deposit. The scutellum borne on an unidentified cuticle fragment is circular, ostiolate, and shows radiating, dichotomously branching, overlapping hyphae (Cookson, 1947), like those seen in *B. ostiolatus*. The scutellum hyphae are infrequently septate, and the area of the ostiole lacks the pseudoparenchyma lining seen in *B. ostiolatus*. The ostiole in *P. masonii* is darkly pigmented, dense, and surrounded by a slightly raised border (Cookson, 1947), which is not seen in *B. ostiolatus*. Hyphae at the scutellum margin of *P. masonii* do not protrude as they do in *B. ostiolatus*.

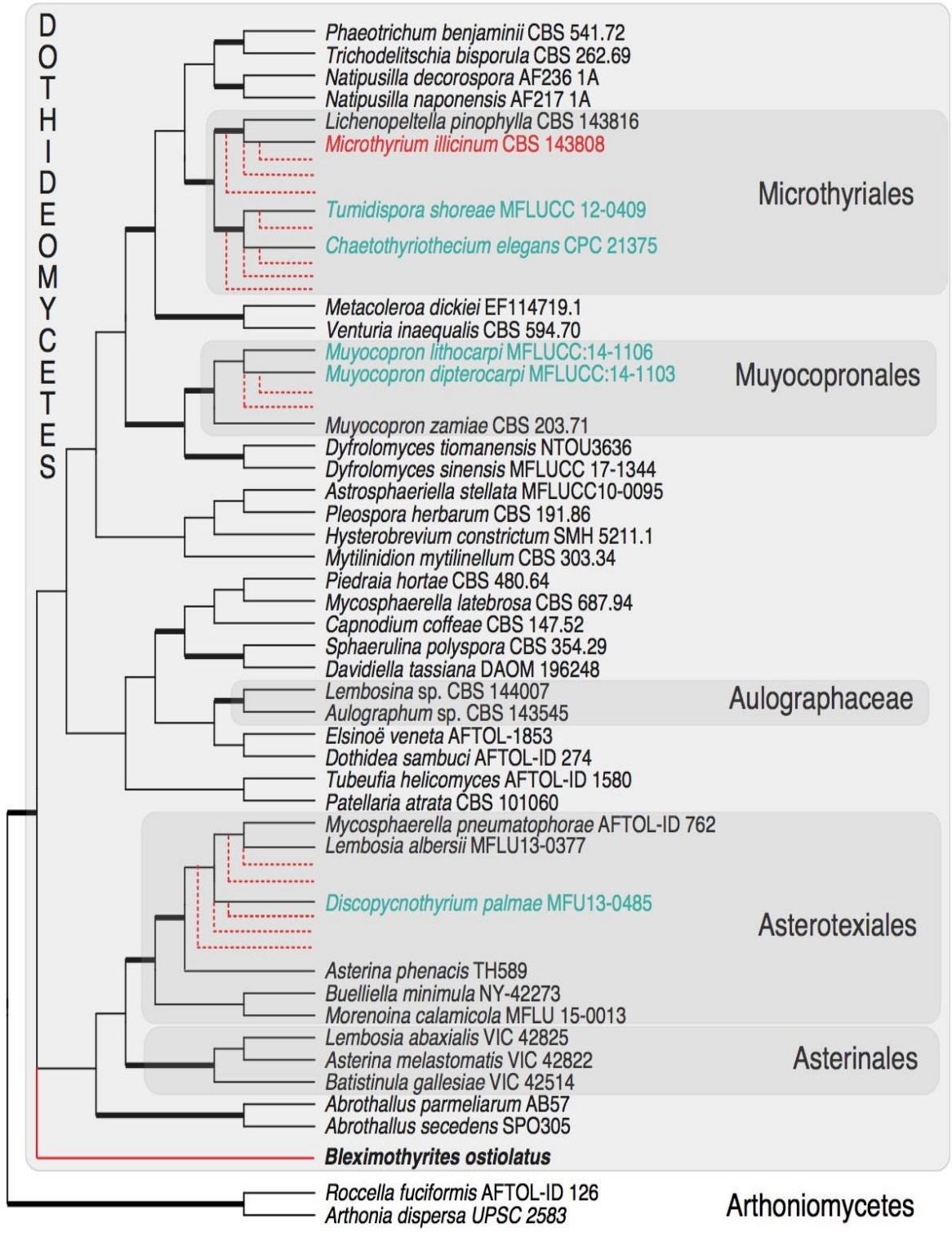
DOTHIDEOMYCETES
Phaeotrichum benjaminii CBS 541.72
Trichodelitschia bisporula CBS 262.69
Natipusilla decorospora AF236 1A
Natipusilla naponensis AF217 1A
Lichenopeltella pinophylla CBS 143816
Microthyrium illicinum CBS 143808
Tumidispora shoreae MFLUCC 12-0409
Chaetothyriothecium elegans CPC 21375
Microthyriales
Metacoleroa dickiei EF114719.1
Venturia inaequalis CBS 594.70
Muyocopron lithocarpi MFLUCC:14-1106
Muyocopron dipterocarpi MFLUCC:14-1103
Muyocopron zamiae CBS 203.71
Muyocopronales
Dyfrolomyces tiomanensis NTOU3636
Dyfrolomyces sinensis MFLUCC 17-1344
Astrosphaeriella stellata MFLUCC10-0095
Pleospora herbarum CBS 191.86
Hysterobrevium constrictum SMH 5211.1
Mytilinidion mytilinellum CBS 303.34
Piedraia hortae CBS 480.64
Mycosphaerella latebrosa CBS 687.94
Capnodium coffeae CBS 147.52
Sphaerulina polyspora CBS 354.29
Davidiella tassiana DAOM 196248
Lembosina sp. CBS 144007
Aulographum sp. CBS 143545
Aulographaceae
Elsinoë veneta AFTOL-1853
Dothidea sambuci AFTOL-ID 274
Tubeufia helicomyces AFTOL-ID 1580
Patellaria atrata CBS 101060
Mycosphaerella pneumatophorae AFTOL-ID 762
Lembosia albersii MFLU13-0377
Discopycnothyrium palmae MFU13-0485
Asterotexiales
Asterina phenacis TH589
Buelliella minimula NY-42273
Morenoina calamicola MFLU 15-0013
Lembosia abaxialis VIC 42825
Asterina melastomatis VIC 42822
Batistinula gallesiae VIC 42514
Asterinales
Abrothallus parmeliarum AB57
Abrothallus secedens SPO305
Bleximothyrites ostiolatus
Roccella fuciformis AFTOL-ID 126
Arthonia dispersa UPSC 2583
Arthoniomycetes

Figure 4.5 Most parsimonious and strict consensus positions of *Bleximothyrites ostiolatus* based on nine morphological characters in constrained phylogeny of Dothideomycetes. Taxon in red shares eight character states with *B. ostiolatus*. Taxa in turquoise share seven character states with *B. ostiolatus*. Dashed branches (red) represent alternative most parsimonious phylogenetic relationships of *B. ostiolatus* within Dothideomycetes: solid branch (red) represents strict consensus position of *B. ostiolatus*. Tree underlying topology corresponds to most likely tree found in maximum likelihood (ML) analysis, used as constraint here; thickened branches indicate ML bootstrap probabilities > 70% and MrBayes posterior probabilities >0.95 obtained in DNA-only phylogenetic analyses.

Selkirk (1975) reported *Plochmopeltinites masonii* from leaves of probable Lauraceae from the Lower Miocene near Kiandra, New South Wales, Australia. These fungi again show radiate, ostiolate scutella with dichotomously branching hyphae that overlap, as in *B. ostiolatus*. The area around their ostiole is too dark to allow accurate description of their hyphal structure. Unlike *B. ostiolatus*, almost every hypha dichotomizes over a short distance in the Selkirk specimen, and the hyphae do not protrude beyond the scutellum. The extensively branching dichotomous hyphae in *P. masonii* do not diverge as much from the radial alignment of the scutellum as they do in *B. ostiolatus*. Selkirk (1975) reported possible intercalary appressoria in *P. masonii* on superficial hyphae, but did not find evidence of *mycélium en palmettes*.

The Dutch Gap sediments from which *B. ostiolatus* originates have also yielded mycelia and scutella of *Protographum luttrellii*, a fly-speck species related to Aulographaceae, Dothideomycetes (Chapter 3). The well-preserved scutella of *P. luttrellii* are distinct from *B. ostiolatus* in that they lack ostioles, originate from multiple generator hyphae, and expand by pseudomonopodial branching. They occur on conifer cuticles, and lack the *mycélium en palmettes*.

4.6.4 Significance of *Bleximothyrites ostiolatus*

Bleximothyrites ostiolatus represents the oldest fossil on plant cuticle that has a complete set of scutellum and mycelium characters of modern thyriothecial fungi–including an ostiole, appressoria, and radiate, dichotomizing hyphal construction. The ostiole indicates that spores were liberated above the scutellum. The large and broken sporocarps suggest that the thallus matured at a time when the host cuticle was still in good condition, although the leaf itself may have been living or dead. Connections between scutella and mycelium with appressoria and subcuticular *mycélium en palmettes* occur in some modern folicolous thyriothecia colonizing living or dead leaves (Ducomet, 1907; Arnaud, 1918). That the host cuticle can be seen here through the ostiole, and in broken sporocarps, indicates that sporocarps lacked a differentiated lower wall, an important character found in most living thyriothecia (Arnaud, 1918; Stevens and Ryan, 1939; Doidge, 1942; Arx and Müller, 1954; Müller and von Arx, 1962; von Arx and Müller, 1975). The scutellum in *B. ostiolatus*, although distinct from that of extant thyriothecia, grew in a similar way, with hyphae that branched dichotomously, radiating from a common central area, occasionally overlapping with adjacent hyphae, but adhering laterally to their neighbors for most of their course (Arnaud, 1918; Stevens and Ryan, 1939; Doidge, 1942; Arx and Müller, 1954; Müller and von Arx, 1962; von Arx and Müller, 1975). The distinct type of branching and overlap found in the distal part of scutellum and the absence of a well-defined margin, are both unique characters of *B. ostiolatus*. However, it is unclear that they represent two distinct characters and they were coded as a single state of the character of scutellum margin.

4.7 Conclusion

The morphological diversity of extant thyriothecial fungi is currently underappreciated, and their fossil record is more extensive than has previously been recognized. In a phylogenetic context, the overall pattern of evolution of thyriothecia in Dothideomycetes is still incompletely understood. Studies combining both DNA and morphology are beginning to add to our knowledge of the phylogeny of these fungi (Hofmann and Piepenbring, 2006, 2008; Hofmann et al., 2010; Guerrero et al., 2011; Hofmann and Piepenbring, 2011; Wu et al., 2011b; Guatimosim et al., 2014b; Hongsanan et al., 2014b; Guatimosim et al., 2015; Hongsanan et al., 2015; Mapook et al., 2016a; Mapook et al., 2016b; Tibpromma et al., 2016; Jayasiri et al., 2018) (Chapter 1). Scoring the morphological characters of fossil and extant thyriothecia is a necessary step toward a more objective interpretation of these remarkable fungi. Fly-speck fungi that form ostiolate and radiate scutella appear to have evolved multiple times within Dothideomycetes. *Bleximothyrites ostiolatus* provides an exceptionally well-preserved example of habit and character state combinations in one of the earliest of the fly-speck lineages.

Chapter 5: Cretaceous fungal scutella from the Lower Potomac Group Zone 1: *Stomatothyrites placocentrus gen. et sp. nov.*, a dothideomycete colonizer of conifer stomata

5.1 Summary

Mesozoic to Cenozoic fungi forming scutella, flat sporocarps borne on leaf surfaces, offer insights into the diversification of filamentous ascomycetes. In a survey of dispersed plant cuticles from the Lower Cretaceous of Virginia, I found a new fungal morphotype consisting of radiate scutella growing from the stomata of leaves of a conifer,. Here, I relate the new morphotype to other fossil groups and to extant taxa. Fragments of conifer cuticles colonized by the fungus were macerated from clays of the Potomac Group, lower Zone 1 (Aptian, 125–113 Ma) and studied using light microscopy. I compared the anatomy of the fossil scutella to extant taxa producing either rhizothyria, asexual sporocarps that release spores from below the outer edge of the scutellum, or thyriothecia, sporocarps with scutella that develop dorsal cracks or an ostiole for the release typically of sexual ascospores. *Stomatothyrites placocentrus gen. et sp. nov.* has a radial arrangement of scutellum hyphae that is characteristic of extant and fossil thyriothecial species in Dothideomycetes (Ascomycota). As in these taxa, its scutellum appears to dehisce by cracks on the dorsal surface. Unusually, these cracks follow the scutellum circumference rather than its radius, and each scutellum arises from a host plant stoma, appearing first as a hyphal columella that broadens into a flat scutellum disc on the leaf surface. Its unique morphology and dehiscence suggest that *Stomatothyrites placocentrus* represents a now-extinct

group of leaf dwelling Dothideomycetes that formed thyriothecia. This discovery contributes to our understanding of the range of character combinations of early epiphyllous Ascomycota.

5.2 Introduction

The available fossil record indicates an increase in the taxonomic diversity of fossilized leaf dwelling fungi from the Cretaceous to the Paleogene (Kalgutkar and Jansonius, 2000; Berbee et al., 2014). Most epiphyllous fossil fungi described from the Cretaceous are microfungi included in phylum Ascomycota (Kalgutkar and Jansonius, 2000; Berbee et al., 2014), identified on the basis of isolated sporocarps (Alvin and Muir, 1970), mycelia (Doubinger and Pons, 1975) and spores (Clarke, 1965). Geologically younger (Eocene) and better-preserved fossil epiphyllous fungi are known with preserved spores, mycelium and sporocarps. Lineages of leaf-inhabiting fungi represented by Eocene fossils include the black mildews (Dilcher, 1965; Selkirk, 1975; Daghlian, 1978; Mandal et al., 2011), fly-speck fungi (Dilcher, 1963; Dilcher, 1965; Lange, 1969; Selkirk, 1975; Smith, 1980, 1984; Phipps and Rember, 2004; Phipps, 2007; Vishnu et al., 2017; Vishnu et al., 2018) and sooty molds (Rikkinen et al., 2003; Schmidt et al., 2014).

Fly-speck fungi are probably the most diverse fungi of those with better characterized fossil records (Kalgutkar and Jansonius, 2000; Taylor et al., 2015). They produce a thyriothecium, a flattened and radiate disc of hyphae called the scutellum, which is appressed to the host cuticle and overlays spore-producing hyphae (Arnaud, 1918; Stevens and Manter, 1925). Analyses of extant taxa show that fly-speck fungi with scutella of radiating hyphae appear to have evolved independently in different orders, mostly in a single class, Dothideomycetes (Wu et al., 2011b; Guatimosim et al., 2015). The diversity of hyphal organization in scutella appears to be useful in distinguishing between species forming scutella (Wu et al., 2011b; Guatimosim et

al., 2015; Mapook et al., 2016b) (Chapters 2, 3). Scutella are all that is preserved in many of these fossils (Elsik, 1978; Kalgutkar and Jansonius, 2000), and analyzing their characters is useful for interpreting their relationships to living fungi (Chapters 2–4).

In surveying angiosperms from the Lower Cretaceous Potomac Group, Upchurch recognized that there was abundant fungal colonization of leaf cuticle surfaces (Upchurch and Doyle, 1981; Upchurch, 1984a, b). Here I process additional Potomac Group (lower Zone 1) clay sediments from the oldest deposits at the Dutch Gap Canal to reveal the abundant fungal remains on gymnosperm leaf cuticles. So far, these sediments have yielded scutella of *Protographum luttrellii* Le Renard, Upchurch, Stockey & Berbee (Chapter 3) and *Bleximothyrites ostiolatus* Le Renard, Upchurch, Stockey & Berbee (Chapter 4), each found on individual fragments of gymnosperms cuticle; these are fossil thyriothecia classified in Dothideomycetes. In this paper, I describe a new genus and species for a common fossil fungal morphotype from the Potomac Group (lower Zone 1) that was abundant on coniferous leaf cuticles, one of which also bears *P. luttrellii*. I compare the characters of the new fossil to previously described fossils that are similar in age or in habit, and to extant thyriothecial and rhizothyrial taxa.

5.3 Material and methods

5.3.1 Fossil fungi

Fossilized plant cuticles occur in an exposure on the south side of Dutch Gap Canal, James River, Virginia (Hickey and Doyle, 1977; Upchurch and Doyle, 1981; Upchurch, 1984b). Prepared sediments came from the base of the sequence in the claybed that is exposed at low tide, also called the *Pseudofrenelopsis parceramosa* bed (37.3760000°, -77.3593000°, locality DMNH 128). This section is dated as lower Zone I of the Potomac Group of the eastern United

States (Brenner, 1963), Lower Cretaceous (Aptian 125–112 Ma), based on the palynoflora (Doyle and Hickey, 1976; Upchurch and Doyle, 1981; Doyle and Upchurch, 2014, and references therein). It yields shoots of the extinct conifer *Pseudofrenelopsis parceramosa* (Fontaine) Watson, along with leaves of the extinct bennettitalean *Dioonites buchianus* (Ettingshausen) Bornemann, conifers included in *Pagiophyllum* Heer, *Podozamites* Braun, *Pityocladus* Seward, shoots of early herbaceous angiosperms (Upchurch and Doyle, 1981; Doyle and Upchurch, 2014; Jud, 2015), and dispersed cuticles of unidentified gymnosperms (Chapters 3, 4)

I used a modified cuticle extraction protocol from Upchurch (1989); (Chapters 3, 4). Briefly, I immersed 200 g of clay in saturated household trisodium phosphate solution (TSP; Rescochem, Québec**)** and added 10% hydrogen peroxide (H_2O_2) for up to 36 h to release cuticles from the matrix, collecting accumulated foam containing organic debris over 3–6 h. Organic debris was rinsed in 70% EtOH, and extracted in two fractions using 200 µm and 90 µm sieves. Silicate rich samples were processed in 20% HF for two days, then washed with water and stored in 50% ethanol. Individual cuticles with attached fungi were removed from solution under a dissecting microscope using an insect pin (size 0, Austerlitz insect pins, Slavkov u Brna, Czech Republic). Dark colored cuticles were further processed in 10% KOH solution, heated to 60 C for up to two days, removing cleared cuticles as early as possible to minimize loss of fungal structures. Cuticles were then mounted in the Eukitt, xylene soluble mounting medium (O. Kindler GmbH, Freiburg, Germany).

5.3.2 Sampling of extant thyriothecia and rhizothyria

I borrowed fungal herbarium specimens of thyriothecia and rhizothyria from the Westerdijk Fungal Biodiversity Institute (CBS), and the herbaria at Oregon State University (OSC), Universidade Federal de Viçosa (VIC), and University of British Columbia (UBC) to prepare semi-permanent slides and document their morphology. For comparison with the fossil, I examined thyriothecia from four lineages of Dothideomycetes thought to have independent origins (Wu et al., 2011b; Guatimosim et al., 2014b; Hongsanan et al., 2014b; Guatimosim et al., 2015; Mapook et al., 2016b) (Chapter 2) : *Lembosina aulographoides* (E. Bommer, M. Rousseau & Sacc.) Theiss. (UBC-F33037), *Microthyrium macrosporum* (Sacc.) Höhn. (UBC-F33039), *Muyocopron smilacis* (De Not.) Sacc. (OSC #93714) and *Rhagadolobiopsis thelypteridis* Guatim. & R.W. Barreto (VIC 31939). To represent extant taxa with rhizothyria, I included *Pirostoma nyssae* Tehon (UBC-F11406) and *Racheliella wingfieldiana* Crous & U. Braun (CBS H-23399). Specimens of *R. wingfieldiana* on coniferous needles could not be sampled *in situ*, together with the cuticle. When the revived host tissue could be cut easily, I prepared peels of host cuticle and epidermal cells, with the fungus in-situ. The peels were obtained by shaving a thin layer of plant tissue parallel to the host surface, up to a few cells thick (i.e., up to ~300µm). Alternatively, I prepared clear nail polish peels following Hosagoudar and Kapoor (1985), in which the fungus is peeled off the substrate in nail polish, and host cells are seen as imprints. These two types of microscope mounts allow us to view the fungus in the same orientation as the fossils (i.e., in dorsal view) and show the position of host stomata relative to the fungus. The morphological characters of living and fossil taxa are summarized in Table 5.1.

5.3.3 Microscopy and image processing

Extant and fossil fungi were observed using a Leica DMRB (Leitz, Germany) DIC microscope and photographed at 200X, 400X or 1000X (under oil immersion) with a Leica DFC420 digital color camera. To more clearly illustrate branching of scutellum hyphae, photographs of different focal planes were stacked in Photoshop CC 2015.1.2 (1990 – 2019, Adobe Systems, San Jose, California) following Harper (2015), using suggestions from Bercovici et al. (2009). Many of the dark fungal structures contrast with the cleared cuticles and benefit from post processing using image adjustment options in Photoshop, to reveal the outline of scutellum hyphae in greater detail.

5.3.4 Terminology

Many fungi in Ascomycota produce both conidia, asexual mitospores, and ascospores, sexual meiospores (Ainsworth et al., 1973; Kirk et al., 2008). They may also produce spermatia, or mitospores that function in fertilization rather than in asexual reproduction (Higgins, 1920; Kirk et al., 2008). Each spore type may be associated with a wide range of sporocarps (Higgins, 1920; Ainsworth et al., 1973). The term sporocarp as used here refers to any pluricellular, sporulating structure, in the absence of details of sporogenesis.

A scutellum, Latin for small shield, is a disc of pigmented hyphae. Scutella that overlie spore production and that are initiated from one or a few dichotomizing hyphae are found in both sexual thyriothecia and asexual rhizothyria and pycnothyria (Nag Raj, 1993; Kirk et al., 2008). Thyriothecia generally produce ascospores that are typically released through a central ostiole, a round opening in the scutellum, or through cracks that open between scutellum hyphae (Arnaud,

1918; Stevens and Ryan, 1939; Eriksson, 1981; Wu et al., 2014a; Guatimosim et al., 2015) (Chapter 2).

Rhizothyria are initiated with a columella, a column of hyphae arising from within the host (Naumov, 1914; Darker, 1965; Nag Raj, 1993). On the leaf surface, hyphal tips of the columella differentiate further to form a radiate scutellum. Spores produced under the scutellum of a rhizothyrium are then released from under the scutellum's distal edge (Naumov, 1914; Darker, 1965). The rhizothyrium takes its name from *Rhizothyrium abietis* Naumov, a species that produces them, but as explained below, similar structures in other taxa are inconsistently named.

The term pycnothyrium refers to radiate scutella that dehisce along their dorsal surface (see footnote, p. 7 in Hughes, 1953c), that are usually borne on superficial mycelium without a columella (Arnaud, 1918; Stevens and Ryan, 1939). Pycnothyria are mitosporic stages of thyriothecium-forming fungi such as *Mahanteshamyces* sp. (Hofmann and Piepenbring, 2008), *Discopycnothyrium palmae* Hongsanan & K.D. Hyde (Hongsanan et al., 2016), and the mitosporic stage of *Microthyrium nolinae* A.W. Ramaley (Ramaley, 1999). In the absence of spores associated with the scutellum of the fossils, I could not distinguish thyriothecia from pycnothyria, and use the more general term thyriothecium for either of these structures.

Sporocarps of Tubakiaceae are sometimes also called rhizothyria (Tehon, 1924; Holdenrieder and Kowalski, 1989; Belisario, 1991; Nag Raj, 1993) but are also referred to as pycnothyria (Munkvold and Neely, 1991; Taylor, 2001; Harrington et al., 2012; Zhang et al., 2015). Similar to *R. abietis*, members of Tubakiaceae release conidia below the distal edge of the scutellum (Naumov, 1914; Darker, 1965). I distinguish rhizothyria from pycnothyria and

thyriothecia by their attachment to the host through a central columella, and by spore release below the distal edge of the scutellum.

A continuous disc refers to scutella that form a continuous cover over spore-bearing tissue, with each scutellum hypha closely appressed to its neighbors. In contrast, a discontinuous disc has some of the peripheral hyphae diverging from their neighbors, resulting in wedge-shaped gaps in the scutellum over the sporogenous tissue. Some scutella growing over stomata have a circular central plate that is raised above the rest of the scutellum. A rim where scutellum hyphae form a depression, change direction, or narrow, sometimes gives a more or less distinct edge or outline to the central plate.

5.4 Results

5.4.1 Description

The fossil thyriothecia occur on conifer leaf cuticles that are amphistomatic (Figs. 1, 2). Because the cuticles of gymnosperms from the Dutch Gap have not been studied in detail, the affinities of the host could not be determined. However, stomata occur in longitudinal rows, and are more numerous on the abaxial than adaxial surfaces (Fig. 5.1G). They have two prominent subsidiary cells with wide, fan-like cuticular flanges (Fig. 5.1E, 5.1F). Stomata lack polar subsidiaries, and can share polar epidermal cells (Figs. 5.1E, 5.1F).

Numerous (over 100) thyriothecial sporocarps of similar morphology have been found on the Dutch Gap cuticles in rows extending out of what appear to be the same host plant (Figs. 5.1A–5.1D, 5.2). Several sporocarps of the same type have also been found isolated in the macerations as they became dislodged from the host cuticles (Fig. 5.3A). The circular scutella, 50–170 μm in diameter, are appressed to the cuticle, forming discrete shield-like structures that

are not confluent with one another (Figs 5.2A, 5.2C). Branching of the hyphae forming the scutella is dichotomous (5.2A, 5.3A–5.3D), and hyphae radiate from the stomatal opening and extend outward (2B, 2D). There is no evidence of superficial mycelium attached to these structures.

Scutella are composed of two zones: a central, compact plate, and a looser marginal zone (Figs 5.2D, 5.3A, 5.3C–5.3F). Hyphae of the central plate, which are 1.5 to 4.5 μm in diameter, radiate outwards from the scutellum centre, branching almost exclusively through isotomous dichotomies (Figs. 5.2A, 5.3A, 5.3C, 5.3D). The side walls of these hyphae are straight and appear to be laterally fused to one another within the plate; they do not overlap with each other.

Hyphae in the marginal zone are narrower than those in the plate. They are 0.8–3 μm in diameter and have a meandering course near the distal edge of the scutellum (Figs. 5.2C, 5.2F, 5.3). Marginal hyphae branch with mostly isotomous branching (Fig. 3B) and less frequently show anisotomous and pseudomonopodial dichotomies (Fig. 5.3A, 5.3C, 5.3D). Hyphae show conspicuous overlap near the edge of the scutellum (Figs. 5.2C, 5.3B–5.3D). Hyphal tips at the appressed margin vary from round to tapering, and may extend beyond the edge of the scutellum, or may be flush with the edge (Figs. 5.2E, 5.2F, 5.3C–5.3F).

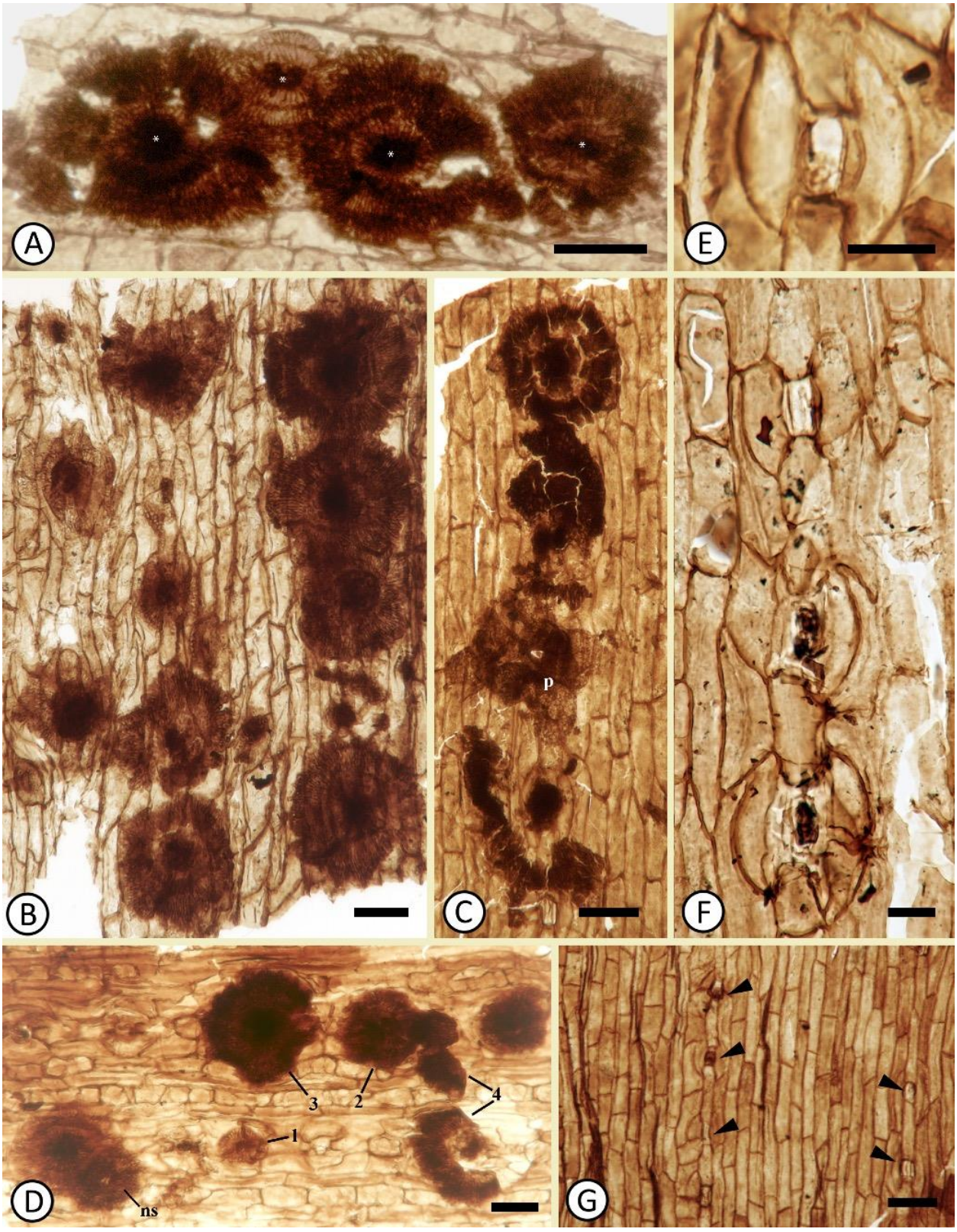
A
E
B
C
p
F
D
3
2
4
1
ns
G

Figure 5.1 *Stomatothyrites placocentrus gen. et sp. nov.* sporocarps aligned above the stomata of coniferous host cuticles.
A, Scutella above stomata of single row, at different stages of development. Note columellae (star) and central plates evident on scutella prior to dehiscence. Holotype, DMNS EPI.53113. B, Scutella above adjacent rows of stomata at different developmental stages preceding dehiscence. Paratype DMNS EPI.53114. C, Scutella at different stages of dehiscence. Note circular fracture in top specimen, remains of margins in bottom specimen, and absence of pigmented underlying wall in dehiscent scutella. Broken pollen grain (p) over two uncolonized stomata. Paratype DMNS EPI.53115. D, Overview of scutellum development. A (1) central plate formed by multiple hyphae; (2) tips of scutellum hyphae have grown beyond the central plate; (3) mature scutellum with dark central plate; (4) mature scutellum cracks open, margin and columella sometimes remaining in place. Paratype DMNS EPI.53116. E–G, Morphology of host cuticle. E, Circular stomatal complexes with prominent subsidiary cells with fan-like cuticular flanges. F, Stomata in rows sharing polar epidermal cells. G, Adaxial side of cuticle with fewer stomata (black arrowheads) separated by elongate polar epidermal cells. Scale bars = 50 µm (A–D, G), 20 µm (E, F).

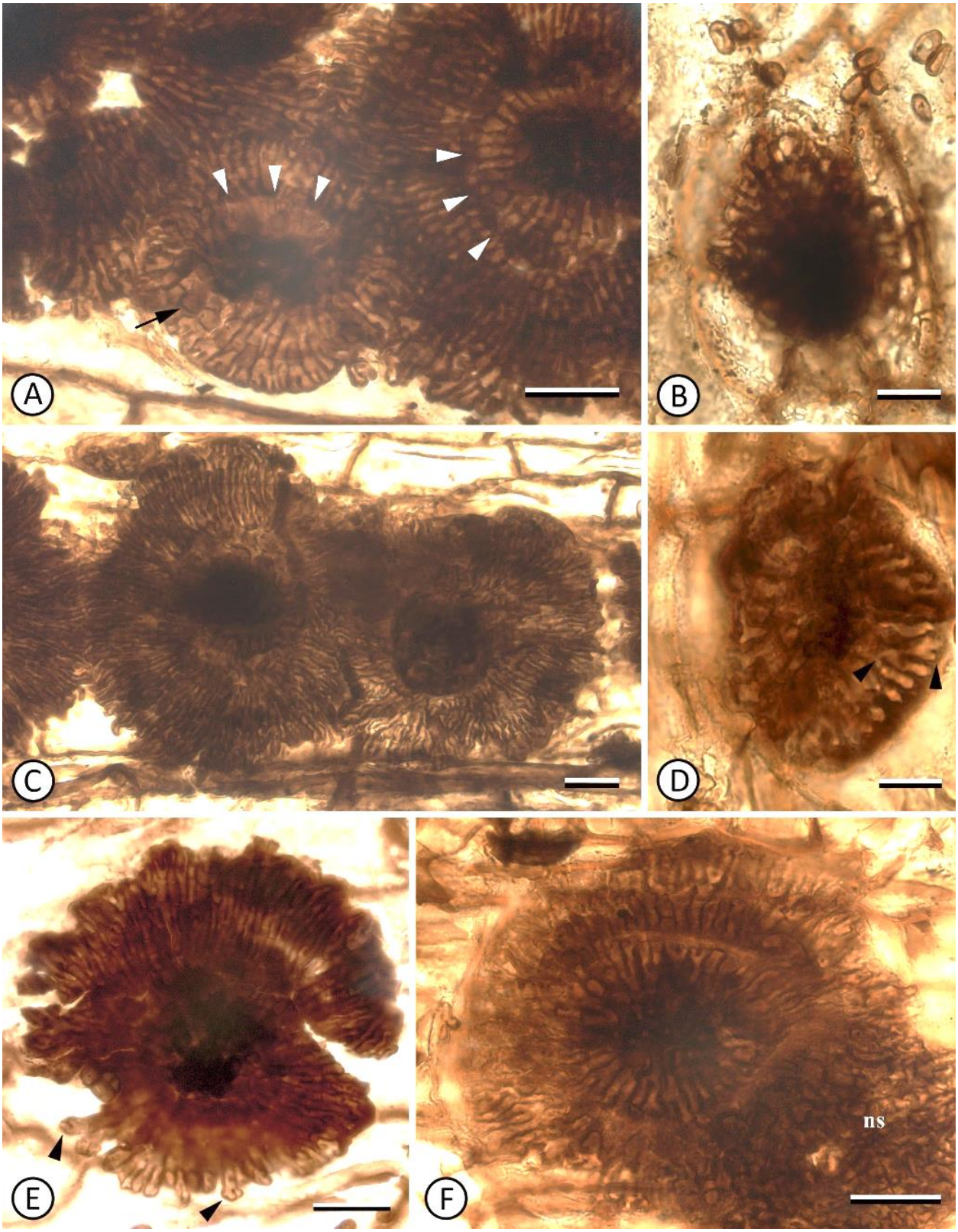
A
B
C
D
E
F
ns

Figure 5.2 Scutella in *Stomatothyrites placocentrus gen. et sp. nov.* in transition from early development to maturity.
A, Young scutella showing dichotomous tip-branching and cross septa (*black arrow*). The central plate (white arrowheads) more conspicuous in larger scutella. Holotype, DMNS EPI.53113. B, Young scutellum without dichotomous branching, multiple hyphae arising from dark, central columella, central plate not fully developed. Paratype DMNS EPI.53117. C, Large, indehiscent scutella with radiating and meandering, distal hyphae. Paratype DMNS EPI.53114. D, Young scutellum with hyphae beginning to form central plate. Note beginning of dichotomous hyphal branching (black arrowheads), shortly after emergence from central columella. Paratype DMNS EPI.53116. E, Dichotomously branching and meandering hyphae that grew beyond the central plate form the distal margin (black arrowheads). Paratype DMNS EPI.53115. F, Scutellum with well-developed central plate. Paratype DMNS EPI.53116. Scale bars = 20 µm (A, C, E, F), 10 µm (B, D).

As they emerge from stomata, the hyphae of the scutellum are of equal diameter. They branch with regular dichotomies, and tend to be flush with one another at the edge of the scutellum (Fig. 5.2A, 5.2B, 5.2D). These are the hyphae that form the central plate. When this scutellum plate reaches a diameter of 40–60 µm, the appearance of the hyphae changes. Beyond the central plate, hyphae exhibit a meandering course, and a distinct line appears that delineates the plate from the marginal rim (Figs. 5.2C, 5.2F. 5.3A–D). I have observed several instances of cross septa at this boundary (Figs. 3*C*, 3*D*, arrowheads). Additionally, differential pigmentation (Figs. 5.1A, 5.3A, 5.3C, 5.3D) can be seen in some specimens separating the two zones of the scutellum. Most scutella that were larger than 100 µm in diameter show a circular fracture at this line that follows the central plate (5.1*C*, 5.3*E*, 5.3*F*). Cracks occur somewhat regularly, and I interpret the characteristic circular cracking as the dehiscence mechanism for these sporocarps.

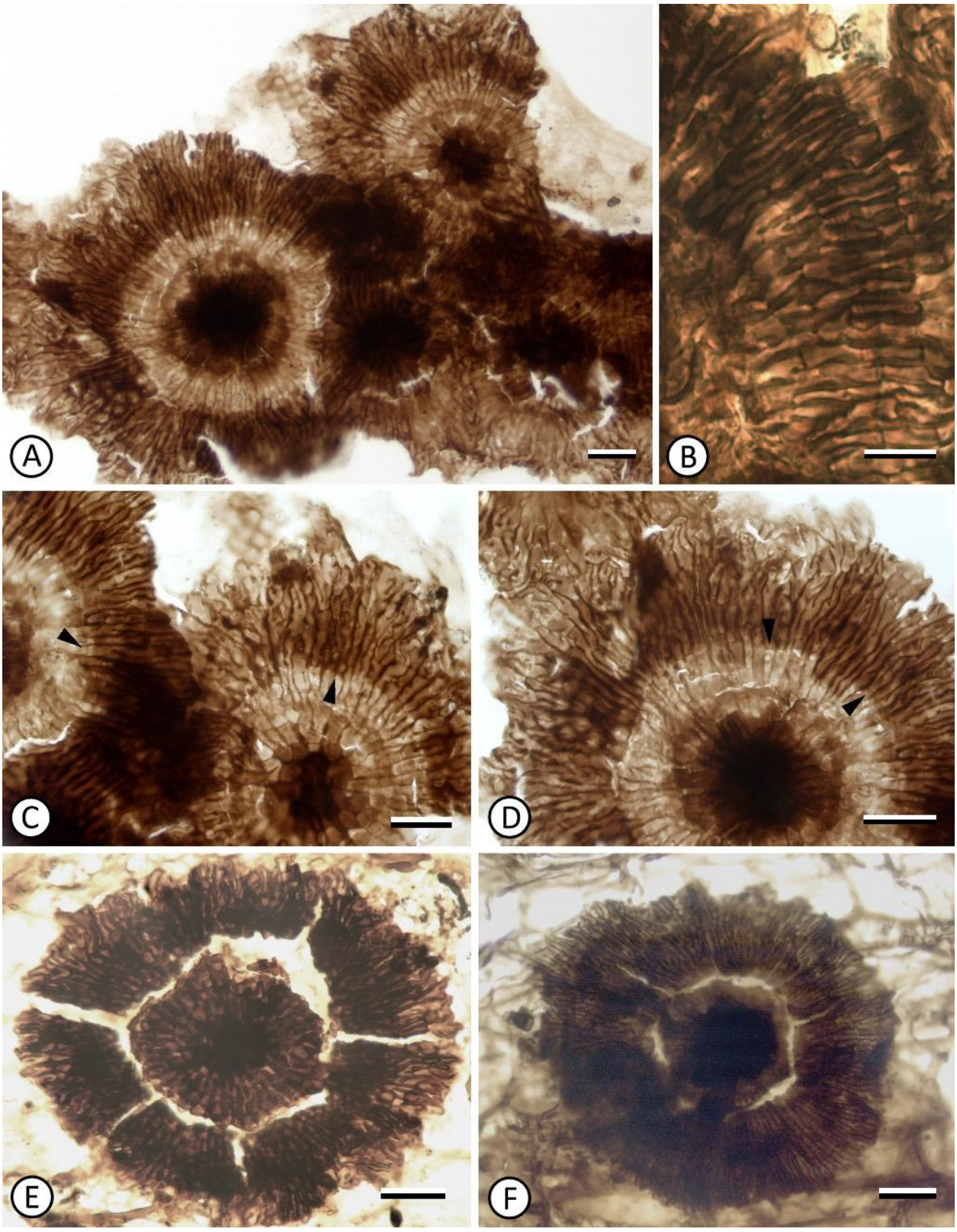
A
B
C
D
E
F

Figure 5.3 Dehiscence of scutellum of *Stomatothyrites placocentrus*.
A, C, D, Scutella dislodged from host cuticle, preserved at start of dehiscence. A, Cracks appear at lightly pigmented edge of central plate of scutella. Paratype DMNS EPI.53118. B, Close up of distal margin of scutella. Meandering hyphae with dichotomous branching and cross septa radiate adjacent to one another. Paratype DMNS EPI.53114. C, D, Columella surrounded by plate of wide and straight hyphae, hyphae distal to plate transition to narrower, branching, parallel and meandering hyphae. Circular fractures (black arrowheads) occur close to transition of hyphal morphology. Paratype DMNS EPI.53118. E, F, Dehiscent scutella showing circular fracture at edge of central plate, propagating along radial walls of hyphae to distal part of the structure. E, Paratype DMNS EPI.53119. F, Paratype DMNS EPI.53120. Scale bars = 20 µm (A, C, E, F), 10 µm (B, D).

5.4.2 Morphological diversity in extant species with thyriothecia

I chose to compare the fossil with living species representing different clades of Dothideomycetes that form round thyriothecia of similar size. I describe the anatomy of illustrated taxa in dorsal view, including scutellum development,

Microthyrium macrosporum (UBC-F33039) is common on *Buxus sempervirens.* It produces a superficial mycelium giving rise to scutella up to 250 µm in diameter on the adaxial and abaxial sides of dead leaves. The scutellum originates from a side branch of a superficial hypha, and develops with successive dichotomously branching of hyphae to form a continuous disc. Scutella in *Microthyrium* open by central ostioles from which spores escape, and as sporulation begins, they remain attached to host tissue at their distal edges. Scutella as small as 110 µm were seen to sporulate. In older scutella, the ostiole and surrounding central area often break away so that only the edge of scutellum remains, anchored to the substrate (Fig. 5.4A). At the distal margin, young scutella without an ostiole exhibit a continuous edge of blunt to slightly dome-shaped hyphal tips (Fig. 5.4A). In contrast, mature scutella (i.e., with a dorsal opening) show hyphae with tapering tips that form a fimbriate margin (Fig. 5.4A).

Lembosina aulographoides (UBC-F33037) was found on living stems of *Rhododendron* cf. *ponticum* in Vancouver. Scutella arise from superficial hyphae, independently of stomata (Fig. 5.4B), forming ellipsoid to elongate ascomata up to 500 µm long and 300 µm wide. Scutella are made of overlapping, pseudomonopodial, dichotomously branching hyphae organized into a continuous disc (Fig. 5.4B). Scutella of *L. aulographoides* open by a longitudinal slit located in the centre of the elongate scutella (Fig. 5.4B). In *L. aulographoides,* scutella can show evidence of dehiscence at an early stage, in structures that are only 165 µm long (Fig. 5.4B). Hyphal tips align at the edge of the distal margin of the scutellum, and the margin appears crenulate throughout development. During sporulation, each side of the scutellum remains attached at the edges, and the centre is lifted up from the host by the developing sporogenous tissue.

Muyocopron smilacis (OSC #93714), collected in New Jersey, occurs on stems of *Smilax* sp., on dead tissue, and forms extensive crusts or a pellicle of confluent scutella, several mm wide (Fig. 5.4C). The edge of the crust often shows small and isolated scutella as small as 150 µm wide, which can show signs of dehiscence (Fig. 5.4D). Crusts of *M. smilacis* include scutella initiated above host stomata and scutella borne on a superficial mycelium. All scutella are formed by dichotomously branching hyphae, resulting in a continuous disc that radiates from the centre. At the distal edge of the scutellum, hyphal tips align to form a more or less crenulate margin (Fig. 5.4D), before merging with other scutella and becoming indistinct (Fig. 5.4C). When arising from stomata, scutella are attached to the host by a columella that appears melanized in the centre of the hyphal disc (Fig. 5.4C). A central plate of hyphae is attached to the columella, reflecting the outline of the underlying stomatal complex with an inconspicuous rim of slightly curving hyphae (Fig. 5.4C). The hyphae of the plate are morphologically similar to

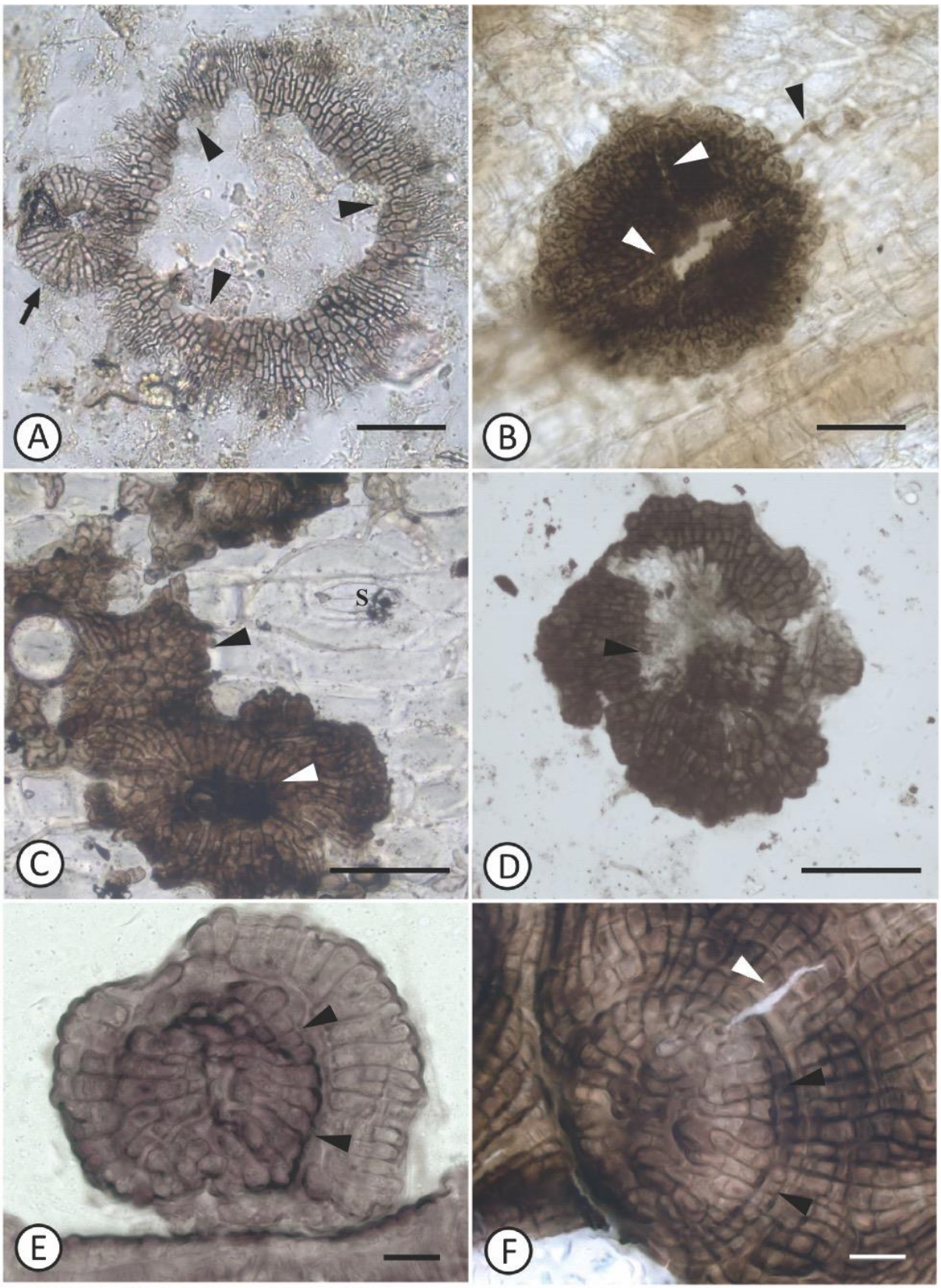
A
B
S
C
D
E
F

Figure 5.4 Morphological diversity of thyriothecial scutella of living species, in dorsal view. A, *Microthyrium macrosporum*, young (black arrow) old and broken (right) scutella. Note distal edge of old scutellum attached to host (black arrowheads), showing fimbriate margin. Specimen UBC-F33039, 12 focal planes (f.p.) stacked. B, *Lembosina aulographoides*, small ellipsoid scutellum with slits of dehiscence (white arrowheads) and attachment to superficial mycelium (black arrowhead). Note absence of stomata in region colonized. Specimen UBC-F33037, eight f.p. stacked. C, D, *Muyocopron smilacis*, on stems of *Smilax* sp., specimen OSC #93714. C, Confluent scutella without apparent columella (black arrowhead) occur beside stomata (S) or on stomata (down), with a columella (white arrowhead); 12 f.p. stacked. D, Small scutellum, dehiscent or broken at centre (black arrowhead), distal edge attached to host; eight f.p. stacked. E, F, *Rhagadolobiopsis thelypteridis*, on leaves of *Thelypteris serrata*, nail polish peels. Specimen VIC 31939. E, Young scutellum showing hyphae arising from elongated columella and forming plate with distinct edge (black arrowheads). Note dichotomous branching in distal part of scutellum; nine f.p. stacked. F, Mature scutellum with central plate (black arrowheads), distal region with similar morphology. Cracking of scutellum is perpendicular to and independent of central plate (white arrowhead); 15 f.p. stacked. Scale bars = 50 µm (A–D), 10 µm (E, F).

to those of plate (Fig.5.4C). At maturity, only a few individual scutella open to release spores through an ostiole, or alternatively, they open through irregular cracking (Fig. 5.4D). I did not observed dehiscence in any of the few, infrequent columellate scutella of *M. smilacis*. These non-dehiscing scutella were always smaller than, confluent with, and distal to, dehiscing scutella (see Luttrell, 1944). As the dehiscing thyriothecium mature, distal regions remain attached to the host, and the scutellum opens dorsally and eventually disintegrates.

Rhagadolobiopsis thelypteridis (VIC 31939) produces scutella arising directly and exclusively from stomata of the fern *Thelypteris serrata* (Cav.) Alston (Fig. 5.4E). Thyriothecia in this taxon are large, up to ca. 1 mm wide. *Rhagadolobiopsis* produces multiple scutella, growing in close proximity and forming a single, larger, compound scutellum. When they merge, scutella are each around 100–200 µm wide (Fig. 5.4E). As they grow out of the stomata, central

plates of hyphae appear above the stomatal complex, with a conspicuous rim of locally depressed hyphae (Fig. 5.4E, 5.4F, black arrowhead). Scutellum hyphae are distally aligned to form a crenulate margin (Fig. 5.4E, 5.4F). In larger scutella, the raised plates are not overgrown by other hyphae (Fig. 5.4F). Compound sporocarps of *R. thelypteridis* open through irregular networks of slits or cracks that tend to run in between multiple scutella, and cracks do not follow the rims of central plates. Columellae and central plates remain in older scutella. The compound scutellum in *Rhagadolobiopsis* is firmly attached to the host substrate, and cannot be removed easily.

5.4.3 Morphology of extant rhizothyrial species

I observed two rhizothyrial species at different stages of development in dorsal view for comparison with the fossil. I borrowed material of the type specimen of *Racheliella wingfieldiana* (CBS H-23399, Tubakiaceae), which was derived from *in vitro* cultures (dried leaves separate from culture and labelled 'Holotype' received from the Westerdijk Institute) rather than from leaves of *Syzygium guineense* (Willd.) DC., its type substrate. The isolate was inoculated onto leaves of *Musa* L. and *Pinus* L. on nutrient agar in culture plates to induce rhizorthyrium formation, then dried and preserved as the herbarium material (P. Crous, personal communication). The dried, colonized leaves of *Musa* sp. and *Pinus* sp. show individual radiate scutella up to 130 µm in diameter surrounded by a mass of conidia oozing in a gelatinous matrix from beneath the distal edges of the scutellum (Fig. 5.5A, arrows). Tips of the scutellum hyphae branch dichotomously. Distal scutellum hyphae diverge from one another and are not aligned at the scutellum margin (Fig. 5.5A). Tips of the marginal hyphae taper and meander slightly (Fig. 5.5A). The scutellum disc is discontinuous, with gaps between hyphae that reveal the underlying conidiogenous cells (Fig. 5.5A). Rhizothyria of *R. wingfieldiana* sometimes occur on stomata

(Figs. 5.5C, stomata in a row labelled “s”), or beside stomata (Figs. 5.5B, stomata labelled “s). The use of autoclaved plant leaves of *Musa* sp. and *Pinus* sp. to trigger the formation of sporocarps may not reflect the interaction of *Racheliella* with its native host *Syzigium guineensis*. Nonetheless it appears that *R. wingfieldiana* does not require host stomata to produce rhizothyria. Rhizothyria are attached to host leaves by a central columella that appears to be entirely superficial and does not extend inside the leaf tissue or through stomata. To observe stomata on cuticle of *Musa*, I cleared the halo of conidia around rhizothyria by quickly vortexing the epidermal peel illustrated in Figure 5.5B in sterile water prior to mounting it on a slide. It appears that, upon disturbance, rhizothyria tend to remain attached by the central columella, and the margin of the scutellum breaks off.

Rhizothyria of *Pirostoma nyssae* (UBC-F11406), collected in Virginia (USA), are produced on the adaxial and abaxial surfaces of leaves of *Nyssa sylvatica*, and are produced near pycnidia (spherical sporocarps), a second asexual stage found in *P. nyssae*. Rhizothyria are up to 120 µm in diameter, radiate, and surrounded by conidia (Fig. 5.5D). The central columella in *P. nyssae* is conspicuous in most specimens (Fig. 5.5A, D, E). It appears as a bundle of hyphae arising perpendicular to the leaf surface, arranged into a cylinder with a central depression. In dorsal view, the columella appears as ring of pigmented cells surrounding an unpigmented circular depression up to 3 µm wide (Fig. 5.5D*,* white arrowhead). As hyphae grow out from the central columella they branch dichotomously to form a continuous disc of hyphae, with a crenulate margin, in young specimens (Fig. 5.5E). Upon sporulating, specimens exhibited a discontinuous disc at the distal edge, exposing underlying conidiogenous cells. Hyphae meander and grow irregularly in distal regions, ending in tapering tips that do not form a continuous margin of the scutellum (Fig. 5.5D). Observed in situ, *P. nyssae* does not appear to colonize or

arise from stomata or substomatal chambers, and it does not form a central plate (Fig. 5.5F). Rhizothyria of *Rhizothyrium abietis*, like those described above, were reported to be 70–200 µm in diameter (Darker, 1965). They produce dense columellae, 10–20 µm wide, that arise through stomata. Columellae give rise to scutella that dehisce around their margin. In the line drawings of Darker (1965), rhizothyria of *R. abietis* radiate from the columella without dichotomous branching and form a scutellum several hyphae thick (Table 5.1).

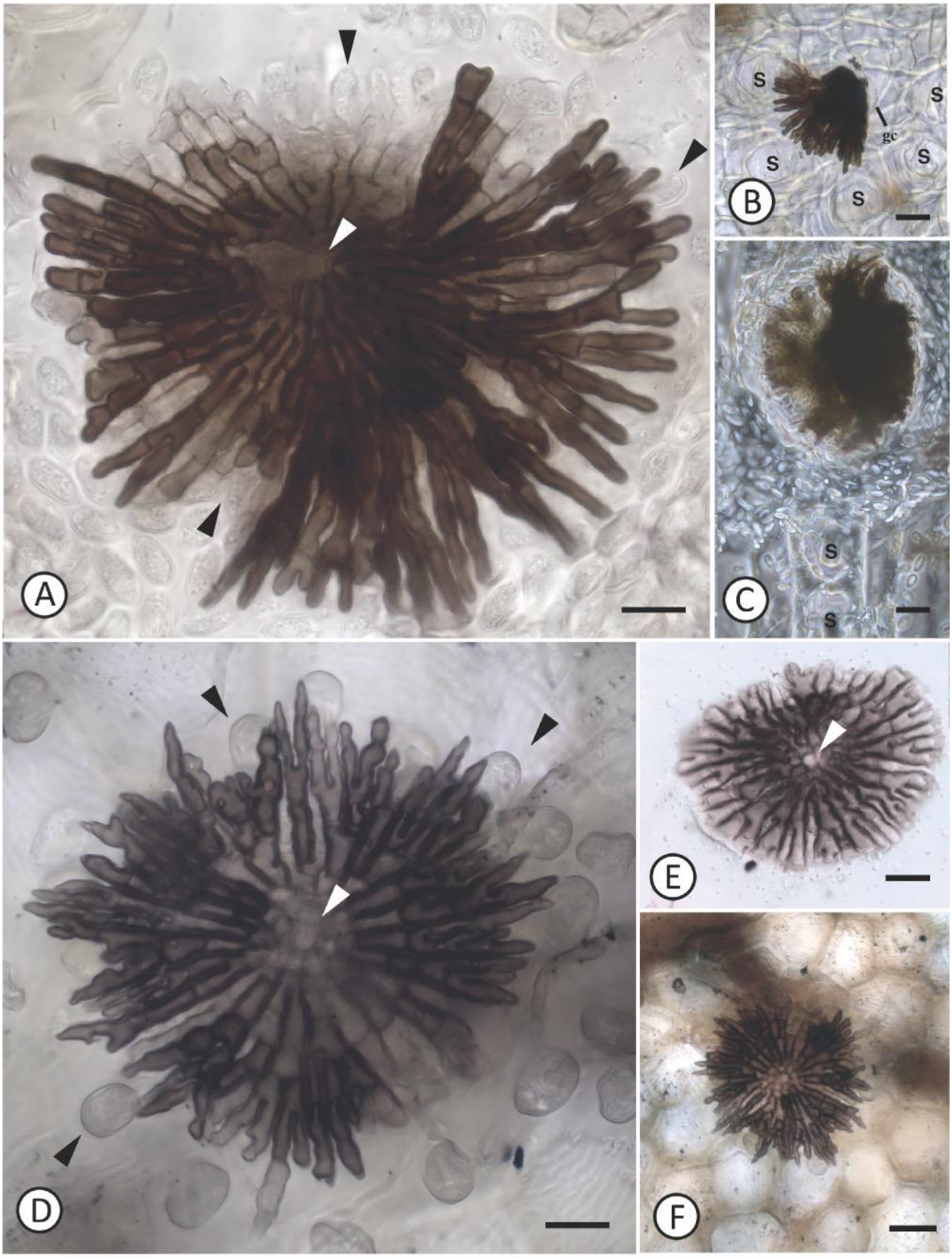
A
B
s
s
s
s
s
gc
C
s
s
D
E
F

Figure 5.5 Scutella of rhizothyria of extant species in dorsal view
A–C, *Racheliella wingfieldiana* CBS H-23399 fruiting on leaves added to growing medium by CBS following isolation. A, Sporocarp on leaves of *Musa* sp. showing conidiogenous cell at distal edge of scutellum (black arrowheads). Discontinuous scutellum made of dichotomously branching hyphae tapering at tip, and central columella (white arrowhead); 16 focal planes (f.p.) stacked. B, Vortexed cuticle of *Musa* sp. showing broken scutellum attached by columella to cuticle, above stoma, surrounded by non-colonized stomata (S); note flange of guard cell (gc) of overgrown stoma; nine f.p. stacked. C, Nail polish peel taken from *Pinus* sp., of scutellum aligned with row of stomata (S), that likely grew above stoma (assuming stomata are evenly spaced). D–F, *Pirostoma nyssae* UBC-F11406 on leaves of *Nyssa sylvatica*. D. Scutellum with central columella (white arrowhead), conidia visible through distal edge of scutellum (black arrowheads). Note scutellum hyphae dichotomously branching in centre, meandering and tapering distally; five f.p. stacked. E, Nail polish peel of young scutellum with central columella (white arrowhead), rounded tips at distal margin and continuous plate of hyphae in the centre; five f.p. stacked. F. Scutellum at lower magnification showing underlying host epidermis without stomata, three f.p. stacked. Scale bars = 10 µm (A, D–F), 20 µm (B, C).

5.5 Taxonomy

Class—Dothideomycetes O. E. Erikss. & Winka

Family—Incertae sedis

Genus—Stomatothyrites Le Renard, Upchurch, Stockey & Berbee *gen. nov.*—

Mycobank number: 832827

Generic diagnosis. Thyriothecial sporocarp circular, arising from host plant stoma, by a dark columella; appressed to host cuticle; discrete, not confluent (Fig. 2*A*–2*C*). Superficial mycelium absent. Scutellum of dichotomously branching hyphae radiate outward from stomatal opening. Substrate, sporocarp size, hyphal pigmentation and branching indicative of Ascomycota.

Etymology. The generic name *stomato-* comes from the Greek to indicate that this taxon is a colonizer of stomata. *Thyr* refers to the thyriothecia it produces (thureos = shield in Greek); and the suffix *-ites* indicates its fossil nature.

Comments*: Stomatothyrites* is distinguished from other fossil taxa by producing individual thyriothecia arising from stomata and dehiscing above stomata. No living genus produces similar structures above stomata.

Type species. Stomatothyrites placocentrus Le Renard, Upchurch, Stockey & Berbee *sp. nov.* (Figs.5. 1A, 5.2A)—Mycobank number: 832828

Figs. 5.1A–D, 2–3

Specific diagnosis. Scutellum hyphae of two growth forms; initially regularly arranged, forming a central plate of roughly trapezoidal cells (Figs. 5.1A–D,5. 2A, B, D); in later stages, hyphae meander producing more elongate cells with lateral lobes or bulges (Figs. 5.2C, 5.2E, 5.2F, 5.3B, 5.3D). Hyphae of central plate, 1.5 to 4.5 µm diameter, radiate, extending from scutellum centre,

wider than hyphae at margin. Plate hyphae branching almost exclusively through isotomous dichotomies (Fig. 5.2A, 5.2D); hyphal side walls straight, laterally abutting within plate without overlap. Marginal hyphae radiate, with meandering side walls and conspicuous overlap; branching with both isotomous and pseudomonopodial dichotomies (Fig. 5.3A–D); diameters (0.8–3 μm); smaller than plate hyphae. Hyphal tips at appressed margin from round to tapering, extend beyond scutellum or flush with edge. Scutella larger than 100 μm open through circular cracks following the edge of central plate; propagating to the scutellum margins (Figs. 5.3E, F). Sporocarp is a radiate thyriothecium, indicative of Dothideomycetes affinities.

Holotype hic designatus. Slide DG-047C deposited in the Department of Earth Sciences, Denver Museum of Nature and Science (DMNS), Denver, CO, under Accession 2019-55-DG-047C, slide #EPI 53113. Specimen is on surface of conifer cuticle, England Finder coordinate N34 with label to right.

Comments: Stomatothyrites placocentrus is distinguished from other fossil taxa by scutella with a central plate, dehiscing by the rim of the plate. Due to its lack of asci and ascospores, the fossil cannot be placed in a living genus.

Paratypes. Stored in DMNS under Accessions 2019-55; cuticle DG-001B (England Finder coordinate T38) under Catalog Number EPI 53114; cuticle DG-049B (England Finder coordinates O44–P44), under EPI 53115; cuticle DG-018B (England Finder coordinate Q37), under EPI 53116; cuticle DG-062A (England Finder coordinate H34), under EPI 53117; cuticle DG-049A (England Finder coordinates Q48–Q49), under EPI 53115; specimen DG-082A (England Finder coordinates R44–R45), under EPI 53118; cuticle DG-080E (England Finder

coordinate M39), under EPI 53119; cuticle DG-073A (England Finder coordinates N45–O46), under EPI 53120.

Type locality. The Dutch Gap Canal (37° 22’ 33.8” N, 77° 21’ 33.6” W; UTM 291098.50 Easting, 4139202.60 Northing, locality DMNH 128), James River, Virginia.

Stratigraphy and age. Potomac Group, lower Zone 1, *Pseudofrenelopsis parceramosa* bed; Lower Cretaceous (Aptian, 125–113 Ma).

Etymology. The species epithet combines *placo-* or shield and *–centrus* for centre, in reference to the conspicuous central plate found in all specimens.

5.6 Discussion

5.6.1 Systematic justification for Stomatothyrites

Molecular systematic studies of thyriothecium forming fungi have shown that thyriothecia with radiate scutella occur in at least five distantly related lineages of Dothideomycetes (Hofmann et al., 2010; Guerrero et al., 2011; Wu et al., 2011b; Guatimosim et al., 2014b; Hongsanan et al., 2014b; Guatimosim et al., 2015; Hongsanan et al., 2015; Mapook et al., 2016a) (Chapter 2). In general, dothideomycete thyriothecia are wider than 100 μm at maturity, and they form individual sporocarps that may be circular or elongate, as shown in *Microthyrium macrosporum* (Figs. 2.4, 5.4A) and *Lembosina aulographoides* (Figs. 2.5Df, 5.4B). Alternatively, they may expand into large, compound sporocarps that result from the merging of more than one scutellum, as in *Rhagadolobiopsis thelypteridis* or *Muyocopron smilacis* (Luttrell, 1944; Guatimosim et al., 2014b). Similar to thyriothecia, and contrasting with rhizothyria illustrated here, *Stomatothyrites* produces scutella with a continuous disc that covers sporogenous tissue without leaving gaps distally. However, I show that continuous discs are also found in immature

rhizothyria of *P. nyssae,* and Braun et al. (2018) showed them to occur in mature rhizothyria of *Involutiscutellula* U. Braun & C. Nakash., *Paratubakia* U. Braun & C. Nakash. and *Sphaerosporothyrium* U. Braun, Crous, O. Moreno-Rico & Marm. While scutella-forming discontinuous discs are only found in rhizothyria, the presence of scutella forming continuous discs is insufficient to distinguish thyriothecia from rhizothyria because they may occur in both structures. The distal area of the scutellum of *Stomatothyrites* appears to preserve better than the central plate, and in this zone, the structure is more firmly attached at the edge than the centre, similar to the remnant of scutella in old thyriothecia of *M. macrosporum*. This suggests that spores could only escape apically, through cracks in its dorsal surface at maturity. Taken together, the continuous disc of the scutellum, the appressed margin of the scutella and the numerous occurrences of circularly opened central plates in *Stomatothyrites* suggest that it formed thyriothecia rather than rhizothyria. Thus, *Stomatothyrites* most likely belongs within the Dothideomycetes.

Table 5.1 Comparison of scutella of *Stomatothyrites placocentrus gen. et sp. nov.* to similar fungi in Dothideomycetes and Sordariomycetes.

Taxon	Scutellum diameter	Scutellum initiation	Scutellum branching	Margin tips	Conti-nuous disc	Attachment to host	Apical dehiscence	Scutellum opens with
Stomatothyrites placocentrus[†]	90–170 µm	Stomata	Dichotomous	crenulate and tapering	yes	Columella and scutellum margin	yes?	circular fracture
Dothideomycetes								
Microthyrium macrosporum	110–250 µm	Superficial mycelium	Dichotomous	blunt then tapering	yes	Scutellum margin	yes	ostiole
Rhagadolobiopsis thelypteridis	400–800 µm	Stomata	Dichotomous	crenulate	yes	Scutellum margin	yes	longitudinal slits
Lembosina aulographoides	up to 350 µm wide	Superficial mycelium	Pseudomono-podial	crenulate	yes	Scutellum margin	yes	longitudinal slits
Muyocopron smilacis	150–700 µm	Stomata and superficial mycelium	Dichotomous	crenulate	yes	Columella or margin	yes or no	ostiole or slits
Sordariomycetes								
Rhizothyrium abietis[1]	70–200µm	Stomata	none	crenulate	yes	Central Columella	no	none
Pirostoma nyssae	50–90 µm	Intracellular mycelium	Dichotomous	crenulate then tapering	no	Central columella	no	none
Racheliella wingfieldiana	60–130 µm	Intracellular mycelium	Dichotomous	tapering	no	Central columella	no	none

[†]fossil

[1] Morphology derived from illustration and dimensions reported in Darker GD (1965)

5.6.2 Comparison to extant Dothideomycetes associated with stomata

Stomatothyrites sporocarps grew directly from host stomata. While folicolous fungi often have the ability to penetrate their host through the stomata (Young, 1926; Bald, 1952; Yirgou and Caldwell, 1963; Turner and Graniti, 1969; Latunde-Dada et al., 1999), few of the taxa initiate their fruiting bodies by growing out of stomatal openings. Initiation of sporocarps from stomata appears to have evolved multiple times within Dothideomycetes. In Dothideomycetes, distantly related, non-thyriothecial genera that initiate sporocarps from stomata include *Ceratocarpia* Rolland (Dodge, 1939), *Nothophaeocryptopus* Videira, C. Nakash. & Crous (Stone et al., 2008), *Stomatogene* Theiss. (Farr, 1989), *Batcheloromyces* Marasas, P.S. van Wyk & Knox-Dav. (Marasas et al., 1975) and *Stigmina* E. Bald. & Cif. (Sutton and Pascoe, 1989). In these taxa, spores are produced in perithecia or sporodochia, round or cup shaped sporocarps where a lower wall is present. *Stomatothyrites placocentrus* differs readily from the above taxa in producing a radiate scutellum, appressed to stomata and without a lower wall.

Of the thyriothecium-forming Dothideomycetes that have been documented with nuclear rDNA sequences, only *Rhagadolobiopsis thelypteridis* produces radiate scutella in stomata (Guatimosim et al., 2014b). This taxon belongs to the order Asterotexiales and is sister to taxa in this order that form thyriothecia initiated from superficial hyphae such as *Asterina* spp., *Lembosia* spp. or *Discopycnothyrium palmae* (Guatimosim et al., 2015; Hongsanan et al., 2016). Sequence data are not yet available for *Muyocopron smilacis,* but it produces radiate scutella that sometimes emerge from stomata. Other *Muyocopron* species form a clade within Dothideomycetes, now named *Muyocopronales* (Mapook et al., 2016b). Of the 10 species of *Muyocopron* published with molecular sequences (Mapook et al., 2016b; Tibpromma et al., 2016; Hernández-Restrepo et al., 2019), none are described as growing directly out of stomata.

Like species with sequence data, *Muyocopron smilacis* produce radiate scutella aggregating into confluent crusts, and containing aseptate ascospores inside bitunicate asci (Luttrell, 1944); and it is possible that all the taxa in *Muyocopron* can colonize stomata. In both *Muyocopron* and *Rhagadolobiopsis*, stomatal colonization leads to confluent sporocarps where scutella do not dehisce individually. In contrast, *Stomatothyrites* produces discrete thyriothecia that may overlap with one another, but which probably dehisce individually rather than collectively after fusing into larger structures.

5.6.3 Comparison to other Cretaceous fungi associated with stomata.

Fungi reported to produce sporocarps arising from stomata include *Xylomites cycadeoideae* Chrysler and Haenseler (1936), *Pteropus brachyphylli* Van der Ham, and pycnidia associated with *Stomiopeltites cretaceus* Alvin and Muir (1970), and Pons and Boureau (1977). Sporocarps of *Xylomites cycadeoideae* from the Raritan Formation (Upper Cretaceous) of New Jersey are found among the leaf bases and dispersed rachides of *Cycadeoidea peridermalis* Chrysler (Chrysler and Haenseler, 1936). The specimens are only described in section view, and so are difficult to compare with *Stomatothyrites*, but they do show a flattened epiphyllous fungus emerging from a stoma. Their hyphal cells, however, are described as isodiametric and 3 μm in diameter; and a radiate scutellum has not been demonstrated for these specimens.

Pteropus brachyphylli (Van der Ham and Dortangs, 2005) was described from the Late Cretaceous, Lower Maastricht Formation of NE Belgium (Fig. 2) on leaves of the cheirolepidiaceous conifer *Brachyphyllum patens* (Miquel) Van der Ham and van Konijnenburg-van Cittert. They were studied in thin section from a fine-grained flint. *Pteropus brachyphylli* consists of stromata arising from the substomatal chamber that grow to fill guard cells and the

stomatal cavity, and then reach the surface of the leaf from the stomata (Van der Ham and Dortangs, 2005). The hyphae located outside the epidermis form a flattened structure that is only illustrated in section view in Van der Ham and Dortangs (2005). Comparisons to the material I contribute are also difficult because the material was studied with thin sections. However, scutellum pigmentation in *P. brachyphylli* obscures individual hyphae, and a radiate scutellum as in *Stomatothyrites* was not evident.

The thyriothecial fungus *Stomiopeltites cretaceus* from the Early Cretaceous English Wealden (Alvin and Muir, 1970) and the Upper Cretaceous (middle Cenomanian) of Anjou, France (Pons and Boureau, 1977) grew with another fungus on the same leaves that formed pycnidia. These pycnidia are associated with stomata, unlike the thyriothecia of *S. cretaceus*. SEM illustrations in Alvin and Muir (1970) do not allow the interpretation of the pycnidial walls, but the Pons and Boureau (1977) specimens are better preserved. They clearly show non-radiate and ostiolate sporocarps associated with stomata, and contrast with the radiate and non-ostiolate sporocarps of *Stomatothyrites.*

5.6.4 Significance of *Stomatothyrites*

Stomatothyrites placocentrus is the most common fossil fungus found on Dutch Gap, Lower Potomac Group Zone 1 cuticles. The unique mode of dehiscence in *Stomatothyrites* does not allow us to infer the type of spores it may have produced, but it does indicate dorsal dehiscence, and probable affinities with thyriothecia of Dothideomycetes. To my knowledge, minute thyriothecial sporocarps associated with stomata of conifers, or other seed plants have not been described before. Illustrated works on extant thyriothecium forming fungi show few taxa that

produce a scutellum above stomata; and all of these differed substantially from *Stomatothyrites* (Arnaud, 1918; Stevens and Manter, 1925; Stevens and Ryan, 1939; Doidge, 1942).

The extensive Kalgutkar and Jansonius fungal database with 1440 entries for species of fossil fungi (Berbee et al., 2014) does not contain any similar stomatal colonizer. This new fossil extends the range of morphological characters known among thyriothecial fungi and adds to the known diversity of thyriothecia on Cretaceous conifers. Rhizothyria are classified in two distant lineages of Ascomycota (Smerlis, 1967; Johnston et al., 2014; Braun et al., 2018), and it is unclear if any characters of rhizothyria that resemble thyriothecia are homologous. Rhizothyria are less systematically informative than radiate thyriothecia. Showing that *S. placocentrus* produced thyriothecia brings this new fossil closer to comparisons based on homology.

Chapter 6: Conclusions

The available fossil record confirms the divergence of crown lineages of Ascomycota before or during the Cretaceous, but otherwise, the Mesozoic record of fungi is still quite sparse and difficult to interpret (Taylor et al., 2015). Documenting fossil and living taxa together is the best way of detecting significant commonalities and of finding characters that carry systematic significance and are present in fossils (Schweitzer, 2003). The integration of newly discovered fossil fungi in an evolutionary scheme compatible with that of living fungi has the potential to improve age estimates for divergence of fungal clades. However, many diagnostic shared characters of fungi are homoplasious, having originated convergently (Berbee and Taylor, 1992; Grube et al., 2004; Tsui and Berbee, 2006; Schmitt et al., 2009; Berbee et al., 2012). My study of living taxa reveals characters of thyriothecia that may be homoplasious but are only found in a single class of Ascomycota: Dothideomycetes. Comparative phylogenetic study of thyriothecia reveals diagnostic apomorphies, derived characters that evolved among Dothideomycetes clades, and suggests a minimum age for crown divergence within this group in the Triassic.

By surveying plant leaf surfaces from the early Cretaceous, I discovered abundant fly-speck fungi on extinct gymnosperms. Among my new species, *Protographum luttrellii* (Chapter 3) has a combination of diagnostic apomorphies found in a single clade of Dothideomycetes, while *Bleximothyrites ostiolatus* (Chapter 4) and *Stomatothyrites placocentrus* (Chapter 5) combine character states homoplasious within Dothideomycetes and autapomorphic character states that could not be found in any living taxon. This suggests that both taxa represent extinct taxa of Dothideomycetes. The morphology of these extinct taxa helps to document ancestral character states of fungi and it provides minimum age for character evolution.

6.1 Strength and significance

The documentation of fungi through time has tended to focus on few, well-preserved fossils of distant phylogenetic affinities, studied by paleontologists with a botanical training (Taylor et al., 2015). I have applied my mycological training to target the sampling of fungi so that I could formally test the phylogenetic relationships of extant fungi with my newly described fossils.

In Chapter 1, I introduce thyriothecial fungi and show the relevance of the online database <https://advance.science.sfu.ca/fungi/fossils/Kalgutkar_and_Jansonius/> (Berbee et al., 2014) in targeting the search for fossils with a good preexisting record. The sorting of fossil taxa through time is a powerful resource to formulate and test hypotheses about the sequence of appearance of fungi through time.

In Chapter 2, I sampled living thyriothecial taxa in Dothideomycetes. Direct observation led me to recognize developmental differences in structure of thyriothecia in this clade that had not been noticed before. I assembled the broadest molecular and morphological dataset for thyriothecial fungi available to date. I scored morphological characters of the taxa using published illustrations and original observations, and reconstructed ancestral character states for clades of Dothideomycetes. Using key examples from the literature, I show the relevance of the newly defined characters for studying fossil thyriothecia. I show that the fossil taxon *Trichothyrites setifer*, from the Ypresian (56–47.8 Ma) of India (Monga et al., 2015), provides the oldest evidence for characters found in *Lichenopeltella pinophylla*, a taxon for which I contributed the first DNA sequence.

In Chapters 3 and 4, 5, I introduce new taxa of fossil thyriothecia and show how the new characters I defined in Chapter 2 have the power to discriminate the new taxa from one another and from other described species of extant taxa. Chapter 3 and 4 formally apply phylogenetically

informative characters from Chapter 2 to test the phylogenetic affinities of the newly described taxa. This is the first time a cladistic interpretation of fossils of epiphyllous fungi has been applied. Chapter 5, in contrast, uses comparative anatomy to define character states among modern taxa that distinguish whether or not radiate scutella are from thyriothecia or from superficially similar structures.

In Chapter 3, the interpretation of *P. luttrellii* owes its significance almost entirely to the characters I found in living Aulographaceae. *Protographum* represents the oldest evidence of thyriothecia that can be linked to a living clade of Dothideomycetes. Prior to this discovery, *T. setifer* (Eocene, 56–47.8 Ma) represented the oldest such evidence (Chapter 2). In Chapter 4, the discovery of *B. ostiolatus* confirms that radiate and ostiolate sporocarps are unique to Dothideomycetes, but nonetheless points to the ambiguity of available sporocarp characters for living taxa, despite the new characters I defined. I revived the concept of *mycélium en palmettes*, showing mycelial characters that currently are not used for identification, while they show potential systematic relevance in addition to the characters of the thyriothecium. The fossil I describe in Chapter 5, *Stomatothyrites placocentrus,* has a unique combination of characters, and in studying this taxon, I contributed to the distinction of rhizothyria from thyriothecia in living taxa. I show that two distantly related lineages of Ascomycota (in different classes) may form radiate sporocarps that look very similar and may need to be found in situ to be distinguished.

6.2 Limits

Working with thyriothecium forming fungi involves numerous limitations. Many modern genera and species of fly-speck fungi have yet to be studied with molecular methods. Among these species there are likely to be examples of convergent evolution that I could not detect, predict, or

include in my analyses. I interpreted ancestral character states of thyriothecia based on characters that I could score. For taxa that I could not observe, the absence of data for a character was sometimes difficult to distinguish from true absence of the same character. Although I justified every morphological state I assigned, it remains possible that the asexual taxa that were scored ambiguously are able to produce structures homologous to those I compared and influence my results.

In order to infer patterns of morphological evolution, a solid phylogenetic hypothesis is often a prerequisite. I chose to work with an under-sampled group of fungi for which phylogenetic relationships were poorly understood (Hofmann and Piepenbring, 2011; Wu et al., 2011b; Hongsanan et al., 2014b). This enabled me to interpret the abundant fossil record of thyriothecial fungi, but I acknowledge that future study of Dothideomycetes phylogenetic relationships may alter interpretations of character evolution among extant and fossil taxa.

For most of the hypotheses that I have made about the phylogenetic distribution of a morphological character, it would take only one new sample of a taxon with an unpredicted combination of character states to significantly change my phylogenetic conclusions. For example, I claim that the distribution of radiate thyriothecia is restricted to Dothideomycetes, but Chapter 4 presents rhizothyria, a radiate type of fungal sporocarp characterized by a columella, and phylogenetically distant from Dothideomycetes. I interpreted the Triassic fossil described by Mishra et al. (2018) as evidence of Dothideomycetes because there was no evidence that the fossil had a columella. If it did have a columella, or if columellate structures of the same age are found, these Triassic fossils might actually represent rhizothyria rather than thyriothecia. If species with radiate sporocarps dehiscing apically are found in living species from clades outside Dothideomycetes in the future, this would contradict my interpretation that these characters in

combination can be used to place fossils in Dothideomycetes. In spite of these limitations, following good systematic practices, I have been clear about my assumptions. My cultures, sequences and character state coding are available for re-interpretation or re-analysis. Where my conclusions are wrong, I have laid the groundwork for future correction.

6.3 Applications

I contributed new DNA sequences for 15 taxa from British Columbia, France, and Costa Rica, and 10 isolates in culture collections (Westerdijk Institute). The large phylogeny of living thyriothecia I inferred is the best available guide to formulate hypotheses about their evolution. I produced a matrix of 11 characters for 323 taxa, and I tested the phylogenetic relationships of six fossil taxa using different versions of the same matrix. The matrix can be used by anyone and all the data and metadata included are available on TreeBase.

Fossils of the Eocene *Trichothyrites setifer* can be used to calibrate the divergence of the clade containing extant *Lichenopeltella pinophylla* from remaining Microthyriales. I suggest it may be premature to use this fossil for age constraints because I only contributed a single DNA sequence for this species. The fossils *P. luttrellii*, *B. ostiolatus* and *S. placocentrus* provide strong evidence for the diversity of Dothideomycetes in the Potomac Group beds of Virginia. The occurrence of *P. luttrellii* in the Aptian Stage of the Lower Cretaceous may prove useful in calibrating the divergence of Aulographaceae from remaining Dothideomycetes, although it will be more informative when the sister clade relationships of the Aulographaceae are more firmly established. If the changes that occurred in the morphology of thyriothecia can be followed through time, they will indicate when lineages of Dothideomycetes diverged from one another.

Given the paucity of fossil evidence used to estimate the age of Ascomycota, many other age estimates of Dothideomycetes will likely be impacted by these new fossil calibrations.

The modified protocol for extracting cuticle builds on pre-existing observations from workers on fossil fungi (Kalgutkar and Jansonius, 2000). I confirm that monitoring pigmented fossil over the oxidation process is key to maximize the imaging of fossil fungi and avoid their disintegration. Additionally, I show that comparative anatomy of scutella is best achieved by preparing stacks of bright field micrographs and observing available sequences of development. The branching of scutellum hyphae is shown to be a rich source of morphological characters if we compare living taxa in the same orientation to the fossils.

6.4 Future directions

Further sampling of thyriothecia will dramatically improve the phylogeny of Dothideomycetes. In phylogenetic analyses, the lack of resolution among the early diverging events of Dothideomycetes always involves clades of thyriothecial fungi (Hofmann and Piepenbring, 2011; Wu et al., 2011b; Hongsanan et al., 2014b). More than ever before, I feel the need to properly characterize these organisms that are hyper-diverse, almost everywhere, and overlooked.

I show that characters of thyriothecia can be used in phylogenetic analyses. I hope that my approach to characters will stimulate similar analyses of additional characters in other groups of fungi with a fossil record. Of the 1004 taxa in Kalgutkar and Jansonius (2000) many fossil characters are quite remarkable and their phylogenetic distribution could be investigated in a similar way. For example, a longitudinal slit in ascospores characterizes the fossil taxa *Hypoxylonites* Elsik and *Spirotremesporites* Dueñas and is also found in living taxa in Xylariales

and Coniochaetales. It may be possible to track the origin and diversification of Xylariales and Coniochaetales by careful analysis of spore types in extant and fossil taxa.

In the course of my study, I described only a small fraction of all the fossils I encountered from my Dutch Gap sample. The abundance of fossils allowed me to choose the most complete specimens. I found that the search for new taxa was very successful, once variation in thyriothecial morphology was understood. The Cretaceous Potomac Group beds extend from the base of the Aptian (125 Ma) through the Cenomanian Stages (94 Ma) of the Cretaceous. They contain leaf and pollen remains that help to document extinct gymnosperms and the rise and diversification of angiosperms (Chapter 1, Fig. 1.7). I examined material from the Aptian, from lower Zone 1. In younger strata, I expect additional taxa of epiphyllous fungi based on a preliminary examination of slides prepared by Gary Upchurch (Texas State University) for his dissertation material. My studies show that it will now be rewarding to further follow the evolution of radiate thyriothecia through this Potomac Group stratigraphic sequence.

Bibliography

AHN, Y.-M., AND C. A. SHEARER. 1999. Taxonomic Revision of *Leptosphaeria vagabunda* and Four Infraspecific Taxa. *Mycologia* 91: 684–693.

AINSWORTH, G. C., F. K. SPARROW, AND A. S. SUSSMAN. 1973. The Fungi, an advanced treatise: a taxonomic review with keys. Ascomycetes and Fungi imperfecti vol. 4B. Academic Press.

AINSWORTH, M. A., S. TAYLOR, AND P. F. CANNON. 2015. Following in the footsteps of Dickie and Leighton: some rarely recorded microfungi on Twinflower leaves including Ceramothyrium linnaeae, new to Britain. *Field Mycology* 16: 5–11.

ALVIN, K. L., AND M. D. MUIR. 1970. An epiphyllous fungus from the Lower Cretaceous. *Biological Journal of the Linnean Society* 2: 55–59.

APTROOT, A., AND R. LÜCKING. 2016. A revisionary synopsis of the Trypetheliaceae (Ascomycota: Trypetheliales). *The Lichenologist* 48: 763–982.

ARIYAWANSA, H. A., K. D. HYDE, S. C. JAYASIRI, B. BUYCK, K. T. CHETHANA, D. Q. DAI, Y. C. DAI, et al. 2015. Fungal diversity notes 111–252—taxonomic and phylogenetic contributions to fungal taxa. *Fungal Diversity* 75: 27–274.

ARNAUD, G. 1917a. Sur quelques microthyriacées. *Compte Rendu de l'Académie des Sciences Paris* 164: 888–890.

ARNAUD, G. 1917b. Sur la famille des microthyriacées. *Compte Rendu de l'Académie des Sciences Paris* 164: 574–577.

ARNAUD, G. 1918. Les Asterinées. Doctorate Ph.D., Faculté des Sciences de Paris, Coulet et Fils, Montpellier.

ARNAUD, G. 1925. Lés Asterinées. IVe partie. *Annales de l'École National d'Agriculture de Montpellier, série 10* 5: 643–722.

ARNOLD, A. E., J. MIADLIKOWSKA, K. L. HIGGINS, S. D. SARVATE, P. GUGGER, A. WAY, V. HOFSTETTER, et al. 2009. A phylogenetic estimation of trophic transition networks for ascomycetous fungi: are lichens cradles of symbiotrophic fungal diversification? *Systematic Biology* 58: 283–297.

ARX, A. J. V., AND E. MÜLLER. 1960. Über die neue Ascomycetengattung *Aulographina*. *Revue de Mycologie* 14: 330–333.

ARX, J. A. V., AND E. MÜLLER. 1954. Die Gattungen der amerosporen Pyrenomyceten. *Beiträge zur Kryptogamenflora der Schweiz* 11: 1–434.

ARZANLOU, M., J. Z. GROENEWALD, W. GAMS, U. BRAUN, H.-D. SHIN, AND P. W. CROUS. 2007. Phylogenetic and morphotaxonomic revision of *Ramichloridium* and allied genera. *Studies in Mycology* 58: 57–93.

ASH, S. 1994. First occurrence of *Czekanowskia* (Gymnospermae, Czekanowskiales) in the United States. *Review of Palaeobotany and Palynology* 81: 129–140.

BAJPAI, U., AND H. K. MAHESHWARI. 1987. Epiphyllous fungi from the Gondwana. *The Palaeobotanist* 36: 210–213.

BAKER, B. J., M. A. LUTZ, S. C. DAWSON, P. L. BOND, AND J. F. BANFIELD. 2004. Metabolically active eukaryotic communities in extremely acidic mine drainage. *Applied and Environmental Microbiology* 70: 6264–6271.

BALD, J. 1952. Stomatal droplets and the penetration of leaves by plant pathogens. *American Journal of Botany*: 97–99.
BALDAUF, S. L. 2003. Phylogeny for the faint of heart: a tutorial. *Trends in Genetics* 19: 345-351.
BALOCH, E., G. GILENSTAM, AND M. WEDIN. 2009. Phylogeny and classification of *Cryptodiscus*, with a taxonomic synopsis of the Swedish species. *Fungal Diversity* 38.
BALOCH, E., G. GILENSTAM, AND M. WEDIN. 2013. The relationships of *Odontotrema* (Odontotremataceae) and the resurrected *Sphaeropezia* (Stictidaceae)—new combinations and three new *Sphaeropezia* species. *Mycologia* 105: 384–397.
BALOCH, E., R. LUCKING, H. T. LUMBSCH, AND M. WEDIN. 2010. Major clades and phylogenetic relationships between lichenized and non-lichenized lineages in Ostropales (Ascomycota: Lecanoromycetes). *Taxon* 59: 1483–1494.
BANNISTER, J. M., J. G. CONRAN, AND D. E. LEE. 2016. Life on the phylloplane: Eocene epiphyllous fungi from Pikopiko Fossil Forest, Southland, New Zealand. *New Zealand Journal of Botany* 54: 412–432.
BARBACKA, M., AND K. BOKA. 2000. The stomatal ontogeny and structure of the Liassic pteridosperm *Sagenopteris* (Caytoniales) from Hungary. *International Journal of Plant Sciences* 161: 149–157.
BARR, M. E. 1968. The Venturiaceae in North America. *Canadian Journal of Botany* 46: 799–864.
BATISTA, A. C. 1959. Monografia dos fungos Micropeltaceae. *Publicações do Instituto de Micologia da Universidade do Recife* 56: 1–519.
BATISTA, A. C., J. L. BEZERRA, T. T. BARROS, AND F. B. LEAL. 1969. Sobre um novo gênero de Microthyriaceae da Nova Caledônia. *Instituto de Micologia, Universidade do Recife* 637.
BEIMFORDE, C., K. FELDBERG, S. NYLINDER, J. RIKKINEN, H. TUOVILA, H. DÖRFELT, M. GUBE, et al. 2014. Estimating the Phanerozoic history of the Ascomycota lineages: Combining fossil and molecular data. *Molecular Phylogenetics and Evolution* 78: 386–398.
BELISARIO, A. 1991. *Dicarpella dryina* sp. nov., teleomorph of *Tubakia dryina*. *Mycotaxon* 41: 147–155.
BERBEE, M., L. LE RENARD, AND D. CARMEAN. 2014. Online access to the Kalgutkar and Jansonius database of fossil fungi. *Palynology* 39: 103–109.
BERBEE, M. L., AND J. W. TAYLOR. 1992. Convergence in ascospore discharge mechanism among pyrenomycete fungi based on 18S ribosomal RNA gene sequence. *Molecular Phylogenetics and Evolution* 1: 59–71.
BERBEE, M. L., AND J. W. TAYLOR. 2010. Dating the molecular clock in fungi – how close are we? *Fungal Biology Reviews* 24: 1–16.
BERBEE, M. L., S. SEKIMOTO, L. LE RENARD, AND J. W. SPATAFORA. 2012. Becoming a fungus: comparative phylogenetic studies of evolution of absorptive nutrition, Mycological Society of America annual meeting, Yale University, New Haven, Connecticut.
BERCOVICI, A., A. HADLEY, AND U. VILLANUEVA-AMADOZ. 2009. Improving depth of field resolution for palynological photomicrography. *Palaeontologia Electronica* 12: 1–12.
BOEHM, E. W., G. MARSON, G. H. MATHIASSEN, A. GARDIENNET, AND C. L. SCHOCH. 2015. An overview of the genus *Glyphium* and its phylogenetic placement in Patellariales. *Mycologia* 107: 607–618.

BOEHM, E. W. A., C. L. SCHOCH, AND J. W. SPATAFORA. 2009a. On the evolution of the Hysteriaceae and Mytilinidiaceae (Pleosporomycetidae, Dothideomycetes, Ascomycota) using four nuclear genes. *Mycological Research* 113: 461–479.

BOEHM, E. W. A., G. K. MUGAMBI, A. N. MILLER, S. M. HUHNDORF, S. MARINCOWITZ, J. W. SPATAFORA, AND C. L. SCHOCH. 2009b. A molecular phylogenetic reappraisal of the Hysteriaceae, Mytilinidiaceae and Gloniaceae (Pleosporomycetidae, Dothideomycetes) with keys to world species. *Studies in Mycology* 64: 49–83–S43.

BOONMEE, S., A. Y. ROSSMAN, J.-K. LIU, W.-J. LI, D.-Q. DAI, J. D. BHAT, E. B. G. JONES, et al. 2014. Tubeufiales, ord. nov., integrating sexual and asexual generic names. *Fungal Diversity* 68: 239–298.

BOONMEE, S., M. J. D'SOUZA, Z. LUO, U. PINRUAN, K. TANAKA, H. SU, D. J. BHAT, et al. 2016. Dictyosporiaceae fam. nov. *Fungal Diversity*: 1–26.

BOSE, T. 2013. Taxonomy and phylogeny of mitosporic Capnodiales and description of a new sooty mold species, Fumiglobus pieridicola, from British Columbia, CanadaText.

BOSE, T., D. R. REYNOLDS, AND M. L. BERBEE. 2014. Common, unsightly and until now undescribed: *Fumiglobus pieridicola* sp. nov., a sooty mold infesting *Pieris japonica* from western North America. *Mycologia* 106: 746–756.

BRAUN, U., S. TAKAMATSU, V. HELUTA, S. LIMKAISANG, R. DIVARANGKOON, R. COOK, AND H. BOYLE. 2006. Phylogeny and taxonomy of powdery mildew fungi of *Erysiphe* sect. Uncinula on *Carpinus* species. *Mycological Progress* 5: 139–153.

BRAUN, U., C. NAKASHIMA, P. W. CROUS, J. Z. GROENEWALD, O. MORENO-RICO, S. ROONEY-LATHAM, C. L. BLOMQUIST, et al. 2018. Phylogeny and taxonomy of the genus *Tubakia* s. lat. *FUSE* 1: 41–99.

BRENNER, G. J. 1963. The spores and pollen of the Potomac Group of Maryland. *Maryland Department of Geology, Mines and Water Resources, Bulletin* 27: 1–215.

BRODO, I. M., S. D. SHARNOFF, AND S. SHARNOFF. 2001. Lichen of North America. Yale University Press.

BRONSON, A. W., A. A. KLYMIUK, R. A. STOCKEY, AND A. M. F. TOMESCU. 2013. A Perithecial Sordariomycete (Ascomycota, Diaporthales) from the Lower Cretaceous of Vancouver Island, British Columbia, Canada. *International Journal of Plant Sciences* 174: 278–292.

BROWN, G. E. 1975. Factors affecting postharvest development of *Colletotrichum gloeosporioides* in citrus fruits. *Phytopathology* 65: 404–409.

CAIN, R. F. 1956. Studies of coprophilous ascomycetes: II *Phaeotrichum*, a new cleistocarpous genus in a new family, and its relationships. *Canadian Journal of Botany* 34: 675–687.

CARRIS, L. M., AND A. P. POOLE. 1993. A New Species of *Protoventuria* on Leaves of *Vaccinium macrocarpon*. *Mycologia* 85: 93–99.

CASTAÑEDA RUIZ, R. F. 1985. Deuteromycotina de Cuba. Hyphomycetes III. Instituto de Investigaciones, "Alejandro de Humboldt", Cuba.

CHANG, Y., S. WANG, S. SEKIMOTO, A. L. AERTS, C. CHOI, A. CLUM, K. M. LABUTTI, et al. 2015. Phylogenomic analyses indicate that early fungi evolved digesting cell walls of algal ancestors of land plants. *Genome Biology and Evolution* 7: 1590–1601.

CHEEWANGKOON, R., J. GROENEWALD, K. HYDE, C. TO-ANUN, AND P. CROUS. 2012. Chocolate spot disease of *Eucalyptus*. *Mycological Progress* 11: 61–69.

CHEEWANGKOON, R., J. Z. GROENEWALD, B. A. SUMMERELL, K. D. HYDE, C. TO-ANUN, AND P. W. CROUS. 2009. Myrtaceae, a cache of fungal biodiversity. *Persoonia* 23: 55–85.

CHOMNUNTI, P., T. W. K. KO, E. CHUKEATIROTE, K. D. HYDE, L. CAI, E. B. G. JONES, R. KODSUEB, et al. 2012. Phylogeny of Chaetothyriaceae in northern Thailand including three new species. *Mycologia* 104: 382–395.
CHOMNUNTI, P., C. SCHOCH, B. AGUIRRE-HUDSON, T. KO-KO, S. HONGSANAN, E. B. G. JONES, R. KODSUEB, et al. 2011. Capnodiaceae. *Fungal Diversity* 51: 103–134.
CHOMNUNTI, P., S. HONGSANAN, B. AGUIRRE-HUDSON, Q. TIAN, D. PERŠOH, M. DHAMI, A. ALIAS, et al. 2014. The sooty moulds. *Fungal Diversity* 66: 1–36.
CHRYSLER, M. A., AND C. M. HAENSELER. 1936. A Cretaceous fungus: *Xylomites cycadeoideae*. *American Journal of Botany* 23: 33–36.
CLARKE, R. T. 1965. Fungal spores from Vermejo Formation coal beds (Upper Cretaceous) of central Colorado. *Mountain Geologist* 2: 85.
CLEMENTS, F. E., AND C. L. SHEAR. 1931. The genera of fungi. (second ed.). New York.
COHEN, K. M., S. FINNEY, AND P. L. GIBBARD. 2019. ICS International Chronostratigraphic Chart 2019/05. (c) International Commission on Stratigraphy, www.stratigraphy.org (visited: 2019/19/12).
COOKSON, I. C. 1947. Fossil fungi from Tertiary deposits in the Southern Hemisphere. Part I. *Proceedings of the Linnean Society of New South Wales* 72: 207–214.
CROUS, P. W. 2009. Taxonomy and phylogeny of the genus *Mycosphaerella* and its anamorphs. *Fungal Diversity* 38: 1–24.
CROUS, P. W., U. BRAUN, AND J. Z. GROENEWALD. 2007a. *Mycosphaerella* is polyphyletic. *Studies in Mycology* 58: 1–32.
CROUS, P. W., J. Z. GROENEWALD, J. P. MANSILLA, G. C. HUNTER, AND M. J. WINGFIELD. 2004. Phylogenetic reassessment of *Mycosphaerella* spp. and their anamorphs occurring on *Eucalyptus*. *Studies in Mycology* 50: 195–214.
CROUS, P. W., M. J. WINGFIELD, J. P. MANSILLA, A. C. ALFENAS, AND J. Z. GROENEWALD. 2006. Phylogenetic reassessment of Mycosphaerella spp. and their anamorphs occurring on Eucalyptus. II. *Studies in Mycology* 55: 99–131.
CROUS, P. W., C. MOHAMMED, M. GLEN, G. J. M. VERKLEY, AND J. Z. GROENEWALD. 2007b. *Eucalyptus* microfungi known from culture. 3. *Eucasphaeria* and *Sympoventuria* genera nova, and new species of *Furcaspora*, *Harknessia*, *Heteroconium* and *Phacidiella*. *Fungal Diversity* 25: 19–36.
CROUS, P. W., R. W. BARRETO, A. C. ALFENAS, R. F. ALFENAS, AND J. Z. GROENEWALD. 2010. What is *Johansonia*? *IMA Fungus* 1: 117–122.
CROUS, P. W., C. L. SCHOCH, K. D. HYDE, A. R. WOOD, C. GUEIDAN, G. S. DE HOOG, AND J. Z. GROENEWALD. 2009. Phylogenetic lineages in the Capnodiales. *Studies in Mycology* 64: 17–47–S17.
CROUS, P. W., J. Z. GROENEWALD, R. G. SHIVAS, J. EDWARDS, K. A. SEIFERT, A. C. ALFENAS, R. F. ALFENAS, et al. 2011. Fungal Planet description sheets: 69–91. *Persoonia : Molecular Phylogeny and Evolution of Fungi* 26: 108–156.
CROUS, P. W., M. J. WINGFIELD, R. K. SCHUMACHER, B. A. SUMMERELL, A. GIRALDO, J. GENÉ, J. GUARRO, et al. 2014. Fungal Planet description sheets: 281–319. *Persoonia* 33: 212–289.
CROUS, P. W., M. J. WINGFIELD, J. J. LE ROUX, D. M. RICHARDSON, D. STRASBERG, R. G. SHIVAS, P. ALVARADO, et al. 2015a. Fungal Planet description sheets: 371–399. *Persoonia* 35: 264–327.

CROUS, P. W., M. J. WINGFIELD, J. GUARRO, M. HERNÁNDEZ-RESTREPO, D. A. SUTTON, K. ACHARYA, P. A. BARBER, et al. 2015b. Fungal Planet description sheets: 320-370. *Persoonia* 34: 167–266.

CROUS, P. W., M. J. WINGFIELD, D. M. RICHARDSON, J. J. LE ROUX, D. STRASBERG, J. EDWARDS, F. ROETS, et al. 2016a. Fungal Planet description sheets: 400–468. *Persoonia* 36: 316–458.

CROUS, P. W., M. J. WINGFIELD, T. I. BURGESS, G. E. S. J. HARDY, C. CRANE, S. BARRETT, J. F. CANO-LIRA, et al. 2016b. Fungal Planet description sheets: 469–557. *Persoonia*.

CURRAH, R., AND M. LOCQUIN-LINARD. 1988. *Spiromastix grisea* sp. nov. and its relationship to other Onygenaceae with helical appendages. *Canadian Journal of Botany* 66: 1135–1137.

DAGHLIAN, C. P. 1978. A new melioloid fungus from the Early Eocene of Texas,. *Palaeontology* 21: 172–176.

DAI, D.-Q., L.-Z. TANG, C. LIU, H.-B. WANG, AND D. K. HYDE. 2018. Studies on Parmulariaceae I. A phylogeny based on available sequence data; introducing Parmulariales ord. nov., and Hemigraphaceae, Melaspileellaceae and Stictographaceae fam. nov. *Phytotaxa* 369: 63–79.

DAMM, U., P. H. FOURIE, AND P. W. CROUS. 2010. *Coniochaeta* (*Lecythophora*), *Collophora* gen. nov. and *Phaeomoniella* species associated with wood necroses of *Prunus* trees. *Persoonia : Molecular Phylogeny and Evolution of Fungi* 24: 60–80.

DARKER, G. D. 1965. The occurence of *Rhizothyrium* on *Abies* and *Tsuga*. *Canadian Journal of Botany* 43: 11–14.

DARRIBA, D., G. L. TABOADA, R. DOALLO, AND D. POSADA. 2012. jModelTest 2: more models, new heuristics and parallel computing. *Nature Methods* 9: 772–772.

DE DIEGO CANDELA, J., A. FORTEZA, D. GARCÍA, G. PRIETO, R. BELLOT, S. VILLAR, AND J. M. CORTINA. 2010. Endocarditis caused by *Arthrographis kalrae*. *The Annals of Thoracic Surgery* 90: e4–e5.

DE LEO, F., C. URZI, AND G. DE HOOG. 1999. Two *Coniosporium* species from rock surface. *Studies in Mycology*: 70–79.

DE SILVA, N., S. LUMYONG, K. HYDE, T. BULGAKOV, A. PHILLIPS, AND J. YAN. 2016. Mycosphere essays 9: defining biotrophs and hemibiotrophs. *Mycosphere* 7: 545–559.

DEARNESS, J. 1924. New and Noteworthy Fungi: III. *Mycologia* 16: 143–176.

DECOCK, C., V. ROBERT, AND A. J. MASUKA. 1998. *Heliocephala zimbabweensis* sp. nov. from Southern Africa. *Mycologia* 90: 330–333.

DENNIS, R. L. 1970. A Middle Pennsylvanian basidiomycete mycelium with clamp connections. *Mycologia* 62: 578–584.

DHANASEKARAN, V., R. JEEWON, AND K. D. HYDE. 2006. Molecular taxonomy, origins and evolution of freshwater ascomycetes. *Fungal Diversity* 23: 351–390.

DIEDERICH, P. 2011. Description of *Abrothallus parmotrematis* sp. nov. (lichenicolous Ascomycota). *Bulletin de la Société des naturalistes luxembourgeois* 112.

DIEDERICH, P., AND M. WEDIN. 2000. The species of *Hemigrapha* (lichenicolous Ascomycetes, Dothideales) on Peltigerales. *Nordic Journal of Botany* 20: 203–214.

DIÉGUEZ-URIBEONDO, J., H. FÖRSTER, A. SOTO-ESTRADA, AND J. E. ADASKAVEG. 2005. Subcuticular-Intracellular Hemibiotrophic and Intercellular Necrotrophic Development of *Colletotrichum acutatum* on Almond. *Phytopathology* 95: 751–758.

DILCHER, D. L. 1963. Eocene epiphyllous fungi. *Science* 142: 667–669.

DILCHER, D. L. 1965. Epiphyllous fungi from Eocene deposits in western Tennessee, U.S.A. *Palaeontographica Abteilung B* 116: 1–54.
DODGE, B. O. 1939. The ascocarp and ascospore formation in *Stevensea wrightii*. *Mycologia* 31: 96–108.
DOIDGE, E. M. 1919. South African Microthyriaceae. *Transactions of the Royal Society of South Africa* 8: 235–282.
DOIDGE, E. M. 1942. A revision of the South African Microthyriaceae. *Bothalia* 4: 273–420.
DOUBINGER, J., AND D. PONS. 1975. Les champignons épiphylles de la formation Guaduas (Maestrichtien, Bassin de Boyecá, Colombie). 95e Congrès national des Société savantes, Reims, 1970. Sciences. v. 3, p. 145-162.
DOYLE, J. A. 2012. Molecular and fossil evidence on the origin of angiosperms. *Annual Review of Earth and Planetary Sciences* 40: 301–326.
DOYLE, J. A., AND L. J. HICKEY. 1976. Pollen and leaves from the mid-Cretaceous Potomac Group and their bearing on early angiosperm evolution. *In* C. B. Beck [ed.], Origin and early evolution of angiosperms, 139–206. Columbia University Press, New York.
DOYLE, J. A., AND G. R. UPCHURCH. 2014. Angiosperm clades in the Potomac Group: what have we learned since 1977? *Bulletin of the Peabody Museum of Natural History* 55: 111–134.
DUCOMET, V. 1907. Recherches sur le développement de quelques champignons parasites à thalle subcuticulaire. Doctorat, Faculté des sciences de Paris, Rennes : impr. de Guillemin et Voisin.
EGIDI, E., G. S. DE HOOG, D. ISOLA, S. ONOFRI, W. QUAEDVLIEG, M. DE VRIES, G. J. M. VERKLEY, et al. 2014. Phylogeny and taxonomy of meristematic rock-inhabiting black fungi in the Dothideomycetes based on multi-locus phylogenies. *Fungal Diversity* 65: 127–165.
ELLIS, J. P. 1976. British *Microthyrium* species and similar fungi. *Transactions of the British Mycological Society* 67: 381–394.
ELLIS, M. B., AND J. P. ELLIS. 1997. Microfungi on land plants, an identification handbook. The Richmond Publishing Co. Ltd.
ELSIK, W. C. 1978. Classification and geologic history of the microthyriaceous fungi, IVth International Palynological Conference (1976–77), 331–342, Lucknow, India.
ELSIK, W. C. 1993. The morphology, taxonomy, classification and geological occurrence of fungal palynomorphs, American Association of Stratigraphic Palynolynologists, Inc., Short Course, October 23–24, 236. unpublished manual.
ELSIK, W. C., AND D. L. DILCHER. 1974. Palynology and age of clays exposed in Lawrence clay pits, Henry County, Tennessee. *Palaeontographica Abteilung B*: 65–87.
EMMETT, R. W., AND D. G. PARBERY. 1975. Appressoria. *Annual Review of Phytopathology* 13: 147–167.
ERIKSSON, O. 1981. The families of bitunicate ascomycetes. *Nordic Journal of Botany* 60: 1–209.
ERIKSSON, O. E., AND K. WINKA. 1997. Supraordinal taxa of Ascomycota. *Myconet* 1: 1–16.
ERTZ, D., AND P. DIEDERICH. 2015. Dismantling Melaspileaceae: a first phylogenetic study of *Buelliella*, *Hemigrapha*, *Karschia*, *Labrocarpon* and *Melaspilea*. *Fungal Diversity* 71: 141–164.
ERTZ, D., B. HEUCHERT, U. BRAUN, C. E. FREEBURY, R. S. COMMON, AND P. DIEDERICH. 2016. Contribution to the phylogeny and taxonomy of the genus *Taeniolella*, with a focus on lichenicolous taxa. *Fungal Biology* 120: 1416–1447.

ESTÉVEZ-GALLARDO, P., L. M. SENDER, U. VILLANUEVA-AMADOZ, C. ARIAS, AND J. B. DIEZ. 2015. New record for the fungus *Mariusia andegavensis* Pons and Boureau (1977) for the Albian of NE Iberian Peninsula: a possible related plant–arthropod interaction. *Historical Biology* 27: 453–459.

ETAYO, J. 2010. Lichenicolous fungi from the western Pyrenees. V. Three new ascomycetes. *Opuscula Philolichenum* 8: 131–139.

FARR, M. 1989. Two new species of tropical fungi. *Memoirs of the New York Botanical Garden* 49: 70–73.

FARR, M. L. 1969. Some "black mildew", "sooty mold", and "fly-speck" fungi and their hyperparasites from Dominica. *Canadian Journal of Botany* 47: 369–381.

FELSENSTEIN, J. 1985. Confidence limits on phylogenies: an approach using the bootstrap. *Evolution* 39: 783–791.

FERNÁNDEZ-BRIME, S., X. LLIMONA, F. LUTZONI, AND E. GAYA. 2013. Phylogenetic study of *Diploschistes* (lichen-forming Ascomycota: Ostropales: Graphidaceae), based on morphological, chemical, and molecular data. *Taxon* 62: 267–280.

FERRER, A., A. N. MILLER, AND C. A. SHEARER. 2011. *Minutisphaera* and *Natipusilla*: two new genera of freshwater Dothideomycetes. *Mycologia* 103: 411–423.

FIRMINO, A. L. 2016. Taxonomy, phylogeny and biogeography of Asterinales on native forest species from Atlantic Forest and Cerrado. Ph.D., Universidade Federal de Viçosa, Viçosa, Minas Gerais - Brazil.

FLORIN, R. 1933. Studien über die Cycadales des Mesozoikums, nebst Erörterungen über die Spaltöffnungsapparate der Bennettitales. *Kung. Svenska Vetenskapakad. Handl. Ser. 3* 12: 1–134.

FRANK, J., P. W. CROUS, J. Z. GROENEWALD, B. OERTEL, K. D. HYDE, P. PHENGSINTHAM, AND H. J. SCHROERS. 2010. *Microcyclospora* and *Microcyclosporella*: novel genera accommodating epiphytic fungi causing sooty blotch on apple. *Persoonia* 24: 93–105.

FRIIS, E. M., P. R. CRANE, AND K. R. PEDERSEN. 2011. Early flowers and angiosperm evolution. Cambridge University Press.

FRISCH, A., G. THOR, AND D. SHEIL. 2014a. Four new Arthoniomycetes from Bwindi Impenetrable National Park, Uganda–supported by molecular data. *Nova Hedwigia* 98: 295–312.

FRISCH, A., G. THOR, D. ERTZ, AND M. GRUBE. 2014b. The Arthonialean challenge: Restructuring Arthoniaceae. *Taxon* 63: 727–744.

FRITZ, J. A., A. SEMINARA, M. ROPER, A. PRINGLE, AND M. P. BRENNER. 2013. A natural O-ring optimizes the dispersal of fungal spores. *Journal of The Royal Society Interface* 10: 20130187.

GACHOMO, E. W., H. W. DEHNE, AND U. STEINER. 2006. Microscopic evidence for the hemibiotrophic nature of *Diplocarpon rosae*, cause of black spot disease of rose. *Physiological and Molecular Plant Pathology* 69: 86–92.

GÄUMANN, E. A. 1952. The fungi. A description of their morphological features and evolutionary development. Hafner Publishing Company, New York.

GIRALDO, A., P. W. CROUS, R. K. SCHUMACHER, R. CHEEWANGKOON, M. GHOBAD-NEJHAD, AND E. LANGER. 2017. The genera of Fungi—G3: *Aleurocystis*, *Blastacervulus*, *Clypeophysalospora*, *Licrostroma*, *Neohendersonia* and *Spumatoria*. *Mycological Progress* 16: 325–348.

GREGUSS, P. 1968. Xylotomy of the living cycads, with a description of their leaves and epidermis. Akadémiai Kiado, Budapest.
GRIGORIEV, I. V., R. NIKITIN, S. HARIDAS, A. KUO, R. OHM, R. OTILLAR, R. RILEY, et al. 2013. MycoCosm portal: gearing up for 1000 fungal genomes. *Nucleic Acids Research* 42: D699–D704.
GROENEWALD, J., C. NAKASHIMA, J. NISHIKAWA, H.-D. SHIN, J.-H. PARK, A. JAMA, M. GROENEWALD, et al. 2013. Species concepts in *Cercospora*: spotting the weeds among the roses. *Studies in Mycology* 75: 115–170.
GRUBE, M., E. BALOCH, AND H. T. LUMBSCH. 2004. The phylogeny of Porinaceae (Ostropomycetidae) suggests a neotenic origin of perithecia in Lecanoromycetes. *Mycological Research* 108: 1111–1118.
GUATIMOSIM, E., P. B. SCHWARTSBURD, AND R. W. BARRETO. 2014a. A new *Inocyclus* species (Parmulariaceae) on the neotropical fern *Pleopeltis astrolepis*. *IMA Fungus* 5: 51–55.
GUATIMOSIM, E., H. J. PINTO, R. W. BARRETO, AND J. PRADO. 2014b. *Rhagadolobiopsis*, a new genus of Parmulariaceae from Brazil with a description of the ontogeny of its ascomata. *Mycologia* 106: 276–281.
GUATIMOSIM, E., A. FIRMINO, J. BEZERRA, O. PEREIRA, R. BARRETO, AND P. CROUS. 2014c. Towards a phylogenetic reappraisal of Parmulariaceae and Asterinaceae (Dothideomycetes). *Persoonia-Molecular Phylogeny and Evolution of Fungi*.
GUATIMOSIM, E., A. FIRMINO, J. BEZERRA, O. PEREIRA, R. BARRETO, AND P. CROUS. 2015. Towards a phylogenetic reappraisal of Parmulariaceae and Asterinaceae (Dothideomycetes). *Persoonia* 35: 230–241.
GUERRERO, Y., T. A. HOFMANN, C. WILLIAMS, M. THINES, AND M. PIEPENBRING. 2011. *Asterotexis cucurbitacearum*, a poorly known pathogen of Cucurbitaceae new to Costa Rica, Grenada and Panama. *Mycology* 2: 87–90.
GUGNANI, H. C. 2003. Ecology and taxonomy of pathogenic aspergilli. *Front Biosci* 8: 346.
HANSEN, K., AND D. H. PFISTER. 2006. Systematics of the Pezizomycetes--the operculate discomycetes. *Mycologia* 98: 1029–1040.
HARPER, C. J. 2015. The diversity and interactions of fungi from the Paleozoic and Mesozoic of Antarctica. Ph.D., University of Kansas, Lawrence, KS.
HARRINGTON, T. C., D. MCNEW, AND H. Y. YUN. 2012. Bur oak blight, a new disease on *Quercus macrocarpa* caused by *Tubakia iowensis* sp. nov. *Mycologia* 104: 79–92.
HARRIS, T. M. 1932. The fossil flora of Scoresby Sound East Greenland. Part 2: Description of seed plants incertae sedis together with a discussion of certain cycadophyte cuticles. *Meddelelser om Gronland* 85: 1–112.
HARRISON, J. C., AND J. A. LANGDALE. 2006. A step by step guide to phylogeny reconstruction. *The Plant Journal* 45: 561-572.
HAYWARD, G. C. 1977. Taxonomy of the lichen families Graphidaceae and Opegraphaceae in New Zealand. *New Zealand Journal of Botany* 15: 565–584.
HERNÁNDEZ-RESTREPO, M., J. D. P. BEZERRA, Y. P. TAN, N. P. WIEDERHOLD, P. W. CROUS, J. GUARRO, AND J. GENÉ. 2019. Re-evaluation of *Mycoleptodiscus* species and morphologically similar fungi. *Persoonia* 42: 205–227.
HIBBETT, D. S. 2007. After the gold rush, or before the flood? Evolutionary morphology of mushroom-forming fungi (Agaricomycetes) in the early 21st century. *Mycological Research* 111: 1001–1018.

HIBBETT, D. S., M. BLACKWELL, T. Y. JAMES, J. W. SPATAFORA, J. W. TAYLOR, AND R. VILGALYS. 2018. Phylogenetic taxon definitions for Fungi, Dikarya, Ascomycota and Basidiomycota. *IMA Fungus* 9: 291–298.
HICKEY, L. J., AND J. A. DOYLE. 1977. Early Cretaceous fossil evidence for angiosperm evolution. *Botanical Review* 43: 2–104.
HIGGINS, B. B. 1920. Morphology and life history of some Ascomycetes with special reference to the presence and function of spermatia. *American Journal of Botany* 7: 435–444.
HOFMANN, T., R. KIRSCHNER, AND M. PIEPENBRING. 2010. Phylogenetic relationships and new records of Asterinaceae (Dothideomycetes) from Panama. *Fungal Diversity* 43: 39–53.
HOFMANN, T. A. 2009. Plant parasitic Asterinaceae and Microthyriaceae from the Neotropics (Panama). Ph.D., Johann Wolfgang Goethe-University, Frankfurt, Germany.
HOFMANN, T. A., AND M. PIEPENBRING. 2006. New records and host plants of fly-speck fungi from Panama. *Fungal Diversity* 22: 55–70.
HOFMANN, T. A., AND M. PIEPENBRING. 2008. New species and records of *Asterina* from Panama. *Mycological Progress* 7: 87–98.
HOFMANN, T. A., AND M. PIEPENBRING. 2011. Biodiversity of *Asterina* species on neotropical host plants: New species and records from Panama. *Mycologia* 103: 1284–1301.
HOLDENRIEDER, O., AND T. KOWALSKI. 1989. Pycnidial formation and pathogenicity in *Tubakia dryina*. *Mycological Research* 92: 166–169.
HOLM, K., AND L. HOLM. 1991. Ascomycetes on *Myrica gale* in Sweden. *Nordic Journal of Botany* 11: 675–687.
HONGSANAN, S., AND D. K. HYDE. 2017. Phylogenetic placement of Micropeltidaceae. *Mycosphere* 8: 1930–1942.
HONGSANAN, S., P. CHOMNUMTI, P. W. CROUS, E. CHUKEATIROTE, AND K. D. HYDE. 2014a. Introducing *Chaetothyriothecium*, a new genus of Microthyriales *Phytotaxa* 161: 157–164.
HONGSANAN, S., A. H. BAHKALI, P. CHOMNUNTI, J.-K. LIU, J.-B. YANG, AND K. D. HYDE. 2016. *Discopycnothyrium palmae* gen. & sp. nov. (Asterinaceae). *Mycotaxon* 131: 859–869.
HONGSANAN, S., Q. TIAN, A. H. BAHKALI, J.-B. YANG, E. H. C. MCKENZIE, P. CHOMNUNTI, AND K. D. HYDE. 2015. Zeloasperisporiales ord. nov., and two new species of *Zeloasperisporium*. *Cryptogamie, Mycologie* 36: 301–317.
HONGSANAN, S., Y.-M. LI, J.-K. LIU, T. HOFMANN, M. PIEPENBRING, J. D. BHAT, S. BOONMEE, et al. 2014b. Revision of genera in Asterinales. *Fungal Diversity* 68: 1–68.
HOSAGOUDAR, V., AND J. KAPOOR. 1985. New technique of mounting meliolaceous fungi. *Indian Phytopathology* 38: 548–549.
HUGHES, S. J. 1953a. Some foliicolous hyphomycetes. *Canadian Journal of Botany* 31: 560–576.
HUGHES, S. J. 1953b. Conidiophores, conidia, and classification. *Canadian Journal of Botany* 31: 577-659.
HUGHES, S. J. 1953c. Fungi from the Gold Coast II. *Mycological Papers* 50: 1–104.
HUGHES, S. J. 1976. Sooty moulds. *Mycologia* 68: 693–820.
HYDE, K. D. 1992a. *Julella avicenniae* (Borse) comb. nov. (Thelenellaceae) from intertidal mangrove wood and miscellaneous fungi from the NE coast of Queensland. *Mycological Research* 96: 939–942.
HYDE, K. D. 1992b. The Genus *Saccardoella* from Intertidal Mangrove Wood. *Mycologia* 84: 803–810.

HYDE, K. D., E. B. G. JONES, J.-K. LIU, H. ARIYAWANSA, E. BOEHM, S. BOONMEE, U. BRAUN, et al. 2013. Families of Dothideomycetes. *Fungal Diversity* 63: 1–313.

HYDE, K. D., S. HONGSANAN, R. JEEWON, D. J. BHAT, E. H. C. MCKENZIE, E. B. G. JONES, R. PHOOKAMSAK, et al. 2016. Fungal diversity notes 367–490: taxonomic and phylogenetic contributions to fungal taxa. *Fungal Diversity* 80: 1–270.

INDERBITZIN, P., Y. R. MEHTA, AND M. L. BERBEE. 2009. *Pleospora* Species with *Stemphylium* Anamorphs: A Four Locus Phylogeny Resolves New Lineages Yet Does Not Distinguish among Species in the *Pleospora herbarum* Clade. *Mycologia* 101: 329–339.

JAMES, T. Y., F. KAUFF, C. L. SCHOCH, P. B. MATHENY, V. HOFSTETTER, C. J. COX, G. CELIO, et al. 2006. Reconstructing the early evolution of Fungi using a six-gene phylogeny. *Nature* 443: 818–822.

JAYASIRI, S., K. HYDE, E. JONES, AND K. S. JIANCHU XU. 2018. Seed decaying Dothideomycetes in Thailand: *Zeloasperisporium pterocarpi* sp. nov.,(Zeloasperisporiaceae, Zeloasperisporiales) on carpel of *Pterocarpus* sp. (Fabaceae) seed pod. *Asian Journal of Mycology* 1: 106–113.

JAYAWARDENA, R. S., H. A. ARIYAWANSA, C. SINGTRIPOP, Y. M. LI, J. YAN, X. LI, S. NILTHONG, AND K. D. HYDE. 2014. A re-assessment of Elsinoaceae (Myriangiales, Dothideomycetes). *2014* 176: 19.

JOHNSTON, P. R., K. A. SEIFERT, J. K. STONE, A. Y. ROSSMAN, AND L. MARVANOVÁ. 2014. Recommendations on generic names competing for use in Leotiomycetes (Ascomycota). *IMA Fungus* 5: 91-120.

JUD, N. A. 2015. Fossil evidence for a herbaceous diversification of early eudicot angiosperms during the Early Cretaceous. *Proceedings of the Royal Society B: Biological Sciences* 282: 20151045.

KALGUTKAR, R. M., AND L. SIGLER. 1995. Some fossil fungal form-taxa from the Maastrichtian and Palaeogene ages. *Mycological Research* 99: 513–522.

KALGUTKAR, R. M., AND J. JANSONIUS. 2000. Synopsis of fossil fungal spores, mycelia and fructifications, AASP Contributions Series, vol. 39, 1–351. American Association of Stratigraphic Palynologists Foundation.

KATOH, K., AND D. M. STANDLEY. 2013. MAFFT Multiple sequence alignment software Version 7: Improvements in performance and usability. *Molecular Biology and Evolution* 30: 772–780.

KAUFF, F., AND B. BÜDEL. 2005. Ascoma Ontogeny and Apothecial Anatomy in the Gyalectaceae (Ostropales, Ascomycota) Support the Re-establishment of the Coenogoniaceae. *The Bryologist* 108: 272–281.

KIRK, P. M., P. F. CANNON, D. W. MINTER, AND J. A. STALPERS. 2008. Ainsworth & Bisby's Dictionary of the Fungi. (10th ed.). CABI Europe, UK.

KOHLMEYER, J. 1966. Neue meerespilze an mangroven. *Berichte der Deutschen Botanischen Gesellschaft* 79: 27–37.

KOHLMEYER, J. 1985. *Caryosporella rhizophorae* gen. et sp. nov. (Massariaceae), a marine Ascomycete from *Rhizophora mangle*. *Proceedings: Plant Sciences* 94: 355–361.

KOHLMEYER, J. 1986. *Ascocratera manglicola* gen. et sp. nov. and key to the marine Loculoascomycetes on mangroves. *Canadian Journal of Botany* 64: 3036–3042.

KOHLMEYER, J., AND S. SCHATZ. 1985. *Aigialus* gen.nov. (Ascomycetes) with two new marine species from mangroves. *Transactions of the British Mycological Society* 85: 699–707.

KOHLMEYER, J., B. VOLKMANN-KOHLMEYER, AND O. E. ERIKSSON. 1996. Fungi on *Juncus roemerianus*. 8. New bitunicate ascomycetes. *Canadian Journal of Botany* 74: 1830–1840.

KRASSILOV, V. A. 1967. Early Cretaceous flora of the southern Primorsk and its significance for the stratigraphy (in Russian). Far East Geological Institute, Moscow.

KRINGS, M., AND T. N. TAYLOR. 2012. Fungal reproductive units enveloped in a hyphal mantle from the Lower Pennsylvanian of Great Britain, and their relevance to our understanding of Carboniferous fungal "sporocarps". *Review of Palaeobotany and Palynology* 175: 1–9.

KRINGS, M., T. N. TAYLOR, AND J. F. WHITE JR. 2011a. Fungal sporocarps from the Carboniferous: An unusual specimen of Traquairia. *Review of Palaeobotany and Palynology* 168: 1–6.

KRINGS, M., N. DOTZLER, J. GALTIER, AND T. TAYLOR. 2011b. Oldest fossil basidiomycete clamp connections. *Mycoscience* 52: 18–23.

KRINGS, M., T. TAYLOR, E. TAYLOR, H. KERP, AND N. DOTZLER. 2014. First record of a fungal "sporocarp" from the Lower Devonian Rhynie chert. *Palaeobiodiversity and Palaeoenvironments* 94: 221–227.

KUMAR, M. 1996. Palynostratigraphy and paleoecology of Early Eocene palynoflora of Rajpardi lignite, Bharuch District, Gujarat. *Palaeobotanist* 43: 110–121.

KUTHUBUTHEEN, A. J., AND A. NAWAWI. 1988. A new species of *Wiesneriomyces* (Hyphomycetes) from submerged decaying leaves. *Transactions of the British Mycological Society* 90: 619–625.

KVACEK, J., H. J. FALCON-LANG, AND J. DASKLOVA. 2005. A new Late Cretaceous ginkgoalean reproductive structure *Nehvizdyella* gen. nov. from the Czech Republic and its whole-plant reconstruction. *American Journal of Botany* 92: 1958–1969.

LANGE, R. T. 1969. Recent and fossil epiphyllous fungi of the *Manginula-Shortensis* group. *Australian Journal of Botany* 17: 565–574.

LARSSON, K.-H. 2007. Re-thinking the classification of corticioid fungi. *Mycological Research* 111: 1040–1063.

LATUNDE-DADA, A., R. O'CONNELL, C. NASH, AND J. LUCAS. 1999. Stomatal penetration of cowpea (*Vigna unguiculata*) leaves by a *Colletotrichum* species causing latent anthracnose. *Plant Pathology* 48: 777–785.

LAWREY, J. D., P. DIEDERICH, M. P. NELSEN, M. SIKAROODI, P. M. GILLEVET, A. M. BRAND, AND P. VAN DEN BOOM. 2011. The obligately lichenicolous genus *Lichenoconium* represents a novel lineage in the Dothideomycetes. *Fungal Biology* 115: 176–187.

LEE, S. B., AND J. W. TAYLOR. 1990. Isolation of DNA from fungal mycelia and single spores. *In* M. A. Innis, D. H. Gelfand, J. J. Sninsky, and T. J. White [eds.], PCR Protocols: A Guide to Methods and Applications, 282–287. Academic Press, San Diego.

LENDEMER, J. C. 2007. The Occurrence of *Endocarpon pallidulum* and *Endocarpon petrolepideum* in Eastern North America. *Evansia* 24: 103–107.

LEWIS, P. O. 2001. A likelihood approach to estimating phylogeny from discrete morphological character data. *Systematic Biology* 50: 913–925.

LIU, J.-K., K. D. HYDE, R. JEEWON, A. J. L. PHILLIPS, S. S. N. MAHARACHCHIKUMBURA, M. RYBERG, Z.-Y. LIU, AND Q. ZHAO. 2017. Ranking higher taxa using divergence times: a case study in Dothideomycetes. *Fungal Diversity* 84: 75–99.

LIU, J.-K., R. PHOOKAMSAK, E. B. G. JONES, Y. ZHANG, T. KO-KO, H.-L. HU, S. BOONMEE, et al. 2011. *Astrosphaeriella* is polyphyletic, with species in *Fissuroma* gen. nov., and *Neoastrosphaeriella* gen. nov. *Fungal Diversity* 51: 135–154.

LIU, J. K., K. D. HYDE, E. B. G. JONES, H. A. ARIYAWANSA, D. J. BHAT, S. BOONMEE, S. S. N. MAHARACHCHIKUMBURA, et al. 2015. Fungal diversity notes 1–110: taxonomic and phylogenetic contributions to fungal species. *Fungal Diversity* 72: 1–197.

LOHMAN, M. L. 1932. Three new Species of *Mytilidion* in the proposed Subgenus, Lophiopsis. *Mycologia* 24: 477–484.

LÜCKING, R., AND E. SÉRUSIAUX. 1996. *Musaespora kalbii* (lichenized Ascomycetes: Melanommatales), a new foliicolous lichen with a pantropical distribution. *Nordic Journal of Botany* 16: 661–668.

LÜCKING, R., APTROOT, A. & THOR, G. 1997. New species or interesting records of foliicolous lichens. II. *Flavobathelium epiphyllum* (lichenized ascomycetes: Melanommatales). *Lichenologist* 29: 221–228.

LUMBSCH, H. T., AND S. D. LEAVITT. 2011. Goodbye morphology? A paradigm shift in the delimitation of species in lichenized fungi. *Fungal Diversity* 50: 59–72.

LUMBSCH, H. T., I. SCHMITT, R. LINDEMUTH, A. MILLER, A. MANGOLD, F. FERNANDEZ, AND S. HUHNDORF. 2005. Performance of four ribosomal DNA regions to infer higher-level phylogenetic relationships of inoperculate euascomycetes (Leotiomyceta). *Molecular Phylogenetics and Evolution* 34: 512–524.

LUTTRELL, E. S. 1944. The morphology of *Myiocopron smilacis* (De Not.) Sacc. *American Journal of Botany* 31: 640–649.

LUTTRELL, E. S. 1946. The genus *Stomiopeltis* (Hemisphaeriaceae). *Mycologia* 38: 565–586.

LUTZONI, F., M. D. NOWAK, M. E. ALFARO, V. REEB, J. MIADLIKOWSKA, M. KRUG, A. E. ARNOLD, et al. 2018. Contemporaneous radiations of fungi and plants linked to symbiosis. *Nature Communications* 9: 5451.

MADDISON, W. P., AND D. R. MADDISON. 2015. Mesquite: a modular system for evolutionary analysis. Version 3.04 http://mesquiteproject.org.

MALLOCH, D., AND L. SIGLER. 1988. The Eremomycetaceae (Ascomycotina). *Canadian Journal of Botany* 66: 1929–1932.

MANAMGODA, D. S., A. Y. ROSSMAN, L. A. CASTLEBURY, P. W. CROUS, H. MADRID, E. CHUKEATIROTE, AND K. D. HYDE. 2014. The genus *Bipolaris*. *Studies in Mycology* 79: 221–288.

MANDAL, A., N. SAMAJPATI, AND S. BERA. 2011. A new species of *Meliolinites* (fossil Meliolales) from the Neogene sediments of sub-Himalayan West Bengal, India. *Nova Hedwigia* 92: 435.

MAPOOK, A., K. HYDE, S. HONGSANAN, C. PHUKHAMSAKDA, J. LI, AND S. BOONMEE. 2016a. Palawaniaceae fam. nov., a new family (Dothideomycetes, Ascomycota) to accommodate *Palawania* species and their evolutionary time estimates. *Mycosphere* 7: 1732–1745.

MAPOOK, A., K. D. HYDE, D.-Q. DAI, J. LI, E. B. G. JONES, A. H. BAHKALI, AND S. BOONMEE. 2016b. Muyocopronales, ord. nov.,(Dothideomycetes, Ascomycota) and a reappraisal of *Muyocopron* species from northern Thailand. *Phytotaxa* 265: 225–237.

MARASAS, W., P. VAN WYK, AND P. KNOX-DAVIES. 1975. *Batcheloromyces*, a new genus of annellidic dematiaceous Hyphomycetes on *Protea cynaroides* in South Africa. *Journal of South African Botany*.

MARTENS, P. 1971. Les Gnetophytes. Borntraeger, Stuttgart.
MARTÍNEZ, A. 1968. Fossil Microthyriales (fungi, Ascomycetes) from the Lower Cretaceous of Santa Cruz Province, Argentina. *Revista de la Asociación Paleontológica Argentina, Ameghiniana* 5: 257–263.
MASSICOTTE, H. B., J. M. TRAPPE, R. L. PETERSON, AND L. H. MELVILLE. 1992. Studies on *Cenococcum geophilum*. II. Sclerotium morphology, germination, and formation in pure culture and growth pouches. *Canadian Journal of Botany* 70: 125–132.
MATHIASSEN, G. H., A. GRANMO, AND T. RÄMÄ. 2015. *Lophium elegans* (Ascomycota), a rare European species.
MCLAUGHLIN, D. J., AND J. W. SPATAFORA. 2015. Systematic and Evolution, Part B. Springer.
MEDJEDOVIĆ, A., J. FRANK, H.-J. SCHROERS, B. OERTEL, AND J. C. BATZER. 2014. *Peltaster cerophilus* is a new species of the apple sooty blotch complex from Europe. *Mycologia* 106: 525–536.
MIADLIKOWSKA, J., F. KAUFF, V. HOFSTETTER, E. FRAKER, M. GRUBE, J. HAFELLNER, V. REEB, et al. 2006. New insights into classification and evolution of the Lecanoromycetes (Pezizomycotina, Ascomycota) from phylogenetic analyses of three ribosomal RNA- and two protein-coding genes. *Mycologia* 98: 1088–1103.
MILLER, M. A., W. PFEIFFER, AND T. SCHWARTZ. 2010. Creating the CIPRES Science Gateway for inference of large phylogenetic trees. Gateway Computing Environments Workshop (GCE), New Orleans, LA: 1–8.
MISHRA, S., N. AGGARWAL, AND N. JHA. 2018. Palaeoenvironmental change across the Permian-Triassic boundary inferred from palynomorph assemblages (Godavari Graben, south India). *Palaeobiodiversity and Palaeoenvironments* 98: 177–204.
MITCHELL, A. 2015. Collecting in collections: a PCR strategy and primer set for DNA barcoding of decades-old dried museum specimens. *Molecular Ecology Resources* 15: 1102–1111.
MONGA, P., M. KUMAR, V. PRASAD, AND Y. JOSHI. 2015. Palynostratigraphy, palynofacies and depositional environment of a lignite-bearing succession at Surkha Mine, Cambay Basin, north-western India. *Acta Palaeobotanica* 55: 183–207.
MOORE, D., G. D. ROBSON, AND A. P. J. TRINCI. 2011. 21st Century Guidebook to Fungi. (Pap/Com ed.). Cambridge University Press, Cambridge.
MUGGIA, L., C. GUEIDAN, K. KNUDSEN, G. PERLMUTTER, AND M. GRUBE. 2013. The Lichen Connections of Black Fungi. *Mycopathologia* 175: 523–535.
MÜLLER, E., AND J. A. VON ARX. 1962. Die Gattungen der didymosporen Pyrenomyceten. *Beiträge zur Kryptogamenflora der Schweiz* 11: 1–922.
MUNKVOLD, G. P., AND D. NEELY. 1991. Development of *Tubakia dryina* on host tissue. *Canadian Journal of Botany* 69: 1865–1871.
MUTHAPPA, B. 1969. Morphology of *Lembosina aulographoides*. *Nova Hedwigia* 17: 165–174.
NAG RAJ, T. 1993. Coelomycetous anamorphs with appendage-bearing conidia. Mycologue Publications.
NAUMOV, M. N. 1914. Description de quelques nouvelles espèces. *Bulletin de la Société Mycologique de France* 30: 423–432.
NELSEN, M., R. LÜCKING, J. MBATCHOU, C. ANDREW, A. SPIELMANN, AND H. T. LUMBSCH. 2011. New insights into relationships of lichen-forming Dothideomycetes. *Fungal Diversity* 51: 155–162.

NELSEN, M. P., R. LÜCKING, M. GRUBE, J. S. MBATCHOU, L. MUGGIA, E. R. PLATA, AND H. T. LUMBSCH. 2009. Unravelling the phylogenetic relationships of lichenised fungi in Dothideomyceta. *Studies in Mycology* 64: 135–144–S134.

NELSEN, M. P., R. LÜCKING, C. J. ANDREW, A. APTROOT, M. E. CÁCERES, J. A. MERCADO-DÍAZ, E. R. PLATA, AND H. T. LUMBSCH. 2014a. Molecular phylogeny reveals the true colours of Myeloconidaceae (Ascomycota: Ostropales). *Australian Systematic Botany* 27: 38–47.

NELSEN, M. P., R. LÜCKING, A. APTROOT, C. J. ANDREW, M. CÁCERES, E. R. PLATA, C. GUEIDAN, et al. 2014b. Elucidating phylogenetic relationships and genus-level classification within the fungal family Trypetheliaceae (Ascomycota: Dothideomycetes). *Taxon* 63: 974–992.

PAGEL, M., AND A. MEADE. 2007. BayesTraits v.2 *Computer program and documentation available at* http://www.evolution.rdg.ac.uk/BayesTraits.html.

PANG, K.-L., K. D. HYDE, S. A. ALIAS, S. SUETRONG, S.-Y. GUO, R. IDID, AND E. GARETH JONES. 2013. Dyfrolomycetaceae, a new family in the Dothideomycetes, Ascomycota. *Cryptogamie, Mycologie* 34: 223–232.

PANT, D. D., AND D. D. NAUTIYAL. 1963. Cuticle and epidermis of recent Cycadales. Leaves, sporangia, and seeds. *Senckenbergiana biologia* 44: 257–348.

PARBERY, D., AND R. EMMETT. 1977. Hypotheses regarding appressoria, spores, survival and phylogeny in parasitic fungi. *Revue de Mycologie* 41: 429–447.

PENNYCOOK, S., AND E. MCKENZIE. 2002. *Scoleciasis atkinsonii*, an earlier name for *Phaeophleospora hebes*; and a note on GH Cunningham's epithets *hebe* and *pseudopanax*. *Mycotaxon* 82: 145–146.

PENTECOST, A. 2014. Growth and development of ascomata in two species of Arthoniales, *Arthonia calcarea* and *Alyxoria varia* (Lichenized Ascomycota: Arthoniaceae and Lecanographaceae). *Nova Hedwigia* 98: 41–49.

PÉREZ-ORTEGA, S., A. SUIJA, A. CRESPO, AND A. DE LOS RÍOS. 2014. Lichenicolous fungi of the genus *Abrothallus* (Dothideomycetes: Abrothallales ordo nov.) are sister to the predominantly aquatic Janhulales. *Fungal Diversity* 64: 295–304.

PERFECT, S. E., AND J. R. GREEN. 2001. Infection structures of biotrophic and hemibiotrophic fungal plant pathogens. *Molecular Plant Pathology* 2: 101–108.

PHIPPS, C. J. 2007. *Entopeltacites remberi* sp. nov. from the Miocene of Clarkia, Idaho, USA. *Review of Palaeobotany and Palynology* 145: 193–200.

PHIPPS, C. J., AND W. C. REMBER. 2004. Epiphyllous fungi from the Miocene of Clarkia, Idaho: reproductive structures. *Review of Palaeobotany and Palynology* 129: 67–79.

PIROZYNSKI, K. A. 1971. Note on *Geastrumia polystigmatis*. *Mycologia* 63: 897–901.

PONS, D., AND E. BOUREAU. 1977. Les champignons épiphylles d'un *Frenelopsis* du Cénomanien moyen de l' Anjou (France). *Revue de Mycologie* 41.

PRIETO, M., AND M. WEDIN. 2013. Dating the diversification of the major lineages of Ascomycota (Fungi). *PLOS ONE* 8: e65576.

QUAN, C., S. G., AND Z. ZHOU. 2010. A new Tertiary *Ginkgo* (Ginkgoaceae) from the Wuyun Formation of Jiayin, Heilongjiang, northeastern China and its paleoenvironmental implications. *American Journal of Botany* 97: 446–457.

RAJA, H. A., AND C. A. SHEARER. 2008. Freshwater Ascomycetes: New and Noteworthy Species from Aquatic Habitats in Florida. *Mycologia* 100: 467–489.

RAJA, H. A., A. N. MILLER, AND C. A. SHEARER. 2012. Freshwater ascomycetes: Natipusillaceae, a new family of tropical fungi, including *Natipusilla bellaspora* sp. nov. from the Peruvian Amazon. *Mycologia* 104: 569–573.

RAJA, H. A., N. H. OBERLIES, M. FIGUEROA, K. TANAKA, K. HIRAYAMA, A. HASHIMOTO, A. N. MILLER, et al. 2013. Freshwater Ascomycetes: *Minutisphaera* (Dothideomycetes) revisited, including one new species from Japan. *Mycologia* 105: 959–976.

RAMALEY, A. W. 1996. *Comminutispora* gen. nov. and Its Hyphospora gen. nov. Anamorph. *Mycologia* 88: 132–136.

RAMALEY, A. W. 1999. Three species of *Microthyrium* from *Nolina*. *Mycotaxon* 70: 7–16.

RAMBAUT, A., AND A. J. DRUMMOND. 2013. Tracer v1.6. Available from: <https://github.com/beast-dev/tracer/releases/tag/v1.6>.

REYNOLDS, D. R., AND G. S. GILBERT. 2005. Epifoliar fungi from Queensland, Australia. *Australian Systematic Botany* 18: 265–289.

RIDDLE, L. W. 1920. Observations on the Genus *Acrospermum*. *Mycologia* 12: 175–181.

RIKKINEN, J., H. DÖRFELT, A. R. SCHMIDT, AND J. WUNDERLICH. 2003. Sooty moulds from European Tertiary amber, with notes on the systematic position of *Rosaria* ('Cyanobacteria'). *Mycological Research* 107: 251–256.

RIVAS PLATA, E., S. PARNMEN, B. STAIGER, A. MANGOLD, A. FRISCH, G. WEERAKOON, J. HERNANDEZ, et al. 2013. A molecular phylogeny of Graphidaceae (Ascomycota, Lecanoromycetes, Ostropales) including 428 species. *MycoKeys* 6.

RONQUIST, F., M. TESLENKO, P. VAN DER MARK, D. L. AYRES, A. DARLING, S. HÖHNA, B. LARGET, et al. 2012. MrBayes 3.2: efficient Bayesian phylogenetic inference and model choice across a large model space. *Systematic Biology* 61: 539–542.

ROPER, M., R. E. PEPPER, M. P. BRENNER, AND A. PRINGLE. 2008. Explosively launched spores of ascomycete fungi have drag-minimizing shapes. *Proceedings of the National Academy of Sciences of the United States of America* 105: 20583–20588.

RUIBAL, C., G. PLATAS, AND G. F. BILLS. 2008. High diversity and morphological convergence among melanised fungi from rock formations in the Central Mountain System of Spain. *Persoonia* 21: 93–110.

RUIBAL, C., C. GUEIDAN, L. SELBMANN, A. A. GORBUSHINA, P. W. CROUS, J. Z. GROENEWALD, L. MUGGIA, et al. 2009. Phylogeny of rock-inhabiting fungi related to Dothideomycetes. *Studies in Mycology* 64: 123–133.

SAMSON, R. A., AND J. MOUCHACCA. 1975. Two new soil-borne cleistothecial ascomycetes. *Canadian Journal of Botany* 53: 1634–1639.

SARTORIS, G. B., AND C. KAUFFMAN. 1925. The development and taxonomic position of *Apiosporina collinsii*. *Papers Mich. Acad. Sci. Arts & Lett* 5: 149–162.

SCHMIDT, A. R., C. BEIMFORDE, L. J. SEYFULLAH, S.-E. WEGE, H. DÖRFELT, V. GIRARD, H. GRABENHORST, et al. 2014. Amber fossils of sooty moulds. *Review of Palaeobotany and Palynology* 200: 53–64.

SCHMITT, I., G. MUELLER, AND H. T. LUMBSCH. 2005. Ascoma morphology is homoplaseous and phylogenetically misleading in some pyrenocarpous lichens. *Mycologia* 97: 362–374.

SCHMITT, I., R. D. PRADO, M. GRUBE, AND H. T. LUMBSCH. 2009. Repeated evolution of closed fruiting bodies is linked to ascoma development in the largest group of lichenized fungi (Lecanoromycetes, Ascomycota). *Molecular Phylogenetics and Evolution* 52: 34–44.

SCHOCH, C. L., C. GUEIDAN, Y. HARADA, S. HATAKEYAMA, K. HIRAYAMA, T. HOSOYA, S. M. HUHNDORF, et al. 2009a. A class-wide phylogenetic assessment of Dothideomycetes. *Studies in Mycology* 64: 1–15.

SCHOCH, C. L., G.-H. SUNG, F. LÓPEZ-GIRÁLDEZ, J. P. TOWNSEND, J. MIADLIKOWSKA, V. HOFSTETTER, B. ROBBERTSE, et al. 2009b. The Ascomycota tree of life: A phylum-wide phylogeny clarifies the origin and evolution of fundamental reproductive and ecological traits. *Systematic Biology* 58: 224–239.

SCHUBERT, K., A. RISCHEL, AND U. BRAUN. 2013. A monograph of *Fusicladium* s. lat. (hyphomycetes). *Schlechtendalia* 9: 1–132.

SCHUBERT, K., J. Z. GROENEWALD, U. BRAUN, J. DIJKSTERHUIS, M. STARINK, C. F. HILL, P. ZALAR, et al. 2007. Biodiversity in the *Cladosporium herbarum* complex (Davidiellaceae, Capnodiales), with standardisation of methods for *Cladosporium* taxonomy and diagnostics. *Studies in Mycology* 58: 105–156.

SCHWEITZER, C. E. 2003. Utility of proxy characters for classification of fossils: An example from the fossil Xanthoidea (Crustacea: Decapoda: Brachyura). *Journal of Paleontology* 77: 1107-1128.

SEAVER, F. J. 1910. Iowa Discomycetes. *Bulletin of the Laboratories of Natural History of the State University of Iowa* 6: 41–131.

SEIFERT, K. A., AND W. GAMS. 2001. The taxonomy of anamorphic Fungi. *In* D. J. McLaughlin, E. G. McLaughlin, and P. A. Lemke [eds.], Systematics and Evolution: Part A, 307-347. Springer Berlin Heidelberg, Berlin, Heidelberg.

SEIFERT, K. A., G. MORGAN-JONES, W. GAMS, AND B. KENDRICK. 2011. The genera of hyphomycetes. CBS-KNAW Fungal Biodiversity Centre Utrecht.

SELBMANN, L., G. S. DE HOOG, A. MAZZAGLIA, E. I. FRIEDMANN, AND S. ONOFRI. 2005. Fungi at the edge of life: cryptoendolithic black fungi from Antarctic desert. *Studies in Mycology*: 1–32.

SELBMANN, L., D. ISOLA, E. EGIDI, L. ZUCCONI, C. GUEIDAN, G. S. DE HOOG, AND S. ONOFRI. 2014. Mountain tips as reservoirs for new rock-fungal entities: Saxomyces gen. nov. and four new species from the Alps. *Fungal Diversity* 65: 167–182.

SELBMANN, L., G. S. DE HOOG, L. ZUCCONI, D. ISOLA, S. RUISI, A. H. G. G. VAN DEN ENDE, C. RUIBAL, et al. 2008. Drought meets acid: three new genera in a dothidealean clade of extremotolerant fungi. *Studies in Mycology* 61: 1–20.

SELKIRK, D. R. 1969. Studies in Australian Tertiary palaeobotany an epiphyllous flora from Kiandra, New South Wales. Ph.D., University of Sydney, Sydney.

SELKIRK, D. R. 1975. Tertiary fossil fungi from Kiandra, New South Wales. *Proceedings of the Linnean Society of New South Wales* 100: 70–94.

SHENOY, B. D., R. JEEWON, W. P. WU, D. J. BHAT, AND K. D. HYDE. 2006. Ribosomal and RPB2 DNA sequence analyses suggest that *Sporidesmium* and morphologically similar genera are polyphyletic. *Mycological Research* 110: 916–928.

SHERWOOD, M. A. 1977. The Ostropalean fungi. *Mycotaxon* 5: 1–277.

SHERWOOD, M. A. 1980. Taxonomic studies in the Phacidales: the genus *Coccomyces* (Rhytismataceae). *Occasional Papers of the Farlow Herbarium of Cryptogamic Botany*: 1–120.

SHIMODAIRA, H. 2002. An approximately unbiased test of phylogenetic tree selection. *Systematic Biology* 51: 492–508.

SHIMODAIRA, H., AND M. HASEGAWA. 2001. CONSEL: for assessing the confidence of phylogenetic tree selection. *Bioinformatics* 17: 1246–1247.
SHOEMAKER, R. A. 1961. *Pyrenophora phaeocomes* (Reb. ex Fr.) Fr. *Canadian Journal of Botany* 39: 901–908.
SLIPPERS, B., P. W. CROUS, S. DENMAN, T. A. COUTINHO, B. D. WINGFIELD, AND M. J. WINGFIELD. 2004. Combined multiple gene genealogies and phenotypic characters differentiate several species previously identified as *Botryosphaeria dothidea*. *Mycologia* 96: 83–101.
SLIPPERS, B., E. BOISSIN, A. J. L. PHILLIPS, J. Z. GROENEWALD, L. LOMBARD, M. J. WINGFIELD, A. POSTMA, et al. 2013. Phylogenetic lineages in the Botryosphaeriales: a systematic and evolutionary framework. *Studies in Mycology* 76: 31–49.
SMERLIS, E. 1967. *Rhizocalyx abietis* Petrak, the perfect state of *Rhizothyrium abietis* Naumoff. *Canadian Journal of Botany* 45: 1715–1717.
SMITH, P. H. 1980. Trichothyriaceous fungi from the early Tertiary of southern England. *Palaeontology* 23: 205–212.
SMITH, P. H. 1984. Fossil fungi from early Tertiary deposits of southern England. Ph.D., University of London, United Kingdom.
SMITH, S. Y., R. S. CURRAH, AND R. A. STOCKEY. 2004. Cretaceous and Eocene poroid hymenophores from Vancouver Island, British Columbia. *Mycologia* 96: 180–186.
SOGONOV, M. V., H.-J. SCHROERS, W. GAMS, J. DIJKSTERHUIS, AND R. C. SUMMERBELL. 2005. The hyphomycete *Teberdinia hygrophila* gen. nov., sp. nov. and related anamorphs of *Pseudeurotium* species. *Mycologia* 97: 695–709.
SPATAFORA, J. W., M. C. AIME, I. V. GRIGORIEV, F. MARTIN, J. E. STAJICH, AND M. BLACKWELL. 2017. The fungal tree of life: from molecular systematics to genome-scale phylogenies, Microbiology Spectrum.
SPOONER, B. M., AND P. M. KIRK. 1990. Observations on some genera of Trichothyriaceae. *Mycological Research* 94: 223–230.
SRIVASTAVA, R. C. 1982. Notes on two interesting fungi from india. *Archiv für Protistenkunde* 125: 331–333.
STAMATAKIS, A. 2014. RAxML version 8: a tool for phylogenetic analysis and post-analysis of large phylogenies. *Bioinformatics* 30: 1312–1313.
STENROOS, S., T. LAUKKA, S. HUHTINEN, P. DÖBBELER, L. MYLLYS, K. SYRJÄNEN, AND J. HYVÖNEN. 2010. Multiple origins of symbioses between ascomycetes and bryophytes suggested by a five-gene phylogeny. *Cladistics* 26: 281–300.
STERFLINGER, K., R. DE BAERE, G. S. DE HOOG, R. DE WACHTER, W. E. KRUMBEIN, AND G. HAASE. 1997. Coniosporium perforans and C. apollinis, two new rock-inhabiting fungi isolated from marble in the Sanctuary of Delos (Cyclades, Greece). *Antonie van Leeuwenhoek* 72: 349–363.
STEVENS, F. L., AND H. W. MANTER. 1925. The Hemisphaeriaceae of British Guiana and Trinidad. *Botanical Gazette* 79: 265–296.
STEVENS, F. L., AND M. H. RYAN. 1939. The Microthyriaceae. The University of Illinois press, Urbana.
STONE, J. K., B. R. CAPITANO, AND J. L. KERRIGAN. 2008. The histopathology of *Phaeocryptopus gaeumannii* on Douglas-fir needles. *Mycologia* 100: 431–444.

SUGIYAMA, J., AND N. AMANO. 1987. Two metacapnodiaceous sooty moulds from Japan: their identity and behavior in pure culture. *Pleomorphic fungi: the diversity and its taxonomic implications*: 141–156.
SUN, C., T. N. TAYLOR, Y. NA, T. LI, AND M. KRINGS. 2015. Unusual preservation of a microthyriaceous fungus (Ascomycota) on *Sphenobaiera* (ginkgophyte foliage) from the Middle Jurassic of China. *Review of Palaeobotany and Palynology* 223: 21–30.
SUNDIN, R., AND A. TEHLER. 1996. The Genus Dendrographa (Roccellaceae). *The Bryologist* 99: 19–31.
SUNDIN, R., AND A. TEHLER. 1998. Phylogenetic studies of the genus *Arthonia*. *The Lichenologist* 30: 381–413.
SUTTON, B. C. 1973. *Pucciniopsis*, *Mycoleptodiscus* and *Amerodiscosiella*. *Transactions of the British Mycological Society* 60: 525–536.
SUTTON, B. C., AND I. G. PASCOE. 1989. Reassessment of *Peltosoma*, *Stigmina* and *Batcheloromyces* and description of *Hyphothyrium* gen. nov. *Mycological Research* 92: 210–222.
SWOFFORD, D. L. 2003. PAUP*. Phylogenetic Analysis Using Parsimony (*and other methods). Version 4.0a165. *Sunderland, MA: Sinauer Associates Inc, software*.
TAKASHIO, M., AND R. VANBREUSEGHEM. 1971. Production of Ascospores by *Piedraia hortai* in Vitro. *Mycologia* 63: 612–618.
TANAKA, K., K. HIRAYAMA, H. YONEZAWA, G. SATO, A. TORIYABE, H. KUDO, A. HASHIMOTO, et al. 2015. Revision of the Massarineae (Pleosporales, Dothideomycetes). *Studies in Mycology* 82: 75–136.
TAYLOR, J. 2001. Pycnothyrium ultrastructure in *Tubakia dryina*. *Mycological Research* 105: 119–121.
TAYLOR, T. N., M. KRINGS, AND E. L. TAYLOR. 2015. Fossil Fungi. (1st ed.). Elsevier/Academic Press Inc., San Diego.
TAYLOR, T. N., H. HASS, H. KERP, M. KRINGS, AND R. T. HANLIN. 2005. Perithecial Ascomycetes from the 400 million year old Rhynie Chert: an example of ancestral polymorphism. *Mycologia* 97: 269–285.
TEHLER, A., AND M. IRESTEDT. 2007. Parallel evolution of lichen growth forms in the family Roccellaceae (Arthoniales, Ascomycota). *Cladistics* 23: 432–454.
TEHON, L. R. 1924. Notes on the parasitic fungi of Illinois. *Mycologia* 16: 135–142.
THAMBUGALA, K. M., H. A. ARIYAWANSA, Y.-M. LI, S. BOONMEE, S. HONGSANAN, Q. TIAN, C. SINGTRIPOP, et al. 2014. Dothideales. *Fungal Diversity* 68: 105–158.
THEISSEN, F. 1914. De Hemisphaerialibus notae supplendae. *Brotéria Série Botânica* 12: 73–96.
TIBPROMMA, S., E. MCKENZIE, S. KARUNARATHNA, P. MORTIMER, J. XU, K. HYDE, AND D. HU. 2016. *Muyocopron garethjonesii* sp. nov. (Muyocopronales, Dothideomycetes) on *Pandanus* sp. *Mycosphere* 7: 1480–1489.
TIBPROMMA, S., K. D. HYDE, R. JEEWON, S. S. N. MAHARACHCHIKUMBURA, J.-K. LIU, D. J. BHAT, E. B. G. JONES, et al. 2017. Fungal diversity notes 491–602: taxonomic and phylogenetic contributions to fungal taxa. *Fungal Diversity* 83: 1–261.
TIFFNEY, B. H., AND E. S. BARGHOORN. 1974. The fossil record of the fungi. Harvard University.
TRAIL, F. 2007. Fungal cannons: explosive spore discharge in the Ascomycota. *FEMS Microbiology Letters* 276: 12–18.

TSUI, C. K. M., AND M. L. BERBEE. 2006. Phylogenetic relationships and convergence of helicosporous fungi inferred from ribosomal DNA sequences. *Molecular Phylogenetics and Evolution* 39: 587–597.
TSUNEDA, A., I. TSUNEDA, AND R. S. CURRAH. 2004. Endoconidiogenesis in *Endoconidioma populi* and *Phaeotheca fissurella*. *Mycologia* 96: 1136–1142.
TSUNEDA, A., M. L. DAVEY, S. HAMBLETON, AND R. S. CURRAH. 2008. *Endosporium*, a new endoconidial genus allied to the Myriangiales. *Botany* 86: 1020–1033.
TURNER, N. C., AND A. GRANITI. 1969. Fusicoccin: a fungal toxin that opens stomata. *Nature* 223: 1070–1071.
UNTEREINER, W. A. 1997. Taxonomy of selected members of the ascomycete genus *Capronia* with notes on Anamorph-teleomorph connections. *Mycologia* 89: 120–131.
UNTEREINER, W. A., N. A. STRAUS, AND D. MALLOCH. 1995. A molecular-morphotaxonomic approach to the systematics of the Herpotrichiellaceae and allied black yeasts. *Mycological Research* 99: 897–913.
UPCHURCH, G. R. 1981. The evolution of the cuticle in early angiosperm leaves from the Lower Cretaceous Potomac Group (Atlantic Coastal Plain, U.S.A.) Doctoral thesis, University of Michigan, Ann Arbor.
UPCHURCH, G. R. 1984a. Cuticle evolution in early Cretaceous angiosperms from the Potomac Group of Virginia and Maryland. *Annals of the Missouri Botanical Garden* 71: 522–550.
UPCHURCH, G. R. 1984b. Cuticular anatomy of angiosperms leaves from the Lower Cretaceous Potomac Group. I. Zone I leaves. *American Journal of Botany* 71: 192–202.
UPCHURCH, G. R. 1989. Dispersed angiosperm cuticles. *In* B. H. Tiffney [ed.], Phytodebris–Notes for a workshop on the study of fragmentary plant remains. paleobotanical section of the Botanical Society of America, 65–92, Toronto.
UPCHURCH, G. R., AND J. A. DOYLE. 1981. Paleoecology of the conifers *Frenelopsis* and *Pseudofrenelopsis* (Cheirolepidiaceae) from the Cretaceous Potomac Group of Maryland and Virginia. *In* R. C. Romans [ed.], Geobotany II. Plenum, New York.
VAN DER HAM, R. W. J. M., AND R. W. DORTANGS. 2005. Structurally preserved ascomycetous fungi from the Maastrichtian type area (NE Belgium). *Review of Palaeobotany and Palynology* 136: 48–62.
VIÉGAS, A. P. 1944. Algun fungos do Brasil II Ascomycetos. *Bragantia* 4: 1–392.
VIJAYA, V., AND S. MURTHY. 2012. Palynomorphs and oribatid mites—From the Denwa Formation, Satpura Basin, Madhya Pradesh, India. *International Journal of Geosciences* 3: 195–205.
VIKRAM, H. C., N. M. RAJ, AND D. MATHEW. 2018. New record of *Chaetasbolisia erysiphoides* from cold arid soils of Zanskar (Kargil), India. *Current science`* 114: 25.
VISHNU, A., M. A. KHAN, M. BERA, D. L. DILCHER, AND S. BERA. 2017. Fossil Asterinaceae in the phyllosphere of the eastern Himalayan Neogene Siwalik forest and their palaeoecological significance. *Botanical Journal of the Linnean Society* 185: 147–167.
VISHNU, A., M. A. KHAN, M. BERA, K. ACHARYA, D. L. DILCHER, AND S. BERA. 2018. Occurrence of *Phoma* Sacc. in the phyllosphere of Neogene Siwalik forest of Arunachal sub-Himalaya and its palaeoecological implications. *Fungal Biology*.
VON ARX, J. A., AND E. MÜLLER. 1975. A re-evalutation of bitunicate ascomycetes with keys to families and genera. *Studies in Mycology* 9: 1–159.

WALL, E., AND P. J. KEANE. 1984. Leaf spot of *Eucalyptus* caused by *Aulographina eucalypti*. *Transactions of the British Mycological Society* 82: 257–273.
WARREN, D. L., A. J. GENEVA, AND R. LANFEAR. 2017. RWTY (R We There Yet): An R package for examining convergence of bayesian phylogenetic analyses. *Molecular Biology and Evolution* 34: 1016–1020.
WATSON, J., AND H. A. CUSACK. 2005. Cycadales of the English Wealden. London.
WEBSTER, J. 1951. Graminicolous pyrenomycetes: I. The conidial stage of *Tubeufia helicomyces*. *Transactions of the British Mycological Society* 34: 304–308.
WEBSTER, J., AND R. WEBER. 2007. Introduction to fungi. Cambridge University Press, New York.
WEDIN, M., H. DÖRING, AND G. GILENSTAM. 2006. *Stictis* s. lat. (Ostropales, Ascomycota) in northern Scandinavia, with a key and notes on morphological variation in relation to lifestyle. *Mycological Research* 110: 773–789.
WIJAYAWARDENE, N., P. CROUS, P. KIRK, D. HAWKSWORTH, S. BOONMEE, U. BRAUN, D.-Q. DAI, et al. 2014. Naming and outline of Dothideomycetes–2014 including proposals for the protection or suppression of generic names. *Fungal Diversity* 69: 1–55.
WILLIAMSON, S. M., C. S. HODGES, AND T. B. SUTTON. 2004. Re-examination of *Peltaster fructicola*, a member of the apple sooty blotch complex. *Mycologia* 96: 885–890.
WOLF, F. A. 1925. Some undescribed fungi on Sourwood, *Oxydendron arboreum* (L.) DC. *Journal of the Elisha Mitchell Scientific Society* 41: 94–99.
WOLF, F. T., AND F. A. WOLF. 1939. A study of *Botryosphaeria ribis* on willow. *Mycologia* 31: 217–227.
WOLLENZIEN, U., G. S. DE HOOG, W. KRUMBEIN, AND J. M. J. UIJTHOF. 1997. *Sarcinomyces petricola*, a new microcolonial fungus from marble in the Mediterranean basin. *Antonie van Leeuwenhoek* 71: 281–288.
WOUDENBERG, J. H. C., J. Z. GROENEWALD, M. BINDER, AND P. W. CROUS. 2013. *Alternaria* redefined. *Studies in Mycology* 75: 171–212.
WU, H., K. D. HYDE, AND H. CHEN. 2011a. Studies on Microthyriaceae: placement of *Actinomyxa*, *Asteritea*, *Cirsosina*, *Polystomellina* and *Stegothyrium*. *Cryptogamie, Mycologie* 32: 3–12.
WU, H., W. M. JAKLITSCH, H. VOGLMAYR, AND K. D. HYDE. 2012. Epitypification, morphology, and phylogeny of *Tothia fuscella*. *Mycotaxon* 118: 203–211.
WU, H., Q. TIAN, W.-J. LI, AND K. HYDE. 2014a. A reappraisal of Microthyriaceae. *Phytotaxa* 176: 201–212.
WU, H., Y. LI, H. A. ARIYAWANSA, W. LI, H. YANG, AND K. D. HYDE. 2014b. A new species of *Microthyrium* from Yunnan, China *2014* 176: 6.
WU, H.-X., C. L. SCHOCH, S. BOONMEE, A. H. BAHKALI, P. CHOMNUNTI, AND K. D. HYDE. 2011b. A reappraisal of Microthyriaceae. *Fungal Diversity* 51: 189–248.
YACHAROEN, S., Q. TIAN, P. CHOMNUNTI, S. BOONMEE, E. CHUKEATIROTE, J. BHAT, AND K. HYDE. 2015. Patellariaceae revisited. *Mycosphere* 6: 290–326.
YANG, H., P. CHOMNUMTI, H. ARYIAWANSA, H.-X. WU, AND K. D. HYDE. 2014. The genus *Phaeosaccardinula* (Chaetothyriales) from Yunnan, China, introducing two new species. *Chiang Mai Journal of Science* 41: 873–884.

YANG, H. L., G. Y. SUN, J. C. BATZER, P. W. CROUS, J. Z. GROENEWALD, AND M. L. GLEASON. 2010. Novel fungal genera and species associated with the sooty blotch and flyspeck complex on apple in China and the USA. *Persoonia* 24: 29–37.

YIRGOU, D., AND R. M. CALDWELL. 1963. Stomatal penetration of wheat seedlings by stem and leaf rust: effect of light and carbon dioxide. *Science* 141: 272–273.

YOUNG, P. A. 1926. Penetration phenomena and facultative parasitism in *Alternaria*, *Diplodia*, and other fungi. *Botanical Gazette* 81: 258–279.

ZHANG, J. Q., Y. ZHANG, Y. P. ZHOU, Z. P. DOU, W. HE, AND P. W. CROUS. 2015. First report of *Tubakia seoraksanensis* parasitizing *Quercus mongolica* in Lesser Khingan Mountains, China. *Plant Disease* 99: 891–891.

ZHANG, Y., P. CROUS, C. SCHOCH, AND K. HYDE. 2012. Pleosporales. *Fungal Diversity* 53: 1–221.

ZHANG, Y., P. CROUS, C. SCHOCH, A. BAHKALI, L. GUO, AND K. HYDE. 2011. A molecular, morphological and ecological re-appraisal of Venturiales—a new order of Dothideomycetes. *Fungal Diversity* 51: 249–277.

ZHAO, W., Y. HOU, J. BAI, W. ZHANG, L. GAO, R. ZHANG, M. L. GLEASON, AND G. SUN. 2016. A new species of *Zasmidium* associated with sooty blotch and flyspeck. *Phytotaxa* 258: 190–194.

Appendices

Appendix A

A1. Isolates included in this study[1]

Order	Taxa	Voucher/Strain	GenBank accession – SSU	GenBank accession - LSU
Abrothallales Pérez-Ort. & Suija	*Abrothallus acetabuli* Diederich	SPO308	KF816215.1	KF816232.1
Abrothallales	*Abrothallus buellianus* De Not.	SPO303	KF816217.1	KF816234.1
Abrothallales	*Abrothallus cladoniae* R. Sant. & D. Hawksw.	AB53	KF816220.1	KF816228.1
Abrothallales	*Abrothallus parmeliarum* (Sommerf.) Arnold	AB36	KF816222.1	KF816229.1
Abrothallales	*Abrothallus parmotrematis* Diederich	AB1	KF816225.1	KF816231.1
Abrothallales	*Abrothallus secedens* Wedin & R. Sant.	SPO305	KF816216.1	KF816236.1
Abrothallales	*Abrothallus suecicus* (Kirschst.) Nordin	AB56	-	KF816226.1
Abrothallales	*Abrothallus usneae* Rabenh.	AB20	KF816223.1	-
Abrothallales	*Lichenoconium lecanorae* (Jaap) D. Hawksw.	strain JL382-10	-	HQ174263.1
Abrothallales	*Abrothallus hypotrachynae* Etayo & Diederich	SPO302	KF816218.1	KF816233.1
Acrospermales Minter, Peredo & A.T. Watson	*Acrospermum compressum* Tode	M151	EU940012.1	EU940084.1
Acrospermales	*Acrospermum graminum* Lib.	M152	EU940013.1	EU940085.1
Acrospermales	*Acrospermum adeanum* Höhn.	M133	EU940031.1	EU940104.1
Arthoniales Henssen ex D. Hawksw. & O.E. Erikss.	*Arthonia dispersa* (Schrad.) Nyl.	UPSC 2583	AY571381.1	AY571381.1
Arthoniales	*Chrysothrix candelaris* (L.) J.R. Laundon	UPS Frisch 11/Se45	-	KF707640.1

Arthoniales	*Combea mollusca* (Ach.) Nyl.	Tehler 7725	AY571380.1	AY571382.1
Arthoniales	*Dendrographa leucophaea* (Tuck.) Darb.	Ornduff 10070 Duke	AF279381.1	AF279382.1
Arthoniales	*Lecanographa amylacea* (Ehrh. ex Pers.) Egea & Torrente	UPS Thor 26176	-	KF707639.1
Arthoniales	*Lichinella iodopulchra* (Couderc ex Croz.) P.P. Moreno & Egea	AFTOL-ID 896	-	DQ782916.1
Arthoniales	*Melarthonis piceae* Frisch & G. Thor	UPS Thor 25995	-	KJ851080.1
Arthoniales	*Opegrapha dolomitica* (Arnold) Clauzade & Cl. Roux ex Torrente & Egea	AFTOL-ID 993	DQ883706.1	-
Arthoniales	*Reichlingia zwackhii* (Sandst.) Frisch & G. Thor	UPS Thor 11/3	-	KF707637.1
Arthoniales	*Roccella fuciformis* (L.) DC.	AFTOL-ID 126	AY584678.1	AY584654.1
Arthoniales	*Roccellographa cretacea* J. Steiner	AFTOL-ID 93	DQ883705.1	DQ883696.1
Arthoniales	*Schismatomma decolorans* (Erichsen) Clauzade & Vězda	DUKE 0047570 Ertz 5003 (BR)	NG_013155.1	NG_027622.1
Arthoniales	*Simonyella variegata* J. Steiner	AFTOL-ID 80	AY584669.1	-
Arthoniales	*Alyxoria varia* (Pers.) Ertz & Tehler	-	AF138853.1	**EU704103.1**
Asterinales M.E. Barr ex D. Hawksw. & O.E. Erikss.	*Alysidiella suttonii* Cheew. & Crous	CBS 124780	-	HM628777.1
Asterinales	*Asterina chrysophylli* Henn.	VIC 42823	-	KP143738.1
Asterinales	*Asterina melastomatis* Lév.	VIC 42822	-	MK251541
Asterinales	*Aulographina eucalypti* (Cooke & Massee) Arx & E. Müll.	CPC 12986	-	HM535600.1

Asterinales	*Batistinula gallesiae* Arx	VIC 42514	-	KM111255.1
Asterinales	*Blastacervulus eucalypti* H.J. Swart	CBS 124759	-	GQ303302.1
Asterinales	*Blastacervulus eucalyptorum* Crous	CPC 29450	-	KY173484.1
Asterinales	*Parmularia styracis* Lév.	VIC 42587	-	KP143730.1
Asterinales	*Prillieuxina baccharidincola* (Rehm) Petr.	VIC 42817	-	KP143735.1
Asterinales	*Lembosia abaxialis* Firmino & R.W. Barreto	VIC 42825	-	KP143737.1
Asterotexiales Firmino, O.L. Pereira & Crous	*Asterina* (Lév.) sp.	MFLU13-0619	-	KM386978.1
Asterotexiales	*Asterina cestricola* (R.W. Ryan) Hosag. & T.K. Abraham	TH 591	GU586209.1	GU586215.1
Asterotexiales	*Asterina cynometrae* Hongsanan & K.D. Hyde	MFLU 13-0373	-	KX845436.1
Asterotexiales	*Asterina fuchsiae* Syd.	TH 590	GU586210.1	GU586216.1
Asterotexiales	*Asterina phenacis* Syd.	TH 589	GU586211.1	GU586217.1
Asterotexiales	*Asterina siphocampyli* Syd.	M-0141060 (PMA)	-	HQ701140.1
Asterotexiales	*Asterina weinmanniae* Syd.	TH592	GU586212.1	GU586218.1
Asterotexiales	*Asterina zanthoxyli* W. Yamam.	TH 561	GU586213.1	GU586219.1
Asterotexiales	**Asterotexiaceae [Firmino, O.L. Pereira & Crous] sp. 1**	UBC-F33036	-	MG844156
Asterotexiales	**Asterotexiaceae sp. 2**	CBS 143813 *	-	MG844162
Asterotexiales	*Asterotexis cucurbitacearum*	PMA M-0141224	-	HQ610510.1
Asterotexiales	*Asterotexis cucurbitacearum* (Rehm) Arx	VIC 42814	-	KP143734.1
Asterotexiales	*Buelliella minimula* (Tuck.) Fink	Lendemer 42273 (NY)	-	KX244961.1

Asterotexiales	*Buelliella physciicola* Poelt & Hafellner	Ertz 19173 (BR)	-	KP456148.1
Asterotexiales	*Buelliella poetschii* Hafellner	Ertz 18116 (BR)	-	KP456150.1
Asterotexiales	*Discopycnothyrium palmae* Hongsanan & K.D. Hyde	MFLU13-0485	-	KM386979.1
Asterotexiales	*Hemigrapha atlantica* Diederich & Wedin	Ertz 14014 (BR)	-	KP456151.1
Asterotexiales	*Inocyclus angularis* Guatim. & R.W. Barreto	VIC 39747	-	KP143731.1
Asterotexiales	*Karschia cezannei* Ertz & Diederich	Ertz 19186(BR)	-	KP456154.1
Asterotexiales	*Karschia talcophila* (Ach.) Körb.	Diederich 16749	-	KP456155.1
Asterotexiales	*Labrocarpon canariense* (D. Hawksw.) Etayo & Pérez-Ort.	Ertz 16907 (BR)	-	KP456158.1
Asterotexiales	*Lembosia albersii* Henn.	MFLU13-0377	-	KM386982.1
Asterotexiales	*Lembosia xyliae* X.Y. Zeng, T., C. Wen & K.D. Hyde	MFLU14-0004	-	KT283685.1
Asterotexiales	*Mahanteshomyces* Hosag. & C.K. Biju sp.	TH 588	GU586214.1	GU586220.1
Asterotexiales	*Melaspilea lekae* Brackel & Kalb	Ertz 17325 (BR)	-	KP456162.1
Asterotexiales	*Melaspileopsis* cf. *diplasiospora* (Nyl.) Ertz & Diederich	Ertz 16625	-	KP456166.1
Asterotexiales	*Morenoina calamicola* S. Konta & K.D. Hyde		KY511427	KY511424
Asterotexiales	*Mycosphaerella pneumatophorae* Kohlm.	AFTOL-ID 762	-	FJ176856.1
Asterotexiales	*Stictographa lentiginosa* (Lyell ex Leight.) Mudd	van den Boom 47621	-	KP456171.1
Asterotexiales	*Taeniolella hawksworthiana* Heuchert, Ertz & Common	Common 9199B (BR)	-	KX244970.1

Asterotexiales	*Taeniolella punctata* M.S. Christ. & D. Hawksw.	Ertz 17390 (BR)	-	KX244972.1
Asterotexiales	*Taeniolella pyrenulae* Heuchert & Diederich	Diederich 17075	-	KX244976.1
Asterotexiales	*Taeniolella* S. Hughes sp.	Ertz 11026 (BR)	-	KX244979.1
Asterotexiales	*Taeniolella toruloides* Heuchert & Diederich	Diederich 17048	-	KX244978.1
Asterotexiales	*Rhagadolobiopsis thelypteridis* Guatim. & R.W. Barreto	EG 156	-	KC171177.1
Aulographaceae Luttr. ex P.M. Kirk, P.F. Cannon & J.C. David	*Aulographum hederae*	CBS 113979	JGI	JGI
Aulographaceae	***Aulographum* Lib. sp.**	CBS 143545 *	MG844146	MG844158
Aulographaceae	***Lembosina aulographoides* E. Bommer, M. Rousseau & Sacc.) Theiss.**	CBS 143809 *	MG844145	MG844157
Aulographaceae	***Lembosina* Theiss. sp.**	CBS 143815 *	-	MG844165
Aulographaceae	***Lembosina* sp.**	CBS 144007 *	-	MG844164
Aulographaceae	*Aulographum hederae* Lib.	MFLUCC13-0001	-	KM386981.1
Botryosphaeriales C.L. Schoch, Crous & Shoemaker	*Botryosphaeria dothidea* (Moug.) Ces. & De Not.	CBS 115476	DQ677998.1	NG_027577.1
Botryosphaeriales	*Kellermania anomala* (Cooke) Höhn.	CBS 132218	KF766259.1	NG_042700.1
Botryosphaeriales	*Kellermania dasylirionicola* Minnis & A.H. Kenn.	CBS 131720	KF766262.1	NG_042703.1
Botryosphaeriales	*Neofusicoccum ribis* (Slippers, Crous & M.J. Wingf.) Crous, Slippers & A.J.L. Phillips	AFTOL-ID 1232	DQ678000.1	DQ678053.1
Botryosphaeriales	*Kellermania yuccifoliorum* A.W. Ramaley	CBS 131726	KF766271.1	NG_042713.1

Caliciales Bessey	*Physcia aipolia* (Ehrh. ex Humb.) Fürnr.	AFTOL-ID 84	DQ782876.1	DQ782904.1
Capnodiales Woron.	*Acidomyces richmondensis* B.J. Baker, M.A. Lutz, S.C. Dawson, P.L. Bond & Banfield	C2	JGI	JGI
Capnodiales	*Arthrocatena tenebrio* Egidi & Selbmann	CCFEE 5413	GU250342.1	GU250385.1
Capnodiales	*Aulographina pinorum* (Desm.) Arx & E. Müll.	CBS 174.90	GU296138.1	GU301802.1
Capnodiales	*Capnobotryella renispora* Sugiy.	CBS 214.90	AF006723.1	GU214398.1
Capnodiales	*Capnodium citri* Berk. & Desm.	CBS 451.66	GU296177.1	AY004337.1
Capnodiales	*Capnodium coffeae* Pat.	CBS 147.52	DQ247808.1	GU214400.1
Capnodiales	*Catenulostroma chromoblastomycosum* Crous & U. Braun	CBS 597.97	GU214516.1	EU019251.2
Capnodiales	*Cercospora zebrina* Pass.	(SSU) STE-U 3955, (LSU) **CBS 118790**	AY251104.2	JQ739815.1
Capnodiales	*Cladosporium bruhnei* Linder	CPC 5101	AY251096.2	GU214408.1
Capnodiales	*Comminutispora agavacearum* A.W. Ramaley	CBS 619.95	Y18699.1	EU981286.1
Capnodiales	*Conidiocarpus caucasicus* Woron.	GUMH937	KC833051.1	KC833050.1
Capnodiales	*Davidiella tassiana* (De Not.) Crous & U. Braun	DAOM 196248	JN939022.1	JN938886.1
Capnodiales	*Elasticomyces elasticus* Zucconi & Selbmann	CCFEE 5320	GU250333.1	GU250376.1
Capnodiales	*Fumiglobus pieridicola* T. Bose	UBC F23788	KC833053.1	KC833052.1
Capnodiales	*Houjia yanglingensis* G.Y. Sun & Crous	YHJN13	-	GQ433631.1

Capnodiales	*Johansonia chapadensis* Crous, R.W. Barreto, Alfenas & R.F. Alfenas	CBS H-20484	-	HQ423450.1
Capnodiales	*Leptoxyphium fumago* (Woron.) R.C. Srivast.	CBS 123.26	GU214535.1	GU301831.1
Capnodiales	*Microcyclospora pomicola* J. Frank, B. Oertel, Schroers & Crous	CPC 16173	GU570559.1	GU570551.1
Capnodiales	*Mycosphaerella latebrosa* (Cooke) J. Schröt.	CBS 687.94	GU214546.1	GU214444.1
Capnodiales	*Passalora fulva* (Cooke) U. Braun & Crous	(SSU) STE-U 3688, (LSU) **CBS 119.46**	AY251109.2	DQ008163.2
Capnodiales	*Peltaster fructicola* Eric M. Johnson, T.B. Sutton & Hodges	strain 11157	KF550926.1	JN573665.1
Capnodiales	*Penidiella columbiana* Crous & U. Braun	CBS 486.80	GU214565.1	EU019274.2
Capnodiales	*Phaeophleospora atkinsonii* (Syd.) Pennycook & McKenzie	CBS 124565	JN938701.1	GU214462.1
Capnodiales	*Phaeotheca fissurella* Sigler, Tsuneda & J.W. Carmich.	CBS 520.89	Y18697.1	GU117900.1
Capnodiales	*Phragmocapnias asiaticus* Chomnunti & K.D. Hyde	MFLUCC10-0062 18S	JN832597.1	JN832612.1
Capnodiales	*Piedraia hortae* Fonseca & Leão	CBS 480.64	AY016349.1	AY016366.1
Capnodiales	*Racodium rupestre* Pers.	L346	EU048575.1	EU048583.1
Capnodiales	*Rasutoria tsugae* (Dearn.) M.E. Barr	EF1147	EF114730.1	EF114705.1
Capnodiales	*Readeriella mirabilis* Syd. & P. Syd.	CBS 116293	EU754110.2	EU019291.2
Capnodiales	*Recurvomyces mirabilis* Selbmann & de Hoog	CCFEE 5264	GU250329.1	GU250372.1

Capnodiales	*Schizothyrium pomi* (Mont. & Fr.) Arx	CBS 228.57	-	KF902007.1
Capnodiales	*Scorias spongiosa* (Schwein.) Fr.	AFTOL-ID 1594	DQ678024.1	DQ678075.1
Capnodiales	*Sphaerulina polyspora* F.A. Wolf	(SSU) STE-U 4301, (LSU) **CBS 354.29**	AY251095.1	GU214501.1
Capnodiales	*Stomiopeltis versicolor* (Desm.) Arx	GA3 23C2b	-	FJ147163.1
Capnodiales	*Teratosphaeria stellenboschiana* (Crous) Crous	CPC 10886	GU214583.1	EU019295.2
Capnodiales	*Uwebraunia communis* (Crous & Mansilla) Crous	CBS 110747	NG_016521.1	GQ852589.1
Capnodiales	*Xenomeris juniperi* (Dearn.) M.E. Barr & E. Müll.	isolate="xejucf"	EF114734.1	EF114709.1
Capnodiales	*Zasmidium anthuriicola* (U. Braun & C.F. Hill) Crous & U. Braun	CBS 118742	GU214595.1	GQ852732.1
Capnodiales	*Mycosphaerella walkeri* R.F. Park & Keane	CPC 11252	GU214593.1	GU214500.1
Chaetothyriales M.E. Barr	*Capronia pilosella* (P. Karst.) E. Müll., Petrini, P.J. Fisher, Samuels & Rossman	AFTOL-ID 657	DQ823106.1	DQ823099.1
Chaetothyriales	*Ceramothyrium carniolicum* (Rehm) Petr.	CBS 175.95	AF346418.1	AY004339.1
Chaetothyriales	*Ceramothyrium podocarpi* Crous	CPC 19826	-	KC005795.1
Chaetothyriales	*Chaetothyrium agathis* Hongsanan & K.D. Hyde	MFLUCC 12 C0113	-	KP744480.1
Chaetothyriales	*Chaetothyrium brischoficola* Chomnunti & K.D. Hyde	MFLU(CC)10-0012	-	HQ895836.1
Chaetothyriales	*Exophiala dermatitidis* (Kano) de Hoog	AFTOL-ID 668	DQ823107.1	DQ823100.1

Chaetothyriales	*Exophiala pisciphila* McGinnis & Ajello	AFTOL-ID 669	DQ823108.1	DQ823101.1
Chaetothyriales	*Phaeosaccardinula dendrocalami* Chomnunti & K.D. Hyde	IFRDCC 2663	-	KF667246.1
Chaetothyriales	*Phaeosaccardinula ficus* Chomnunti & K.D. Hyde	MFLU(CC)10-0009	-	HQ895837.1
Chaetothyriales	*Sarcinomyces petricola* Wollenz. & de Hoog	CBS 101157	FJ358318.1	FJ358249.1
Chaetothyriales	*Ceramothyrium linnaeae* (Dearn.) S. Hughes	UPSC 2646	AF022715.1	-
Dothideales Lindau	*Aureobasidium subglaciale* (Zalar, de Hoog & Gunde-Cim.) Zalar, de Hoog & Gunde-Cim.	EXF-2481	JGI	JGI
Dothideales	*Dothidea insculpta* Wallr.	CBS 189.58	DQ247810.1	NG_027643.1
Dothideales	*Stylodothis puccinioides* (DC.) Arx & E. Müll.	CBS 193.58	NG_013130.1	NG_027594.1
Dothideales	*Sydowia polyspora* (Bref. & Tavel) E. Müll.	AFTOL-ID 178	AY544718.1	AY544675.1
Dothideales	*Dothidea sambuci* (Pers.) Fr.	AFTOL-ID 274	AY544739.1	AY544681.1
Dyfrolomycetales K.L. Pang, K.D. Hyde & E.B.G. Jones	*Dyfrolomyces rhizophorae* (K.D. Hyde) K.D. Hyde, K.L. Pang, Alias, Suetrong & E.B.G. Jones	JK 5349A	GU479766.1	GU479799.1
Dyfrolomycetales	*Dyfrolomyces tiomanensis* K.L. Pang, Alias, K.D. Hyde, Suetrong & E.B.G. Jones	NTOU3636	KC692155.1	KC692156.1
Erysiphales E. Warming	*Erysiphe mori* (I. Miyake) U. Braun & S. Takam.	MUMHS77	AB033484.2	AB022418.1

Eurotiales G.W. Martin ex Benny & Kimbr.	*Aspergillus fumigatus* Fresen.	(SSU) **JCM1738** (LSU) HP044	AB008401.1	KT323254.1
Eurotiales	*Aspergillus niger* Tiegh.	ATCC 1015	JGI	JGI
Eurotiales	*Monascus purpureus* Went	AFTOL-ID 426	DQ782881.1	DQ782908.1
Eurotiales	*Aspergillus nidulans* (Eidam) G. Winter	ATCC 10074	U77377.1	KC146369.1
Helotiales Nannf. ex Korf & Lizoň	*Cudoniella clavus* Alb. & Schwein.) Dennis	AFTOL-ID 166	DQ470992.1	DQ470944.1
Helotiales	*Mollisia cinerea* (Batsch) P. Karst.	AFTOL-ID 76	DQ470990.1	DQ470942.1
Helotiales	*Monilinia laxa* (Aderh. & Ruhland) Honey	CBS 122031	AY544714.1	NG_027608.1
Hysteriales Lindau	*Hysterobrevium constrictum* (N. Amano) E. Boehm & C.L. Schoch	SMH 5211.1	GU397361.1	GQ221905.2
Hysteriales	*Psiloglonium araucanum* (Speg.) E. Boehm, Marinc. & C.L. Schoch	CBS 112412	FJ161133.2	FJ161172.2
Hysteriales	*Psiloglonium clavisporum* (Seaver) E. Boehm, C.L. Schoch & Spatafora	GKM L172A	GU323192.1	GU323204.1
Hysteriales	*Hysterobrevium smilacis* (Schwein.) E. Boehm & C.L. Schoch	CBS 114601	FJ161135.2	FJ161174.2
Lecanorales Nannf.	*Cladonia caroliniana*	AFTOL-ID 3	AY584664.1	AY584640.1
Lecanorales	*Lecanora hybocarpa* (Tuck.) Brodo	AFTOL-ID 639	DQ782883.1	DQ782910.1
Licheno-stigmatales Ertz, Diederich & Lawrey	*Cf. Arthoniales sp.*	GU250325.1	GU250325.1	-
Licheno-stigmatales	*Dothideomycetes sp.*	TRN 213	GU324008.1	-
Licheno-stigmatales	*Lichenostigma maureri* Hafellner	Diederich 17326	-	KF176953.1

Licheno-stigmatales	*Phaeococcomycetaceae* McGinnis & Schell sp.	TRN 529	GU324016.1	GU323987.1
Licheno-stigmatales	*Phaeococcomycetaceae* sp.	TRN 456	GU324015.1	GU323986.1
Licheno-stigmatales	*Phaeococcomycetaceae* sp.	TRN 452	GU324014.1	GU323985.1
Licheno-stigmatales	***Seuratia millardetii* (Racib.) Meeker**	UBC-F33043	MG844150	MG844163
Licheno-stigmatales	*Teratosphaeriaceae* Crous & U. Braun 2007 sp.	D007 09	GU250359.1	GU250402.1
Microthyriales G. Arnaud	*Chaetothyriothecium elegans* Hongsanan & K.D. Hyde	CPC 21375	-	KF268420.1
Microthyriales	*Heliocephala gracilis* (R.F. Castañeda) R.F. Castañeda & Unter.	MUCL 41200	HQ333479.1	HQ333479.1
Microthyriales	***Lichenopeltella pinophylla* (Höhn.) P.M. Kirk & Minter**	UBC-F33032	-	VUL.316
Microthyriales	***Microthyrium illicinum* De Not.**	CBS 143808 *	MG844144	MG844151
Microthyriales	***Microthyrium macrosporum* (Sacc.) Höhn.**	CBS 143810 *	MG844147	MG844159
Microthyriales	*Microthyrium microscopicum* Desm.	CBS 115976	GU296175.1	GU301846.1
Microthyriales	*Stomiopeltis betulae* J.P. Ellis	CBS 114420	GU214701.1	GU214701.1
Microthyriales	*Tumidispora shoreae* Hongsanan & K.D. Hyde	MFLUCC 12-0409	-	KT314074.1
Microthyriales	*Heliocephala zimbabweensis* Decock, V. Robert & Masuka	MUCL 40019	HQ333481.1	HQ333481.1

Monoblastiales Lücking, M.P. Nelsen & K.D. Hyde	*Acrocordia subglobosa* (Vězda) Poelt & Vězda	HTL940	JN887373.1	JN887392.1
Monoblastiales	*Anisomeridium phaeospermum* R.C. Harris 1995	MPN539	JN887374.1	JN887394.1
Monoblastiales	*Funbolia dimorpha* Crous & Seifert	CPC 14170	-	JF951156.1
Monoblastiales	*Heleiosa barbatula* Kohlm., Volkm.-Kohlm. & O.E. Erikss.	JK 5548I	GU479753.1	GU479787.1
Monoblastiales	*Megalotremis verrucosa* (Makhija & Patw.) Aptroot	MPN104	JN887383.1	GU327718.1
Monoblastiales	*Musaespora kalbii* Lücking & Sérus.	MPN243	JN887391.1	JN887406.1
Monoblastiales	*Anisomeridium ubianum* (Vain.) R.C. Harris	MPN94	JN887379.1	GU327709.1
Muyocopronales Mapook, Boonmee & K.D. Hyde	*Arxiella dolichandrae* Crous	CBS 138853	-	KP004477.1
Muyocopronales	*Muyocopron castanopsis* Mapook, Boonmee & K.D. Hyde	MFLUCC 14-1108	KU726968.1	KU726965.1
Muyocopronales	*Muyocopron dipterocarpi*	MFLUCC 14-110	KU726969.1	KU726966.1
Muyocopronales	*Muyocopron garethjonesii* Tibpromma, Karun. & K.D. Hyde	MFLU 16-2664	KY070275.1	KY070274.1
Muyocopronales	*Muyocopron lithocarpi* Mapook, Boonmee & K.D. Hyde	MFLUCC 14-1106	KU726970.1	KU726967.1
Muyocopronales	*Mycoleptodiscus indicus* (V.P. Sahni) B. Sutton	UAMH 8520	-	GU980695.1
Muyocopronales	*Paramycoleptodiscus albiziae* Crous & M.J. Wingf.	CPC 27552	-	KX228330.1
Muyocopronales	*Muyocopron* Speg. *sp.*	MFLU (CC) 10-0041	JQ036226.1	JQ036230.1

Myriangiales	*Elsinoe veneta* (Burkh.) Jenkins	AFTOL-ID 1853	DQ767651.1	DQ767658.1
Myriangiales Starbäck	*Endosporium aviarium* Tsuneda	UAMH 10530	EU304349.1	EU304351.1
Myriangiales	*Endosporium populi-tremuloides* Tsuneda	UAMH 10529	EU304346.1	EU304348.1
Myriangiales	*Myriangium hispanicum* J.B. Martínez	CBS 247.33	GU296180.1	GU301854.1
Myriangiales	*Myriangium duriaei* Mont. & Berk.	CBS 260.36	JGI	JGI
Mytilinidiales E. Boehm, C.L. Schoch & Spatafora	*Cenococcum geophilum* Fr.	JGI 1.58 v2.0	JGI	JGI
Mytilinidiales	*Lepidopterella palustris* Shearer & J.L. Crane	CBS 459.81	JGI	JGI
Mytilinidiales	*Lophium elegans* H. Zogg	EB 0366	GU323184.1	GU323210.1
Mytilinidiales	*Lophium mytilinum* (Pers.) Fr.	AFTOL-ID 1609	DQ678030.1	DQ678081.1
Mytilinidiales	*Mytilinidion mytilinellum* (Fr.) H. Zogg	CBS 303.34	FJ161144.2	FJ161184.2
Mytilinidiales	*Mytilinidion scolecosporum* M.L. Lohman	CBS 305.34	FJ161146.2	FJ161186.2
Natipusillales Raja, Shearer, A.N. Mill. & K.D. Hyde	*Natipusilla bellaspora* Raja, Shearer & A.N. Mill.	PE91 1a	JX474868.1	JX474863.1
Natipusillales	*Natipusilla decorospora* A. Ferrer, A.N. Mill. & Shearer	AF236 1A	HM196376.1	HM196369.1
Natipusillales	*Natipusilla naponensis* A. Ferrer, A.N. Mill. & Shearer	AF217 1A	HM196378.1	HM196371.1
Natipusillales	*Natipusilla limonensis* A. Ferrer, A.N. Mill. & Shearer	AF286 1A	HM196377.1	HM196370.1
Onygenales Cif. ex Benny & Kimbr.	*Spiromastix warcupii* Kuehn & G.F. Orr	AFTOL-ID 430	DQ782882.1	DQ782909.1

Ostropales Nannf.	*Absconditella sphagnorum* Vězda & Poelt	T. Laukka 52 (TUR)	EU940022.1	EU940095.1
Ostropales	*Acarosporina microspora* (R.W. Davidson & R.C. Lorenz) Sherwood	AFTOL-ID 78	AY584667.1	AY584643.1
Ostropales	*Cryptodiscus gloeocapsa* (Nitschke ex Arnold) Baloch, Gilenstam & Wedin	TSB 30770	AF465456.1	AF465440.1
Ostropales	*Diploschistes cinereocaesius* (Sw.) Vain.	DUKE 0047509	DQ883790.1	DQ883790.1
Ostropales	*Diploschistes ocellatus* (Fr.) Norman	Spain 995	NG_013126.1	NG_027624.1
Ostropales	*Diploschistes rampoddensis* (Nyl.) Zahlbr.	-	AF274111.1	AF274094.1
Ostropales	*Diploschistes thunbergianus* (Ach.) Lumbsch & Vězda	Eldridge 3800 (F)	AF274112.1	AF274095.1
Ostropales	*Dyplolabia afzelii* (Ach.) A. Massal.	Luecking 26509a	-	HQ639628.1
Ostropales	*Fissurina insidiosa* C. Knight & Mitt.	AFTOL-ID 1662	DQ973022.1	DQ973045.1
Ostropales	*Fissurina marginata* Staiger	DNA3418	-	JX421493.1
Ostropales	*Gyalecta hypoleuca* (Ach.) Zahlbr.	TSB 20801	AF465460.1	AF465453.1
Ostropales	*Gyalecta ulmi* (Sw.) Zahlbr.	Scheidegger 30.05.1998 (Duke)	AF465464.1	AF465463.1
Ostropales	***Micropeltis* [Mont.] sp.**	UBC-F33034	-	MG844154
Ostropales	*Micropeltis zingiberaceicola* Henn.	IFRDCC 2264	JQ036222.1	JQ036227.1
Ostropales	*Odontotrema phacidioides* Nyl.	Palice 11440	-	HM244770.1
Ostropales	*Porina farinosa* C. Knight	Lucking Pan-02 (F)	-	KJ449332.1

Ostropales	*Porina guentheri* (Flot.) Zahlbr.	Lutzoni 97.10.09-10(Duke)	AF279404.1	AF279405.1
Ostropales	***Scolecopeltidium* F. [Stevens & Manter] sp. 2**	UBC-F33035	-	MG844155
Ostropales	***Scolecopeltidium* sp. 1**	UBC-F33033	-	MG844153
Ostropales	*Sphaeropezia arctoalpina* (Döbbeler & Poelt) Baloch, Gilenstam & Wedin	Baloch SW057 (S)	-	HM244760.1
Ostropales	*Stictis radiata* (L.) Pers.	-	U20610.1	**AF356663.1**
Ostropales	*Trapelia placodioides* Coppins & P. James	-	AF119500.2	AF274103
Ostropales	*Diploschistes muscorum* (Scop.) R. Sant.	Palice 2805 (HB Palice)	-	AY300836.1
Patellariales D. Hawksw. & O.E. Erikss.	*Glyphium elatum* (Grev.) H. Zogg	EB 0342	KM220935.1	KM220938.1
Patellariales	*Hysteropatella clavispora* (Peck) Höhn.	CBS 247.34	DQ678006.1	AY541493.1
Patellariales	*Patellaria atrata* (Hedw.) Fr.	CBS 101060	JGI	JGI
Patellariales	*Hysteropatella elliptica* (Fr.) Rehm	CBS 935.97, AFTOL-ID 1790	EF495114.1	DQ767657.1
Pertusariales M. Choisy ex D. Hawksw. & O.E. Erikss.	*Dibaeis baeomyces* (L. f.) Rambold & Hertel	(SSU) taxon 83478, (LSU) **Lutzoni 93.08.20**	AF113712.1	KJ462342.1
Pertusariales	*Pertusaria dactylina* (Ach.) Nyl.	AFTOL-ID 224	DQ782880.1	DQ782907.1
Phaeotrichales Ariyaw., Jian K. Liu & K.D. Hyde	*Trichodelitschia bisporula* (P. Crouan & H. Crouan) Munk ex N. Lundq.	CBS 262.69	JGI	JGI

Phaeotrichales	*Phaeotrichum benjaminii* Malloch & Cain	CBS 541.72	AY016348.1	AY004340.1
Pleosporales Luttr. ex M.E. Barr	*Aigialus grandis* Kohlm. & S. Schatz	JK 5244A	NG_016503.1	GU301793.1
Pleosporales	*Alternaria alternata* (Fr.) Keissl.	SRC1lrK2f	HM216191.1	HM216200.1
Pleosporales	*Arthopyrenia salicis* A. Massal.	CBS 368.94	AY538333.1	AY538339.1
Pleosporales	*Ascocratera manglicola*	JK 5262C	GU296136.1	GU301799.1
Pleosporales	*Astrosphaeriella stellata* (Pat.) Sacc.	MFLUCC10-0095	JN846741.1	JN846720.1
Pleosporales	*Astrosphaeriella vesuvius* (Berk. & Broome) D. Hawksw. & Boise	LF-157	KP814137.1	KP814136.1
Pleosporales	*Bipolaris maydis* (Y. Nisik. & C. Miyake) Shoemaker	AFTOL-ID 54	AY544727.1	AY544645.1
Pleosporales	*Chaetasbolisia erysiphoides* (Griffon & Maubl.) Griffon & Maubl.	CBS 148.94	EU754041.1	EU754140.1
Pleosporales	*Cheirosporium triseriale* L. Cai & K.D. Hyde	HMAS 180703	-	EU413954.1
Pleosporales	*Dictyocheirospora rotunda* M.J. D'souza, Bhat & K.D. Hyde	DLUCC 0577	-	KY320517.1
Pleosporales	*Dictyosporium elegans* Corda	NBRC 32502	DQ018079.1	DQ018100.1
Pleosporales	*Halojulella avicenniae*	JK 5326A	GU479756.1	GU479790.1
Pleosporales	*Halojulella avicenniae* (Borse) Suetrong, K.D. Hyde & E.B.G. Jones	BCC 18422	GU371831.1	GU371823.1
Pleosporales	*Jalapriya pulchra* M.J. D'souza, Hong Y. Su, Z.L. Luo & K.D. Hyde	SB-2016c isolate LQXM47	KU179110.1	KU179109.1

Pleosporales	*Leptosphaeria heterospora* (De Not.) Niessl	CBS 644.86	AY016354.1	AY016369.1
Pleosporales	*Pleospora herbarum* (Pers.) Rabenh.	CBS 191.86	DQ247812.1	JX681120.1
Pleosporales	*Pseudocoleophoma polygonicola* Kaz. Tanaka & K. Hiray.	KT 731	AB797256.1	AB807546.1
Pleosporales	*Pseudodictyosporium wauense* Matsush.	NBRC 30078	DQ018083.1	DQ018105.1
Pleosporales	*Pyrenophora phaeocomes* (Rebent.) Fr.	AFTOL-ID 283	DQ499595.1	NG_027575.1
Pyrenulales Fink ex D. Hawksw. & O.E. Erikss.	*Pyrenula pseudobufonia* (Rehm) R.C. Harris	Reeb VR (DUKE)	AY641001.1	AY640962.1
Pyrenulales	*Pyrgillus javanicus* (Mont. & Bosch) Nyl.	AFTOL-ID 342	DQ823110.1	DQ823103.1
Rhytismatales M.E. Barr ex Minter	*Coccomyces dentatus* (J.C. Schmidt & Kunze) Sacc.	AFTOL-ID 147	AY544701.1	AY544657.1
Strigulales Lücking, M.P. Nelsen & K.D. Hyde	*Flavobathelium epiphyllum* Lücking, Aptroot & G. Thor	MPN67	JN887382.1	GU327717.1
Strigulales	*Phyllobathelium anomalum* Lücking	MPN242	JN887386.1	GU327722.1
Strigulales	*Strigula jamesii* (Swinscow) R.C. Harris	MPN548	JN887388.1	JN887404.1
Strigulales	*Strigula nemathora* Mont.	MPN72	JN887389.1	JN887405.1
Strigulales	*Strigula schizospora* R. Sant.	MPN73	JN887390.1	-
Strigulales	*Taeniolella exilis* (P. Karst.) S. Hughes	CBS122902	-	KX244968.1
Strigulales	*Phyllobathelium firmum* (Stirt.) Vězda	MPN545	JN887387.1	JN887401.1

Trypetheliales Lücking, Aptroot & Sipman	*Astrothelium megaspermum* (Mont.) Aptroot & Lücking	AFTOL-ID 2094	GU561841.1	FJ267702.1
Trypetheliales	*Mycomicrothelia hemisphaerica* (Müll. Arg.) D. Hawksw.	MPN102	JN887384.1	GU327719.1
Trypetheliales	*Mycomicrothelia miculiformis* (Nyl. ex Müll. Arg.) D. Hawksw.	MPN101B	JN887385.1	GU327720.1
Trypetheliales	*Trypethelium eluteriae* Spreng.	CBS 132375	JGI	JGI
Trypetheliales	*Trypethelium nitidiusculum* (Nyl.) R.C. Harris	AFTOL-ID 2099	GU561842.1	GU561856.1
Tubeufiales Boonmee & K.D. Hyde	*Helicomyces roseus* Link	AFTOL-ID 1613	DQ678032.1	DQ678083.1
Tubeufiales	*Tubeufia cerea* (Berk. & M.A. Curtis) Höhn.	AFTOL-ID 1316	DQ471034.1	DQ470982.1
Tubeufiales	*Tubeufia helicomyces* Höhn.	AFTOL-ID 1580	DQ767649.1	DQ767654.1
Tubeufiales	*Wiesneriomyces conjunctosporus* Kuthub. & Nawawi	BCC18525	KJ425436.1	KJ425450.1
Tubeufiales	*Tubeufia paludosa* (P. Crouan & H. Crouan) Rossman	CBS 120503	GU296203.1	GU301877.1
Umbilicariales J.C. Wei & Q.M. Zhou	*Umbilicaria mammulata* (Ach.) Tuck.	(SSU)Wei 96042, 1996, (LSU)**AFTOL-ID 645**	AY648114.1	DQ782912.1
Venturiales Y. Zhang ter, C.L. Schoch & K.D. Hyde	*Apiosporina collinsii* (Schwein.) Höhn.	CBS 118973	GU296135.1	GU301798.1
Venturiales	*Aulographina pinorum* (Desm.) Arx & E. Müll.	CBS 655.86	-	KF902102.1

Venturiales	*Dibotryon morbosum* (Schwein.) Theiss. & Syd.	Oregon-non-cultivated 'dimosp'	EF114718.1	EF114694.1
Venturiales	*Fusicladium oleagineum* (Castagne) Ritschel & U. Braun	CBS 113427	KF766251.1	KF766331.1
Venturiales	*Gibbera conferta* (Fr.) Petr.	CBS 191.53	GU296150.1	GU301814.1
Venturiales	*Metacoleroa dickiei* (Berk. & Broome) Petr.	Oregon-non-cultivated	EF114719.1	EF114695.1
Venturiales	*Protoventuria barriae* Carris & A.P. Poole	ATCC 90285	EF114728.1	JQ036232.1
Venturiales	***Stomiopeltis* [Theiss.] sp.**	CBS 143811 *	MG844148	MG844160
Venturiales	***Stomiopeltis* sp.**	UBC-F33041	MG844149	MG844161
Venturiales	*Tothia fuscella* (Sacc.) Bat.	CBS 130266	JGI	JGI
Venturiales	*Tyrannosorus pinicola* (Petrini & P.J. Fisher) Unter. & Malloch	AFTOL-ID 1235	DQ471025.1	DQ470974.1
Venturiales	*Venturia inaequalis* (Cooke) G. Winter	CBS 594.70	KF156093.1	GU301879.1
Venturiales	*Venturia pyrina* Aderh.	ICMP 11032	JGI	JGI
Venturiales	*Veronaeopsis simplex* (Papendorf) Arzanlou & Crous	CBS 588.66	KF156095.1	EU041877.1
Venturiales	*Sympoventuria capensis* Crous & Seifert	CBS 120136	KF156094.1	KF156104.1
Verrucariales Mattick ex D. Hawksw. & O.E. Erikss.	*Endocarpon pallidulum* (Nyl.) Nyl.	AFTOL-ID 661	DQ823097.1	DQ823104.1
Verrucariales	*Staurothele frustulenta* Vain.	AFTOL-ID 697	DQ823105.1	DQ823098.1
Zeloasperisporiales Hongsanan & K.D. Hyde	*Zeloasperisporium cliviae* Crous	CPC 25145	-	KR476781.1

Zeloasperisporiales	*Zeloasperisporium eucalyptorum* Cheew. & Crous	CBS 124809	-	GQ303329.1
Zeloasperisporiales	*Zeloasperisporium ficusicola* Hongsanan & K.D. Hyde	MFLUCC 15-0222	KT387736.1	KT387735.1
Zeloasperisporiales	*Zeloasperisporium searsiae* Crous & A.R. Wood	CPC 25880	-	KT950866.1
Zeloasperisporiales	*Zeloasperisporium siamense* (Boonmee, H.X. Wu & K.D. Hyde) Hongsanan & K.D. Hyde	IFRDCC 2194	JQ036223.1	JQ036228.1
Zeloasperisporiales	*Zeloasperisporium wrightiae* Hongsanan & K.D. Hyde	MFLUCC 15-0215	KT387746.1	KT387742.1
Incertae sedis	*Arthrographis kalrae* (R.P. Tewari & Macph.) Sigler & J.W. Carmich.	IFM 52423 (YRL)	-	AB116544.1
Incertae sedis	*Caryosporella rhizophorae* Kohlm.	JK 5386C	GU479750.1	GU479784.1
Incertae sedis	*Collophora africana* Damm & Crous	CBS 120872	GQ154630.1	GQ154609.1
Incertae sedis	*Coniosporium apollinis* Sterfl.	CBS 352.97	GU250916.1	GU250895.1
Incertae sedis	*Coniosporium uncinatum* De Leo, Urzì & de Hoog	CBS 100212	GU250922.1	GU250902.1
Incertae sedis	*Cryomyces antarcticus* Selbmann, de Hoog, Mazzaglia, Friedmann & Onofri	CCFEE 536	GU250321.1	GU250365.1
Incertae sedis	*Cryomyces minteri* Selbmann, de Hoog, Mazzaglia, Friedmann & Onofri	CCFEE 5187	KC315858.1	GU250369.1
Incertae sedis	*Dothideomycetes* [O.E. Erikss. & Winka] sp.	CCFEE5460	GU250349.1	GU250391.1
Incertae sedis	*Dothideomycetes* sp.	CCFEE5416	GU250344.1	GU250387.1

Incertae sedis	*Encephalographa elisae* A. Massal.	EB 0347	GU397358.1	GU397343.1
Incertae sedis	*Eremomyces bilateralis* Malloch & Cain	CBS 781.70	JGI	JGI
Incertae sedis	*Farlowiella carmichaeliana* (Berk.) Sacc.	CBS 164.76	GU296129.1	GU301791.1
Incertae sedis	*Hysterographium fraxini* (Pers.) De Not.	CBS 109.43	FJ161132.2	FJ161171.2
Incertae sedis	*Lichenothelia calcarea* Henssen	L1324	KC015082.1	KC015062.1
Incertae sedis	*Lichenothelia convexa* Henssen	L1609	KC015086.1	KC015071.1
Incertae sedis	*Lineolata rhizophorae* (Kohlm. & E. Kohlm.) Kohlm. & Volkm.-Kohlm.	CBS 641.66	GU479758.1	GU479792.1
Incertae sedis	*Minutisphaera fimbriatispora* Shearer, A.N. Mill. & A. Ferrer	G155.1	JX474865.1	JX474859.1
Incertae sedis	*Minutisphaera japonica* Kaz. Tanaka, Raja & Shearer	KTC 2738	AB733434.1	NG_042338.1
Incertae sedis	*Pseudeurotium hygrophilum* (Sogonov, W. Gams, Summerb. & Schroers) Minnis & D.L. Lindner	isolate 229	JQ780655.1	JQ780654.1
Incertae sedis	*Rhexothecium globosum* Samson & Mouch.	CBS 955.73	-	HG004544.1
Incertae sedis	*Saxomyces alpinus* Zucconi & Selbmann	CCFEE 5466	GU250350.1	GU250392.1
Incertae sedis	*Saxomyces penninicus* Zucconi & Onofri	CCFEE 5495	KC315875.1	KC315864.1
Incertae sedis	*Geastrumia polystigmatis* Bat. & M.L. Farr	strain NC4 1.8F1a	-	FJ147177.1

[1]Isolates included in this study. Bolded taxa represent newly contributed taxa, bolded voucher/strain represent identifier used in phylogenetic trees presented, authorities in square bracket apply to Genus, Family, Order or Class level rather than species. When LSU ans SSU were derived from 2 different studies, bolded voucher represents the identifier used to refer to the taxon, CBS number follower by a star (*) represent newly deposited culture to the Westerdijk Institute, accessions labelled JGI refers to sequences extracted from JGI genomes project, for which no genbank accession exists.

A.2 JGI sequence data retrieved from Mycocosm portal

Taxon/strain	Blast target	SSU Sequence length (bp)	SSU assembly	LSU Sequence length (bp)	LSU Assembly	Publication	Genome project PI
Acidomyces richmondensis C2	Assembly	1729	8 scaffolds, 2 bp conflicts	2995	6 scaffolds, 1 bp conflicts	Mosier et al. (2016)	Singer, Steven - Berkeley Lab, USA
Aspergillus niger ATCC 1015	Assembly	1738	Single scaffold	3424	Single scaffold	Andersen et al. (2011)	Baker, Scott - Environmental Molecular Sciences Laboratory, USA
Aulographum hederae CBS 113979	Assembly	1791	Single scaffold with SSU and LSU	2934	Single scaffold with SSU and LSU	permission granted	Spatafora, Joseph - Oregon State University, USA
Aureobasidium subglacialis EXF-2481	EST	1731	5 clusters	3092	3 clusters	Gostincar et al. (2014)	Gunde-Cimerman, Nina - University of Ljubljana, Department of Biology, Slovenia
Cenococcum geophilum strain 1.58	Assembly + EST	1737	Single scaffold for both regions	3610	1 scaffold + 3 clusters	Peter et al. (2016)	Martin, Francis - INRA Nancy, France

Eremomyces bilateralis CBS 781.70		1729	Single cluster	2875	Single cluster	permission granted	Crous, Pedro and Binder, Manfred - CBS-KNAW, Netherlands
Lepidopterella palustris CBS 459.81	EST	1728	2 clusters	2951	2 clusters	Peter et al. (2016)	Spatafora, Joseph
Myriangium duriaei CBS 260.36	Genbank + Assembly	1703	genbank sequence	2969	1 scaffold	permission granted	Spatafora, Joseph
Patellaria atrata CBS 101060	Assembly + EST	1477	single scaffold from assembly	3011	Contig of 4 ESTs	permission granted	Spatafora, Joseph
Tothia fuscella CBS 130266	Assembly	1738	Single scaffold, big insert	1125	Single scaffold	permission granted	Binder, Manfred
Trichodelitschia bisporula CBS 262.69		1731	5 clusters, 1bp conflict	3015	3 clusters	permission granted	Binder, Manfred
Trypethelium eluteriae MPN111	EST	1122	Single cluster	3292	2 clusters	McDonald et al. (2013)	Binder, Manfred
Venturia pirina ICMP 11032	EST	1725	Single scaffold	3158	Single scaffold	Cooke et al. (2014)	Deng, Cecilia - The New Zealand Institute for Plant & Food Research Limited, New Zealand

A3. Matrix of characters used in my ancestral character state reconstructions

Matrix of morphological characters states following code in Table 2 with (**I)** Habitat- Substrate, (**II**) Lichenized, (**III**) Sporocarp type, (**IV**) Differentiated lower wall, (**V**) Dehiscence type, (**VI**) Sporogenous tissue outline, (**VII**) Radiating scutellum, (**VIII**) Scutellum branching and septation, (**IX**) Appressed margin, (**X**) Lateral appressoria, (**XI**) Sporocarp initiation. Illustrations for thyriothecia were only analyzed if a sequence was available from the same specimen, ensuring that morphology and sequence were correctly paired.

Taxon	**I**	**II**	**III**	**IV**	**V**	**VI**	**VII**	**VIII**	**IX**	**X**	**XI**	**Ref.**	**Illustration**
Abrothallus acetabuli SPO308	2	0	0	1	4	0	0	0	0	0	?	(Pérez-Ortega et al., 2014)	all *Abrothallus* in (Pérez-Ortega et al., 2014) coded similarly
Abrothallus buellianus SPO303	2	0	0	1	4	0	0	0	0	0	?	(Pérez-Ortega et al., 2014)	"
Abrothallus cladoniae AB53	2	0	0	1	4	0	0	0	0	0	?	(Pérez-Ortega et al., 2014)	"
Abrothallus hypotrachynae SPO302	2	0	0	1	4	0	0	0	0	0	?	(Pérez-Ortega et al., 2014)	"
Abrothallus parmeliarum AB36	2	0	0	1	4	0	0	0	0	0	?	(Pérez-Ortega et al., 2014)	"

Taxon	I	II	III	IV	V	VI	VII	VIII	IX	X	XI	Ref.	Illustration
Abrothallus parmotrematis AB1	2	0	0	1	4	0	0	0	0	0	?	(Diederich, 2011)	"
Abrothallus secedens SPO305	2	0	0	1	4	0	0	0	0	0	?	(Pérez-Ortega et al., 2014)	"
Abrothallus suecicus AB56	2	0	0	1	4	0	0	0	0	0	?	(Pérez-Ortega et al., 2014)	"
Abrothallus usneae AB20	2	0	0	1	4	0	0	0	0	0	?	(Pérez-Ortega et al., 2014)	"
Absconditella sphagnorum EU940095.1	4	0	0	1	4	0	0	0	0	0	?	(Stenroos et al., 2010)	Fig. 3b
Acarosporina microspora AFTOL-ID 78	3	0	0	1	4	0	0	0	0	0	?	(Sherwood, 1977)	p. 36
Acidomyces richmondensis JGI	?	0	?	?	?	?	0	?	?	0	?	(Baker et al., 2004)	Fig. 8
Acrocordia subglobosa HTL940	0 *	1	1	1	0	0	0	0	0	0	?		Based on *A. cavata* morphology UBC L47305
Acrospermum adeanum M133	1	0	1	1	0	0	0	0	0	0	?	(Stenroos et al., 2010)	Fig. 3a
Acrospermum compressum M151	1	0	1	1	0	0	0	0	0	0	?	(Riddle, 1920)	Fig. 6–12
Acrospermum graminum M152	1	0	1	1	0	0	0	0	0	0	?		link

Taxon	I	II	III	IV	V	VI	VII	VIII	IX	X	XI	Ref.	Illustration
Aigialus grandis JK 5244A	3	0	1	1	0	0	0	0	0	0	?	(Kohlmeyer and Schatz, 1985)	Fig. 1–3
Alternaria alternata SRC1lrK2f	1	0	1	1	?	0	0	?	0	0	?	(Woudenberg et al., 2013)	Based on genus description
Alysidiella suttonii CBS 124780	1	0	?	?	?	?	0	?	?	0	?	(Cheewangkoon et al., 2012)	Fig. 3
Alyxoria varia EU704103.1	3	1	0	1	2	1	0	0	0	0	?	(Brodo et al., 2001) (Pentecost, 2014)	Fig. 551
Anisomeridium phaeospermum MPN539	3	1	1	1	0	0	0	0	0	0	?	(Nelsen et al., 2011)	Figs. 2c; 3b
Anisomeridium ubianum MPN94	3	1	1	1	0	0	0	0	0	0	?	(Nelsen et al., 2011)	derived from *A phaeospermum*
Apiosporina collinsii CBS 118973	1	0	1	1	3	0	0	0	0	0	?	(Sartoris and Kauffman, 1925)	Pl. XVI
Arthonia dispersa UPSC 2583	3	1	0	0	2	1	0	0	0	0	?	(Brodo et al., 2001) (Sundin and Tehler, 1998)	from genus description
Arthopyrenia salicis CBS 368.94	3	0	1	1	0	0	0	0	0	0	?		link
Arthrocatena tenebrio CCFEE 5413	0	0	?	?	?	?	0	?	?	0	?	(Egidi et al., 2014)	Figs. 15d–15g
Arthrographis kalrae IFM 52423(YRL)	?	0	?	?	?	?	0	?	?	0	?	(de Diego Candela et al., 2010)	Fig. 3

Taxon	I	II	III	IV	V	VI	VII	VIII	IX	X	XI	Ref.	Illustration
Arxiella dolichandrae CBS 138853	1	0	?	?	?	?	0	?	?	0	?	(Crous et al., 2014)	p. 226
Ascocratera manglicola JK 5262C	3	0	1	1	0	0	0	0	0	0	?	(Kohlmeyer, 1986)	Figs. 1–7
Aspergillus fumigatus JCM1738	?	0	3	1	3	0	0	0	0	0	?		link
Aspergillus niger ATCC 1015	?	0	3	1	3	0	0	0	0	0	?		link
Asterina cestricola TH 591	1	0	2	0	1	0	1	1	1	1	1	(Hofmann et al., 2010)	Fig. 3.1
Asterina chrysophylli VIC 42823	1	0	2	0	1	0	1	1	1	1	1	(Guatimosim et al., 2014c)	Fig. 4
Asterina cynometrae MFLU 13-0373	1	0	2	0	1	0	1	1	1	1	1	(Hyde et al., 2016)	Fig. 2
Asterina fuchsiae TH 590	1	0	2	0	1	0	1	1	1	1	1	(Hofmann and Piepenbring, 2008)	Fig. 6
Asterina melastomatis VIC 42822	1	0	2	0	1	0	1	1	1	1	1	(Guatimosim et al., 2014c)	Fig. 3
Asterina phenacis TH 589	1	0	2	0	1	0	1	1	1	1	1	(Hofmann and Piepenbring, 2008)	Fig. 8
Asterina siphocampyli M 0141060 PMA	1	0	2	0	1	0	1	1	1	1	1	(Hofmann and Piepenbring, 2011)	Fig. 7

Taxon	I	II	III	IV	V	VI	VII	VIII	IX	X	XI	Ref.	Illustration
Asterina sp. MFLU13-0619	1	0	2	0	1	0	1	1	1	1	1	(Hongsanan et al., 2014b)	Fig. 5
Asterina weinmanniae TH592	1	0	2	0	1	0	1	1	1	1	1	(Hofmann et al., 2010)	Fig. 3
Asterina zanthoxyli TH 561	1	0	2	0	1	0	1	1	1	1	1	(Hofmann et al., 2010)	Fig. 4
Asterotexiaceae sp.1 UBC-F33036	1	0	2	0	0	0	1	1	1	0	1		Personal collection
Asterotexiaceae sp.2 CBS 143813	1	0	2	0	1	0	1	?	1	0	0		Personal collection
Asterotexis cucurbitacearum PMA M-0141224	1	0	2	0	1	1	1	?	1	0	2	(Guerrero et al., 2011)	Figs. 1–2
Asterotexis cucurbitacearum VIC 42814	1	0	2	0	1	1	1	?	1	0	2	(Guatimosim et al., 2014c)	Fig. 8
Astrosphaeriella stellata MFLUCC10-0095	1	0	1	1	0	0	0	0	0	0	?	(Liu et al., 2011)	Fig. 2
Astrosphaeriella vesuvius LF-157	3	0	1	1	0	0	0	0	0	0	?	(Liu et al., 2011)	Derived from *A. stellata*
Astrothelium nitidiusculum AFTOL-ID 2099	3	1	1	1	0	0	0	0	0	0	?	(Aptroot and Lücking, 2016)	Figs.1; 3A; 4D; 4B; 6A
Aulographina eucalypti CPC 12986	1	0	?	?	?	?	?	?	?	0	?	(Wall and Keane, 1984)	Figs. 1–7

Taxon	I	II	III	IV	V	VI	VII	VIII	IX	X	XI	Ref.	Illustration
Aulographina pinorum CBS 174.90	1	0	?	?	?	?	?	?	?	0	?	(Arx and Müller, 1960)	*Abb. 1*
Aulographina pinorum CBS 655.86	?	0	?	?	?	?	?	?	?	0	?	(Arx and Müller, 1960)	*Abb. 1*
Aulographum hederae CBS 113979	1	0	2	0	1	1	1	3	1	0	4	(Wu et al., 2011b)	Fig. 23
Aulographum hederae MFLUCC13-0001	1	0	2	0	1	1	1	3	1	0	4	(Wu et al., 2011b)	Fig. 23
Aulographum sp. CBS 143545	1	0	2	0	1	1	1	3	1	0	4		Personal collection
Aureobasidium subglaciale EXF-2481	?	0	?	?	?	?	0	?	?	0	?		link
Batistinula gallesiae B VIC 42514	1	0	2	0	1	0	1	1	1	1	1	(Guatimosim et al., 2014c)	Fig. 5
Bipolaris maydis AFTOL-ID 54	?	0	1	1	?	0	0	?	0	0	?	(Manamgoda et al., 2014)	Fig. 22
Blastacervulus eucalypti CBS 124759	1	0	?	?	?	?	0	?	?	0	?	(Cheewangkoon et al., 2009)	Fig. 4
Blastacervulus eucalyptorum CPC 29450	1	0	?	?	?	?	0	?	?	0	?	(Crous et al., 2016b)	p. 292

Taxon	I	II	III	IV	V	VI	VII	VIII	IX	X	XI	Ref.	Illustration
Botryosphaeria dothidea CBS 115476	3	0	1	1	0	0	0	0	0	0	?	(Slippers et al., 2004)	Figs. 1–7
Buelliella minimula Lendemer 42273(NY)	2	0	0	1	4	0	0	0	0	0	?	(Ertz and Diederich, 2015)	Figs. 4a; 5a
Buelliella physciicola Ertz 19173(BR)	2	0	0	1	4	0	0	0	0	0	?	(Ertz and Diederich, 2015)	Figs. 4b; 5c
Buelliella poetschii Ertz 18116(BR)	2	0	0	1	4	0	0	0	0	0	?	(Ertz and Diederich, 2015)	Figs. 4c; 5d
Capnobotryella renispora CBS 214.90	1	0	1	?	0	?	0	?	?	0	?	(Sugiyama and Amano, 1987) (Seifert et al., 2011)	Fig. 7.5–7.8, and Pl. 170A in (Seifert et al., 2011)
Capnodium citri CBS 451.66	1	0	1	1	0	?	0	?	0	0	?	(Chomnunti et al., 2011)	Fig. 9
Capnodium coffeae CBS 147.52	1	0	1	1	0	0	0	0	0	0	?	(Chomnunti et al., 2011)	Following genus description
Capronia pilosella AFTOL-ID 657	3	0	1	1	0	0	0	0	0	0	?	(Untereiner, 1997)	Figs. 14–19
Caryosporella rhizophorae JK 5386C	3	0	1	1	**0**	0	0	0	0	0	?	(Kohlmeyer, 1985)	Figs. 1–5

Taxon	I	II	III	IV	V	VI	VII	VIII	IX	X	XI	Ref.	Illustration
Catenulostroma chromoblastomycosum CBS 597.97	?	0	?	?	?	?	0	?	?	0	?	(Crous et al., 2007a)	Fig. 6
Cenococcum geophilum JGI 1.58 v2.0	4	0	?	?	?	?	0	?	?	0	?	(Massicotte et al., 1992)	NA
Ceramothyrium carniolicum CBS 175.95	1	0	?	?	?	0	?	?	?	0	?	(Chomnunti et al., 2012)	Derived from *C. thailandicum*, Fig. 3
Ceramothyrium linnaeae UPSC 2646	1	0	1	1	?	0	0	4	3	0	?	(Ainsworth et al., 2015)	Fig. 7
Ceramothyrium podocarpi CPC 19826	1	0	?	?	?	?	?	?	?	0	?	(Chomnunti et al., 2012)	Derived from *C. thailandicum*, Fig. 3
Cercospora zebrina CBS 118790	?	0	1	1	0	0	0	?	0	0	?	(Groenewald et al., 2013)	
Cf. Arthoniales sp. CCFEE 5176	0	0	?	?	?	?	0	?	?	0	?	(Selbmann et al., 2005)	none
cf. *Stomiopeltis* sp. 1 CBS 143811	1	0	2	0	0	0	1	4	1	0	?		Personal collection
cf. *Stomiopeltis* sp. 2 UBC-F33041	1	0	2	0	0	0	1	4	1	0	?		Personal collection

Taxon	I	II	III	IV	V	VI	VII	VIII	IX	X	XI	Ref.	Illustration
Chaetasbolisia erysiphoides CBS 148.94	0	0	?	?	0	?	0	?	?	0	?	(Vikram et al., 2018)	Figs. 1–2
Chaetothyriothecium elegans CPC 21375	1	0	2	?	0	?	1	?	?	0	?	(Hongsanan et al., 2014a)	Fig. 2
Chaetothyrium agathis MFLUCC 12 C0113	1	0	1	1	3	0	0	0	0	0	?	(Liu et al., 2015)	Fig. 132
Chaetothyrium brischoficola MFLUCC 10-0012	1	0	1	1	3	0	0	0	0	0	?	(Chomnunti et al., 2012)	Derived from *C. thailandicum*, Fig. 3
Cheirosporium triseriale HMAS 180703	3	0	?	?	?	?	0	?	?	0	?	(Boonmee et al., 2016)	Fig. 3
Chrysothrix candelaris KF707640.1	0				4						?		link
Cladonia caroliniana AFTOL-ID 3	0	1	0	1	4	0	0	0	0	0	?	(Brodo et al., 2001)	Fig. 220
Cladosporium bruhnei CPC 5101	?		?	?	?	?		?	?		?	(Schubert et al., 2007)	Fig. 9
Coccomyces dentatus AFTOL-ID 147	1	0	0	1	4	0	0	0	0	0	?	(Sherwood, 1980)	Fig. 19
Collophora africana CBS 120872	3	0	?	?	?	?	0	?	?	0	?	(Damm et al., 2010)	Fig. 7

Taxon	I	II	III	IV	V	VI	VII	VIII	IX	X	XI	Ref.	Illustration
Combea mollusca Tehler 7725	0	1	0	1	4	0	0	0	0	0	?		link
Comminutispora agavacearum CBS 619.95	1	0	?	1	?	?	0	?	0	0	?	(Ramaley, 1996)	Figs. 1–3
Conidiocarpus caucasicus GUMH937	?	0	1	1	0	?	0	?	0	0	?	(Bose, 2013)	Fig. 10
Coniosporium apollinis CBS 352.97	0	0	?	?	?	?	0	?	?	0	?	(Sterflinger et al., 1997)	Fig. 5
Coniosporium uncinatum CBS 100212	0	0	?	?	?	?	0	?	?	0	?	(De Leo et al., 1999)	Pl. 2
Cryomyces antarcticus CCFEE 536	0	0	?	?	?	?	0	?	?	0	?	(Selbmann et al., 2005)	Fig. 9
Cryomyces minteri CCFEE 5187	0	0	?	?	?	?	0	?	?	0	?	(Selbmann et al., 2005)	Fig. 10
Cryptodiscus gloeocapsa TSB 30770	3	1	0	1	4	0	0	0	0	0	?	(Baloch et al., 2009)	Fig. 3b
Cudoniella clavus AFTOL-ID 166	3	0	0	1	4	0	0	0	0	0	?	(Ellis and Ellis, 1997)	Pl. 36 Fig. 347
Davidiella tassiana DAOM 196248	1	0	1	1	0	0	0	0	0	0	?	(Schubert et al., 2007)	Fig. 18

Taxon	I	II	III	IV	V	VI	VII	VIII	IX	X	XI	Ref.	Illustration
Dendrographa leucophaea Ornduff 10070 Duke	0	1	0	1	4	0	0	0	0	0	?	(Sundin and Tehler, 1996)	Figs. 2–3; 9–14
Dibaeis baeomyces Lutzoni 93.08.20(Duke)	0	1	0	1	4	0	0	0	0	0	?		link
Dibotryon morbosum EF114694.1	1	0	1	1	0	0	0	0	0	0	?	(Zhang et al., 2011)	Fig. 5
Dictyocheirospora rotunda MFLUCC 0577	3	0	?	?	?	?	0	0	?	0	?	(Boonmee et al., 2016)	Fig. 4
Dictyosporium elegans NBRC 32502	3	0	?	?	?	?	0	0	?	0	?	(Boonmee et al., 2016)	Fig. 10
Diploschistes cinereocaesius DUKE 0047509	0	1	0	?	4	0	0	0	?	0	?	(Fernández-Brime et al., 2013)	derived from genus description
Diploschistes muscorum Palice 2805 (HB Palice)	0	1	0	?	4	0	0	0	?	0	?	(Fernández-Brime et al., 2013)	derived from genus description
Diploschistes ocellatus Spain 995	0	1	0	1	4	0	0	0	0	0	?	(Fernández-Brime et al., 2013)	derived from genus description
Diploschistes rampoddensis AF274094.1	0	1	0	?	4	0	0	0	?	0	?	(Fernández-Brime et al., 2013)	derived from genus description

Taxon	I	II	III	IV	V	VI	VII	VIII	IX	X	XI	Ref.	Illustration
Diploschistes thunbergianus Eldridge 3800(F)	0	1	0	?	4	0	0	0	?	0	?	(Fernández-Brime et al., 2013)	derived from genus description
Discopycnothyrium palmae MFLU13-0485	1	0	2	?	0	0	1	?	?	0	1	(Hongsanan et al., 2016)	Fig. 1
Dothidea insculpta CBS 189.58	1	0	1	1	0	0	0	0	0	0	?	(Thambugala et al., 2014)	Fig. 3
Dothidea sambuci AFTOL-ID 274	1	0	1	1	0	0	0	0	0	0	?	(Thambugala et al., 2014)	Fig. 2
Dothideomycetes sp. CCFEE5416	0	0	?	?	?	?	0	?	?	0	?	(Selbmann et al., 2008)	none
Dothideomycetes sp. CCFEE5460	0	0	?	?	?	?	0	?	?	0	?	(Selbmann et al., 2005)	none
Dothideomycetes sp. TRN 213	0	0	?	?	?	?	0	?	?	0	?	(Ruibal et al., 2008)	none
Dyfrolomyces rhizophorae JK 5349A	3	0	1	1	0	0	0	0	0	0	?	(Hyde, 1992b)	Figs. 17–20
Dyfrolomyces tiomanensis NTOU3636	3	0	1	1	0	0	0	0	0	0	?	(Pang et al., 2013)	Figs. 2–4
Dyplolabia afzelii Luecking 26509a	3	1	0	1	4	1	0	0	0	0	?	(Baloch et al., 2010; Rivas Plata et al., 2013)	Fig. 2a in (Rivas Plata et al., 2013), link

Taxon	I	II	III	IV	V	VI	VII	VIII	IX	X	XI	Ref.	Illustration
Elasticomyces elasticus CCFEE 5320	2	0	?	?	?	?	0	?	?	0	?	(Selbmann et al., 2008)	Fig. 7
Elsinoe veneta AFTOL-ID 1853	1	0	1	1	0	0	0	?	0	0	?	(Jayawardena et al., 2014)	p. 129
Emericella nidulans ATCC 10074	?	0	3	1	3	0	0	?	0	0	?	(Gugnani, 2003)	p. 6
Encephalographa elisae EB 0347	0	1	0	?	2	1	0	?	?	0	?	(Ertz and Diederich, 2015)	Fig. 3n
Endocarpon pallidulum AFTOL-ID 661	0	1	0	1	4	0	0	0	0	0	?	(Lendemer, 2007)	Fig. 3 right
Endosporium aviarium UAMH 10530	?	0	?	?	?	?	0	?	?	0	?	(Tsuneda et al., 2008)	Figs. 25–37
Endosporium populi-tremuloides UAMH 10529	?	0	?	?	?	?	0	?	?	0	?	(Tsuneda et al., 2008)	Figs. 1–24
Eremomyces bilateralis CBS 781.70	?	0	3	1	3	0	0	0	0	0	?	(Malloch and Sigler, 1988)	Fig. 8
Erysiphe mori MUMHS77	1	0	3	1	3	0	0	0	0	0	?	(Braun et al., 2006)	treated as similar to Erisyphe sect. Uncinula

Taxon	I	II	III	IV	V	VI	VII	VIII	IX	X	XI	Ref.	Illustration
Exophiala dermatitidis AFTOL-ID 668	?	0	1	1	0	?	0	?	0	0	?	(Untereiner et al., 1995)	Fig. 3
Exophiala pisciphila AFTOL-ID 669	?	0	1	1	0	?	0	?	0	0	?	(Untereiner et al., 1995)	Fig. 4
Farlowiella carmichaeliana CBS 164.76	3	0	0	1	2	0	0	0	0	0	?	(Ellis and Ellis, 1997)	Pl. 11 Fig. 102
Fissurina insidiosa AFTOL-ID 1662	3	1	0	1	2	1	0	0	0	0	?	(Hayward, 1977)	Figs. 6A; 8B
Fissurina marginata DNA3418	3	1	0	1	2	1	0	0	0	0	?	(Hayward, 1977)	Coded similarly to *F. insidiosa*
Flavobathelium epiphyllum MPN67	1	1	1	1	**0**	0	0	0	0	0	?	(Lücking, 1997)	Figs. 1–2
Fumiglobus pieridicola UBC F23788	1	0	1	1	0	?	0	?	0	0	?	(Bose et al., 2014)	Figs. 2–3
Funbolia dimorpha CPC 14170	3	0	?	?	?	?	0	?	?	0	?	(Crous et al., 2011)	p.114
Fusicladium oleaginum CBS 113427	1	0	?	?	?	?	0	?	?	0	?	(Schubert et al., 2013)	Fig. 35
Geastrumia polystigmatis FJ147177.1	1	0	?	0	1	?	0	?	0	0	?	(Pirozynski, 1971)	Figs. 1–2
Gibbera conferta CBS 191.53	1	0	1	1	3	0	0	0	0	0	?	(Barr, 1968)	Fig. 3

Taxon	I	II	III	IV	V	VI	VII	VIII	IX	X	XI	Ref.	Illustration
Glyphium elatum EB 0342	1	0	0	1	2	0	0	0	0	0	?	(Boehm et al., 2015)	Figs. 1;7
Gyalecta hypoleuca TSB 20801	0	1	0	1	4	0	0	0	0	0	?	(Kauff and Büdel, 2005)	coded as *G. ulmi*
Gyalecta ulmi AF465463.1	3	1	0	1	4	0	0	0	0	0	?	(Kauff and Büdel, 2005)	Figs. 1A–2A
Halojulella avicenniae BCC 18422	3	0	1	1	0	0	0	0	0	0	?	(Hyde, 1992a)	Figs. 1–11
Halojulella avicenniae JK 5326A	3	0	1	1	0	0	0	0	0	0	?	(Hyde, 1992a)	Figs. 1–11
Heleiosa barbatula JK 5548I	1	0	1	1	0	0	0	0	0	0	?	(Kohlmeyer et al., 1996)	Figs. 1–12
Helicomyces roseus AFTOL-ID 1613	3	0	1	1	0	0	0	0	0	0	?	(Tsui and Berbee, 2006)	Fig. 1H
Heliocephala gracilis MUCL 41200	3	0	?	?	?	?	0	?	?	0	?	(Castañeda Ruiz, 1985)	Figs. 10–11
Heliocephala zimbabweensis MUCL 40019	3	0	?	?	?	?	0	?	?	0	?	(Decock et al., 1998)	Fig. 1
Hemigrapha atlantica Ertz 14014 (BR)	2	0	2	0	1	1	1	?	2	0	?	(Diederich and Wedin, 2000)	Fig. 5
Houjia yanglingensis YHJN13	1	0	?	?	?	?	0	?	?	0	?	(Yang et al., 2010)	Fig. 5

Taxon	I	II	III	IV	V	VI	VII	VIII	IX	X	XI	Ref.	Illustration
Hysterobrevium constrictum SMH 5211.1	1	0	0	1	2	1	0	0	0	0	?	(Boehm et al., 2009b)	Figs. 5A–5E
Hysterobrevium smilacis CBS 114601	1	0	0	1	2	1	0	0	0	0	?	(Boehm et al., 2009b)	Figs. 5F–5I
Hysterographium fraxini CBS 109.43	1	0	0	1	2	1	0	0	0	0	?	(Ellis and Ellis, 1997)	Fig. 610
Hysteropatella clavispora CBS 247.34	3	0	0	1	2	1	0	0	0	0	?	(Seaver, 1910)	Pl. 35
Hysteropatella elliptica CBS 935.97	1	0	0	1	2	1	0	0	0	0	?	(Yacharoen et al., 2015)	As *H.prostii* Fig. 7
Inocyclus angularis VIC 39747	1	0	2	1	2	1	1	?	1	0	?	(Guatimosim et al., 2014a)	Figs. 1–2
Jalapriya pulchra AF465463.1	3	0	?	?	?	?	0	?	?	0	?	(Boonmee et al., 2016)	Fig. 14
Johansonia chapadiensis CBS H-20484	1	0	0	1	4	0	0	0	0	0	?	(Crous et al., 2010)	Fig. 2
Karschia cezannei Ertz 19186 (BR)	3	0	0	1	4	0	0	0	0	0	?	(Ertz and Diederich, 2015)	Figs. 4h; 5i
Karschia talcophila Diederich 16749	2	0	0	1	4	0	0	0	0	0	?	(Ertz and Diederich, 2015)	Figs. 4g; 5n
Kellermania anomala CBS 132218	3	0	1	1	0	?	0	?	0	0	?	(Slippers et al., 2013)	Based on *K. yuccigena*, Fig. 7

Taxon	I	II	III	IV	V	VI	VII	VIII	IX	X	XI	Ref.	Illustration
Kellermania dasylirionicola CBS 131720	3	0	1	1	0	?	0	?	0	0	?	(Slippers et al., 2013)	Based on *K. yuccigena*, Fig. 7
Kellermania yuccifoliorum CBS 131726	3	0	1	1	0	?	0	?	0	0	?	(Slippers et al., 2013)	Based on *K. yuccigena*, Fig. 7
Labrocarpon canariense Ertz 16907(BR)	2	0	0	?	2	0	0	0	?	0	?	(Ertz and Diederich, 2015)	Fig. 4i
Laurera megasperma AFTOL-ID 2094	3	1	1	1	0	0	0	0	0	0	?	(Nelsen et al., 2014b)	Fig.1O
Lecanographa amylacea UPS Thor 26176	3	1	0	1	4	1	0	0	0	0	?		link
Lecanora hybocarpa AFTOL-ID 639	3	1	0	1	4	0	0	0	0	0	?		link
Lembosia abaxialis VIC 42825	1	0	2	0	1	1	1	1	1	1	1	(Guatimosim et al., 2014c)	Fig. 6
Lembosia albersii MFLU13-0377	1	0	2	0	1	1	1	1	1	1	1	(Hongsanan et al., 2014b)	Fig. 18
Lembosia xyliae MFLU14-0004	1	0	2	0	1	1	1	1	1	1	1	(Ariyawansa et al., 2015)	Fig. 7
Lembosina aulographoides CBS 143809	1	0	2	0	1	1	1	3	1	0	4		Personal collection
Lembosina sp. 1 CBS 144007	1	0	2	0	1	1	1	3	1	0	4		personal collection

Taxon	I	II	III	IV	V	VI	VII	VIII	IX	X	XI	Ref.	Illustration
Lembosina sp. 2 CBS 143815	1	0	2	0	1	1	1	3	1	0	4		personal collection
Lepidopterella palustris CBS 459.81	3	0	3	1	3	0	0	0	0	0	?	(Raja and Shearer, 2008)	Figs. 71–80
Leptosphaeria heterospora CBS 644.86	1	0	1	1	0	0	0	0	0	0	?	(Ahn and Shearer, 1999)	Figs. 17–23
Leptoxyphium fumago CBS 123.26	1	0	1	1	0	0	0	0	0	0	?	(Srivastava, 1982)	Figs. 4–7
Lichenoconium lecanorae JL382-10	2	0	1	1	0	?	0	?	0	0	?	(Lawrey et al., 2011)	Figs. 5Q–5S
Lichenopeltella pinophylla UBC-F33032	1	0	2	1	0	0	1	?	2	0	0		personal collection
Lichenostigma maureri Diederich 17326	0	0	0	1	4	?	0	0	0	0	?		link
Lichenothelia calcarea L1324	0	0	0	1	4	?	0	0	0	0	?	(Muggia et al., 2013)	Fig. 1
Lichenothelia convexa L1609	0	0	0	1	4	?	0	0	0	0	?	(Muggia et al., 2013)	Fig. 1
Lichinella iodopulchra AFTOL-ID 896	0	1	0	1	4	0	0	0	0	0	?		link
Lineolata rhizophorae CBS 641.66	3	0	1	1	0	0	0	0	0	0	?	(Zhang et al., 2012)	Fig. 48

Taxon	I	II	III	IV	V	VI	VII	VIII	IX	X	XI	Ref.	Illustration
Lophium elegans EB 0366	1	0	0	1	2	?	0	0	0	0	?	(Mathiassen et al., 2015)	Fig. 1
Lophium mytilinum AFTOL-ID 1609	1	0	0	1	2	?	0	0	0	0	?	(Boehm et al., 2009a)	Fig. 1R; 1X
Mahanteshomyces sp. TH 588	1	0	2	0	1	0	1	1	1	1	1	(Hofmann, 2009)	Fig. 3.80
Megalotremis verrucosa MPN104	0	1	1	?	0	0	0	0	?	0	?	(Hyde et al., 2013)	Based on *M. laterale* and *M. cauliflora*, Figs. 80h–i
Melarthonis piceae UPS Thor25995	3	1	0	1	4	?	0	0	0	0	?	(Frisch et al., 2014b)	Figs. 4D; 4G
Melaspilea lekae Ertz 17325(BR)	2	0	0	1	4	0	0	0	0	0	?	(Ertz and Diederich, 2015)	Fig. 4r
Melaspileopsis cf. *diplasiospora* Ertz 16625	3	0	0	0	2	1	0	0	0	0	?	(Ertz and Diederich, 2015)	Figs. 4o; 5s
Metacoleroa dickiei EF114695.1	1	0	1	?	0	0	0	0	?	0	?	(Barr, 1968)	Fig. 8
Microcyclospora pomicola CPC 16173	1	0	?	?	?	?	0	?	?	0	?	(Frank et al., 2010)	Fig. 6
Micropeltis sp. UBC-F33034	1	0	2	0	0	0	0	4	3	0	?		Personal collection
Micropeltis zingiberacicola IFRDCC 2264	1	0	2	0	0	0	0	4	3	0	?	(Wu et al., 2011b)	Fig. 11

Taxon	I	II	III	IV	V	VI	VII	VIII	IX	X	XI	Ref.	Illustration
Microthyrium illicinum CBS 143808	1	0	2	0	0	0	1	2	2	0	0		Personal collection
Microthyrium macrosporum CBS 143810	1	0	2	0	0	0	1	2	2	0	0		Personal collection
Microthyrium microscopicum CBS 115976	1	0	2	0	0	0	1	2	2	0	?	(Wu et al., 2011b)	Fig. 3
Minutisphaera fimbriatispora G155.1	3	0	1	1	**0**	0	0	0	0	0	?	(Raja et al., 2013)	Figs. 22–27
Minutisphaera japonica KTC 2738	3	0	1	1	**0**	0	0	0	0	0	?	(Raja et al., 2013)	Figs. 3–21
Mollisia cinerea AFTOL-ID 76	4	0	0	1	4	0	0	0	0	0	?	(Ellis and Ellis, 1997)	Pl. 4 Fig. 30
Monascus purpureus AFTOL-ID 426	?	0	3	1	3	0	0	0	0	0	?		yeast
Monilinia laxa CBS 122031	4	0	0	1	4	0	0	0	0	0	?	(Ellis and Ellis, 1997)	based on *M. cinerea*
Morenoina calamicola MFLUCC 14-1162	1	0	2	0	1	1	1	1	1	0	1	(Tibpromma et al., 2017)	Fig. 2
Musaespora kalbii MPN243	1	1	1	1	0	0	0	0	0	0	?	(Lücking and Sérusiaux, 1996)	Figs. 1–2
Muyocopron castanopsis MFLUCC 14-1108	1	0	2	0	0	0	1	?	1	0	?	(Mapook et al., 2016b)	Fig. 2

Taxon	I	II	III	IV	V	VI	VII	VIII	IX	X	XI	Ref.	Illustration
Muyocopron dipterocarpi MFLUCC 14-110	1	0	2	0	0	0	1	?	1	0	?	(Mapook et al., 2016b)	Fig. 3
Muyocopron garethjonesii MFLU 16-2664	1	0	2	0	0	0	1	?	1	0	?	(Tibpromma et al., 2016)	Fig. 2
Muyocopron lithocarpi MFLUCC 10-0041	1	0	2	0	0	0	1	?	1	0	?	(Mapook et al., 2016b)	Fig. 4
Muyocopron lithocarpi MFLUCC 14-1106	1	0	2	0	0	0	1	?	1	0	?	(Mapook et al., 2016b)	Fig. 4
Mycoleptodiscus indicus UAMH 8520	1	0	?	?	?	?	1	?	?	0	?	(Sutton, 1973)	Fig. 3
Mycomicrothelia hemisphaerica MPN102	3	1	1	1	0	0	0	0	0	0	?	(Nelsen et al., 2009)	Based on *M. modesta* Fig. 3B
Mycomicrothelia miculiformis MPN101B	3	1	1	1	0	0	0	0	0	0	?	(Nelsen et al., 2009)	Based on *M. modesta* Fig. 3B
Mycosphaerella latebrosa CBS 687.94	1	0	1	1	0	0	0	0	0	0	?	(Crous et al., 2009)	none
Mycosphaerella pneumatophorae AFTOL-ID 762	3	0	1	1	1	0	0	0	0	0	?	(Kohlmeyer, 1966)	Fig. 87a

Taxon	I	II	III	IV	V	VI	VII	VIII	IX	X	XI	Ref.	Illustration
Mycosphaerella walkeri CPC 11252	1	0	1	1	0	0	0	0	0	0	?	(Crous et al., 2006)	Based on *M. sumatrensis*, Fig. 25
Myriangium duriaei CBS 260.36	3	0	1	1	0	0	0	0	0	0	?	(Hyde et al., 2013)	Fig. 86
Myriangium hispanicum CBS 247.33	3	0	1	1	0	0	0	0	0	0	?	(Hyde et al., 2013)	Based on *M. duriaei*
Mytilinidion mytilinellum CBS 303.34	1	0	0	1	2	0	0	0	0	0	?	(Hyde et al., 2013)	Fig. 87
Mytilinidion scolecosporum CBS 305.34	3	0	0	1	2	0	0	0	0	0	?	(Lohman, 1932)	Pl. 17A
Natipusilla bellaspora PE91 1a	3	0	3	1	3	0	0	0	0	0	?	(Raja et al., 2012)	Figs. 1–12
Natipusilla decorospora AF236 1A	3	0	3	1	3	0	0	0	0	0	?	(Ferrer et al., 2011)	Figs. 11–16
Natipusilla limonensis AF286 1A	3	0	3	1	3	0	0	0	0	0	?	(Ferrer et al., 2011)	Figs. 17–23
Natipusilla naponensis AF217 1A	3	0	3	1	3	0	0	0	0	0	?	(Ferrer et al., 2011)	Figs. 24–30
Neofusicoccum ribis AFTOL-ID 1232	3	0	1	1	0	0	0	0	0	0	?	(Wolf and Wolf, 1939)	Figs. 2-3

Taxon	I	II	III	IV	V	VI	VII	VIII	IX	X	XI	Ref.	Illustration
Odontotrema phacidioides Palice 11440	3	1	0	1	4	?	0	0	0	0	?	(Baloch et al., 2013)	Fig. 3F
Opegrapha dolomitica AFTOL-ID 993	0	1	0	1	2	1	0	0	0	0	?	(Brodo et al., 2001)	Based on *O. varia* Fig. 551
Paramycoleptodiscus albizziae CPC 27552	1	0	?	?	?	?	1	?	?	0	?	(Crous et al., 2016a)	p. 370
Parmularia styracis VIC 42587	1	0	2	1	1	1	1	?	1	0	?	(Guatimosim et al., 2014c)	Fig.2
Passalora fulva CBS 119.46	1	0	?	?	?	?	0	?	?	0	?	(Crous, 2009)	Fig.6A
Patellaria atrata CBS 101060	3	0	0	1	2	0	0	0	0	0	?	(Ellis and Ellis, 1997)	Pl.5 Fig. 45
Peltaster fructicola JN573665.1	1	0	2	0	1	0	0	?	?	0	?	(Williamson et al., 2004)	Figs. 5–8
Penidiella columbiana CBS 486.80	1	0	?	?	?	?	0	?	?	0	?	(Crous et al., 2007a)	Fig. 8
Pertusaria dactylina AFTOL-ID 224	0	1	0	1	4	0	0	0	0	0	?	(Brodo et al., 2001)	Fig. 629
Phaeococcomycetaceae sp. TRN 452	0	0	?	?	?	?	0	?	?	0	?	(Ruibal et al., 2008)	none
Phaeococcomycetaceae sp. TRN 456	0	0	?	?	?	?	0	?	?	0	?	(Ruibal et al., 2008)	none

Taxon	I	II	III	IV	V	VI	VII	VIII	IX	X	XI	Ref.	Illustration
Phaeococcomycetaceae sp. TRN 529	0	0	?	?	?	?	0	?	?	0	?	(Ruibal et al., 2008)	none
Phaeophleospora atkinsonii CBS 124565	1	0	1	?	0	?	0	?	?	0	?	(Pennycook and McKenzie, 2002)	none
Phaeosaccardinula dendrocalami IFRDCC 2663	1	0	1	1	0	0	0	0	0	0	?	(Yang et al., 2014)	Fig. 3
Phaeosaccardinula ficus MFLUCC 10-0009	1	0	1	1	0	0	0	0	0	0	?	(Chomnunti et al., 2012)	Fig. 3
Phaeotheca fissurella CBS 520.89	?	0	?	?	?	?	0	?	?	0	?	(Tsuneda et al., 2004)	Figs. 1–5
Phaeotrichum benjaminii CBS 541.72	?	0	3	1	3	0	0	0	0	0	?	(Cain, 1956)	Based on *P. hystricinum*, Figs. 1–11
Phragmocapnias asiaticus MFLUCC10-0062	1	0	1	1	0	0	0	0	0	0	?	(Chomnunti et al., 2011)	Fig. 5
Phyllobathelium anomalum MPN242	1	1	1	1	0	0	0	0	0	0	?	(Nelsen et al., 2009)	Based on *P. firmum* Fig. 3M
Phyllobathelium firmum MPN545	1	1	1	1	0	0	0	0	0	0	?	(Nelsen et al., 2009)	Fig. 3M
Physcia aipolia AFTOL-ID 84	3	1	0	1	4	0	0	0	0	0	?	(Brodo et al., 2001)	Fig. 659

Taxon	I	II	III	IV	V	VI	VII	VIII	IX	X	XI	Ref.	Illustration
Piedraia hortae CBS 480.64	?	0	3	1	3	0	0	0	0	0	?	(Takashio and Vanbreuseghem, 1971)	Figs. 1–2
Pleospora herbarum CBS 191.86	1	0	1	1	0	0	0	0	0	0	?	(Inderbitzin et al., 2009)	Fig. 1
Porina farinosa MPN35	1	1	1	1	0	0	0	0	0	0	?	(Nelsen et al., 2014a)	Fig. 4
Porina guentheri AF279405.1	1	1	1	1	0	0	0	0	0	0	?	(Nelsen et al., 2014a)	Based on *P. farinosa* Fig. 4
Prillieuxina baccharidincola VIC 42817	1	0	2	0	1	0	1	?	3	0	1	(Guatimosim et al., 2014c)	Fig. 7
Protoventuria barriae ATCC 90285	1	0	1	1	?	0	0	0	0	0	?	(Carris and Poole, 1993)	Figs.1–6; 7; 9; 10
Pseudeurotium hygrophilum JQ780654.1	0	0	3	?	3	?	0	0	?	0	?	(Sogonov et al., 2005)	Figs. 1–2
Pseudocoleophoma polygonicola KT 731	3	0	1	1	0	0	0	0	0	0	?	(Tanaka et al., 2015)	Fig. 5
Pseudodictyosporium wauense NBRC 30078	3	0	?	?	?	?	0	?	?	0	?	(Boonmee et al., 2016)	Fig. 15
Psiloglonium araucanum CBS 112412	1	0	0	1	2	1	0	0	0	0	?	(Boehm et al., 2009b)	Figs. 8N–8Q

Taxon	I	II	III	IV	V	VI	VII	VIII	IX	X	XI	Ref.	Illustration
Psiloglonium clavisporum GKM L172A	1	0	0	1	2	1	0	0	0	0	?	(Boehm et al., 2009b)	Figs. 8E–8H
Pyrenophora phaeocomes AFTOL-ID 283	1	0	1	1	0	0	0	0	0	0	?	(Shoemaker, 1961)	Figs. 1–11
Pyrenula pseudobufonia AY640962.1	3	1	1	1	0	0	0	0	0	0	?		link
Pyrgillus javanicus AFTOL-ID 342	3	1	1	1	0	0	0	0	0	0	?		link
Racodium rupestre L346	0	1	?	?	?	?	0	?	?	0	?		link
Rasutoria tsugae EF1147	1	0	1	1	0	0	0	0	0	0	?	(Dearness, 1924)	none
Readeriella mirabilis CBS 116293	1	0	1	?	0	?	0	?	?	0	?	(Crous et al., 2007a)	Fig. 18
Recurvomyces mirabilis CCFEE 5264	0	0	?	?	?	?	0	?	?	0	?	(Selbmann et al., 2008)	Fig. 1
Reichlingia zwackhii KF707637.1	?	1	0	?	2	?	0	0	?	0	?	(Frisch et al., 2014a)	Based on *R. syncesioides*, Figs. 2b; 3a–3c
Rhagadolobiopsis thelypteridis EG 156	1	0	2	1	1	1	1	?	1	0	3	(Guatimosim et al., 2014b)	Fig. 1–2

Taxon	I	II	III	IV	V	VI	VII	VIII	IX	X	XI	Ref.	Illustration
Rhexothecium globosum CBS 955.73	?	0	3	1	3	0	0	0	0	0	?	(Samson and Mouchacca, 1975)	Fig. 6
Roccella fuciformis AFTOL-ID 126	0	1	0	?	4	0	0	0	?	0	?		link
Roccellographa cretacea AFTOL-ID 93	0	1	0	1	2	0	0	0	0	0	?	(Tehler and Irestedt, 2007)	none, following genus description
Sarcinomyces petricola CBS 101157	0	0	?	?	?	?	0	?	?	0	?	(Wollenzien et al., 1997)	Figs. 1–11
Saxomyces alpinus CCFEE 5466	0	0	?	?	?	?	0	?	?	0	?	(Selbmann et al., 2014)	Figs. 3–4
Saxomyces penninicus CCFEE 5495	0	0	?	?	?	?	0	?	?	0	?	(Selbmann et al., 2014)	Fig. 5
Schismatomma decolorans DUKE-0047570	0	1	0	?	4	0	0	0	?	0	?		link
Schizothyrium pomi CBS 228.57	1	0	2	0	1	0	0	4	3	0	?		Based on *Schizothyrium gaultheriae* UBC-F3143
Scolecopeltidium sp. 1 UBC-F33033	1	0	2	0	0	0	0	4	3	0	?		Personal collection
Scolecopeltidium sp. 2 UBC-F33035	1	0	2	0	0	0	0	4	3	0	?		Personal collection

Taxon	I	II	III	IV	V	VI	VII	VIII	IX	X	XI	Ref.	Illustration
Scorias spongiosa AFTOL-ID 1594	1	0	1	1	0	0	0	0	0	0	?	(Chomnunti et al., 2011)	Figs. 12–13
Seuratia millardetii UBC-F33043	1	?	0	1	4	0	0	?	?	0	?		Personal collection
Simonyella variegata AFTOL-ID 80	0	1	0	?	4	0	0	0	?	0	?		link1, link2
Sphaeropeziza arctoalpina Baloch SW057(S)	4	0	0	1	4	0	0	0	0	0	?	(Baloch et al., 2013)	Fig. 5A
Sphaerulina polyspora CBS 354.29	1	0	1	1	0	0	0	0	0	0	?	(Wolf, 1925)	Figs. 8; 11–14; 16-17
Spiromastix warcupii AFTOL-ID 430	0	0	3	1	3	0	0	0	0	0	?	(Currah and Locquin-Linard, 1988)	Based on *S.grisea*, Figs. 1–6
Staurothele frustulenta AFTOL-ID 697	0	1	1	1	0	0	0	0	0	0	?		link
Stictis radiata AF356663.1	3	0	0	1	4	?	0	0	0	0	?	(Wedin et al., 2006)	Fig. 2I
Stictographa lentiginosa 47621	2	0	0	1	2	1	0	0	0	0	?	(Ertz and Diederich, 2015)	Fig. 4q
Stomiopeltis betulae CBS 114420	1	0	?	?	?	0	?	?	?	0	?		Never illustrated

Taxon	I	II	III	IV	V	VI	VII	VIII	IX	X	XI	Ref.	Illustration
Stomiopeltis versicolor GA3 23C2b	1	0	?	?	?	?	?	?	?	0	?		Never illustrated
Strigula jamesii MPN548	1	1	1	1	**0**	0	0	0	0	0	?		Based on *S. nemathora*. link
Strigula nemathora MPN72	1	1	1	1	**0**	0	0	0	0	0	?		link
Strigula schizospora MPN73	1	1	1	1	**0**	0	0	0	0	0	?		Based on *S. nemathora*
Stylodothis puccinioides CBS 193.58	1	0	1	1	0	0	0	0	0	0	?	(Müller and von Arx, 1962)	*Abb.* 144
Sydowia polyspora AFTOL-ID 178	1	0	1	?	0	?	0	?	?	0	?	(Ellis and Ellis, 1997)	Pl. 76 Fig. 778
Sympoventuria capensis CBS 120136	1	0	1	1	0	0	0	0	0	0	?	(Crous et al., 2007b)	Fig. 8
Taeniolella exilis CBS122902	3	0	?	?	?	?	0	?	?	0	?	(Ertz et al., 2016)	Figs. 5–6
Taeniolella hawksworthiana Common 9199B(BR)	2	0	?	?	?	?	0	?	?	0	?	(Ertz et al., 2016)	Figs. 7-8
Taeniolella punctata Ertz 17390(BR)	2	0	?	?	?	?	0	?	?	0	?	(Ertz et al., 2016)	Figs. 9–11

Taxon	I	II	III	IV	V	VI	VII	VIII	IX	X	XI	Ref.	Illustration
Taeniolella pyrenulae Diederich 17075	2	0	?	?	?	?	0	?	?	0	?	(Ertz et al., 2016)	Figs. 12–13
Taeniolella sp. Ertz 11026(BR)	2	0	?	?	?	?	0	?	?	0	?	(Ertz et al., 2016)	Figs. 14–15
Taeniolella toruloides Diederich 17048	2	0	?	?	?	?	0	?	?	0	?	(Ertz et al., 2016)	Figs. 16–17
Teratosphaeria stellenboschiana CPC 10886	1	0	1	?	0	?	0	?	?	0	?	(Crous et al., 2006)	Fig. 5
Teratosphaeriaceae sp. D007 09	0	0	?	?	?	?	0	?	?	0	?	(Ruibal et al., 2009)	none
Tothia fuscella CBS 130266	1	0	2	0	0	0	1	4	1	0	?	(Wu et al., 2012)	Fig. 2
Trapelia placodioides AF274103	0	1	0	1	4	0	0	0	0	0	?	(Brodo et al., 2001)	Based on *T. involuta*, Fig. 841
Trichodelitschia bisporula CBS 262.69	?				0						?		Based on *T. minuta*, link
Trypethelium eluteriae CBS 132375	3	1	1	1	0	0	0	0	0	0	?	(Aptroot and Lücking, 2016)	Figs. 7J; 8E; 10G; 56B–L
Tubeufia cerea AFTOL-ID 1316	3	0	1	1	0	0	0	0	0	0	?	(Boonmee et al., 2014)	Fig. 23

Taxon	I	II	III	IV	V	VI	VII	VIII	IX	X	XI	Ref.	Illustration
Tubeufia helicomyces AFTOL-ID 1580	3	0	1	1	0	0	0	0	0	0	?	(Webster, 1951)	Figs.1–2
Tubeufia paludosa CBS 120503	3	0	1	1	0	0	0	0	0	0	?	(Boonmee et al., 2014)	Fig. 22
Tumidispora shoreae MFLUCC 12-0409	1	0	2	0	0	0	1	2	2	0	?	(Ariyawansa et al., 2015)	Fig. 39
Tyrannosorus pinicola AFTOL-ID 1235	?	0	1	1	0	0	0	0	0	0	?	(Untereiner et al., 1995)	Figs. 6–10
Umbilicaria mammulata AFTOL-ID 645	0	1	0	1	4	0	0	0	0	0	?	(Brodo et al., 2001)	Fig. 865
Uwebraunia commune CBS 110747	1	0	?	?	?	?	0	?	?	0	?	(Crous et al., 2004)	Figs. 3–6
Venturia inaequalis CBS 594.70	1	0	1	1	0	0	0	0	0	0	?	(Hyde et al., 2013)	Fig. 131
Venturia pyrina ICMP 11032	1	0	1	1	0	0	0	0	0	0	?		
Veronaeopsis simplex CBS 588.66	1	0	?	?	?	?	0	?	?	0	?	(Arzanlou et al., 2007)	Figs. 17C; 35
Wiesneriomyces conjunctosporus BCC18525	1	0	?	?	?	?	0	?	?	0	?	(Kuthubutheen and Nawawi, 1988)	Figs. 1–11
Xenomeris juniperi EF114709.1	1	0	1	1	?	?	0	0	0	0	?	(Müller and von Arx, 1962)	Based on *X. raetica*, *Abb.* 177

Taxon	I	II	III	IV	V	VI	VII	VIII	IX	X	XI	Ref.	Illustration
Zasmidium anthuriicola CBS 118742	1	0	?	?	?	?	?	?	?	0	?	(Zhao et al., 2016)	Based on *Z. litseae*, Fig. 2
Zeloasperisporium cliviae CPC 25145	1	0	?	?	?	?	?	?	?	0	?	(Crous et al., 2015b)	p. 214
Zeloasperisporium eucalyptorum CBS 124809	1	0	?	?	?	?	?	?	?	0	?	(Cheewangkoon et al., 2009)	Fig. 26
Zeloasperisporium ficusicola MFLUCC 15-0222	1	0	2	0	?	0	1	2	2	0	?	(Hongsanan et al., 2015)	Fig. 2
Zeloasperisporium searsiae CPC 25880	1	0	2	?	?	0	1	?	?	0	?	(Crous et al., 2015a)	p. 280
Zeloasperisporium siamense IFRDCC 2194	1	0	2	0	?	0	1	2	2	0	?	(Wu et al., 2011b)	Fig. 15
Zeloasperisporium wrightiae MFLUCC 15-0215	1	0	2	0	?	0	1	2	2	0	?	(Hongsanan et al., 2015)	Fig. 4

A.4 Results from CONSEL for six topologies tested against most likely tree

Test Statistic	Approximately Unbiased test	Kishino Hasegawa Test	Bootstrap probability	Constraint
55.9	0.086	0.06	0.029	Asterinales and Asterotexiales monophyletic
102.3	0.011	0.006	0.002	Microthyriales + Zeloasperisporiales monophyletic
161	3.00E-04	0	2.00E-05	*Lembosia* monophyletic
1242.2	4.00E-06	0	1.00E-05	Radiate thyriothecia monophyletic
419.2	2.00E-80	0	4.00E-21	*Asterina* spp. monophyletic

A.5 Detailed output of ancestral state reconstruction

Output of ancestral state reconstruction for each of 208 nodes performed in Mesquite (white rows) and in BayesTraits V3 (grey rows). Nodes labelled in the first column correspond to the 11 nodes labelled on Fig. 1 and the second column lists a name in duplicate for the 208 nodes reconstructed with each method (proportional likelihoods, followed by posterior probability).

		Substrate					Lichenized	
	State	Saxicolous	Superficial on plants	Lichenicolous	Immersed on plants	Other	no	yes
Labelled in Fig.1	Node/StateCode	0	1	2	3	4	0	1
	NLeotio	0.0006	0.0000	0.0000	0.9993	0.0001	1.0000	0.0000
	NLeotio	0.1682	0.0003	0.0000	0.6718	0.1598	0.9999	0.0001
	NEuroAll	0.0950	0.0039	0.0026	0.8960	0.0026	0.4620	0.5380
	NEuroAll	0.7542	0.0045	0.0012	0.1284	0.1117	0.5232	0.4768
	NOnyEuro	0.0000	0.0000	0.0000	0.0000	0.0000	0.9875	0.0125
	NOnyEuro	0.8253	0.0032	0.0008	0.0364	0.1344	0.9978	0.0022
	NEuro1	0.0000	0.0000	0.0000	0.0000	0.0000	0.9999	0.0001
	NEuro1	0.6523	0.0037	0.0001	0.0083	0.3357	0.9998	0.0002
	NEuro2	0.0000	0.0000	0.0000	0.0000	0.0000	1.0000	0.0000
	NEuro2	0.6030	0.0153	0.0001	0.0069	0.3747	0.9999	0.0001
	NEuro3	0.0000	0.0000	0.0000	0.0000	0.0000	1.0000	0.0000

NEuro3	0.5866	0.0589	0.0004	0.0110	0.3431	0.9996	0.0004
NPyrVeChae	0.0899	0.0061	0.0016	0.9009	0.0016	0.2727	0.7273
NPyrVeChae	0.6328	0.0036	0.0004	0.1988	0.1645	0.0554	0.9446
NPyren	0.0123	0.0018	0.0013	0.9833	0.0013	0.0221	0.9779
NPyren	0.0982	0.0151	0.0019	0.7219	0.1628	0.0024	0.9976
NVerChae	0.2107	0.0314	0.0026	0.7528	0.0026	0.2894	0.7106
NVerChae	0.8859	0.0005	0.0003	0.0502	0.0631	0.5136	0.4864
NVerru	0.9809	0.0013	0.0007	0.0163	0.0007	0.0041	0.9959
NVerru	0.9562	0.0002	0.0002	0.0071	0.0363	0.0003	0.9997
NCthyrL	0.1525	0.0825	0.0020	0.7610	0.0020	0.9968	0.0032
NCthyrL	0.7889	0.0011	0.0001	0.0976	0.1123	0.9998	0.0002
NHerpo1	0.0000	0.0000	0.0000	0.0000	0.0000	1.0000	0.0000
NHerpo1	0.6194	0.0002	0.0000	0.2921	0.0883	0.9999	0.0001
NHerpo2	0.0000	0.0000	0.0000	0.0000	0.0000	1.0000	0.0000
NHerpo2	0.4731	0.0008	0.0001	0.3871	0.1389	0.9997	0.0003
NCthyr01	0.1872	0.4844	0.0049	0.3185	0.0049	0.9999	0.0001
NCthyr01	0.6779	0.0276	0.0004	0.0254	0.2687	0.9993	0.0007
NCthyr02	0.0087	0.9757	0.0005	0.0146	0.0005	1.0000	0.0000
NCthyr02	0.4367	0.1155	0.0003	0.0209	0.4267	0.9999	0.0001
NCthyr03	0.0000	0.0000	0.0000	0.0000	0.0000	1.0000	0.0000
NCthyr03	0.5536	0.0480	0.0012	0.1108	0.2864	0.9992	0.0008
NCthyr04	0.0000	0.9999	0.0000	0.0000	0.0000	1.0000	0.0000
NCthyr04	0.0013	0.9489	0.0007	0.0003	0.0489	0.9999	0.0001
NCthyr05	0.0000	0.9999	0.0000	0.0000	0.0000	1.0000	0.0000
NCthyr05	0.2624	0.3346	0.0004	0.0116	0.3911	0.9999	0.0001
NCthyr06	0.0000	1.0000	0.0000	0.0000	0.0000	1.0000	0.0000
NCthyr06	0.3362	0.2529	0.0005	0.0241	0.3863	0.9998	0.0002

NCthyr07	0.0000	0.0000	0.0000	0.0000	0.0000	1.0000	0.0000
NCthyr07	0.6176	0.0501	0.0003	0.1065	0.2256	1.0000	0.0000
NLecano	0.0240	0.0001	0.0000	0.9759	0.0000	0.0178	0.9822
NLecano	0.8322	0.0008	0.0001	0.0912	0.0757	0.0176	0.9824
NLeca1	0.0262	0.0039	0.0005	0.9690	0.0005	0.0015	0.9985
NLeca1	0.4590	0.0398	0.0010	0.1630	0.3373	0.0005	0.9995
NLeca2	0.0584	0.0317	0.0021	0.9058	0.0021	0.0000	1.0000
NLeca2	0.4677	0.0455	0.0009	0.1012	0.3846	0.0003	0.9997
NLeca3	0.0791	0.0238	0.0023	0.8925	0.0023	0.0000	1.0000
NLeca3	0.6072	0.0037	0.0003	0.2138	0.1750	0.0005	0.9995
NUAO	0.0533	0.0002	0.0002	0.9460	0.0003	0.0073	0.9927
NUAO	0.8099	0.0003	0.0001	0.1115	0.0782	0.0170	0.9830
NUmbi1	0.8652	0.0015	0.0015	0.1303	0.0015	0.0006	0.9994
NUmbi1	0.9114	0.0006	0.0005	0.0316	0.0559	0.0006	0.9994
NUmbi2	0.9696	0.0013	0.0013	0.0264	0.0013	0.0001	0.9999
NUmbi2	0.8582	0.0032	0.0020	0.0518	0.0848	0.0023	0.9977
NOstropo	0.0289	0.0002	0.0000	0.9706	0.0004	0.0138	0.9862
NOstropo	0.3808	0.0016	0.0001	0.4512	0.1664	0.2777	0.7223
NMpeltout1	0.0069	0.0026	0.0003	0.9815	0.0087	0.9879	0.0121
NMpeltout1	0.1361	0.0283	0.0004	0.5200	0.3152	0.9991	0.0009
NMpeltout2	0.0005	0.0002	0.0001	0.9986	0.0006	0.9995	0.0005
NMpeltout2	0.0313	0.0036	0.0005	0.8412	0.1235	0.9987	0.0013
NMpeltout3	0.0066	0.0160	0.0015	0.9210	0.0550	0.9922	0.0078
NMpeltout3	0.2562	0.1751	0.0028	0.2036	0.3623	0.9863	0.0137
NMpeltout4	0.0069	0.0095	0.0054	0.2647	0.7134	0.9986	0.0014
NMpeltout4	0.2909	0.1314	0.0035	0.2182	0.3561	0.9926	0.0074
NMpeltout5	0.0071	0.0266	0.0023	0.9113	0.0526	0.9914	0.0086

	NMpeltout5	0.2050	0.2422	0.0071	0.1706	0.3750	0.8747	0.1253
	NMpelt1	0.0004	0.9945	0.0004	0.0041	0.0006	1.0000	0.0000
	NMpelt1	0.0061	0.8717	0.0027	0.0015	0.1181	0.9997	0.0003
	NMpelt2	0.0001	0.9992	0.0001	0.0005	0.0001	1.0000	0.0000
	NMpelt2	0.0128	0.8404	0.0053	0.0040	0.1375	0.9988	0.0012
	NMpelt3	0.0001	0.9995	0.0001	0.0003	0.0001	1.0000	0.0000
	NMpelt3	0.0124	0.8343	0.0051	0.0037	0.1445	0.9989	0.0011
	NOstro1	0.2157	0.0135	0.0052	0.7604	0.0052	0.0000	1.0000
	NOstro1	0.6424	0.0036	0.0005	0.1926	0.1610	0.0007	0.9993
	NOstro2	0.0037	0.0006	0.0005	0.9947	0.0005	0.0000	1.0000
	NOstro2	0.0239	0.0026	0.0004	0.8611	0.1121	0.0004	0.9996
	NOstro3	0.8311	0.0063	0.0047	0.1533	0.0047	0.0000	1.0000
	NOstro3	0.8706	0.0023	0.0015	0.0473	0.0784	0.0019	0.9981
	NOstro4	0.9999	0.0000	0.0000	0.0001	0.0000	0.0000	1.0000
	NOstro4	0.9914	0.0000	0.0000	0.0006	0.0080	0.0000	1.0000
	NOstro5	1.0000	0.0000	0.0000	0.0000	0.0000	0.0000	1.0000
	NOstro5	0.9954	0.0000	0.0000	0.0003	0.0043	0.0000	1.0000
	NOstro6	1.0000	0.0000	0.0000	0.0000	0.0000	0.0000	1.0000
	NOstro6	0.9980	0.0000	0.0000	0.0001	0.0019	0.0000	1.0000
NODE 1	**NDothArTry**	**0.0035**	**0.0000**	**0.0000**	**0.9965**	**0.0000**	**0.8877**	**0.1123**
	NDothArTry	**0.8204**	**0.0001**	**0.0000**	**0.0869**	**0.0926**	**0.8240**	**0.1760**
	NArthTryp	0.0095	0.0002	0.0002	0.9899	0.0002	0.8116	0.1884
	NArthTryp	0.7340	0.0036	0.0006	0.1372	0.1247	0.1907	0.8093
	NTryp1	0.0039	0.0032	0.0032	0.9864	0.0032	0.0386	0.9614
	NTryp1	0.1754	0.0296	0.0037	0.6117	0.1797	0.0035	0.9965
	NTryp2	0.0006	0.0006	0.0006	0.9975	0.0006	0.0004	0.9996
	NTryp2	0.0342	0.0040	0.0005	0.8370	0.1243	0.0007	0.9993

NTryp3	0.0025	0.0023	0.0023	0.9907	0.0023	0.0070	0.9930
NTryp3	0.1638	0.0334	0.0044	0.6149	0.1835	0.0056	0.9944
NTryp4	0.0003	0.0003	0.0003	0.9988	0.0003	0.0001	0.9999
NTryp4	0.0226	0.0025	0.0003	0.8628	0.1117	0.0004	0.9996
NArtho01	0.0434	0.0005	0.0004	0.9552	0.0004	0.8054	0.1946
NArtho01	0.8392	0.0007	0.0001	0.0807	0.0794	0.2856	0.7144
NArtho02	0.9624	0.0076	0.0006	0.0289	0.0006	0.9974	0.0026
NArtho02	0.8815	0.0045	0.0002	0.0053	0.1086	0.9090	0.0910
NSeurat	0.9523	0.0240	0.0013	0.0211	0.0013	0.0000	0.0000
NSeurat	0.6132	0.0636	0.0014	0.0253	0.2965	0.5732	0.4268
NArthRock	0.9975	0.0005	0.0001	0.0019	0.0001	0.9999	0.0001
NArthRock	0.9654	0.0001	0.0001	0.0048	0.0296	0.9996	0.0004
NArtho03	0.0254	0.0002	0.0002	0.9742	0.0002	0.0342	0.9658
NArtho03	0.5164	0.0031	0.0011	0.3420	0.1375	0.0085	0.9915
NArtho04	0.0835	0.0044	0.0044	0.9033	0.0044	0.0005	0.9995
NArtho04	0.4530	0.0041	0.0004	0.3461	0.1963	0.0008	0.9992
NArtho05	0.0184	0.0000	0.0000	0.9815	0.0000	0.0021	0.9979
NArtho05	0.4534	0.0041	0.0036	0.3710	0.1679	0.0004	0.9996
NArtho06	0.0000	0.0000	0.0000	0.0000	0.0000	0.0001	0.9999
NArtho06	0.0647	0.0250	0.1061	0.4685	0.3358	0.0005	0.9995
NArtho07	0.0292	0.0002	0.0002	0.9700	0.0002	0.0000	1.0000
NArtho07	0.5312	0.0014	0.0001	0.2845	0.1828	0.0002	0.9998
NArtho08	0.0033	0.0001	0.0001	0.9963	0.0001	0.0000	1.0000
NArtho08	0.0319	0.0044	0.0006	0.8590	0.1040	0.0007	0.9993
NArtho09	0.9166	0.0015	0.0015	0.0790	0.0015	0.0000	1.0000
NArtho09	0.9028	0.0007	0.0006	0.0363	0.0596	0.0006	0.9994
NArtho10	0.9761	0.0019	0.0019	0.0180	0.0019	0.0002	0.9998

NArtho10	0.7917	0.0074	0.0035	0.0911	0.1063	0.0041	0.9959
NArtho11	0.9978	0.0001	0.0001	0.0019	0.0001	0.0000	1.0000
NArtho11	0.9248	0.0004	0.0005	0.0246	0.0496	0.0004	0.9996
NArtho12	0.9995	0.0001	0.0001	0.0004	0.0001	0.0000	1.0000
NArtho12	0.9144	0.0008	0.0007	0.0239	0.0602	0.0010	0.9990
NArtho13	0.9990	0.0002	0.0002	0.0005	0.0002	0.0000	1.0000
NArtho13	0.9008	0.0014	0.0009	0.0343	0.0627	0.0010	0.9990
NArtho14	1.0000	0.0000	0.0000	0.0000	0.0000	0.0000	1.0000
NArtho14	0.9847	0.0000	0.0000	0.0013	0.0139	0.0001	0.9999
NArtho15	1.0000	0.0000	0.0000	0.0000	0.0000	0.0000	1.0000
NArtho15	0.9898	0.0000	0.0000	0.0007	0.0094	0.0000	1.0000
NDothid	0.0034	0.0000	0.0000	0.9966	0.0000	1.0000	0.0000
NDothid	0.7130	0.0001	0.0001	0.1080	0.1789	1.0000	0.0000
NPate	0.0003	0.0008	0.0004	0.9984	0.0000	1.0000	0.0000
NPate	0.0355	0.0416	0.0007	0.5253	0.3969	0.9997	0.0003
NAbro1	0.0001	0.0001	0.9958	0.0039	0.0001	1.0000	0.0000
NAbro1	0.0000	0.0000	0.9992	0.0000	0.0007	0.9999	0.0001
NAbro2	0.0000	0.0000	1.0000	0.0000	0.0000	1.0000	0.0000
NAbro2	0.0000	0.0000	0.9994	0.0000	0.0006	0.9999	0.0001
NTube1	0.0000	0.0000	0.0000	1.0000	0.0000	1.0000	0.0000
NTube1	0.0105	0.0009	0.0001	0.9013	0.0872	0.9997	0.0003
NTube2	0.0000	0.0000	0.0000	1.0000	0.0000	1.0000	0.0000
NTube2	0.0161	0.0017	0.0003	0.8901	0.0918	0.9994	0.0006
NBotry1	0.0000	0.0000	0.0000	1.0000	0.0000	1.0000	0.0000
NBotry1	0.0032	0.0003	0.0000	0.9453	0.0512	0.9999	0.0001
NBotry2	0.0000	0.0000	0.0000	1.0000	0.0000	1.0000	0.0000
NBotry2	0.0043	0.0004	0.0001	0.9417	0.0536	0.9998	0.0002

	NBotry3	0.0000	0.0000	0.0000	1.0000	0.0000	1.0000	0.0000
	NBotry3	0.0003	0.0000	0.0000	0.9917	0.0080	1.0000	0.0000
	NCapnodX	0.4576	0.0306	0.0001	0.5116	0.0001	1.0000	0.0000
	NCapnodX	0.5761	0.0043	0.0001	0.0583	0.3612	0.9999	0.0001
	NDothi1	0.0000	0.0000	0.0000	0.0000	0.0000	1.0000	0.0000
	NDothi1	0.0688	0.0794	0.0400	0.4136	0.3982	0.9995	0.0005
	NMyri1	0.0280	0.0964	0.0015	0.8727	0.0015	1.0000	0.0000
	NMyri1	0.0435	0.2369	0.0025	0.1843	0.5328	0.9996	0.0004
	NMyri2	0.0007	0.0022	0.0001	0.9970	0.0001	1.0000	0.0000
	NMyri2	0.0110	0.0011	0.0002	0.9044	0.0833	0.9996	0.0004
	NCapnod0	0.0000	0.0000	0.0000	0.0000	0.0000	1.0000	0.0000
	NCapnod0	0.4705	0.0271	0.0021	0.0122	0.4882	0.9979	0.0021
	NCapnod1	0.4782	0.1825	0.0013	0.3366	0.0013	1.0000	0.0000
	NCapnod1	0.4599	0.0310	0.0013	0.0101	0.4978	0.9960	0.0040
	NCapnod2	0.0000	0.0000	0.0000	0.0000	0.0000	0.9962	0.0038
	NCapnod2	0.5863	0.0326	0.0273	0.0327	0.3210	0.6065	0.3935
	NCapnod3	0.0543	0.9101	0.0001	0.0354	0.0001	1.0000	0.0000
	NCapnod3	0.2568	0.1640	0.0005	0.0084	0.5702	0.9999	0.0001
	NCapnod4	0.0225	0.9624	0.0001	0.0148	0.0001	1.0000	0.0000
	NCapnod4	0.1030	0.5719	0.0037	0.0046	0.3168	0.9993	0.0007
NODE 2	**NCapnod5**	**0.0538**	**0.9106**	**0.0001**	**0.0354**	**0.0001**	**1.0000**	**0.0000**
	NCapnod5	**0.3160**	**0.1103**	**0.0003**	**0.0105**	**0.5629**	**0.9999**	**0.0001**
	NAsteOut1	0.1552	0.7110	0.0029	0.1280	0.0029	1.0000	0.0000
	NAsteOut1	0.4257	0.0985	0.0004	0.0215	0.4538	0.9997	0.0003
	NAsteOut2	0.0000	0.0004	0.0000	0.9996	0.0000	1.0000	0.0000
	NAsteOut2	0.1892	0.2219	0.0085	0.1506	0.4297	0.9985	0.0015
	NAsteOut3	0.0000	0.0000	0.0000	0.0000	0.0000	1.0000	0.0000

	NAsteOut3	0.1671	0.0705	0.0082	0.2983	0.4559	1.0000	0.0000
	NAsteOut4	0.0000	0.0000	0.0000	0.0000	0.0000	1.0000	0.0000
	NAsteOut4	0.0659	0.0132	0.0014	0.6512	0.2684	1.0000	0.0000
	NAste1	0.0049	0.9229	0.0049	0.0626	0.0049	0.9999	0.0001
	NAste1	0.0314	0.7655	0.0122	0.0121	0.1787	0.9966	0.0034
NODE 3	**NAste2**	**0.0000**	**1.0000**	**0.0000**	**0.0000**	**0.0000**	**1.0000**	**0.0000**
	NAste2	**0.0011**	**0.9463**	**0.0006**	**0.0002**	**0.0518**	**0.9999**	**0.0001**
	NAste3	0.0000	1.0000	0.0000	0.0000	0.0000	1.0000	0.0000
	NAste3	0.0016	0.9319	0.0008	0.0003	0.0653	0.9999	0.0001
	NAste4	0.0000	1.0000	0.0000	0.0000	0.0000	1.0000	0.0000
	NAste4	0.0079	0.8676	0.0034	0.0023	0.1188	0.9993	0.0007
	NAste5	0.0000	1.0000	0.0000	0.0000	0.0000	1.0000	0.0000
	NAste5	0.0007	0.9725	0.0004	0.0002	0.0262	0.9999	0.0001
	NAste6	0.0000	1.0000	0.0000	0.0000	0.0000	1.0000	0.0000
	NAste6	0.0001	0.9934	0.0001	0.0000	0.0064	1.0000	0.0000
	NAste7	0.0000	1.0000	0.0000	0.0000	0.0000	1.0000	0.0000
	NAste7	0.0002	0.9832	0.0001	0.0001	0.0164	1.0000	0.0000
	NAste8	0.0000	1.0000	0.0000	0.0000	0.0000	1.0000	0.0000
	NAste8	0.0002	0.9862	0.0001	0.0001	0.0134	1.0000	0.0000
	NCapno01	0.0005	0.9993	0.0000	0.0002	0.0000	1.0000	0.0000
	NCapno01	0.1373	0.2549	0.0002	0.0027	0.6049	0.9999	0.0001
	NCapno02	0.0001	0.9998	0.0000	0.0000	0.0000	1.0000	0.0000
	NCapno02	0.0209	0.7694	0.0050	0.0040	0.2006	0.9989	0.0011
	NCapno03	0.0000	1.0000	0.0000	0.0000	0.0000	1.0000	0.0000
	NCapno03	0.0006	0.9685	0.0003	0.0001	0.0305	0.9999	0.0001
	NCapno04	0.0000	1.0000	0.0000	0.0000	0.0000	1.0000	0.0000
	NCapno04	0.0015	0.9417	0.0008	0.0003	0.0556	0.9999	0.0001

NCapno05	0.0000	1.0000	0.0000	0.0000	0.0000	1.0000	0.0000
NCapno05	0.0003	0.9822	0.0002	0.0001	0.0172	1.0000	0.0000
NCapno06	1.0000	0.0000	0.0000	0.0000	0.0000	1.0000	0.0000
NCapno06	0.0000	0.9960	0.0000	0.0000	0.0039	1.0000	0.0000
NCapno07	0.0002	0.9997	0.0000	0.0000	0.0000	1.0000	0.0000
NCapno07	0.2215	0.0778	0.0001	0.0127	0.6879	0.9999	0.0001
NTerato01	0.0019	0.9970	0.0010	0.0001	0.0001	1.0000	0.0000
NTerato01	0.2998	0.0605	0.0003	0.0108	0.6286	0.9999	0.0001
NTerato02	0.0007	0.9987	0.0004	0.0001	0.0001	1.0000	0.0000
NTerato02	0.0381	0.7469	0.0137	0.0140	0.1872	0.9961	0.0039
NTerato03	0.0000	0.0000	0.0000	0.0000	0.0000	1.0000	0.0000
NTerato03	0.4097	0.0052	0.0001	0.0291	0.5559	1.0000	0.0000
NTerato04	0.0000	0.0000	0.0000	0.0000	0.0000	1.0000	0.0000
NTerato04	0.2988	0.0469	0.0090	0.1314	0.5139	0.9998	0.0002
NTerato05	0.0000	0.0000	0.0000	0.0000	0.0000	1.0000	0.0000
NTerato05	0.4866	0.0045	0.0005	0.0487	0.4597	1.0000	0.0000
NTerato06	0.0000	0.0000	0.0000	0.0000	0.0000	1.0000	0.0000
NTerato06	0.3393	0.0478	0.0114	0.1282	0.4733	0.9998	0.0002
NTerato07	0.0000	0.0000	0.0000	0.0000	0.0000	1.0000	0.0000
NTerato07	0.5960	0.0051	0.0047	0.0504	0.3439	0.9999	0.0001
NTerato08	0.0000	0.0000	0.0000	0.0000	0.0000	1.0000	0.0000
NTerato08	0.4154	0.0431	0.0181	0.1241	0.3993	0.9998	0.0002
NTerato09	0.0000	0.0000	0.0000	0.0000	0.0000	1.0000	0.0000
NTerato09	0.4025	0.0642	0.0408	0.1735	0.3189	0.9978	0.0022
NTerato10	0.3134	0.4873	0.1863	0.0065	0.0065	1.0000	0.0000
NTerato10	0.6286	0.0082	0.0217	0.0361	0.3055	0.9998	0.0002
NTerato11	0.0000	0.0000	0.0000	0.0000	0.0000	1.0000	0.0000

NTerato11	0.2813	0.0823	0.1871	0.0823	0.3669	0.9997	0.0003
NCapnod6	0.0000	1.0000	0.0000	0.0000	0.0000	1.0000	0.0000
NCapnod6	0.0375	0.1837	0.0006	0.0726	0.7055	0.9999	0.0001
NSchiz	0.0000	1.0000	0.0000	0.0000	0.0000	1.0000	0.0000
NSchiz	0.0075	0.8517	0.0026	0.0029	0.1354	0.9995	0.0005
NMcspha1	0.0000	0.9978	0.0000	0.0021	0.0000	1.0000	0.0000
NMcspha1	0.0640	0.0197	0.0004	0.2935	0.6224	1.0000	0.0000
NMcspha2	0.0000	0.0000	0.0000	0.0000	0.0000	1.0000	0.0000
NMcspha2	0.1515	0.1033	0.0105	0.1721	0.5626	0.9995	0.0005
NMcspha3	0.0000	0.0000	0.0000	0.0000	0.0000	1.0000	0.0000
NMcspha3	0.1296	0.2053	0.0359	0.1202	0.5090	0.9995	0.0005
NMcspha4	0.0001	0.9595	0.0001	0.0401	0.0001	1.0000	0.0000
NMcspha4	0.0233	0.0138	0.0006	0.5682	0.3942	1.0000	0.0000
NMcspha5	0.0000	0.0000	0.0000	0.0000	0.0000	1.0000	0.0000
NMcspha5	0.0894	0.3079	0.0250	0.0701	0.5075	0.9998	0.0002
NMcspha6	0.0002	0.0734	0.0002	0.9260	0.0002	1.0000	0.0000
NMcspha6	0.0102	0.0018	0.0001	0.7915	0.1964	0.9999	0.0001
NMcspha7	0.0000	0.0003	0.0000	0.9997	0.0000	1.0000	0.0000
NMcspha7	0.0105	0.0008	0.0001	0.8510	0.1376	1.0000	0.0000
NMcspha9	0.0000	0.0000	0.0000	0.0000	0.0000	1.0000	0.0000
NMcspha9	0.0051	0.0003	0.0000	0.9091	0.0853	0.9999	0.0001
NMcspha8	0.0000	0.0000	0.0000	1.0000	0.0000	1.0000	0.0000
NMcspha8	0.1091	0.0475	0.0105	0.4691	0.3638	0.9999	0.0001
NMonOut1	0.1170	0.0068	0.0010	0.8743	0.0010	0.9958	0.0042
NMonOut1	0.5988	0.0167	0.0013	0.2422	0.1410	0.6751	0.3249
NMonOut2	0.1353	0.0099	0.0058	0.8432	0.0058	0.9791	0.0209
NMonOut2	0.4604	0.0321	0.0049	0.3187	0.1838	0.5106	0.4894

	NMono	0.0667	0.0886	0.0007	0.8433	0.0007	0.9714	0.0286
	NMono	0.3161	0.0461	0.0004	0.2157	0.4217	0.5561	0.4439
	NPleo1	0.0000	0.0001	0.0000	0.9999	0.0000	1.0000	0.0000
	NPleo1	0.4079	0.0103	0.0003	0.3344	0.2471	0.9997	0.0003
	NStrig1	0.0015	0.0621	0.0015	0.9335	0.0015	0.9993	0.0007
	NStrig1	0.4143	0.1166	0.0022	0.1966	0.2704	0.9441	0.0559
	NStrig2	0.0015	0.8983	0.0015	0.0972	0.0015	0.9817	0.0183
	NStrig2	0.3947	0.2499	0.0032	0.1555	0.1966	0.7790	0.2210
	NStrig3	0.0004	0.9905	0.0004	0.0083	0.0004	0.2760	0.7240
	NStrig3	0.3960	0.2461	0.0031	0.1554	0.1994	0.6783	0.3217
	NStrig4	0.0000	0.0000	0.0000	0.0000	0.0000	0.2698	0.7302
	NStrig4	0.4060	0.2197	0.0045	0.1620	0.2078	0.6936	0.3064
	NStrig5	0.0001	0.9994	0.0001	0.0003	0.0001	0.0039	0.9961
	NStrig5	0.0136	0.8379	0.0056	0.0043	0.1386	0.0006	0.9994
	NStrig6	0.0000	0.9997	0.0000	0.0002	0.0000	0.0027	0.9973
	NStrig6	0.0068	0.8697	0.0030	0.0017	0.1189	0.0002	0.9998
	NStrig7	0.0000	0.9999	0.0000	0.0000	0.0000	0.0002	0.9998
	NStrig7	0.0088	0.8588	0.0037	0.0024	0.1262	0.0003	0.9997
	NStrig8	0.0000	0.9999	0.0000	0.0000	0.0000	0.0000	1.0000
	NStrig8	0.0060	0.8805	0.0027	0.0016	0.1092	0.0003	0.9997
	NADM01	0.0009	0.9527	0.0009	0.0446	0.0009	0.9995	0.0005
	NADM01	0.0770	0.6047	0.0103	0.0539	0.2542	0.9982	0.0018
	NADM02	0.0001	0.9990	0.0001	0.0007	0.0001	1.0000	0.0000
	NADM02	0.0118	0.8381	0.0049	0.0032	0.1420	0.9993	0.0007
	NADM03	0.0001	0.9997	0.0001	0.0001	0.0001	1.0000	0.0000
	NADM03	0.0209	0.7975	0.0082	0.0068	0.1665	0.9980	0.0020
NODE 4	**NADM04**	**0.0024**	**0.9346**	**0.0024**	**0.0581**	**0.0024**	**0.9999**	**0.0001**

	NADM04	**0.1436**	**0.2986**	**0.0099**	**0.1806**	**0.3672**	**0.9949**	**0.0051**
	NADM05	0.0023	0.0207	0.0023	0.9723	0.0023	0.9999	0.0001
	NADM05	0.0456	0.0056	0.0007	0.8113	0.1367	0.9980	0.0020
	NADM06	0.0001	0.9995	0.0001	0.0003	0.0001	1.0000	0.0000
	NADM06	0.0072	0.8212	0.0022	0.0020	0.1673	0.9997	0.0003
	NADM07	0.0000	0.9998	0.0000	0.0001	0.0000	1.0000	0.0000
	NADM07	0.0152	0.8219	0.0061	0.0047	0.1521	0.9986	0.0014
NODE 5	**NADM08**	**0.0000**	**1.0000**	**0.0000**	**0.0000**	**0.0000**	**1.0000**	**0.0000**
	NADM08	**0.0071**	**0.6762**	**0.0010**	**0.0019**	**0.3138**	**0.9998**	**0.0002**
	NADM11	0.0000	1.0000	0.0000	0.0000	0.0000	1.0000	0.0000
	NADM11	0.0115	0.3777	0.0007	0.0029	0.6072	0.9998	0.0002
	NADM12	1.0000	0.0000	0.0000	0.0000	0.0000	1.0000	0.0000
	NADM12	0.0112	0.1489	0.0006	0.0025	0.8369	0.9999	0.0001
	NADM09	0.0000	1.0000	0.0000	0.0000	0.0000	1.0000	0.0000
	NADM09	0.0024	0.9275	0.0012	0.0006	0.0682	0.9998	0.0002
	NADM10	0.0000	0.0000	0.0000	0.0000	0.0000	1.0000	0.0000
	NADM10	0.0000	0.9977	0.0000	0.0000	0.0022	1.0000	0.0000
	NPleo2	0.0000	0.0001	0.0000	0.9996	0.0003	1.0000	0.0000
	NPleo2	0.0325	0.0023	0.0001	0.6110	0.3541	0.9998	0.0002
	NMyti1	0.0006	0.0045	0.0006	0.9731	0.0213	1.0000	0.0000
	NMyti1	0.0798	0.0143	0.0003	0.2057	0.6999	0.9995	0.0005
	NMyti2	0.0051	0.0867	0.0051	0.4664	0.4367	1.0000	0.0000
	NMyti2	0.0708	0.0330	0.0004	0.0321	0.8637	0.9995	0.0005
	NMyti3	0.0003	0.9093	0.0003	0.0873	0.0028	1.0000	0.0000
	NMyti3	0.0597	0.1304	0.0001	0.0195	0.7903	1.0000	0.0000
	NHyster	0.0000	0.0000	0.0000	1.0000	0.0000	1.0000	0.0000
	NHyster	0.0009	0.0001	0.0000	0.9739	0.0251	1.0000	0.0000

	NPleo3	0.0000	0.0000	0.0000	1.0000	0.0000	1.0000	0.0000
	NPleo3	0.0107	0.0006	0.0001	0.9090	0.0796	0.9998	0.0002
	NDicty1	0.0000	0.0000	0.0000	0.9999	0.0000	1.0000	0.0000
	NDicty1	0.0071	0.0007	0.0001	0.9214	0.0708	0.9997	0.0003
	NDicty2	0.0000	0.0000	0.0000	1.0000	0.0000	1.0000	0.0000
	NDicty2	0.0015	0.0002	0.0000	0.9790	0.0192	0.9999	0.0001
	NPleo4	0.0000	0.0000	0.0000	1.0000	0.0000	1.0000	0.0000
	NPleo4	0.0006	0.0000	0.0000	0.9779	0.0215	1.0000	0.0000
NODE 6	**NMVP**	**0.0032**	**0.9815**	**0.0003**	**0.0147**	**0.0003**	**1.0000**	**0.0000**
	NMVP	**0.1307**	**0.4321**	**0.0096**	**0.1142**	**0.3135**	**0.9998**	**0.0002**
	NVent1	0.0002	0.9963	0.0000	0.0034	0.0000	1.0000	0.0000
	NVent1	0.0602	0.4073	0.0070	0.0960	0.4295	0.9995	0.0005
	NStom1	0.0000	0.9996	0.0000	0.0003	0.0000	1.0000	0.0000
	NStom1	0.0134	0.8421	0.0056	0.0043	0.1346	0.9987	0.0013
	NStom2	0.0000	1.0000	0.0000	0.0000	0.0000	1.0000	0.0000
	NStom2	0.0009	0.9566	0.0005	0.0002	0.0417	0.9999	0.0001
	NVent2	0.0001	0.9872	0.0001	0.0124	0.0001	1.0000	0.0000
	NVent2	0.0418	0.1816	0.0097	0.3249	0.4422	0.9999	0.0001
	NVent3	0.0000	0.0000	0.0000	0.0000	0.0000	1.0000	0.0000
	NVent3	0.1463	0.1003	0.1071	0.3883	0.2581	0.9990	0.0010
	NMThyrX	0.0000	0.0000	0.0000	0.0000	0.0000	1.0000	0.0000
	NMThyrX	0.1613	0.3755	0.0167	0.1436	0.3030	0.9996	0.0004
	NPhaeo	0.0000	0.0000	0.0000	0.0000	0.0000	1.0000	0.0000
	NPhaeo	0.1485	0.1985	0.0420	0.3270	0.2840	0.9997	0.0003
NODE 7	**NMThyr1**	**0.0021**	**0.9842**	**0.0004**	**0.0130**	**0.0004**	**1.0000**	**0.0000**
	NMThyr1	**0.1687**	**0.4273**	**0.0126**	**0.1141**	**0.2773**	**0.9986**	**0.0014**
	NMThyr2	0.0005	0.9959	0.0004	0.0028	0.0004	1.0000	0.0000

NMThyr2	0.1244	0.5303	0.0146	0.0854	0.2453	0.9977	0.0023
NMThyr3	0.0010	0.9955	0.0010	0.0014	0.0010	0.9998	0.0002
NMThyr3	0.0696	0.6636	0.0254	0.0317	0.2097	0.9932	0.0068
NMThyr4	0.0007	0.9973	0.0007	0.0007	0.0007	0.9999	0.0001
NMThyr4	0.0582	0.6950	0.0207	0.0248	0.2014	0.9933	0.0067
NMTSup	0.0008	0.9914	0.0008	0.0062	0.0008	1.0000	0.0000
NMTSup	0.1627	0.3507	0.0095	0.1835	0.2935	0.9991	0.0009
NMThyr5	0.0000	0.0000	0.0000	0.0000	0.0000	1.0000	0.0000
NMThyr5	0.1773	0.3159	0.0224	0.1908	0.2936	0.9954	0.0046
NMThyr6	0.0022	0.9720	0.0022	0.0215	0.0022	1.0000	0.0000
NMThyr6	0.1348	0.3031	0.0092	0.1801	0.3728	0.9959	0.0041
NHelio	0.0001	0.0011	0.0001	0.9985	0.0001	1.0000	0.0000
NHelio	0.0030	0.0003	0.0000	0.9521	0.0446	0.9999	0.0001
NZelo1	0.0060	0.9551	0.0048	0.0294	0.0048	0.9998	0.0002
NZelo1	0.2032	0.3003	0.0214	0.1960	0.2791	0.9804	0.0196
NNati	0.0022	0.0084	0.0022	0.9850	0.0022	0.9999	0.0001
NNati	0.0489	0.0054	0.0007	0.8070	0.1380	0.9983	0.0017
NZelo2	1.0000	0.0000	0.0000	0.0000	0.0000	1.0000	0.0000
NZelo2	0.0035	0.9020	0.0006	0.0020	0.0919	0.9999	0.0001
NZelo3	0.0000	1.0000	0.0000	0.0000	0.0000	1.0000	0.0000
NZelo3	0.0147	0.8115	0.0023	0.0129	0.1586	0.9999	0.0001
NZelo4	0.0000	1.0000	0.0000	0.0000	0.0000	1.0000	0.0000
NZelo4	0.0001	0.9957	0.0000	0.0000	0.0042	1.0000	0.0000
NZelo5	0.0000	0.0000	0.0000	0.0000	0.0000	1.0000	0.0000
NZelo5	0.1339	0.2845	0.0228	0.2208	0.3379	0.9997	0.0003
NZelo6	0.0000	0.0000	0.0000	0.0000	0.0000	1.0000	0.0000
NZelo6	0.1056	0.4064	0.0484	0.1250	0.3147	0.9999	0.0001

NODE 8	**NAulo1**	**0.0202**	**0.9459**	**0.0108**	**0.0123**	**0.0108**	**0.9990**	**0.0010**
	NAulo1	**0.0753**	**0.6522**	**0.0264**	**0.0356**	**0.2105**	**0.9903**	**0.0097**
	NLembo	0.0001	0.9998	0.0001	0.0001	0.0001	1.0000	0.0000
	NLembo	0.0021	0.9362	0.0010	0.0005	0.0602	0.9998	0.0002
	NAulo2	0.0000	1.0000	0.0000	0.0000	0.0000	1.0000	0.0000
	NAulo2	0.0005	0.9703	0.0003	0.0001	0.0288	1.0000	0.0000
	NAstx01	0.0072	0.9816	0.0086	0.0020	0.0006	1.0000	0.0000
	NAstx01	0.0170	0.5106	0.2444	0.0048	0.2232	0.9998	0.0002
NODE 9	**NAstx02**	**0.0042**	**0.9845**	**0.0096**	**0.0012**	**0.0004**	**1.0000**	**0.0000**
	NAstx02	**0.0197**	**0.4694**	**0.2689**	**0.0064**	**0.2356**	**0.9998**	**0.0002**
	NMelas01	0.0043	0.8716	0.1188	0.0028	0.0025	1.0000	0.0000
	NMelas01	0.0472	0.1456	0.5365	0.0351	0.2356	0.9990	0.0010
	NMelas02	0.0003	0.0109	0.9883	0.0003	0.0003	1.0000	0.0000
	NMelas02	0.0003	0.0003	0.9955	0.0002	0.0036	0.9995	0.0005
	NMelas03	0.0000	0.0004	0.9996	0.0000	0.0000	1.0000	0.0000
	NMelas03	0.0003	0.0003	0.9955	0.0002	0.0036	0.9995	0.0005
	NMelas04	0.0000	0.0000	1.0000	0.0000	0.0000	1.0000	0.0000
	NMelas04	0.0003	0.0003	0.9956	0.0002	0.0036	0.9995	0.0005
	NMelas05	0.0000	0.0000	1.0000	0.0000	0.0000	1.0000	0.0000
	NMelas05	0.0001	0.0000	0.9985	0.0001	0.0013	0.9998	0.0002
	NMelas06	0.0000	0.0000	1.0000	0.0000	0.0000	1.0000	0.0000
	NMelas06	0.0001	0.0000	0.9983	0.0001	0.0015	0.9998	0.0002
	NMelas07	0.0000	0.0000	1.0000	0.0000	0.0000	1.0000	0.0000
	NMelas07	0.0000	0.0000	0.9991	0.0000	0.0008	0.9999	0.0001
	NMelas08	0.0000	0.0000	1.0000	0.0000	0.0000	1.0000	0.0000
	NMelas08	0.0002	0.0001	0.9972	0.0002	0.0022	0.9994	0.0006
	NMelas09	0.0000	0.0000	1.0000	0.0000	0.0000	1.0000	0.0000

	NMelas09	0.0003	0.0003	0.9955	0.0002	0.0036	0.9995	0.0005
	NMelas10	0.0000	0.0000	1.0000	0.0000	0.0000	1.0000	0.0000
	NMelas10	0.0001	0.0001	0.9982	0.0001	0.0016	0.9997	0.0003
	NMelas11	0.0000	0.0000	1.0000	0.0000	0.0000	1.0000	0.0000
	NMelas11	0.0000	0.0000	0.9995	0.0000	0.0004	0.9999	0.0001
	NMelas12	0.0000	0.0000	1.0000	0.0000	0.0000	1.0000	0.0000
	NMelas12	0.0001	0.0000	0.9989	0.0001	0.0009	0.9998	0.0002
	NMelas13	0.0008	0.0008	0.9969	0.0008	0.0008	0.9998	0.0002
	NMelas13	0.0029	0.0018	0.9844	0.0028	0.0081	0.9932	0.0068
	NAstx03	0.0007	0.9974	0.0015	0.0003	0.0002	1.0000	0.0000
	NAstx03	0.0314	0.7018	0.0745	0.0119	0.1805	0.9974	0.0026
NODE 10	**NAstx04**	**0.0000**	**1.0000**	**0.0000**	**0.0000**	**0.0000**	**1.0000**	**0.0000**
	NAstx04	**0.0014**	**0.9375**	**0.0008**	**0.0003**	**0.0600**	**0.9999**	**0.0001**
	NAstx05	0.0000	0.9998	0.0002	0.0000	0.0000	1.0000	0.0000
	NAstx05	0.0074	0.7079	0.0779	0.0029	0.2040	0.9999	0.0001
	NAstx06	0.0000	0.9995	0.0004	0.0001	0.0000	1.0000	0.0000
	NAstx06	0.0271	0.4827	0.1078	0.0228	0.3596	0.9996	0.0004
	NAstx07	0.0001	0.9994	0.0002	0.0001	0.0001	1.0000	0.0000
	NAstx07	0.0338	0.7699	0.0131	0.0116	0.1716	0.9981	0.0019
	NAstx08	0.0000	1.0000	0.0000	0.0000	0.0000	1.0000	0.0000
	NAstx08	0.0009	0.9583	0.0005	0.0002	0.0400	0.9999	0.0001
	NAstx09	0.0002	0.9991	0.0002	0.0002	0.0002	1.0000	0.0000
	NAstx09	0.0434	0.7403	0.0162	0.0170	0.1830	0.9961	0.0039
	NAstx10	0.0000	1.0000	0.0000	0.0000	0.0000	1.0000	0.0000
	NAstx10	0.0009	0.9739	0.0005	0.0002	0.0246	0.9999	0.0001
	NAstx11	0.0001	0.9892	0.0088	0.0018	0.0001	1.0000	0.0000
	NAstx11	0.0370	0.2802	0.1470	0.0672	0.4686	0.9997	0.0003

	NAstx14	0.0093	0.8117	0.0157	0.1540	0.0093	0.9999	0.0001
	NAstx14	0.1162	0.1279	0.0443	0.4173	0.2943	0.9904	0.0096
	NAstx15	0.0850	0.6331	0.0861	0.1109	0.0850	0.9867	0.0133
	NAstx15	0.1483	0.4659	0.0527	0.1020	0.2310	0.9575	0.0425
	NAstx12	0.0001	0.9777	0.0214	0.0007	0.0001	1.0000	0.0000
	NAstx12	0.0104	0.3488	0.3489	0.0072	0.2847	0.9999	0.0001
	NAstx13	0.0008	0.1594	0.8380	0.0009	0.0008	1.0000	0.0000
	NAstx13	0.0019	0.0374	0.9102	0.0021	0.0483	0.9994	0.0006
CHARACTERS		**Sporocarp Type**				**Lower Wall**		
	State	**Apothecioid**	**Perithecioid**	**Thyriothecioid**	**Cleistothecioid**	**Undifferen-tiated**	**Differen-tiated**	
Labelled in Fig.1	**Node/StateCode**	0	1	2	3	0	1	
	NLeotio	0.9728	0.0004	0.0004	0.0265	0.0000	0.0000	
	NLeotio	0.2062	0.0198	0.1056	0.6684	0.8973	0.1027	
	NEuroAll	0.4949	0.2823	0.0134	0.2094	0.0003	0.9997	
	NEuroAll	0.0942	0.4345	0.0216	0.4497	0.3058	0.6942	
	NOnyEuro	0.0160	0.0098	0.0019	0.9722	0.0004	0.9996	
	NOnyEuro	0.0255	0.0454	0.0145	0.9146	0.1691	0.8309	
	NEuro1	0.0001	0.0001	0.0000	0.9998	0.0000	1.0000	
	NEuro1	0.0015	0.0040	0.0007	0.9938	0.0319	0.9681	
	NEuro2	0.0000	0.0000	0.0000	1.0000	0.0000	1.0000	
	NEuro2	0.0012	0.0033	0.0006	0.9948	0.0283	0.9717	
	NEuro3	0.0000	0.0000	0.0000	1.0000	0.0000	1.0000	
	NEuro3	0.0033	0.0074	0.0017	0.9876	0.0504	0.9496	
	NPyrVeChae	0.0221	0.9691	0.0014	0.0073	0.0003	0.9997	

NPyrVeChae	0.0609	0.8075	0.0050	0.1266	0.2390	0.7610
NPyren	0.0027	0.9956	0.0005	0.0011	0.0009	0.9991
NPyren	0.0665	0.7783	0.0124	0.1428	0.2741	0.7259
NVerChae	0.0079	0.9915	0.0002	0.0005	0.0001	0.9999
NVerChae	0.0964	0.7598	0.0037	0.1402	0.1720	0.8280
NVerru	0.0260	0.9726	0.0006	0.0007	0.0001	0.9999
NVerru	0.3850	0.4376	0.0062	0.1711	0.0727	0.9273
NCthyrL	0.0000	1.0000	0.0000	0.0000	0.0000	1.0000
NCthyrL	0.0151	0.8741	0.0009	0.1099	0.2110	0.7890
NHerpo1	0.0000	1.0000	0.0000	0.0000	0.0000	1.0000
NHerpo1	0.0011	0.9916	0.0001	0.0072	0.0120	0.9880
NHerpo2	0.0000	1.0000	0.0000	0.0000	0.0000	1.0000
NHerpo2	0.0048	0.9718	0.0006	0.0228	0.0383	0.9617
NCthyr01	0.0000	0.0000	0.0000	0.0000	0.0000	0.0000
NCthyr01	0.1187	0.4950	0.0120	0.3744	0.6046	0.3954
NCthyr02	0.0000	1.0000	0.0000	0.0000	0.0000	1.0000
NCthyr02	0.0378	0.7131	0.0173	0.2318	0.3964	0.6036
NCthyr03	0.0000	1.0000	0.0000	0.0000	0.0000	0.0000
NCthyr03	0.1508	0.2329	0.2545	0.3618	0.6078	0.3922
NCthyr04	0.0000	1.0000	0.0000	0.0000	0.0000	1.0000
NCthyr04	0.0018	0.9881	0.0002	0.0099	0.0158	0.9842
NCthyr05	0.0000	1.0000	0.0000	0.0000	0.0000	1.0000
NCthyr05	0.0319	0.8206	0.0179	0.1295	0.2559	0.7441
NCthyr06	0.0000	1.0000	0.0000	0.0000	0.0000	1.0000
NCthyr06	0.0612	0.7166	0.0474	0.1748	0.3494	0.6506
NCthyr07	0.0000	1.0000	0.0000	0.0000	0.0000	0.0000
NCthyr07	0.1717	0.2435	0.3079	0.2769	0.6114	0.3886

NLecano	1.0000	0.0000	0.0000	0.0000	0.0000	1.0000
NLecano	0.9210	0.0145	0.0007	0.0637	0.0809	0.9191
NLeca1	0.9996	0.0003	0.0000	0.0001	0.0001	0.9999
NLeca1	0.7509	0.1060	0.0058	0.1373	0.1538	0.8462
NLeca2	0.9963	0.0034	0.0002	0.0002	0.0000	1.0000
NLeca2	0.7104	0.1325	0.0049	0.1522	0.1246	0.8754
NLeca3	0.9992	0.0007	0.0001	0.0001	0.0001	0.9999
NLeca3	0.9252	0.0135	0.0033	0.0580	0.1498	0.8502
NUAO	1.0000	0.0000	0.0000	0.0000	0.0000	1.0000
NUAO	0.9738	0.0025	0.0006	0.0231	0.0928	0.9072
NUmbi1	1.0000	0.0000	0.0000	0.0000	0.0000	1.0000
NUmbi1	0.9270	0.0115	0.0036	0.0579	0.1653	0.8347
NUmbi2	0.9996	0.0001	0.0001	0.0001	0.0004	0.9996
NUmbi2	0.8596	0.0321	0.0137	0.0946	0.2180	0.7820
NOstropo	1.0000	0.0000	0.0000	0.0000	0.0000	1.0000
NOstropo	0.9727	0.0022	0.0006	0.0245	0.1137	0.8863
NMpeltout1	1.0000	0.0000	0.0000	0.0000	0.0001	0.9999
NMpeltout1	0.9081	0.0072	0.0067	0.0780	0.2513	0.7487
NMpeltout2	0.9999	0.0000	0.0000	0.0000	0.0001	0.9999
NMpeltout2	0.9397	0.0088	0.0030	0.0484	0.1182	0.8818
NMpeltout3	0.9997	0.0000	0.0003	0.0000	0.0007	0.9993
NMpeltout3	0.6677	0.0433	0.0836	0.2054	0.4741	0.5259
NMpeltout4	0.9997	0.0001	0.0001	0.0001	0.0005	0.9995
NMpeltout4	0.7854	0.0345	0.0370	0.1430	0.3454	0.6546
NMpeltout5	0.9912	0.0005	0.0077	0.0005	0.0115	0.9885
NMpeltout5	0.4479	0.0724	0.2470	0.2327	0.5610	0.4390
NMpelt1	0.0038	0.0003	0.9957	0.0003	0.9933	0.0067

	NMpelt1	0.0008	0.0022	0.9815	0.0155	0.9793	0.0207
	NMpelt2	0.0004	0.0001	0.9995	0.0001	0.9990	0.0010
	NMpelt2	0.0026	0.0063	0.9636	0.0275	0.9599	0.0401
	NMpelt3	0.0002	0.0000	0.9997	0.0000	0.9993	0.0007
	NMpelt3	0.0024	0.0059	0.9643	0.0275	0.9628	0.0372
	NOstro1	0.9995	0.0003	0.0001	0.0001	0.0005	0.9995
	NOstro1	0.9021	0.0164	0.0050	0.0764	0.3158	0.6842
	NOstro2	0.9998	0.0001	0.0001	0.0001	0.0002	0.9998
	NOstro2	0.9525	0.0064	0.0022	0.0389	0.0962	0.9038
	NOstro3	0.9997	0.0001	0.0001	0.0001	0.0000	0.0000
	NOstro3	0.8639	0.0282	0.0109	0.0970	0.3977	0.6023
	NOstro4	1.0000	0.0000	0.0000	0.0000	0.0000	0.0000
	NOstro4	0.9954	0.0004	0.0001	0.0041	0.8314	0.1686
	NOstro5	1.0000	0.0000	0.0000	0.0000	0.0000	0.0000
	NOstro5	0.9977	0.0002	0.0001	0.0020	0.8134	0.1866
	NOstro6	1.0000	0.0000	0.0000	0.0000	0.0000	0.0000
	NOstro6	0.9991	0.0001	0.0000	0.0008	0.8088	0.1912
NODE 1	**NDothArTry**	**0.9998**	**0.0002**	**0.0000**	**0.0000**	**0.0000**	**1.0000**
	NDothArTry	**0.6743**	**0.0486**	**0.0006**	**0.2764**	**0.4036**	**0.5964**
	NArthTryp	0.9984	0.0013	0.0002	0.0002	0.0001	0.9999
	NArthTryp	0.6180	0.0854	0.0134	0.2832	0.4522	0.5478
	NTryp1	0.0703	0.9104	0.0096	0.0096	0.0046	0.9954
	NTryp1	0.1352	0.6348	0.0271	0.2030	0.4078	0.5922
	NTryp2	0.0010	0.9979	0.0005	0.0005	0.0011	0.9989
	NTryp2	0.0210	0.9074	0.0032	0.0684	0.1255	0.8745
	NTryp3	0.0177	0.9748	0.0038	0.0038	0.0034	0.9966
	NTryp3	0.1243	0.6505	0.0294	0.1958	0.3728	0.6272

NTryp4	0.0002	0.9994	0.0002	0.0002	0.0005	0.9995
NTryp4	0.0135	0.9339	0.0019	0.0508	0.0909	0.9091
NArtho01	1.0000	0.0000	0.0000	0.0000	0.0000	1.0000
NArtho01	0.6989	0.0242	0.0082	0.2688	0.4416	0.5584
NArtho02	0.0000	0.0000	0.0000	0.0000	0.0000	0.0000
NArtho02	0.3148	0.0985	0.0666	0.5201	0.5505	0.4495
NSeurat	0.9999	0.0000	0.0000	0.0000	0.0001	0.9999
NSeurat	0.6915	0.0444	0.0272	0.2368	0.3084	0.6916
NArthRock	0.0000	0.0000	0.0000	0.0000	0.0000	0.0000
NArthRock	0.0693	0.1590	0.2168	0.5549	0.7303	0.2697
NArtho03	0.9999	0.0000	0.0000	0.0000	0.0017	0.9983
NArtho03	0.9147	0.0104	0.0035	0.0714	0.3456	0.6544
NArtho04	0.9995	0.0002	0.0002	0.0002	0.0006	0.9994
NArtho04	0.9283	0.0113	0.0040	0.0564	0.1390	0.8610
NArtho05	1.0000	0.0000	0.0000	0.0000	0.0082	0.9918
NArtho05	0.9443	0.0079	0.0026	0.0453	0.3703	0.6297
NArtho06	0.9998	0.0001	0.0001	0.0001	0.0000	0.0000
NArtho06	0.9461	0.0077	0.0026	0.0436	0.9550	0.0450
NArtho07	1.0000	0.0000	0.0000	0.0000	0.0004	0.9996
NArtho07	0.9617	0.0042	0.0011	0.0330	0.1833	0.8167
NArtho08	0.9999	0.0000	0.0000	0.0000	0.0001	0.9999
NArtho08	0.9419	0.0107	0.0041	0.0433	0.1044	0.8956
NArtho09	0.9999	0.0000	0.0000	0.0000	0.0003	0.9997
NArtho09	0.9169	0.0134	0.0043	0.0654	0.3563	0.6437
NArtho10	0.9988	0.0004	0.0004	0.0004	0.0000	0.0000
NArtho10	0.7858	0.0551	0.0242	0.1348	0.5543	0.4457
NArtho11	1.0000	0.0000	0.0000	0.0000	0.0000	1.0000

NArtho11	0.9337	0.0097	0.0030	0.0537	0.2956	0.7044
NArtho12	0.9999	0.0000	0.0000	0.0000	0.0001	0.9999
NArtho12	0.9129	0.0147	0.0053	0.0672	0.1662	0.8338
NArtho13	0.9997	0.0001	0.0001	0.0001	0.0002	0.9998
NArtho13	0.9096	0.0172	0.0066	0.0667	0.3740	0.6260
NArtho14	1.0000	0.0000	0.0000	0.0000	0.0000	0.0000
NArtho14	0.9903	0.0009	0.0003	0.0085	0.3868	0.6132
NArtho15	1.0000	0.0000	0.0000	0.0000	0.0000	0.0000
NArtho15	0.9942	0.0005	0.0002	0.0051	0.3580	0.6420
NDothid	0.9950	0.0050	0.0000	0.0000	0.0000	1.0000
NDothid	0.6352	0.0746	0.0007	0.2895	0.4191	0.5809
NPate	1.0000	0.0000	0.0000	0.0000	0.0000	1.0000
NPate	0.9793	0.0021	0.0006	0.0180	0.0507	0.9493
NAbro1	0.9998	0.0002	0.0000	0.0000	0.0000	1.0000
NAbro1	0.6657	0.2563	0.0014	0.0766	0.0107	0.9893
NAbro2	1.0000	0.0000	0.0000	0.0000	0.0000	1.0000
NAbro2	0.9941	0.0007	0.0001	0.0051	0.0121	0.9879
NTube1	0.0000	0.0000	0.0000	0.0000	0.0000	1.0000
NTube1	0.3489	0.4802	0.0149	0.1560	0.5234	0.4766
NTube2	0.0001	0.9999	0.0000	0.0000	0.0000	1.0000
NTube2	0.0098	0.9512	0.0014	0.0377	0.0670	0.9330
NBotry1	0.0000	1.0000	0.0000	0.0000	0.0000	0.0000
NBotry1	0.0018	0.9872	0.0002	0.0108	0.0175	0.9825
NBotry2	0.0000	1.0000	0.0000	0.0000	0.0000	0.0000
NBotry2	0.0025	0.9841	0.0003	0.0130	0.0212	0.9788
NBotry3	0.0000	1.0000	0.0000	0.0000	0.0000	1.0000
NBotry3	0.0002	0.9988	0.0000	0.0011	0.0016	0.9984

	NCapnodX	0.0001	0.9999	0.0000	0.0000	0.0000	1.0000
	NCapnodX	0.2386	0.2392	0.0011	0.5212	0.6538	0.3462
	NDothi1	0.0000	0.0000	0.0000	0.0000	0.0000	0.0000
	NDothi1	0.2317	0.4809	0.0398	0.2476	0.4685	0.5315
	NMyri1	0.0000	0.0000	0.0000	0.0000	0.0000	0.0000
	NMyri1	0.2857	0.3542	0.0178	0.3423	0.3663	0.6337
	NMyri2	0.0000	1.0000	0.0000	0.0000	0.0000	1.0000
	NMyri2	0.0065	0.9640	0.0008	0.0287	0.0501	0.9499
	NCapnod0	0.0000	0.0000	0.0000	0.0000	0.0000	1.0000
	NCapnod0	0.2302	0.2341	0.0095	0.5263	0.5639	0.4361
	NCapnod1	0.0000	0.0000	0.0000	0.0000	0.0000	0.0000
	NCapnod1	0.2164	0.2561	0.0090	0.5186	0.6004	0.3996
	NCapnod2	0.0000	0.0000	0.0000	0.0000	0.0000	0.0000
	NCapnod2	0.4678	0.0766	0.0841	0.3714	0.6384	0.3616
	NCapnod3	0.0000	1.0000	0.0000	0.0000	0.0000	1.0000
	NCapnod3	0.0631	0.5025	0.0134	0.4210	0.5623	0.4377
	NCapnod4	0.0000	0.9996	0.0004	0.0000	0.0006	0.9994
	NCapnod4	0.0387	0.6625	0.0428	0.2560	0.3759	0.6241
NODE 2	**NCapnod5**	**0.0000**	**1.0000**	**0.0000**	**0.0000**	**0.0000**	**1.0000**
	NCapnod5	**0.0843**	**0.4501**	**0.0147**	**0.4509**	**0.6483**	**0.3517**
	NAsteOut1	0.0000	0.0000	0.0000	0.0000	0.0000	0.0000
	NAsteOut1	0.1364	0.3882	0.0527	0.4227	0.6277	0.3723
	NAsteOut2	0.0000	0.9997	0.0002	0.0000	0.0001	0.9999
	NAsteOut2	0.1238	0.3917	0.1993	0.2852	0.5430	0.4570
	NAsteOut3	0.0000	0.0000	0.0000	0.0000	0.0000	0.0000
	NAsteOut3	0.1878	0.5808	0.0416	0.1897	0.3493	0.6507
	NAsteOut4	0.0000	1.0000	0.0000	0.0000	0.0000	1.0000

	NAsteOut4	0.0107	0.9654	0.0007	0.0232	0.0422	0.9578
	NAste1	0.0033	0.0515	0.9420	0.0033	0.3583	0.6417
	NAste1	0.0207	0.0293	0.7963	0.1537	0.8089	0.1911
NODE 3	**NAste2**	**0.0000**	**0.0000**	**1.0000**	**0.0000**	**0.9728**	**0.0272**
	NAste2	**0.0377**	**0.0157**	**0.7250**	**0.2217**	**0.9574**	**0.0426**
	NAste3	0.0000	0.0000	1.0000	0.0000	0.9998	0.0002
	NAste3	0.0002	0.0006	0.9939	0.0052	0.9947	0.0053
	NAste4	0.0000	0.0000	1.0000	0.0000	0.9999	0.0001
	NAste4	0.0014	0.0036	0.9761	0.0188	0.9763	0.0237
	NAste5	0.0000	0.0000	1.0000	0.0000	1.0000	0.0000
	NAste5	0.0001	0.0003	0.9971	0.0024	0.9978	0.0022
	NAste6	0.0000	0.0000	0.0000	0.0000	0.0000	0.0000
	NAste6	0.4064	0.0599	0.1017	0.4319	0.6872	0.3128
	NAste7	0.0000	0.0000	0.0000	0.0000	0.0000	0.0000
	NAste7	0.4126	0.0596	0.0857	0.4421	0.6797	0.3203
	NAste8	0.0000	0.0000	0.0000	0.0000	0.0000	0.0000
	NAste8	0.4426	0.0664	0.1265	0.3645	0.6514	0.3486
	NCapno01	0.0000	1.0000	0.0000	0.0000	0.0000	1.0000
	NCapno01	0.0589	0.5166	0.0004	0.4240	0.6855	0.3145
	NCapno02	0.0000	1.0000	0.0000	0.0000	0.0000	1.0000
	NCapno02	0.0211	0.8748	0.0024	0.1017	0.1876	0.8124
	NCapno03	0.0000	1.0000	0.0000	0.0000	0.0000	1.0000
	NCapno03	0.0008	0.9942	0.0001	0.0049	0.0078	0.9922
	NCapno04	0.0000	1.0000	0.0000	0.0000	0.0000	1.0000
	NCapno04	0.0021	0.9864	0.0003	0.0113	0.0184	0.9816
	NCapno05	0.0000	1.0000	0.0000	0.0000	0.0000	1.0000
	NCapno05	0.0005	0.9967	0.0001	0.0028	0.0042	0.9958

NCapno06	0.0000	1.0000	0.0000	0.0000	0.0000	1.0000
NCapno06	0.0001	0.9994	0.0000	0.0005	0.0007	0.9993
NCapno07	0.0000	1.0000	0.0000	0.0000	0.0000	1.0000
NCapno07	0.1426	0.3428	0.0017	0.5130	0.9210	0.0790
NTerato01	0.0000	1.0000	0.0000	0.0000	0.0000	0.0000
NTerato01	0.1105	0.4134	0.0034	0.4727	0.8709	0.1291
NTerato02	0.0000	0.0000	0.0000	0.0000	0.0000	0.0000
NTerato02	0.2680	0.3125	0.0700	0.3495	0.7065	0.2935
NTerato03	0.0000	1.0000	0.0000	0.0000	0.0000	0.0000
NTerato03	0.0945	0.4387	0.0010	0.4657	0.8307	0.1693
NTerato04	0.0000	0.0000	0.0000	0.0000	0.0000	0.0000
NTerato04	0.2055	0.4918	0.0316	0.2710	0.7654	0.2346
NTerato05	0.0000	0.9999	0.0001	0.0000	0.0000	1.0000
NTerato05	0.1274	0.3610	0.0024	0.5092	0.7820	0.2180
NTerato06	0.0001	0.9884	0.0113	0.0002	0.0000	0.0000
NTerato06	0.2536	0.3974	0.0458	0.3033	0.5291	0.4709
NTerato07	0.0000	0.0000	0.0000	0.0000	0.0000	0.0000
NTerato07	0.1615	0.2570	0.0099	0.5717	0.8286	0.1714
NTerato08	0.0001	0.9976	0.0002	0.0021	0.0000	0.0000
NTerato08	0.0967	0.5038	0.0111	0.3883	0.7248	0.2752
NTerato09	0.0000	0.0000	0.0000	0.0000	0.0000	0.0000
NTerato09	0.2257	0.1038	0.0725	0.5979	0.5788	0.4212
NTerato10	0.0000	0.0000	0.0000	0.0000	0.0000	0.0000
NTerato10	0.3271	0.0952	0.0608	0.5169	0.7712	0.2288
NTerato11	0.0000	0.0000	0.0000	0.0000	0.0000	0.0000
NTerato11	0.3458	0.1039	0.1123	0.4380	0.7348	0.2652
NCapnod6	0.0014	0.9969	0.0016	0.0001	0.0002	0.9998

NCapnod6	0.3581	0.1686	0.0379	0.4354	0.7573	0.2427
NSchiz	0.2102	0.5450	0.2397	0.0051	0.0166	0.9834
NSchiz	0.3496	0.0438	0.3865	0.2200	0.6609	0.3391
NMcspha1	0.0000	0.0000	0.0000	0.0000	0.0000	0.0000
NMcspha1	0.2627	0.2984	0.0060	0.4329	0.7070	0.2930
NMcspha2	0.0000	0.0000	0.0000	0.0000	0.0000	0.0000
NMcspha2	0.4018	0.0941	0.0547	0.4495	0.7818	0.2182
NMcspha3	0.0000	0.0000	0.0000	0.0000	0.0000	0.0000
NMcspha3	0.4283	0.0845	0.0933	0.3939	0.7603	0.2397
NMcspha4	0.0000	0.9999	0.0000	0.0000	0.0000	1.0000
NMcspha4	0.1412	0.6331	0.0042	0.2215	0.4875	0.5125
NMcspha5	0.0000	0.0000	0.0000	0.0000	0.0000	0.0000
NMcspha5	0.2211	0.4913	0.0314	0.2561	0.4385	0.5615
NMcspha6	0.0000	0.0000	0.0000	0.0000	0.0000	0.0000
NMcspha6	0.1720	0.5723	0.0178	0.2379	0.5068	0.4932
NMcspha7	0.0000	1.0000	0.0000	0.0000	0.0000	1.0000
NMcspha7	0.0007	0.9941	0.0001	0.0050	0.1354	0.8646
NMcspha9	0.0000	1.0000	0.0000	0.0000	0.0000	1.0000
NMcspha9	0.0014	0.9903	0.0002	0.0081	0.2787	0.7213
NMcspha8	0.0000	1.0000	0.0000	0.0000	0.0000	0.0000
NMcspha8	0.0011	0.9924	0.0001	0.0063	0.0122	0.9878
NMonOut1	0.8533	0.1436	0.0016	0.0016	0.0003	0.9997
NMonOut1	0.3207	0.4677	0.0175	0.1941	0.3914	0.6086
NMonOut2	0.8302	0.1606	0.0046	0.0046	0.0000	0.0000
NMonOut2	0.3843	0.3107	0.0576	0.2473	0.5092	0.4908
NMono	0.0114	0.9877	0.0004	0.0004	0.0001	0.9999
NMono	0.0159	0.8995	0.0185	0.0661	0.3304	0.6696

	NPleo1	0.9946	0.0051	0.0000	0.0003	0.0000	1.0000
	NPleo1	0.4066	0.2472	0.0142	0.3320	0.1999	0.8001
	NStrig1	0.8835	0.1079	0.0018	0.0067	0.0001	0.9999
	NStrig1	0.3423	0.3053	0.0173	0.3351	0.2375	0.7625
	NStrig2	0.0651	0.9269	0.0063	0.0017	0.0005	0.9995
	NStrig2	0.2529	0.4131	0.0169	0.3171	0.2556	0.7444
	NStrig3	0.0046	0.9946	0.0006	0.0003	0.0002	0.9998
	NStrig3	0.2545	0.4151	0.0159	0.3145	0.2257	0.7743
	NStrig4	0.0000	0.0000	0.0000	0.0000	0.0000	0.0000
	NStrig4	0.2669	0.3884	0.0190	0.3258	0.2399	0.7601
	NStrig5	0.0001	0.9997	0.0001	0.0001	0.0002	0.9998
	NStrig5	0.0188	0.9175	0.0028	0.0609	0.1111	0.8889
	NStrig6	0.0001	0.9999	0.0000	0.0000	0.0001	0.9999
	NStrig6	0.0090	0.9474	0.0010	0.0426	0.0863	0.9137
	NStrig7	0.0000	0.9999	0.0000	0.0000	0.0001	0.9999
	NStrig7	0.0117	0.9384	0.0015	0.0483	0.0934	0.9066
	NStrig8	0.0000	0.9999	0.0000	0.0000	0.0001	0.9999
	NStrig8	0.0081	0.9565	0.0011	0.0342	0.0594	0.9406
	NADM01	0.0123	0.9607	0.0258	0.0012	0.0216	0.9784
	NADM01	0.0716	0.6564	0.0510	0.2211	0.4749	0.5251
	NADM02	0.0002	0.9994	0.0003	0.0001	0.0005	0.9995
	NADM02	0.0162	0.9185	0.0019	0.0634	0.1304	0.8696
	NADM03	0.0000	0.9999	0.0001	0.0000	0.0002	0.9998
	NADM03	0.0283	0.8818	0.0044	0.0856	0.1594	0.8406
NODE 4	**NADM04**	**0.0063**	**0.8467**	**0.1447**	**0.0023**	**0.1809**	**0.8191**
	NADM04	**0.1068**	**0.3238**	**0.2386**	**0.3308**	**0.6633**	**0.3367**
	NADM05	0.0005	0.9962	0.0029	0.0004	0.0059	0.9941

	NADM05	0.0283	0.8821	0.0044	0.0852	0.1587	0.8413
	NADM06	0.0000	0.0000	0.0000	0.0000	0.0000	0.0000
	NADM06	0.0508	0.0271	0.5667	0.3554	0.9291	0.0709
	NADM07	0.0000	0.0000	0.0000	0.0000	0.0000	0.0000
	NADM07	0.1560	0.0677	0.1926	0.5837	0.6443	0.3557
NODE 5	**NADM08**	**0.0002**	**0.0086**	**0.9911**	**0.0002**	**0.9867**	**0.0133**
	NADM08	**0.0014**	**0.0015**	**0.9720**	**0.0252**	**0.9901**	**0.0099**
	NADM11	0.0000	0.0001	0.9999	0.0000	0.9997	0.0003
	NADM11	0.0200	0.0032	0.9168	0.0599	0.9778	0.0222
	NADM12	0.0000	0.0000	0.0000	0.0000	1.0000	0.0000
	NADM12	0.1344	0.0091	0.7315	0.1250	0.9429	0.0571
	NADM09	0.0000	0.0001	0.9999	0.0000	0.9997	0.0003
	NADM09	0.0004	0.0012	0.9911	0.0073	0.9927	0.0073
	NADM10	0.0000	0.0000	1.0000	0.0000	0.0000	0.0000
	NADM10	0.0000	0.0000	0.9999	0.0001	0.9999	0.0001
	NPleo2	0.9956	0.0039	0.0000	0.0005	0.0000	1.0000
	NPleo2	0.3636	0.1219	0.0072	0.5073	0.1298	0.8702
	NMyti1	0.9823	0.0031	0.0006	0.0141	0.0001	0.9999
	NMyti1	0.1815	0.0842	0.0489	0.6855	0.3351	0.6649
	NMyti2	0.0000	0.0000	0.0000	0.0000	0.0000	0.0000
	NMyti2	0.3102	0.1129	0.1439	0.4330	0.4128	0.5872
	NMyti3	1.0000	0.0000	0.0000	0.0000	0.0000	1.0000
	NMyti3	0.9974	0.0002	0.0000	0.0024	0.0063	0.9937
	NHyster	1.0000	0.0000	0.0000	0.0000	0.0000	1.0000
	NHyster	0.9973	0.0002	0.0001	0.0024	0.0057	0.9943
	NPleo3	0.0135	0.9860	0.0002	0.0002	0.0000	1.0000
	NPleo3	0.0046	0.9649	0.0004	0.0300	0.0867	0.9133

	NDicty1	0.0000	0.0000	0.0000	0.0000	0.0000	0.0000
	NDicty1	0.0271	0.7137	0.1111	0.1481	0.5342	0.4658
	NDicty2	0.0000	0.0000	0.0000	0.0000	0.0000	0.0000
	NDicty2	0.0634	0.4149	0.3463	0.1754	0.8042	0.1958
	NPleo4	0.0000	1.0000	0.0000	0.0000	0.0000	1.0000
	NPleo4	0.0003	0.9971	0.0000	0.0026	0.0041	0.9959
NODE 6	**NMVP**	**0.0086**	**0.0172**	**0.9690**	**0.0053**	**0.5693**	**0.4307**
	NMVP	**0.0248**	**0.1948**	**0.4519**	**0.3285**	**0.6401**	**0.3599**
	NVent1	0.0034	0.0313	0.9630	0.0023	0.5782	0.4218
	NVent1	0.0691	0.2537	0.4810	0.1962	0.7418	0.2582
	NStom1	0.0003	0.0019	0.9976	0.0002	0.9626	0.0374
	NStom1	0.0029	0.0068	0.9626	0.0278	0.9571	0.0429
	NStom2	0.0000	0.0000	1.0000	0.0000	0.9997	0.0003
	NStom2	0.0002	0.0005	0.9961	0.0033	0.9972	0.0028
	NVent2	0.0001	0.9960	0.0038	0.0001	0.0025	0.9975
	NVent2	0.1982	0.5587	0.1491	0.0939	0.2601	0.7399
	NVent3	0.0000	0.0000	0.0000	0.0000	0.0000	0.0000
	NVent3	0.2299	0.4829	0.1344	0.1528	0.4696	0.5304
	NMThyrX	0.0054	0.0169	0.9678	0.0099	0.5845	0.4155
	NMThyrX	0.0309	0.1928	0.3998	0.3765	0.5577	0.4423
	NPhaeo	0.0065	0.3282	0.1198	0.5455	0.0040	0.9960
	NPhaeo	0.0121	0.2572	0.0023	0.7285	0.0306	0.9694
NODE 7	**NMThyr1**	**0.0031**	**0.0095**	**0.9785**	**0.0089**	**0.8352**	**0.1648**
	NMThyr1	**0.0314**	**0.1488**	**0.5504**	**0.2694**	**0.6149**	**0.3851**
	NMThyr2	0.0003	0.0005	0.9988	0.0004	0.9566	0.0434
	NMThyr2	0.0289	0.0776	0.7599	0.1336	0.6993	0.3007
	NMThyr3	0.0005	0.0005	0.9985	0.0005	0.9520	0.0480

	NMThyr3	0.0196	0.0404	0.8425	0.0974	0.6765	0.3235
	NMThyr4	0.0003	0.0003	0.9990	0.0003	0.9876	0.0124
	NMThyr4	0.0159	0.0332	0.8643	0.0866	0.8075	0.1925
	NMTSup	0.0001	0.0001	0.9998	0.0001	0.0000	0.0000
	NMTSup	0.0783	0.1602	0.5564	0.2051	0.7145	0.2855
	NMThyr5	0.0001	0.0001	0.9997	0.0001	0.0000	0.0000
	NMThyr5	0.1751	0.2208	0.3788	0.2253	0.5546	0.4454
	NMThyr6	0.0000	0.0000	0.0000	0.0000	0.0000	0.0000
	NMThyr6	0.0794	0.1433	0.5798	0.1975	0.7663	0.2337
	NHelio	0.0000	0.0000	0.0000	0.0000	0.0000	0.0000
	NHelio	0.2547	0.3282	0.2597	0.1574	0.5217	0.4783
	NZelo1	0.0055	0.0100	0.9600	0.0245	0.9326	0.0674
	NZelo1	0.1124	0.1747	0.4484	0.2645	0.5605	0.4395
	NNati	0.0015	0.0016	0.0075	0.9894	0.0131	0.9869
	NNati	0.0233	0.0438	0.0120	0.9210	0.1813	0.8187
	NZelo2	0.0000	0.0000	1.0000	0.0000	0.0000	0.0000
	NZelo2	0.0012	0.0100	0.9788	0.0100	0.8170	0.1830
	NZelo3	0.0000	0.0000	1.0000	0.0000	0.9952	0.0048
	NZelo3	0.0107	0.0497	0.9048	0.0347	0.8817	0.1183
	NZelo4	0.0000	0.0000	1.0000	0.0000	1.0000	0.0000
	NZelo4	0.0000	0.0000	0.9997	0.0002	0.9998	0.0002
	NZelo5	0.0000	0.0000	0.0000	0.0000	0.0000	0.0000
	NZelo5	0.1771	0.3722	0.3162	0.1345	0.6900	0.3100
	NZelo6	0.0000	0.0000	0.0000	0.0000	0.0000	0.0000
	NZelo6	0.1353	0.2919	0.4712	0.1016	0.7695	0.2305
NODE 8	**NAulo1**	**0.0088**	**0.0045**	**0.9823**	**0.0045**	**0.9702**	**0.0298**
	NAulo1	**0.0236**	**0.0464**	**0.8257**	**0.1043**	**0.7544**	**0.2456**

	NLembo	0.0000	0.0000	0.9999	0.0000	0.9998	0.0002
	NLembo	0.0004	0.0010	0.9924	0.0063	0.9937	0.0063
	NAulo2	0.0000	0.0000	1.0000	0.0000	1.0000	0.0000
	NAulo2	0.0001	0.0002	0.9979	0.0018	0.9985	0.0015
	NAstx01	0.0000	0.0000	0.0000	0.0000	0.8948	0.1052
	NAstx01	0.3458	0.0611	0.3208	0.2723	0.9310	0.0690
NODE 9	**NAstx02**	**0.1819**	**0.0002**	**0.8177**	**0.0001**	**0.8969**	**0.1031**
	NAstx02	**0.3258**	**0.0503**	**0.3661**	**0.2578**	**0.9178**	**0.0822**
	NMelas01	0.2546	0.0014	0.7426	0.0014	0.7860	0.2140
	NMelas01	0.7766	0.0281	0.0564	0.1389	0.7037	0.2963
	NMelas02	0.9919	0.0002	0.0078	0.0002	0.0185	0.9815
	NMelas02	0.9362	0.0069	0.0042	0.0527	0.6427	0.3573
	NMelas03	0.9998	0.0000	0.0002	0.0000	0.0000	0.0000
	NMelas03	0.9333	0.0073	0.0044	0.0550	0.6535	0.3465
	NMelas04	1.0000	0.0000	0.0000	0.0000	0.0100	0.9900
	NMelas04	0.9249	0.0095	0.0057	0.0599	0.6541	0.3459
	NMelas05	0.0000	0.0000	0.0000	0.0000	0.0000	0.0000
	NMelas05	0.4899	0.1930	0.1248	0.1923	0.3467	0.6533
	NMelas06	0.0000	0.0000	0.0000	0.0000	0.0000	0.0000
	NMelas06	0.5096	0.1838	0.1213	0.1854	0.3349	0.6651
	NMelas07	1.0000	0.0000	0.0000	0.0000	0.0003	0.9997
	NMelas07	0.9203	0.0143	0.0069	0.0585	0.1151	0.8849
	NMelas08	0.0000	0.0000	0.0000	0.0000	0.0000	0.0000
	NMelas08	0.7017	0.1011	0.0624	0.1348	0.2435	0.7565
	NMelas09	1.0000	0.0000	0.0000	0.0000	0.0114	0.9886
	NMelas09	0.9225	0.0118	0.0065	0.0592	0.6630	0.3370
	NMelas10	1.0000	0.0000	0.0000	0.0000	0.0042	0.9958

	NMelas10	0.7759	0.0691	0.0383	0.1168	0.2412	0.7588
	NMelas11	0.0000	0.0000	0.0000	0.0000	0.0000	0.0000
	NMelas11	0.3529	0.3205	0.1770	0.1496	0.4242	0.5758
	NMelas12	0.0000	0.0000	0.0000	0.0000	0.0000	0.0000
	NMelas12	0.3541	0.3206	0.1758	0.1495	0.4094	0.5906
	NMelas13	0.9987	0.0004	0.0004	0.0004	0.0022	0.9978
	NMelas13	0.8145	0.0449	0.0190	0.1216	0.2922	0.7078
	NAstx03	0.0199	0.0005	0.9792	0.0005	0.9833	0.0167
	NAstx03	0.0059	0.0139	0.9316	0.0486	0.9129	0.0871
NODE 10	**NAstx04**	**0.0000**	**0.0000**	**1.0000**	**0.0000**	**1.0000**	**0.0000**
	NAstx04	**0.0002**	**0.0006**	**0.9948**	**0.0045**	**0.9946**	**0.0054**
	NAstx05	0.0001	0.0000	0.9999	0.0000	0.9988	0.0012
	NAstx05	0.0004	0.0022	0.9860	0.0113	0.9889	0.0111
	NAstx06	0.0000	0.0000	1.0000	0.0000	0.9986	0.0014
	NAstx06	0.0040	0.0233	0.9257	0.0471	0.9526	0.0474
	NAstx07	0.0001	0.0001	0.9998	0.0001	0.9821	0.0179
	NAstx07	0.0060	0.0149	0.9248	0.0543	0.6082	0.3918
	NAstx08	0.0000	0.0000	1.0000	0.0000	1.0000	0.0000
	NAstx08	0.0002	0.0005	0.9961	0.0032	0.9972	0.0028
	NAstx09	0.0001	0.0001	0.9996	0.0001	0.9504	0.0496
	NAstx09	0.0103	0.0226	0.9004	0.0667	0.5434	0.4566
	NAstx10	0.0000	0.0000	1.0000	0.0000	1.0000	0.0000
	NAstx10	0.0002	0.0004	0.9969	0.0025	0.9973	0.0027
	NAstx11	0.0000	0.0003	0.9997	0.0000	0.9970	0.0030
	NAstx11	0.0207	0.0962	0.7692	0.1139	0.9766	0.0234
	NAstx14	0.0060	0.1190	0.8691	0.0059	0.7077	0.2923
	NAstx14	0.0797	0.5004	0.2472	0.1727	0.8353	0.1647

NAstx15	0.0535	0.0792	0.8137	0.0535	0.4218	0.5782
NAstx15	0.0888	0.1285	0.6047	0.1780	0.4539	0.5461
NAstx12	0.0000	0.0000	1.0000	0.0000	0.9987	0.0013
NAstx12	0.0092	0.0049	0.9526	0.0333	0.9838	0.0162
NAstx13	0.0017	0.0001	0.9981	0.0001	0.9960	0.0040
NAstx13	0.1706	0.0351	0.6210	0.1733	0.8289	0.1711

CHARACTERS		**Sporocarp dehiscence**				**Locule enlargement**	
	State	**Ostiole**	**Irregular slit**	**Regular slit**	**None**	**Exposed**	**Circular**	**Elongated**
Labelled in Fig.1	**Node/StateCode**	0	1	2	3	4	0	1
NLeotio		0.0062	0.0006	0.0006	0.0461	0.9465	0.0000	0.0000
NLeotio		0.0044	0.0021	0.5385	0.1376	0.3175	0.8142	0.1858
NEuroAll		0.3140	0.0124	0.0124	0.1971	0.4641	0.9998	0.0002
NEuroAll		0.3799	0.0167	0.2102	0.3507	0.0425	0.5173	0.4827
NOnyEuro		0.0106	0.0019	0.0019	0.9706	0.0150	0.9997	0.0003
NOnyEuro		0.0633	0.0082	0.0842	0.8250	0.0193	0.6074	0.3926
NEuro1		0.0001	0.0000	0.0000	0.9998	0.0001	1.0000	0.0000
NEuro1		0.0099	0.0018	0.0233	0.9633	0.0017	0.8024	0.1976
NEuro2		0.0000	0.0000	0.0000	1.0000	0.0000	1.0000	0.0000
NEuro2		0.0081	0.0016	0.0184	0.9705	0.0014	0.8275	0.1725
NEuro3		0.0000	0.0000	0.0000	1.0000	0.0000	1.0000	0.0000
NEuro3		0.0150	0.0023	0.0275	0.9520	0.0031	0.7825	0.2175
NPyrVeChae		0.9683	0.0014	0.0014	0.0079	0.0212	0.9998	0.0002
NPyrVeChae		0.6530	0.0086	0.1893	0.1325	0.0167	0.5498	0.4502
NPyren		0.9951	0.0005	0.0005	0.0012	0.0026	0.9994	0.0006
NPyren		0.6224	0.0172	0.1984	0.1403	0.0218	0.5406	0.4594

NVerChae	0.9899	0.0002	0.0002	0.0017	0.0081	0.9999	0.0001
NVerChae	0.6699	0.0061	0.1577	0.1380	0.0282	0.6392	0.3608
NVerru	0.9716	0.0006	0.0006	0.0010	0.0261	0.9999	0.0001
NVerru	0.4417	0.0126	0.2031	0.1392	0.2034	0.7375	0.2625
NCthyrL	0.9962	0.0000	0.0000	0.0033	0.0004	1.0000	0.0000
NCthyrL	0.7743	0.0017	0.0589	0.1616	0.0035	0.7946	0.2054
NHerpo1	1.0000	0.0000	0.0000	0.0000	0.0000	0.0000	0.0000
NHerpo1	0.9718	0.0002	0.0124	0.0154	0.0002	0.9053	0.0947
NHerpo2	1.0000	0.0000	0.0000	0.0000	0.0000	0.0000	0.0000
NHerpo2	0.9259	0.0011	0.0362	0.0360	0.0008	0.8221	0.1779
NCthyr01	0.0000	0.0000	0.0000	0.0000	0.0000	0.0000	0.0000
NCthyr01	0.3816	0.0127	0.1372	0.4104	0.0581	0.7104	0.2896
NCthyr02	0.9501	0.0004	0.0004	0.0487	0.0005	1.0000	0.0000
NCthyr02	0.3766	0.0127	0.0544	0.5390	0.0172	0.8337	0.1663
NCthyr03	0.0000	0.0000	0.0000	0.0000	0.0000	0.0000	0.0000
NCthyr03	0.5525	0.1629	0.0811	0.0979	0.1056	0.7364	0.2636
NCthyr04	0.9999	0.0000	0.0000	0.0001	0.0000	1.0000	0.0000
NCthyr04	0.9666	0.0004	0.0154	0.0174	0.0003	0.9101	0.0899
NCthyr05	0.0518	0.0004	0.0004	0.9471	0.0004	1.0000	0.0000
NCthyr05	0.1502	0.0134	0.0216	0.8036	0.0112	0.8925	0.1075
NCthyr06	0.0000	0.0000	0.0000	0.0000	0.0000	1.0000	0.0000
NCthyr06	0.2313	0.0391	0.0305	0.6733	0.0259	0.8706	0.1294
NCthyr07	0.0000	0.0000	0.0000	0.0000	0.0000	1.0000	0.0000
NCthyr07	0.4958	0.2966	0.0105	0.1111	0.0859	0.9610	0.0390
NLecano	0.0038	0.0000	0.0000	0.0001	0.9961	1.0000	0.0000
NLecano	0.0091	0.0018	0.0707	0.0267	0.8917	0.5818	0.4182
NLeca1	0.0026	0.0001	0.0001	0.0001	0.9972	0.9999	0.0001

NLeca1	0.0937	0.0112	0.1576	0.0898	0.6477	0.5935	0.4065
NLeca2	0.0054	0.0002	0.0002	0.0002	0.9941	1.0000	0.0000
NLeca2	0.1213	0.0109	0.1768	0.1032	0.5877	0.6164	0.3836
NLeca3	0.0011	0.0001	0.0001	0.0001	0.9987	1.0000	0.0000
NLeca3	0.0078	0.0048	0.0526	0.0295	0.9053	0.6188	0.3812
NUAO	0.0001	0.0000	0.0000	0.0000	0.9999	1.0000	0.0000
NUAO	0.0010	0.0011	0.0233	0.0114	0.9631	0.6116	0.3884
NUmbi1	0.0000	0.0000	0.0000	0.0000	0.9999	1.0000	0.0000
NUmbi1	0.0056	0.0052	0.0516	0.0290	0.9087	0.6008	0.3992
NUmbi2	0.0001	0.0001	0.0001	0.0001	0.9995	0.9997	0.0003
NUmbi2	0.0188	0.0160	0.0826	0.0530	0.8296	0.6118	0.3882
NOstropo	0.0000	0.0000	0.0000	0.0000	1.0000	1.0000	0.0000
NOstropo	0.0010	0.0009	0.0232	0.0103	0.9645	0.6066	0.3934
NMpeltout1	0.0000	0.0000	0.0000	0.0000	1.0000	1.0000	0.0000
NMpeltout1	0.0064	0.0021	0.0531	0.0234	0.9151	0.5922	0.4078
NMpeltout2	0.0000	0.0000	0.0000	0.0000	0.9999	0.0000	0.0000
NMpeltout2	0.0044	0.0041	0.0409	0.0243	0.9263	0.6612	0.3388
NMpeltout3	0.0003	0.0000	0.0000	0.0000	0.9997	1.0000	0.0000
NMpeltout3	0.0711	0.0118	0.1638	0.0802	0.6731	0.5424	0.4576
NMpeltout4	0.0001	0.0001	0.0001	0.0001	0.9996	0.9998	0.0002
NMpeltout4	0.0362	0.0128	0.1176	0.0612	0.7723	0.5525	0.4475
NMpeltout5	0.0077	0.0005	0.0005	0.0005	0.9906	0.9999	0.0001
NMpeltout5	0.1848	0.0255	0.2149	0.1215	0.4534	0.5348	0.4652
NMpelt1	0.9957	0.0003	0.0003	0.0003	0.0036	0.9999	0.0001
NMpelt1	0.8579	0.0017	0.0758	0.0630	0.0016	0.6641	0.3359
NMpelt2	0.9995	0.0000	0.0000	0.0000	0.0004	0.9999	0.0001
NMpelt2	0.8250	0.0043	0.0917	0.0749	0.0041	0.6889	0.3111

	NMpelt3	0.9997	0.0000	0.0000	0.0000	0.0002	0.9999	0.0001
	NMpelt3	0.8247	0.0039	0.0918	0.0760	0.0036	0.6768	0.3232
	NOstro1	0.0006	0.0002	0.0012	0.0002	0.9977	0.9758	0.0242
	NOstro1	0.0097	0.0092	0.1088	0.0410	0.8312	0.4636	0.5364
	NOstro2	0.0016	0.0015	0.0442	0.0015	0.9511	0.0202	0.9798
	NOstro2	0.0083	0.0107	0.3411	0.0364	0.6035	0.1244	0.8756
	NOstro3	0.0002	0.0001	0.0003	0.0001	0.9993	0.9948	0.0052
	NOstro3	0.0157	0.0134	0.0853	0.0508	0.8348	0.5646	0.4354
	NOstro4	0.0000	0.0000	0.0000	0.0000	1.0000	1.0000	0.0000
	NOstro4	0.0002	0.0002	0.0032	0.0022	0.9942	0.9367	0.0633
	NOstro5	0.0000	0.0000	0.0000	0.0000	1.0000	1.0000	0.0000
	NOstro5	0.0001	0.0001	0.0016	0.0011	0.9971	0.9680	0.0320
	NOstro6	0.0000	0.0000	0.0000	0.0000	1.0000	1.0000	0.0000
	NOstro6	0.0000	0.0000	0.0006	0.0004	0.9989	0.9875	0.0125
NODE 1	**NDothArTry**	**0.1476**	**0.0001**	**0.0002**	**0.0006**	**0.8515**	**1.0000**	**0.0000**
	NDothArTry	**0.0701**	**0.0070**	**0.6266**	**0.1397**	**0.1566**	**0.2031**	**0.7969**
	NArthTryp	0.1300	0.0004	0.0005	0.0007	0.8684	0.9995	0.0005
	NArthTryp	0.0516	0.0155	0.2064	0.0864	0.6401	0.4196	0.5804
	NTryp1	0.9115	0.0089	0.0089	0.0089	0.0619	0.9967	0.0033
	NTryp1	0.4691	0.0382	0.2532	0.1780	0.0616	0.5043	0.4957
	NTryp2	0.9976	0.0005	0.0005	0.0005	0.0009	0.9992	0.0008
	NTryp2	0.8018	0.0050	0.1047	0.0836	0.0049	0.6601	0.3399
	NTryp3	0.9730	0.0036	0.0036	0.0036	0.0161	0.9976	0.0024
	NTryp3	0.4957	0.0381	0.2405	0.1717	0.0541	0.5142	0.4858
	NTryp4	0.9992	0.0002	0.0002	0.0002	0.0002	0.9996	0.0004
	NTryp4	0.8468	0.0031	0.0792	0.0681	0.0028	0.7027	0.2973
	NArtho01	0.0020	0.0000	0.0001	0.0000	0.9978	0.9973	0.0027

NArtho01	0.0041	0.0022	0.0734	0.0274	0.8928	0.4192	0.5808
NArtho02	0.0000	0.0000	0.0000	0.0000	0.0000	0.0000	0.0000
NArtho02	0.0132	0.0055	0.0883	0.0560	0.8370	0.4842	0.5158
NSeurat	0.0004	0.0000	0.0000	0.0000	0.9995	0.0000	0.0000
NSeurat	0.0092	0.0060	0.0691	0.0417	0.8740	0.5025	0.4975
NArthRock	0.0000	0.0000	0.0000	0.0000	0.0000	0.0000	0.0000
NArthRock	0.0287	0.0311	0.1770	0.1258	0.6375	0.4686	0.5314
NArtho03	0.0003	0.0000	0.0004	0.0000	0.9993	0.9534	0.0466
NArtho03	0.0054	0.0054	0.1049	0.0295	0.8548	0.3758	0.6242
NArtho04	0.0002	0.0002	0.0002	0.0002	0.9993	0.0000	0.0000
NArtho04	0.0058	0.0052	0.0479	0.0284	0.9127	0.4785	0.5215
NArtho05	0.0002	0.0001	0.0019	0.0001	0.9976	0.6052	0.3948
NArtho05	0.0071	0.0084	0.1434	0.0334	0.8078	0.3315	0.6685
NArtho06	0.0010	0.0010	0.9854	0.0010	0.0118	0.0000	0.0000
NArtho06	0.0042	0.0095	0.9349	0.0133	0.0381	0.2195	0.7805
NArtho07	0.0000	0.0000	0.0006	0.0000	0.9993	0.5962	0.4038
NArtho07	0.0023	0.0025	0.0670	0.0190	0.9091	0.2800	0.7200
NArtho08	0.0002	0.0002	0.0019	0.0002	0.9976	0.0694	0.9306
NArtho08	0.0093	0.0098	0.0751	0.0319	0.8737	0.1137	0.8863
NArtho09	0.0000	0.0000	0.0008	0.0000	0.9991	0.8552	0.1448
NArtho09	0.0082	0.0083	0.1283	0.0375	0.8177	0.5502	0.4498
NArtho10	0.0024	0.0024	0.0144	0.0024	0.9784	0.8559	0.1441
NArtho10	0.0408	0.0381	0.1524	0.0852	0.6835	0.5297	0.4703
NArtho11	0.0001	0.0001	0.0014	0.0001	0.9984	0.9959	0.0041
NArtho11	0.0064	0.0067	0.1571	0.0332	0.7966	0.5785	0.4215
NArtho12	0.0007	0.0007	0.0201	0.0007	0.9779	0.9992	0.0008
NArtho12	0.0159	0.0202	0.4915	0.0489	0.4235	0.6116	0.3884

NArtho13	0.0001	0.0001	0.0003	0.0001	0.9994	0.9992	0.0008
NArtho13	0.0100	0.0092	0.0954	0.0375	0.8480	0.6049	0.3951
NArtho14	0.0000	0.0000	0.0000	0.0000	1.0000	1.0000	0.0000
NArtho14	0.0004	0.0004	0.0068	0.0043	0.9880	0.8798	0.1202
NArtho15	0.0000	0.0000	0.0000	0.0000	1.0000	1.0000	0.0000
NArtho15	0.0002	0.0002	0.0040	0.0027	0.9928	0.9294	0.0706
NDothid	0.9480	0.0000	0.0027	0.0000	0.0492	1.0000	0.0000
NDothid	0.1049	0.0131	0.7138	0.1488	0.0194	0.1808	0.8192
NPate	0.0163	0.0002	0.9795	0.0002	0.0037	0.9986	0.0014
NPate	0.0010	0.0026	0.9782	0.0052	0.0130	0.3046	0.6954
NAbro1	0.1300	0.0001	0.0014	0.0001	0.8683	1.0000	0.0000
NAbro1	0.3617	0.0043	0.1080	0.0845	0.4415	0.4627	0.5373
NAbro2	0.0017	0.0000	0.0000	0.0000	0.9983	1.0000	0.0000
NAbro2	0.0004	0.0002	0.0045	0.0028	0.9921	0.8835	0.1165
NTube1	1.0000	0.0000	0.0000	0.0000	0.0000	0.0000	0.0000
NTube1	0.4339	0.0685	0.1878	0.2744	0.0354	0.4935	0.5065
NTube2	1.0000	0.0000	0.0000	0.0000	0.0000	1.0000	0.0000
NTube2	0.8827	0.0023	0.0600	0.0531	0.0019	0.7587	0.2413
NBotry1	0.0000	0.0000	0.0000	0.0000	0.0000	0.0000	0.0000
NBotry1	0.9614	0.0004	0.0175	0.0204	0.0003	0.5968	0.4032
NBotry2	0.0000	0.0000	0.0000	0.0000	0.0000	0.0000	0.0000
NBotry2	0.9561	0.0006	0.0207	0.0222	0.0004	0.8849	0.1151
NBotry3	1.0000	0.0000	0.0000	0.0000	0.0000	1.0000	0.0000
NBotry3	0.9960	0.0000	0.0016	0.0023	0.0000	0.4239	0.5761
NCapnodX	1.0000	0.0000	0.0000	0.0000	0.0000	1.0000	0.0000
NCapnodX	0.7442	0.0032	0.1410	0.1096	0.0020	0.4106	0.5894
NDothi1	0.0000	0.0000	0.0000	0.0000	0.0000	0.0000	0.0000

	NDothi1	0.6933	0.0305	0.1337	0.1078	0.0347	0.5110	0.4890
	NMyri1	0.0000	0.0000	0.0000	0.0000	0.0000	0.0000	0.0000
	NMyri1	0.6097	0.0238	0.2001	0.1295	0.0368	0.5668	0.4332
	NMyri2	1.0000	0.0000	0.0000	0.0000	0.0000	1.0000	0.0000
	NMyri2	0.9073	0.0015	0.0463	0.0437	0.0012	0.7879	0.2121
	NCapnod0	0.0000	0.0000	0.0000	0.0000	0.0000	0.0000	0.0000
	NCapnod0	0.6155	0.0198	0.1559	0.1955	0.0133	0.4826	0.5174
	NCapnod1	0.0000	0.0000	0.0000	0.0000	0.0000	0.0000	0.0000
	NCapnod1	0.6294	0.0223	0.1448	0.1925	0.0110	0.4902	0.5098
	NCapnod2	0.0000	0.0000	0.0000	0.0000	0.0000	0.0000	0.0000
	NCapnod2	0.3949	0.1386	0.1782	0.1870	0.1013	0.4367	0.5633
	NCapnod3	1.0000	0.0000	0.0000	0.0000	0.0000	1.0000	0.0000
	NCapnod3	0.7339	0.0247	0.0710	0.1675	0.0029	0.6175	0.3825
	NCapnod4	0.9996	0.0003	0.0000	0.0000	0.0000	1.0000	0.0000
	NCapnod4	0.7218	0.0545	0.0719	0.1465	0.0054	0.6762	0.3238
NODE 2	**NCapnod5**	**1.0000**	**0.0000**	**0.0000**	**0.0000**	**0.0000**	**1.0000**	**0.0000**
	NCapnod5	**0.6825**	**0.0314**	**0.0903**	**0.1904**	**0.0054**	**0.5605**	**0.4395**
	NAsteOut1	0.0000	0.0000	0.0000	0.0000	0.0000	0.0000	0.0000
	NAsteOut1	0.5919	0.0932	0.1024	0.1866	0.0258	0.5508	0.4492
	NAsteOut2	0.9997	0.0002	0.0000	0.0000	0.0000	1.0000	0.0000
	NAsteOut2	0.4227	0.2691	0.1070	0.1790	0.0222	0.5401	0.4599
	NAsteOut3	0.0000	0.0000	0.0000	0.0000	0.0000	0.0000	0.0000
	NAsteOut3	0.7342	0.0868	0.0647	0.0797	0.0346	0.7240	0.2760
	NAsteOut4	1.0000	0.0000	0.0000	0.0000	0.0000	1.0000	0.0000
	NAsteOut4	0.9713	0.0026	0.0144	0.0104	0.0013	0.9457	0.0543
	NAste1	0.0532	0.9367	0.0034	0.0034	0.0034	0.9847	0.0153
	NAste1	0.0355	0.8591	0.0167	0.0831	0.0055	0.4671	0.5329

NODE 3								
	NAste2	**0.0015**	**0.9981**	**0.0001**	**0.0001**	**0.0001**	**0.9985**	**0.0015**
	NAste2	**0.0510**	**0.8477**	**0.0068**	**0.0903**	**0.0042**	**0.4827**	**0.5173**
	NAste3	0.0000	1.0000	0.0000	0.0000	0.0000	0.9988	0.0012
	NAste3	0.0005	0.9938	0.0005	0.0052	0.0001	0.5528	0.4472
	NAste4	0.0000	1.0000	0.0000	0.0000	0.0000	0.9942	0.0058
	NAste4	0.0030	0.9784	0.0020	0.0161	0.0006	0.3547	0.6453
	NAste5	0.0000	1.0000	0.0000	0.0000	0.0000	0.2790	0.7210
	NAste5	0.0003	0.9972	0.0002	0.0023	0.0001	0.0452	0.9548
	NAste6	0.0000	0.0000	0.0000	0.0000	0.0000	0.0000	0.0000
	NAste6	0.3627	0.2674	0.1001	0.1668	0.1031	0.4778	0.5222
	NAste7	0.0000	0.0000	0.0000	0.0000	0.0000	0.0000	0.0000
	NAste7	0.3644	0.2271	0.1114	0.1940	0.1031	0.4423	0.5577
	NAste8	0.0000	0.0000	0.0000	0.0000	0.0000	0.0000	0.0000
	NAste8	0.3652	0.2515	0.1018	0.1626	0.1190	0.5103	0.4897
	NCapno01	1.0000	0.0000	0.0000	0.0000	0.0000	1.0000	0.0000
	NCapno01	0.7113	0.0037	0.0772	0.2057	0.0022	0.5496	0.4504
	NCapno02	1.0000	0.0000	0.0000	0.0000	0.0000	0.0000	0.0000
	NCapno02	0.8021	0.0043	0.0968	0.0930	0.0038	0.5238	0.4762
	NCapno03	1.0000	0.0000	0.0000	0.0000	0.0000	1.0000	0.0000
	NCapno03	0.9815	0.0002	0.0079	0.0103	0.0001	0.7865	0.2135
	NCapno04	1.0000	0.0000	0.0000	0.0000	0.0000	1.0000	0.0000
	NCapno04	0.9611	0.0005	0.0179	0.0202	0.0003	0.6193	0.3807
	NCapno05	1.0000	0.0000	0.0000	0.0000	0.0000	0.0000	0.0000
	NCapno05	0.9902	0.0001	0.0043	0.0053	0.0001	0.6370	0.3630
	NCapno06	1.0000	0.0000	0.0000	0.0000	0.0000	0.0000	0.0000
	NCapno06	0.9982	0.0000	0.0008	0.0011	0.0000	0.7616	0.2384
	NCapno07	1.0000	0.0000	0.0000	0.0000	0.0000	1.0000	0.0000

NCapno07	0.5003	0.0214	0.1471	0.3097	0.0215	0.5586	0.4414
NTerato01	1.0000	0.0000	0.0000	0.0000	0.0000	0.0000	0.0000
NTerato01	0.5212	0.0167	0.1658	0.2787	0.0176	0.4791	0.5209
NTerato02	0.0000	0.0000	0.0000	0.0000	0.0000	0.0000	0.0000
NTerato02	0.3299	0.1423	0.2118	0.2098	0.1063	0.4866	0.5134
NTerato03	1.0000	0.0000	0.0000	0.0000	0.0000	0.0000	0.0000
NTerato03	0.5146	0.0213	0.1425	0.2969	0.0247	0.5209	0.4791
NTerato04	0.0000	0.0000	0.0000	0.0000	0.0000	0.0000	0.0000
NTerato04	0.5708	0.0798	0.1415	0.1605	0.0475	0.5817	0.4183
NTerato05	0.0000	0.0000	0.0000	0.0000	0.0000	0.0000	0.0000
NTerato05	0.3652	0.0585	0.1516	0.3472	0.0775	0.5252	0.4748
NTerato06	0.0000	0.0000	0.0000	0.0000	0.0000	0.0000	0.0000
NTerato06	0.2083	0.2195	0.1155	0.2815	0.1753	0.5960	0.4040
NTerato07	0.0000	0.0000	0.0000	0.0000	0.0000	0.0000	0.0000
NTerato07	0.4325	0.0396	0.1570	0.3041	0.0669	0.5157	0.4843
NTerato08	0.9976	0.0001	0.0001	0.0020	0.0001	0.0000	0.0000
NTerato08	0.5799	0.0168	0.1385	0.2424	0.0224	0.5609	0.4391
NTerato09	0.0000	0.0000	0.0000	0.0000	0.0000	0.0000	0.0000
NTerato09	0.1658	0.1038	0.1631	0.4355	0.1318	0.5281	0.4719
NTerato10	0.0000	0.0000	0.0000	0.0000	0.0000	0.0000	0.0000
NTerato10	0.2434	0.1809	0.1243	0.2712	0.1802	0.5525	0.4475
NTerato11	0.0000	0.0000	0.0000	0.0000	0.0000	0.0000	0.0000
NTerato11	0.2369	0.2281	0.1063	0.2444	0.1842	0.5931	0.4069
NCapnod6	0.9969	0.0016	0.0001	0.0001	0.0014	1.0000	0.0000
NCapnod6	0.2930	0.1441	0.1340	0.3011	0.1278	0.6717	0.3283
NSchiz	0.5439	0.2380	0.0049	0.0049	0.2083	1.0000	0.0000
NSchiz	0.0438	0.4795	0.0583	0.1597	0.2587	0.7625	0.2375

NMcspha1	0.0000	0.0000	0.0000	0.0000	0.0000	0.0000	0.0000
NMcspha1	0.4698	0.0380	0.1763	0.2568	0.0591	0.5790	0.4210
NMcspha2	0.0000	0.0000	0.0000	0.0000	0.0000	0.0000	0.0000
NMcspha2	0.2031	0.1575	0.1684	0.2944	0.1767	0.4969	0.5031
NMcspha3	0.0000	0.0000	0.0000	0.0000	0.0000	0.0000	0.0000
NMcspha3	0.1885	0.2197	0.1376	0.2655	0.1887	0.5433	0.4567
NMcspha4	0.9999	0.0000	0.0000	0.0000	0.0000	1.0000	0.0000
NMcspha4	0.7075	0.0122	0.1229	0.1368	0.0207	0.6888	0.3112
NMcspha5	0.0000	0.0000	0.0000	0.0000	0.0000	0.0000	0.0000
NMcspha5	0.5464	0.0863	0.1470	0.1652	0.0551	0.7012	0.2988
NMcspha6	0.0000	0.0000	0.0000	0.0000	0.0000	0.0000	0.0000
NMcspha6	0.6371	0.0450	0.1347	0.1484	0.0349	0.6739	0.3261
NMcspha7	1.0000	0.0000	0.0000	0.0000	0.0000	1.0000	0.0000
NMcspha7	0.9804	0.0002	0.0083	0.0110	0.0001	0.8206	0.1794
NMcspha9	1.0000	0.0000	0.0000	0.0000	0.0000	1.0000	0.0000
NMcspha9	0.9710	0.0003	0.0128	0.0157	0.0002	0.7711	0.2289
NMcspha8	1.0000	0.0000	0.0000	0.0000	0.0000	0.0000	0.0000
NMcspha8	0.9778	0.0002	0.0099	0.0119	0.0002	0.9356	0.0644
NMonOut1	0.9853	0.0004	0.0039	0.0004	0.0102	0.9990	0.0010
NMonOut1	0.3258	0.0298	0.3053	0.1339	0.2052	0.4732	0.5268
NMonOut2	0.9558	0.0037	0.0260	0.0037	0.0108	0.9682	0.0318
NMonOut2	0.2415	0.0892	0.3264	0.1610	0.1819	0.4941	0.5059
NMono	0.9998	0.0000	0.0001	0.0000	0.0001	0.9999	0.0001
NMono	0.6605	0.0042	0.2632	0.0672	0.0050	0.5686	0.4314
NPleo1	0.9665	0.0000	0.0323	0.0009	0.0003	1.0000	0.0000
NPleo1	0.1019	0.0041	0.7488	0.0685	0.0767	0.3085	0.6915
NStrig1	0.9637	0.0004	0.0338	0.0016	0.0005	0.9930	0.0070

	NStrig1	0.1401	0.0091	0.6777	0.0844	0.0887	0.3577	0.6423
	NStrig2	0.9980	0.0001	0.0017	0.0001	0.0001	0.9994	0.0006
	NStrig2	0.2522	0.0061	0.5716	0.0917	0.0783	0.3881	0.6119
	NStrig3	0.9997	0.0000	0.0002	0.0000	0.0000	0.9998	0.0002
	NStrig3	0.2572	0.0066	0.5648	0.0911	0.0802	0.3978	0.6022
	NStrig4	0.0000	0.0000	0.0000	0.0000	0.0000	0.0000	0.0000
	NStrig4	0.2326	0.0106	0.5710	0.0961	0.0897	0.3941	0.6059
	NStrig5	0.9998	0.0001	0.0001	0.0001	0.0001	0.9999	0.0001
	NStrig5	0.8223	0.0045	0.0931	0.0757	0.0044	0.6911	0.3089
	NStrig6	0.9999	0.0000	0.0000	0.0000	0.0000	1.0000	0.0000
	NStrig6	0.8541	0.0019	0.0779	0.0643	0.0018	0.6698	0.3302
	NStrig7	0.9999	0.0000	0.0000	0.0000	0.0000	1.0000	0.0000
	NStrig7	0.8446	0.0027	0.0824	0.0679	0.0025	0.6749	0.3251
	NStrig8	0.9999	0.0000	0.0000	0.0000	0.0000	1.0000	0.0000
	NStrig8	0.8928	0.0019	0.0540	0.0498	0.0015	0.7692	0.2308
	NADM01	0.9997	0.0001	0.0001	0.0001	0.0001	0.9998	0.0002
	NADM01	0.5904	0.0176	0.2282	0.1396	0.0243	0.5184	0.4816
	NADM02	0.9999	0.0000	0.0000	0.0000	0.0000	0.9999	0.0001
	NADM02	0.7976	0.0035	0.1106	0.0847	0.0036	0.6135	0.3865
	NADM03	0.9999	0.0000	0.0000	0.0000	0.0000	0.9999	0.0001
	NADM03	0.7581	0.0068	0.1288	0.0993	0.0070	0.6149	0.3851
NODE 4	**NADM04**	**0.9999**	**0.0000**	**0.0000**	**0.0000**	**0.0000**	**0.9999**	**0.0001**
	NADM04	**0.4563**	**0.0541**	**0.2627**	**0.1649**	**0.0620**	**0.5090**	**0.4910**
	NADM05	0.9994	0.0001	0.0001	0.0001	0.0001	0.9996	0.0004
	NADM05	0.7588	0.0068	0.1284	0.0989	0.0071	0.6165	0.3835
	NADM06	0.0000	0.0000	0.0000	0.0000	0.0000	0.0000	0.0000
	NADM06	0.3997	0.1068	0.2535	0.1719	0.0680	0.5475	0.4525

	NADM07	0.0000	0.0000	0.0000	0.0000	0.0000	0.0000	0.0000
	NADM07	0.0385	0.4640	0.1727	0.1366	0.1882	0.3797	0.6203
NODE 5	**NADM08**	**1.0000**	**0.0000**	**0.0000**	**0.0000**	**0.0000**	**1.0000**	**0.0000**
	NADM08	**0.8253**	**0.0015**	**0.1220**	**0.0480**	**0.0033**	**0.7748**	**0.2252**
	NADM11	1.0000	0.0000	0.0000	0.0000	0.0000	1.0000	0.0000
	NADM11	0.6651	0.0075	0.2285	0.0686	0.0304	0.7955	0.2045
	NADM12	1.0000	0.0000	0.0000	0.0000	0.0000	1.0000	0.0000
	NADM12	0.3950	0.0381	0.3183	0.0778	0.1708	0.8438	0.1562
	NADM09	1.0000	0.0000	0.0000	0.0000	0.0000	1.0000	0.0000
	NADM09	0.9454	0.0008	0.0260	0.0272	0.0006	0.8650	0.1350
	NADM10	0.0000	0.0000	0.0000	0.0000	0.0000	0.0000	0.0000
	NADM10	0.9990	0.0000	0.0004	0.0006	0.0000	0.9969	0.0031
	NPleo2	0.6735	0.0004	0.3181	0.0076	0.0004	0.9992	0.0008
	NPleo2	0.0659	0.0025	0.7339	0.1215	0.0761	0.2444	0.7556
	NMyti1	0.4428	0.0052	0.4146	0.1322	0.0052	0.9998	0.0002
	NMyti1	0.0924	0.0053	0.3312	0.3524	0.2186	0.5163	0.4837
	NMyti2	0.0000	0.0000	0.0000	0.0000	0.0000	0.0000	0.0000
	NMyti2	0.1013	0.0056	0.3640	0.1820	0.3471	0.5079	0.4921
	NMyti3	0.0001	0.0000	0.9999	0.0000	0.0000	1.0000	0.0000
	NMyti3	0.0000	0.0001	0.9982	0.0007	0.0009	0.6952	0.3048
	NHyster	0.0009	0.0000	0.9991	0.0000	0.0000	0.0020	0.9980
	NHyster	0.0001	0.0002	0.9982	0.0006	0.0009	0.0051	0.9949
	NPleo3	0.9952	0.0001	0.0045	0.0001	0.0001	0.9993	0.0007
	NPleo3	0.8838	0.0009	0.0613	0.0532	0.0008	0.6382	0.3618
	NDicty1	0.0000	0.0000	0.0000	0.0000	0.0000	0.0000	0.0000
	NDicty1	0.3602	0.0065	0.0747	0.5462	0.0123	0.5037	0.4963
	NDicty2	0.0000	0.0000	0.0000	0.0000	0.0000	0.0000	0.0000

	NDicty2	0.0633	0.0181	0.0340	0.8522	0.0324	0.3660	0.6340
	NPleo4	1.0000	0.0000	0.0000	0.0000	0.0000	1.0000	0.0000
	NPleo4	0.7534	0.0050	0.0522	0.1746	0.0147	0.9541	0.0459
NODE 6	**NMVP**	**0.9992**	**0.0001**	**0.0000**	**0.0005**	**0.0001**	**1.0000**	**0.0000**
	NMVP	**0.5699**	**0.0058**	**0.2118**	**0.1999**	**0.0126**	**0.5421**	**0.4579**
	NVent1	0.9999	0.0000	0.0000	0.0000	0.0000	1.0000	0.0000
	NVent1	0.6564	0.0249	0.1836	0.1154	0.0196	0.5594	0.4406
	NStom1	0.9999	0.0000	0.0000	0.0000	0.0000	1.0000	0.0000
	NStom1	0.8251	0.0048	0.0915	0.0741	0.0046	0.7021	0.2979
	NStom2	1.0000	0.0000	0.0000	0.0000	0.0000	1.0000	0.0000
	NStom2	0.9735	0.0003	0.0120	0.0139	0.0002	0.9263	0.0737
	NVent2	1.0000	0.0000	0.0000	0.0000	0.0000	1.0000	0.0000
	NVent2	0.4946	0.1281	0.1754	0.1211	0.0807	0.5797	0.4203
	NVent3	0.0000	0.0000	0.0000	0.0000	0.0000	0.0000	0.0000
	NVent3	0.3119	0.1952	0.1989	0.1758	0.1182	0.4579	0.5421
	NMThyrX	0.9962	0.0001	0.0001	0.0035	0.0001	1.0000	0.0000
	NMThyrX	0.4917	0.0095	0.2102	0.2631	0.0255	0.5379	0.4621
	NPhaeo	0.9187	0.0008	0.0008	0.0789	0.0008	1.0000	0.0000
	NPhaeo	0.3060	0.0023	0.0563	0.6314	0.0040	0.8479	0.1521
NODE 7	**NMThyr1**	**0.9931**	**0.0005**	**0.0005**	**0.0054**	**0.0005**	**0.9999**	**0.0001**
	NMThyr1	**0.4582**	**0.0243**	**0.2284**	**0.2317**	**0.0575**	**0.5232**	**0.4768**
	NMThyr2	0.9991	0.0002	0.0002	0.0004	0.0002	0.9997	0.0003
	NMThyr2	0.4494	0.0364	0.2776	0.1717	0.0649	0.5100	0.4900
	NMThyr3	0.9980	0.0005	0.0005	0.0005	0.0005	0.9989	0.0011
	NMThyr3	0.5106	0.0306	0.2431	0.1689	0.0468	0.5089	0.4911
	NMThyr4	0.9987	0.0003	0.0003	0.0003	0.0003	0.9992	0.0008
	NMThyr4	0.5794	0.0225	0.2168	0.1518	0.0296	0.5270	0.4730

	NMTSup	0.9989	0.0003	0.0003	0.0003	0.0003	0.9998	0.0002
	NMTSup	0.3740	0.0699	0.2797	0.1792	0.0973	0.5330	0.4670
	NMThyr5	0.0000	0.0000	0.0000	0.0000	0.0000	0.9997	0.0003
	NMThyr5	0.2372	0.1367	0.2520	0.1919	0.1822	0.5533	0.4467
	NMThyr6	0.0000	0.0000	0.0000	0.0000	0.0000	0.0000	0.0000
	NMThyr6	0.4354	0.0591	0.2495	0.1778	0.0782	0.5283	0.4717
	NHelio	0.0000	0.0000	0.0000	0.0000	0.0000	0.0000	0.0000
	NHelio	0.1529	0.1737	0.2585	0.2267	0.1882	0.3578	0.6422
	NZelo1	0.0000	0.0000	0.0000	0.0000	0.0000	0.9986	0.0014
	NZelo1	0.2254	0.0977	0.2284	0.2729	0.1756	0.5034	0.4966
	NNati	0.0072	0.0015	0.0015	0.9884	0.0015	0.9993	0.0007
	NNati	0.0685	0.0081	0.0918	0.8133	0.0183	0.5816	0.4184
	NZelo2	0.0000	0.0000	0.0000	0.0000	0.0000	1.0000	0.0000
	NZelo2	0.1890	0.1028	0.2413	0.3344	0.1326	0.8826	0.1174
	NZelo3	0.0000	0.0000	0.0000	0.0000	0.0000	1.0000	0.0000
	NZelo3	0.1900	0.0913	0.2461	0.3572	0.1155	0.8052	0.1948
	NZelo4	0.0000	0.0000	0.0000	0.0000	0.0000	1.0000	0.0000
	NZelo4	0.1953	0.1026	0.2144	0.3380	0.1497	0.9937	0.0063
	NZelo5	0.0000	0.0000	0.0000	0.0000	0.0000	0.0000	0.0000
	NZelo5	0.1787	0.1518	0.1805	0.3155	0.1735	0.4315	0.5685
	NZelo6	0.0000	0.0000	0.0000	0.0000	0.0000	0.0000	0.0000
	NZelo6	0.2022	0.1703	0.1439	0.2900	0.1936	0.5456	0.4544
NODE 8	**NAulo1**	**0.0252**	**0.9483**	**0.0088**	**0.0088**	**0.0089**	**0.0494**	**0.9506**
	NAulo1	**0.0422**	**0.8312**	**0.0275**	**0.0872**	**0.0119**	**0.4362**	**0.5638**
	NLembo	0.0001	0.9998	0.0000	0.0000	0.0000	0.0002	0.9998
	NLembo	0.0008	0.9927	0.0005	0.0059	0.0001	0.0251	0.9749
	NAulo2	0.0000	1.0000	0.0000	0.0000	0.0000	0.0000	1.0000

	NAulo2	0.0002	0.9977	0.0001	0.0019	0.0000	0.0065	0.9935
	NAstx01	0.0102	0.9796	0.0075	0.0006	0.0021	0.0000	0.0000
	NAstx01	0.0058	0.8825	0.0563	0.0467	0.0087	0.3690	0.6310
NODE 9	**NAstx02**	**0.0055**	**0.9841**	**0.0081**	**0.0004**	**0.0020**	**1.0000**	**0.0000**
	NAstx02	**0.0083**	**0.8380**	**0.0830**	**0.0554**	**0.0152**	**0.3687**	**0.6313**
	NMelas01	0.0042	0.8980	0.0794	0.0017	0.0167	0.9993	0.0007
	NMelas01	0.0188	0.1510	0.6123	0.0694	0.1484	0.2810	0.7190
	NMelas02	0.0017	0.0781	0.7706	0.0015	0.1481	0.9950	0.0050
	NMelas02	0.0062	0.0489	0.7215	0.0448	0.1786	0.2466	0.7534
	NMelas03	0.0009	0.0303	0.7537	0.0008	0.2142	0.9996	0.0004
	NMelas03	0.0067	0.0511	0.7071	0.0466	0.1884	0.2587	0.7413
	NMelas04	0.0002	0.0025	0.3708	0.0002	0.6264	0.9998	0.0002
	NMelas04	0.0083	0.0549	0.6877	0.0506	0.1985	0.2539	0.7461
	NMelas05	0.0000	0.0000	0.0000	0.0000	0.0000	0.0000	0.0000
	NMelas05	0.0891	0.1774	0.1318	0.1928	0.4088	0.4403	0.5597
	NMelas06	0.0000	0.0000	0.0000	0.0000	0.0000	0.0000	0.0000
	NMelas06	0.0885	0.1880	0.1239	0.1878	0.4117	0.4592	0.5408
	NMelas07	0.0001	0.0002	0.0063	0.0001	0.9932	1.0000	0.0000
	NMelas07	0.0081	0.0230	0.0351	0.0488	0.8850	0.6988	0.3012
	NMelas08	0.0000	0.0000	0.0000	0.0000	0.0000	0.0000	0.0000
	NMelas08	0.0522	0.1123	0.0817	0.1133	0.6404	0.5811	0.4189
	NMelas09	0.0002	0.0014	0.3586	0.0002	0.6394	0.9982	0.0018
	NMelas09	0.0093	0.0565	0.6914	0.0498	0.1930	0.2541	0.7459
	NMelas10	0.0006	0.0009	0.0968	0.0006	0.9010	0.9994	0.0006
	NMelas10	0.0417	0.0904	0.2824	0.1053	0.4802	0.3845	0.6155
	NMelas11	0.0000	0.0000	0.0000	0.0000	0.0000	0.0000	0.0000
	NMelas11	0.1614	0.2377	0.1301	0.1704	0.3004	0.3994	0.6006

	NMelas12	0.0000	0.0000	0.0000	0.0000	0.0000	0.0000	0.0000
	NMelas12	0.1696	0.2533	0.1312	0.1570	0.2889	0.4303	0.5697
	NMelas13	0.0012	0.0012	0.0142	0.0012	0.9823	0.9989	0.0011
	NMelas13	0.0265	0.0221	0.1079	0.0671	0.7765	0.5464	0.4536
	NAstx03	0.0007	0.9980	0.0010	0.0001	0.0003	0.9998	0.0002
	NAstx03	0.0118	0.9386	0.0076	0.0394	0.0026	0.5561	0.4439
NODE 10	**NAstx04**	**0.0000**	**1.0000**	**0.0000**	**0.0000**	**0.0000**	**1.0000**	**0.0000**
	NAstx04	**0.0019**	**0.9905**	**0.0008**	**0.0067**	**0.0002**	**0.7761**	**0.2239**
	NAstx05	0.0000	1.0000	0.0000	0.0000	0.0000	0.9997	0.0003
	NAstx05	0.0007	0.9908	0.0012	0.0071	0.0002	0.6640	0.3360
	NAstx06	0.0000	1.0000	0.0000	0.0000	0.0000	0.9990	0.0010
	NAstx06	0.0030	0.9739	0.0046	0.0173	0.0011	0.5165	0.4835
	NAstx07	0.0006	0.9901	0.0080	0.0006	0.0006	0.0497	0.9503
	NAstx07	0.0400	0.6995	0.1323	0.0952	0.0331	0.3851	0.6149
	NAstx08	0.0000	1.0000	0.0000	0.0000	0.0000	0.0001	0.9999
	NAstx08	0.0004	0.9961	0.0003	0.0032	0.0001	0.0103	0.9897
	NAstx09	0.0018	0.9647	0.0298	0.0018	0.0018	0.0244	0.9756
	NAstx09	0.0511	0.5601	0.2253	0.1041	0.0593	0.3862	0.6138
	NAstx10	0.0000	1.0000	0.0000	0.0000	0.0000	0.0000	1.0000
	NAstx10	0.0003	0.9971	0.0003	0.0022	0.0001	0.0098	0.9902
	NAstx11	0.0000	0.9999	0.0000	0.0000	0.0000	0.9996	0.0004
	NAstx11	0.0026	0.9781	0.0021	0.0152	0.0020	0.5549	0.4451
	NAstx14	0.0000	0.0000	0.0000	0.0000	0.0000	0.9976	0.0024
	NAstx14	0.0459	0.8236	0.0292	0.0844	0.0170	0.5541	0.4459
	NAstx15	0.0758	0.7429	0.0605	0.0605	0.0605	0.5541	0.4459
	NAstx15	0.1659	0.4301	0.1316	0.1851	0.0873	0.4751	0.5249
	NAstx12	0.0000	1.0000	0.0000	0.0000	0.0000	0.9994	0.0006

	NAstx12	0.0017	0.9765	0.0021	0.0163	0.0034	0.5501	0.4499
	NAstx13	0.0001	0.9982	0.0001	0.0001	0.0016	0.9849	0.0151
	NAstx13	0.0272	0.7038	0.0371	0.1171	0.1148	0.2450	0.7550
CHARACTERS		**Radiate**		**Patterns of branching and septation**				
	State	**no**	**yes**	**Pseudo-parenchyma**	**Isotomous overlapping**	**Anisotomous no overlap**	**Monopodial overlapping**	**Un-traceable**
Labelled in Fig.1	**Node/ StateCode**	0	1	0	1	2	3	4
	NLeotio	1.0000	0.0000	1.0000	0.0000	0.0000	0.0000	0.0000
	NLeotio	0.9996	0.0004	0.1614	0.0291	0.5684	0.0885	0.1526
	NEuroAll	1.0000	0.0000	1.0000	0.0000	0.0000	0.0000	0.0000
	NEuroAll	0.9810	0.0190	0.2717	0.1302	0.2227	0.1820	0.1933
	NOnyEuro	0.9999	0.0001	1.0000	0.0000	0.0000	0.0000	0.0000
	NOnyEuro	0.9882	0.0118	0.4229	0.0750	0.2248	0.1243	0.1530
	NEuro1	1.0000	0.0000	1.0000	0.0000	0.0000	0.0000	0.0000
	NEuro1	0.9989	0.0011	0.6014	0.0298	0.1943	0.0792	0.0954
	NEuro2	1.0000	0.0000	1.0000	0.0000	0.0000	0.0000	0.0000
	NEuro2	0.9991	0.0009	0.5228	0.0379	0.2084	0.1146	0.1164
	NEuro3	1.0000	0.0000	0.0000	0.0000	0.0000	0.0000	0.0000
	NEuro3	0.9977	0.0023	0.3854	0.0579	0.2318	0.1717	0.1533
	NPyrVeChae	1.0000	0.0000	1.0000	0.0000	0.0000	0.0000	0.0000
	NPyrVeChae	0.9905	0.0095	0.2544	0.1155	0.2363	0.1927	0.2012
	NPyren	0.9999	0.0001	1.0000	0.0000	0.0000	0.0000	0.0000
	NPyren	0.9743	0.0257	0.3483	0.1019	0.2254	0.1502	0.1741
	NVerChae	1.0000	0.0000	1.0000	0.0000	0.0000	0.0000	0.0000

NVerChae	0.9949	0.0051	0.2089	0.0944	0.2746	0.2077	0.2145
NVerru	1.0000	0.0000	1.0000	0.0000	0.0000	0.0000	0.0000
NVerru	0.9962	0.0038	0.6369	0.0340	0.1807	0.0597	0.0887
NCthyrL	1.0000	0.0000	1.0000	0.0000	0.0000	0.0000	0.0000
NCthyrL	0.9986	0.0014	0.0884	0.0844	0.3529	0.2596	0.2147
NHerpo1	1.0000	0.0000	0.0000	0.0000	0.0000	0.0000	0.0000
NHerpo1	0.9996	0.0004	0.1428	0.0270	0.4785	0.2372	0.1145
NHerpo2	1.0000	0.0000	0.0000	0.0000	0.0000	0.0000	0.0000
NHerpo2	0.9982	0.0018	0.2878	0.0345	0.3947	0.1495	0.1335
NCthyr01	1.0000	0.0000	0.0000	0.0000	0.0000	0.0000	0.0000
NCthyr01	0.9829	0.0171	0.1286	0.1730	0.2422	0.2290	0.2272
NCthyr02	1.0000	0.0000	1.0000	0.0000	0.0000	0.0000	0.0000
NCthyr02	0.9287	0.0713	0.2028	0.1087	0.2907	0.2007	0.1971
NCthyr03	0.0000	0.0000	0.0000	0.0000	0.0000	0.0000	0.0000
NCthyr03	0.5851	0.4149	0.1942	0.1805	0.2485	0.2314	0.1454
NCthyr04	1.0000	0.0000	1.0000	0.0000	0.0000	0.0000	0.0000
NCthyr04	0.9993	0.0007	0.8600	0.0092	0.0836	0.0180	0.0292
NCthyr05	1.0000	0.0000	1.0000	0.0000	0.0000	0.0000	0.0000
NCthyr05	0.9244	0.0756	0.2938	0.0840	0.2792	0.1535	0.1895
NCthyr06	1.0000	0.0000	0.9989	0.0000	0.0000	0.0000	0.0011
NCthyr06	0.8403	0.1597	0.2352	0.1064	0.2754	0.1832	0.1997
NCthyr07	0.0000	0.0000	0.0000	0.0000	0.0000	0.0000	0.0000
NCthyr07	0.5446	0.4554	0.1065	0.1916	0.2599	0.2578	0.1841
NLecano	1.0000	0.0000	1.0000	0.0000	0.0000	0.0000	0.0000
NLecano	0.9987	0.0013	0.5444	0.0479	0.2091	0.0833	0.1153
NLeca1	1.0000	0.0000	1.0000	0.0000	0.0000	0.0000	0.0000
NLeca1	0.9934	0.0066	0.4714	0.0645	0.2195	0.1068	0.1379

NLeca2	1.0000	0.0000	1.0000	0.0000	0.0000	0.0000	0.0000
NLeca2	0.9962	0.0038	0.5114	0.0544	0.2142	0.0938	0.1261
NLeca3	1.0000	0.0000	1.0000	0.0000	0.0000	0.0000	0.0000
NLeca3	0.9930	0.0070	0.4861	0.0615	0.2165	0.1017	0.1342
NUAO	1.0000	0.0000	1.0000	0.0000	0.0000	0.0000	0.0000
NUAO	0.9985	0.0015	0.5459	0.0454	0.2096	0.0839	0.1153
NUmbi1	1.0000	0.0000	1.0000	0.0000	0.0000	0.0000	0.0000
NUmbi1	0.9923	0.0077	0.4638	0.0666	0.2197	0.1091	0.1409
NUmbi2	0.9999	0.0001	1.0000	0.0000	0.0000	0.0000	0.0000
NUmbi2	0.9761	0.0239	0.4208	0.0832	0.2207	0.1219	0.1534
NOstropo	1.0000	0.0000	1.0000	0.0000	0.0000	0.0000	0.0000
NOstropo	0.9988	0.0012	0.5128	0.0493	0.2162	0.0949	0.1268
NMpeltout1	1.0000	0.0000	1.0000	0.0000	0.0000	0.0000	0.0000
NMpeltout1	0.9987	0.0013	0.3623	0.0756	0.2374	0.1464	0.1784
NMpeltout2	1.0000	0.0000	1.0000	0.0000	0.0000	0.0000	0.0000
NMpeltout2	0.9930	0.0070	0.5389	0.0505	0.2074	0.0851	0.1181
NMpeltout3	1.0000	0.0000	1.0000	0.0000	0.0000	0.0000	0.0000
NMpeltout3	0.9945	0.0055	0.2166	0.1271	0.2263	0.2096	0.2205
NMpeltout4	1.0000	0.0000	1.0000	0.0000	0.0000	0.0000	0.0000
NMpeltout4	0.9852	0.0148	0.3058	0.1078	0.2262	0.1698	0.1903
NMpeltout5	1.0000	0.0000	0.9980	0.0000	0.0000	0.0000	0.0019
NMpeltout5	0.9797	0.0203	0.1750	0.1537	0.2147	0.2282	0.2283
NMpelt1	1.0000	0.0000	0.0009	0.0000	0.0000	0.0000	0.9991
NMpelt1	0.9978	0.0022	0.0063	0.1204	0.1595	0.3350	0.3787
NMpelt2	1.0000	0.0000	0.0000	0.0000	0.0000	0.0000	1.0000
NMpelt2	0.9935	0.0065	0.0107	0.1048	0.1659	0.2721	0.4466
NMpelt3	1.0000	0.0000	0.0000	0.0000	0.0000	0.0000	1.0000

	NMpelt3	0.9939	0.0061	0.0096	0.1052	0.1735	0.2850	0.4267
	NOstro1	1.0000	0.0000	1.0000	0.0000	0.0000	0.0000	0.0000
	NOstro1	0.9897	0.0103	0.3791	0.0894	0.2260	0.1397	0.1658
	NOstro2	1.0000	0.0000	1.0000	0.0000	0.0000	0.0000	0.0000
	NOstro2	0.9949	0.0051	0.5802	0.0433	0.1966	0.0743	0.1056
	NOstro3	1.0000	0.0000	1.0000	0.0000	0.0000	0.0000	0.0000
	NOstro3	0.9790	0.0210	0.3824	0.0908	0.2252	0.1370	0.1647
	NOstro4	1.0000	0.0000	1.0000	0.0000	0.0000	0.0000	0.0000
	NOstro4	0.9996	0.0004	0.8972	0.0057	0.0647	0.0123	0.0201
	NOstro5	1.0000	0.0000	1.0000	0.0000	0.0000	0.0000	0.0000
	NOstro5	0.9998	0.0002	0.9446	0.0028	0.0360	0.0062	0.0104
	NOstro6	1.0000	0.0000	1.0000	0.0000	0.0000	0.0000	0.0000
	NOstro6	0.9999	0.0001	0.9763	0.0011	0.0156	0.0026	0.0043
NODE 1	**NDothArTry**	**1.0000**	**0.0000**	**1.0000**	**0.0000**	**0.0000**	**0.0000**	**0.0000**
	NDothArTry	**0.9994**	**0.0006**	**0.1291**	**0.2142**	**0.2368**	**0.1817**	**0.2381**
	NArthTryp	1.0000	0.0000	1.0000	0.0000	0.0000	0.0000	0.0000
	NArthTryp	0.9883	0.0117	0.1246	0.1715	0.2135	0.2531	0.2372
	NTryp1	0.9993	0.0007	0.9999	0.0000	0.0000	0.0000	0.0000
	NTryp1	0.9544	0.0456	0.2508	0.1515	0.2144	0.1874	0.1960
	NTryp2	0.9998	0.0002	1.0000	0.0000	0.0000	0.0000	0.0000
	NTryp2	0.9923	0.0077	0.5323	0.0527	0.2066	0.0880	0.1204
	NTryp3	0.9995	0.0005	1.0000	0.0000	0.0000	0.0000	0.0000
	NTryp3	0.9454	0.0546	0.2746	0.1375	0.2185	0.1779	0.1915
	NTryp4	0.9999	0.0001	1.0000	0.0000	0.0000	0.0000	0.0000
	NTryp4	0.9950	0.0050	0.5929	0.0408	0.1942	0.0705	0.1016
	NArtho01	1.0000	0.0000	1.0000	0.0000	0.0000	0.0000	0.0000
	NArtho01	0.9980	0.0020	0.0992	0.1387	0.2261	0.2837	0.2524

NArtho02	1.0000	0.0000	0.0000	0.0000	0.0000	0.0000	0.0000
NArtho02	0.9986	0.0014	0.0242	0.1916	0.1698	0.3568	0.2576
NSeurat	1.0000	0.0000	0.0000	0.0000	0.0000	0.0000	0.0000
NSeurat	0.9920	0.0080	0.1015	0.2165	0.1823	0.2805	0.2192
NArthRock	1.0000	0.0000	0.0000	0.0000	0.0000	0.0000	0.0000
NArthRock	0.9981	0.0019	0.0237	0.1700	0.1824	0.3520	0.2719
NArtho03	1.0000	0.0000	1.0000	0.0000	0.0000	0.0000	0.0000
NArtho03	0.9944	0.0056	0.3989	0.0821	0.2226	0.1374	0.1591
NArtho04	0.9999	0.0001	1.0000	0.0000	0.0000	0.0000	0.0000
NArtho04	0.9912	0.0088	0.5077	0.0574	0.2126	0.0948	0.1276
NArtho05	1.0000	0.0000	1.0000	0.0000	0.0000	0.0000	0.0000
NArtho05	0.9946	0.0054	0.4596	0.0670	0.2205	0.1109	0.1420
NArtho06	1.0000	0.0000	1.0000	0.0000	0.0000	0.0000	0.0000
NArtho06	0.9939	0.0061	0.5672	0.0458	0.1997	0.0778	0.1096
NArtho07	1.0000	0.0000	1.0000	0.0000	0.0000	0.0000	0.0000
NArtho07	0.9973	0.0027	0.5197	0.0536	0.2110	0.0920	0.1237
NArtho08	1.0000	0.0000	1.0000	0.0000	0.0000	0.0000	0.0000
NArtho08	0.9920	0.0080	0.6149	0.0440	0.1735	0.0699	0.0977
NArtho09	1.0000	0.0000	1.0000	0.0000	0.0000	0.0000	0.0000
NArtho09	0.9915	0.0085	0.3982	0.0838	0.2257	0.1319	0.1604
NArtho10	0.9998	0.0002	1.0000	0.0000	0.0000	0.0000	0.0000
NArtho10	0.9591	0.0409	0.3136	0.1189	0.2227	0.1621	0.1828
NArtho11	1.0000	0.0000	1.0000	0.0000	0.0000	0.0000	0.0000
NArtho11	0.9939	0.0061	0.4451	0.0711	0.2214	0.1164	0.1460
NArtho12	1.0000	0.0000	1.0000	0.0000	0.0000	0.0000	0.0000
NArtho12	0.9887	0.0113	0.4657	0.0666	0.2197	0.1077	0.1403
NArtho13	1.0000	0.0000	1.0000	0.0000	0.0000	0.0000	0.0000

NArtho13	0.9881	0.0119	0.4473	0.0745	0.2162	0.1165	0.1455
NArtho14	1.0000	0.0000	1.0000	0.0000	0.0000	0.0000	0.0000
NArtho14	0.9992	0.0008	0.8235	0.0115	0.1053	0.0226	0.0372
NArtho15	1.0000	0.0000	1.0000	0.0000	0.0000	0.0000	0.0000
NArtho15	0.9995	0.0005	0.8865	0.0067	0.0702	0.0137	0.0228
NDothid	1.0000	0.0000	1.0000	0.0000	0.0000	0.0000	0.0000
NDothid	0.9995	0.0005	0.1664	0.2356	0.2447	0.1379	0.2154
NPate	1.0000	0.0000	1.0000	0.0000	0.0000	0.0000	0.0000
NPate	0.9985	0.0015	0.6799	0.0268	0.1690	0.0493	0.0750
NAbro1	1.0000	0.0000	1.0000	0.0000	0.0000	0.0000	0.0000
NAbro1	0.9996	0.0004	0.3558	0.2908	0.1421	0.0936	0.1177
NAbro2	1.0000	0.0000	1.0000	0.0000	0.0000	0.0000	0.0000
NAbro2	0.9997	0.0003	0.8420	0.0108	0.0974	0.0187	0.0310
NTube1	1.0000	0.0000	0.0000	0.0000	0.0000	0.0000	0.0000
NTube1	0.9980	0.0020	0.3259	0.1698	0.2243	0.1299	0.1501
NTube2	1.0000	0.0000	1.0000	0.0000	0.0000	0.0000	0.0000
NTube2	0.9965	0.0035	0.6584	0.0320	0.1708	0.0558	0.0830
NBotry1	1.0000	0.0000	0.0000	0.0000	0.0000	0.0000	0.0000
NBotry1	0.9993	0.0007	0.2675	0.1981	0.2500	0.1342	0.1502
NBotry2	1.0000	0.0000	0.0000	0.0000	0.0000	0.0000	0.0000
NBotry2	0.9990	0.0010	0.8246	0.0120	0.1026	0.0234	0.0374
NBotry3	1.0000	0.0000	1.0000	0.0000	0.0000	0.0000	0.0000
NBotry3	0.9999	0.0001	0.1031	0.3937	0.2148	0.1900	0.0983
NCapnodX	1.0000	0.0000	1.0000	0.0000	0.0000	0.0000	0.0000
NCapnodX	0.9997	0.0003	0.0286	0.1702	0.1904	0.3238	0.2869
NDothi1	1.0000	0.0000	0.0000	0.0000	0.0000	0.0000	0.0000
NDothi1	0.9972	0.0028	0.1594	0.1674	0.2464	0.1960	0.2309

	NMyri1	1.0000	0.0000	0.0000	0.0000	0.0000	0.0000	0.0000
	NMyri1	0.9977	0.0023	0.1168	0.1775	0.2241	0.2287	0.2529
	NMyri2	1.0000	0.0000	0.0000	0.0000	0.0000	0.0000	0.0000
	NMyri2	0.9977	0.0023	0.2915	0.1295	0.2288	0.1514	0.1987
	NCapnod0	1.0000	0.0000	0.0000	0.0000	0.0000	0.0000	0.0000
	NCapnod0	0.9993	0.0007	0.0453	0.1392	0.2264	0.2993	0.2898
	NCapnod1	1.0000	0.0000	0.0000	0.0000	0.0000	0.0000	0.0000
	NCapnod1	0.9995	0.0005	0.0504	0.1336	0.2325	0.2908	0.2927
	NCapnod2	1.0000	0.0000	0.0000	0.0000	0.0000	0.0000	0.0000
	NCapnod2	0.9963	0.0037	0.1126	0.1985	0.2132	0.2597	0.2160
	NCapnod3	1.0000	0.0000	1.0000	0.0000	0.0000	0.0000	0.0000
	NCapnod3	0.9963	0.0037	0.0876	0.0999	0.2680	0.2390	0.3056
	NCapnod4	1.0000	0.0000	0.0000	0.0000	0.0000	0.0000	0.0000
	NCapnod4	0.9947	0.0053	0.2816	0.0849	0.2435	0.1686	0.2213
NODE 2	**NCapnod5**	**1.0000**	**0.0000**	**1.0000**	**0.0000**	**0.0000**	**0.0000**	**0.0000**
	NCapnod5	**0.9957**	**0.0043**	**0.0595**	**0.1154**	**0.2443**	**0.2616**	**0.3191**
	NAsteOut1	1.0000	0.0000	0.0000	0.0000	0.0000	0.0000	0.0000
	NAsteOut1	0.9835	0.0165	0.0877	0.1370	0.2413	0.2446	0.2894
	NAsteOut2	0.9932	0.0068	0.9998	0.0002	0.0000	0.0000	0.0000
	NAsteOut2	0.5413	0.4587	0.1925	0.2021	0.2099	0.1871	0.2084
	NAsteOut3	1.0000	0.0000	0.0000	0.0000	0.0000	0.0000	0.0000
	NAsteOut3	1.0000	0.0000	0.4713	0.1025	0.1639	0.1063	0.1559
	NAsteOut4	1.0000	0.0000	1.0000	0.0000	0.0000	0.0000	0.0000
	NAsteOut4	1.0000	0.0000	0.8920	0.0125	0.0433	0.0190	0.0332
	NAste1	0.1343	0.8657	0.0000	0.0000	0.0000	0.0000	0.0000
	NAste1	0.0074	0.9926	0.0569	0.4541	0.1332	0.1756	0.1803
NODE 3	**NAste2**	**0.0977**	**0.9023**	**0.0020**	**0.9980**	**0.0000**	**0.0000**	**0.0000**

	NAste2	**0.0329**	**0.9671**	**0.0279**	**0.5613**	**0.1185**	**0.1364**	**0.1560**
	NAste3	0.0004	0.9996	0.0000	0.0000	0.0000	0.0000	0.0000
	NAste3	0.0001	0.9999	0.0352	0.6158	0.1005	0.1109	0.1376
	NAste4	0.0001	0.9999	0.0001	0.9999	0.0000	0.0000	0.0000
	NAste4	0.0005	0.9995	0.0126	0.7735	0.0557	0.0688	0.0894
	NAste5	0.0000	1.0000	0.0000	1.0000	0.0000	0.0000	0.0000
	NAste5	0.0001	0.9999	0.0005	0.9623	0.0095	0.0113	0.0164
	NAste6	1.0000	0.0000	0.0000	0.0000	0.0000	0.0000	0.0000
	NAste6	0.9898	0.0102	0.1715	0.1976	0.2386	0.2020	0.1903
	NAste7	1.0000	0.0000	0.0000	0.0000	0.0000	0.0000	0.0000
	NAste7	0.9837	0.0163	0.1642	0.1822	0.2491	0.2023	0.2022
	NAste8	0.0000	0.0000	0.0000	0.0000	0.0000	0.0000	0.0000
	NAste8	0.7345	0.2655	0.2068	0.1876	0.2191	0.2066	0.1798
	NCapno01	1.0000	0.0000	1.0000	0.0000	0.0000	0.0000	0.0000
	NCapno01	0.9996	0.0004	0.0257	0.0977	0.2348	0.2788	0.3631
	NCapno02	1.0000	0.0000	0.0000	0.0000	0.0000	0.0000	0.0000
	NCapno02	0.9939	0.0061	0.1741	0.1415	0.2338	0.2134	0.2372
	NCapno03	1.0000	0.0000	1.0000	0.0000	0.0000	0.0000	0.0000
	NCapno03	0.9997	0.0003	0.5345	0.0456	0.1982	0.0841	0.1376
	NCapno04	1.0000	0.0000	1.0000	0.0000	0.0000	0.0000	0.0000
	NCapno04	0.9992	0.0008	0.2965	0.1026	0.2454	0.1486	0.2069
	NCapno05	1.0000	0.0000	0.0000	0.0000	0.0000	0.0000	0.0000
	NCapno05	0.9998	0.0002	0.2781	0.1531	0.1967	0.1570	0.2151
	NCapno06	1.0000	0.0000	0.0000	0.0000	0.0000	0.0000	0.0000
	NCapno06	1.0000	0.0000	0.4903	0.0861	0.1643	0.0995	0.1599
	NCapno07	1.0000	0.0000	1.0000	0.0000	0.0000	0.0000	0.0000
	NCapno07	0.9997	0.0003	0.0173	0.0955	0.2186	0.2807	0.3879

NTerato01	1.0000	0.0000	0.0000	0.0000	0.0000	0.0000	0.0000
NTerato01	0.9991	0.0009	0.0396	0.1397	0.2195	0.2685	0.3326
NTerato02	1.0000	0.0000	0.0000	0.0000	0.0000	0.0000	0.0000
NTerato02	0.9801	0.0199	0.1156	0.2325	0.1871	0.2381	0.2267
NTerato03	1.0000	0.0000	0.0000	0.0000	0.0000	0.0000	0.0000
NTerato03	0.9980	0.0020	0.0503	0.1108	0.2528	0.2305	0.3556
NTerato04	1.0000	0.0000	0.0000	0.0000	0.0000	0.0000	0.0000
NTerato04	0.9987	0.0013	0.1339	0.1731	0.2265	0.1958	0.2707
NTerato05	1.0000	0.0000	1.0000	0.0000	0.0000	0.0000	0.0000
NTerato05	0.9829	0.0171	0.0748	0.1167	0.2539	0.2293	0.3254
NTerato06	0.0000	0.0000	0.0000	0.0000	0.0000	0.0000	0.0000
NTerato06	0.6191	0.3809	0.2668	0.1146	0.2455	0.1454	0.2278
NTerato07	1.0000	0.0000	0.0000	0.0000	0.0000	0.0000	0.0000
NTerato07	0.9992	0.0008	0.0621	0.1551	0.2160	0.2546	0.3123
NTerato08	1.0000	0.0000	0.0000	0.0000	0.0000	0.0000	0.0000
NTerato08	0.9984	0.0016	0.1419	0.1736	0.2108	0.2132	0.2604
NTerato09	1.0000	0.0000	0.0000	0.0000	0.0000	0.0000	0.0000
NTerato09	0.9882	0.0118	0.1807	0.1638	0.2208	0.2080	0.2268
NTerato10	1.0000	0.0000	0.0000	0.0000	0.0000	0.0000	0.0000
NTerato10	0.9988	0.0012	0.0937	0.1756	0.2128	0.2235	0.2943
NTerato11	1.0000	0.0000	0.0000	0.0000	0.0000	0.0000	0.0000
NTerato11	0.9981	0.0019	0.1281	0.1901	0.2046	0.2058	0.2714
NCapnod6	1.0000	0.0000	1.0000	0.0000	0.0000	0.0000	0.0000
NCapnod6	0.9992	0.0008	0.0543	0.0724	0.2527	0.2278	0.3928
NSchiz	1.0000	0.0000	0.9972	0.0000	0.0000	0.0000	0.0028
NSchiz	0.9971	0.0029	0.0939	0.0632	0.2545	0.1792	0.4093
NMcspha1	1.0000	0.0000	0.0000	0.0000	0.0000	0.0000	0.0000

NMcspha1	0.9964	0.0036	0.0899	0.0957	0.2687	0.2184	0.3274
NMcspha2	1.0000	0.0000	0.0000	0.0000	0.0000	0.0000	0.0000
NMcspha2	0.9109	0.0891	0.1067	0.1732	0.2114	0.2326	0.2761
NMcspha3	0.0000	0.0000	0.0000	0.0000	0.0000	0.0000	0.0000
NMcspha3	0.7632	0.2368	0.1481	0.1762	0.2131	0.2040	0.2584
NMcspha4	1.0000	0.0000	1.0000	0.0000	0.0000	0.0000	0.0000
NMcspha4	0.9970	0.0030	0.2053	0.0712	0.2876	0.1602	0.2757
NMcspha5	0.0000	0.0000	0.0000	0.0000	0.0000	0.0000	0.0000
NMcspha5	0.8145	0.1855	0.3340	0.0962	0.2478	0.1281	0.1939
NMcspha6	1.0000	0.0000	0.0000	0.0000	0.0000	0.0000	0.0000
NMcspha6	0.9990	0.0010	0.1954	0.0899	0.2727	0.1673	0.2747
NMcspha7	1.0000	0.0000	1.0000	0.0000	0.0000	0.0000	0.0000
NMcspha7	0.9997	0.0003	0.3108	0.0638	0.2711	0.1172	0.2371
NMcspha9	1.0000	0.0000	0.0000	0.0000	0.0000	0.0000	0.0000
NMcspha9	0.9995	0.0005	0.3198	0.0791	0.2624	0.1166	0.2220
NMcspha8	1.0000	0.0000	0.0000	0.0000	0.0000	0.0000	0.0000
NMcspha8	0.9996	0.0004	0.2978	0.1230	0.2274	0.1287	0.2231
NMonOut1	1.0000	0.0000	1.0000	0.0000	0.0000	0.0000	0.0000
NMonOut1	0.9855	0.0145	0.2891	0.1332	0.2186	0.1717	0.1874
NMonOut2	0.9997	0.0003	0.0000	0.0000	0.0000	0.0000	0.0000
NMonOut2	0.9299	0.0701	0.2090	0.1856	0.2048	0.1985	0.2020
NMono	1.0000	0.0000	1.0000	0.0000	0.0000	0.0000	0.0000
NMono	0.9985	0.0015	0.4035	0.0967	0.2209	0.1152	0.1637
NPleo1	1.0000	0.0000	1.0000	0.0000	0.0000	0.0000	0.0000
NPleo1	0.9939	0.0061	0.3898	0.0817	0.2322	0.1274	0.1689
NStrig1	1.0000	0.0000	1.0000	0.0000	0.0000	0.0000	0.0000
NStrig1	0.9902	0.0098	0.3763	0.0902	0.2296	0.1347	0.1692

	NStrig2	1.0000	0.0000	1.0000	0.0000	0.0000	0.0000	0.0000
	NStrig2	0.9826	0.0174	0.3603	0.0968	0.2287	0.1404	0.1738
	NStrig3	1.0000	0.0000	1.0000	0.0000	0.0000	0.0000	0.0000
	NStrig3	0.9914	0.0086	0.3840	0.0891	0.2296	0.1307	0.1665
	NStrig4	0.9999	0.0001	0.0000	0.0000	0.0000	0.0000	0.0000
	NStrig4	0.9873	0.0127	0.3722	0.0956	0.2285	0.1344	0.1693
	NStrig5	1.0000	0.0000	1.0000	0.0000	0.0000	0.0000	0.0000
	NStrig5	0.9931	0.0069	0.5695	0.0474	0.1945	0.0791	0.1095
	NStrig6	1.0000	0.0000	1.0000	0.0000	0.0000	0.0000	0.0000
	NStrig6	0.9974	0.0026	0.5830	0.0413	0.1984	0.0731	0.1042
	NStrig7	1.0000	0.0000	1.0000	0.0000	0.0000	0.0000	0.0000
	NStrig7	0.9961	0.0039	0.5777	0.0430	0.1985	0.0748	0.1061
	NStrig8	1.0000	0.0000	1.0000	0.0000	0.0000	0.0000	0.0000
	NStrig8	0.9970	0.0030	0.6771	0.0286	0.1661	0.0512	0.0771
	NADM01	0.9982	0.0018	1.0000	0.0000	0.0000	0.0000	0.0000
	NADM01	0.7025	0.2975	0.2046	0.1567	0.2150	0.2122	0.2114
	NADM02	1.0000	0.0000	1.0000	0.0000	0.0000	0.0000	0.0000
	NADM02	0.9953	0.0047	0.5026	0.0561	0.2162	0.0963	0.1289
	NADM03	1.0000	0.0000	1.0000	0.0000	0.0000	0.0000	0.0000
	NADM03	0.9895	0.0105	0.4737	0.0642	0.2190	0.1050	0.1380
NODE 4	**NADM04**	**0.9739**	**0.0261**	**0.0000**	**0.0000**	**0.0000**	**0.0000**	**0.0000**
	NADM04	**0.2228**	**0.7772**	**0.1142**	**0.2138**	**0.1899**	**0.2599**	**0.2223**
	NADM05	0.9995	0.0005	1.0000	0.0000	0.0000	0.0000	0.0000
	NADM05	0.9895	0.0105	0.4755	0.0641	0.2184	0.1046	0.1374
	NADM06	0.2129	0.7871	0.0000	0.0000	0.0000	0.0000	0.0000
	NADM06	0.0129	0.9871	0.0092	0.2197	0.1334	0.4128	0.2249
	NADM07	0.2190	0.7810	0.0000	0.0000	0.0000	0.0000	0.0000

	NADM07	0.2649	0.7351	0.0243	0.3197	0.1526	0.3058	0.1976
NODE 5	**NADM08**	**0.0019**	**0.9981**	**0.0000**	**0.0000**	**0.0000**	**0.0000**	**0.0000**
	NADM08	**0.0002**	**0.9998**	**0.0071**	**0.1101**	**0.1425**	**0.4681**	**0.2723**
	NADM11	0.0000	1.0000	0.0000	0.0000	0.0000	0.0000	0.0000
	NADM11	0.0002	0.9998	0.0150	0.1026	0.1484	0.4250	0.3090
	NADM12	0.0000	1.0000	0.0000	0.0000	0.0000	0.0000	0.0000
	NADM12	0.0000	1.0000	0.0393	0.1101	0.1258	0.4118	0.3130
	NADM09	0.0000	1.0000	0.0000	0.0000	0.0000	0.0000	0.0000
	NADM09	0.0002	0.9998	0.0188	0.1090	0.1487	0.3736	0.3498
	NADM10	0.0000	1.0000	0.0000	0.0000	0.0000	0.0000	0.0000
	NADM10	0.0000	1.0000	0.0495	0.1161	0.0758	0.3387	0.4199
	NPleo2	1.0000	0.0000	1.0000	0.0000	0.0000	0.0000	0.0000
	NPleo2	0.9990	0.0010	0.4032	0.1172	0.2221	0.0969	0.1605
	NMyti1	1.0000	0.0000	1.0000	0.0000	0.0000	0.0000	0.0000
	NMyti1	0.9973	0.0027	0.1395	0.3098	0.1916	0.1347	0.2243
	NMyti2	1.0000	0.0000	0.0000	0.0000	0.0000	0.0000	0.0000
	NMyti2	0.9971	0.0029	0.0477	0.5039	0.1320	0.1037	0.2127
	NMyti3	1.0000	0.0000	1.0000	0.0000	0.0000	0.0000	0.0000
	NMyti3	0.9999	0.0001	0.8873	0.0050	0.0758	0.0119	0.0200
	NHyster	1.0000	0.0000	1.0000	0.0000	0.0000	0.0000	0.0000
	NHyster	0.9998	0.0002	0.9119	0.0040	0.0587	0.0094	0.0160
	NPleo3	1.0000	0.0000	1.0000	0.0000	0.0000	0.0000	0.0000
	NPleo3	0.9988	0.0012	0.5589	0.0455	0.2066	0.0787	0.1103
	NDicty1	1.0000	0.0000	1.0000	0.0000	0.0000	0.0000	0.0000
	NDicty1	0.9985	0.0015	0.3665	0.1062	0.2510	0.1162	0.1601
	NDicty2	1.0000	0.0000	1.0000	0.0000	0.0000	0.0000	0.0000
	NDicty2	0.9997	0.0003	0.2581	0.1744	0.2539	0.1388	0.1749

	NPleo4	1.0000	0.0000	1.0000	0.0000	0.0000	0.0000	0.0000
	NPleo4	0.9999	0.0001	0.4100	0.1175	0.2100	0.1101	0.1524
NODE 6	**NMVP**	**0.9626**	**0.0374**	**0.9989**	**0.0000**	**0.0009**	**0.0000**	**0.0003**
	NMVP	**0.0560**	**0.9440**	**0.1365**	**0.1227**	**0.2280**	**0.2484**	**0.2644**
	NVent1	0.9374	0.0626	0.9904	0.0000	0.0003	0.0000	0.0092
	NVent1	0.1407	0.8593	0.0741	0.0978	0.2339	0.2578	0.3364
	NStom1	0.0470	0.9530	0.0161	0.0001	0.0001	0.0001	0.9837
	NStom1	0.0010	0.9990	0.0115	0.1003	0.1678	0.2506	0.4698
	NStom2	0.0002	0.9998	0.0000	0.0000	0.0000	0.0000	1.0000
	NStom2	0.0001	0.9999	0.0005	0.0230	0.0757	0.0789	0.8218
	NVent2	0.9999	0.0001	1.0000	0.0000	0.0000	0.0000	0.0000
	NVent2	0.6211	0.3789	0.5565	0.0395	0.1325	0.1322	0.1392
	NVent3	1.0000	0.0000	0.0000	0.0000	0.0000	0.0000	0.0000
	NVent3	0.9947	0.0053	0.3407	0.0959	0.2012	0.1832	0.1790
	NMThyrX	0.9574	0.0426	0.9898	0.0000	0.0100	0.0000	0.0002
	NMThyrX	0.1147	0.8853	0.1912	0.1316	0.2257	0.2188	0.2327
	NPhaeo	0.9998	0.0002	1.0000	0.0000	0.0000	0.0000	0.0000
	NPhaeo	0.9986	0.0014	0.7761	0.0163	0.1268	0.0312	0.0497
NODE 7	**NMThyr1**	**0.8079**	**0.1921**	**0.1849**	**0.0001**	**0.8148**	**0.0001**	**0.0001**
	NMThyr1	**0.0541**	**0.9459**	**0.1633**	**0.1656**	**0.2139**	**0.2259**	**0.2313**
	NMThyr2	0.0754	0.9246	0.0018	0.0000	0.9981	0.0000	0.0000
	NMThyr2	0.0095	0.9905	0.1362	0.2242	0.1904	0.2379	0.2113
	NMThyr3	0.0082	0.9918	0.0000	0.0000	0.0000	0.0000	0.0000
	NMThyr3	0.0059	0.9941	0.1404	0.2262	0.1934	0.2296	0.2104
	NMThyr4	0.0013	0.9987	0.0001	0.0000	0.9999	0.0000	0.0000
	NMThyr4	0.0057	0.9943	0.1141	0.2079	0.2036	0.2485	0.2258
	NMTSup	0.0568	0.9432	0.0000	0.0000	0.0000	0.0000	0.0000

	NMTSup	0.1007	0.8993	0.1317	0.1885	0.2050	0.2503	0.2244
	NMThyr5	0.0000	0.0000	0.0000	0.0000	0.0000	0.0000	0.0000
	NMThyr5	0.2319	0.7681	0.1925	0.1834	0.1969	0.2193	0.2079
	NMThyr6	0.0666	0.9334	0.0000	0.0000	0.0000	0.0000	0.0000
	NMThyr6	0.1869	0.8131	0.1152	0.1763	0.2303	0.2436	0.2346
	NHelio	0.9991	0.0009	0.0000	0.0000	0.0000	0.0000	0.0000
	NHelio	0.9993	0.0007	0.3413	0.1233	0.1550	0.1575	0.2229
	NZelo1	0.7845	0.2155	0.1442	0.0001	0.8556	0.0001	0.0001
	NZelo1	0.2195	0.7805	0.1896	0.1945	0.2035	0.2079	0.2046
	NNati	0.9983	0.0017	0.9980	0.0001	0.0018	0.0001	0.0001
	NNati	0.9902	0.0098	0.4369	0.0728	0.2230	0.1181	0.1492
	NZelo2	0.0000	1.0000	0.0000	0.0000	0.0000	0.0000	0.0000
	NZelo2	0.0002	0.9998	0.1352	0.0474	0.4977	0.1407	0.1789
	NZelo3	0.0000	1.0000	0.0018	0.0000	0.9982	0.0000	0.0000
	NZelo3	0.0027	0.9973	0.0707	0.0467	0.5749	0.1312	0.1766
	NZelo4	0.0000	1.0000	0.0000	0.0000	1.0000	0.0000	0.0000
	NZelo4	0.0000	1.0000	0.0001	0.0009	0.9901	0.0030	0.0059
	NZelo5	0.0000	0.0000	0.0000	0.0000	0.0000	0.0000	0.0000
	NZelo5	0.1938	0.8062	0.2143	0.1018	0.2793	0.1987	0.2059
	NZelo6	0.0000	0.0000	0.0000	0.0000	0.0000	0.0000	0.0000
	NZelo6	0.2270	0.7730	0.1472	0.0833	0.4231	0.1621	0.1843
NODE 8	**NAulo1**	**0.0300**	**0.9700**	**0.0088**	**0.0009**	**0.0007**	**0.9890**	**0.0007**
	NAulo1	**0.0086**	**0.9914**	**0.1017**	**0.2321**	**0.1728**	**0.2848**	**0.2087**
	NLembo	0.0001	0.9999	0.0000	0.0000	0.0000	1.0000	0.0000
	NLembo	0.0001	0.9999	0.0019	0.0324	0.0556	0.8457	0.0644
	NAulo2	0.0000	1.0000	0.0000	0.0000	0.0000	1.0000	0.0000
	NAulo2	0.0000	1.0000	0.0004	0.0162	0.0339	0.9111	0.0383

	NAstx01	0.9724	0.0276	0.0000	0.0000	0.0000	0.0000	0.0000
	NAstx01	0.4235	0.5765	0.1262	0.2986	0.1787	0.1860	0.2105
NODE 9	**NAstx02**	**0.9435**	**0.0565**	**0.9545**	**0.0454**	**0.0000**	**0.0001**	**0.0000**
	NAstx02	**0.3453**	**0.6547**	**0.1312**	**0.3019**	**0.1787**	**0.1811**	**0.2071**
	NMelas01	0.9454	0.0546	0.9549	0.0449	0.0000	0.0001	0.0000
	NMelas01	0.8364	0.1636	0.3208	0.1162	0.2287	0.1512	0.1831
	NMelas02	0.9995	0.0005	0.9999	0.0001	0.0000	0.0000	0.0000
	NMelas02	0.9876	0.0124	0.4171	0.0650	0.2329	0.1265	0.1585
	NMelas03	1.0000	0.0000	1.0000	0.0000	0.0000	0.0000	0.0000
	NMelas03	0.9876	0.0124	0.4099	0.0659	0.2338	0.1294	0.1609
	NMelas04	1.0000	0.0000	1.0000	0.0000	0.0000	0.0000	0.0000
	NMelas04	0.9877	0.0123	0.4027	0.0671	0.2344	0.1324	0.1634
	NMelas05	1.0000	0.0000	0.0000	0.0000	0.0000	0.0000	0.0000
	NMelas05	0.9987	0.0013	0.2052	0.1219	0.2420	0.2085	0.2225
	NMelas06	1.0000	0.0000	0.0000	0.0000	0.0000	0.0000	0.0000
	NMelas06	0.9987	0.0013	0.2258	0.1197	0.2426	0.1980	0.2139
	NMelas07	1.0000	0.0000	1.0000	0.0000	0.0000	0.0000	0.0000
	NMelas07	0.9994	0.0006	0.5172	0.0473	0.2153	0.0898	0.1304
	NMelas08	1.0000	0.0000	0.0000	0.0000	0.0000	0.0000	0.0000
	NMelas08	0.9969	0.0031	0.3650	0.0926	0.2301	0.1386	0.1736
	NMelas09	1.0000	0.0000	1.0000	0.0000	0.0000	0.0000	0.0000
	NMelas09	0.9876	0.0124	0.4064	0.0672	0.2344	0.1291	0.1629
	NMelas10	1.0000	0.0000	1.0000	0.0000	0.0000	0.0000	0.0000
	NMelas10	0.9982	0.0018	0.3007	0.0772	0.2576	0.1644	0.2001
	NMelas11	1.0000	0.0000	0.0000	0.0000	0.0000	0.0000	0.0000
	NMelas11	0.9995	0.0005	0.2349	0.1355	0.2185	0.1800	0.2311
	NMelas12	1.0000	0.0000	0.0000	0.0000	0.0000	0.0000	0.0000

	NMelas12	0.9988	0.0012	0.2512	0.1383	0.2186	0.1743	0.2177
	NMelas13	0.9998	0.0002	1.0000	0.0000	0.0000	0.0000	0.0000
	NMelas13	0.9665	0.0335	0.3386	0.1081	0.2240	0.1529	0.1764
	NAstx03	0.0843	0.9157	0.3216	0.6780	0.0001	0.0001	0.0001
	NAstx03	0.0021	0.9979	0.0510	0.5245	0.1130	0.1502	0.1613
NODE 10	**NAstx04**	**0.0000**	**1.0000**	**0.0000**	**0.9999**	**0.0000**	**0.0000**	**0.0000**
	NAstx04	**0.0001**	**0.9999**	**0.0013**	**0.8761**	**0.0271**	**0.0429**	**0.0525**
	NAstx05	0.0004	0.9996	0.3026	0.6974	0.0000	0.0000	0.0000
	NAstx05	0.0001	0.9999	0.0529	0.5201	0.1182	0.1321	0.1766
	NAstx06	0.0002	0.9998	0.3106	0.6894	0.0000	0.0000	0.0000
	NAstx06	0.0022	0.9978	0.1683	0.1740	0.2056	0.2210	0.2311
	NAstx07	0.0000	1.0000	0.0000	0.0000	0.0000	0.0000	0.0000
	NAstx07	0.0015	0.9985	0.1169	0.2814	0.1676	0.2259	0.2083
	NAstx08	0.0000	1.0000	0.0000	0.0000	0.0000	0.0000	0.0000
	NAstx08	0.0001	0.9999	0.2162	0.1446	0.1889	0.2232	0.2271
	NAstx09	0.0001	0.9999	0.0000	0.0000	0.0000	0.0000	0.0000
	NAstx09	0.0033	0.9967	0.1196	0.2825	0.1688	0.2222	0.2070
	NAstx10	0.0000	1.0000	0.0000	1.0000	0.0000	0.0000	0.0000
	NAstx10	0.0001	0.9999	0.0008	0.9642	0.0089	0.0107	0.0155
	NAstx11	0.0004	0.9996	0.7648	0.2349	0.0001	0.0001	0.0001
	NAstx11	0.0222	0.9778	0.2287	0.1239	0.2157	0.2063	0.2255
	NAstx14	0.0766	0.9234	0.7772	0.2220	0.0003	0.0003	0.0003
	NAstx14	0.5583	0.4417	0.3028	0.1212	0.2193	0.1672	0.1895
	NAstx15	0.0406	0.9594	0.0000	0.0000	0.0000	0.0000	0.0000
	NAstx15	0.0484	0.9516	0.1800	0.2160	0.1931	0.2077	0.2032
	NAstx12	0.0002	0.9998	0.0000	0.0000	0.0000	0.0000	0.0000
	NAstx12	0.0037	0.9963	0.2358	0.1266	0.1996	0.2099	0.2282

	NAstx13	0.0017	0.9983	0.0000	0.0000	0.0000	0.0000	0.0000
	NAstx13	0.1219	0.8781	0.2556	0.1223	0.2155	0.1928	0.2137
CHARACTERS		**Margin**				**Lateral appressoria**		
	State	**Not appressed**	**Crenulate**	**Entire**	**Anastomo-sing**	**no**	**yes**	
Labelled in Fig.1	**Node/StateCode**	0	1	2	3	0	1	
	NLeotio	0.0000	0.0000	0.0000	0.0000	1.0000	0.0000	
	NLeotio	0.8092	0.0005	0.0905	0.0998	0.9971	0.0029	
	NEuroAll	1.0000	0.0000	0.0000	0.0000	1.0000	0.0000	
	NEuroAll	0.4594	0.0334	0.2522	0.2550	0.9025	0.0975	
	NOnyEuro	1.0000	0.0000	0.0000	0.0000	1.0000	0.0000	
	NOnyEuro	0.5570	0.0148	0.2137	0.2145	0.9440	0.0560	
	NEuro1	1.0000	0.0000	0.0000	0.0000	1.0000	0.0000	
	NEuro1	0.7746	0.0012	0.1086	0.1156	0.9932	0.0068	
	NEuro2	1.0000	0.0000	0.0000	0.0000	1.0000	0.0000	
	NEuro2	0.7960	0.0010	0.0977	0.1053	0.9941	0.0059	
	NEuro3	1.0000	0.0000	0.0000	0.0000	1.0000	0.0000	
	NEuro3	0.7430	0.0024	0.1241	0.1305	0.9869	0.0131	
	NPyrVeChae	1.0000	0.0000	0.0000	0.0000	1.0000	0.0000	
	NPyrVeChae	0.5094	0.0180	0.2351	0.2375	0.9423	0.0577	
	NPyren	0.9999	0.0000	0.0000	0.0000	1.0000	0.0000	
	NPyren	0.4719	0.0314	0.2478	0.2489	0.8919	0.1081	
	NVerChae	1.0000	0.0000	0.0000	0.0000	1.0000	0.0000	
	NVerChae	0.5799	0.0077	0.2040	0.2084	0.9713	0.0287	
	NVerru	1.0000	0.0000	0.0000	0.0000	1.0000	0.0000	
	NVerru	0.6884	0.0037	0.1520	0.1559	0.9796	0.0204	

NCthyrL	1.0000	0.0000	0.0000	0.0000	1.0000	0.0000
NCthyrL	0.6489	0.0021	0.1650	0.1839	0.9935	0.0065
NHerpo1	1.0000	0.0000	0.0000	0.0000	1.0000	0.0000
NHerpo1	0.8718	0.0003	0.0599	0.0680	0.9975	0.0025
NHerpo2	1.0000	0.0000	0.0000	0.0000	1.0000	0.0000
NHerpo2	0.7739	0.0015	0.1090	0.1156	0.9898	0.0102
NCthyr01	0.0000	0.0000	0.0000	0.0000	1.0000	0.0000
NCthyr01	0.4053	0.0130	0.2772	0.3045	0.9785	0.0215
NCthyr02	1.0000	0.0000	0.0000	0.0000	1.0000	0.0000
NCthyr02	0.4391	0.0022	0.2539	0.3048	0.9957	0.0043
NCthyr03	0.0000	0.0000	0.0000	0.0000	1.0000	0.0000
NCthyr03	0.4180	0.0101	0.2808	0.2911	0.9767	0.0233
NCthyr04	1.0000	0.0000	0.0000	0.0000	1.0000	0.0000
NCthyr04	0.8742	0.0005	0.0591	0.0661	0.9959	0.0041
NCthyr05	0.9999	0.0000	0.0000	0.0001	1.0000	0.0000
NCthyr05	0.4777	0.0011	0.2226	0.2987	0.9973	0.0027
NCthyr06	0.9981	0.0000	0.0000	0.0018	1.0000	0.0000
NCthyr06	0.4177	0.0022	0.2448	0.3353	0.9948	0.0052
NCthyr07	0.0000	0.0000	0.0000	0.0000	1.0000	0.0000
NCthyr07	0.2792	0.0009	0.2939	0.4260	0.9986	0.0014
NLecano	1.0000	0.0000	0.0000	0.0000	1.0000	0.0000
NLecano	0.6516	0.0025	0.1696	0.1763	0.9904	0.0096
NLeca1	1.0000	0.0000	0.0000	0.0000	1.0000	0.0000
NLeca1	0.5745	0.0101	0.2064	0.2089	0.9620	0.0380
NLeca2	1.0000	0.0000	0.0000	0.0000	1.0000	0.0000
NLeca2	0.6027	0.0062	0.1941	0.1969	0.9735	0.0265
NLeca3	1.0000	0.0000	0.0000	0.0000	1.0000	0.0000

NLeca3	0.5825	0.0095	0.2031	0.2049	0.9595	0.0405
NUAO	1.0000	0.0000	0.0000	0.0000	1.0000	0.0000
NUAO	0.6396	0.0031	0.1754	0.1820	0.9877	0.0123
NUmbi1	1.0000	0.0000	0.0000	0.0000	1.0000	0.0000
NUmbi1	0.5652	0.0114	0.2111	0.2123	0.9541	0.0459
NUmbi2	1.0000	0.0000	0.0000	0.0000	1.0000	0.0000
NUmbi2	0.5272	0.0253	0.2237	0.2239	0.9070	0.0930
NOstropo	1.0000	0.0000	0.0000	0.0000	1.0000	0.0000
NOstropo	0.6362	0.0026	0.1746	0.1866	0.9911	0.0089
NMpeltout1	1.0000	0.0000	0.0000	0.0000	1.0000	0.0000
NMpeltout1	0.5404	0.0060	0.2145	0.2391	0.9861	0.0139
NMpeltout2	1.0000	0.0000	0.0000	0.0000	1.0000	0.0000
NMpeltout2	0.6122	0.0075	0.1898	0.1906	0.9644	0.0356
NMpeltout3	1.0000	0.0000	0.0000	0.0000	1.0000	0.0000
NMpeltout3	0.4077	0.0265	0.2610	0.3048	0.9522	0.0478
NMpeltout4	1.0000	0.0000	0.0000	0.0000	1.0000	0.0000
NMpeltout4	0.4599	0.0260	0.2481	0.2660	0.9256	0.0744
NMpeltout5	0.9966	0.0001	0.0001	0.0032	1.0000	0.0000
NMpeltout5	0.3437	0.0576	0.2717	0.3270	0.9077	0.0923
NMpelt1	0.0015	0.0000	0.0000	0.9984	1.0000	0.0000
NMpelt1	0.0667	0.0272	0.3179	0.5882	0.9838	0.0162
NMpelt2	0.0001	0.0000	0.0000	0.9999	1.0000	0.0000
NMpelt2	0.0624	0.0311	0.2869	0.6197	0.9671	0.0329
NMpelt3	0.0000	0.0000	0.0000	1.0000	1.0000	0.0000
NMpelt3	0.0629	0.0299	0.3070	0.6003	0.9682	0.0318
NOstro1	1.0000	0.0000	0.0000	0.0000	1.0000	0.0000
NOstro1	0.4627	0.0323	0.2521	0.2529	0.9364	0.0636

	NOstro2	1.0000	0.0000	0.0000	0.0000	1.0000	0.0000
	NOstro2	0.6450	0.0057	0.1735	0.1759	0.9729	0.0271
	NOstro3	0.0000	0.0000	0.0000	0.0000	1.0000	0.0000
	NOstro3	0.3997	0.0653	0.2696	0.2654	0.9091	0.0909
	NOstro4	0.0000	0.0000	0.0000	0.0000	1.0000	0.0000
	NOstro4	0.0998	0.1070	0.4875	0.3056	0.9978	0.0022
	NOstro5	0.0000	0.0000	0.0000	0.0000	1.0000	0.0000
	NOstro5	0.1185	0.0432	0.5270	0.3113	0.9990	0.0010
	NOstro6	0.0000	0.0000	0.0000	0.0000	1.0000	0.0000
	NOstro6	0.1616	0.0747	0.4658	0.2979	0.9996	0.0004
NODE 1	**NDothArTry**	**1.0000**	**0.0000**	**0.0000**	**0.0000**	**1.0000**	**0.0000**
	NDothArTry	**0.4136**	**0.0044**	**0.3141**	**0.2678**	**0.9955**	**0.0045**
	NArthTryp	1.0000	0.0000	0.0000	0.0000	1.0000	0.0000
	NArthTryp	0.3340	0.0463	0.3189	0.3008	0.9422	0.0578
	NTryp1	0.9997	0.0001	0.0001	0.0001	1.0000	0.0000
	NTryp1	0.3974	0.0725	0.2629	0.2673	0.8085	0.1915
	NTryp2	0.9999	0.0000	0.0000	0.0000	1.0000	0.0000
	NTryp2	0.6095	0.0084	0.1904	0.1917	0.9612	0.0388
	NTryp3	0.9998	0.0001	0.0001	0.0001	1.0000	0.0000
	NTryp3	0.4076	0.0658	0.2619	0.2648	0.8130	0.1870
	NTryp4	1.0000	0.0000	0.0000	0.0000	1.0000	0.0000
	NTryp4	0.6538	0.0051	0.1695	0.1717	0.9738	0.0262
	NArtho01	1.0000	0.0000	0.0000	0.0000	1.0000	0.0000
	NArtho01	0.2673	0.0327	0.3674	0.3326	0.9860	0.0140
	NArtho02	0.0000	0.0000	0.0000	0.0000	1.0000	0.0000
	NArtho02	0.1211	0.0924	0.4386	0.3478	0.9900	0.0100
	NSeurat	0.0000	0.0000	0.0000	0.0000	1.0000	0.0000

NSeurat	0.1999	0.1000	0.3697	0.3303	0.9603	0.0397
NArthRock	0.0000	0.0000	0.0000	0.0000	1.0000	0.0000
NArthRock	0.1259	0.1309	0.4247	0.3185	0.9870	0.0130
NArtho03	1.0000	0.0000	0.0000	0.0000	1.0000	0.0000
NArtho03	0.4990	0.0180	0.2406	0.2424	0.9637	0.0363
NArtho04	1.0000	0.0000	0.0000	0.0000	1.0000	0.0000
NArtho04	0.5902	0.0098	0.1997	0.2003	0.9563	0.0437
NArtho05	1.0000	0.0000	0.0000	0.0000	1.0000	0.0000
NArtho05	0.5177	0.0181	0.2304	0.2338	0.9665	0.0335
NArtho06	0.0000	0.0000	0.0000	0.0000	1.0000	0.0000
NArtho06	0.3681	0.0590	0.2848	0.2881	0.9686	0.0314
NArtho07	1.0000	0.0000	0.0000	0.0000	1.0000	0.0000
NArtho07	0.5597	0.0109	0.2136	0.2158	0.9786	0.0214
NArtho08	1.0000	0.0000	0.0000	0.0000	1.0000	0.0000
NArtho08	0.6880	0.0080	0.1491	0.1548	0.9637	0.0363
NArtho09	1.0000	0.0000	0.0000	0.0000	1.0000	0.0000
NArtho09	0.3826	0.0551	0.2828	0.2795	0.9460	0.0540
NArtho10	0.0000	0.0000	0.0000	0.0000	1.0000	0.0000
NArtho10	0.2551	0.1817	0.2825	0.2807	0.8504	0.1496
NArtho11	1.0000	0.0000	0.0000	0.0000	1.0000	0.0000
NArtho11	0.4142	0.0403	0.2770	0.2685	0.9586	0.0414
NArtho12	1.0000	0.0000	0.0000	0.0000	1.0000	0.0000
NArtho12	0.5592	0.0128	0.2140	0.2140	0.9456	0.0544
NArtho13	1.0000	0.0000	0.0000	0.0000	1.0000	0.0000
NArtho13	0.3248	0.0694	0.3232	0.2825	0.9414	0.0586
NArtho14	0.0000	0.0000	0.0000	0.0000	1.0000	0.0000
NArtho14	0.2037	0.0699	0.4585	0.2679	0.9953	0.0047

NArtho15	0.0000	0.0000	0.0000	0.0000	1.0000	0.0000
NArtho15	0.3073	0.1016	0.3816	0.2095	0.9973	0.0027
NDothid	1.0000	0.0000	0.0000	0.0000	1.0000	0.0000
NDothid	0.4193	0.0015	0.3229	0.2563	0.9989	0.0011
NPate	1.0000	0.0000	0.0000	0.0000	1.0000	0.0000
NPate	0.7253	0.0020	0.1333	0.1394	0.9895	0.0105
NAbro1	1.0000	0.0000	0.0000	0.0000	1.0000	0.0000
NAbro1	0.8816	0.0003	0.0547	0.0634	0.9975	0.0025
NAbro2	1.0000	0.0000	0.0000	0.0000	1.0000	0.0000
NAbro2	0.8614	0.0003	0.0650	0.0733	0.9978	0.0022
NTube1	1.0000	0.0000	0.0000	0.0000	1.0000	0.0000
NTube1	0.5985	0.0362	0.1883	0.1770	0.9877	0.0123
NTube2	1.0000	0.0000	0.0000	0.0000	1.0000	0.0000
NTube2	0.7104	0.0036	0.1399	0.1461	0.9812	0.0188
NBotry1	0.0000	0.0000	0.0000	0.0000	1.0000	0.0000
NBotry1	0.8446	0.0006	0.0731	0.0817	0.9959	0.0041
NBotry2	0.0000	0.0000	0.0000	0.0000	1.0000	0.0000
NBotry2	0.8430	0.0007	0.0742	0.0821	0.9945	0.0055
NBotry3	1.0000	0.0000	0.0000	0.0000	1.0000	0.0000
NBotry3	0.9778	0.0000	0.0097	0.0125	0.9996	0.0004
NCapnodX	1.0000	0.0000	0.0000	0.0000	1.0000	0.0000
NCapnodX	0.1874	0.0078	0.3803	0.4245	0.9975	0.0025
NDothi1	0.0000	0.0000	0.0000	0.0000	1.0000	0.0000
NDothi1	0.2181	0.0631	0.3596	0.3592	0.9843	0.0157
NMyri1	0.0000	0.0000	0.0000	0.0000	1.0000	0.0000
NMyri1	0.3323	0.0206	0.3154	0.3317	0.9862	0.0138
NMyri2	1.0000	0.0000	0.0000	0.0000	1.0000	0.0000

	NMyri2	0.7426	0.0023	0.1243	0.1307	0.9868	0.0132
	NCapnod0	1.0000	0.0000	0.0000	0.0000	1.0000	0.0000
	NCapnod0	0.3289	0.0075	0.3112	0.3524	0.9948	0.0052
	NCapnod1	0.0000	0.0000	0.0000	0.0000	1.0000	0.0000
	NCapnod1	0.3049	0.0105	0.3224	0.3622	0.9950	0.0050
	NCapnod2	0.0000	0.0000	0.0000	0.0000	1.0000	0.0000
	NCapnod2	0.1803	0.0796	0.3589	0.3811	0.9803	0.0197
	NCapnod3	1.0000	0.0000	0.0000	0.0000	1.0000	0.0000
	NCapnod3	0.4511	0.0077	0.2456	0.2955	0.9696	0.0304
	NCapnod4	0.0000	0.0000	0.0000	0.0000	1.0000	0.0000
	NCapnod4	0.5365	0.0122	0.2111	0.2402	0.9646	0.0354
NODE 2	**NCapnod5**	**1.0000**	**0.0000**	**0.0000**	**0.0000**	**1.0000**	**0.0000**
	NCapnod5	**0.3888**	**0.0116**	**0.2746**	**0.3250**	**0.9615**	**0.0385**
	NAsteOut1	0.0000	0.0000	0.0000	0.0000	1.0000	0.0000
	NAsteOut1	0.3724	0.0326	0.2783	0.3167	0.8946	0.1054
	NAsteOut2	0.9999	0.0001	0.0000	0.0000	1.0000	0.0000
	NAsteOut2	0.2659	0.1301	0.3094	0.2945	0.2767	0.7233
	NAsteOut3	0.0000	0.0000	0.0000	0.0000	1.0000	0.0000
	NAsteOut3	0.5862	0.0324	0.1679	0.2134	0.9999	0.0001
	NAsteOut4	1.0000	0.0000	0.0000	0.0000	1.0000	0.0000
	NAsteOut4	0.9142	0.0011	0.0337	0.0510	0.9998	0.0002
	NAste1	0.0230	0.9755	0.0006	0.0010	0.9990	0.0010
	NAste1	0.0410	0.4511	0.2218	0.2861	0.0265	0.9735
NODE 3	**NAste2**	**0.0004**	**0.9990**	**0.0000**	**0.0005**	**0.9919**	**0.0081**
	NAste2	**0.0200**	**0.2767**	**0.3041**	**0.3992**	**0.0066**	**0.9934**
	NAste3	0.0001	0.9983	0.0000	0.0016	0.9737	0.0263
	NAste3	0.0032	0.3464	0.2206	0.4298	0.0132	0.9868

NAste4	0.0000	0.9998	0.0000	0.0002	0.0898	0.9102
NAste4	0.0017	0.7995	0.0882	0.1106	0.0002	0.9998
NAste5	0.0000	1.0000	0.0000	0.0000	0.0000	1.0000
NAste5	0.0001	0.9878	0.0071	0.0051	0.0000	1.0000
NAste6	0.0000	0.0000	0.0000	0.0000	1.0000	0.0000
NAste6	0.2551	0.0671	0.2722	0.4056	0.9997	0.0003
NAste7	0.0000	0.0000	0.0000	0.0000	1.0000	0.0000
NAste7	0.2376	0.0450	0.2890	0.4285	0.9991	0.0009
NAste8	0.0000	0.0000	0.0000	0.0000	1.0000	0.0000
NAste8	0.3014	0.0623	0.2544	0.3819	0.9992	0.0008
NCapno01	1.0000	0.0000	0.0000	0.0000	1.0000	0.0000
NCapno01	0.4229	0.0011	0.2456	0.3304	0.9971	0.0029
NCapno02	1.0000	0.0000	0.0000	0.0000	1.0000	0.0000
NCapno02	0.5867	0.0069	0.1992	0.2072	0.9685	0.0315
NCapno03	1.0000	0.0000	0.0000	0.0000	1.0000	0.0000
NCapno03	0.9124	0.0002	0.0398	0.0476	0.9982	0.0018
NCapno04	1.0000	0.0000	0.0000	0.0000	1.0000	0.0000
NCapno04	0.8511	0.0006	0.0699	0.0783	0.9954	0.0046
NCapno05	1.0000	0.0000	0.0000	0.0000	1.0000	0.0000
NCapno05	0.9538	0.0001	0.0208	0.0253	0.9989	0.0011
NCapno06	1.0000	0.0000	0.0000	0.0000	1.0000	0.0000
NCapno06	0.9895	0.0000	0.0046	0.0059	0.9998	0.0002
NCapno07	1.0000	0.0000	0.0000	0.0000	1.0000	0.0000
NCapno07	0.2833	0.0024	0.3072	0.4071	0.9976	0.0024
NTerato01	0.0000	0.0000	0.0000	0.0000	1.0000	0.0000
NTerato01	0.3320	0.0114	0.3029	0.3537	0.9934	0.0066
NTerato02	0.0000	0.0000	0.0000	0.0000	1.0000	0.0000

NTerato02	0.3139	0.0962	0.2854	0.3044	0.9129	0.0871
NTerato03	0.0000	0.0000	0.0000	0.0000	1.0000	0.0000
NTerato03	0.3667	0.0038	0.2845	0.3450	0.9989	0.0011
NTerato04	0.0000	0.0000	0.0000	0.0000	1.0000	0.0000
NTerato04	0.3893	0.0347	0.2706	0.3054	0.9924	0.0076
NTerato05	1.0000	0.0000	0.0000	0.0000	1.0000	0.0000
NTerato05	0.3844	0.0040	0.2841	0.3275	0.9981	0.0019
NTerato06	0.0000	0.0000	0.0000	0.0000	1.0000	0.0000
NTerato06	0.5190	0.0191	0.2212	0.2407	0.9922	0.0078
NTerato07	0.0000	0.0000	0.0000	0.0000	1.0000	0.0000
NTerato07	0.3222	0.0127	0.3080	0.3572	0.9949	0.0051
NTerato08	0.0000	0.0000	0.0000	0.0000	1.0000	0.0000
NTerato08	0.4030	0.0279	0.2707	0.2984	0.9880	0.0120
NTerato09	0.0000	0.0000	0.0000	0.0000	1.0000	0.0000
NTerato09	0.3897	0.0443	0.2765	0.2895	0.9439	0.0561
NTerato10	0.0000	0.0000	0.0000	0.0000	1.0000	0.0000
NTerato10	0.3518	0.0289	0.2839	0.3354	0.9924	0.0076
NTerato11	0.0000	0.0000	0.0000	0.0000	1.0000	0.0000
NTerato11	0.3917	0.0400	0.2580	0.3104	0.9894	0.0106
NCapnod6	1.0000	0.0000	0.0000	0.0000	1.0000	0.0000
NCapnod6	0.2847	0.0031	0.2994	0.4128	0.9957	0.0043
NSchiz	0.9953	0.0000	0.0000	0.0046	1.0000	0.0000
NSchiz	0.2010	0.0074	0.2738	0.5178	0.9838	0.0162
NMcspha1	0.0000	0.0000	0.0000	0.0000	1.0000	0.0000
NMcspha1	0.3898	0.0057	0.2951	0.3094	0.9979	0.0021
NMcspha2	0.0000	0.0000	0.0000	0.0000	1.0000	0.0000
NMcspha2	0.3289	0.0411	0.3059	0.3242	0.9834	0.0166

NMcspha3	0.0000	0.0000	0.0000	0.0000	1.0000	0.0000
NMcspha3	0.3634	0.0493	0.2838	0.3035	0.9842	0.0158
NMcspha4	1.0000	0.0000	0.0000	0.0000	1.0000	0.0000
NMcspha4	0.5167	0.0041	0.2344	0.2448	0.9983	0.0017
NMcspha5	0.0000	0.0000	0.0000	0.0000	1.0000	0.0000
NMcspha5	0.5381	0.0164	0.2199	0.2255	0.9923	0.0077
NMcspha6	0.0000	0.0000	0.0000	0.0000	1.0000	0.0000
NMcspha6	0.5000	0.0105	0.2393	0.2502	0.9958	0.0042
NMcspha7	1.0000	0.0000	0.0000	0.0000	1.0000	0.0000
NMcspha7	0.7006	0.0019	0.1376	0.1598	0.9983	0.0017
NMcspha9	1.0000	0.0000	0.0000	0.0000	1.0000	0.0000
NMcspha9	0.6331	0.0077	0.1709	0.1883	0.9969	0.0031
NMcspha8	0.0000	0.0000	0.0000	0.0000	1.0000	0.0000
NMcspha8	0.9025	0.0003	0.0449	0.0523	0.9975	0.0025
NMonOut1	1.0000	0.0000	0.0000	0.0000	1.0000	0.0000
NMonOut1	0.4208	0.0595	0.2602	0.2596	0.9114	0.0886
NMonOut2	0.0000	0.0000	0.0000	0.0000	1.0000	0.0000
NMonOut2	0.3168	0.1491	0.2670	0.2670	0.7752	0.2248
NMono	1.0000	0.0000	0.0000	0.0000	1.0000	0.0000
NMono	0.4235	0.0210	0.3036	0.2519	0.9889	0.0111
NPleo1	1.0000	0.0000	0.0000	0.0000	1.0000	0.0000
NPleo1	0.5119	0.0167	0.2381	0.2332	0.9935	0.0065
NStrig1	1.0000	0.0000	0.0000	0.0000	1.0000	0.0000
NStrig1	0.4746	0.0217	0.2538	0.2499	0.9808	0.0192
NStrig2	1.0000	0.0000	0.0000	0.0000	1.0000	0.0000
NStrig2	0.4582	0.0270	0.2595	0.2553	0.9788	0.0212
NStrig3	1.0000	0.0000	0.0000	0.0000	1.0000	0.0000

	NStrig3	0.4778	0.0217	0.2525	0.2481	0.9779	0.0221
	NStrig4	0.0000	0.0000	0.0000	0.0000	1.0000	0.0000
	NStrig4	0.4652	0.0273	0.2558	0.2518	0.9664	0.0336
	NStrig5	1.0000	0.0000	0.0000	0.0000	1.0000	0.0000
	NStrig5	0.6401	0.0074	0.1747	0.1777	0.9654	0.0346
	NStrig6	1.0000	0.0000	0.0000	0.0000	1.0000	0.0000
	NStrig6	0.6505	0.0039	0.1714	0.1742	0.9819	0.0181
	NStrig7	1.0000	0.0000	0.0000	0.0000	1.0000	0.0000
	NStrig7	0.6460	0.0048	0.1733	0.1758	0.9770	0.0230
	NStrig8	1.0000	0.0000	0.0000	0.0000	1.0000	0.0000
	NStrig8	0.7203	0.0029	0.1360	0.1408	0.9835	0.0165
	NADM01	0.9980	0.0019	0.0000	0.0000	1.0000	0.0000
	NADM01	0.3289	0.0982	0.2854	0.2875	0.9285	0.0715
	NADM02	1.0000	0.0000	0.0000	0.0000	1.0000	0.0000
	NADM02	0.5911	0.0072	0.2002	0.2015	0.9694	0.0306
	NADM03	1.0000	0.0000	0.0000	0.0000	1.0000	0.0000
	NADM03	0.5640	0.0119	0.2121	0.2119	0.9488	0.0512
NODE 4	**NADM04**	**0.9452**	**0.0541**	**0.0004**	**0.0004**	**1.0000**	**0.0000**
	NADM04	**0.1833**	**0.2439**	**0.2829**	**0.2899**	**0.8854**	**0.1146**
	NADM05	0.9995	0.0005	0.0000	0.0000	1.0000	0.0000
	NADM05	0.5654	0.0119	0.2114	0.2113	0.9489	0.0511
	NADM06	0.0000	0.0000	0.0000	0.0000	1.0000	0.0000
	NADM06	0.0280	0.3871	0.2950	0.2899	0.9857	0.0143
	NADM07	0.0000	0.0000	0.0000	0.0000	1.0000	0.0000
	NADM07	0.1487	0.0683	0.3488	0.4343	0.9620	0.0380
NODE 5	**NADM08**	**0.0041**	**0.9958**	**0.0000**	**0.0000**	**1.0000**	**0.0000**
	NADM08	**0.0007**	**0.9086**	**0.0530**	**0.0377**	**0.9924**	**0.0076**

	NADM11	0.0000	1.0000	0.0000	0.0000	1.0000	0.0000
	NADM11	0.0071	0.7391	0.1623	0.0916	0.9934	0.0066
	NADM12	0.0000	1.0000	0.0000	0.0000	1.0000	0.0000
	NADM12	0.0507	0.4071	0.3636	0.1786	0.9978	0.0022
	NADM09	0.0000	1.0000	0.0000	0.0000	1.0000	0.0000
	NADM09	0.0002	0.9653	0.0202	0.0142	0.9928	0.0072
	NADM10	0.0000	0.0000	0.0000	0.0000	1.0000	0.0000
	NADM10	0.0000	0.9992	0.0005	0.0003	0.9999	0.0001
	NPleo2	1.0000	0.0000	0.0000	0.0000	1.0000	0.0000
	NPleo2	0.5198	0.0063	0.2225	0.2514	0.9934	0.0066
	NMyti1	1.0000	0.0000	0.0000	0.0000	1.0000	0.0000
	NMyti1	0.3028	0.0380	0.2974	0.3618	0.9837	0.0163
	NMyti2	0.0000	0.0000	0.0000	0.0000	1.0000	0.0000
	NMyti2	0.2268	0.0889	0.2830	0.4013	0.9846	0.0154
	NMyti3	1.0000	0.0000	0.0000	0.0000	1.0000	0.0000
	NMyti3	0.8937	0.0001	0.0488	0.0573	0.9990	0.0010
	NHyster	1.0000	0.0000	0.0000	0.0000	1.0000	0.0000
	NHyster	0.9178	0.0001	0.0375	0.0446	0.9989	0.0011
	NPleo3	1.0000	0.0000	0.0000	0.0000	1.0000	0.0000
	NPleo3	0.6540	0.0024	0.1697	0.1739	0.9909	0.0091
	NDicty1	0.0000	0.0000	0.0000	0.0000	1.0000	0.0000
	NDicty1	0.1573	0.0723	0.4887	0.2817	0.9913	0.0087
	NDicty2	0.0000	0.0000	0.0000	0.0000	1.0000	0.0000
	NDicty2	0.0210	0.2296	0.5863	0.1631	0.9981	0.0019
	NPleo4	1.0000	0.0000	0.0000	0.0000	1.0000	0.0000
	NPleo4	0.9300	0.0001	0.0314	0.0385	0.9992	0.0008
NODE 6	**NMVP**	**0.9964**	**0.0014**	**0.0022**	**0.0000**	**1.0000**	**0.0000**

	NMVP	**0.1369**	**0.2633**	**0.3188**	**0.2810**	**0.9831**	**0.0169**
	NVent1	0.9828	0.0163	0.0009	0.0001	1.0000	0.0000
	NVent1	0.0387	0.5239	0.2420	0.1953	0.9806	0.0194
	NStom1	0.0263	0.9733	0.0002	0.0002	1.0000	0.0000
	NStom1	0.0021	0.9007	0.0545	0.0426	0.9659	0.0341
	NStom2	0.0001	0.9999	0.0000	0.0000	1.0000	0.0000
	NStom2	0.0001	0.9816	0.0109	0.0074	0.9970	0.0030
	NVent2	1.0000	0.0000	0.0000	0.0000	1.0000	0.0000
	NVent2	0.2577	0.2053	0.2805	0.2565	0.9979	0.0021
	NVent3	0.0000	0.0000	0.0000	0.0000	1.0000	0.0000
	NVent3	0.2282	0.1509	0.3225	0.2984	0.9727	0.0273
	NMThyrX	0.9820	0.0007	0.0171	0.0001	1.0000	0.0000
	NMThyrX	0.2369	0.1888	0.2990	0.2753	0.9659	0.0341
	NPhaeo	1.0000	0.0000	0.0000	0.0000	1.0000	0.0000
	NPhaeo	0.8010	0.0012	0.0951	0.1027	0.9920	0.0080
NODE 7	**NMThyr1**	**0.2081**	**0.0003**	**0.7913**	**0.0003**	**1.0000**	**0.0000**
	NMThyr1	**0.2052**	**0.2376**	**0.2886**	**0.2686**	**0.9285**	**0.0715**
	NMThyr2	0.0056	0.0002	0.9941	0.0002	1.0000	0.0000
	NMThyr2	0.1808	0.2992	0.2589	0.2610	0.9084	0.0916
	NMThyr3	0.0003	0.0000	0.9996	0.0000	1.0000	0.0000
	NMThyr3	0.2357	0.2260	0.2744	0.2640	0.8365	0.1635
	NMThyr4	0.0000	0.0000	0.9999	0.0000	1.0000	0.0000
	NMThyr4	0.2074	0.2006	0.3076	0.2844	0.8685	0.1315
	NMTSup	0.0000	0.0000	0.0000	0.0000	1.0000	0.0000
	NMTSup	0.1332	0.2908	0.2864	0.2895	0.9493	0.0507
	NMThyr5	0.0000	0.0000	0.0000	0.0000	1.0000	0.0000
	NMThyr5	0.1442	0.2960	0.2733	0.2865	0.9037	0.0963

	NMThyr6	0.0000	0.0000	0.0000	0.0000	1.0000	0.0000
	NMThyr6	0.1488	0.2299	0.3270	0.2943	0.9075	0.0925
	NHelio	0.0000	0.0000	0.0000	0.0000	1.0000	0.0000
	NHelio	0.0897	0.2656	0.3348	0.3099	0.9961	0.0039
	NZelo1	0.1418	0.0002	0.8578	0.0002	1.0000	0.0000
	NZelo1	0.2696	0.2013	0.2657	0.2635	0.7489	0.2511
	NNati	0.9966	0.0002	0.0030	0.0002	1.0000	0.0000
	NNati	0.5409	0.0138	0.2226	0.2227	0.9472	0.0528
	NZelo2	0.0000	0.0000	0.0000	0.0000	1.0000	0.0000
	NZelo2	0.0634	0.1252	0.6163	0.1951	0.9981	0.0019
	NZelo3	0.0030	0.0000	0.9970	0.0000	1.0000	0.0000
	NZelo3	0.0336	0.0841	0.6755	0.2067	0.9970	0.0030
	NZelo4	0.0000	0.0000	1.0000	0.0000	1.0000	0.0000
	NZelo4	0.0002	0.0003	0.9896	0.0099	0.9998	0.0002
	NZelo5	0.0000	0.0000	0.0000	0.0000	1.0000	0.0000
	NZelo5	0.0848	0.1740	0.4602	0.2810	0.9904	0.0096
	NZelo6	0.0000	0.0000	0.0000	0.0000	1.0000	0.0000
	NZelo6	0.0918	0.1604	0.5252	0.2225	0.9954	0.0046
NODE 8	**NAulo1**	**0.0148**	**0.9816**	**0.0018**	**0.0018**	**0.9999**	**0.0001**
	NAulo1	**0.0280**	**0.7173**	**0.1329**	**0.1218**	**0.8329**	**0.1671**
	NLembo	0.0000	1.0000	0.0000	0.0000	1.0000	0.0000
	NLembo	0.0002	0.9698	0.0176	0.0125	0.9939	0.0061
	NAulo2	0.0000	1.0000	0.0000	0.0000	1.0000	0.0000
	NAulo2	0.0000	0.9888	0.0067	0.0045	0.9985	0.0015
	NAstx01	0.9777	0.0222	0.0000	0.0000	1.0000	0.0000
	NAstx01	0.0939	0.2602	0.3475	0.2984	0.1548	0.8452
NODE 9	**NAstx02**	**0.9529**	**0.0470**	**0.0001**	**0.0000**	**1.0000**	**0.0000**

	NAstx02	0.0792	0.3152	0.3264	0.2792	0.1269	0.8731
	NMelas01	0.9536	0.0462	0.0001	0.0001	1.0000	0.0000
	NMelas01	0.2237	0.1187	0.3370	0.3206	0.9645	0.0355
	NMelas02	0.9999	0.0001	0.0000	0.0000	1.0000	0.0000
	NMelas02	0.3090	0.0518	0.3198	0.3195	0.9819	0.0181
	NMelas03	0.0000	0.0000	0.0000	0.0000	1.0000	0.0000
	NMelas03	0.3014	0.0554	0.3223	0.3209	0.9819	0.0181
	NMelas04	1.0000	0.0000	0.0000	0.0000	1.0000	0.0000
	NMelas04	0.3064	0.0511	0.3214	0.3211	0.9824	0.0176
	NMelas05	0.0000	0.0000	0.0000	0.0000	1.0000	0.0000
	NMelas05	0.2129	0.1193	0.3230	0.3448	0.9917	0.0083
	NMelas06	0.0000	0.0000	0.0000	0.0000	1.0000	0.0000
	NMelas06	0.2323	0.1197	0.3112	0.3368	0.9918	0.0082
	NMelas07	1.0000	0.0000	0.0000	0.0000	1.0000	0.0000
	NMelas07	0.5531	0.0153	0.2135	0.2181	0.9955	0.0045
	NMelas08	0.0000	0.0000	0.0000	0.0000	1.0000	0.0000
	NMelas08	0.4072	0.0733	0.2573	0.2621	0.9830	0.0170
	NMelas09	1.0000	0.0000	0.0000	0.0000	1.0000	0.0000
	NMelas09	0.3145	0.0528	0.3160	0.3167	0.9817	0.0183
	NMelas10	1.0000	0.0000	0.0000	0.0000	1.0000	0.0000
	NMelas10	0.2840	0.0678	0.3181	0.3301	0.9899	0.0101
	NMelas11	0.0000	0.0000	0.0000	0.0000	1.0000	0.0000
	NMelas11	0.1988	0.2559	0.2117	0.3336	0.9968	0.0032
	NMelas12	0.0000	0.0000	0.0000	0.0000	1.0000	0.0000
	NMelas12	0.2244	0.2670	0.1961	0.3125	0.9929	0.0071
	NMelas13	0.9999	0.0000	0.0000	0.0000	1.0000	0.0000
	NMelas13	0.4624	0.0390	0.2488	0.2498	0.8720	0.1280

	NAstx03	0.1454	0.8446	0.0095	0.0005	0.9725	0.0275
	NAstx03	0.0074	0.8124	0.0989	0.0813	0.0016	0.9984
NODE 10	**NAstx04**	**0.0000**	**1.0000**	**0.0000**	**0.0000**	**0.0002**	**0.9998**
	NAstx04	**0.0002**	**0.9701**	**0.0176**	**0.0121**	**0.0001**	**0.9999**
	NAstx05	0.0935	0.8834	0.0230	0.0001	0.9734	0.0266
	NAstx05	0.0013	0.8202	0.1122	0.0663	0.0405	0.9595
	NAstx06	0.0892	0.8974	0.0134	0.0000	0.9986	0.0014
	NAstx06	0.0160	0.5030	0.3001	0.1808	0.8350	0.1650
	NAstx07	0.0010	0.9988	0.0002	0.0000	0.9991	0.0009
	NAstx07	0.0071	0.8336	0.0846	0.0748	0.2608	0.7392
	NAstx08	0.0000	1.0000	0.0000	0.0000	1.0000	0.0000
	NAstx08	0.0001	0.9822	0.0105	0.0072	0.9970	0.0030
	NAstx09	0.0002	0.9997	0.0000	0.0000	0.9972	0.0028
	NAstx09	0.0117	0.8044	0.0973	0.0866	0.2065	0.7935
	NAstx10	0.0000	1.0000	0.0000	0.0000	0.0000	1.0000
	NAstx10	0.0001	0.9876	0.0072	0.0051	0.0000	1.0000
	NAstx11	0.0919	0.8953	0.0128	0.0000	1.0000	0.0000
	NAstx11	0.0493	0.2347	0.4579	0.2581	0.9720	0.0280
	NAstx14	0.1316	0.8570	0.0105	0.0009	1.0000	0.0000
	NAstx14	0.3109	0.1285	0.3048	0.2558	0.8518	0.1482
	NAstx15	0.0319	0.9521	0.0089	0.0071	0.9984	0.0016
	NAstx15	0.1078	0.5071	0.1967	0.1885	0.6799	0.3201
	NAstx12	0.0904	0.8954	0.0141	0.0000	1.0000	0.0000
	NAstx12	0.0149	0.3657	0.4215	0.1978	0.9967	0.0033
	NAstx13	0.1583	0.6568	0.1837	0.0012	1.0000	0.0000
	NAstx13	0.1200	0.0521	0.5671	0.2608	0.9807	0.0193
CHARACTERS			**Sporocarp Initiation**				

Labelled in Fig.1	State	Meristogenous lateral	Meristogenous intercalary	Meristogenous from spores	From stomata	Symphiogenous
	Node/StateCode	0	1	2	3	4
	NLeotio	0.0000	0.0000	0.0000	0.0000	0.0000
	NLeotio	0.1818	0.1883	0.2008	0.2146	0.2145
	NEuroAll	0.0000	0.0000	0.0000	0.0000	0.0000
	NEuroAll	0.2000	0.1997	0.2001	0.2000	0.2001
	NOnyEuro	0.0000	0.0000	0.0000	0.0000	0.0000
	NOnyEuro	0.2001	0.1959	0.2022	0.1993	0.2024
	NEuro1	0.0000	0.0000	0.0000	0.0000	0.0000
	NEuro1	0.2010	0.1847	0.2090	0.1938	0.2115
	NEuro2	0.0000	0.0000	0.0000	0.0000	0.0000
	NEuro2	0.2066	0.1849	0.2061	0.1925	0.2099
	NEuro3	0.0000	0.0000	0.0000	0.0000	0.0000
	NEuro3	0.2077	0.1884	0.2037	0.1960	0.2042
	NPyrVeChae	0.0000	0.0000	0.0000	0.0000	0.0000
	NPyrVeChae	0.1997	0.1998	0.2004	0.1999	0.2002
	NPyren	0.0000	0.0000	0.0000	0.0000	0.0000
	NPyren	0.1999	0.2000	0.1996	0.2004	0.2000
	NVerChae	0.0000	0.0000	0.0000	0.0000	0.0000
	NVerChae	0.1982	0.1983	0.2028	0.1995	0.2011
	NVerru	0.0000	0.0000	0.0000	0.0000	0.0000
	NVerru	0.1901	0.2185	0.1905	0.1955	0.2054
	NCthyrL	0.0000	0.0000	0.0000	0.0000	0.0000
	NCthyrL	0.1888	0.1867	0.2217	0.1986	0.2042

NHerpo1	0.0000	0.0000	0.0000	0.0000	0.0000
NHerpo1	0.1565	0.1804	0.2555	0.2000	0.2076
NHerpo2	0.0000	0.0000	0.0000	0.0000	0.0000
NHerpo2	0.1985	0.1804	0.2253	0.2041	0.1917
NCthyr01	0.0000	0.0000	0.0000	0.0000	0.0000
NCthyr01	0.1956	0.1920	0.2146	0.1952	0.2025
NCthyr02	0.0000	0.0000	0.0000	0.0000	0.0000
NCthyr02	0.1889	0.1859	0.2345	0.1882	0.2025
NCthyr03	0.0000	0.0000	0.0000	0.0000	0.0000
NCthyr03	0.1915	0.1938	0.2248	0.1895	0.2002
NCthyr04	0.0000	0.0000	0.0000	0.0000	0.0000
NCthyr04	0.1740	0.1712	0.2736	0.1720	0.2092
NCthyr05	0.0000	0.0000	0.0000	0.0000	0.0000
NCthyr05	0.1788	0.1842	0.2596	0.1777	0.1997
NCthyr06	0.0000	0.0000	0.0000	0.0000	0.0000
NCthyr06	0.1798	0.1828	0.2554	0.1801	0.2019
NCthyr07	0.0000	0.0000	0.0000	0.0000	0.0000
NCthyr07	0.1417	0.2046	0.3162	0.1381	0.1994
NLecano	0.0000	0.0000	0.0000	0.0000	0.0000
NLecano	0.2000	0.1977	0.2010	0.2007	0.2006
NLeca1	0.0000	0.0000	0.0000	0.0000	0.0000
NLeca1	0.1992	0.1950	0.2028	0.2006	0.2024
NLeca2	0.0000	0.0000	0.0000	0.0000	0.0000
NLeca2	0.1991	0.1940	0.2030	0.2012	0.2028
NLeca3	0.0000	0.0000	0.0000	0.0000	0.0000
NLeca3	0.1990	0.1939	0.2023	0.2022	0.2027
NUAO	0.0000	0.0000	0.0000	0.0000	0.0000

NUAO	0.2000	0.1986	0.2008	0.2005	0.2001
NUmbi1	0.0000	0.0000	0.0000	0.0000	0.0000
NUmbi1	0.1999	0.1996	0.2004	0.2006	0.1995
NUmbi2	0.0000	0.0000	0.0000	0.0000	0.0000
NUmbi2	0.1996	0.1953	0.2049	0.2007	0.1996
NOstropo	0.0000	0.0000	0.0000	0.0000	0.0000
NOstropo	0.1998	0.1975	0.2016	0.2004	0.2007
NMpeltout1	0.0000	0.0000	0.0000	0.0000	0.0000
NMpeltout1	0.2000	0.1979	0.2013	0.2002	0.2006
NMpeltout2	0.0000	0.0000	0.0000	0.0000	0.0000
NMpeltout2	0.1997	0.1940	0.2047	0.2003	0.2012
NMpeltout3	0.0000	0.0000	0.0000	0.0000	0.0000
NMpeltout3	0.2000	0.1995	0.2003	0.2000	0.2001
NMpeltout4	0.0000	0.0000	0.0000	0.0000	0.0000
NMpeltout4	0.1999	0.1992	0.2007	0.2000	0.2002
NMpeltout5	0.0000	0.0000	0.0000	0.0000	0.0000
NMpeltout5	0.2000	0.1996	0.2003	0.2000	0.2001
NMpelt1	0.0000	0.0000	0.0000	0.0000	0.0000
NMpelt1	0.1993	0.1970	0.2026	0.2001	0.2010
NMpelt2	0.0000	0.0000	0.0000	0.0000	0.0000
NMpelt2	0.1983	0.1966	0.2055	0.1987	0.2008
NMpelt3	0.0000	0.0000	0.0000	0.0000	0.0000
NMpelt3	0.1993	0.1965	0.2035	0.2003	0.2004
NOstro1	0.0000	0.0000	0.0000	0.0000	0.0000
NOstro1	0.1999	0.2000	0.2001	0.2000	0.2000
NOstro2	0.0000	0.0000	0.0000	0.0000	0.0000
NOstro2	0.1988	0.2001	0.2015	0.2007	0.1988

	NOstro3	0.0000	0.0000	0.0000	0.0000	0.0000
	NOstro3	0.1999	0.1999	0.2003	0.1998	0.2001
	NOstro4	0.0000	0.0000	0.0000	0.0000	0.0000
	NOstro4	0.1907	0.1991	0.2194	0.2059	0.1849
	NOstro5	0.0000	0.0000	0.0000	0.0000	0.0000
	NOstro5	0.1865	0.2017	0.2280	0.2039	0.1799
	NOstro6	0.0000	0.0000	0.0000	0.0000	0.0000
	NOstro6	0.1830	0.2136	0.2279	0.1992	0.1764
NODE 1	**NDothArTry**	**0.0000**	**0.0000**	**0.0000**	**0.0000**	**0.0000**
	NDothArTry	**0.2003**	**0.2034**	**0.1923**	**0.2076**	**0.1963**
	NArthTryp	0.0000	0.0000	0.0000	0.0000	0.0000
	NArthTryp	0.1993	0.1976	0.2001	0.2006	0.2024
	NTryp1	0.0000	0.0000	0.0000	0.0000	0.0000
	NTryp1	0.2000	0.2000	0.2000	0.2000	0.2000
	NTryp2	0.0000	0.0000	0.0000	0.0000	0.0000
	NTryp2	0.1970	0.1840	0.2183	0.1945	0.2062
	NTryp3	0.0000	0.0000	0.0000	0.0000	0.0000
	NTryp3	0.1999	0.2000	0.2001	0.1999	0.2001
	NTryp4	0.0000	0.0000	0.0000	0.0000	0.0000
	NTryp4	0.1996	0.1916	0.2115	0.1938	0.2035
	NArtho01	0.0000	0.0000	0.0000	0.0000	0.0000
	NArtho01	0.1998	0.1964	0.2017	0.1996	0.2025
	NArtho02	0.0000	0.0000	0.0000	0.0000	0.0000
	NArtho02	0.1993	0.1937	0.2029	0.1988	0.2053
	NSeurat	0.0000	0.0000	0.0000	0.0000	0.0000
	NSeurat	0.1997	0.1956	0.2020	0.2000	0.2027
	NArthRock	0.0000	0.0000	0.0000	0.0000	0.0000

NArthRock	0.1991	0.1927	0.2031	0.1980	0.2071
NArtho03	0.0000	0.0000	0.0000	0.0000	0.0000
NArtho03	0.1997	0.1982	0.2012	0.1997	0.2012
NArtho04	0.0000	0.0000	0.0000	0.0000	0.0000
NArtho04	0.1979	0.1941	0.2042	0.1982	0.2056
NArtho05	0.0000	0.0000	0.0000	0.0000	0.0000
NArtho05	0.1996	0.1976	0.2018	0.1992	0.2018
NArtho06	0.0000	0.0000	0.0000	0.0000	0.0000
NArtho06	0.1997	0.1925	0.2055	0.1966	0.2057
NArtho07	0.0000	0.0000	0.0000	0.0000	0.0000
NArtho07	0.1989	0.1954	0.2039	0.1977	0.2040
NArtho08	0.0000	0.0000	0.0000	0.0000	0.0000
NArtho08	0.1985	0.1843	0.2113	0.1773	0.2288
NArtho09	0.0000	0.0000	0.0000	0.0000	0.0000
NArtho09	0.1999	0.1990	0.2005	0.1999	0.2007
NArtho10	0.0000	0.0000	0.0000	0.0000	0.0000
NArtho10	0.1998	0.1995	0.2004	0.1998	0.2005
NArtho11	0.0000	0.0000	0.0000	0.0000	0.0000
NArtho11	0.1998	0.1983	0.2010	0.1996	0.2014
NArtho12	0.0000	0.0000	0.0000	0.0000	0.0000
NArtho12	0.1993	0.1975	0.2017	0.1989	0.2027
NArtho13	0.0000	0.0000	0.0000	0.0000	0.0000
NArtho13	0.1990	0.1953	0.2023	0.1977	0.2057
NArtho14	0.0000	0.0000	0.0000	0.0000	0.0000
NArtho14	0.1953	0.1778	0.2073	0.1767	0.2429
NArtho15	0.0000	0.0000	0.0000	0.0000	0.0000
NArtho15	0.1926	0.1685	0.2069	0.1556	0.2763

NDothid	0.0000	0.0000	0.0000	0.0000	0.0000
NDothid	0.1997	0.2073	0.1871	0.2126	0.1933
NPate	0.0000	0.0000	0.0000	0.0000	0.0000
NPate	0.2057	0.2038	0.1962	0.1972	0.1972
NAbro1	0.0000	0.0000	0.0000	0.0000	0.0000
NAbro1	0.2138	0.2258	0.1913	0.1963	0.1728
NAbro2	0.0000	0.0000	0.0000	0.0000	0.0000
NAbro2	0.2010	0.2029	0.1922	0.2028	0.2011
NTube1	0.0000	0.0000	0.0000	0.0000	0.0000
NTube1	0.2016	0.1970	0.1984	0.2034	0.1996
NTube2	0.0000	0.0000	0.0000	0.0000	0.0000
NTube2	0.2057	0.2044	0.1909	0.2037	0.1954
NBotry1	0.0000	0.0000	0.0000	0.0000	0.0000
NBotry1	0.2022	0.1874	0.2026	0.2110	0.1968
NBotry2	0.0000	0.0000	0.0000	0.0000	0.0000
NBotry2	0.2237	0.1850	0.2103	0.1988	0.1822
NBotry3	0.0000	0.0000	0.0000	0.0000	0.0000
NBotry3	0.1959	0.1635	0.1923	0.2559	0.1924
NCapnodX	0.0000	0.0000	0.0000	0.0000	0.0000
NCapnodX	0.2008	0.1941	0.2018	0.2023	0.2010
NDothi1	0.0000	0.0000	0.0000	0.0000	0.0000
NDothi1	0.2012	0.1977	0.1973	0.2051	0.1988
NMyri1	0.0000	0.0000	0.0000	0.0000	0.0000
NMyri1	0.1996	0.1958	0.2029	0.2024	0.1992
NMyri2	0.0000	0.0000	0.0000	0.0000	0.0000
NMyri2	0.2132	0.2056	0.1846	0.2040	0.1926
NCapnod0	0.0000	0.0000	0.0000	0.0000	0.0000

	NCapnod0	0.2012	0.1953	0.2007	0.2032	0.1996
	NCapnod1	0.0000	0.0000	0.0000	0.0000	0.0000
	NCapnod1	0.2013	0.1951	0.2005	0.2037	0.1993
	NCapnod2	0.0000	0.0000	0.0000	0.0000	0.0000
	NCapnod2	0.2019	0.1965	0.1994	0.2051	0.1971
	NCapnod3	0.0000	0.0000	0.0000	0.0000	0.0000
	NCapnod3	0.2017	0.1942	0.1996	0.2051	0.1993
	NCapnod4	0.0000	0.0000	0.0000	0.0000	0.0000
	NCapnod4	0.2017	0.1954	0.1987	0.2049	0.1993
NODE 2	**NCapnod5**	**0.0000**	**0.0000**	**0.0000**	**0.0000**	**0.0000**
	NCapnod5	**0.2013**	**0.1948**	**0.1993**	**0.2048**	**0.1998**
	NAsteOut1	0.0000	0.0000	0.0000	0.0000	0.0000
	NAsteOut1	0.2015	0.1957	0.1994	0.2038	0.1996
	NAsteOut2	0.0000	0.0000	0.0000	0.0000	0.0000
	NAsteOut2	0.2010	0.1968	0.1996	0.2031	0.1995
	NAsteOut3	0.0000	0.0000	0.0000	0.0000	0.0000
	NAsteOut3	0.2094	0.1358	0.1757	0.3064	0.1727
	NAsteOut4	0.0000	0.0000	0.0000	0.0000	0.0000
	NAsteOut4	0.2073	0.1419	0.1676	0.3037	0.1795
	NAste1	0.0000	0.0000	0.0000	0.0000	0.0000
	NAste1	0.2000	0.2078	0.1961	0.1999	0.1962
NODE 3	**NAste2**	**0.0001**	**0.9999**	**0.0000**	**0.0000**	**0.0000**
	NAste2	**0.2001**	**0.2317**	**0.1799**	**0.2066**	**0.1818**
	NAste3	0.0000	1.0000	0.0000	0.0000	0.0000
	NAste3	0.1871	0.3299	0.1449	0.1832	0.1549
	NAste4	0.0000	1.0000	0.0000	0.0000	0.0000
	NAste4	0.1972	0.2639	0.1694	0.1942	0.1752

NAste5	0.0000	1.0000	0.0000	0.0000	0.0000
NAste5	0.0848	0.7141	0.0542	0.0832	0.0637
NAste6	0.0000	0.0000	0.0000	0.0000	0.0000
NAste6	0.2020	0.1484	0.1793	0.2900	0.1803
NAste7	0.0000	0.0000	0.0000	0.0000	0.0000
NAste7	0.2037	0.1545	0.1911	0.2696	0.1810
NAste8	0.0000	0.0000	0.0000	0.0000	0.0000
NAste8	0.2023	0.1516	0.1819	0.2768	0.1875
NCapno01	0.0000	0.0000	0.0000	0.0000	0.0000
NCapno01	0.1999	0.1946	0.1987	0.2072	0.1996
NCapno02	0.0000	0.0000	0.0000	0.0000	0.0000
NCapno02	0.2003	0.1975	0.1994	0.2027	0.2000
NCapno03	0.0000	0.0000	0.0000	0.0000	0.0000
NCapno03	0.2051	0.1743	0.1826	0.2462	0.1918
NCapno04	0.0000	0.0000	0.0000	0.0000	0.0000
NCapno04	0.2046	0.1838	0.1901	0.2294	0.1922
NCapno05	0.0000	0.0000	0.0000	0.0000	0.0000
NCapno05	0.2088	0.1575	0.1649	0.2869	0.1820
NCapno06	0.0000	0.0000	0.0000	0.0000	0.0000
NCapno06	0.2057	0.1438	0.1647	0.3193	0.1665
NCapno07	0.0000	0.0000	0.0000	0.0000	0.0000
NCapno07	0.1993	0.1941	0.1982	0.2090	0.1993
NTerato01	0.0000	0.0000	0.0000	0.0000	0.0000
NTerato01	0.1996	0.1956	0.1979	0.2081	0.1988
NTerato02	0.0000	0.0000	0.0000	0.0000	0.0000
NTerato02	0.2000	0.1997	0.1997	0.2005	0.2001
NTerato03	0.0000	0.0000	0.0000	0.0000	0.0000

NTerato03	0.1993	0.1931	0.1954	0.2156	0.1966
NTerato04	0.0000	0.0000	0.0000	0.0000	0.0000
NTerato04	0.1990	0.1923	0.1933	0.2217	0.1937
NTerato05	0.0000	0.0000	0.0000	0.0000	0.0000
NTerato05	0.1997	0.1954	0.1959	0.2122	0.1968
NTerato06	0.0000	0.0000	0.0000	0.0000	0.0000
NTerato06	0.1998	0.1920	0.1914	0.2223	0.1945
NTerato07	0.0000	0.0000	0.0000	0.0000	0.0000
NTerato07	0.2002	0.1968	0.1977	0.2075	0.1978
NTerato08	0.0000	0.0000	0.0000	0.0000	0.0000
NTerato08	0.1989	0.1963	0.1976	0.2096	0.1977
NTerato09	0.0000	0.0000	0.0000	0.0000	0.0000
NTerato09	0.1997	0.1992	0.1998	0.2014	0.1999
NTerato10	0.0000	0.0000	0.0000	0.0000	0.0000
NTerato10	0.2012	0.1968	0.1933	0.2133	0.1954
NTerato11	0.0000	0.0000	0.0000	0.0000	0.0000
NTerato11	0.2006	0.1941	0.1894	0.2223	0.1936
NCapnod6	0.0000	0.0000	0.0000	0.0000	0.0000
NCapnod6	0.1989	0.1947	0.1985	0.2080	0.1998
NSchiz	0.0000	0.0000	0.0000	0.0000	0.0000
NSchiz	0.1985	0.1963	0.1976	0.2080	0.1997
NMcspha1	0.0000	0.0000	0.0000	0.0000	0.0000
NMcspha1	0.1990	0.1936	0.1975	0.2113	0.1986
NMcspha2	0.0000	0.0000	0.0000	0.0000	0.0000
NMcspha2	0.2010	0.1969	0.1985	0.2048	0.1988
NMcspha3	0.0000	0.0000	0.0000	0.0000	0.0000
NMcspha3	0.2016	0.1934	0.1933	0.2138	0.1979

NMcspha4	0.0000	0.0000	0.0000	0.0000	0.0000
NMcspha4	0.1974	0.1926	0.1949	0.2176	0.1974
NMcspha5	0.0000	0.0000	0.0000	0.0000	0.0000
NMcspha5	0.1979	0.1931	0.1929	0.2204	0.1957
NMcspha6	0.0000	0.0000	0.0000	0.0000	0.0000
NMcspha6	0.1974	0.1930	0.1949	0.2178	0.1969
NMcspha7	0.0000	0.0000	0.0000	0.0000	0.0000
NMcspha7	0.1961	0.1866	0.1898	0.2358	0.1918
NMcspha9	0.0000	0.0000	0.0000	0.0000	0.0000
NMcspha9	0.1966	0.1873	0.1899	0.2338	0.1924
NMcspha8	0.0000	0.0000	0.0000	0.0000	0.0000
NMcspha8	0.1956	0.1810	0.1833	0.2523	0.1878
NMonOut1	0.0000	0.0000	0.0000	0.0000	0.0000
NMonOut1	0.2001	0.1996	0.2000	0.2000	0.2002
NMonOut2	0.0000	0.0000	0.0000	0.0000	0.0000
NMonOut2	0.2000	0.1999	0.2000	0.2000	0.2000
NMono	0.0000	0.0000	0.0000	0.0000	0.0000
NMono	0.2007	0.2021	0.1986	0.2003	0.1983
NPleo1	0.0000	0.0000	0.0000	0.0000	0.0000
NPleo1	0.1999	0.1988	0.1995	0.2013	0.2005
NStrig1	0.0000	0.0000	0.0000	0.0000	0.0000
NStrig1	0.2000	0.1988	0.1997	0.2011	0.2004
NStrig2	0.0000	0.0000	0.0000	0.0000	0.0000
NStrig2	0.1999	0.1989	0.1997	0.2012	0.2003
NStrig3	0.0000	0.0000	0.0000	0.0000	0.0000
NStrig3	0.1999	0.1988	0.1997	0.2012	0.2004
NStrig4	0.0000	0.0000	0.0000	0.0000	0.0000

	NStrig4	0.2000	0.1989	0.1996	0.2012	0.2003
	NStrig5	0.0000	0.0000	0.0000	0.0000	0.0000
	NStrig5	0.2113	0.2008	0.1884	0.1975	0.2020
	NStrig6	0.0000	0.0000	0.0000	0.0000	0.0000
	NStrig6	0.2004	0.1979	0.1983	0.2026	0.2008
	NStrig7	0.0000	0.0000	0.0000	0.0000	0.0000
	NStrig7	0.2005	0.1974	0.1981	0.2029	0.2011
	NStrig8	0.0000	0.0000	0.0000	0.0000	0.0000
	NStrig8	0.2021	0.2004	0.1927	0.2092	0.1956
	NADM01	0.0000	0.0000	0.0000	0.0000	0.0000
	NADM01	0.2000	0.2001	0.1999	0.2000	0.1999
	NADM02	0.0000	0.0000	0.0000	0.0000	0.0000
	NADM02	0.2006	0.2001	0.1998	0.2001	0.1994
	NADM03	0.0000	0.0000	0.0000	0.0000	0.0000
	NADM03	0.2007	0.2004	0.1996	0.2005	0.1989
NODE 4	**NADM04**	**0.0000**	**0.0000**	**0.0000**	**0.0000**	**0.0000**
	NADM04	**0.2001**	**0.2004**	**0.1998**	**0.1999**	**0.1998**
	NADM05	0.0000	0.0000	0.0000	0.0000	0.0000
	NADM05	0.2012	0.2054	0.1961	0.2008	0.1964
	NADM06	0.0000	0.0000	0.0000	0.0000	0.0000
	NADM06	0.2020	0.2061	0.1958	0.1989	0.1971
	NADM07	0.0000	0.0000	0.0000	0.0000	0.0000
	NADM07	0.2018	0.2064	0.1950	0.1994	0.1974
NODE 5	**NADM08**	**0.0000**	**0.0000**	**0.0000**	**0.0000**	**0.0000**
	NADM08	**0.2060**	**0.2125**	**0.1902**	**0.1963**	**0.1950**
	NADM11	0.0000	0.0000	0.0000	0.0000	0.0000
	NADM11	0.2119	0.2279	0.1810	0.1845	0.1947

	NADM12	0.0000	0.0000	0.0000	0.0000	0.0000
	NADM12	0.2356	0.2619	0.1554	0.1571	0.1900
	NADM09	0.0000	0.0000	0.0000	0.0000	0.0000
	NADM09	0.2172	0.2224	0.1779	0.1893	0.1932
	NADM10	0.0000	0.0000	0.0000	0.0000	0.0000
	NADM10	0.2649	0.2714	0.1258	0.1493	0.1887
	NPleo2	0.0000	0.0000	0.0000	0.0000	0.0000
	NPleo2	0.1993	0.1949	0.2007	0.2016	0.2035
	NMyti1	0.0000	0.0000	0.0000	0.0000	0.0000
	NMyti1	0.1987	0.2019	0.1889	0.2128	0.1976
	NMyti2	0.0000	0.0000	0.0000	0.0000	0.0000
	NMyti2	0.1889	0.2015	0.1673	0.2452	0.1971
	NMyti3	0.0000	0.0000	0.0000	0.0000	0.0000
	NMyti3	0.1687	0.1714	0.1865	0.2319	0.2416
	NHyster	0.0000	0.0000	0.0000	0.0000	0.0000
	NHyster	0.1935	0.1764	0.2265	0.1684	0.2352
	NPleo3	0.0000	0.0000	0.0000	0.0000	0.0000
	NPleo3	0.2004	0.2012	0.1979	0.2006	0.1999
	NDicty1	0.0000	0.0000	0.0000	0.0000	0.0000
	NDicty1	0.2424	0.2087	0.1799	0.1864	0.1828
	NDicty2	0.0000	0.0000	0.0000	0.0000	0.0000
	NDicty2	0.3631	0.2002	0.1364	0.1474	0.1529
	NPleo4	0.0000	0.0000	0.0000	0.0000	0.0000
	NPleo4	0.3157	0.2060	0.1544	0.1653	0.1586
NODE 6	**NMVP**	**0.0000**	**0.0000**	**0.0000**	**0.0000**	**0.0000**
	NMVP	**0.2003**	**0.1982**	**0.2005**	**0.2010**	**0.2000**
	NVent1	0.0000	0.0000	0.0000	0.0000	0.0000

	NVent1	0.2006	0.1944	0.2020	0.2044	0.1986
	NStom1	0.0000	0.0000	0.0000	0.0000	0.0000
	NStom1	0.2024	0.1948	0.2024	0.2021	0.1983
	NStom2	0.0000	0.0000	0.0000	0.0000	0.0000
	NStom2	0.2208	0.1737	0.2129	0.2086	0.1840
	NVent2	0.0000	0.0000	0.0000	0.0000	0.0000
	NVent2	0.2242	0.1483	0.2089	0.2664	0.1522
	NVent3	0.0000	0.0000	0.0000	0.0000	0.0000
	NVent3	0.2021	0.2100	0.1964	0.2006	0.1910
	NMThyrX	0.0000	0.0000	0.0000	0.0000	0.0000
	NMThyrX	0.2003	0.1993	0.2002	0.2003	0.1999
	NPhaeo	0.0000	0.0000	0.0000	0.0000	0.0000
	NPhaeo	0.2204	0.1975	0.1938	0.2050	0.1833
NODE 7	**NMThyr1**	**0.0000**	**0.0000**	**0.0000**	**0.0000**	**0.0000**
	NMThyr1	**0.2001**	**0.1993**	**0.2003**	**0.2002**	**0.2000**
	NMThyr2	0.0000	0.0000	0.0000	0.0000	0.0000
	NMThyr2	0.2000	0.1998	0.2001	0.2001	0.2000
	NMThyr3	0.9157	0.0767	0.0025	0.0025	0.0025
	NMThyr3	0.2001	0.1999	0.2000	0.2000	0.2000
	NMThyr4	1.0000	0.0000	0.0000	0.0000	0.0000
	NMThyr4	0.2005	0.2000	0.1998	0.2000	0.1997
	NMTSup	0.0000	0.0000	0.0000	0.0000	0.0000
	NMTSup	0.2000	0.1995	0.2002	0.2003	0.2001
	NMThyr5	0.0000	0.0000	0.0000	0.0000	0.0000
	NMThyr5	0.1997	0.1995	0.2004	0.2006	0.1997
	NMThyr6	0.0000	0.0000	0.0000	0.0000	0.0000
	NMThyr6	0.1999	0.1991	0.2003	0.2005	0.2002

	NHelio	0.0000	0.0000	0.0000	0.0000	0.0000
	NHelio	0.1985	0.1861	0.2047	0.2329	0.1777
	NZelo1	0.0000	0.0000	0.0000	0.0000	0.0000
	NZelo1	0.2000	0.2000	0.2000	0.2000	0.2000
	NNati	0.0000	0.0000	0.0000	0.0000	0.0000
	NNati	1.0000	1.0000	3.0000	3.0000	0.1999
	NZelo2	0.0000	0.0000	0.0000	0.0000	0.0000
	NZelo2	0.1906	0.2078	0.2115	0.2286	0.1615
	NZelo3	0.0000	0.0000	0.0000	0.0000	0.0000
	NZelo3	0.1948	0.2036	0.2040	0.2235	0.1741
	NZelo4	0.0000	0.0000	0.0000	0.0000	0.0000
	NZelo4	0.1822	0.2273	0.2019	0.2646	0.1240
	NZelo5	0.0000	0.0000	0.0000	0.0000	0.0000
	NZelo5	0.1974	0.2060	0.2008	0.2081	0.1876
	NZelo6	0.0000	0.0000	0.0000	0.0000	0.0000
	NZelo6	0.1929	0.2160	0.1975	0.2259	0.1677
NODE 8	**NAulo1**	**0.0040**	**0.0207**	**0.0040**	**0.0040**	**0.9673**
	NAulo1	**0.1999**	**0.1990**	**0.2005**	**0.1999**	**0.2008**
	NLembo	0.0000	0.0000	0.0000	0.0000	0.9999
	NLembo	0.1379	0.1177	0.1670	0.1389	0.4385
	NAulo2	0.0000	0.0000	0.0000	0.0000	1.0000
	NAulo2	0.1159	0.0971	0.1463	0.1169	0.5237
	NAstx01	0.0000	0.0000	0.0000	0.0000	0.0000
	NAstx01	0.2004	0.2018	0.1988	0.2000	0.1990
NODE 9	**NAstx02**	**0.0009**	**0.9989**	**0.0000**	**0.0000**	**0.0001**
	NAstx02	**0.2004**	**0.2019**	**0.1988**	**0.2000**	**0.1989**
	NMelas01	0.0000	0.0000	0.0000	0.0000	0.0000

NMelas01	0.2004	0.1991	0.1999	0.2005	0.2000
NMelas02	0.0000	0.0000	0.0000	0.0000	0.0000
NMelas02	0.2007	0.1984	0.2000	0.2008	0.2001
NMelas03	0.0000	0.0000	0.0000	0.0000	0.0000
NMelas03	0.2007	0.1982	0.2002	0.2007	0.2002
NMelas04	0.0000	0.0000	0.0000	0.0000	0.0000
NMelas04	0.2007	0.1981	0.2002	0.2008	0.2003
NMelas05	0.0000	0.0000	0.0000	0.0000	0.0000
NMelas05	0.1992	0.1942	0.2059	0.1984	0.2023
NMelas06	0.0000	0.0000	0.0000	0.0000	0.0000
NMelas06	0.1991	0.1940	0.2073	0.1980	0.2016
NMelas07	0.0000	0.0000	0.0000	0.0000	0.0000
NMelas07	0.2007	0.1923	0.2099	0.1972	0.1998
NMelas08	0.0000	0.0000	0.0000	0.0000	0.0000
NMelas08	0.2002	0.1959	0.2054	0.1979	0.2006
NMelas09	0.0000	0.0000	0.0000	0.0000	0.0000
NMelas09	0.2007	0.1981	0.2001	0.2007	0.2004
NMelas10	0.0000	0.0000	0.0000	0.0000	0.0000
NMelas10	0.1997	0.1945	0.2034	0.2003	0.2021
NMelas11	0.0000	0.0000	0.0000	0.0000	0.0000
NMelas11	0.2052	0.1881	0.2289	0.2009	0.1769
NMelas12	0.0000	0.0000	0.0000	0.0000	0.0000
NMelas12	0.2084	0.1909	0.2174	0.2013	0.1821
NMelas13	0.0000	0.0000	0.0000	0.0000	0.0000
NMelas13	0.2000	0.2002	0.2001	0.1999	0.1998
NAstx03	0.0007	0.9992	0.0000	0.0000	0.0000
NAstx03	0.2015	0.2085	0.1951	0.1992	0.1957

NODE 10						
	NAstx04	**0.0000**	**1.0000**	**0.0000**	**0.0000**	**0.0000**
	NAstx04	**0.1969**	**0.2658**	**0.1701**	**0.1929**	**0.1744**
	NAstx05	0.0041	0.9954	0.0003	0.0001	0.0000
	NAstx05	0.2120	0.2506	0.1694	0.1929	0.1751
	NAstx06	0.0285	0.9682	0.0026	0.0005	0.0003
	NAstx06	0.2271	0.2020	0.1883	0.1932	0.1894
	NAstx07	0.0169	0.9258	0.0517	0.0029	0.0027
	NAstx07	0.2000	0.1994	0.2004	0.2000	0.2002
	NAstx08	0.0000	0.0004	0.9995	0.0000	0.0000
	NAstx08	0.0986	0.0675	0.6032	0.1029	0.1278
	NAstx09	0.0000	0.0000	0.0000	0.0000	0.0000
	NAstx09	0.2001	0.1997	0.2001	0.2001	0.2000
	NAstx10	0.0000	1.0000	0.0000	0.0000	0.0000
	NAstx10	0.0734	0.7518	0.0470	0.0722	0.0555
	NAstx11	0.3292	0.6607	0.0034	0.0048	0.0019
	NAstx11	0.2647	0.1966	0.1766	0.1830	0.1792
	NAstx14	0.0000	0.0000	0.0000	0.0000	0.0000
	NAstx14	0.2133	0.1997	0.1946	0.1970	0.1954
	NAstx15	0.1503	0.3805	0.0572	0.3553	0.0568
	NAstx15	0.1999	0.1997	0.1997	0.2011	0.1996
	NAstx12	0.0000	0.0000	0.0000	0.0000	0.0000
	NAstx12	0.3542	0.1788	0.1515	0.1598	0.1557
	NAstx13	0.0000	0.0000	0.0000	0.0000	0.0000
	NAstx13	0.2216	0.1983	0.1857	0.2023	0.1920

A.6 Consensus tree from MrBayes analysis

Results from four runs of eight chains each, running 160 million generations and sampling every 5000 trees, from which 50% of the samples were discarded as burn-in. Posterior probabilities mapped on branches, clades are labelled and ordered as in Fig. 1.

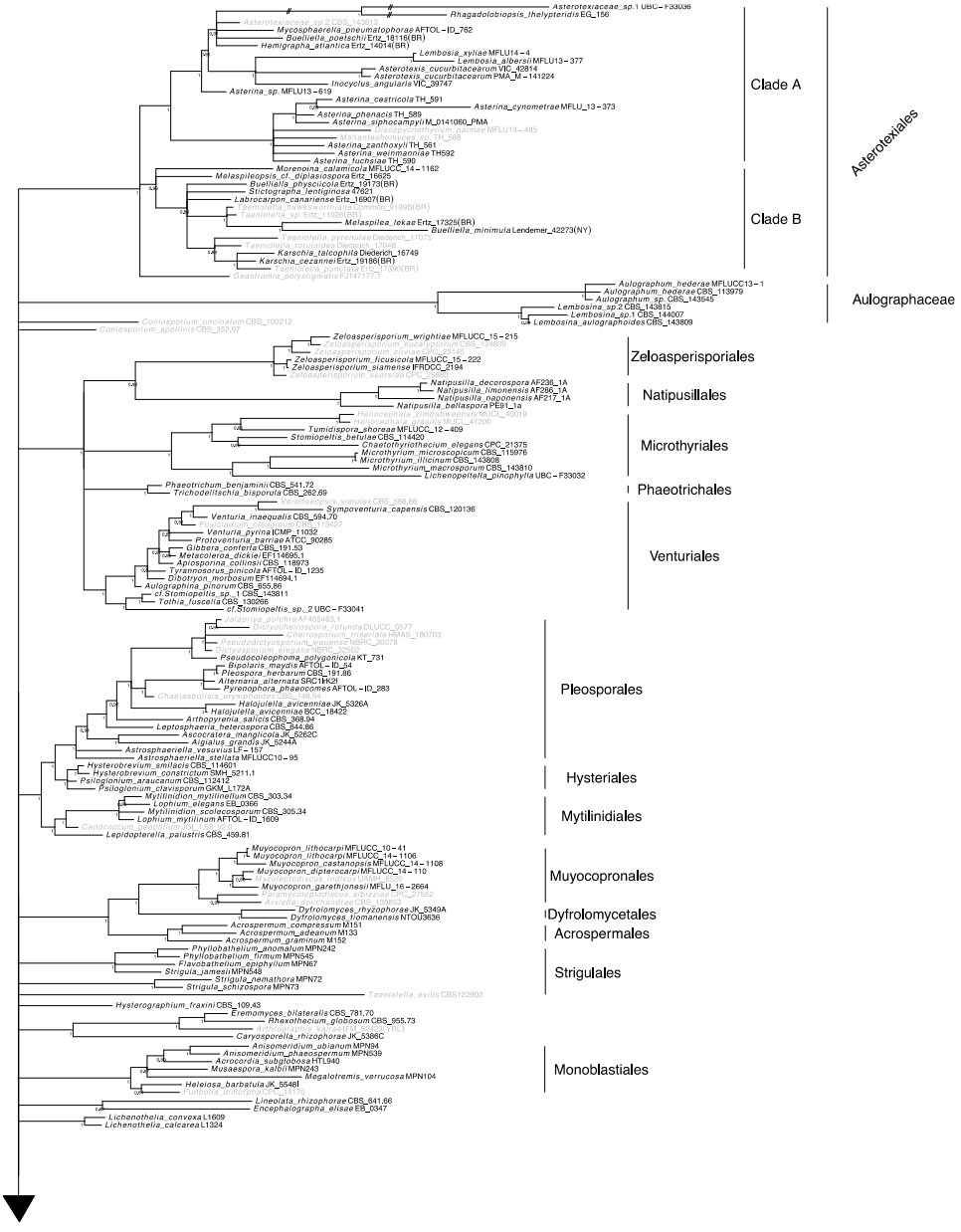

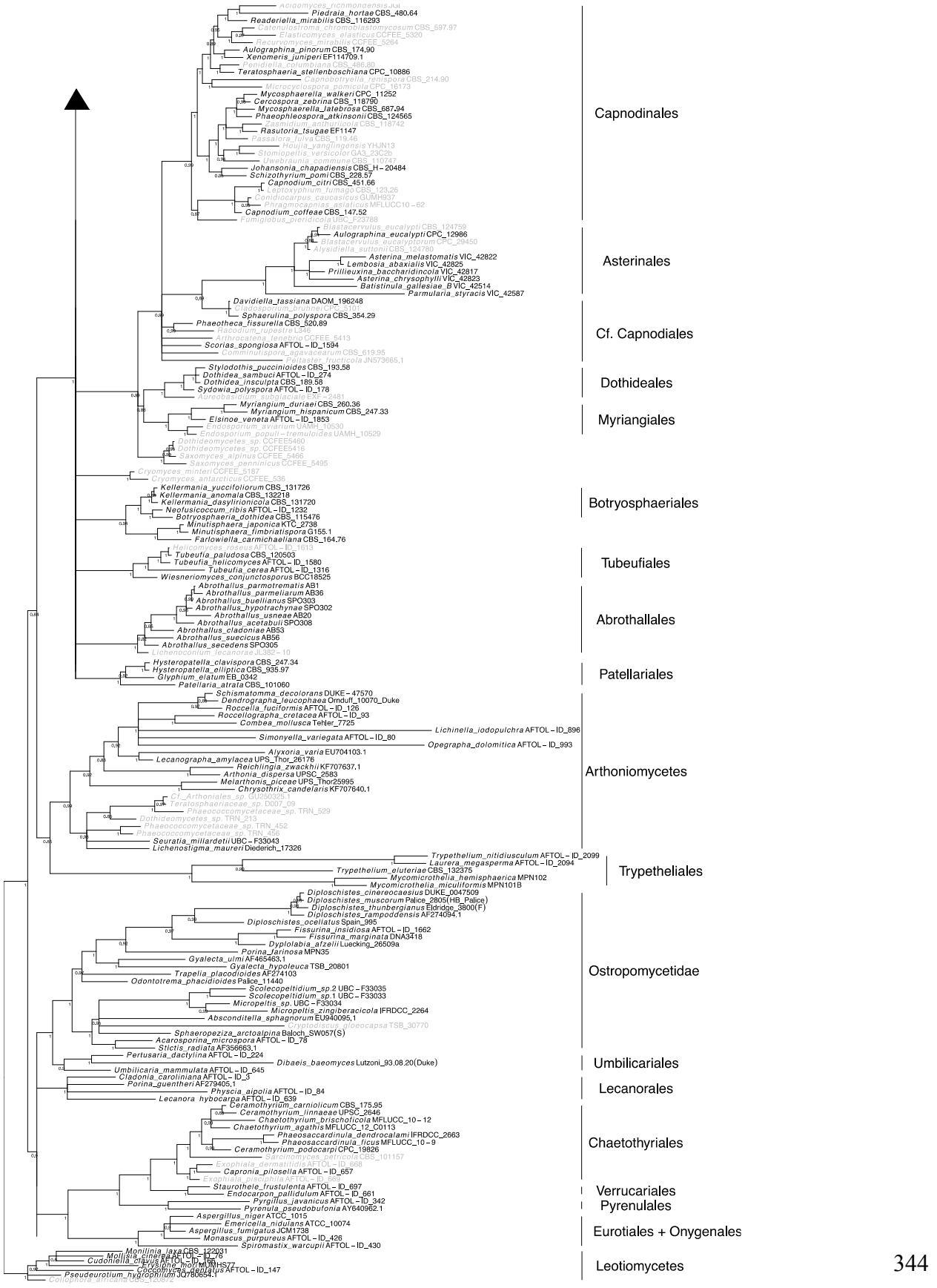
Capnodinales
Asterinales
Cf. Capnodiales
Dothideales
Myriangiales
Botryosphaeriales
Tubeufiales
Abrothallales
Patellariales
Arthoniomycetes
Trypetheliales
Ostropomycetidae
Umbilicariales
Lecanorales
Chaetothyriales
Verrucariales
Pyrenulales
Eurotiales + Onygenales
Leotiomycetes

A.7 Maximum likelihood phylogeny labelled with codes for nodes

Maximum likelihood phylogeny labelled with codes for nodes reconstructed in ancestral character state analyses. Most likely tree obtained out of 4000 independent ML searches of a 4552 bp alignment of LSU and SSU rDNA data for 320 taxa, with bootstrap support > 70% in red and a posterior probability > 0.95.

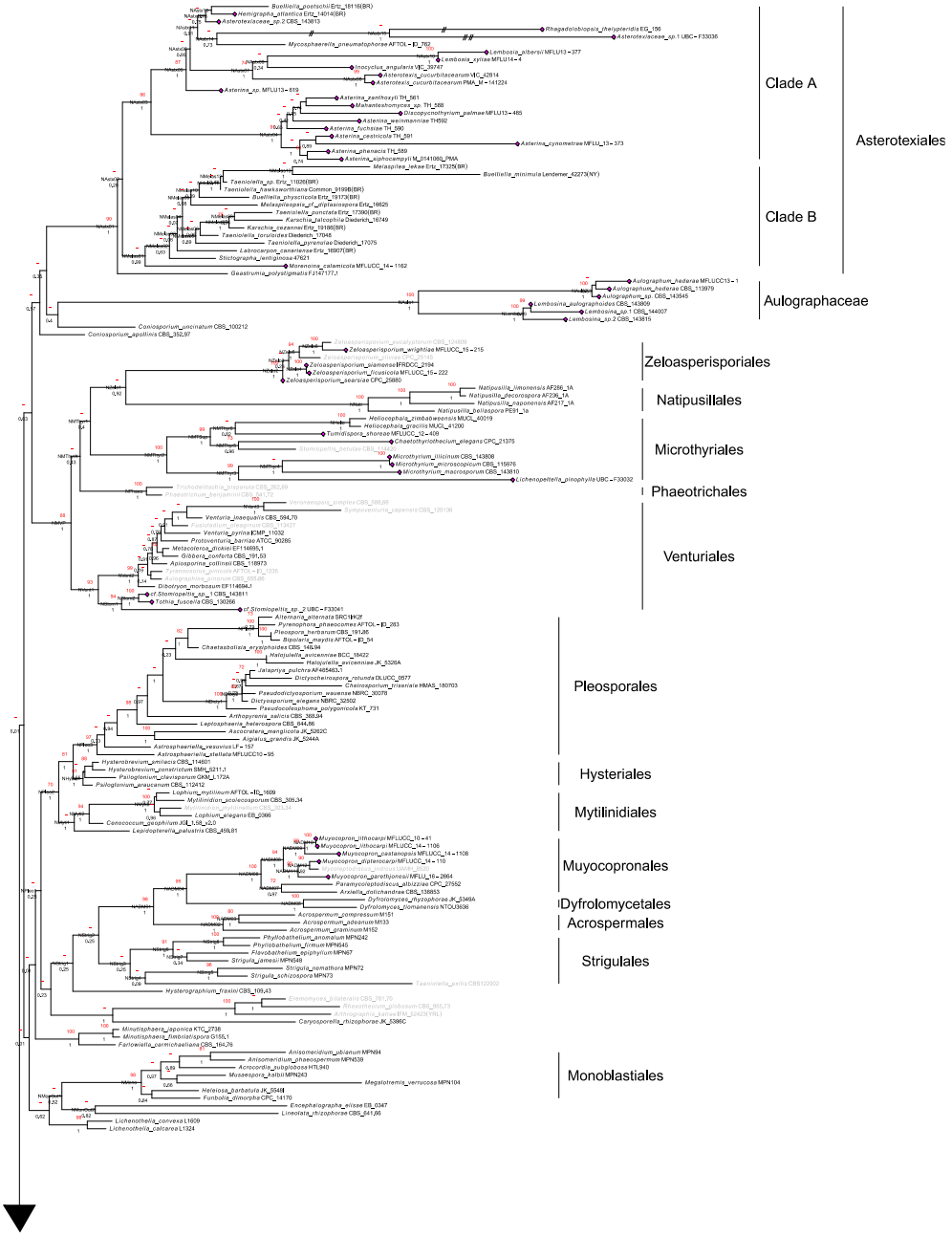

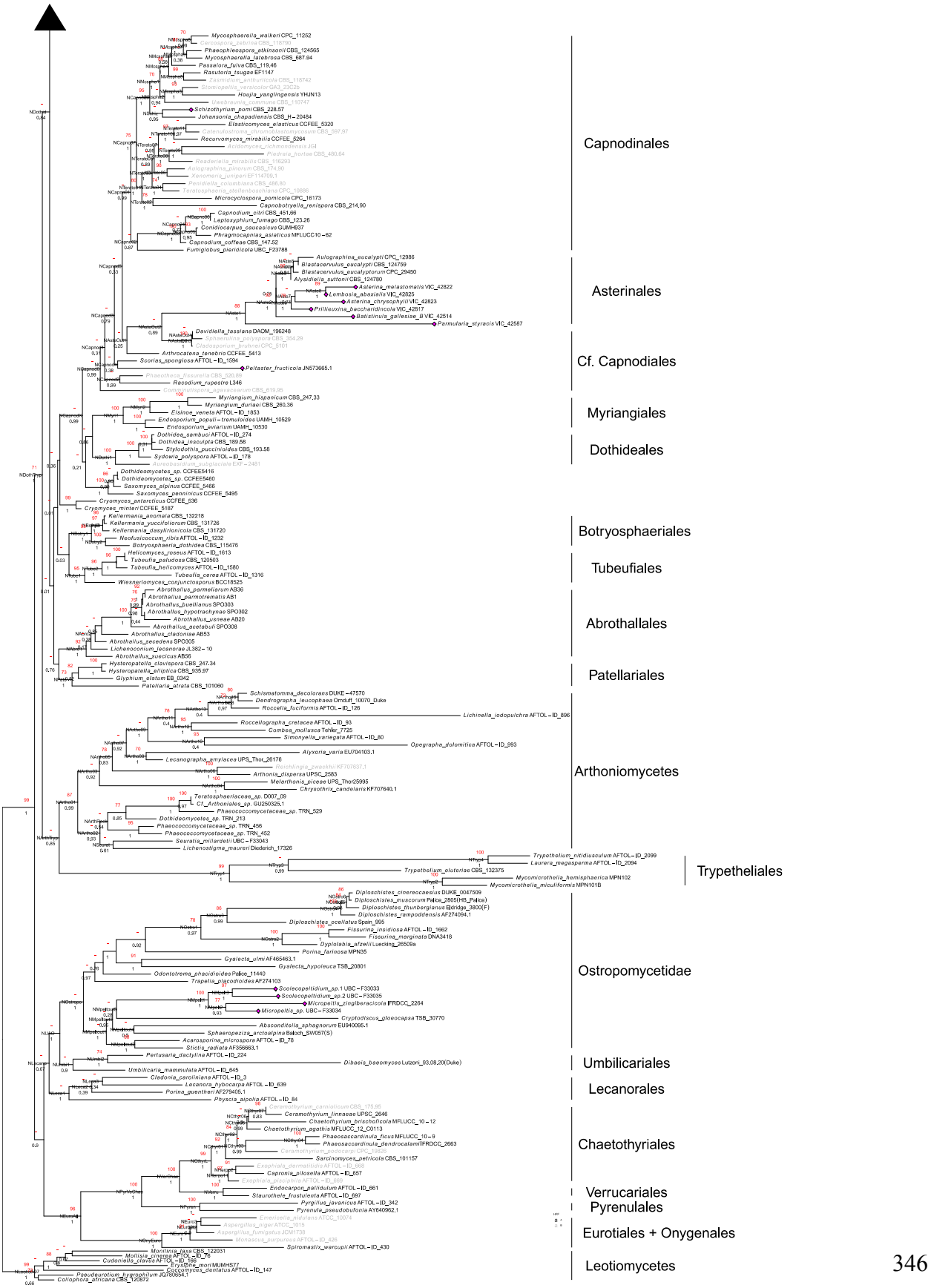
Capnodinales
Asterinales
Cf. Capnodiales
Myriangiales
Dothideales
Botryosphaeriales
Tubeufiales
Abrothallales
Patellariales
Arthoniomycetes
Trypetheliales
Ostropomycetidae
Umbilicariales
Lecanorales
Chaetothyriales
Verrucariales
Pyrenulales
Eurotiales + Onygenales
Leotiomycetes

Appendices A.8–A.18 Ancestral character state reconstructions for (I) Substrate

Ancestral character state reconstructions over most likely topology for 11 morphological characters: proportional likelihoods from MK1 analysis are reported in red pie charts, and posterior probabilities from BayesTraits V3 analysis reported in yellow pie charts. Both were mapped for nodes that could be reconstructed in each tree. In each tree, names in grey indicate taxa that could not be coded for the character, with ancestral states that could not be reconstructed. Bootstrap support >0.7 is reported in red and posterior probabilities >0.95 in black.

A.8 Ancestral character state reconstructions for (I) Substrate: *saxicolous*, *folicolous*, *lichenicolous*, *lignicolous and corticolous* or *other*.

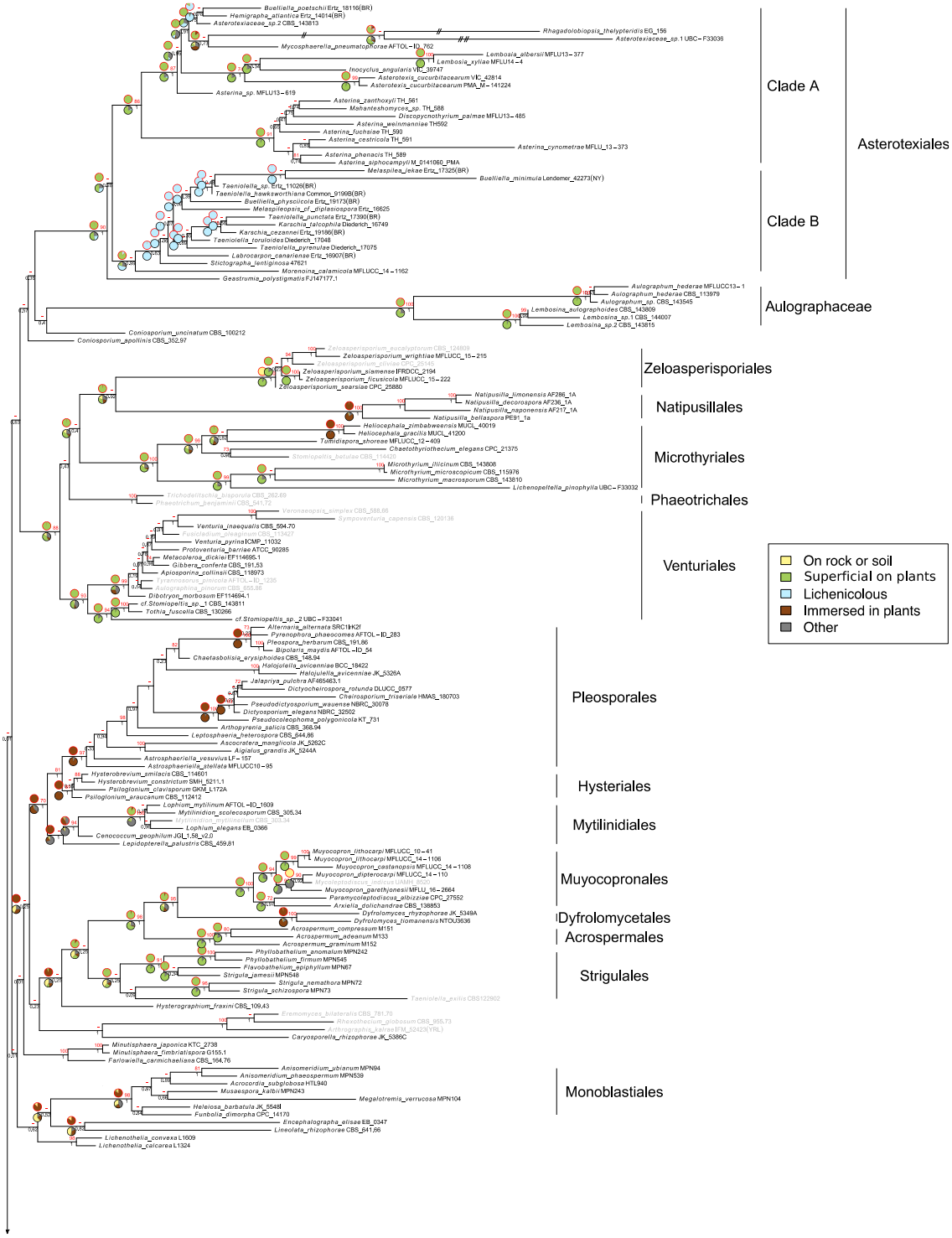

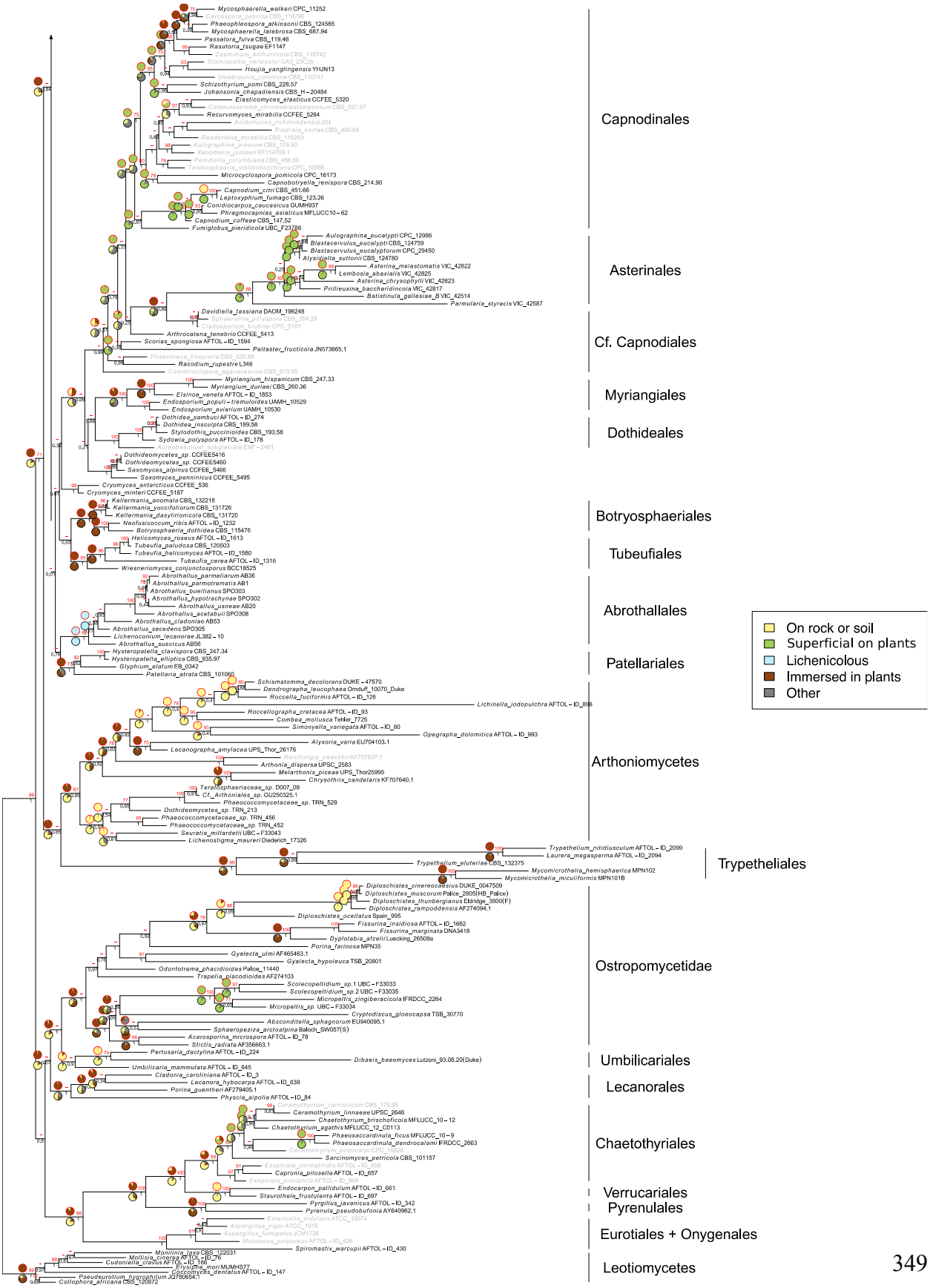
Capnodinales
Asterinales
Cf. Capnodiales
Myriangiales
Dothideales
Botryosphaeriales
Tubeufiales
Abrothallales
Patellariales
Arthoniomycetes
Trypetheliales
Ostropomycetidae
Umbilicariales
Lecanorales
Chaetothyriales
Verrucariales
Pyrenulales
Eurotiales + Onygenales
Leotiomycetes
On rock or soil
Superficial on plants
Lichenicolous
Immersed in plants
Other

A.9 Ancestral character states reconstruction (II), as *lichenized* or *non-lichenized*

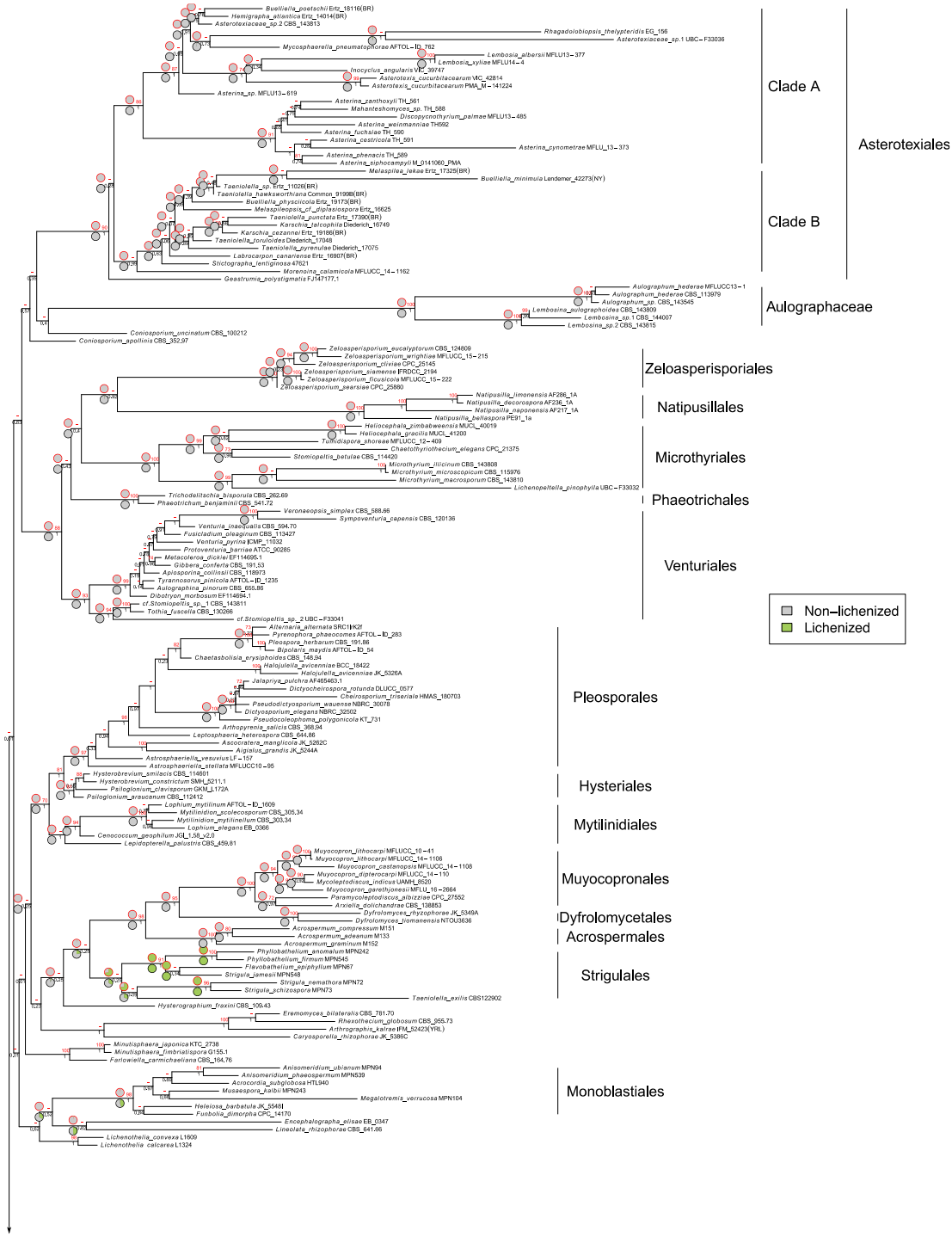

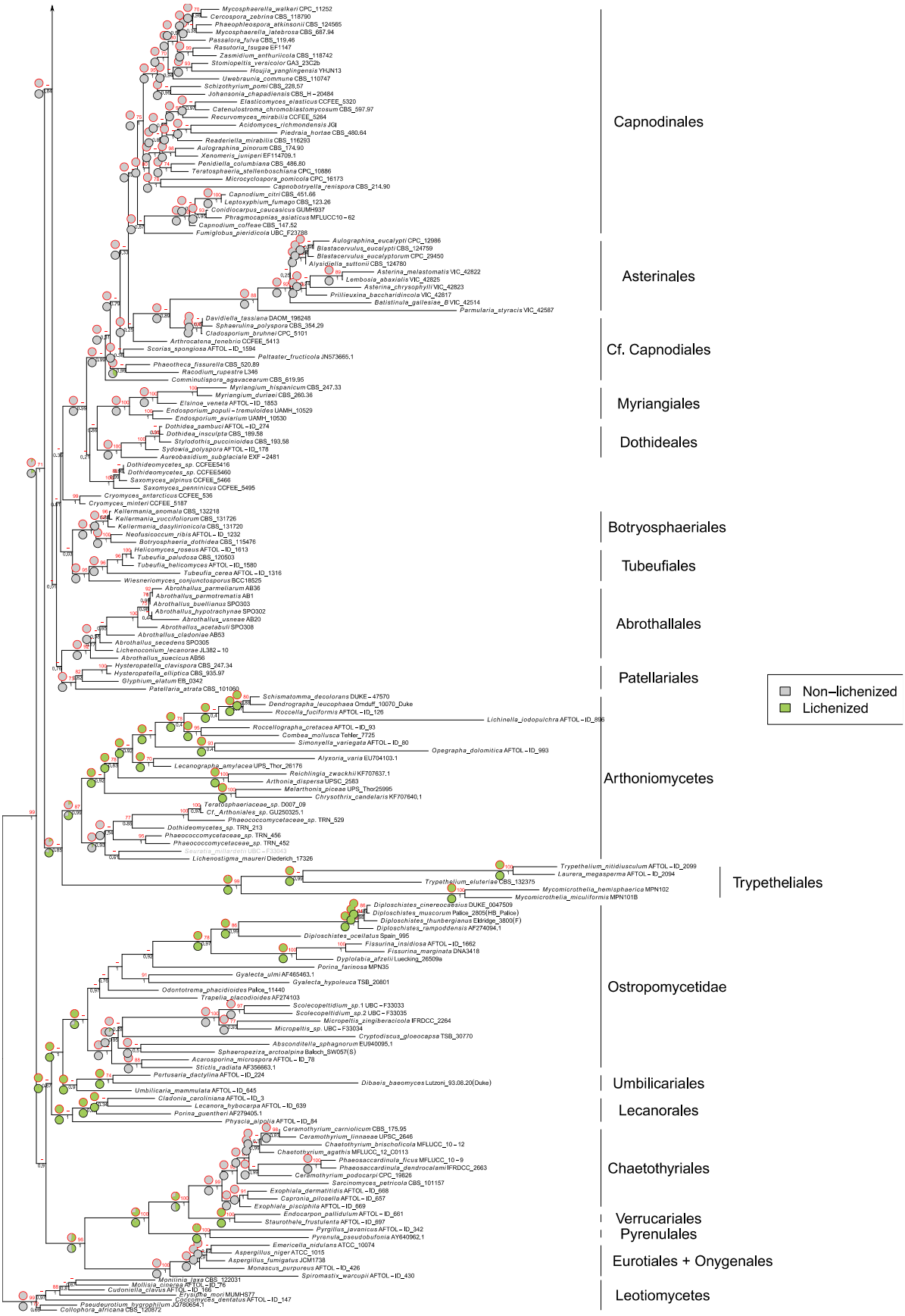
Capnodinales
Asterinales
Cf. Capnodiales
Myriangiales
Dothideales
Botryosphaeriales
Tubeufiales
Abrothallales
Patellariales
Arthoniomycetes
Trypetheliales
Ostropomycetidae
Umbilicariales
Lecanorales
Chaetothyriales
Verrucariales
Pyrenulales
Eurotiales + Onygenales
Leotiomycetes
Non–lichenized
Lichenized

A. 10 Ancestral character state reconstruction for (III) sporocarp type, *apothecioid, perithecioid, thyriothecioid* or *cleistothecioid*

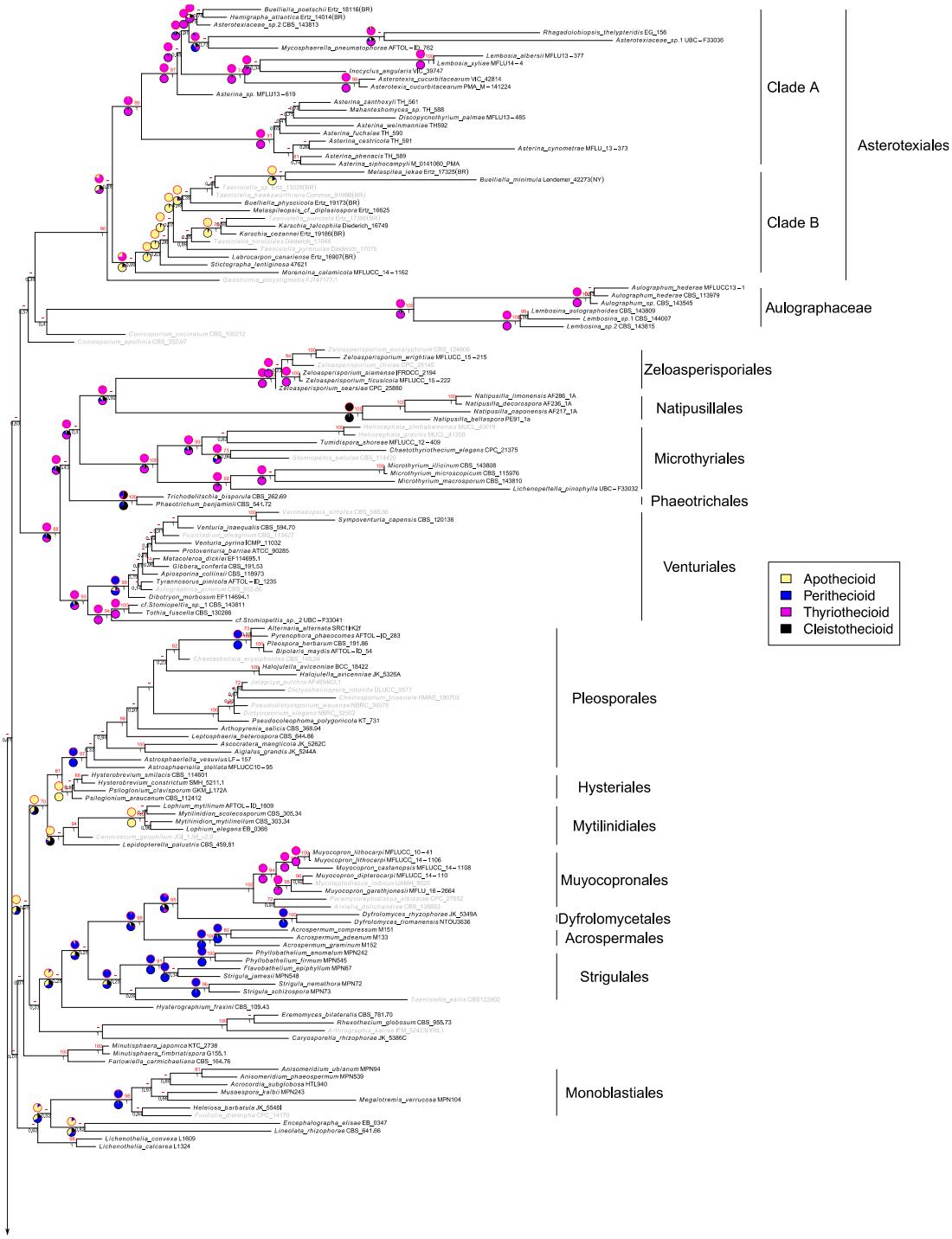

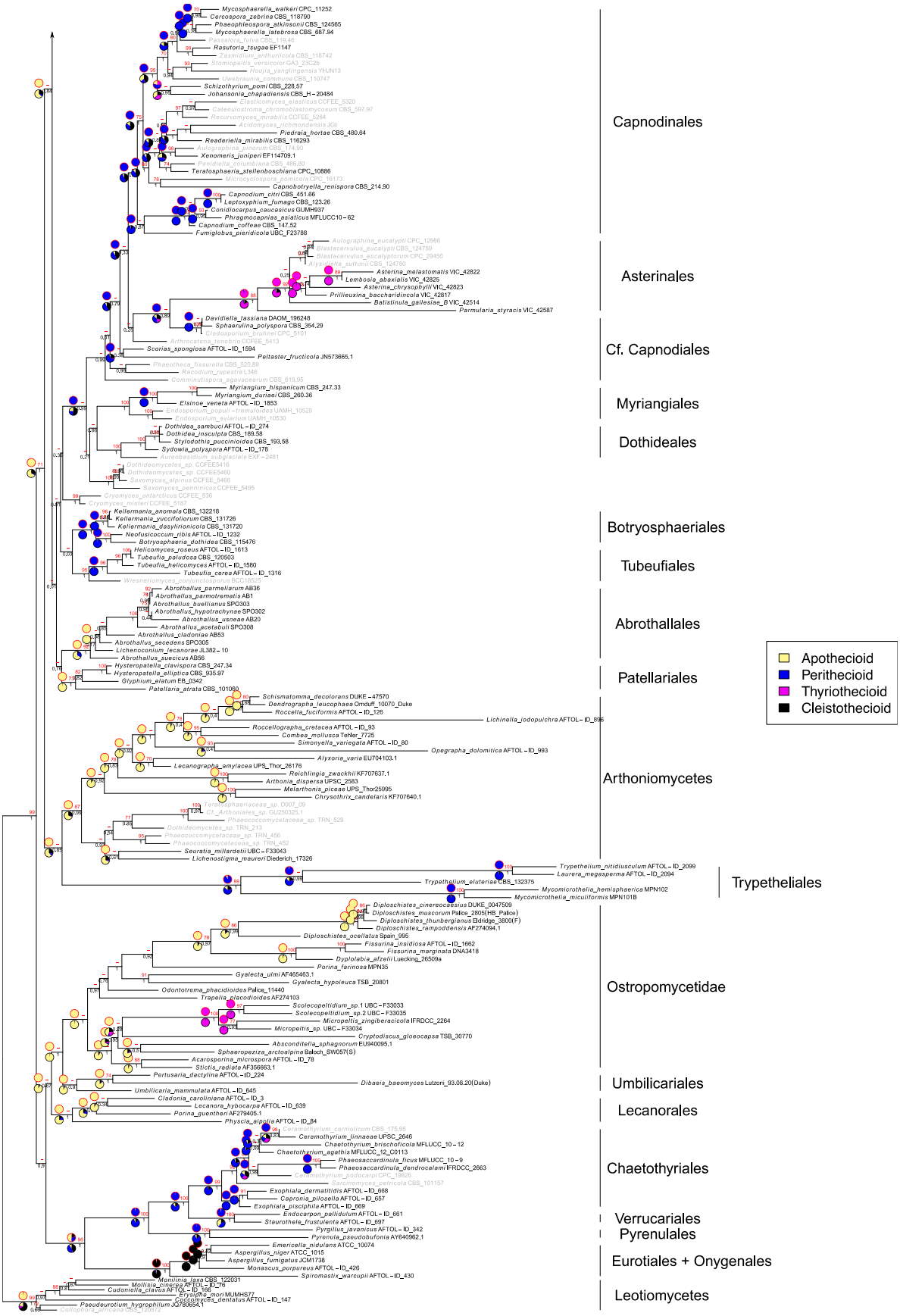
Capnodinales
Asterinales
Cf. Capnodiales
Myriangiales
Dothideales
Botryosphaeriales
Tubeufiales
Abrothallales
Patellariales
Arthoniomycetes
Trypetheliales
Ostropomycetidae
Umbilicariales
Lecanorales
Chaetothyriales
Verrucariales
Pyrenulales
Eurotiales + Onygenales
Leotiomycetes
Apothecioid
Perithecioid
Thyriothecioid
Cleistothecioid

A.11 Ancestral character state reconstruction for the *presence* or *absence* of a (IV) lower wall differentiation

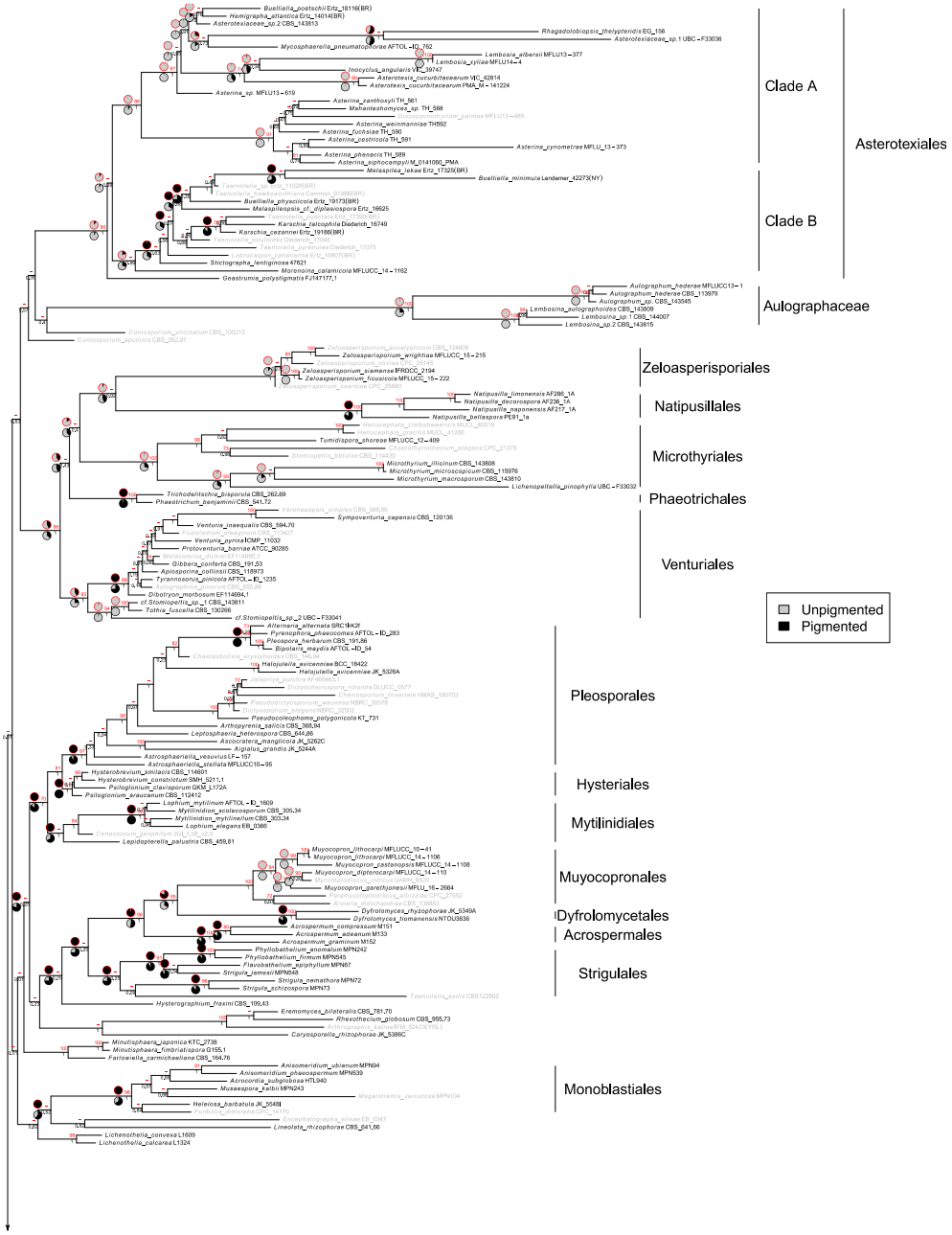

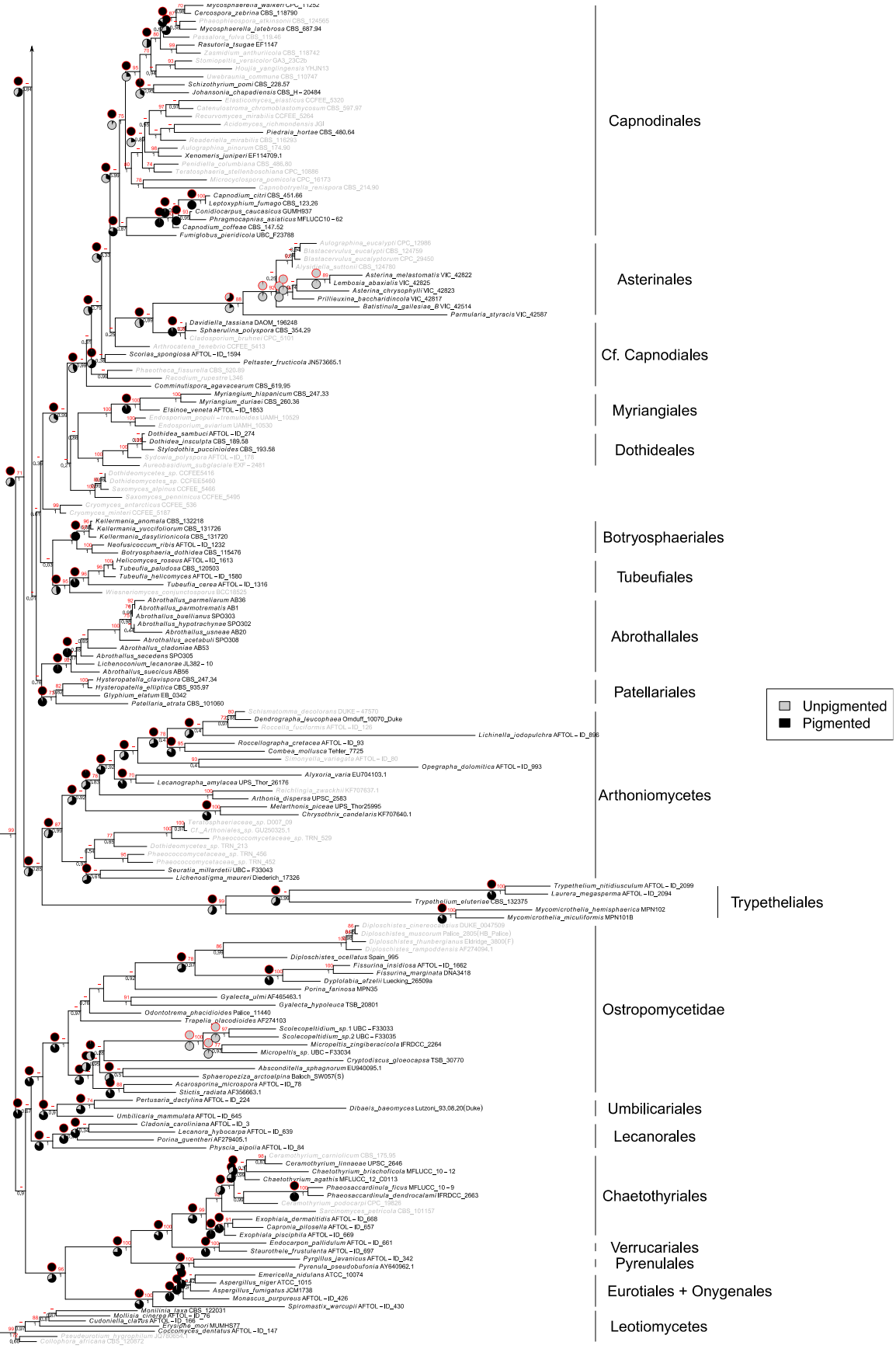
Capnodinales
Asterinales
Cf. Capnodiales
Myriangiales
Dothideales
Botryosphaeriales
Tubeufiales
Abrothallales
Patellariales
Arthoniomycetes
Trypetheliales
Ostropomycetidae
Umbilicariales
Lecanorales
Chaetothyriales
Verrucariales
Pyrenulales
Eurotiales + Onygenales
Leotiomycetes
Unpigmented
Pigmented

A.12 Ancestral character state reconstruction for (V) sporocarp dehiscence: with *ostiole*, *irregular slit*, *regular slit*, *no dehiscence* or *exposed at maturity*

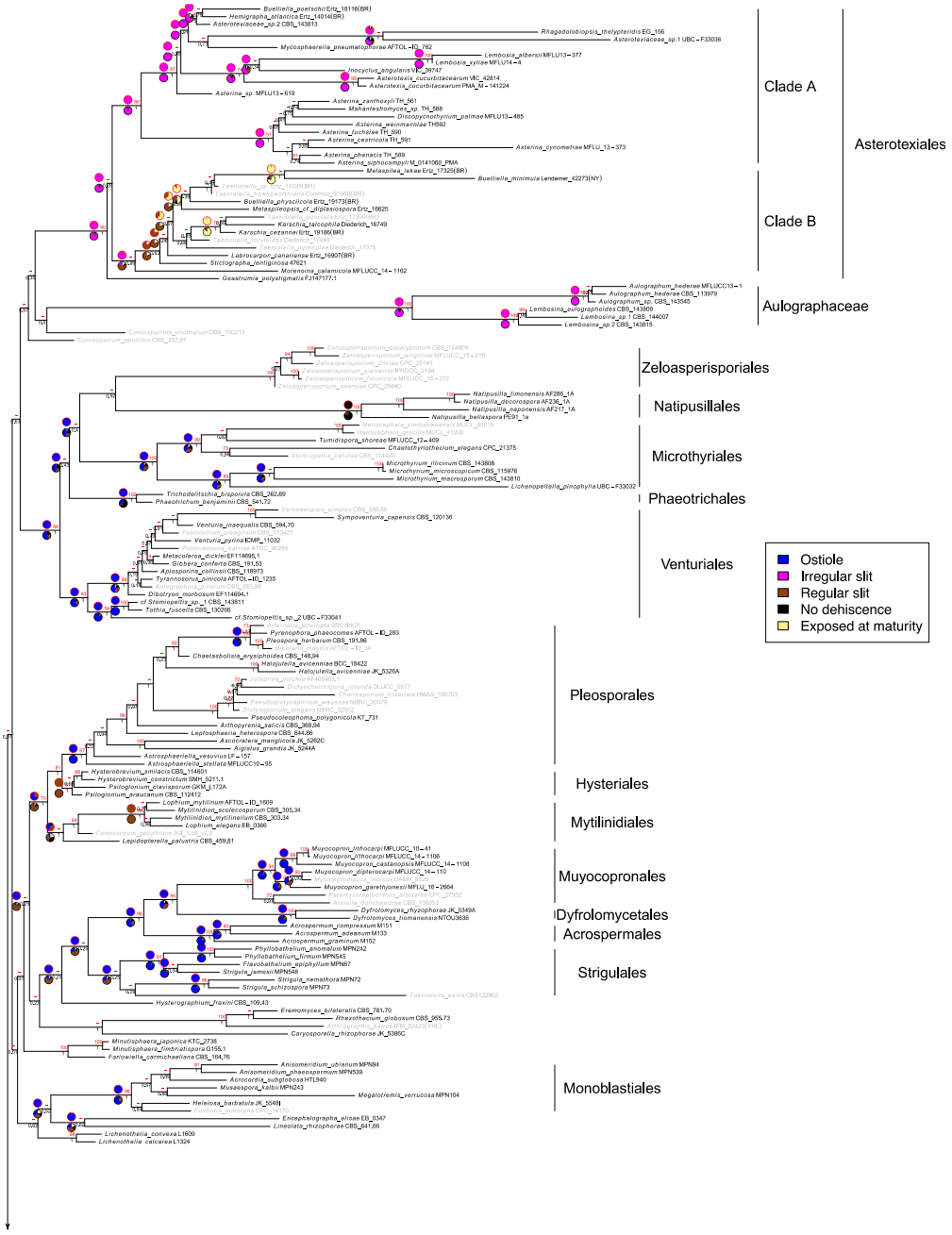

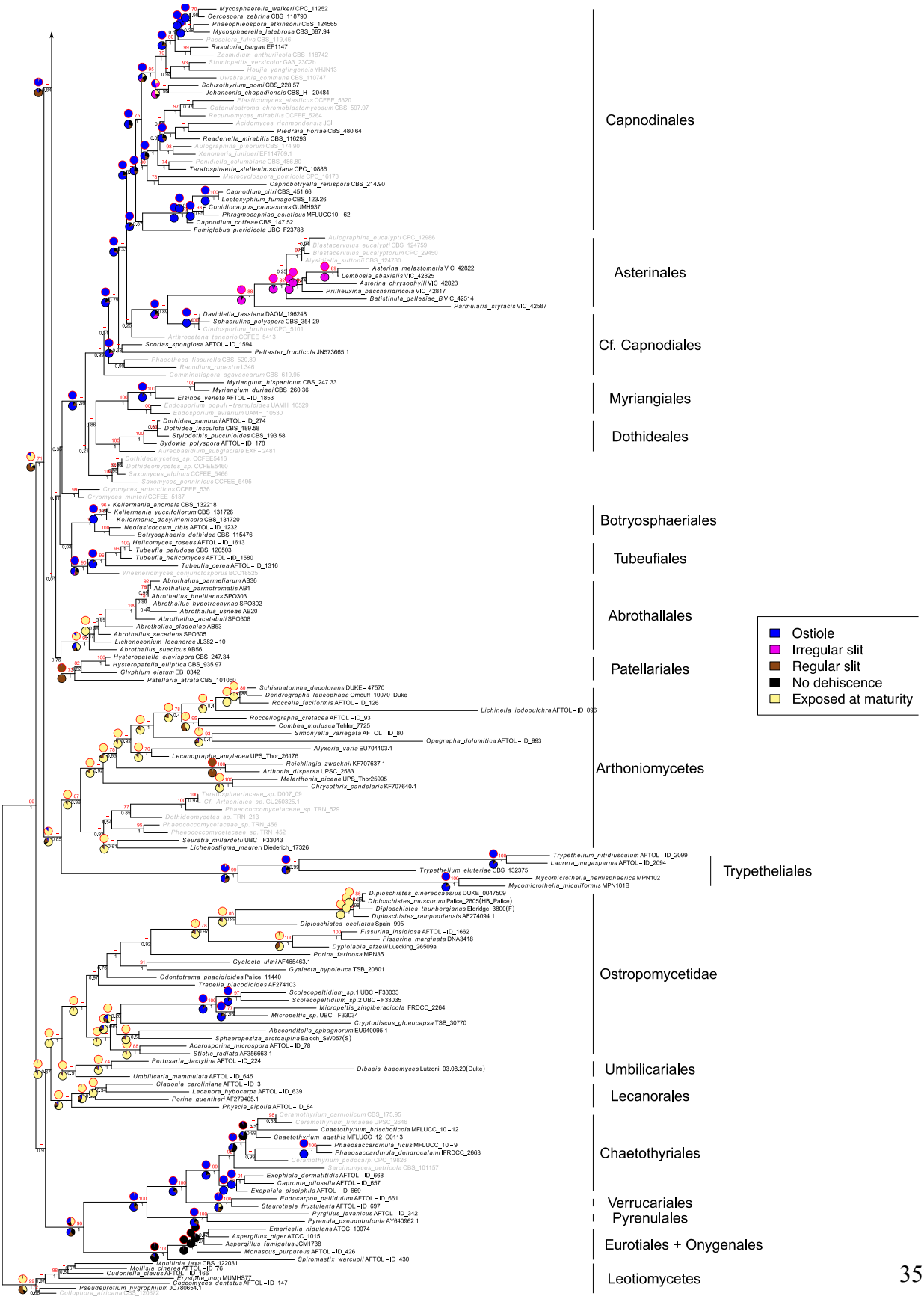
Capnodinales
Asterinales
Cf. Capnodiales
Myriangiales
Dothideales
Botryosphaeriales
Tubeufiales
Abrothallales
Patellariales
Arthoniomycetes
Trypetheliales
Ostropomycetidae
Umbilicariales
Lecanorales
Chaetothyriales
Verrucariales
Pyrenulales
Eurotiales + Onygenales
Leotiomycetes
Ostiole
Irregular slit
Regular slit
No dehiscence
Exposed at maturity

A.13 Ancestral character state reconstruction for (VI) sporogenous tissue outline: *circular* or *elongate*

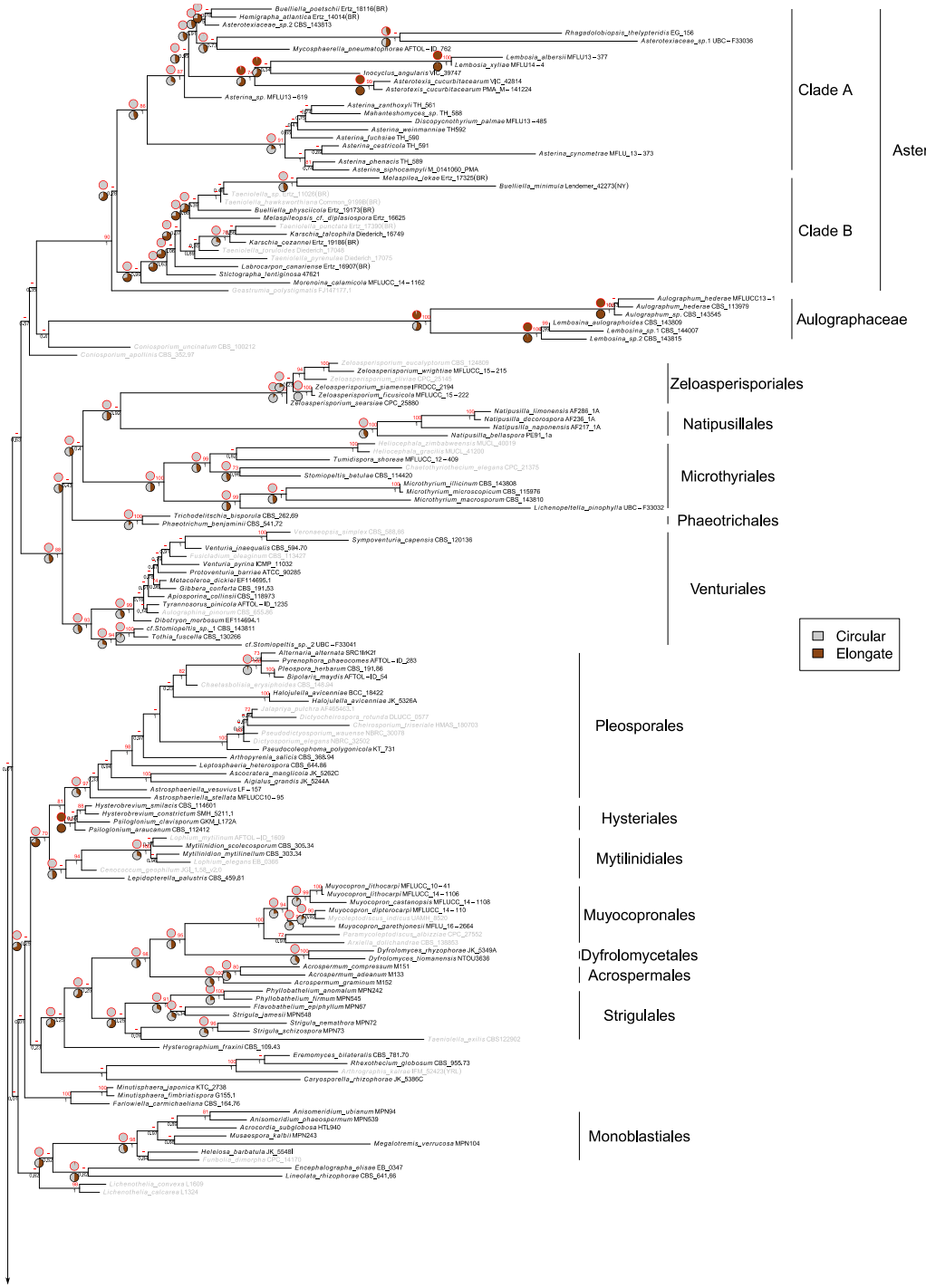

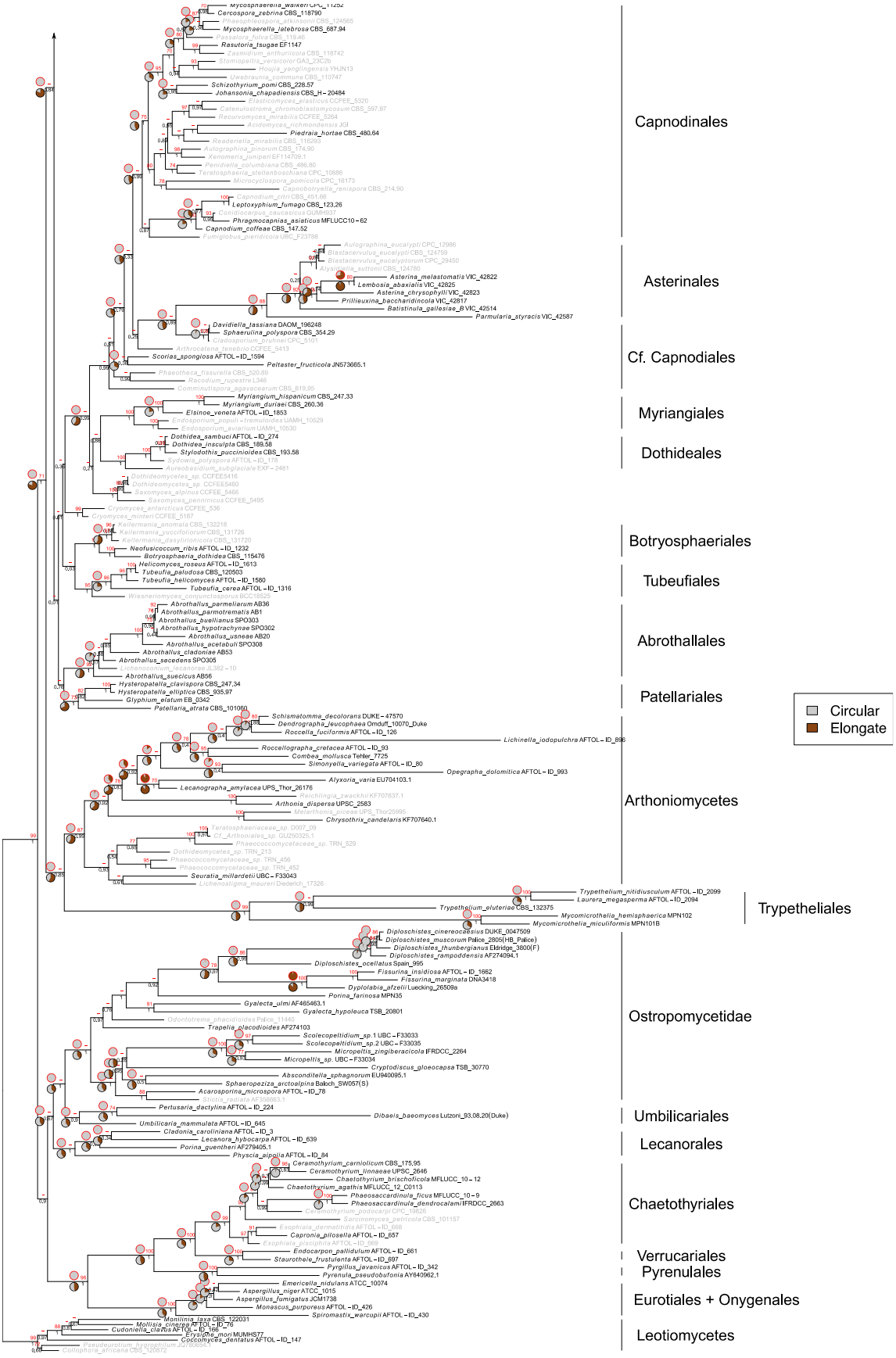
Capnodinales
Asterinales
Cf. Capnodiales
Myriangiales
Dothideales
Botryosphaeriales
Tubeufiales
Abrothallales
Patellariales
Arthoniomycetes
Trypetheliales
Ostropomycetidae
Umbilicariales
Lecanorales
Chaetothyriales
Verrucariales
Pyrenulales
Eurotiales + Onygenales
Leotiomycetes
Circular
Elongate

A.14 Ancestral character state reconstruction for *presence* or *absence* of a (VII) radiate sporocarp

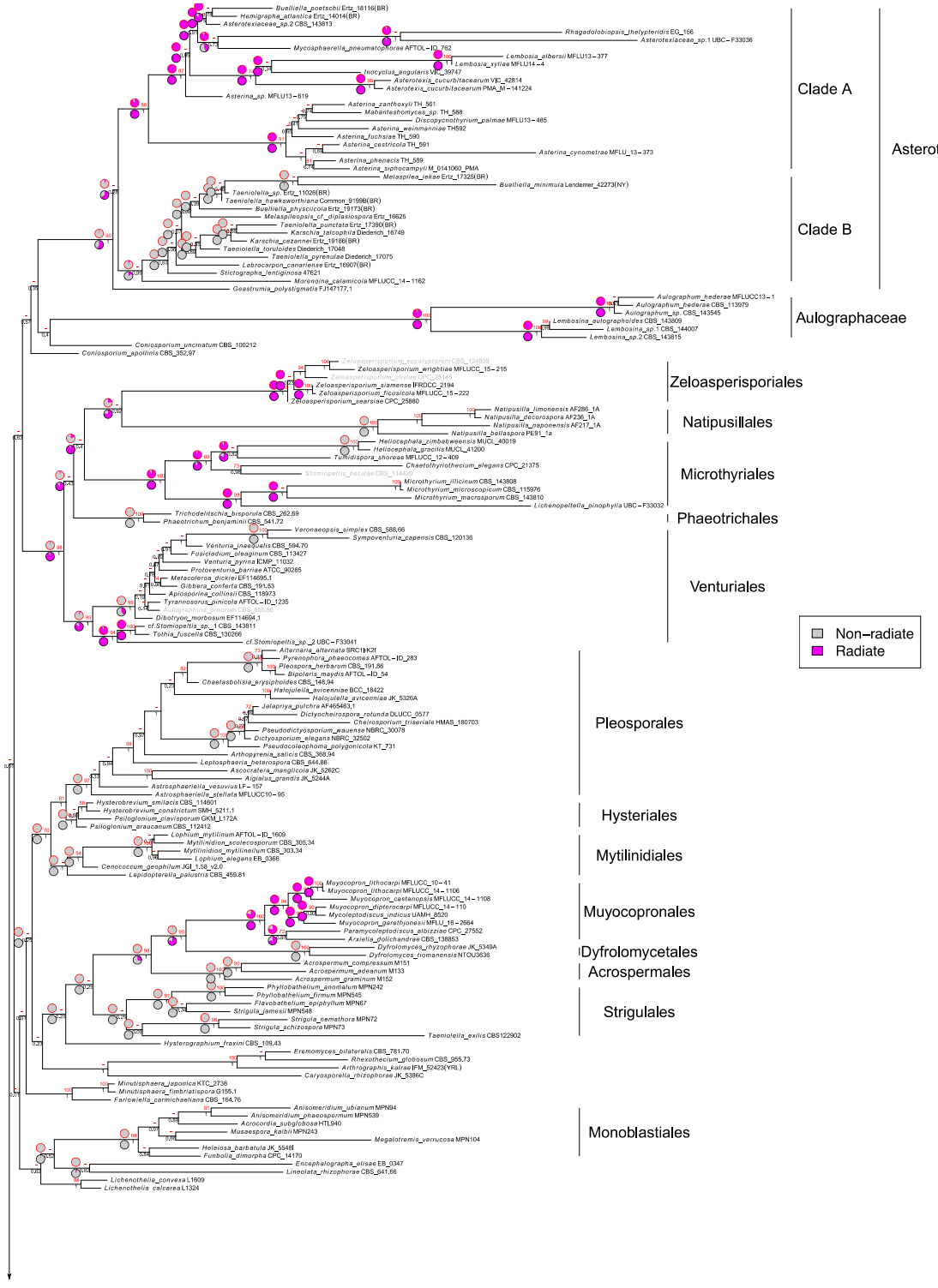

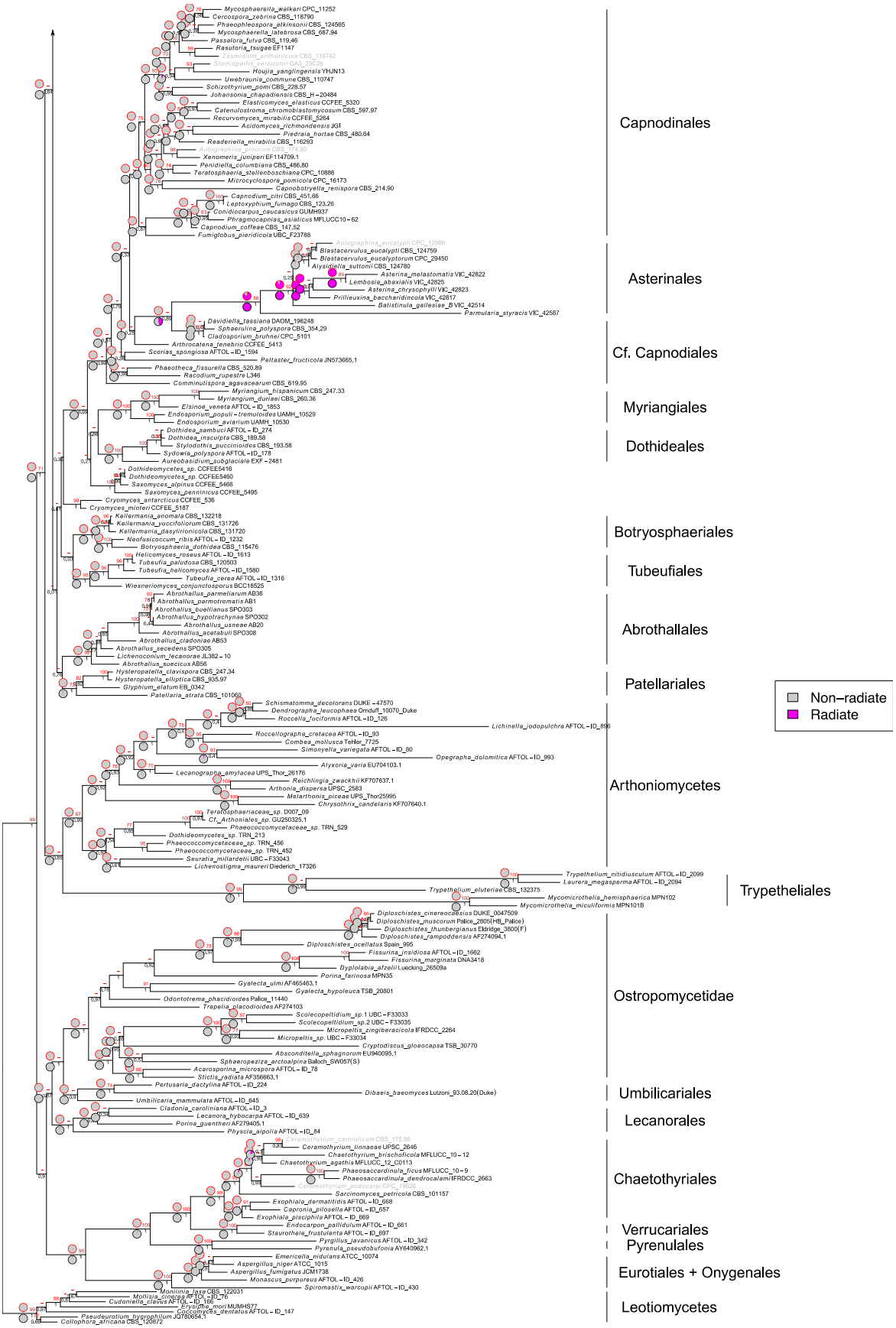
Capnodinales
Asterinales
Cf. Capnodiales
Myriangiales
Dothideales
Botryosphaeriales
Tubeufiales
Abrothallales
Patellariales
Arthoniomycetes
Trypetheliales
Ostropomycetidae
Umbilicariales
Lecanorales
Chaetothyriales
Verrucariales
Pyrenulales
Eurotiales + Onygenales
Leotiomycetes
Non–radiate
Radiate

A.15 Ancestral character state reconstruction for (VIII) scutellum branching: pseudoparenchymatous (no scutellum), or scutella that are *isotomous*, *anisotomous*, *pseudomonopodial* or *untraceable*

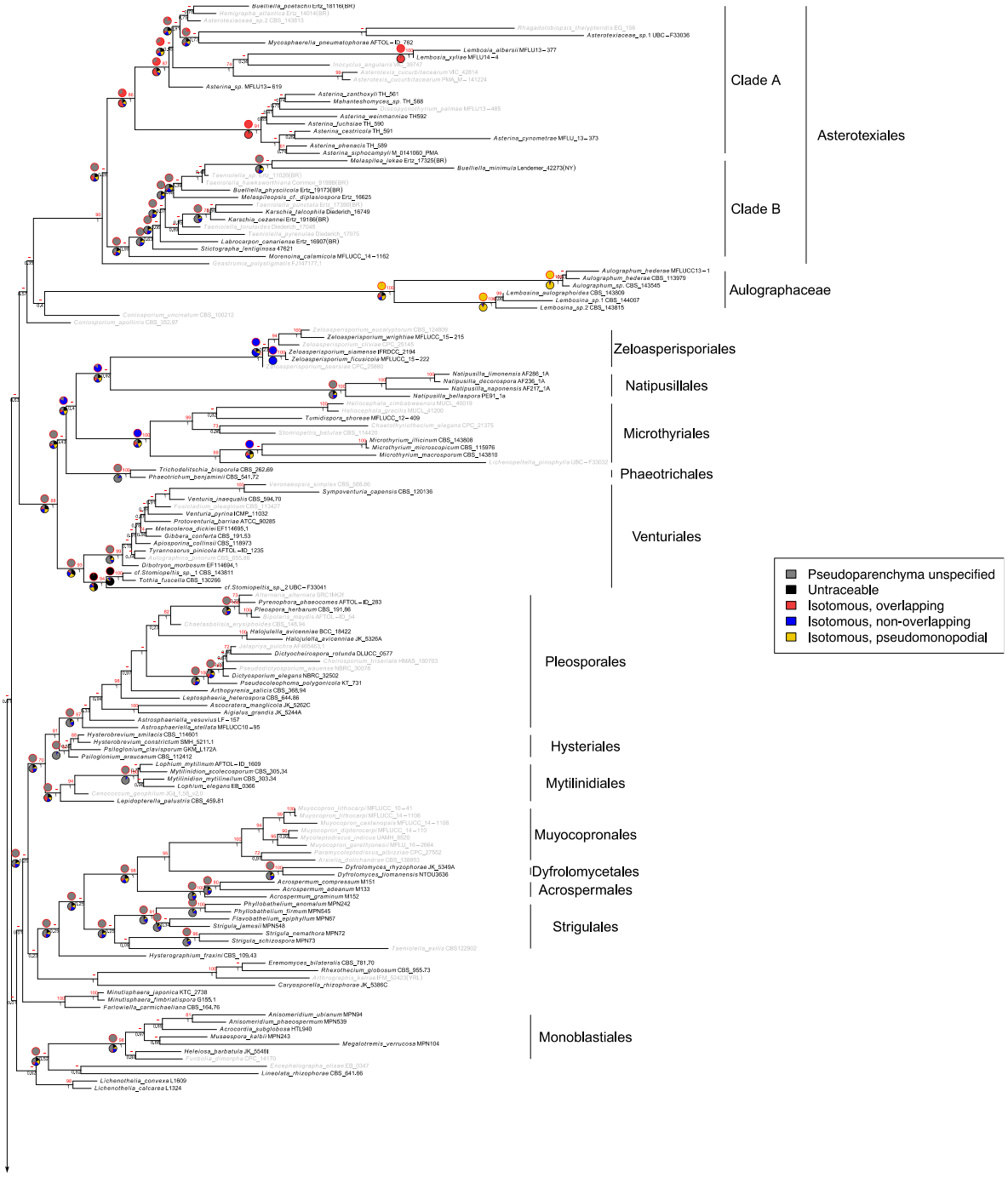

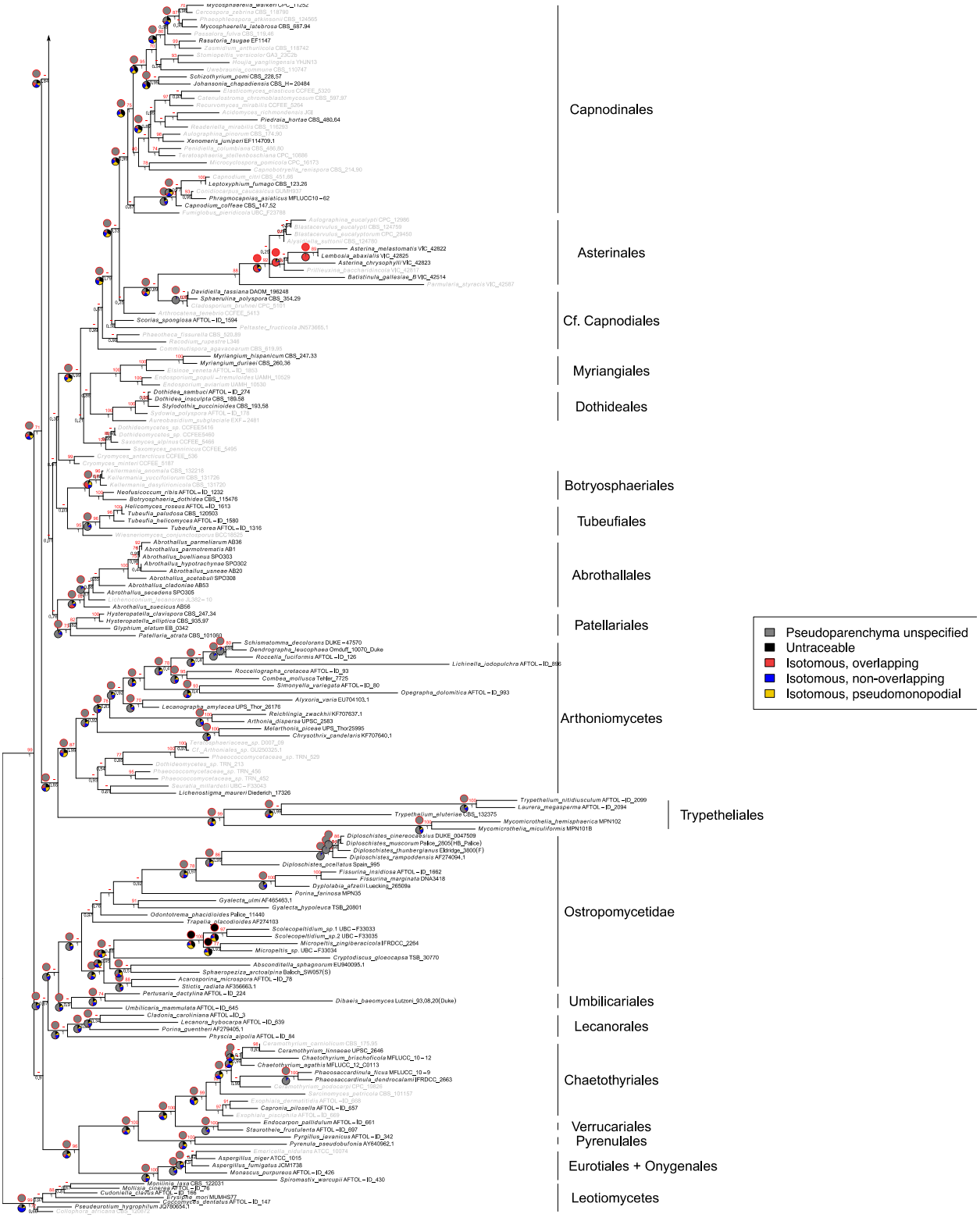
Capnodinales
Asterinales
Cf. Capnodiales
Myriangiales
Dothideales
Botryosphaeriales
Tubeufiales
Abrothallales
Patellariales
Arthoniomycetes
Trypetheliales
Ostropomycetidae
Umbilicariales
Lecanorales
Chaetothyriales
Verrucariales
Pyrenulales
Eurotiales + Onygenales
Leotiomycetes
Pseudoparenchyma unspecified
Untraceable
Isotomous, overlapping
Isotomous, non-overlapping
Isotomous, pseudomonopodial

A.16 Ancestral character state reconstruction for (IX) margin of sporocarp: either a distal margin *not appressed* or an appressed margin that is *crenulate*, *entire* or *anastomosing*

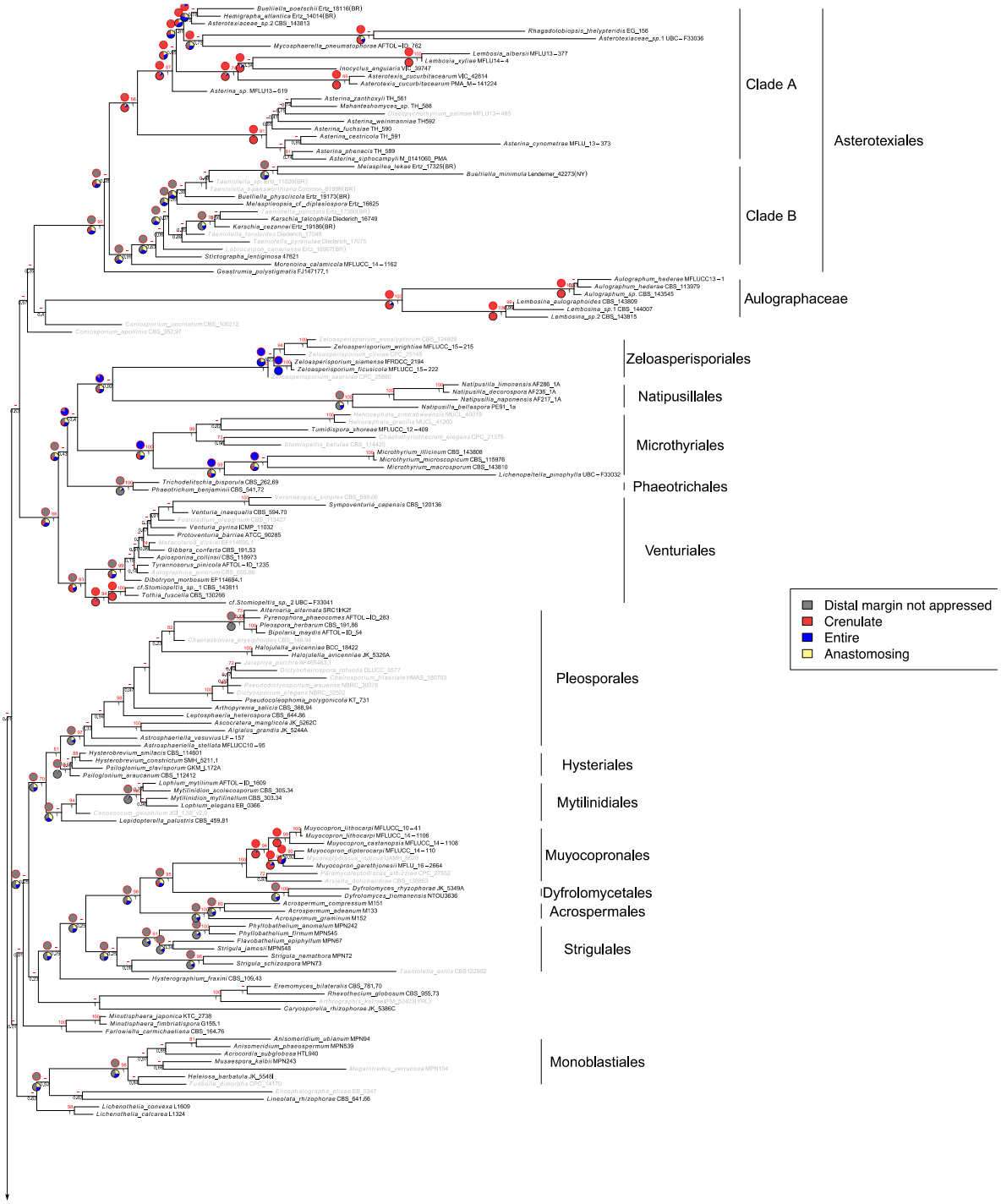

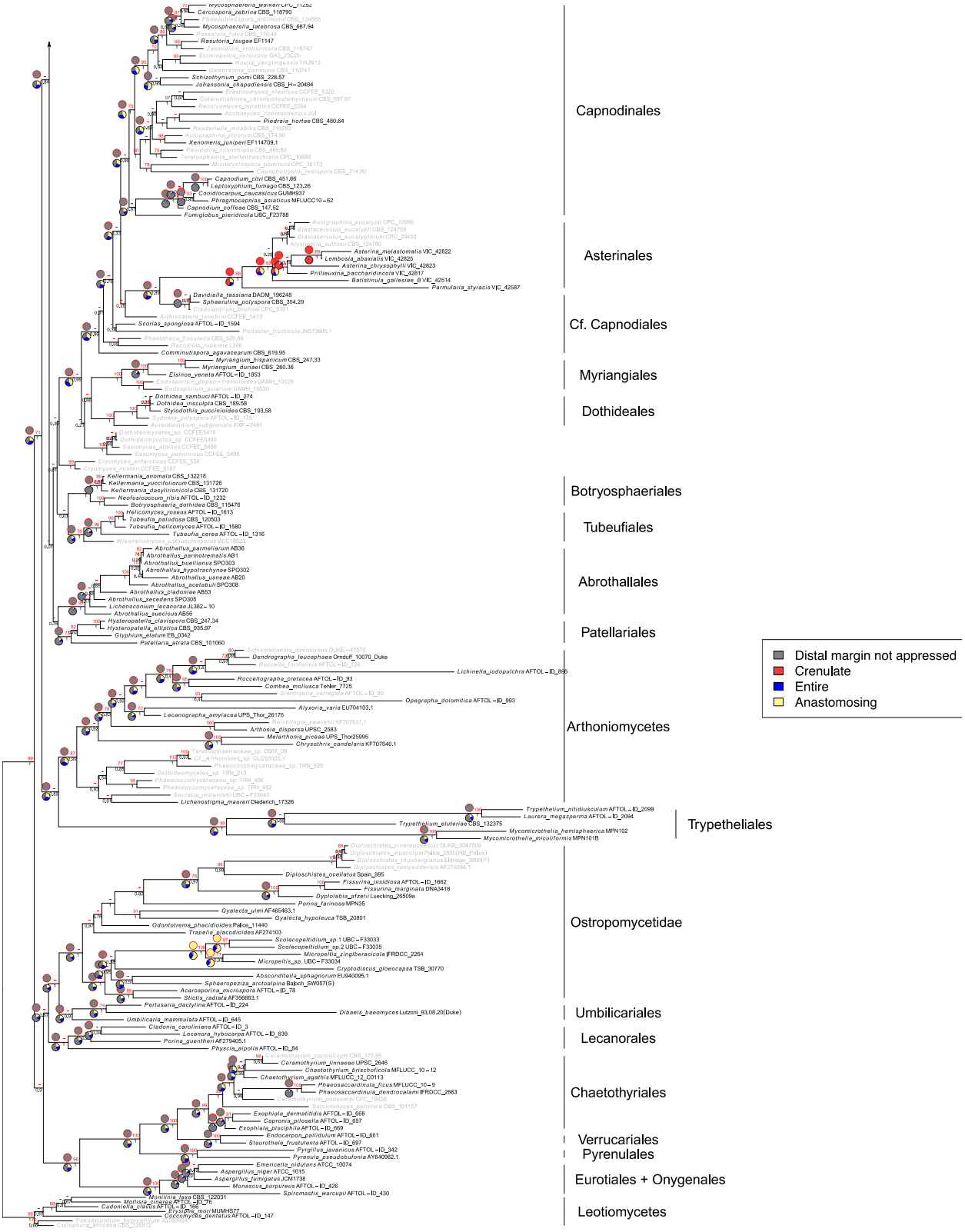
Capnodiales
Asterinales
Cf. Capnodiales
Myriangiales
Dothideales
Botryosphaeriales
Tubeufiales
Abrothallales
Patellariales
Arthoniomycetes
Trypetheliales
Ostropomycetidae
Umbilicariales
Lecanorales
Chaetothyriales
Verrucariales
Pyrenulales
Eurotiales + Onygenales
Leotiomycetes
Distal margin not appressed
Crenulate
Entire
Anastomosing

A.17 Ancestral character state reconstruction for the *presence* or *absence* of (X) lateral appressoria on superficial mycelium

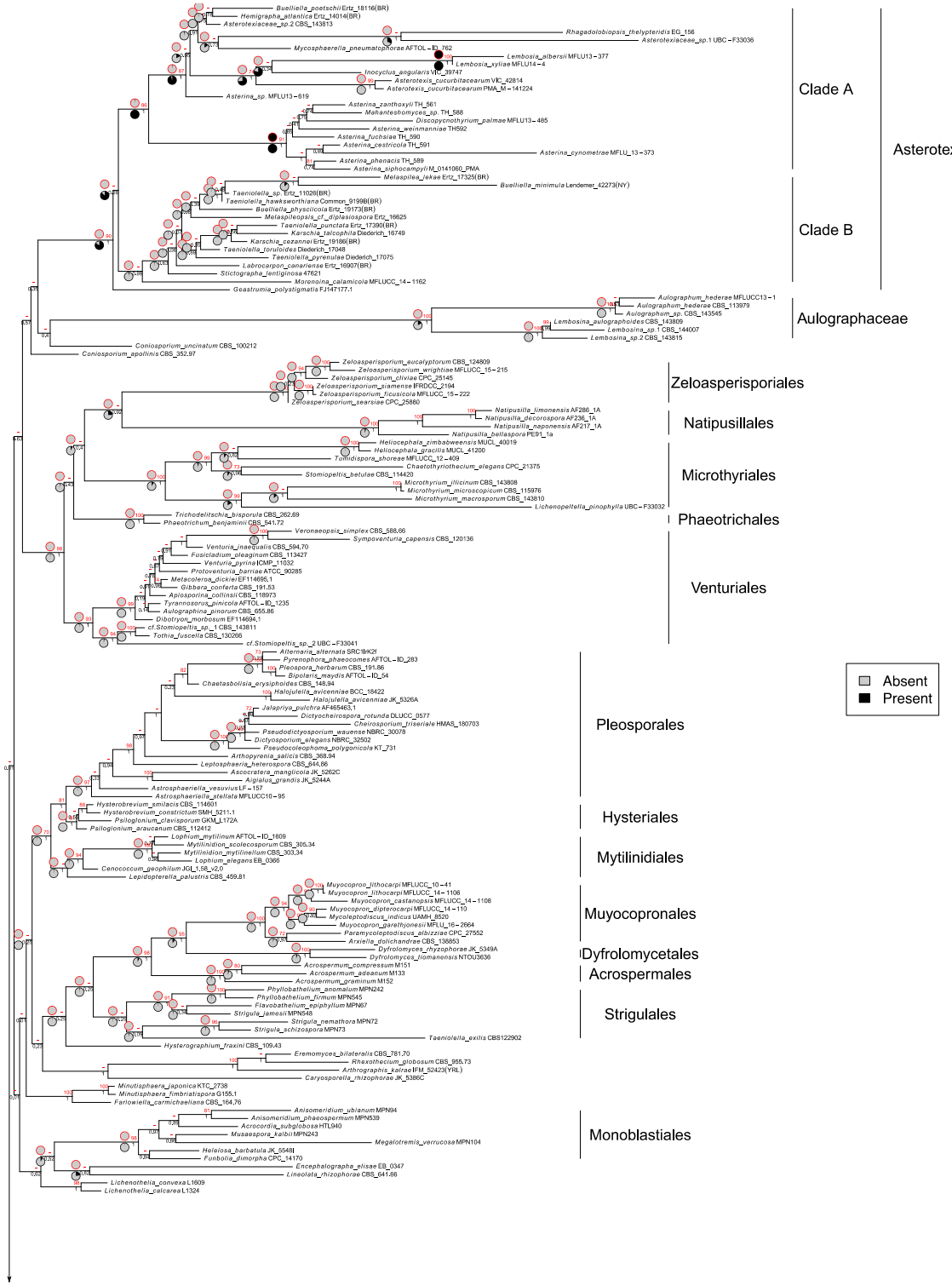

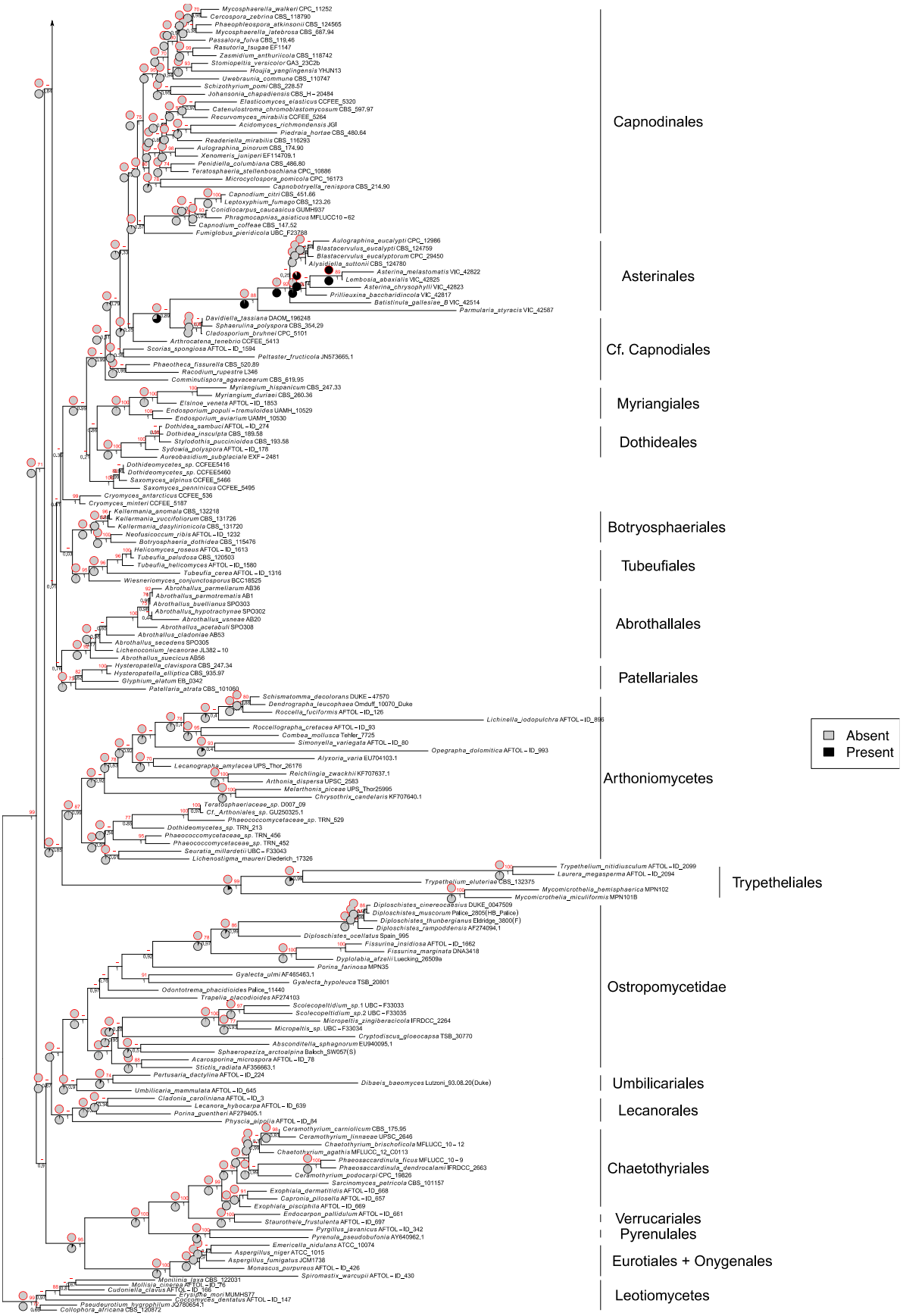
Capnodinales
Asterinales
Cf. Capnodiales
Myriangiales
Dothideales
Botryosphaeriales
Tubeufiales
Abrothallales
Patellariales
Arthoniomycetes
Trypetheliales
Ostropomycetidae
Umbilicariales
Lecanorales
Chaetothyriales
Verrucariales
Pyrenulales
Eurotiales + Onygenales
Leotiomycetes
Absent
Present

A.18 Ancestral character state reconstruction for (XI) Sporocarp initiation: *at tip of generator hypha*, *intercalary on generator hypha*, *from spore*, *from host stomata* or from *coordinated generator hyphae*.

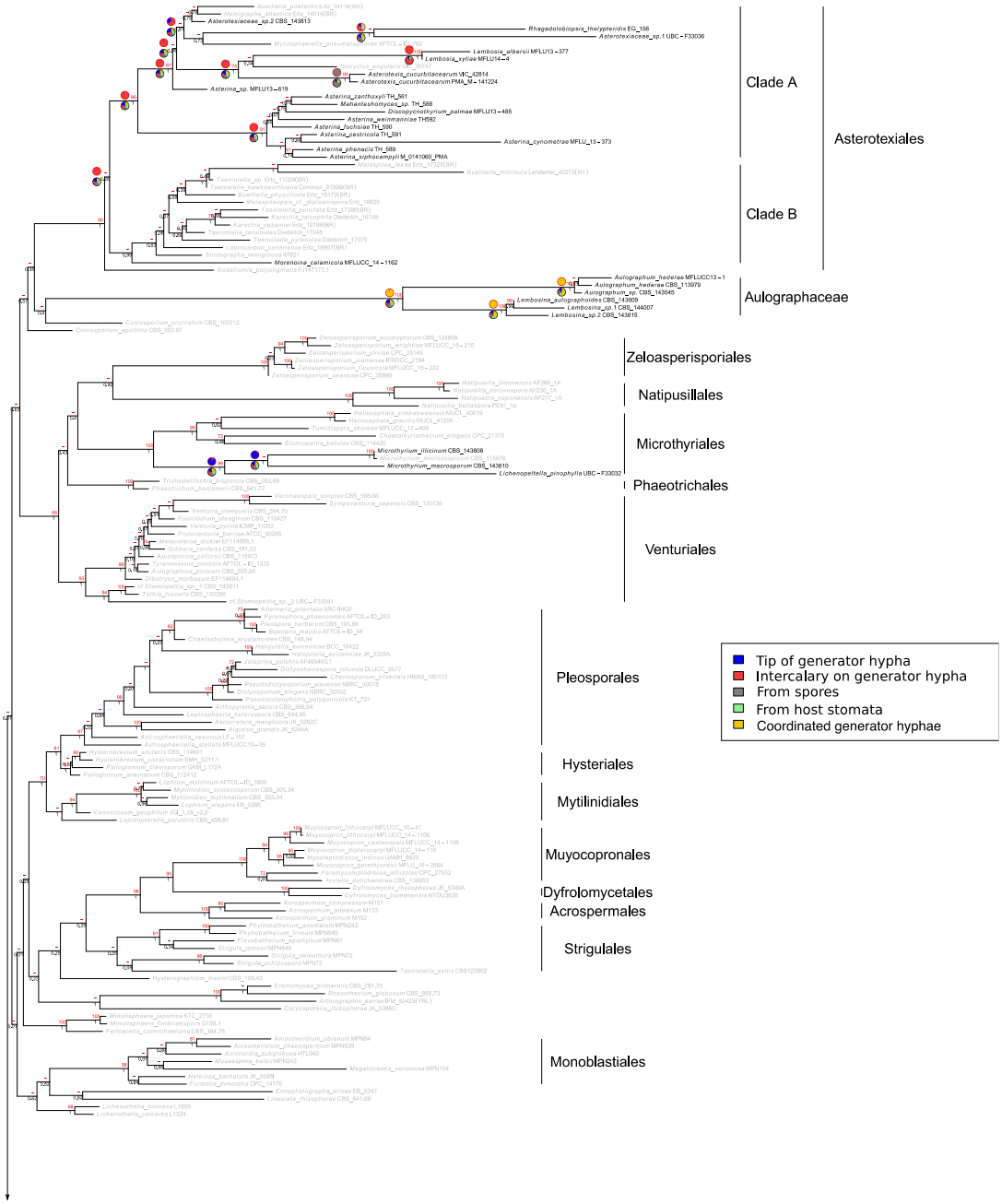

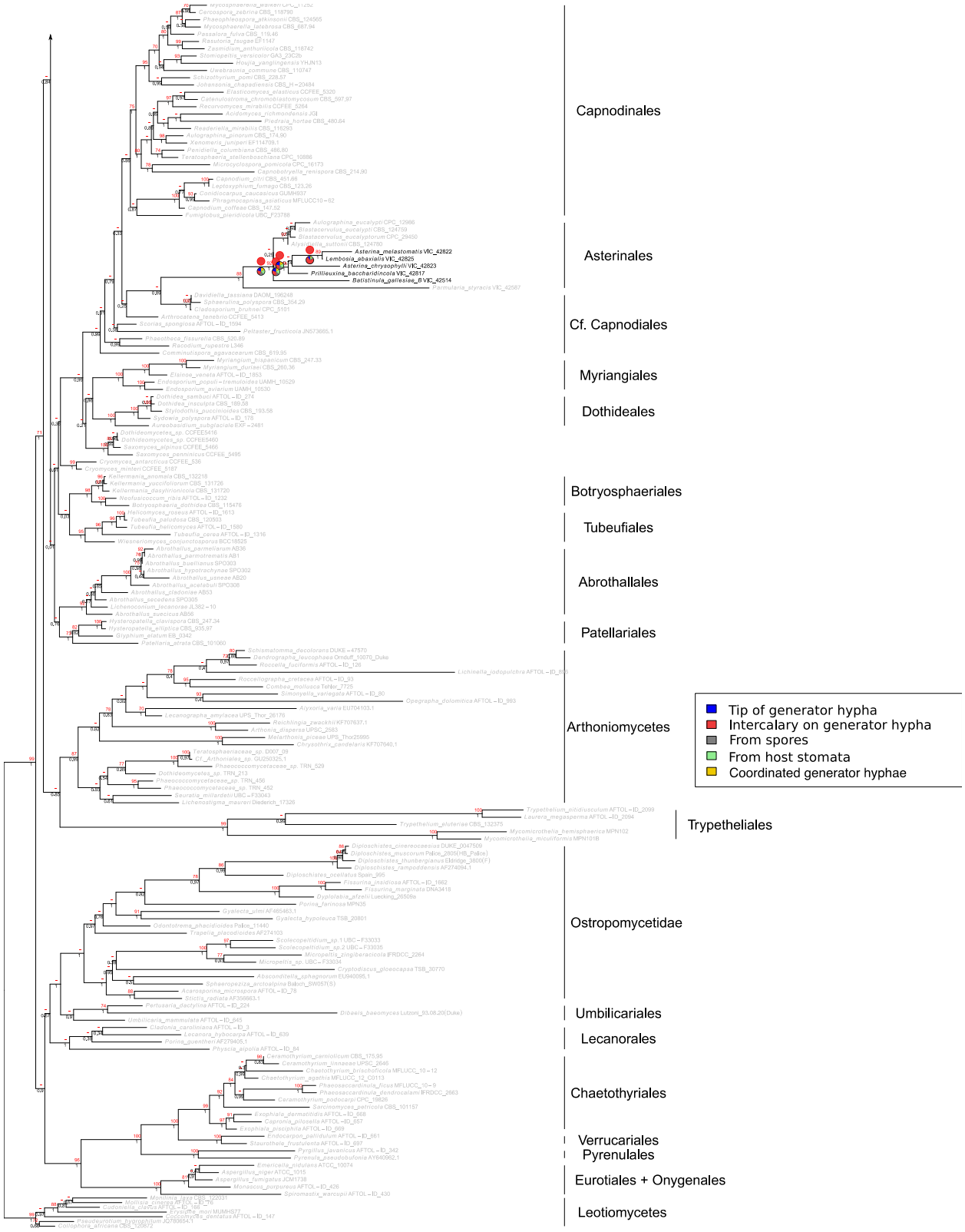
Capnodinales
Asterinales
Asterina_melastomatis VIC_42822
Lembosia_abaxialis VIC_42825
Asterina_chrysophylli VIC_42823
Prillieuxina_baccharidincola VIC_42817
Batistinula_gallesiae_B VIC_42514
Cf. Capnodiales
Myriangiales
Dothideales
Botryosphaeriales
Tubeufiales
Abrothallales
Patellariales
Arthoniomycetes
Tip of generator hypha
Intercalary on generator hypha
From spores
From host stomata
Coordinated generator hyphae
Trypetheliales
Ostropomycetidae
Umbilicariales
Lecanorales
Chaetothyriales
Verrucariales
Pyrenulales
Eurotiales + Onygenales
Leotiomycetes

A.19 Consensus of 28 equally most parsimonious phylogenetic positions of the Triassic "fungal thallus" form India described in Mishra et al. (2018).

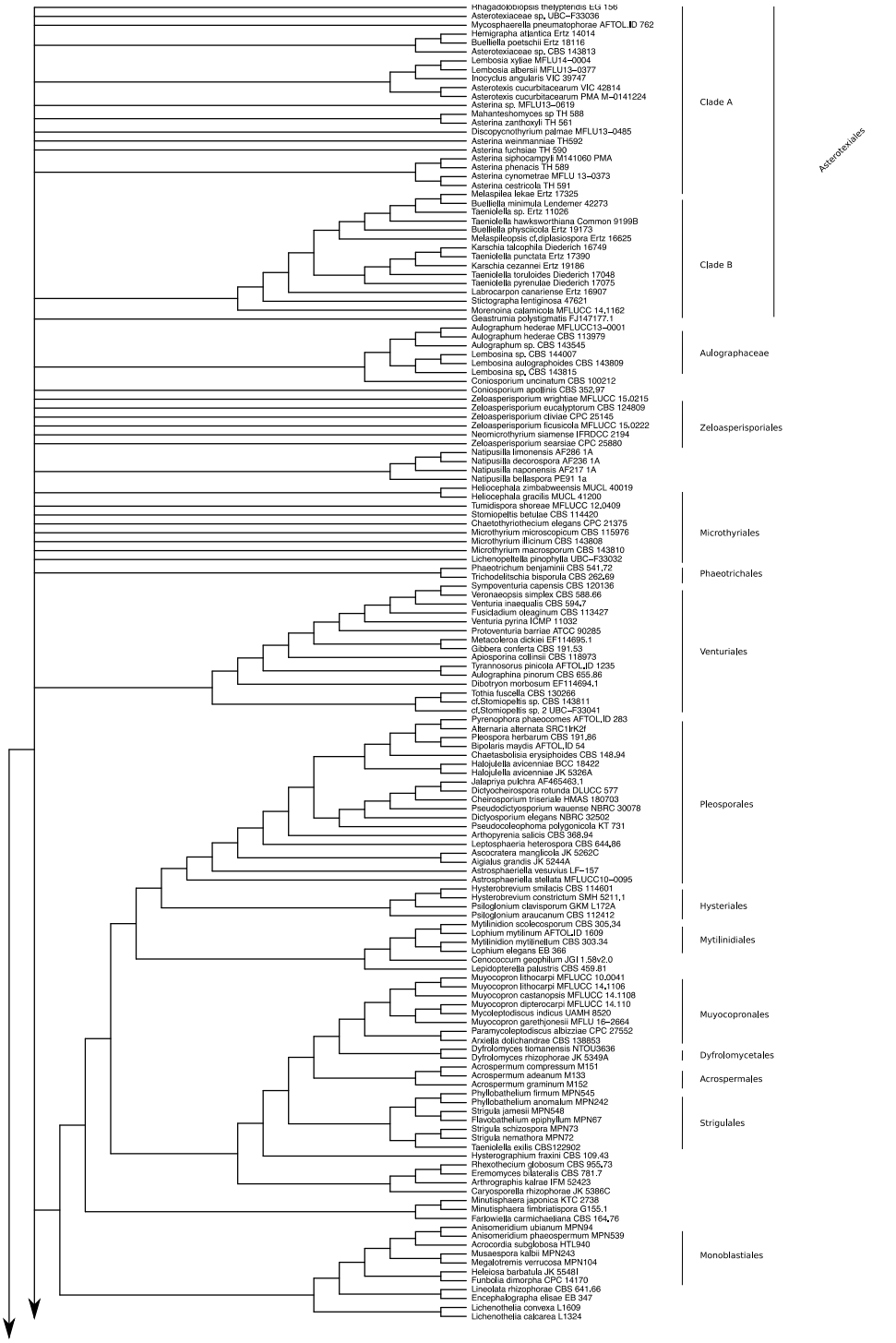

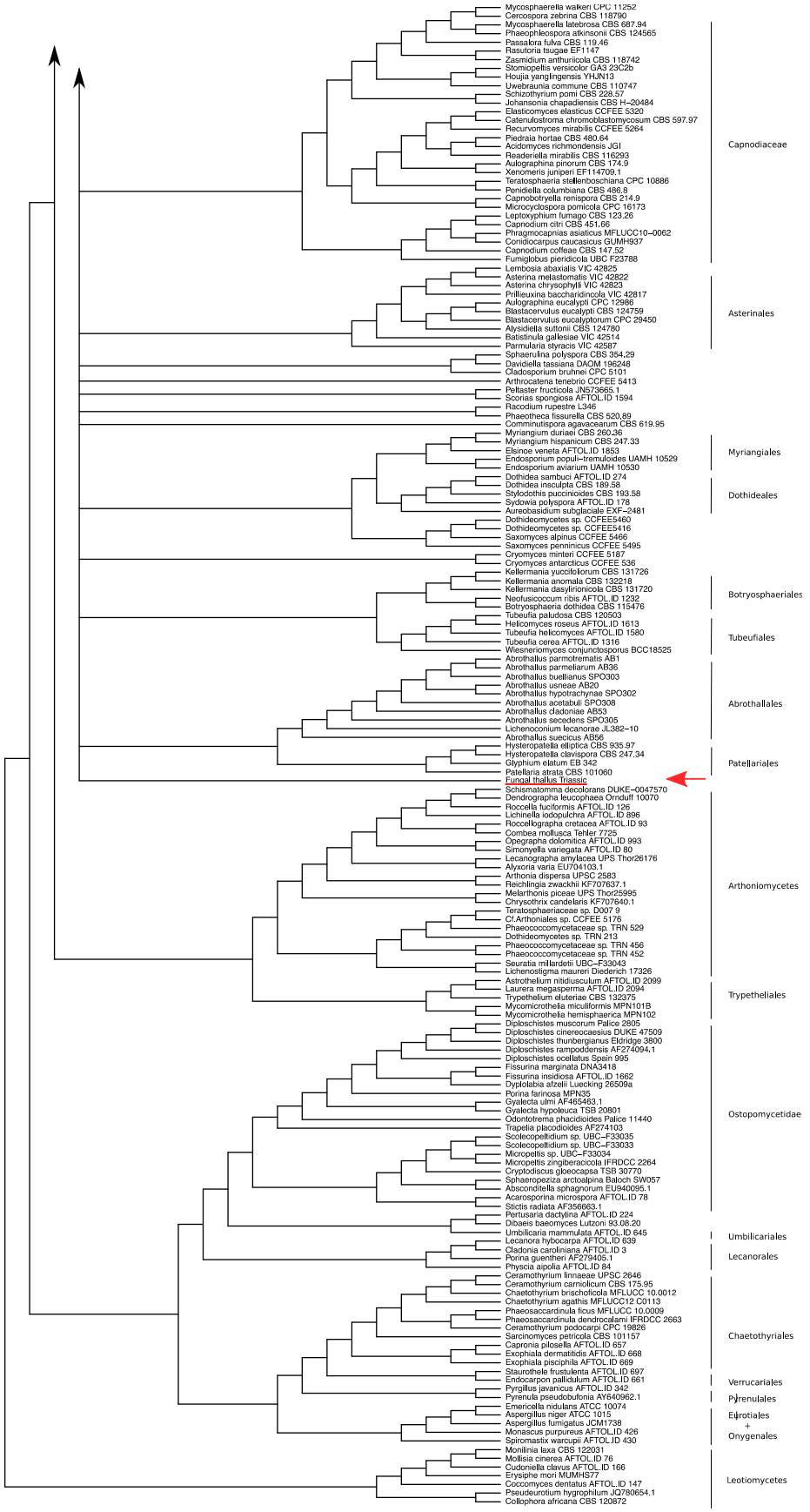
Mycosphaerella walkeri CPC 11252
Cercospora zebrina CBS 118790
Mycosphaerella latebrosa CBS 687.94
Phaeophleospora atkinsonii CBS 124565
Passalora fulva CBS 119.46
Rasutoria tsugae EF1147
Zasmidium anthuriicola CBS 118742
Stomiopeltis versicolor GA3 23C2b
Houjia yangIngensis YHJN13
Uwebraunia commune CBS 110747
Schizothyrium pomi CBS 228.57
Johansonia chapadiensis CBS H–20484
Elasticomyces elasticus CCFEE 5320
Catenulostroma chromoblastomycosum CBS 597.97
Recurvomyces mirabilis CCFEE 5264
Piedraia hortae CBS 480.64
Acidomyces richmondensis JGI
Readeriella mirabilis CBS 116293
Aulographina pinorum CBS 174.9
Xenomeris juniperi EF114709.1
Teratosphaeria stellenboschiana CPC 10886
Peridiella columbiana CBS 486.8
Capnobotryella renispora CBS 214.9
Microcyclospora pomicola CPC 16173
Leptoxyphium fumago CBS 123.26
Capnodium citri CBS 451.66
Phragmocapnias asiaticus MFLUCC10–0062
Conidiocarpus caucasicus GUMH937
Capnodium coffeae CBS 147.52
Fumiglobus pieridicola UBC F23788
Capnodiaceae
Lembosia abaxialis VIC 42825
Asterina metastomatis VIC 42822
Asterina chrysophylli VIC 42823
Prillieuxina baccharidincola VIC 42817
Aulographina eucalypti CPC 12986
Blastacervulus eucalypti CBS 124759
Blastacervulus eucalyptorum CPC 29450
Alysidiella suttonii CBS 124780
Batistinula gallesiae VIC 42514
Parmularia styracis VIC 42587
Asterinales
Sphaerulina polyspora CBS 354.29
Davidiella tassiana DAOM 196248
Cladosporium bruhnei CPC 5101
Arthrocatena tenebrio CCFEE 5413
Peltaster fructicola JN573665.1
Scorias spongiosa AFTOL-ID 1594
Racodium rupestre L346
Phaeotheca fissurella CBS 520.89
Comminutispora agavacearum CBS 619.95
Myriangium duriaei CBS 260.36
Myriangium hispanicum CBS 247.33
Elsinoe veneta AFTOL-ID 1853
Endosporium populi–tremuloides UAMH 10529
Endosporium aviarium UAMH 10530
Myriangiales
Dothidea sambuci AFTOL-ID 274
Dothidea insculpta CBS 189.58
Stylodothis puccinioides CBS 193.58
Sydowia polyspora AFTOL-ID 178
Aureobasidium subglaciale EXF–2481
Dothideomycetes sp. CCFEE5460
Dothideomycetes sp. CCFEE5416
Saxomyces alpinus CCFEE 5466
Saxomyces penninicus CCFEE 5495
Dothideales
Cryomyces minteri CCFEE 5187
Cryomyces antarcticus CCFEE 536
Kellermania yuccifoliorum CBS 131726
Kellermania anomala CBS 132218
Kellermania dasyliriicola CBS 131720
Neofusicoccum ribis AFTOL-ID 1232
Botryosphaeria dothidea CBS 115476
Botryosphaeriales
Tubeufia paludosa CBS 120503
Helicomyces roseus AFTOL-ID 1613
Tubeufia helicomyces AFTOL-ID 1580
Tubeufia cerea AFTOL-ID 1316
Wiesneriomyces conjunctosporus BCC18525
Tubeufiales
Abrothallus parmotrematis AB1
Abrothallus parmeliarum AB36
Abrothallus buellianus SPO303
Abrothallus usneae AB20
Abrothallus hypotrachynae SPO302
Abrothallus acetabuli SPO308
Abrothallus dadoniae AB53
Abrothallus secedens SPO305
Lichenoconium lecanorae JL382–10
Abrothallus suecicus AB56
Abrothallales
Hysteropatella elliptica CBS 935.97
Hysteropatella clavispora CBS 247.34
Glyphium elatum EB 342
Patellaria atrata CBS 101060
Patellariales
Fungal thallus Triassic
Schismatomma decolorans DUKE–0047570
Dendrographa leucophaea Ornduff 10070
Roccella fuciformis AFTOL-ID 126
Lichinella iodopulchra AFTOL-ID 896
Roccellographa cretacea AFTOL-ID 93
Combea mollusca Tehler 7725
Opegrapha dolomitica AFTOL-ID 993
Simonyella variegata AFTOL-ID 80
Lecanographa amylacea UPS Thor26176
Alyxoria varia EU704103.1
Arthonia dispersa UPSC 2583
Reichlingia zwackhii KF707637.1
Melarthonis piceae UPS Thor25995
Chrysothrix candelaris KF707640.1
Teratosphaeriaceae sp. D007 9
Cf.Arthoniales sp. CCFEE 5176
Phaeococcomycetaceae sp. TRN 529
Dothideomycetes sp. TRN 213
Phaeococcomycetaceae sp. TRN 456
Phaeococcomycetaceae sp. TRN 452
Seuratia millardetii UBC–F33043
Lichenostigma maureri Diederich 17326
Arthoniomycetes
Astrothelium nidiusculum AFTOL-ID 2099
Laurera megasperma AFTOL-ID 2094
Trypethelium eluteriae CBS 132375
Mycomicrothelia miculiformis MPN101B
Mycomicrothelia hemisphaerica MPN102
Trypetheliales
Diploschistes muscorum Palice 2805
Diploschistes cinereocaesius DUKE 47509
Diploschistes thunbergianus Eldridge 3800
Diploschistes rampoddensis AF274094.1
Diploschistes ocellatus Spain 995
Fissurina marginata DNA3418
Fissurina insidiosa AFTOL-ID 1662
Dyplolabia afzelii Luecking 26509a
Porina farinosa MPN35
Gyalecta ulmi AF465463.1
Gyalecta hypoleuca TSB 20801
Odontotrema phacidioides Palice 11440
Trapelia placodioides AF274103
Scolecopeltidium sp. UBC–F33035
Scolecopeltidium sp. UBC–F33033
Micropeltis sp. UBC–F33034
Micropeltis zingiberaciocola IFRDCC 2264
Cryptodiscus gloeocapsa TSB 30770
Sphaeropeziza arctoalpina Baloch SW057
Absconditella sphagnorum EU940095.1
Acarosporina microspora AFTOL-ID 78
Stictis radiata AF356663.1
Ostopomycetidae
Pertusaria dactylina AFTOL-ID 224
Dibaeis baeomyces Lutzoni 93.08.20
Umbilicaria mammulata AFTOL-ID 645
Umbilicariales
Lecanora hybocarpa AFTOL-ID 639
Cladonia caroliniana AFTOL-ID 3
Porina guentheri AF279405.1
Physcia aipolia AFTOL-ID 84
Lecanorales
Ceramothyrium linnaeae UPSC 2646
Ceramothyrium carniolicum CBS 175.95
Chaetothyrium brischoficola MFLUCC 10.0012
Chaetothyrium agathis MFLUCC12 C0113
Phaeosaccardinula ficus MFLUCC 10.0009
Phaeosaccardinula dendrocalami IFRDCC 2663
Ceramothyrium podocarpi CPC 19826
Sarcinomyces petricola CBS 101157
Capronia pilosella AFTOL-ID 657
Exophiala dermatitidis AFTOL-ID 668
Exophiala pisciphila AFTOL-ID 669
Chaetothyriales
Staurothele frustulenta AFTOL-ID 697
Endocarpon pallidulum AFTOL-ID 661
Verrucariales
Pyrgillus javanicus AFTOL-ID 342
Pyrenula pseudobufonia AY640962.1
Pyrenulales
Emericella nidulans ATCC 10074
Aspergillus niger ATCC 1015
Aspergillus fumigatus JCM1738
Monascus purpureus AFTOL-ID 426
Spiromastix warcupii AFTOL-ID 430
Eurotiales + Onygenales
Monilinia laxa CBS 122031
Mollisia cinerea AFTOL-ID 76
Cudoniella clavus AFTOL-ID 166
Erysiphe mori MUMHS77
Coccomyces dentatus AFTOL-ID 147
Pseudeurotium hygrophilum JQ790654.1
Collophora africana CBS 120872
Leotiomycetes

A.20 Consensus of 16 equally most parsimonious phylogenetic positions of *Trichothyrites setifer* from the Eocene of India described in Monga et al. (2015).

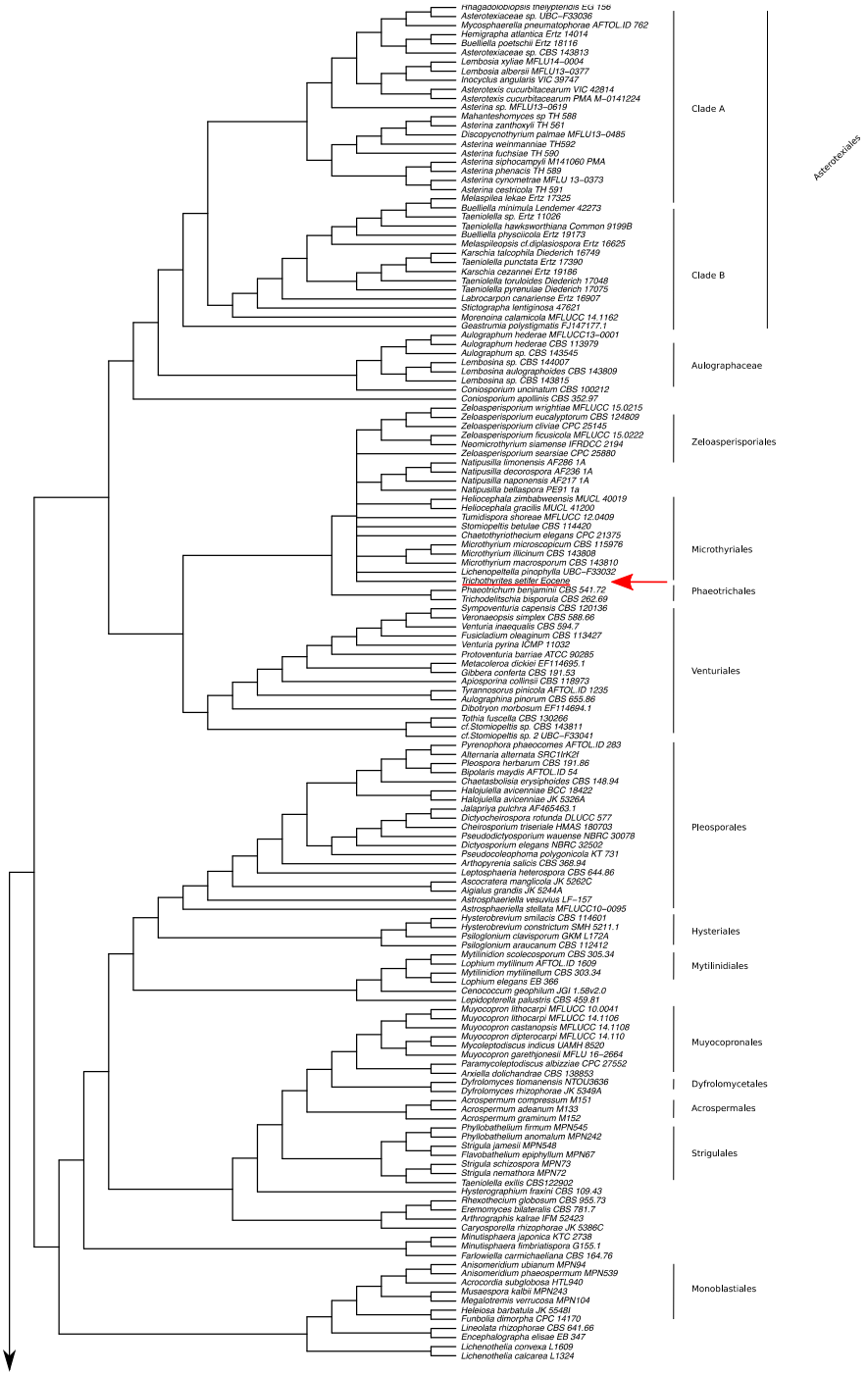

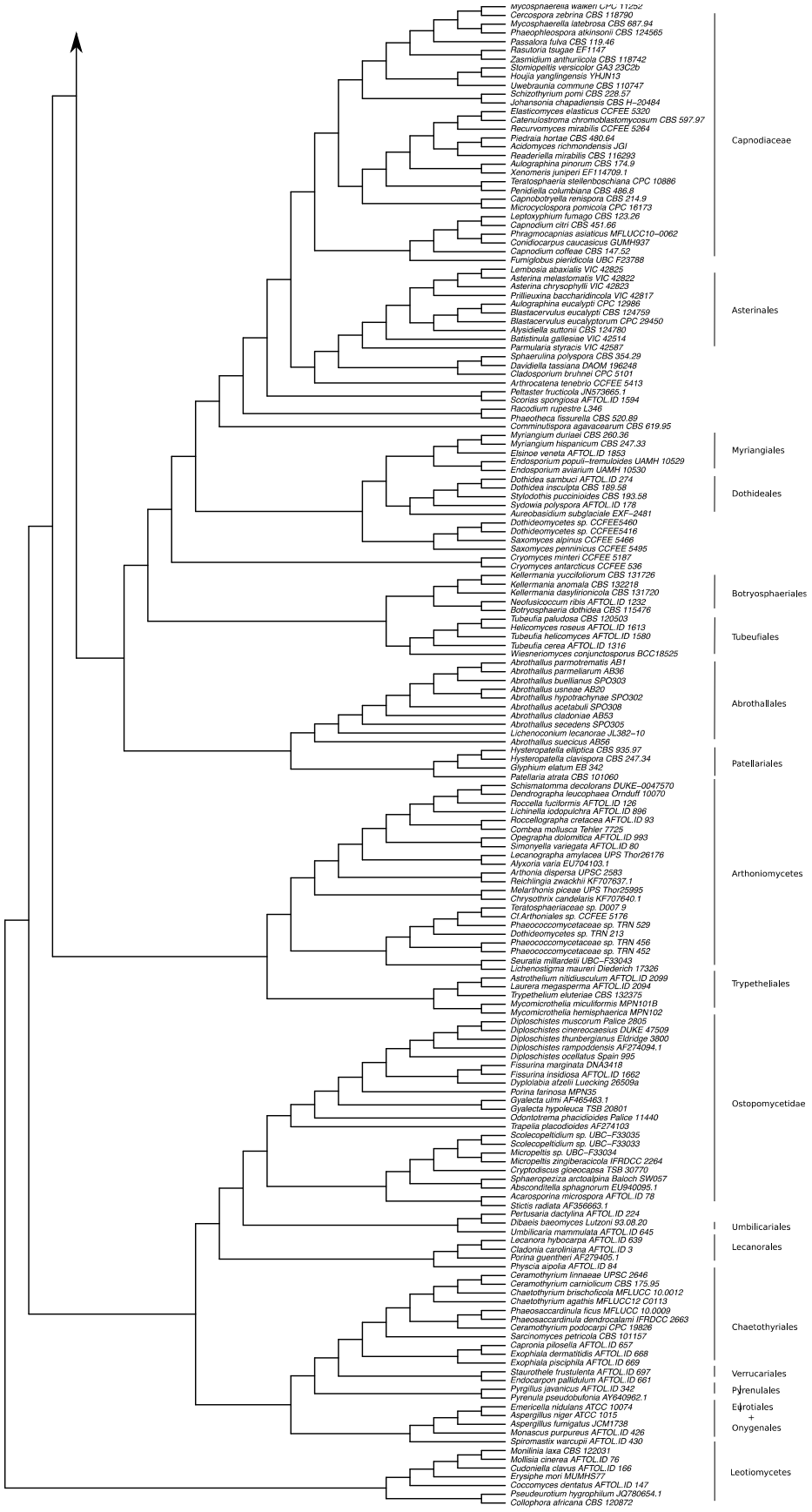
Mycosphaerella walkeri UPS 112b2
Cercospora zebrina CBS 118790
Mycosphaerella latebrosa CBS 687.94
Phaeophleospora atkinsonii CBS 124565
Passalora fulva CBS 119.46
Rasutoria tsugae EF1147
Zasmidium anthuricola CBS 118742
Stomiopeltis versicolor GA3 23C2b
Houjia yanglingensis YHJN13
Uwebraunia commune CBS 110747
Schizothyrium pomi CBS 228.57
Johansonia chapadiensis CBS H–20484
Elasticomyces elasticus CCFEE 5320
Catenulostroma chromoblastomycosum CBS 597.97
Recurvomyces mirabilis CCFEE 5264
Piedraia hortae CBS 480.64
Acidomyces richmondensis JGI
Readeriella mirabilis CBS 116293
Aulographina pinorum CBS 174.9
Xenomeris juniperi EF114709.1
Teratosphaeria stellenboschiana CPC 10886
Penidiella columbiana CBS 486.8
Capnobotryella renispora CBS 214.9
Microcyclospora pomicola CPC 16173
Leptoxyphium fumago CBS 123.26
Capnodium citri CBS 451.66
Phragmocapnias asiaticus MFLUCC10–0062
Conidiocarpus caucasicus GUMH937
Capnodium coffeae CBS 147.52
Fumiglobus pieridicola UBC F23788
Capnodiaceae
Lembosia abaxialis VIC 42825
Asterina melastomatis VIC 42822
Asterina chrysophylli VIC 42823
Prillieuxina baccharidincola VIC 42817
Aulographina eucalypti CPC 12986
Blastacervulus eucalypti CBS 124759
Blastacervulus eucalyptorum CPC 29450
Alysidiella suttonii CBS 124780
Batistinula gallesiae VIC 42514
Parmularia styracis VIC 42587
Asterinales
Sphaerulina polyspora CBS 354.29
Davidiella tassiana DAOM 196248
Cladosporium brunnei CPC 5101
Arthrocatena tenebrio CCFEE 5413
Peltaster fructicola JN573665.1
Scorias spongiosa AFTOL ID 1594
Racodium rupestre L346
Phaeotheca fissurella CBS 520.89
Comminutispora agavacearum CBS 619.95
Myriangium duriaei CBS 260.36
Myriangium hispanicum CBS 247.33
Elsinoe veneta AFTOL ID 1853
Endosporium populi–tremuloides UAMH 10529
Endosporium aviarium UAMH 10530
Myriangiales
Dothidea sambuci AFTOL ID 274
Dothidea insculpta CBS 189.58
Stylodothis puccinioides CBS 193.58
Sydowia polyspora AFTOL ID 178
Aureobasidium subglaciale EXF–2481
Dothideomycetes sp. CCFEE5460
Dothideomycetes sp. CCFEE5416
Saxomyces alpinus CCFEE 5466
Saxomyces penninicus CCFEE 5495
Dothideales
Cryomyces minteri CCFEE 5187
Cryomyces antarcticus CCFEE 536
Kellermania yuccifoliorum CBS 131726
Kellermania anomala CBS 132218
Kellermania dasylirionicola CBS 131720
Neofusicoccum ribis AFTOL ID 1232
Botryosphaeria dothidea CBS 115476
Botryosphaeriales
Tubeufia paludosa CBS 120503
Helicomyces roseus AFTOL ID 1613
Tubeufia helicomyces AFTOL ID 1580
Tubeufia cerea AFTOL ID 1316
Wiesneriomyces conjunctosporus BCC18525
Tubeufiales
Abrothallus parmotrematis AB1
Abrothallus parmeliarum AB36
Abrothallus buellianus SPO303
Abrothallus usneae AB20
Abrothallus hypotrachynae SPO302
Abrothallus acetabuli SPO308
Abrothallus cladoniae AB53
Abrothallus secedens SPO305
Lichenoconium lecanorae JL382–10
Abrothallus suecicus AB56
Abrothallales
Hysteropatella elliptica CBS 935.97
Hysteropatella clavispora CBS 247.34
Glyphium elatum EB 342
Patellaria atrata CBS 101060
Patellariales
Schismatomma decolorans DUKE–0047570
Dendrographa leucophaea Ornduff 10070
Roccella fuciformis AFTOL ID 126
Lichinella iodopulchra AFTOL ID 896
Roccellographa cretacea AFTOL ID 93
Combea mollusca Tehler 7725
Opegrapha dolomitica AFTOL ID 993
Simonyella variegata AFTOL ID 80
Lecanographa amylacea UPS Thor26176
Alyxoria varia EU704103.1
Arthonia dispersa UPSC 2583
Reichlingia zwackhii KF707637.1
Melarthonis piceae UPS Thor25995
Chrysothrix candelaris KF707640.1
Teratosphaeriaceae sp. D007 9
Cf.Arthoniales sp. CCFEE 5176
Phaeococcomycetaceae sp. TRN 529
Dothideomycetes sp. TRN 213
Phaeococcomycetaceae sp. TRN 456
Phaeococcomycetaceae sp. TRN 452
Seuratia millardetii UBC–F33043
Lichenostigma maureri Diederich 17326
Arthoniomycetes
Astrothelium nitidiusculum AFTOL ID 2099
Laurera megasperma AFTOL ID 2094
Trypethelium eluteriae CBS 132375
Mycomicrothelia miculiformis MPN101B
Mycomicrothelia hemisphaerica MPN102
Trypetheliales
Diploschistes muscorum Palice 2805
Diploschistes cinereocaesius DUKE 47509
Diploschistes thunbergianus Eldridge 3800
Diploschistes rampoddensis AF274094.1
Diploschistes ocellatus Spain 995
Fissurina marginata DNA3418
Fissurina insidiosa AFTOL ID 1662
Dyplolabia afzelii Luecking 26509a
Porina farinosa MPN35
Gyalecta ulmi AF465463.1
Gyalecta hypoleuca TSB 20801
Odontotrema phacidioides Palice 11440
Trapelia placodioides AF274103
Scolecopeltidium sp. UBC–F33035
Scolecopeltidium sp. UBC–F33033
Micropeltis sp. UBC–F33034
Micropeltis zingiberacicola IFRDCC 2264
Cryptodiscus gloeocapsa TSB 30770
Sphaeropezia arctoalpina Baloch SW057
Absconditella sphagnorum EU940095.1
Acarosporina microspora AFTOL ID 78
Stictis radiata AF356663.1
Ostopomycetidae
Pertusaria dactylina AFTOL ID 224
Dibaeis baeomyces Lutzoni 93.08.20
Umbilicariales
Umbilicaria mammulata AFTOL ID 645
Lecanora hybocarpa AFTOL ID 639
Lecanorales
Cladonia carolliniana AFTOL ID 3
Porina guentheri AF279405.1
Physcia aipolia AFTOL ID 84
Ceramothyrium linnaeae UPSC 2646
Ceramothyrium carniolicum CBS 175.95
Chaetothyrium brischoficola MFLUCC 10.0012
Chaetothyrium agathis MFLUCC12 C0113
Phaeosaccardinula ficus MFLUCC 10.0009
Phaeosaccardinula dendrocalami IFRDCC 2663
Ceramothyrium podocarpi CPC 19826
Sarcinomyces petricola CBS 101157
Capronia pilosella AFTOL ID 657
Exophiala dermatitidis AFTOL ID 668
Exophiala pisciphila AFTOL ID 669
Chaetothyriales
Staurothele frustulenta AFTOL ID 697
Endocarpon pallidulum AFTOL ID 661
Verrucariales
Pyrgillus javanicus AFTOL ID 342
Pyrenulales
Pyrenula pseudobufonia AY640962.1
Emericella nidulans ATCC 10074
Aspergillus niger ATCC 1015
Aspergillus fumigatus JCM1738
Monascus purpureus AFTOL ID 426
Spiromastix warcupii AFTOL ID 430
Eurotiales + Onygenales
Monilinia laxa CBS 122031
Mollisia cinerea AFTOL ID 76
Cudoniella clavus AFTOL ID 166
Erysiphe mori MUMHS77
Coccomyces dentatus AFTOL ID 147
Pseudeurotium hygrophilum JQ780654.1
Collophora africana CBS 120872
Leotiomycetes

A.21 Consensus of 23 equally most parsimonious phylogenetic positions of *Asterina eocenica* from the Eocene of USA, described in Dilcher (1965).

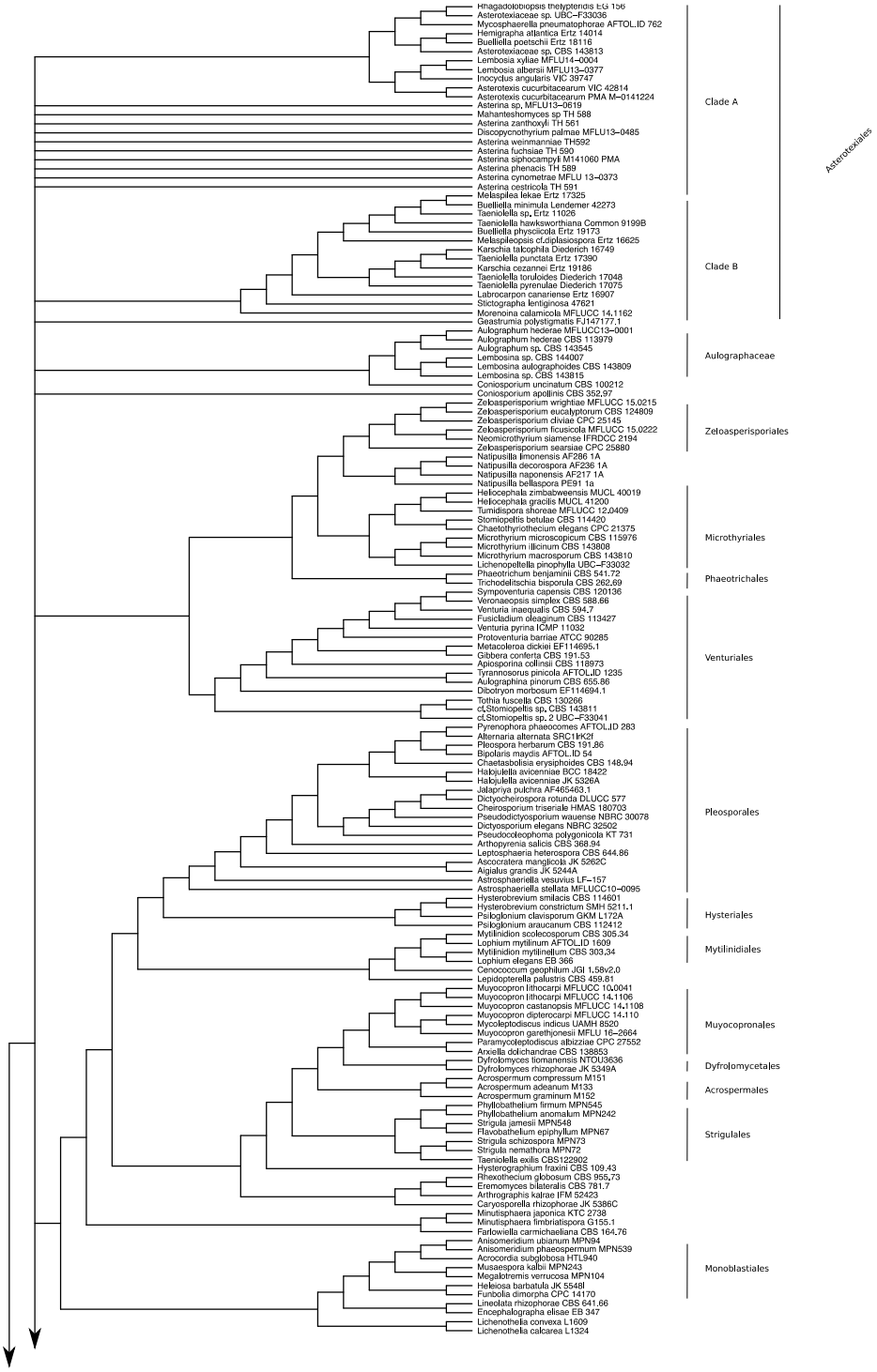

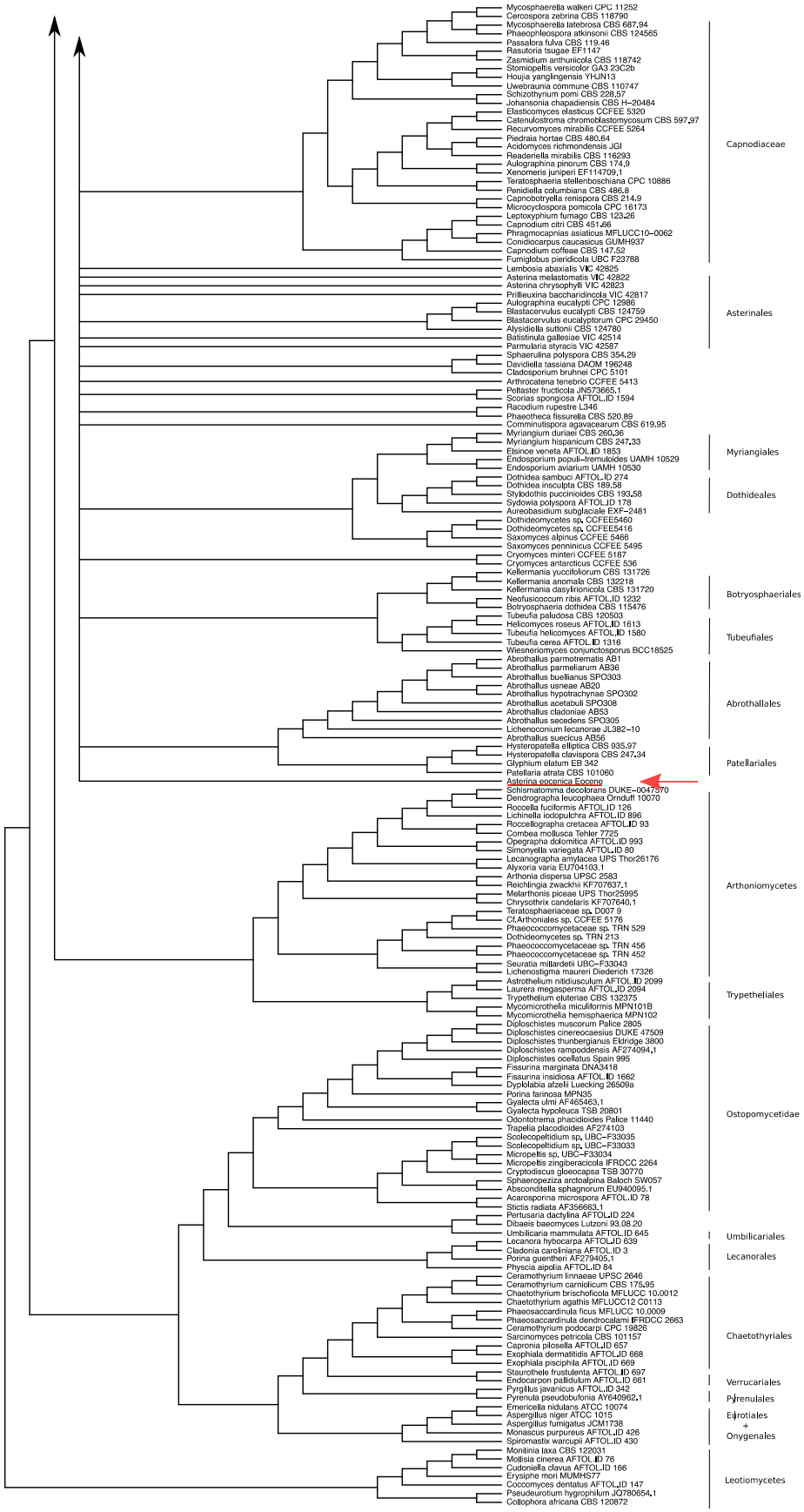
Mycosphaerella walkeri CPC 11252
Cercospora zebrina CBS 118790
Mycosphaerella latebrosa CBS 687.94
Phaeophleospora atkinsonii CBS 124565
Passalora fulva CBS 119.46
Rasutoria tsugae EF1147
Zasmidium anthuriicola CBS 118742
Stomiopeltis versicolor GA3 23C2b
Houjia yanglingensis YHJN13
Uwebraunia commune CBS 110747
Schizothyrium pomi CBS 228.57
Johansonia chapadiensis CBS H–20484
Elasticomyces elasticus CCFEE 5320
Catenulostroma chromoblastomycosum CBS 597.97
Recurvomyces mirabilis CCFEE 5264
Piedraia hortae CBS 480.64
Acidomyces richmondensis JGI
Readeriella mirabilis CBS 116293
Aulographina pinorum CBS 174.9
Xenomeris juniperi EF114709.1
Teratosphaeria stellenboschiana CPC 10886
Peridiella columbiana CBS 466.8
Capnobotryella renispora CBS 214.9
Microcyclospora pomicola CPC 16173
Leptoxyphium fumago CBS 123.26
Capnodium citri CBS 451.66
Phragmocapnias asiaticus MFLUCC10–0062
Conidiocarpus caucasicus GUMH937
Capnodium coffeae CBS 147.52
Fumiglobus pieridicola UBC F23788
Capnodiaceae
Lembosia abaxialis VIC 42825
Asterina melastomatis VIC 42822
Asterina chrysophylli VIC 42823
Prillieuxina baccharidincola VIC 42817
Aulographina eucalypti CPC 12986
Blastacervulus eucalypti CBS 124759
Blastacervulus eucalyptorum CPC 29450
Alysidiella suttonii CBS 124780
Batistinula gallesiae VIC 42514
Parmularia styracis VIC 42587
Asterinales
Sphaerulina polyspora CBS 354.29
Davidiella tassiana DAOM 196248
Cladosporium bruhnei CPC 5101
Arthrocatena tenebrio CCFEE 5413
Peltaster fructicola JN573665.1
Scorias spongiosa AFTOL-ID 1594
Racodium rupestre L346
Phaeotheca fissurella CBS 520.89
Comminutispora agavacearum CBS 619.95
Myriangium duriaei CBS 260.36
Myriangium hispanicum CBS 247.33
Elsinoe veneta AFTOL-ID 1853
Endosporium populi–tremuloides UAMH 10529
Endosporium aviarium UAMH 10530
Myriangiales
Dothidea sambuci AFTOL-ID 274
Dothidea insculpta CBS 189.58
Stydothis puccinioides CBS 193.58
Sydowia polyspora AFTOL-ID 178
Aureobasidium subglaciale EXF–2481
Dothideomycetes sp. CCFEE5460
Dothideomycetes sp. CCFEE5416
Saxomyces alpinus CCFEE 5466
Saxomyces penninicus CCFEE 5495
Dothideales
Cryomyces minteri CCFEE 5187
Cryomyces antarcticus CCFEE 536
Kellermania yuccifoliorum CBS 131726
Kellermania anomala CBS 132218
Kellermania dasylirionicola CBS 131720
Neofusicoccum ribis AFTOL-ID 1232
Botryosphaeria dothidea CBS 115476
Botryosphaeriales
Tubeufia paludosa CBS 120503
Helicomyces roseus AFTOL-ID 1613
Tubeufia helicomyces AFTOL-ID 1580
Tubeufia cerea AFTOL-ID 1316
Wiesneriomyces conjunctosporus BCC18525
Tubeufiales
Abrothallus parmotrematis AB1
Abrothallus parmeliarum AB36
Abrothallus buellianus SPO303
Abrothallus usneae AB20
Abrothallus hypotrachynae SPO302
Abrothallus acetabuli SPO308
Abrothallus cladoniae AB53
Abrothallus secedens SPO305
Lichenoconium lecanorae JL382–10
Abrothallus suecicus AB56
Abrothallales
Hysteropatella elliptica CBS 935.97
Hysteropatella clavispora CBS 247.34
Glyphium elatum EB 342
Patellaria atrata CBS 101060
Asterina eocenica Eocene
Patellariales
Schismatomma decolorans DUKE–0047870
Dendrographa leucophaea Orduff 10070
Roccella fuciformis AFTOL-ID 126
Lichinella iodopulchra AFTOL-ID 896
Roccellographa cretacea AFTOL-ID 93
Combea mollusca Tehler 7725
Opegrapha dolomitica AFTOL-ID 993
Simonyella variegata AFTOL-ID 80
Lecanographa amylacea UPS Thor26176
Alyxoria varia EU704103.1
Arthonia dispersa UPSC 2583
Reichlingia zwackhii KF707637.1
Melarthonis piceae UPS Thor25995
Chrysothrix candelaris KF707640.1
Teratosphaeriaceae sp. D007 9
CtArthoniales sp. CCFEE 5176
Phaeococcomycetaceae sp. TRN 529
Dothideomycetes sp. TRN 213
Phaeococcomycetaceae sp. TRN 456
Phaeococcomycetaceae sp. TRN 452
Seuratia millardetii UBC–F33043
Lichenostigma maureri Diederich 17326
Arthoniomycetes
Astrothelium nitidiusculum AFTOL-ID 2099
Laurera megasperma AFTOL-ID 2094
Trypethelium eluteriae CBS 132375
Mycomicrothelia miculiformis MPN101B
Mycomicrothelia hemisphaerica MPN102
Trypetheliales
Diploschistes muscorum Palice 2805
Diploschistes cinereocaesius DUKE 47509
Diploschistes thunbergianus Eldridge 3800
Diploschistes rampodensis AF274094.1
Diploschistes ocellatus Spain 995
Fissurina marginata DNA3418
Fissurina insidiosa AFTOL-ID 1662
Dyplolabia afzelii Luecking 26509a
Porina farinosa MPN35
Gyalecta ulmi AF465463.1
Gyalecta hypoleuca TSB 20801
Odontotrema phacidioides Palice 11440
Trapelia placodioides AF274103
Scolecopeltidium sp. UBC–F33035
Scolecopeltidium sp. UBC–F33033
Micropeltis sp. UBC–F33034
Micropeltis zingiberacicola IFRDCC 2264
Cryptodiscus gloeocapsa TSB 30770
Sphaeropeziza arctoalpina Baloch SW057
Absconditella sphagnorum EU940095.1
Acarosporina microspora AFTOL-ID 78
Stictis radiata AF356663.1
Ostopomycetidae
Pertusaria dactylina AFTOL-ID 224
Dibaeis baeomyces Lutzoni 93.08.20
Umbilicaria mammulata AFTOL-ID 645
Umbilicariales
Lecanora hybocarpa AFTOL-ID 639
Cladonia caroliniana AFTOL-ID 3
Porina guentheri AF279405.1
Physcia aipolia AFTOL-ID 84
Lecanorales
Ceramothyrium linnaeae UPSC 2646
Ceramothyrium carnidicum CBS 175.95
Chaetothyrium brischoficola MFLUCC 10.0012
Chaetothyrium agathis MFLUCC12 C0113
Phaeosaccardinula ficus MFLUCC 10.0009
Phaeosaccardinula dendrocalami IFRDCC 2663
Ceramothyrium podocarpi CPC 19826
Sarcinomyces petricola CBS 101157
Capronia pilosella AFTOL-ID 657
Exophiala dermatitidis AFTOL-ID 668
Exophiala piscipihila AFTOL-ID 669
Chaetothyriales
Staurothele frustulenta AFTOL-ID 697
Endocarpon pallidulum AFTOL-ID 661
Verrucariales
Pyrgillus javanicus AFTOL-ID 342
Pyrenula pseudobufonia AY640962.1
Pyrenulales
Emericella nidulans ATCC 10074
Aspergillus niger ATCC 1015
Aspergillus fumigatus JCM1738
Monascus purpureus AFTOL-ID 426
Spiromastix warcupii AFTOL-ID 430
Eurotiales + Onygenales
Monilinia laxa CBS 122031
Mollisia cinerea AFTOL-ID 76
Cudoniella clavus AFTOL-ID 166
Erysiphe mori MUMHS77
Coccomyces dentatus AFTOL-ID 147
Pseudeurotium hygrophilum JQ780654.1
Collophora africana CBS 120872
Leotiomycetes

A.22 Consensus of the 18 equally most parsimonious phylogenetic trees placing *Asterina eocenica* with taxa in Asterotexiales.

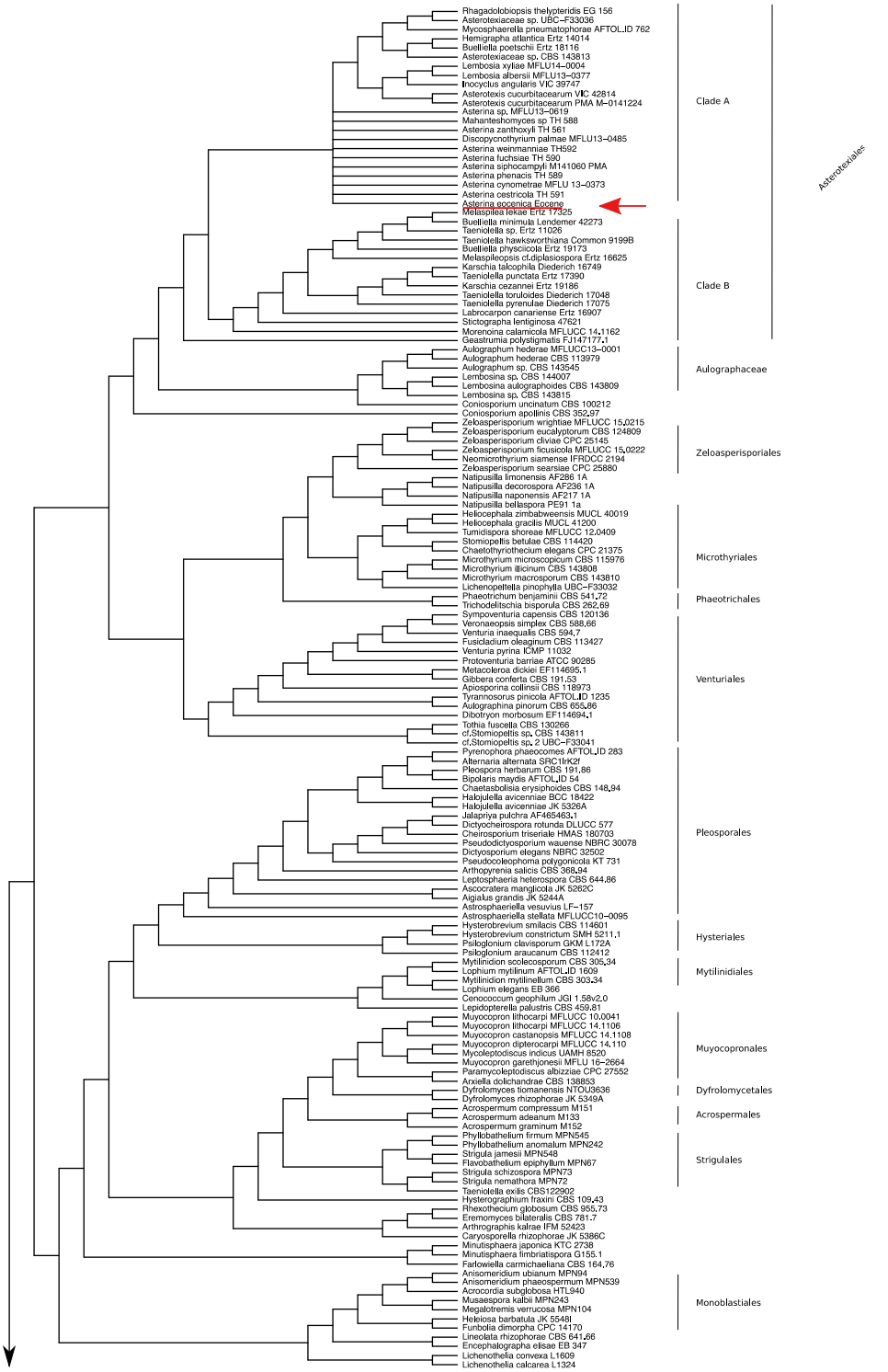

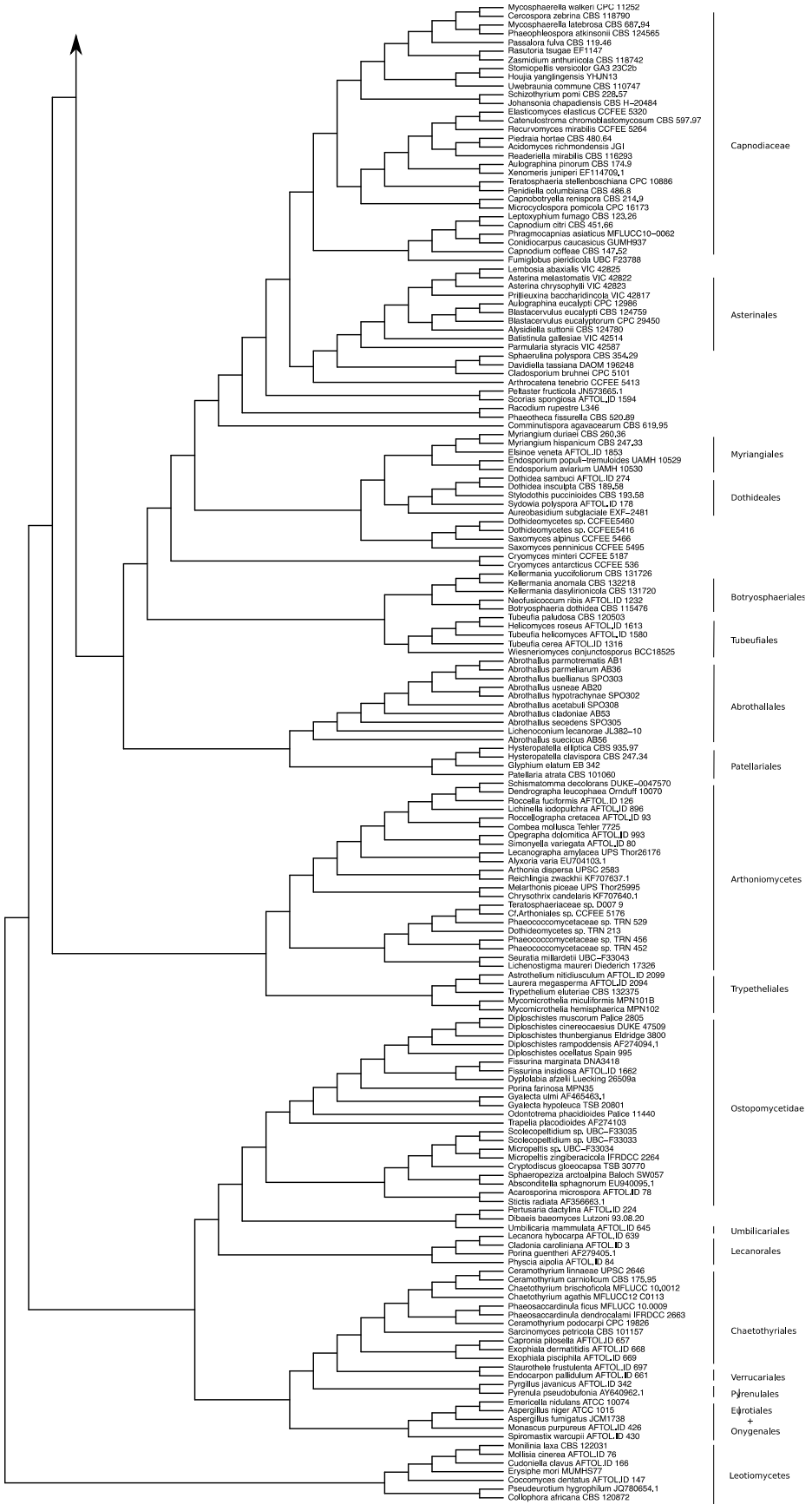
Mycosphaerella walkeri CPC 11252
Cercospora zebrina CBS 118790
Mycosphaerella latebrosa CBS 687.94
Phaeophleospora atkinsonii CBS 124565
Passalora fulva CBS 119.46
Rasutoria tsugae EF1147
Zasmidium anthuriicola CBS 118742
Stomiopeltis versicolor GA3 23C2b
Houjia yanglingensis YHJN13
Uwebraunia commune CBS 110747
Schizothyrium pomi CBS 228.57
Johansonia chapadiensis CBS H–20484
Elasticomyces elasticus CCFEE 5320
Catenulostroma chromoblastomycosum CBS 597.97
Recurvomyces mirabilis CCFEE 5264
Piedraia hortae CBS 480.64
Acidomyces richmondensis JGI
Readeriella mirabilis CBS 116293
Aulographina pinorum CBS 174.9
Xenomeris juniperi EF114709.1
Teratosphaeria stellenboschiana CPC 10886
Penidiella columbiana CBS 486.8
Capnobotryella renispora CBS 214.9
Microcyclospora pomicola CPC 16173
Leptoxyphium fumago CBS 123.26
Capnodium citri CBS 451.66
Phragmocapnias asiaticus MFLUCC10–0062
Conidiocarpus caucasicus GUMH937
Capnodium coffeae CBS 147.52
Fumiglobus pieridicola UBC F23788
Capnodiaceae
Lembosia abaxialis VIC 42825
Asterina metastomatis VIC 42822
Asterina chrysophylli VIC 42823
Prillieuxina baccharidincola VIC 42817
Aulographina eucalypti CPC 12986
Blastacervulus eucalypti CBS 124759
Blastacervulus eucalyptorum CPC 29450
Alysidiella suttonii CBS 124780
Batistinula gallesiae VIC 42514
Parmularia styracis VIC 42587
Asterinales
Sphaerulina polyspora CBS 354.29
Davidiella tassiana DAOM 196248
Cladosporium bruhnei CPC 5101
Arthrocatena tenebrio CCFEE 5413
Peltaster fructicola JN573665.1
Scorias spongiosa AFTOL_ID 1594
Racodium rupestre L346
Phaeotheca fissurella CBS 520.89
Comminutispora agavacearum CBS 619.95
Myriangium duriaei CBS 260.36
Myriangium hispanicum CBS 247.33
Elsinoe veneta AFTOL_ID 1853
Endosporium populi–tremuloides UAMH 10529
Endosporium aviarium UAMH 10530
Myriangiales
Dothidea sambuci AFTOL_ID 274
Dothidea insculpta CBS 189.58
Stylodothis puccinioides CBS 193.58
Sydowia polyspora AFTOL_ID 178
Aureobasidium subglaciale EXF–2481
Dothideomycetes sp. CCFEE5460
Dothideomycetes sp. CCFEE5416
Saxomyces alpinus CCFEE 5466
Saxomyces penninicus CCFEE 5495
Dothideales
Cryomyces minteri CCFEE 5187
Cryomyces antarcticus CCFEE 536
Kellermania yuccifoliorum CBS 131726
Kellermania anomala CBS 132218
Kellermania dasylirionicola CBS 131720
Neofusicoccum ribis AFTOL_ID 1232
Botryosphaeria dothidea CBS 115476
Botryosphaeriales
Tubeufia paludosa CBS 120503
Helicomyces roseus AFTOL_ID 1613
Tubeufia helicomyces AFTOL_ID 1580
Tubeufia cerea AFTOL_ID 1316
Wiesneriomyces conjunctosporus BCC18525
Tubeufiales
Abrothallus parmotrematis AB1
Abrothallus parmeliarum AB36
Abrothallus buellianus SPO303
Abrothallus usnese AB20
Abrothallus hypotrachynae SPO302
Abrothallus acetabuli SPO308
Abrothallus cladoniae AB53
Abrothallus secedens SPO305
Lichenoconium lecanorae JL382–10
Abrothallus suecicus AB56
Abrothallales
Hysteropatella elliptica CBS 935.97
Hysteropatella clavispora CBS 247.34
Glyphium elatum EB 342
Patellaria atrata CBS 101060
Patellariales
Schismatomma decolorans DUKE–0047570
Dendrographa leucophaea Ornduff 10070
Roccella fuciformis AFTOL_ID 126
Lichinella iodopulchra AFTOL_ID 896
Roccellographa cretacea AFTOL_ID 93
Combea mollusca Tehler 7725
Opegrapha dolomitica AFTOL_ID 993
Simonyella variegata AFTOL_ID 80
Lecanographa amylacea UPS Thor26176
Alyxoria varia EU704103.1
Arthonia dispersa UPSC 2583
Reichlingia zwackhii KF707637.1
Melarthonis piceae UPS Thor25995
Chrysothrix candelaris KF707640.1
Teratosphaeriaceae sp. D007 9
Cf.Arthoniales sp. CCFEE 5176
Phaeococcomycetaceae sp. TRN 529
Dothideomycetes sp. TRN 213
Phaeococcomycetaceae sp. TRN 456
Phaeococcomycetaceae sp. TRN 452
Seuratia millardetii UBC–F33043
Lichenostigma maureri Diederich 17326
Arthoniomycetes
Astrothelium nitidiusculum AFTOL_ID 2099
Laurera megasperma AFTOL_ID 2094
Trypethelium eluteriae CBS 132375
Mycomicrothelia miculiformis MPN101B
Mycomicrothelia hemisphaerica MPN102
Trypetheliales
Diploschistes muscorum Palice 2805
Diploschistes cinereocaesius DUKE 47509
Diploschistes thunbergianus Eldridge 3800
Diploschistes rampoddensis AF274094.1
Diploschistes ocellatus Spain 995
Fissurina marginata DNA3418
Fissurina insidiosa AFTOL_ID 1662
Dyplolabia afzelii Luecking 26509a
Porina farinosa MPN35
Gyalecta ulmi AF465463.1
Gyalecta hypoleuca TSB 20801
Odontotrema phacidioides Palice 11440
Trapelia placodioides AF274103
Scolecopeltidium sp. UBC–F33035
Scolecopeltidium sp. UBC–F33033
Micropeltis sp. UBC–F33034
Micropeltis zingiberacicola IFRDCC 2264
Cryptodiscus gloeocapsa TSB 30770
Sphaeropeziza arctoalpina Baloch SW057
Absconditella sphagnorum EU940095.1
Acarosporina microspora AFTOL_ID 78
Stictis radiata AF356683.1
Pertusaria dactylina AFTOL_ID 224
Dibaeis baeomyces Lutzoni 93.08.20
Ostopomycetidae
Umbilicaria mammulata AFTOL_ID 645
Umbilicariales
Lecanora hybocarpa AFTOL_ID 639
Cladonia caroliniana AFTOL_ID 3
Porina guentheri AF279405.1
Lecanorales
Physcia aipolia AFTOL_ID 84
Ceramothyrium linnaeae UPSC 2646
Ceramothyrium carniolicum CBS 175.95
Chaetothyrium brischoficola MFLUCC 10.0012
Chaetothyrium agathis MFLUCC12 C0113
Phaeosaccardinula ficus MFLUCC 10.0009
Phaeosaccardinula dendrocalami IFRDCC 2663
Ceramothyrium podocarpi CPC 19826
Sarcinomyces petricola CBS 101157
Capronia pilosella AFTOL_ID 657
Exophiala dermatitidis AFTOL_ID 668
Exophiala pisciphila AFTOL_ID 669
Chaetothyriales
Staurothele frustulenta AFTOL_ID 897
Endocarpon pallidulum AFTOL_ID 661
Verrucariales
Pyrgillus javanicus AFTOL_ID 342
Pyrenula pseudobufonia AY640962.1
Pyrenulales
Emericella nidulans ATCC 10074
Aspergillus niger ATCC 1015
Aspergillus fumigatus JCM1738
Monascus purpureus AFTOL_ID 426
Spiromastix warcupii AFTOL_ID 430
Eurotiales + Onygenales
Monilinia laxa CBS 122031
Moliisia cinerea AFTOL_ID 76
Cudoniella clavus AFTOL_ID 166
Erysiphe mori MUMHS77
Coccomyces dentatus AFTOL_ID 147
Pseudeurotium hygrophilum JQ780654.1
Collophora africana CBS 120872
Leotiomycetes

A.23 Consensus of the 5 equally most parsimonious phylogenetic trees placing *Asterina eocenica* with taxa in Asterinales.

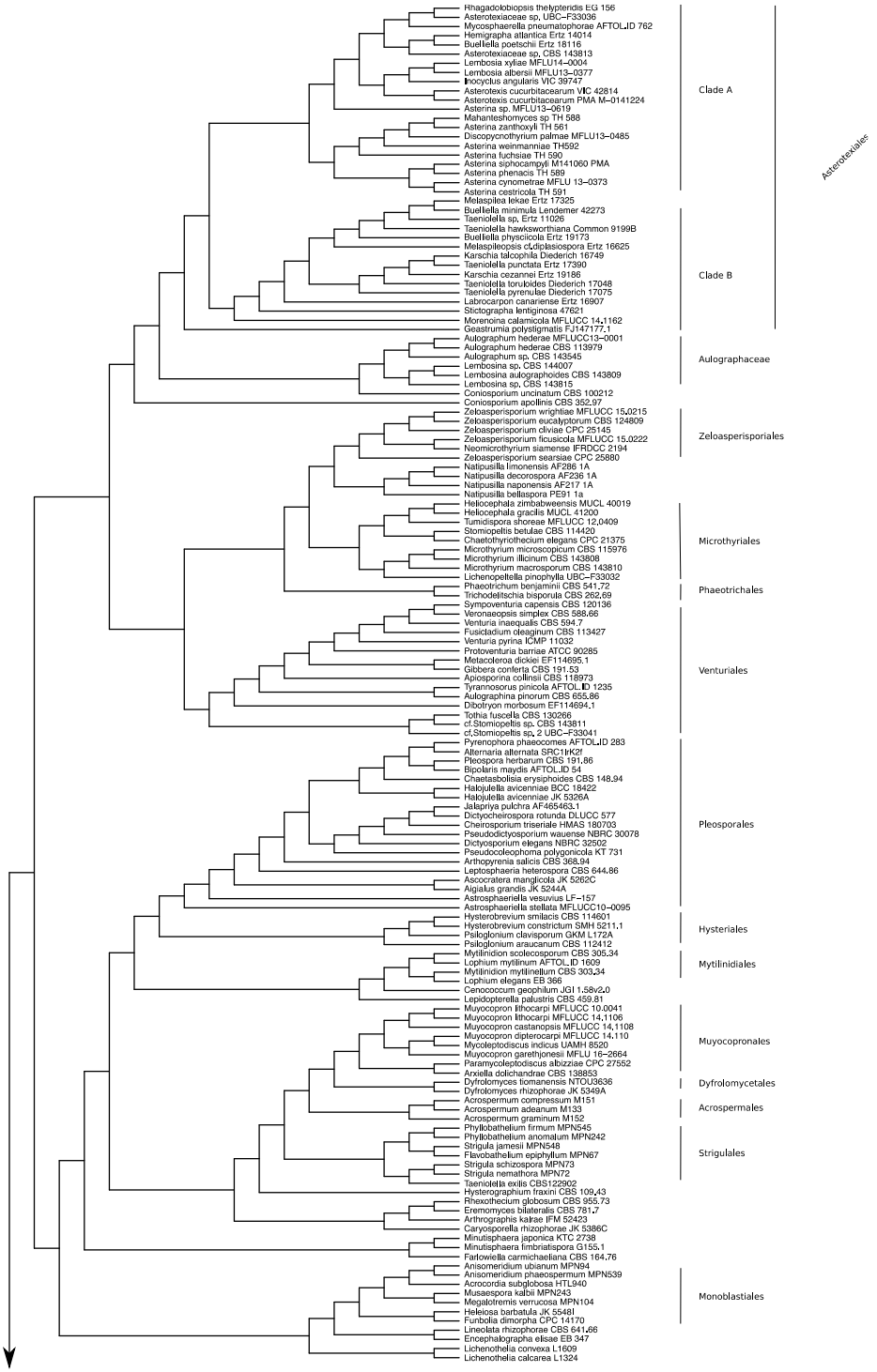

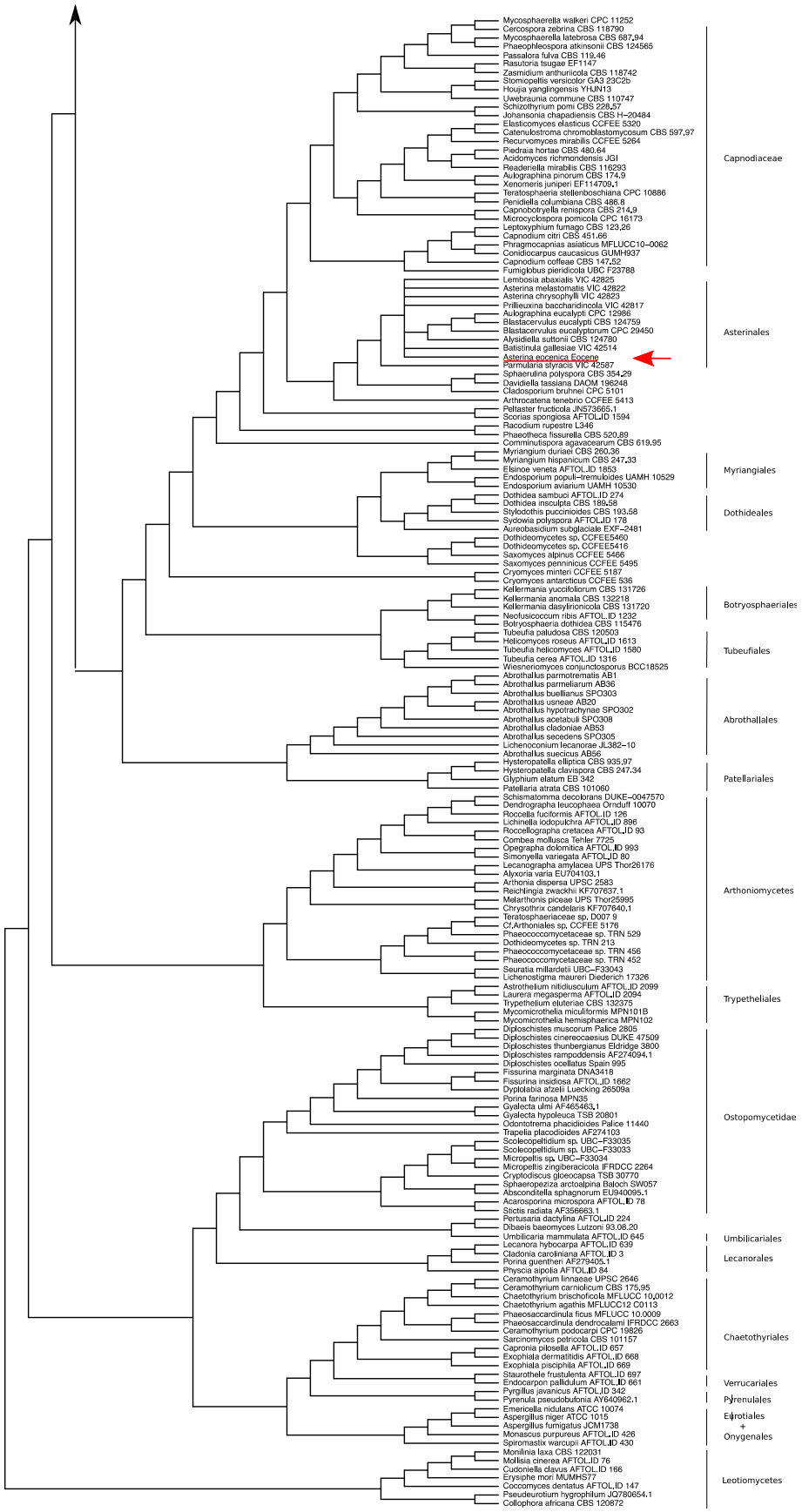
Mycosphaerella walkeri CPC 11252
Cercospora zebrina CBS 118790
Mycosphaerella latebrosa CBS 687.94
Phaeophleospora atkinsonii CBS 124565
Passalora fulva CBS 119.46
Rasutoria tsugae EF1147
Zasmidium anthuriicola CBS 118742
Stomiopeltis versicolor GA3 23C2b
Houjia yangtingensis YHJN13
Uwebraunia commune CBS 110747
Schizothyrium pomi CBS 228.57
Johansonia chapadiensis CBS H-20484
Elasticomyces elasticus CCFEE 5320
Catenulostroma chromoblastomycosum CBS 597.97
Recurvomyces mirabilis CCFEE 5264
Piedraia hortae CBS 480.64
Acidomyces richmondensis JGI
Readeriella mirabilis CBS 116293
Aulographina pinorum CBS 174.9
Xenomeris juniperi EF114709.1
Teratosphaeria stellenboschiana CPC 10886
Penidiella columbiana CBS 486.8
Capnobotryella renispora CBS 214.9
Microcyclospora pomicola CPC 16173
Leptoxyphium fumago CBS 123.26
Capnodium citri CBS 451.66
Phragmocapnias asiaticus MFLUCC10-0062
Conidiocarpus caucasicus GUMH937
Capnodium coffeae CBS 147.52
Fumiglobus pieridicola UBC F23788
Capnodiaceae
Lembosia abaxialis VIC 42825
Asterina melastomatis VIC 42822
Asterina chrysophylli VIC 42823
Prillieuxina baccharidincola VIC 42817
Aulographina eucalypti CPC 12986
Blastacervulus eucalypti CBS 124759
Blastacervulus eucalyptorum CPC 29450
Alysidiella suttonii CBS 124780
Batistinula gallesiae VIC 42514
Asterina eocenica Eocene
Parmularia styracis VIC 42587
Asterinales
Sphaerulina polyspora CBS 354.29
Davidiella tassiana DAOM 196248
Cladosporium bruhnei CPC 5101
Arthrocatena tenebrio CCFEE 5413
Peltaster fructicola JN573665.1
Scorias spongiosa AFTOL_ID 1594
Racodium rupestre L346
Phaeotheca fissurella CBS 520.89
Comminutispora agavacearum CBS 619.95
Myriangium duriaei CBS 260.36
Myriangium hispanicum CBS 247.33
Elsinoe veneta AFTOL_ID 1853
Endosporium populi-tremuloides UAMH 10529
Endosporium aviarium UAMH 10530
Myriangiales
Dothidea sambuci AFTOL_ID 274
Dothidea insculpta CBS 189.58
Stylodothis puccinioides CBS 193.58
Sydowia polyspora AFTOL_ID 178
Aureobasidium subglaciale EXF-2481
Dothideales
Dothideomycetes sp. CCFEE5460
Dothideomycetes sp. CCFEE5416
Saxomyces alpinus CCFEE 5466
Saxomyces penninicus CCFEE 5495
Cryomyces minteri CCFEE 5187
Cryomyces antarcticus CCFEE 536
Kellermania yuccifoliorum CBS 131726
Kellermania anomala CBS 132218
Kellermania dasyliriicola CBS 131720
Botryosphaeriales
Neofusicoccum ribis AFTOL_ID 1232
Botryosphaeria dothidea CBS 115476
Tubeufia paludosa CBS 120503
Helicomyces roseus AFTOL_ID 1613
Tubeufia helicomyces AFTOL_ID 1580
Tubeufia cerea AFTOL_ID 1316
Tubeufiales
Wiesneriomyces conjunctosporus BCC18525
Abrothallus parmotrematis AB1
Abrothallus parmeliarum AB36
Abrothallus buellianus SPO303
Abrothallus usneae AB20
Abrothallus hypotrachynae SPO302
Abrothallus acetabuli SPO308
Abrothallus cladoniae AB53
Abrothallus secedens SPO305
Lichenoconium lecanorae JL382-10
Abrothallus suecicus AB56
Abrothallales
Hysteropatella elliptica CBS 935.97
Hysteropatella clavispora CBS 247.34
Glyphium elatum EB 342
Patellaria atrata CBS 101060
Patellariales
Schismatomma decolorans DUKE-0047570
Dendrographa leucophaea Ornduff 10070
Roccella fuciformis AFTOL_ID 126
Lichinella iodopulchra AFTOL_ID 896
Roccellographa cretacea AFTOL_ID 93
Combea mollusca Tehler 7725
Opegrapha dolomitica AFTOL_ID 993
Simonyella variegata AFTOL_ID 80
Lecanographa amylacea UPS Thor26176
Alyxoria varia EU704103.1
Arthonia dispersa UPSC 2583
Reichlingia zwackhii KF707637.1
Melarthonis piceae UPS Thor25995
Chrysothrix candelaris KF707640.1
Teratosphaeriaceae sp. D007 9
Cf.Arthoniales sp. CCFEE 5176
Phaeococcomycetaceae sp. TRN 529
Dothideomycetes sp. TRN 213
Phaeococcomycetaceae sp. TRN 456
Phaeococcomycetaceae sp. TRN 452
Seuratia millardetii UBC-F33043
Lichenostigma maureri Diederich 17326
Arthoniomycetes
Astrothelium nitidiusculum AFTOL_ID 2099
Laurera megasperma AFTOL_ID 2094
Trypethelium eluteriae CBS 132375
Mycomicrothelia miculiformis MPN101B
Mycomicrothelia hemisphaerica MPN102
Trypetheliales
Diploschistes muscorum Palice 2805
Diploschistes cinereocaesius DUKE 47509
Diploschistes thunbergianus Eldridge 3800
Diploschistes rampoddensis AF274094.1
Diploschistes ocellatus Spain 995
Fissurina marginata DNA3418
Fissurina insidiosa AFTOL_ID 1662
Dyplolabia afzelii Lueking 26509a
Porina farinosa MPN35
Gyalecta ulmi AF465463.1
Gyalecta hypoleuca TSB 20801
Odontotrema phacidioides Palice 11440
Trapelia placodioides AF274103
Sclerocpeltidium sp. UBC-F33035
Sclerocpeltidium sp. UBC-F33033
Micropeltis sp. UBC-F33034
Micropeltis zingiberacicola IFRDCC 2264
Cryptodiscus gloeocapsa TSB 30770
Sphaeropeziza arctoalpina Baloch SW057
Absconditella sphagnorum EU940095.1
Acarosporina microspora AFTOL_ID 78
Stictis radiata AF356663.1
Ostopomycetidae
Pertusaria dactylina AFTOL_ID 224
Dibaeis baeomyces Lutzoni 93.08.20
Umbilicaria mammulata AFTOL_ID 645
Umbilicariales
Lecanora hybocarpa AFTOL_ID 639
Cladonia caroliniana AFTOL_ID 3
Porina guentheri AF279405.1
Lecanorales
Physcia aipolia AFTOL_ID 84
Ceramothyrium linnaeae UPSC 2646
Ceramothyrium carniolicum CBS 175.95
Chaetothyrium brischoficola MFLUCC 10.0012
Chaetothyrium agathis MFLUCC12 C0113
Phaeosaccardinula ficus MFLUCC 10.0009
Phaeosaccardinula dendrocalami IFRDCC 2663
Ceramothyrium podocarpi CPC 19826
Sarcinomyces petricola CBS 101157
Capronia pilosella AFTOL_ID 657
Exophiala dermatitidis AFTOL_ID 668
Exophiala pisciphila AFTOL_ID 669
Chaetothyriales
Staurothele frustulenta AFTOL_ID 697
Endocarpon pallidulum AFTOL_ID 661
Verrucariales
Pyrgillus javanicus AFTOL_ID 342
Pyrenulales
Pyrenula pseudobufonia AY640962.1
Emericella nidulans ATCC 10074
Aspergillus niger ATCC 1015
Aspergillus fumigatus JCM1738
Monascus purpureus AFTOL_ID 426
Spiromastix warcupii AFTOL_ID 430
Eurotiales + Onygenales
Monilinia laxa CBS 122031
Mollisia cinerea AFTOL_ID 76
Cudoniella clavus AFTOL_ID 166
Erysiphe mori MUMHS77
Coccomyces dentatus AFTOL_ID 147
Pseudeurotium hygrophilum JQ780654.1
Callophora africana CBS 120872
Leotiomycetes

Appendix B

B.1 Isolates used in phylogenetic analyses

Order	Taxa	Voucher/Strain	GenBank accession - SSU	GenBank accession - LSU
Asterotexiales	**Asterotexiaceae Firmino, O.L. Pereira & Crous sp. 1**	UBC-F33036*	-	MG844156
Asterotexiales	*Mycosphaerella pneumatophorae* Kohlm.	AFTOL-ID 762	-	FJ176856.1
Asterotexiales	*Lembosia albersii* Henn.	MFLU13-0377	-	KM386982.1
Asterotexiales	*Asterina phenacis* Syd.	TH 589	GU586211.1	GU586217.1
Asterotexiales	*Melaspilea lekae* Brackel & Kalb	Ertz 17325 (BR)	-	KP456162.1
Asterotexiales	*Buelliella minimula* (Tuck.) Fink	Lendemer 42273 (NY)	-	KX244961.1
Asterotexiales	*Morenoina calamicola* S. Konta & K.D. Hyde		KY511427	KY511424
Aulographaceae	***Aulographum* Lib. sp.**	CBS 143545*	MG844146	MG844158
Aulographaceae	***Lembosina* Theiss. sp.**	CBS 144007*	-	MG844164
Natipusillales	*Natipusilla decorospora* A. Ferrer, A.N. Mill. & Shearer	AF236 1A	HM196376.1	HM196369.1
Natipusillales	*Natipusilla naponensis* A. Ferrer, A.N. Mill. & Shearer	AF217 1A	HM196378.1	HM196371.1
Microthyriales	*Tumidispora shoreae* Hongsanan & K.D. Hyde	MFLUCC 12-0409	-	KT314074.1
Microthyriales	*Chaetothyriothecium elegans*	CPC 21375	-	KF268420.1

	Hongsanan & K.D. Hyde			
Microthyriales	***Microthyrium illicinum* De Not.**	CBS 143808 *	MG844144	MG844151
Microthyriales	***Lichenopeltella pinophylla* (Höhn.) P.M. Kirk & Minter**	UBC-F33032*	-	MG844152
Phaeotrichales	*Phaeotrichum benjaminii* Malloch & Cain	CBS 541.72	AY016348.1	AY004340.1
Phaeotrichales	*Trichodelitschia bisporula* (P. Crouan & H. Crouan) Munk ex N. Lundq.	CBS 262.69	JGI	JGI
Venturiales	*Venturia inaequalis* (Cooke) G. Winter	CBS 594.70	KF156093.1	GU301879.1
Venturiales	*Metacoleroa dickiei* (Berk. & Broome) Petr.	Oregon-non-cultivated	EF114719.1	EF114695.1
Pleosporales	*Pleospora herbarum* (Pers.) Rabenh.	CBS 191.86	DQ247812.1	JX681120.1
Pleosporales	*Astrosphaeriella stellata* (Pat.) Sacc.	MFLUCC10-0095	JN846741.1	JN846720.1
Hysteriales	*Hysterobrevium constrictum* (N. Amano) E. Boehm & C.L. Schoch	SMH 5211.1	GU397361.1	GQ221905.2
Mytilinidiales	*Lophium mytilinum* (Pers.) Fr.	AFTOL-ID 1609	DQ678030.1	DQ678081.1
Mytilinidiales	*Mytilinidion mytilinellum* (Fr.) H. Zogg	CBS 303.34	FJ161144.2	FJ161184.2

* Newly sequenced specimen

Capnodiales	*Mycosphaerella latebrosa* (Cooke) J. Schröt.	CBS 687.94	GU214546.1	GU214444.1
Capnodiales	*Capnodium coffeae* Pat.	CBS 147.52	DQ247808.1	GU214400.1
Asterinales	*Lembosia abaxialis* Firmino & R.W. Barreto	VIC 42825	-	KP143737.1
Asterinales	*Asterina melastomatis* Lév.	VIC 42822	-	MK251541
Asterinales	*Batistinula gallesiae* Arx	VIC 42514	-	KM111255.1
Capnodiales	*Sphaerulina polyspora* F.A. Wolf	(SSU) STE-U 4301	AY251095.1	GU214501.1
		(LSU) **CBS 354.29**		
Capnodiales	*Davidiella tassiana* (De Not.) Crous & U. Braun	DAOM 196248	JN939022.1	JN938886.1
Tubeufiales	*Tubeufia helicomyces*	AFTOL-ID 1580	DQ767649.1	DQ767654.1
Patellariales	*Patellaria atrata* (Hedw.) Fr.	CBS 101060	JGI	JGI
Arthoniales	*Roccella fuciformis* (L.) DC.	AFTOL-ID 126	AY584678.1	AY584654.1
Arthoniales	*Arthonia dispersa* (Schrad.) Nyl.	UPSC 2583	AY571381.1	AY571381.1

B.2 Character matrix used in parsimony analysis

Characters scored include I - HAB, substrate or habitat (0= on rock or soil, 1= superficial on plants, 2= lichenicolous or 3= immersed in plants); II - SPO, sporocarp type (0= apothecioid, perithecioid, 1= thyriothecioid, 2= cleistothecioid); III - DEH, dehiscence (0= ostiole, 1= irregular slit, 2= regular slit, 3= no dehiscence; 4= exposed at maturity); IV - LOC, locule circumference (0= circular,1= elongate); V - BRA, scutellum hyphal branching (0= pseudoparenchyma, 1= isotomous dichotomies; 2= pseudomonopodial dichotomies); VI-MAR, appressed margin of scutellum (0= not appressed, 1= crenulate, 2= entire) and VII - APP, lateral appressoria (0= present, 1= absent). Taxon morphology is either from direct observation or interpretation of the figures referenced in the last two columns. Thyriothecial taxa and their states are in bold

Taxon name	**I - HAB**	**II - SPO**	**III - DEH**	**IV - LOC**	**V - BRA**	**VI - MAR**	**VII - APP**	**Reference**	**Illustration for character information**
Asterotexiaceae sp. CBS 143813	**1**	**2**	**0**	**0**	**1**	**1**	**0**		This study
Mycosphaerella pneumatophorae AFTOL-ID 762	3	1	1	0	0	0	0	(Kohlmeyer, 1966)	Fig. 87a
***Lembosia albersii* MFLU13-0377**	**1**	**2**	**1**	**1**	**1**	**1**	**1**	(Hongsanan et al., 2014b)	Fig. 18
***Asterina phenacis* TH 589**	**1**	**2**	**1**	**0**	**1**	**1**	**1**	(Hofmann and Piepenbring, 2008)	Fig. 8

Buelliella minimula Lendemer 42273(NY)	2	0	4	0	0	0	0	(Ertz and Diederich, 2015)	Figs. 4a-5a
***Morenoina calamicola* MFLUCC 14-1162**	**1**	**2**	**1**	**1**	**1**	**1**	**0**	(Tibpromma et al., 2017)	Fig. 2
***Aulographum* sp. CBS 143545**	**1**	**2**	**1**	**1**	**2**	**1**	**0**		This study
***Lembosina* sp. 2 CBS 143815**	**1**	**2**	**1**	**1**	**2**	**1**	**0**		This study
Natipusilla decorospora AF236 1A	3	3	3	0	0	0	0	(Ferrer et al., 2011)	Figs. 11–16
Natipusilla naponensis AF217 1A	3	3	3	0	0	0	0	(Ferrer et al., 2011)	Figs. 24–30
***Tumidispora shoreae* MFLUCC 12-0409**	**1**	**2**	**0**	**0**	**1**	**?**	**0**		Fig. 39
***Chaetothyriothecium elegans* CPC 21375**	**1**	**2**	**0**	**0**	**1**	**?**	**0**	(Ariyawansa et al., 2015)	Fig. 2
***Lichenopeltella pinophylla* UBC-F33032**	**1**	**2**	**0**	**0**	**1**	**2**	**0**		This study
***Microthyrium ilicinum* CBS 143808**	**1**	**2**	**0**	**0**	**1**	**2**	**0**		This study
Phaeotrichum benjaminii CBS 541.72	?	3	3	0	0	0	0	(Cain, 1956)	Based on *P. hystricinum*, Figs.1–11
Trichodelitschia bisporula CBS 262.69	?	1	0	0	0	0	0		Based on *T. minuta* at ascofrance.org
Venturia inaequalis CBS 594.70	1	1	0	0	0	0	0	(Hyde et al., 2013)	Fig. 131
Metacoleroa dickiei EF114695.1	1	1	0	0	0	?	0	(Barr, 1968)	Fig. 8

Pleospora herbarum CBS 191.86	1	1	0	0	0	0	0	(Inderbitzin et al., 2009)	Fig. 1
Astrosphaeriella stellata MFLUCC10-0095	1	1	0	0	0	0	0	(Liu et al., 2011)	Fig. 2
Hysterobrevium constrictum SMH 5211.1	1	0	2	1	0	0	0	(Boehm et al., 2009b)	Figs. 5A–E
Mytilinidion mytilinellum CBS 303.34	1	0	2	0	0	0	0	(Hyde et al., 2013)	Fig. 87
Mycosphaerella latebrosa CBS 687.94	1	1	0	0	0	0	0	(Crous et al., 2009)	none
Piedraia hortae CBS 480.64	?	3	3	0	0	0	0	(Takashio and Vanbreuseghem, 1971)	Figs. 1-2
Capnodium coffeae CBS 147.52	1	1	0	0	0	0	0	(Chomnunti et al., 2014)	Following genus description
***Lembosia abaxialis* VIC 42825**	**1**	**2**	**1**	**1**	**1**	**1**	**1**	(Guatimosim et al., 2015)	Fig. 6, this study
***Asterina melastomatis* VIC 42822**	**1**	**2**	**1**	**0**	**1**	**1**	**1**	(Guatimosim et al., 2015)	Fig. 3, this study
***Batistinula gallesiae* VIC 42514**	**1**	**2**	**1**	**0**	**1**	**1**	**1**	(Guatimosim et al., 2015)	Fig. 5, This study
Sphaerulina polyspora CBS 354.29	1	1	0	0	0	0	0	(Wolf, 1925)	Figs. 8;11–14; 16-17
Davidiella tassiana DAOM 196248	1	1	0	0	0	0	0	(Schubert et al., 2007)	Fig. 18
Elsinoe veneta AFTOL-ID 1853	1	1	0	0	?	0	0	(Jayawardena et al., 2014)	p. 129
Dothidea sambuci AFTOL-ID 274	1	1	0	0	0	0	0	(Thambugala et al., 2014)	Fig. 2
Tubeufia helicomyces AFTOL-ID 1580	3	1	0	0	0	0	0	(Webster, 1951)	Figs. 1-2

Patellaria atrata CBS 101060	3	0	2	0	0	0	0		Pl. 5 Fig. 45
Roccella fuciformis AFTOL-ID 126	0	0	4	0	0	?	0	(Ellis and Ellis, 1997)	link
Arthonia dispersa UPSC 2583	3	0	2	1	0	0	0	(Brodo et al., 2001)	from genus description and link

Appendix C

C.1 List of taxa and accessions included in phylogenetic analysis

Taxa in bold represent thyriothecium-forming fungi.

Order	Taxa	Voucher/Strain	GenBank accession - SSU	GenBank accession - LSU
Abrothallales	*Abrothallus parmeliarum* (Sommerf.) Arnold 1874	AB57	KF816221.1	KF816227.1
Abrothallales	*Abrothallus secedens* Wedin & R. Sant. 1994	SPO305	KF816216.1	KF816236.1
Arthoniales	*Roccella fuciformis* (L.) DC.	AFTOL-ID 126	AY584678.1	AY584654.1
Arthoniales	*Arthonia dispersa* (Schrad.) Nyl.	UPSC 2583	AY571381.1	AY571381.1
Asterinales	***Lembosia abaxialis* Firmino & R.W. Barreto**	VIC 42825	-	KP143737.1
Asterinales	***Asterina melastomatis* Lév.**	VIC 42822	-	MK251541
Asterinales	***Batistinula gallesiae* Arx**	VIC 42514	-	KM111255.1
Asterotexiales	*Mycosphaerella pneumatophorae* Kohlm.	AFTOL-ID 762	-	FJ176856.1
Asterotexiales	***Lembosia albersii* Henn.**	MFLU13-0377	-	KM386982.1
Asterotexiales	***Asterina phenacis* Syd.**	TH 589	GU586211.1	GU586217.1
Asterotexiales	***Discopycnothyrium palmae* Hongsanan & K.D. Hyde**	SH-2014	-	KM386979.1
Asterotexiales	*Buelliella minimula* (Tuck.) Fink	Lendemer 42273 (NY)	-	KX244961.1

Asterotexiales	***Morenoina calamicola* S. Konta & K.D. Hyde**		KY511427	KY511424
Aulographaceae	***Aulographum* Lib. sp.**	CBS 143545	MG844146	MG844158
Aulographaceae	***Lembosina* Theiss. sp.**	CBS 144007	-	MG844164
Capnodiales	*Mycosphaerella latebrosa* (Cooke) J. Schröt.	CBS 687.94	GU214546.1	GU214444.1
Capnodiales	*Capnodium coffeae* Pat.	CBS 147.52	DQ247808.1	GU214400.1
Capnodiales	*Sphaerulina polyspora* F.A. Wolf	(SSU) STE-U 4301	AY251095.1	GU214501.1
		(LSU) **CBS 354.29**		
Capnodiales	*Davidiella tassiana* (De Not.) Crous & U. Braun	DAOM 196248	JN939022.1	JN938886.1
Dothideales	*Dothidea sambuci* (Pers.) Fr.	AFTOL-ID 274	AY544722.1	AY544681.1
Dyfrolomycetales	*Dyfrolomyces tiomanensis* K.L. Pang, Alias, K.D. Hyde, Suetrong & E.B.G. Jones	NTOU3636	KC692155.1	KC692156.1
Dyfrolomycetales	*Dyfrolomyces sinensis* Samarak., Tennakoon & K.D. Hyde	MFLUCC 17-1344	MG836700.1	MG836699.1
Hysteriales	*Hysterobrevium constrictum* (N. Amano) E. Boehm & C.L. Schoch	SMH 5211.1	GU397361.1	GQ221905.2
Microthyriales	***Tumidispora shoreae* Hongsanan & K.D. Hyde**	MFLUCC 12-0409	-	KT314074.1
Microthyriales	***Chaetothyriothecium elegans* Hongsanan & K.D. Hyde**	CPC 21375	-	KF268420.1
Microthyriales	***Microthyrium illicinum* De Not.**	CBS 143808 *	MG844144	MG844151
Microthyriales	***Lichenopeltella pinophylla* (Höhn.) P.M. Kirk & Minter**	CBS 143816	-	

Muyocopronales	***Muyocopron dipterocarpi* Mapook, Boonmee & K.D. Hyde**	MFLUCC:14-1103	KU726969.1	KU726966.1
Muyocopronales	***Muyocopron lithocarpi* Mapook, Boonmee & K.D. Hyde**	MFLUCC:14-1106	KU726970.1	KU726967.1
Muyocopronales	*Muyocopron zamiae* Hern.-Restr. & Crous	CBS 203.71	-	MK487727.1
	Elsinoë veneta (Burkh.) Jenkins	AFTOL-ID 1853	DQ767651.1	DQ767658.1
Mytilinidiales	*Lophium mytilinum* (Pers.) Fr.	AFTOL-ID 1609	DQ678030.1	DQ678081.1
Natipusillales	*Natipusilla decorospora* A. Ferrer, A.N. Mill. & Shearer	AF236 1A	HM196376.1	HM196369.1
Natipusillales	*Natipusilla naponensis* A. Ferrer, A.N. Mill. & Shearer	AF217 1A	HM196378.1	HM196371.1
Patellariales	*Patellaria atrata* (Hedw.) Fr.	CBS 101060	JGI	JGI
Phaeotrichales	*Trichodelitschia bisporula* (P. Crouan & H. Crouan) Munk ex N. Lundq.	CBS 262.69	JGI	JGI
Phaeotrichales	*Phaeotrichum benjaminii* Malloch & Cain	CBS 541.72	AY016348.1	AY004340.1
Pleosporales	*Pleospora herbarum* (Pers.) Rabenh.	CBS 191.86	DQ247812.1	JX681120.1
Pleosporales	*Astrosphaeriella stellata* (Pat.) Sacc.	MFLUCC10-0095	JN846741.1	JN846720.1
Tubeufiales	*Tubeufia helicomyces*	AFTOL-ID 1580	DQ767649.1	DQ767654.1
Venturiales	*Venturia inaequalis* (Cooke) G. Winter	CBS 594.70	KF156093.1	GU301879.1
Venturiales	*Metacoleroa dickiei* (Berk. & Broome) Petr.	Oregon-non-cultivated	EF114719.1	EF114695.1

C.2 Maximum likelihood phylogeny

Most likely topology of 41 extant Dothideomycetes and two outgroup taxa in Arthoniomycetes; numbers on branches represent support out of 1000 bootstrap replicated.

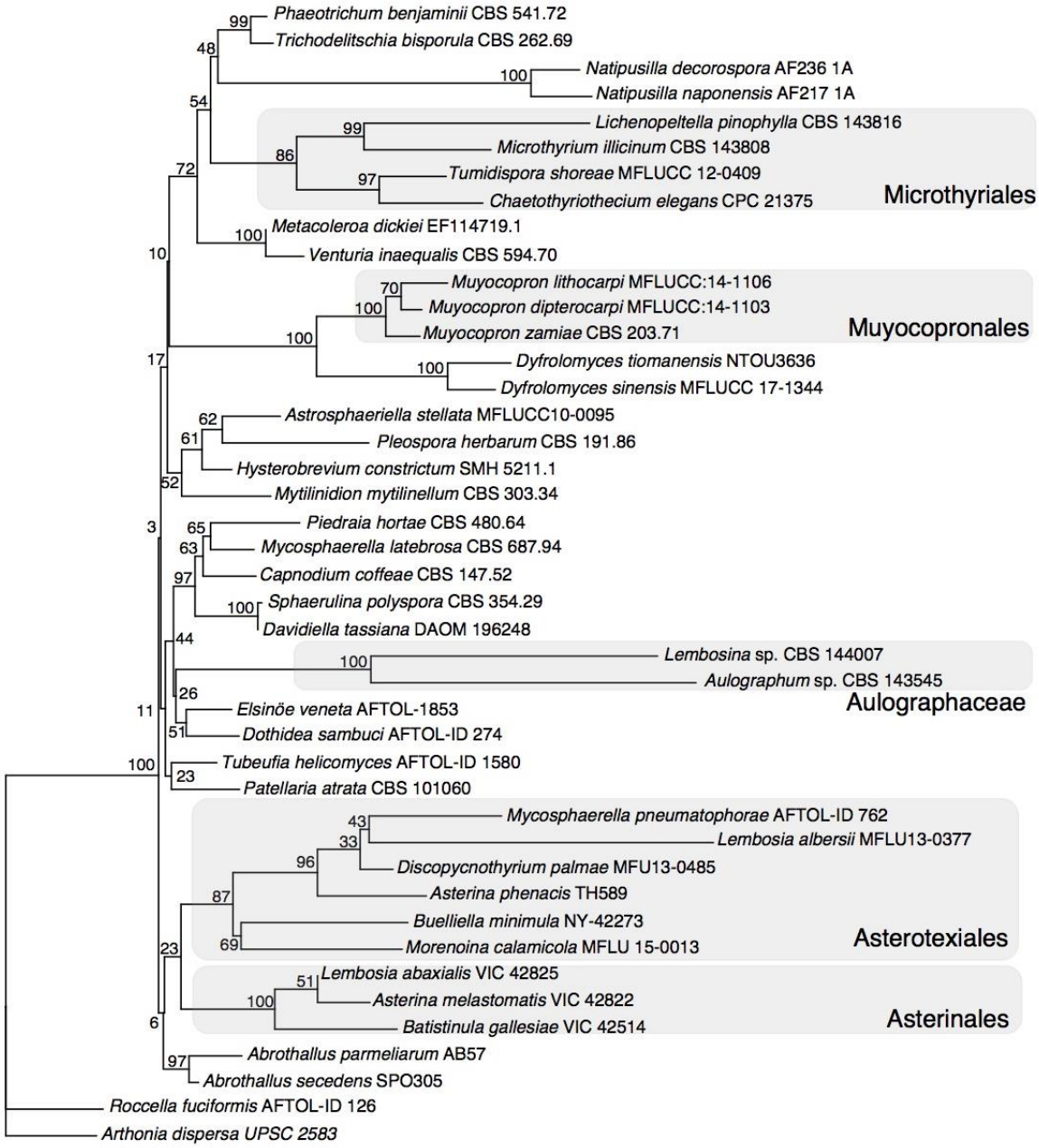

C.3 Bayesian inference of phylogeny

Maxixmum clade credibility topology obtained from the posterior distribution of trees from Mr.Bayes runs; numbers on branches indicate posterior probabilities.

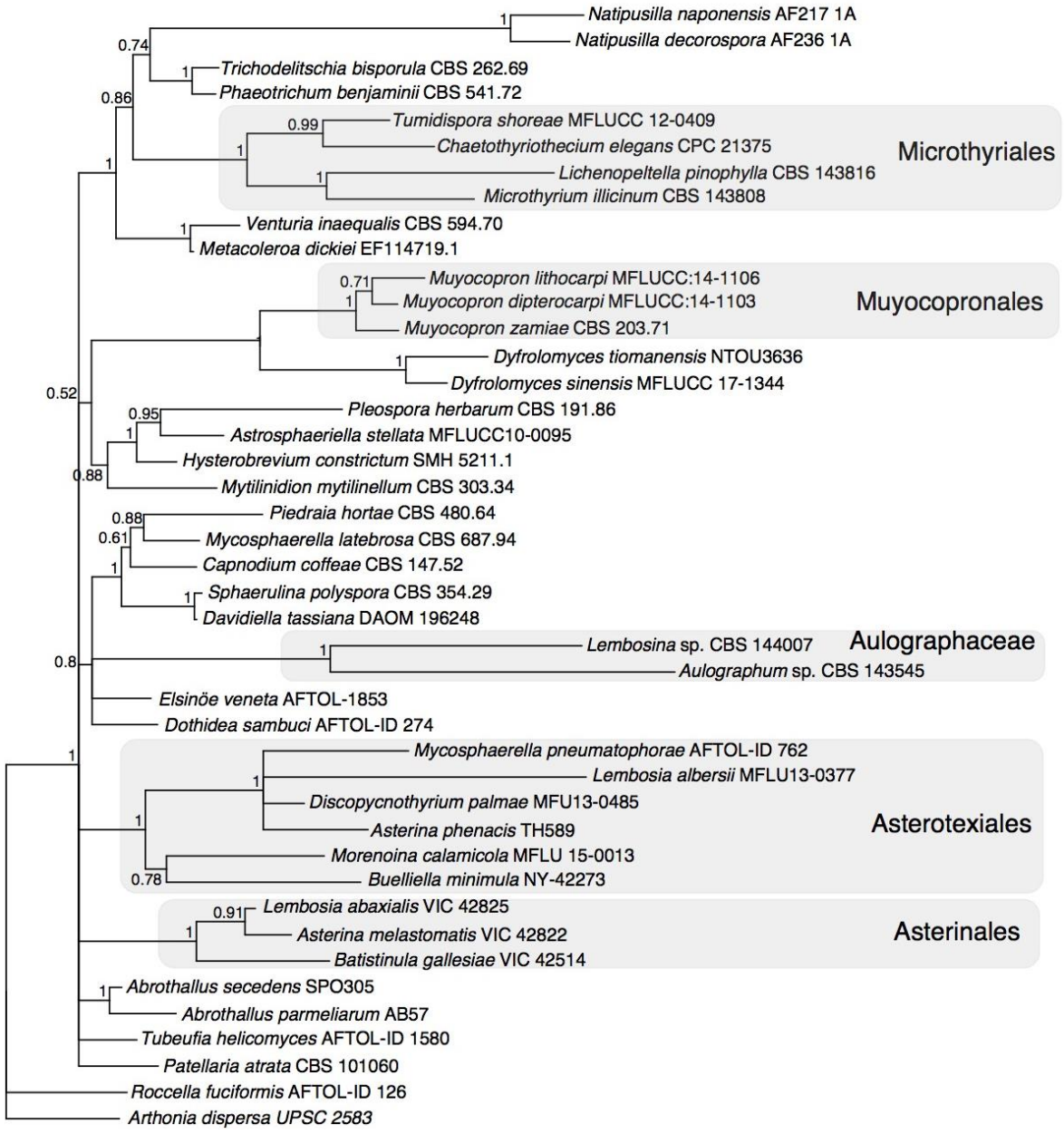

C.4 Character matrix used for parsimony analysis

Taxon	HAB	SPO	LW	OST	OL	RAD	BRA	MAR	APP	Reference
Bleximothyrites otiolatus †	1	2	0	1	0	1	1	3	1	personal observation
Abrothallus parmeliarum	2	0	1	0	0	0	0	0	?	(Pérez-Ortega et al., 2014)
Abrothallus secedens	2	0	1	0	0	0	0	0	?	(Pérez-Ortega et al., 2014)
Arthonia dispersa	3	0	0	0	1	0	0	0	?	(Sundin and Tehler, 1998; Brodo et al., 2001)
Roccella fuciformis	0	0	1	0	0	0	0	?	?	link
Asterina melastomatis	1	2	0	0	0	1	1	1	1	personal observation.
Batistinula gallesiae	1	2	0	0	0	1	1	1	1	personal observation.
Lembosia abaxialis	1	2	0	1	1	1	1	1	1	(Guatimosim et al., 2015)
Asterina phenacis	1	2	0	0	0	1	1	1	1	(Hofmann and Piepenbring, 2008)
Buelliella minimula	2	0	1	0	0	0	0	0	?	(Ertz and Diederich, 2015)
Discopycnothyrium palmae	1	2	0	1	0	1	1	1	?	(Hongsanan et al., 2016)
Lembosia albersii	1	2	0	0	1	1	1	1	1	(Hongsanan et al., 2014b)
Morenoina calamicola	1	2	0	0	1	1	1	1	?	(Tibpromma et al., 2017)
Mycosphaerella pneumatophorae	3	1	1	1	0	0	0	0	?	(Kohlmeyer, 1966)
Aulographum sp.	1	2	0	1	1	1	2	1	1	personal observation.
Lembosina sp.	1	2	0	1	1	1	2	1	1	personal observation.

Taxon	HAB	SPO	LW	OST	OL	RAD	BRA	MAR	APP	Reference
Capnodium coffeae	1	1	1	1	0	0	0	0	?	(Chomnunti et al., 2011)
Davidiella tassiana	1	1	1	1	0	0	0	0	?	(Schubert et al., 2007)
Mycosphaerella latebrosa	1	1	1	1	0	0	0	0	?	(Crous et al., 2009)
Piedraia hortae	?	3	1	0	0	0	0	0	?	(Takashio and Vanbreuseghem, 1971)
Sphaerulina polyspora	1	1	1	1	0	0	0	0	?	(Wolf, 1925)
Dothidea sambuci	1	1	1	1	0	0	0	0	?	(Thambugala et al., 2014)
Dyfrolomyces sinensis	3	1	1	1	0	0	0	0	?	(Pang et al., 2013)
Dyfrolomyces tiomanensis	3	1	1	1	0	0	0	0	?	(Pang et al., 2013)
Hysterobrevium constrictum	1	0	1	1	1	0	0	0	?	(Boehm et al., 2009b)
Chaetothyriothecium elegans	1	2	0	1	0	1	1	?	?	(Hongsanan et al., 2014a)
Lichenopeltella pinophylla	1	2	1	1	0	1	1	2	0	personal observation
Microthyrium illicinum	1	2	0	1	0	1	1	2	1	personal observation.
Tumidispora shoreae	1	2	0	1	0	1	1	?	?	(Ariyawansa et al., 2015)
Muyocopron dipterocarpi	1	2	0	1	1	1	1	1	?	(Mapook et al., 2016b)
Muyocopron lithocarpi	1	2	0	1	1	1	1	1	?	(Mapook et al., 2016b)
Muyocopron zamiae	1	?	?	?	1	0	0	0	?	(Hernández-Restrepo et al., 2019)

Taxon	HAB	SPO	LW	OST	OL	RAD	BRA	MAR	APP	Reference
Elsinoë veneta	1	1	1	1	0	0	0	0	?	(Jayawardena et al., 2014)
Mytilinidion mytilinellum	1	0	1	0	0	0	0	0	?	(Hyde et al., 2013)
Natipusilla decorospora	3	3	1	1	0	0	0	0	?	(Ferrer et al., 2011)
Natipusilla naponensis	3	3	1	1	0	0	0	0	?	(Ferrer et al., 2011)
Patellaria atrata	3	0	1	0	0	0	0	0	?	(Ellis and Ellis, 1997)
Trichodelitschia bisporula	?	3	1	0	0	0	0	0	?	link
Phaeotrichum benjaminii	?	1	1	1	0	0	0	0	?	(Cain, 1956)
Astrosphaeriella stellata	1	1	1	1	0	0	0	0	?	(Liu et al., 2011)
Pleospora herbarum	1	1	1	1	0	0	0	0	?	(Inderbitzin et al., 2009)
Tubeufia helicomyces	3	1	1	1	0	0	0	0	?	(Webster, 1951)
Metacoleroa dickiei	1	1	1	1	0	0	0	?	?	(Barr, 1968)
Venturia inaequalis	1	1	1	1	0	0	0	0	1	(Hyde et al., 2013)

†Fossil taxon

HAB - Substrate: 0 = saxicolous; 1 = superficial on plants; 2 = lichenicolous; 3 = immersed on plants; SPO - Sporocarp type: 0 = apothecioid; 1 = perithecioid; 2 = thyriothecioid; 3 = cleisothecioid; LW - Lower wall: 0 = undifferientiated; 1 = differentiated; OST- Ostiole: 0 = absent; 1 = present; OL - Sporocarp outline: 0 = circular; 1 = ellipsoid to elongate; RAD: 0 = non-radiate; 1 = radiate BRA - Scutellum branching: 0 = pseudoparenchymatous; 1 = isotomous dichotomies; 2 = pseudomonopodial dichotomies; MAR - Margin: 0 = margin not appressed; 1 = crenulate, aligned; 2 = entire, aligned; 3 = diverging from radius; APP - Appressoria: 0 = absent; 1 = present; Column 'Ref.' indicate reference used to score fungus, 'obs.' indicate taxa score from direct observation